

Dissertation zur Erlangung des Doktorgrades
der Fakultät für Chemie und Pharmazie
der Ludwig-Maximilians-Universität München

**Synthesis of Tri- and Tetracyclic Azaheterocycles from
1,4-Dihydropyridines and their Use for the Development of
GAT Inhibitors**

Heinrich-Karl Andreas Rudy

aus Essen, Deutschland

2020

Erklärung

Diese Dissertation wurde im Sinne von § 7 der Promotionsordnung vom 28. November 2011 von Herrn Prof. Dr. Klaus T. Wanner betreut.

Eidesstattliche Versicherung

Diese Dissertation wurde eigenständig und ohne unerlaubte Hilfe erarbeitet.

München, 26.10.2020

Heinrich-Karl Rudy

Dissertation eingereicht am 26.10.2020

1. Gutachter Prof. Dr. Klaus T. Wanner

2. Gutachter Prof. Dr. Franz F. Paintner

Mündliche Prüfung am 27.11.2020

Die vorliegende Arbeit entstand in der Zeit von März 2015 bis November 2020 am
Department Pharmazie – Zentrum für Pharmaforschung – der
Ludwig-Maximilians-Universität München auf Anregung und unter Leitung von

Herrn Prof. Dr. Klaus T. Wanner

Für die hervorragende und äußerst engagierte Betreuung und Förderung meiner
Arbeit sowie die ausgezeichneten Forschungsbedingungen möchte ich mich bei
Herrn Prof. Dr. Klaus T. Wanner sehr herzlich bedanken.

Herrn Prof. Dr. Franz Paintner danke ich sehr herzlich für
die Übernahme des Koreferats.

This cumulative thesis is based on the following original publications

First publication:

Heinrich-Karl A. Rudy, and Klaus T. Wanner, *Synthesis* **2019**, *51*, 4296–4310.

“Accessing Tricyclic Imines Comprising a 2-Azabicyclo[2.2.2]octane Scaffold by Intramolecular Hetero-Diels–Alder Reaction of 4-Alkenyl-Substituted *N*-Silyl-1,4-dihydropyridines”

Second publication:

Heinrich-Karl A. Rudy, Peter Mayer, and Klaus T. Wanner, *Eur. J. Org. Chem.* **2020**, 3599–3612.

“Synthesis of 1,5-Ring-Fused Imidazoles from Cyclic Imines and TosMIC – Identification of in situ Generated *N*-Methyleneformamide as a Catalyst in the van Leusen Imidazole Synthesis”

Manuscript of the third publication:

Heinrich-Karl A. Rudy, Georg Höfner, and Klaus T. Wanner, *Med. Chem. Res.* **2020**, accepted.

“Synthesis and biological evaluation of novel *N*-substituted nipecotic acid derivatives with tricyclic cage structures in the lipophilic domain as GABA uptake inhibitors”

Reprinted with permission. Copyright of the publications belong to the publishers.

Parts of this thesis have also been presented at international conferences

Poster presentation and short talk at the “International PhD Students and Postdocs Meeting of the German Pharmaceutical Society – DPhG” 2019, Darmstadt.

Heinrich-Karl A. Rudy, and Klaus T. Wanner

“Synthesis of tricyclic imines comprising a 2-azabicyclo[2.2.2]octane scaffold via 4- ω -alkenyl substituted *N*-silyl-1,4-dihydropyridines”

Danksagung

Mein herzlicher Dank für die angenehme Arbeitsatmosphäre, die kollegiale Zusammenarbeit und die schöne gemeinsame Zeit in und neben der Arbeit gilt allen aktuellen und ehemaligen Mitarbeitern des Arbeitskreises.

Meinen Laborpartnern Krisztián Tóth, Janina Andreß und Valentin Nitsche möchte ich für die gute Laboratmosphäre und die unvergessliche Zeit in Labor C1.050B danken. Auch meinen übrigen Kollegen: Simone Huber, Sebastian „Rappi“ Rappenglück, Michael „Michi“ Böck, Mark Währa, Jürgen Gabriel, Thomas Ackermann, Sonja Sichler, Patrick Neiens, Maren Jung, Tobias Hauke, Tamara Bernauer, Herrn Li, Adrian Müller-Deku, Alex Sailer, Ines Trübenbach, Janin Germer, Matthias Frei und Hannah Kipka möchte ich von ganzem Herzen für die gemeinsamen wissenschaftlichen Diskussionen, Mittagessen, Kaffeepausen, Studentenfeiern, Tagungen, Praktikumsaufsichten und alle weiteren außeruniversitären Aktivitäten danken. Ohne euch wären diese sicherlich nicht annähernd so stimmungsvoll und erfolgreich verlaufen.

Einen großen Dank möchte ich auch den Oberassistenten aussprechen. Vielen Dank an Jörg Pabel für die vielen Gespräche zu wissenschaftlichen Fragen, deine Hilfe bei PC-Problemen, die erfolgreiche Zusammenarbeit im Praktikum sowie zahlreiche Abende in der Teeküche. Lars Allmendinger möchte ich zunächst einmal für seine wirklich einzigartige Art und Weise danken; bleib so wie du bist. Daneben danke ich ihm für seinen unermüdlichen Einsatz meine zahlreichen NMR Wünsche zu erfüllen. An dieser Stelle auch ein großes Dankeschön an Claudia Glas für die verlässliche und schnelle Aufnahme unzähliger Spektren für mich. Der Riege von der biologischen Prüfung, Silke Duensing-Kropp, Miriam Sandner und Tanja Franz möchte ich für die Testung der von mir synthetisierten Substanzen danken. Georg Höfner und Thomas Wein danke ich für die Ratschläge zu biologischen Testergebnissen.

Den zahlreichen helfenden Händen im Arbeitskreis, Katharina Heimberger, Anne Kärtner und Gerd Bauschke, möchte ich für ihre Hilfe und Unterstützung im Laboralltag danken. Meinen Freunden aus dem Studium danke ich herzlich für die vielen Aktivitäten die wir gemeinsam neben der Promotion erlebt haben.

Ein ganz besonderer Dank gilt auch meiner Familie, mit der ich während meiner Promotionszeit viele schöne Momente erleben konnte, die immer für mich da war und dank deren Unterstützung letztendlich meine Promotion möglich wurde.

Mein größter Dank gilt jedoch Katrin für die wundervolle Zeit zusammen. Danke dafür, dass du mich immer wieder zum Lachen bringst und mir jeden Tag aufs Neue Rückhalt gibst.

Table of Contents

1	INTRODUCTION	1
1.1	1,4-Dihydropyridines	1
1.1.1	<i>N</i> -Silyl protected 1,4-dihydropyridines.....	3
1.2	Fused and bridged polycyclic compounds	7
1.2.1	2-Azabicyclo[2.2.2]octanes	8
1.2.2	1,5-Ring-fused Imidazoles.....	11
1.3	GABAergic neurotransmission and treatment of GABA related diseases.....	16
1.3.1	GABA transporters	18
1.3.2	GAT inhibitors	22
2	AIMS AND SCOPE	26
3	SUMMUARY OF MANUSCRIPTS AND PUBLISHED RESULTS	29
3.1	First publication: “Accessing Tricyclic Imines Comprising a 2-Azabicyclo[2.2.2]octane Scaffold by Intramolecular Hetero-Diels–Alder Reaction of 4-Alkenyl-Substituted <i>N</i> -Silyl-1,4-dihydropyridines”	29
3.2	Second Publication: “Synthesis of 1,5-Ring-Fused Imidazoles from Cyclic Imines and TosMIC – Identification of in situ Generated <i>N</i> -Methyleneformamide as a Catalyst in the van Leusen Imidazole Synthesis”	31
3.3	Third Publication: “Synthesis and biological evaluation of novel <i>N</i> -substituted nipecotic acid derivatives with tricyclic cage structures in the lipophilic domain as GABA uptake inhibitors”.....	33
4	FURTHER EXPERIMENTS.....	35
4.1	Synthesis of polycyclic lactams.....	35
5	SUMMARY OF THE THESIS	42
6	LIST OF ABBREVIATIONS	45
7	LITERATURE.....	47
8	PUBLICATIONS AND MANUSCRIPTS.....	53
8.1	First publication.....	54

8.2	Second publication	100
8.3	Manuscript of the third publication	145

1 Introduction

1.1 1,4-Dihydropyridines

The 1,4-dihydropyridine (1,4-DHP) scaffold **1** is a structural element present in a multitude of drugs, synthetic intermediates and natural products. The importance of 1,4-DHPs can be highlighted by two major discoveries – the identification of the 1,4-DHP scaffold in nicotinamide adenine dinucleotide (NADH) (**2**) and the finding of the antihypertensive effect of many 1,4-DHPs.¹

NADH (**2**) is an essential coenzyme which together with its phosphorylated counterpart NADPH and their oxidized forms, i.e. NAD^+ and NADP^+ , takes part in cellular metabolism and energy production. Being responsible for many enzymatic redox reactions, NADH (**2**) and NAD^+ play a vital role as hydride-donating or hydride-accepting coenzymes, respectively.²

The possibility to treat cardiovascular diseases with compounds inheriting a 1,4-DHP nucleus was recognized by Bossert and Vater at Bayer AG and has led to the development of a multitude of drugs such as Nifedipine (**3**) or Nimodipin (**4**).^{1a,3} Nifedipine (**3**) (Adalat®), the first generation of DHP-based calcium channel blockers, is still in use for the treatment of angina pectoris.⁴ Later on, with the second and third generation of dihydropyridine type calcium antagonists including Nimodipine (**4**), drugs with improved pharmacokinetics were introduced to address angina pectoris, hypertension, posthemorrhagic cerebral vasospasm and supraventricular tachycardia.^{1a,3a}

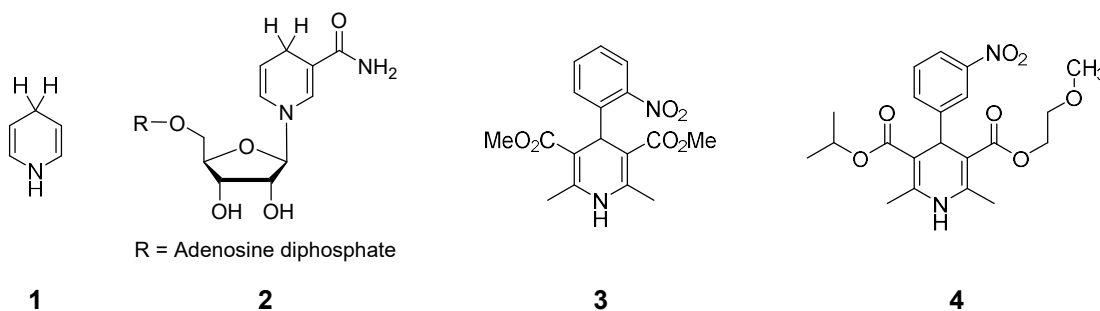
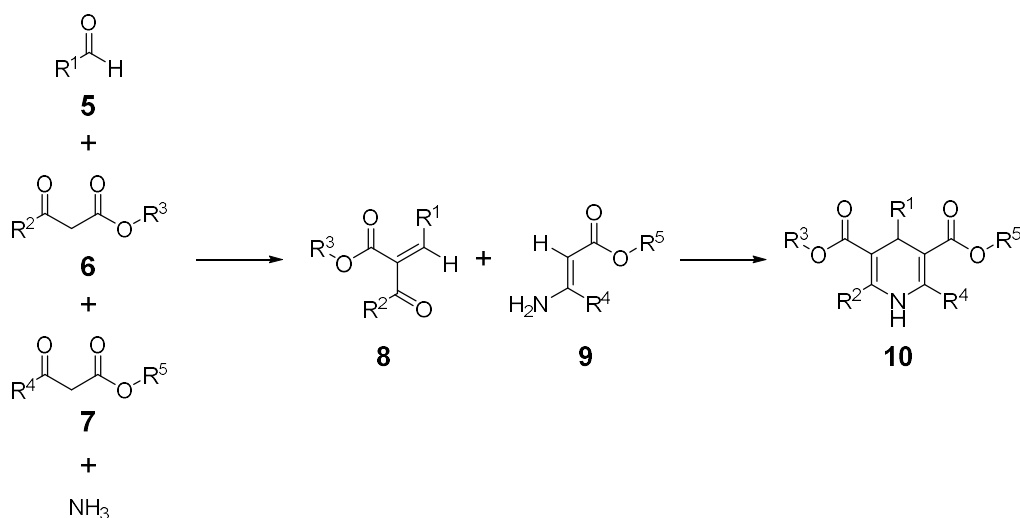


Figure 1 Structures of 1,4-dihydropyridine (**1**), NADH (**2**), the drug Nifedipine (**3**) and Nimodipine (**4**).

Besides their use as cardiovascular agents, 1,4-DHPs have been suggested as promising multidrug-resistance-reversing agents in cancer chemotherapy, as antimycobacterial and anticonvulsant agents. Even neurodegenerative diseases as Parkinson's disease (PD) and dementia may be treated with highly lipophilic 1,4-DHPs, for instance with Nimodipin (**4**), which can enter the brain and prevent cerebral ischemia.^{1b,3a}

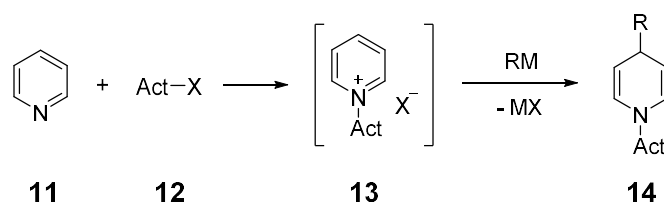
Already in 1882 the first syntheses of 1,4-dihydropyridines were reported by Hantzsch.⁵ A simple condensation reaction of an aldehyde (**5**), a β -ketoester (**6**) and ammonia led to the desired polysubstituted 1,4-dihydropyridine. For the synthesis of a symmetric Hantzsch-type 1,4-DHP such as Nifedipine (**3**) simply two equivalents of the β -ketoester are used in this one pot multicomponent condensation reaction. The selective synthesis of asymmetric 1,4-DHPs can be achieved by the reaction of precondensed intermediates (**8** + **9**) formed from aldehyde **5** and β -ketoester **6** (\rightarrow **8**) or ammonia and another β -ketoester **7** (\rightarrow **9**) structurally different from the first one.^{1b,4}



Scheme 1 General scheme for Hantzsch-type dihydropyridine syntheses.

Another common approach to access 1,4-DHPs is the addition of nucleophiles to pyridinium salts **13**. To obtain these, initially pyridines (**11**) have to be reacted with an electrophile. Commonly *N*-acylpyridinium or *N*-alkylpyridinium salts are generated which are then reacted with organometallics, often organocuprates, to ensure a preferred addition of the nucleophile to the 4-position (\rightarrow **14**) of the former pyridine (**11**). However, also organozinc, organotin and organomagnesium

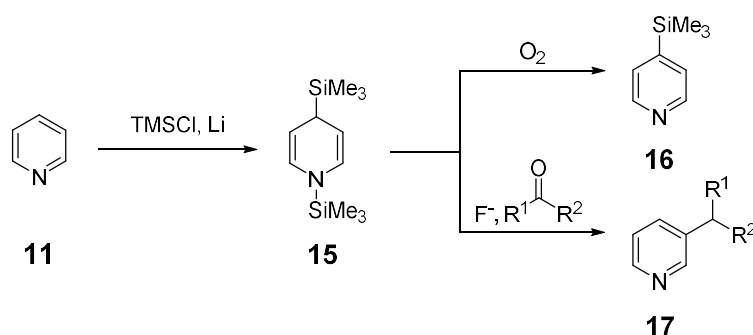
compounds have been employed in syntheses of 1,4-DHPs from pyridinium salts. The selectivity for the nucleophilic 4-addition to the pyridinium salt depends on the activating agent, the substitution pattern of the pyridine ring and the nature of the organometallic species. With substituents in the 3-position of the pyridinium species serving as chiral auxiliaries even diastereoselective syntheses of 1,4-DHPs have been exploited.⁶



Scheme 2 1,4-Addition of an organometallic reagent to a pyridinium salt (**13**) (Act = activator).

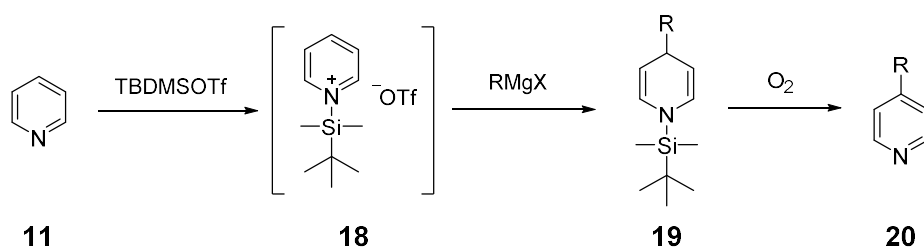
1.1.1 *N*-Silyl protected 1,4-dihydropyridines

A variation of the aforementioned possibilities to access 1,4-DHPs via pyridinium salts, although far less explored, is the synthesis of 1,4-DHPs starting from *N*-silyl pyridinium ions. Subsequent trapping of these with nucleophiles may grant access to *N*-silyl protected 1,4-DHPs. A first example for the preparation of such a 1,4-DHP can be found in the synthesis of 1,4-bis(trimethylsilyl)-1,4-dihydropyridine (**15**) by Sulzbach. By the addition of pyridine (**11**) to a trimethylsilyl chloride/ lithium dispersion the 1,4-DHP **15** could be obtained which was easily oxidized to 4-trimethylsilylpyridine (**16**) by oxygen in the next step.⁷ The usefulness of 1,4-DHP **15** was later on demonstrated by Tsuge et al. who used 1,4-DHP **15** as starting material in syntheses of 3-substituted pyridine derivatives (**17**).⁸



Scheme 3 Synthesis and applications of 1,4-bis(trimethylsilyl)-1,4-dihydropyridine (**15**).

With the discovery of Akiba et al. that by the reaction of pyridine (**11**) via the corresponding pyridinium ion **18** generated *in situ* upon treatment with silyl triflate with grignard reagents 4-substituted pyridine derivatives **20** can be accessed in high yields and with high regioselectivities, for the first time a convenient synthetic approach towards 4-substituted pyridines **20** via *N*-silyl 1,4-DHPs was found. As the for the activation initially used trimethylsilyl triflate was prone to attack by the employed nucleophile and therefore could not adequately serve its function as pyridine activator, leading to low yields and excessive side product formation, for subsequent reactions sterically more demanding *tert*-butyldimethylsilyl triflate (TBDMSOTf) was used. Thus, Pyridine (**11**) activated by TBDMSOTf was reacted with a variety of alkyl and aryl grignard reagents to form 4-monosubstituted *N*-silyl-1,4-DHPs **19**, which were then oxidized by oxygen to the corresponding 4-substituted pyridine derivatives **20**.⁹

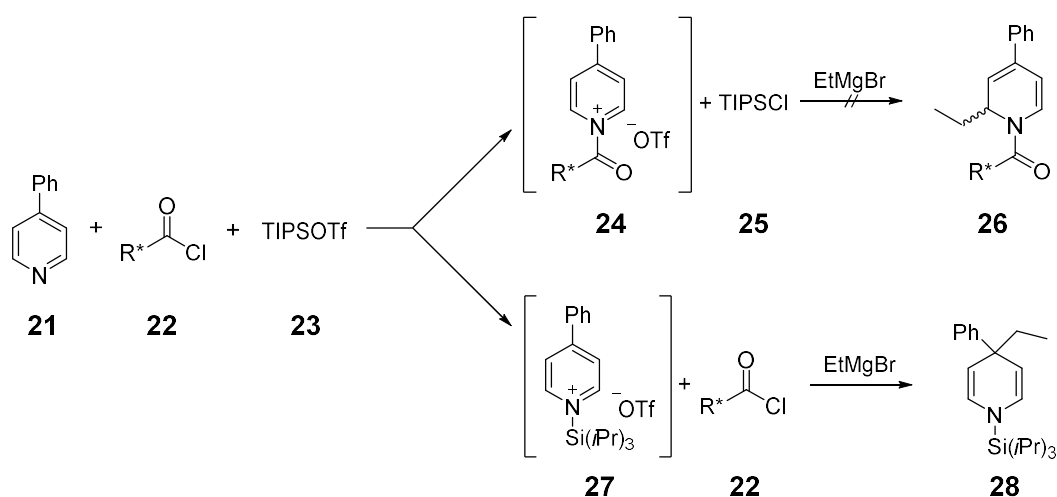


Scheme 4 Preparation of 4-substituted pyridines (**20**) via 4-monosubstituted *N*-silyl-1,4-DHPs (**19**) according to Akiba et al.⁹

Analogously, Bennasar et al. activated methyl nicotinate by reaction with TBDMSOTf and added a phenyl residue to the formed pyridinium ion via a grignard

reagent to obtain a 4-phenyl substituted *N*-silyl-1,4-DHP, which was then further processed to an asymmetrically substituted Hantzsch dihydropyridine.¹⁰ The concept of activating a nitrogen containing heterocycle with a silyl triflate was extended by Mani et al. on quinoline. They generated several quinolinium salts with different silyl triflates and studied the addition of ethylmagnesium bromide to these.¹¹

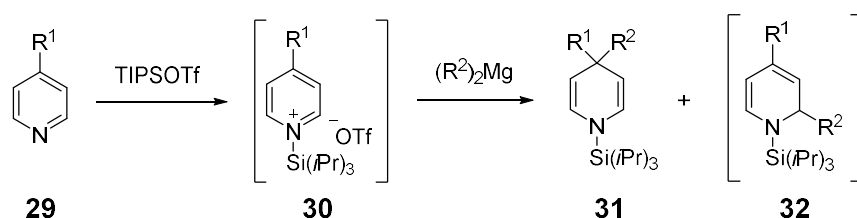
During studies on the diastereoselective 2-addition of ethylmagnesium bromide to 4-phenylpyridine (**21**), after its activation by reaction with a chiral acid chloride (**22**) to give *N*-acyl pyridinium ion **24**, Bräckow observed an unexpected formation of a 4,4-disubstituted *N*-silyl 1,4-DHP **28**. The silyl species triisopropylsilyl triflate (TIPSOTf, **23**), originally added to promote the formation of the *N*-acylpyridinium salt **24** by an equilibrium shift, had given rise to the formation of *N*-silyl pyridinium salt **27** in a side reaction. The addition of the grignard reagent to this pyridinium salt **27** had then finally led to the formation of the 4,4-disubstituted *N*-silyl 1,4-DHP **28**.¹²



Scheme 5 Studies on the alkylation of *N*-acyl pyridinium salts in presence of TIPSOTf by Bräckow et al.¹²

Further investigation of this side reaction revealed that also *n*-butyl and benzyl grignards could be added to pyridinium salt **27** leading to the corresponding 4,4-disubstituted *N*-silyl 1,4-DHPs whereas the alkylation of **27** failed with methyl- and phenyl grignards, organocuprates, organolithium and organozinc compounds. With the application of bisorganomagnesium compounds instead of grignard reagents and hence an exclusion of halide ions, which were assumed to shift the

equilibrium of the pyridinium salt formation to the side of the pyridine because of their higher nucleophilicity as compared to triflate, this type of reaction could finally be developed to a convenient method for the alkylation of 4-substituted pyridinium salts. After an initial activation of the 4-substituted pyridine derivatives **29** with TIPSOTf followed by trapping of the intermediate pyridinium ions **30** with bisorganomagnesium compounds for the first time many 4,4-disubstituted *N*-silyl 1,4-DHPs **31** could be obtained in high yields and with a good regioselectivity for the addition of the nucleophile. However, allyl, methyl and phenyl derived bisorganomagnesium compounds led predominantly to the formation of 2,4-disubstituted 1,2-DHPs (**32**) and their oxidized pyridine counterparts as main products.¹³



Scheme 6 Synthesis of 4,4-disubstituted 1,4-DHPs (**31**) according to Bräckow et al.¹³

The described method was later successfully applied by Sperger et al. to the synthesis of 4-mono and 4,4-disubstituted 1,4-dihyronicotinates starting from methyl nicotinate¹⁴ and with the work of Schmaunz et al. the scope of the method was further broadened.¹⁵ Finally Rappenglück et al. used the method to introduce a *tert*-butyl residue in the 4-position of varying 3-substituted pyridine derivatives employing bis(*tert*-butyl)magnesium as nucleophile. The initially obtained 3,4-disubstituted *N*-silyl 1,4-DHPs were then transferred in a successive oxidation reaction with sulfur in naphthalene to the desired 3,4-disubstituted pyridines with a *tert*-butyl moiety in 4-position.¹⁶

1.2 Fused and bridged polycyclic compounds

Polycycles are ubiquitous structural elements involved in almost every aspect of life. Prominent polycyclic compounds with fused cycles are the nucleobases adenine and guanine, as part of the DNA essential for the storage of the genetic information, or cholesterol which is an important component of cell walls and serves as precursor for all steroid hormones.¹⁷ Also in medicine and drug development polycycles are of considerable importance. Due to the protruding relevance of nitrogen containing heterocycles in bioactive substances, in many pharmaceutically applied polycyclic compounds *N*-heterocyclic subunits can be found. In 2014 out of 1100 FDA approved small molecule drugs 640 substances contained a *N*-heterocycle, with the latter being part of a polycyclic scaffold in approximately 200 cases.¹⁸

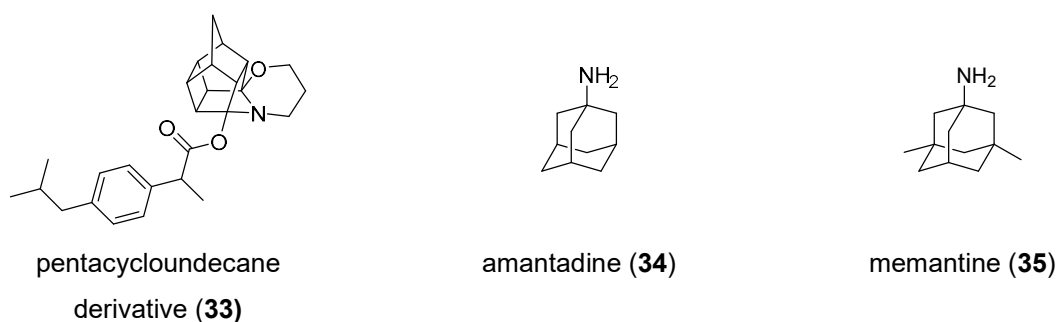


Figure 2 Structures of polycyclic compounds applied in medicine or as pharmacological tool.

Based on their molecular properties polycycles inheriting bridges or displaying cage like structures are especially interesting for drug development and application. Bridges reduce the flexibility of polycyclic scaffolds and in consequence also of the attached substituents, leading to structures of high rigidity with well-defined three-dimensional geometries. This improves binding to a target as due to a decrease of the structural flexibility the conformational entropy penalty is lowered.¹⁹ Furthermore, the stiffening brings about structures of high stability what may slow down their metabolic degradation. Polycyclic cages are often hydrocarbon rich structures with high lipophilicity and thus can facilitate the crossing of the blood brain barrier (BBB), which makes them particularly appealing as structural element in drugs addressing neurological diseases. Hence, polycyclic cage compounds may be used as carrier molecules to deliver drugs to the brain. A pharmacological tool prepared for this purpose is the pentacycloundecane derivative **33**, which was

designed as a prodrug for an in-brain ibuprofen release to counteract inflammation which often plays an important role in neurodegenerative diseases.^{19a,19b,20} However, bridged polycycles are also applied to address neurodegenerative diseases directly. For instance, the structurally simple cage compound amantadine (**34**) is used to lessen symptoms of Parkinson's disease or the structurally closely related memantine (**35**), bearing two additional methyl groups at the bridge heads, is applied to treat neurodegenerative symptoms of Alzheimer disease (AD).²¹

1.2.1 2-Azabicyclo[2.2.2]octanes

The occurrence of the isoquinuclidine {2-azabicyclo[2.2.2]octane} ring system **36** in many natural products with interesting pharmacological properties has drawn considerable attention to this bridged bicyclic scaffold.²² Important representatives of substances incorporating a 2-azabicyclo[2.2.2]octane skeleton are the alkaloids dioscorine (**37**) and ibogaine (**38**). The toxic alkaloid dioscorine (**37**) can be found in tropical yam tuber and shows antifeedant and insecticidal properties, most likely due to its interaction with the nicotinic acetylcholine receptor leading to a suppression of the respective neuronal signal transduction.²³ Ibogaine (**38**), a psychoactive alkaloid, has been extensively investigated for its antiaddictive properties and might offer new perspectives in the development of pharmacotherapies countering drug addiction.²⁴

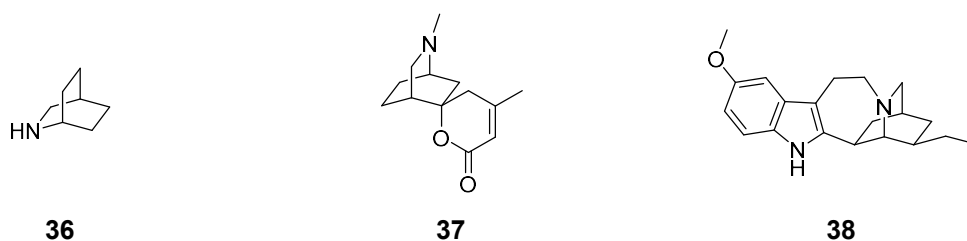
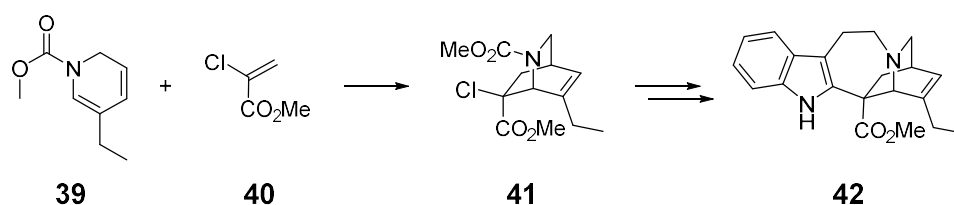


Figure 3 Structures of 2-azabicyclo[2.2.2]octane (**36**), dioscorine (**37**) and ibogaine (**38**).

As a consequence of the biological importance of the isoquinuclidine scaffold, a multitude of synthetic routes for its construction were developed, mostly relying on an intramolecular ring closure or a Diels-Alder cycloaddition reaction.^{22,25} In case of the construction of 2-azabicyclo[2.2.2]octanes via cycloaddition reactions

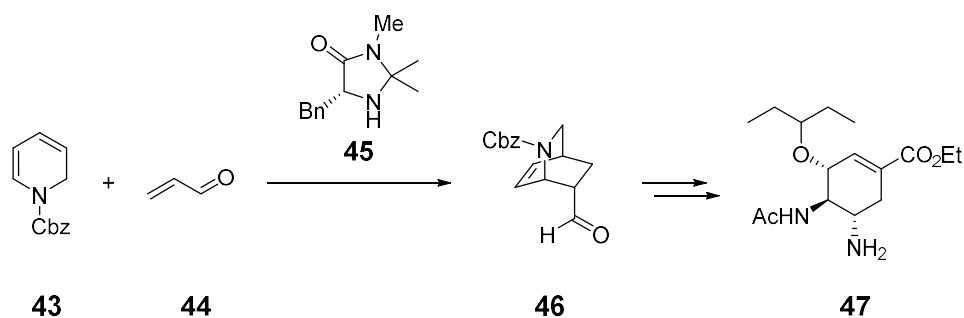
pyridines,²⁶ pyridones,²⁷ 1,2-dihydropyridines²⁸ or 1,4-dihydropyridines^{15a,29} were employed as starting material for the generation of 2-azabutadienes serving as reaction intermediates.

An example for the formation of an isoquinuclidine scaffold via a Diels-Alder reaction of a 1,2-dihydropyridine derivative can be found in the total synthesis of catharanthine (**42**) by Raucher and Bray from 1985. They employed *N*-methoxycarbonyl-5-ethyl-1,2-dihydropyridine (**39**) as diene and methyl 2-chloroacrylate (**40**) as dienophile in a cycloaddition reaction to access the 2-azabicyclo[2.2.2]octane core **41** of catharanthine (**42**).³⁰ As the Iboga alkaloid catharanthine (**42**) can be employed as precursor for the synthesis of vinblastine and vincristine, two strong anticancer chemotherapeutic agents, synthetic ways to access this alkaloid with its bridged skeleton continue to be investigated.³⁰⁻³¹



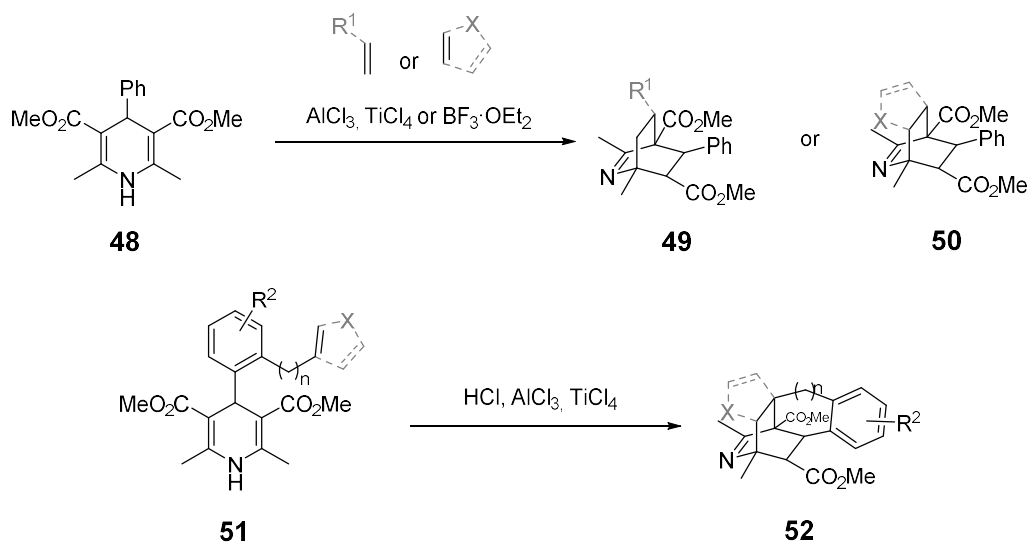
Scheme 7 Preparation of the 2-azabicyclo[2.2.2]octane core **41** of catharanthine (**42**) according to Raucher and Bray.³⁰

The isoquinuclidine scaffold also proved to be a highly useful and versatile intermediate in the synthesis of the antiviral drug oseltamivir (**47**) (Tamiflu®) reported by Fukuyama et al. The 2-azabicyclo[2.2.2]octane intermediate **46** was obtained similar to the synthesis of catharanthine (**42**), via an Diels-Alder reaction of the 1,2-dihydropyridine **43** with acroleine (**44**) as the dienophile. In order to access the formation of the desired enantiomer, Fukuyama et al. performed an asymmetric Diels-Alder reaction employing imidazolidinone **45** (MacMillan) as catalyst.³²



Scheme 8 Application of an 2-azabicyclo[2.2.2]octane intermediate in the synthesis of oseltamivir (**47**) by Fukuyama et al.³² (Cbz \equiv benzyloxycarbonyl)

Diels-Alder reactions to build up an isoquinuclidine scaffold starting from 1,4-DHPs require an activation of the 1,4-DHP system to a 2-azadiene before the cycloaddition reaction can take place. Hartman et al. described a variety of inter- and intramolecular Diels-Alder reactions with 4-aryl substituted Hantzsch type 1,4-DHPs.^{29a,29b}

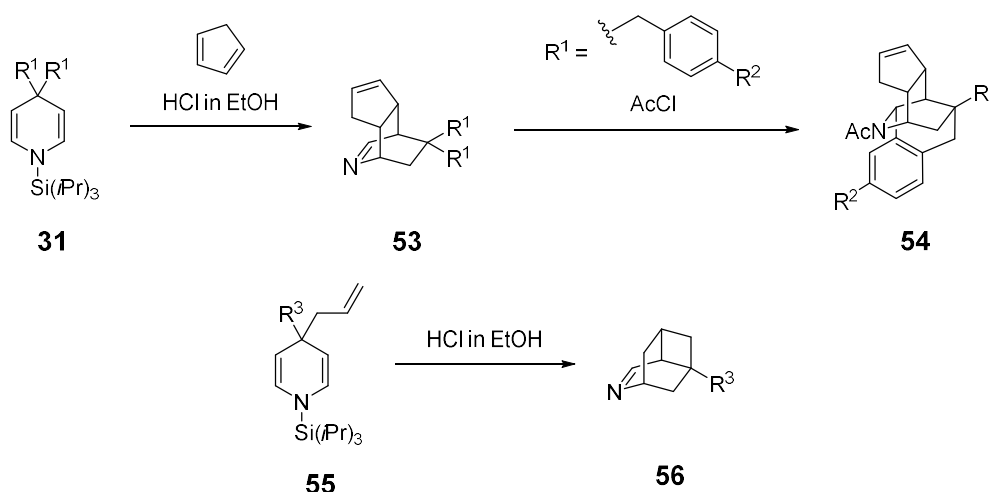


Scheme 9 Inter- and intramolecular Diels-Alder reactions with Hantzsch type 1,4-DHPs performed by Hartman et al.²⁹

To activate the 1,4-DHPs (**48** or **51**) and generate the required 2-azadiene intermediates, they employed either Brønsted (HCl) or Lewis acids (TiCl₄, AlCl₃, BF₃ · OEt₂). For intermolecular cycloaddition reactions dienophiles like styrene and cyclopentadiene but also heteroaromatics as furan or thiophene were used.^{29c,29d}

To carry out intramolecular cyclization reactions first suitable precursors such as **51** were prepared, e.g. 4-aryl substituted 1,4-DHPs that carried either a heteroaromatic or an alkenyl function in the *ortho*-position of the 4-aryl residue, which then gave access to highly substituted 2-azabicyclo[2.2.2]octanes **52**.^{29a,29b}

Further inter- and intramolecular Diels-Alder reactions with 1,4-DHPs were carried out by Schmaunz in our group. She employed 4,4-disubstituted *N*-silyl-1,4-DHPs as **31** or **55** as starting material and generated the necessary 2-azadiene system by adding HCl in ethanol. For the successive cycloaddition reaction either cyclopentadiene or an ω -alkenyl moiety attached to the 4-position of the former 1,4-DHP were utilized as dienophile. That way several tricyclic compounds, **53** or **56**, inheriting a 2-azabicyclo[2.2.2]octane skeleton could be obtained, of which compounds **53** served as excellent precursors in subsequent intramolecular Friedel-Crafts type cyclization reactions to access polycycles **54** containing a 7,8-benzomorphane subunit.^{15a}



Scheme 10 Inter- and intramolecular Diels-Alder reactions with *N*-silyl-1,4-DHPs performed by Schmaunz.^{15a}

1.2.2 1,5-Ring-fused Imidazoles

The heterocyclic motif of imidazoles is a basic structural element in chemistry that is found in almost every aspect of life.³³ Hence it is not surprising that also 1,5-ring-fused imidazole derivatives **57** are quite common. A search on imidazoles fused to another ring system in 1- and 5-position, without restrictions to composition and size of the second cycle, revealed more than half a million hits on this structural

motif in the SciFinder® database.³⁴ An important substance incorporating a 1,5-ring-fused imidazole substructure is the imidazo-benzodiazepine drug Flumazenil (**58**). In contrast to structurally related benzodiazepine pharmaceuticals Flumazenil (**58**) acts as an antagonist at the benzodiazepine receptor and consequently is able to attenuate or suspend the effects of drugs binding to the same target. As a result, Flumazenil (**58**) is used to antagonize the sedative effect of benzodiazepines post operational or in case of an intoxication. It further may help to reduce benzodiazepine tolerance and consequently could be used to manage benzodiazepine withdrawal.³⁵

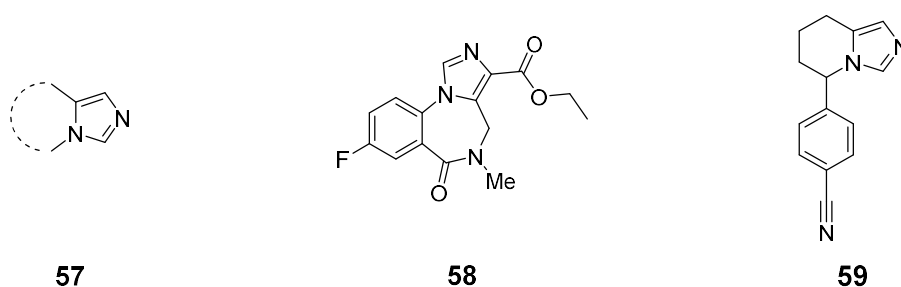
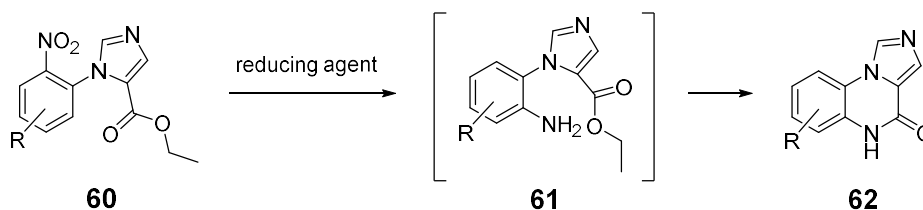


Figure 4 Structures of a 1,5-ring-fused imidazole **57**, Flumazenil (**58**) and Fadrozole (**59**).

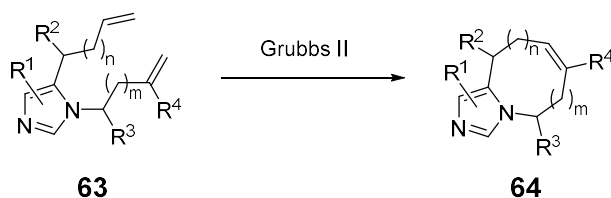
Another example for a drug with a 1,5-ring-fused imidazole is the non-steroidal aromatase inhibitor Fadrozole (**59**) used in the treatment of hormone-responsive breast cancer. As Fadrozole (**59**) is a highly potent reversible inhibitor of the enzyme complex responsible for the aromatization of the estrogen precursors, it may effectively suppress estrogen production in postmenopausal women and accordingly inhibit the growth of hormone receptor-sensitive breast cancer.³⁶

Though the many synthetic methods addressing the preparation of 1,5-ring-fused imidazoles are highly variable, usually the synthetic approaches either demand the construction of the second cycle that is fused to the imidazole ring or, vice versa, the imidazole ring is to be attached to a given ring system. An example for the construction of the second cycle starting from an imidazole derivative can be found in the work of Chen et al. and Pierre et al.³⁷ They employed 1-aryl substituted 5-ethoxycarbonylimidazole derivatives **60** as starting material. Upon reduction of the *ortho*-nitro group of the aryl substituent this compound, **60**, could be cyclized via an intramolecular aminolysis of the ester function yielding **62**.



Scheme 11 Construction of 1,5-ring-fused imidazoles via an intramolecular reductive cyclization reaction according Chen et al. and Pierre et al.³⁷

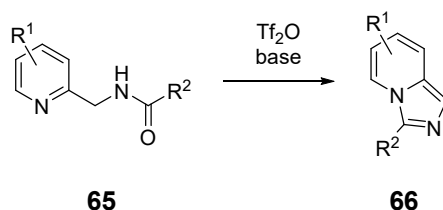
The construction of the anellated cycle of 1,5-ring-fused imidazoles via intramolecular cyclization of 1,5-disubstituted imidazole derivatives was studied extensively by Gracias et al. For instance, they used imidazole derivatives substituted in 1- and 5-position with moieties carrying a terminal alkene function, **63**, for ring-closing metathesis reactions giving **64**.³⁸ In further studies 1,5-disubstituted imidazoles displaying an alkynyl and an ω -alkenyl moiety were employed for enyne metathesis reactions.³⁹ Other approaches to access 1,5-ring-fused imidazoles starting from 1,5-disubstituted imidazoles included intramolecular Heck reactions or alkyne-azide cycloaddition reactions.⁴⁰ By the described methods the imidazole precursors could be efficiently transformed into 1,5-ring-fused imidazoles exhibiting diversely substituted 6-, 7- and 8-membered ring systems.



Scheme 12 Application of ring-closing metathesis reactions for the construction of 1,5-ring-fused imidazoles according to Gracias et al.³⁸

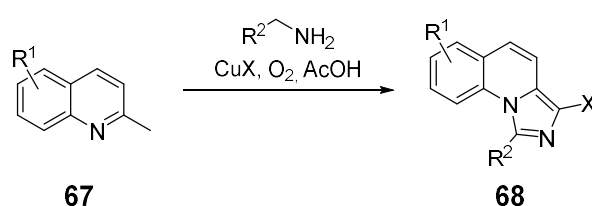
One among the many methods describing the preparation of the imidazole subunit within 1,5-ring-fused imidazole derivatives starting from nitrogen containing cyclic precursors was presented by Charette and Pelletier. They used *N*-(2-pyridylmethyl)amides **65** as starting materials in an intramolecular cyclodehydration/ aromatization reaction. After an initial activation of the amide by triflic acid anhydride a nucleophilic attack of the pyridine nitrogen on the former carbonyl carbon atom led to a cyclized intermediate, which finally reacted to **66**.

Applying this method a multitude of imidazo[1,5-*a*]pyridines **66** were synthesized. Yet, the method also proved to be suitable for the preparation of imidazo[1,5-*a*]pyrazines, imidazo[1,5-*a*]quinolines and imidazo[1,5-*a*]isoquinolines.⁴¹



Scheme 13 Synthesis of Imidazo[1,5-*a*]pyridines **66** according to Charette and Pelletier.⁴¹

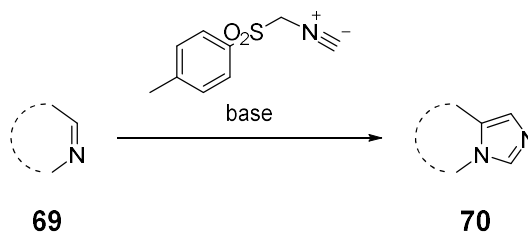
For the synthesis of 1,5-ring-fused imidazoles by attaching the imidazole unit to an aromatic *N*-heterocycle also 2-methylquinolines **67**, 1-methylisoquinolines or 2-methylpyridines may serve as starting materials. Reddy et al. employed these substances in copper-promoted double oxidative C-H amination reactions with aliphatic amines to obtain the desired 1,5-ring-fused imidazole derivatives **68**. The method gave access to a great variety of 1,5-annulated imidazoles carrying an additional aromatic, heteroaromatic or aliphatic residue in 2-position and a halide in 4-position allowing further modification.⁴²



Scheme 14 Method for the synthesis of 1,5-ring-fused imidazole derivatives according to Reddy et al.⁴²

The van Leusen imidazole synthesis is a common, well-known method for the preparation of imidazoles. Consequently, it was also utilized for the preparation of 1,5-ring-fused imidazoles. For the construction of an imidazole ring via the van Leusen imidazole synthesis besides the reagent tosylmethyl isocyanide (TosMIC) in combination with a base an imine is required. Thus for the preparation of the

1,5-ring-fused imidazoles **70** cyclic imines **69** had to be employed as starting materials.⁴³ As cyclic imines are relatively rare as compared to their acyclic counterparts relatively few syntheses of the described ring-fused imidazoles were conducted via the van Leusen methodology.⁴⁴ By means of these syntheses imidazobenzodiazepine derivatives,⁴⁵ imidazo β -carboline derivatives⁴⁶ or imidazopyrazinones⁴⁷ were obtained, the latter of which served as intermediates in the synthesis of inhibitors for potential cancer treatment.



Scheme 15 General scheme for a van Leusen imidazole synthesis starting from a cyclic imine **70**.

1.3 GABAergic neurotransmission and treatment of GABA related diseases

The proper functioning of the mammalian central nervous system (CNS) is highly dependent on the fine-tuned interaction of excitatory and inhibitory neurotransmitters. As a result, an imbalance within this system may lead to severe neurological disorders. The most important inhibitory neurotransmitter in the CNS is γ -aminobutyric acid (**71**) (GABA, Figure 5)⁴⁸ and a malfunction in GABAergic neurotransmission is associated with a multitude of neurological diseases like Alzheimer's disease (AD),⁴⁹ Parkinson's disease (PD),⁵⁰ depression⁵¹ or epilepsy.⁵² An isolated view on epilepsy alone demonstrates the importance of GABA related disorders as in 2019 more than 50 million people worldwide were affected by epileptic seizures. Though up to 70% of these sick people could become seizure free in case of an appropriate and low-cost medical supply with antiepileptic drugs still 30% of the patients continue to have seizures.⁵³ As even those patients who are responsive to the treatment of their epilepsy are often affected by complex psychiatric, behavioral, cognitive or social problems the development of more potent pharmaceuticals with less side-effects remains an ongoing task in pharmaceutical industry and research.^{53b}

The neurotransmitter GABA (**71**) is synthesized in the presynaptic neurons via enzymatic decarboxylation of glutamate by glutamic acid decarboxylase (GAD) and successively stored in synaptic vesicles. Responsible for the transportation into these vesicles is the vesicular neurotransmitter transporter (VGAT). With an arriving action potential, the increasing calcium concentration in the presynaptic neuron triggers the release of GABA (**71**) from the storage vesicles into the synaptic cleft by exocytosis.^{48,54} In the synaptic cleft GABA (**71**) can bind to two GABA receptors denominated as GABA_A and GABA_B which can be found in the membrane of the pre- and the postsynaptic neuron. However, the GABA_A receptor is predominantly localized on post-synaptic neurons and mediates upon GABA-binding a chloride ion influx into the neuron consequently leading to a hyperpolarization of the neuron that inhibits neural signal transmission. In contrast, GABA_B receptors can be found in the membrane of pre- and postsynaptic neurons. They are G-protein coupled receptors (GPCR) and their function varies depending on the membrane they are located on. Pre-synaptic GABA_B receptors provoke a reduction in the calcium current at the nerve terminal upon GABA binding and hence reduce the probability for further calcium dependent GABA exocytosis. Contrary to this, an activation of GABA_B

receptors located on the post-synaptic neuron leads to the hyperpolarization of the neuron by a downstream activation of potassium ion channels resulting in a facilitated efflux of this ion.^{48,54-55}

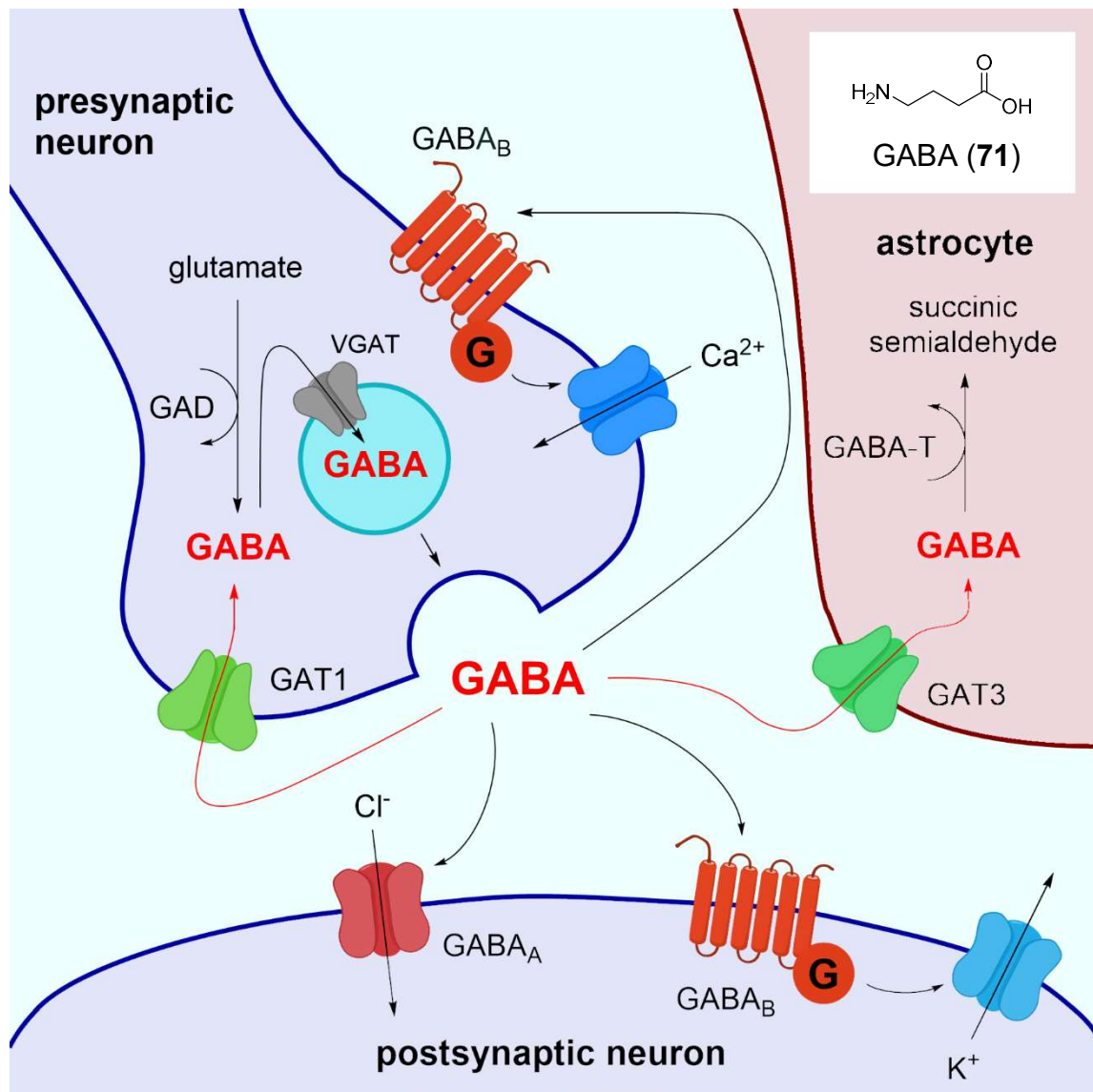


Figure 5 Schematic representation of the GABAergic neurotransmission.

The inactivation of the GABAergic neurotransmission is mainly accomplished by removal of GABA (71) from the synaptic cleft into the presynaptic neuron or neighboring astrocytes. This is realized by high-affinity GABA transporters (GATs) located in the plasma membrane. GABA is mostly transported back into the presynaptic neuron where the majority is reutilized as neurotransmitter after reuptake into vesicles, though GABA may here also be metabolized into succinic semialdehyde by GABA transaminase (GABA-T) and then further degraded. This

degradation process likewise takes place in the glia cells surrounding the synaptic cleft.^{54,56}

The above described pathways involved in the GABAergic neurotransmission offer several possibilities to influence the GABA mediated inhibitory effect and consequently they were addressed to treat neurological diseases connected with a reduced GABAergic signaling. For instance, benzodiazepines, such as Diazepam (**72**), act as allosteric modulators of the GABA_A receptors and enhance the chloride-ion dependent hyperpolarization by a structural change of the GABA_A receptor that increases the agonist efficacy of GABA.⁵⁷ The drug Baclofen (**73**) acts as a GABA_B receptor agonist and thus is used to reduce the excitability of excitatory neurons in people suffering from spasticity. In order to keep up and enhance the GABAergic neurotransmission also the degradation of GABA may be blocked which can be achieved with Vigabatrin (**74**) which irreversibly binds to GABA transaminase (GABA-T)^{55b}. Finally, the removal of GABA from the synaptic cleft may be suppressed by inhibition of the GABA transporters and thus a prolonged effect of GABA can take place. Yet, so far only the GAT inhibitor Tiagabine (**75**) has been introduced to the market and is used as add-on therapy in the management of epileptic seizures.⁵⁸

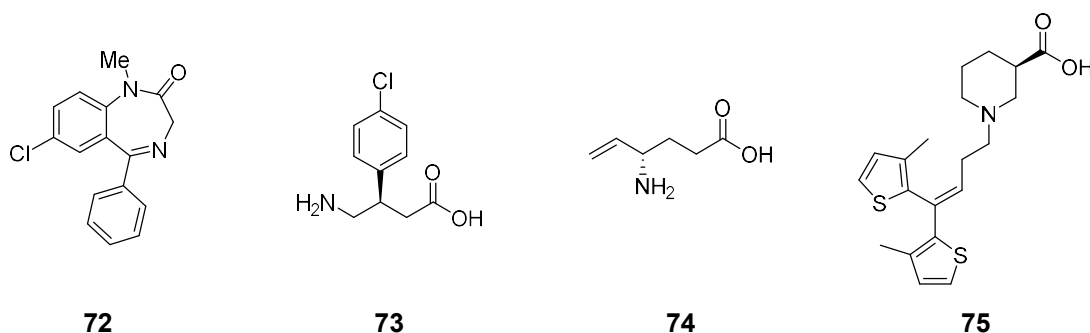


Figure 6 Drugs interfering with the GABAergic neurotransmission and enhancing GABAergic signaling.

1.3.1 GABA transporters

GABA transporters exist in form of four subtypes which are termed GAT1, BGT1, GAT2 and GAT3 according to the nomenclature proposed by the Gene Nomenclature Committee of the Human Genome Organization (HUGO).⁵⁹ In addition to this species independent denomination system also species specific

denotations of the GABA transporters can be frequently found in literature in which a prefix indicating the species of origin, such as r for rat, is added to the transporter name.⁶⁰ However, the nomenclature of GATs originating from mouse tissue differs from the above-mentioned system as they are entitled mGAT1 (\equiv GAT1), mGAT2 (\equiv BGT1), mGAT3 (\equiv GAT2) and mGAT4 (\equiv GAT3).^{60d} As the GATs in the biological test system used for my study were cloned from mice, for the sake of consistency the denomination mGAT1-mGAT4 will be applied in this dissertation.

For the understanding of the function of mGAT1-mGAT4 within the body the expression pattern of the GATs is of utter importance. It was found that the GABA transporter subtypes mGAT2 and mGAT3 are only weakly expressed in the brain but occur in high concentrations in kidney and liver. Based on their low expression in the brain, mGAT2 and mGAT3 are considered to play no significant role in the termination of the GABAergic signaling.⁶¹ In contrast, mGAT1 can be found in all parts of the brain where it is predominately located on presynaptic GABAergic neurons.^{60c,61c} Also mGAT4 is expressed throughout the CNS albeit at lower concentrations as compared to mGAT1. As mGAT4 is located on the membranes of astrocytes neighboring GABAergic neurons it mediates glial GABA uptake and consequently GABA metabolization whereas mGAT1 is responsible for the reuptake of GABA into presynaptic neurons which is predominantly followed by GABA recycling.^{60b,61c,62} Hence mGAT1 and mGAT4 remain as promising targets for the treatment of diseases involving a reduced GABAergic signalling.

As member of the solute carrier family 6 (SLC6) the four GATs employ the co-transport of sodium and chloride ions as driving force to translocate their substrate GABA through the cell membrane. In consequence, they and the remaining 16 members of this gene family, who likewise make use of the co-transport of sodium ions as driving force, are also termed neurotransmitter sodium symporters (NSS).⁶³ For the transport of GABA by GATs a stoichiometry of two sodium ions and one chloride ion per equivalent of GABA was assumed for a long time, yet more recent findings suggest a stoichiometry of 3:1:1 ($\text{Na}^+:\text{Cl}^-:\text{GABA}$).⁶⁴

Though so far no three-dimensional structure of the GATs was elucidated the structure and functioning of these SLC6 transporters is generally well understood. After the initial isolation of rGAT1 from rat brain and subsequent sequencing and

cloning by Guastella et al. the remaining GATs were cloned and sequenced and showed a high degree of amino acid identity among each other (52%-68%).^{62a,65} A high degree of amino acid sequence identity was also observed for the substrate binding site of prokaryotic leucine transporter LeuT_{Aa} from the bacteria *Aquifex aeolicus* with the substrate binding site of the transporters of the SLC6 family. Accordingly, this transporter accounts as valuable model for the comprehension of the three-dimensional structure and functioning of the eukaryotic SLC6-transporters, especially as LeuT_{Aa} has been crystallized in presence of its substrate and two sodium ions by Yamashita et al. in 2005.⁶⁶ With the more recently conducted successful crystallizations and X-ray structure analyses of the dopamine transporter from *Drosophila melanogaster* (dDAT) and the human serotonin transporter (hSERT), both being eukaryotic SLC6-transporters, the solidity of LeuT_{Aa} as homology model for the understanding of SLC6-transporters was confirmed.⁶⁷

The structure of the LeuT_{Aa} transporter is determined by twelve transmembrane helices (TM1-TM12) that are connected by loops in the intra- and extracellular space. Both the amino- and the carboxy-terminus are located intracellularly and within the first ten helices an internal structural repeat occurs among TM1-5 and TM6-10. These two sets of helices are arranged in a C₂-pseudosymmetric manner leading to an antiparallel orientation of TM6-10 as compared to TM1-5.^{66b}

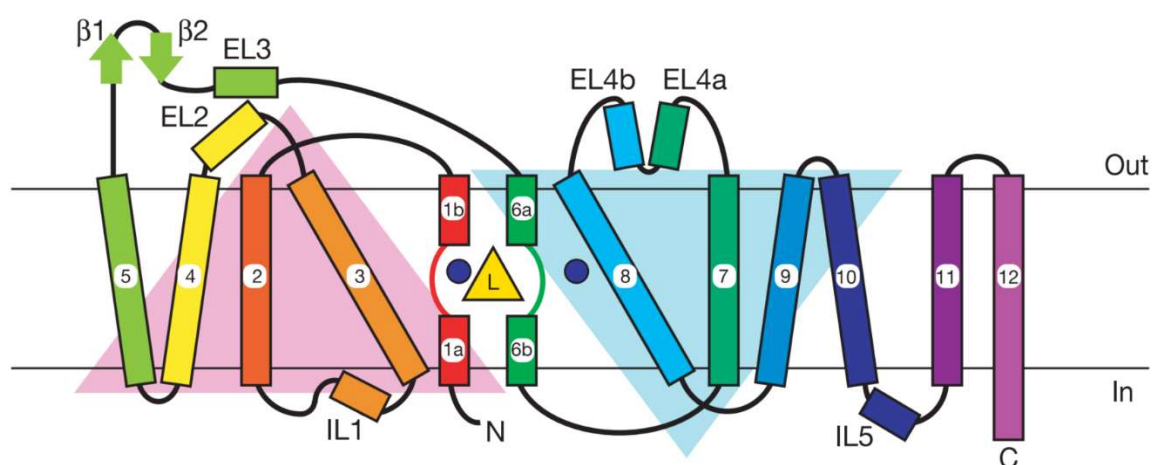


Figure 7 Secondary structure of the LeuT_{Aa} transporter. The position of the binding site (S1) is indicated by the substrate leucine (yellow triangle) and two sodium ions (blue circles).^{66b}

The primary substrate binding site (S1) is located roughly in the middle of the membrane bilayer within the four transmembrane helices TM1, TM3, TM6 and TM8. Two of these helices, TM1 and TM6, are unwound halfway across the membrane allowing additional hydrogen bonding and ion coordination with the substrate and the sodium ions at the binding site.^{66b}

With the crystallization of LeuT_{Aa} by Yamashita et al.^{66b} and subsequent crystallographic analyses of this transporter in different states with and without a substrate or inhibitor bound by Gouaux et al.⁶⁸ for a long time assumed transport mechanism according to the “alternating access model” for the SLC6-transporters could be verified.⁶⁹ According to the findings the transporter first displays an outward-open conformation with a funnel-like cavity allowing the substrate and co-substrates to access the central binding site (S1). A direct passage through the transporter is blocked by a closed intracellular gate consisting of amino acids from TM1, TM6 and TM8 within this state. Upon substrate binding conformational changes mediate the closure of the extracellular gate, trapping the substrate and sodium ions in the binding site. Starting from this outward-occluded state further conformational changes lead to the opening of the intracellular gate resulting in an inward-open state of the transporter finally allowing substrate release.^{66b,68}

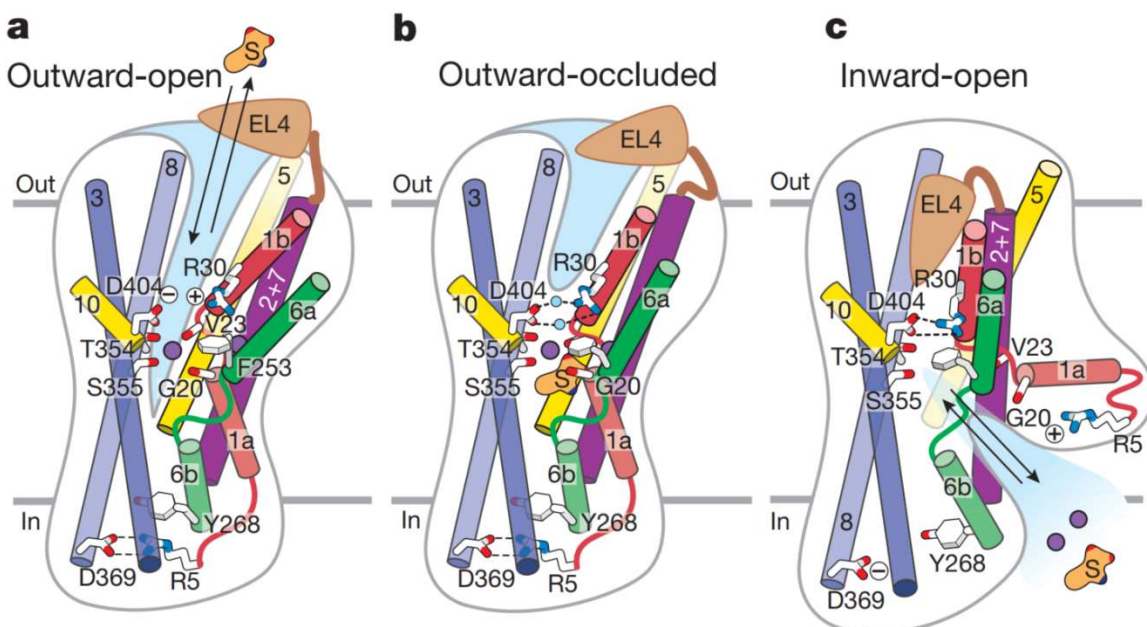


Figure 8 Schematic of the transport mechanism in LeuT_{Aa} according to Gouaux et al.^{68a}

In addition to the substrate binding site (S1) at the bottom of the extracellular vestibule above the extracellular gate a second binding site (S2) in LeuT_{Aa} exists.^{63b} This binding site (S2) is assumed to be able to accommodate another substrate molecule which upon binding could trigger conformational changes that are responsible for the release of the substrate from the central binding site (S1) into the cytoplasm.⁷⁰ Though the hypothesis of the second binding site being responsible for the allosteric release of the substrate is still under debate,⁷¹ the importance of S2 in LeuT_{Aa} as binding pocket for non-competitive inhibitors was unequivocally proven.^{71a,72} Recently, with the crystallization of hSERT, an allosteric binding site located above the extracellular gate was identified in the structure of a transporter of the SLC6-family directly.^{67c}

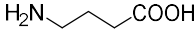
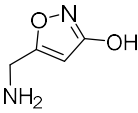
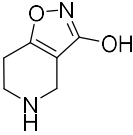
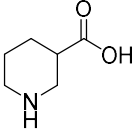
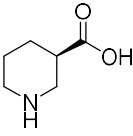
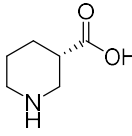
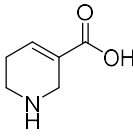
1.3.2 GAT inhibitors

Seeing that a dysregulation in GABAergic neurotransmission is involved in a multitude of neurological disorders the possibility to influence GABA concentrations by inhibition of the GABA transporters and hence to restore a proper function of the GABAergic system was intensively investigated.

One of the first compounds identified to inhibit the GABA uptake was the alkaloid muscimol (**76**) from the fly agaric mushroom. Muscimol (**76**) acts as a GABA analogue and binds not only to GATs but also to GABA_A where it displays potent receptor agonist activity. Attempts to retain the GAT activity of muscimol (**76**) and selectively address the GAT transporters led to the first selective, yet still only mildly potent GABA reuptake inhibitor THPO (**77**). Within THPO (**77**) the amino function was rigidized in a ring and its spatial orientation relative to the isoxazol-3-ol was altered.^{58b} A further conversion of this isoxazol-3-ol subunit in THPO (**77**) to a bioisosteric carboxylic acid function led to the generation of nipecotic acid (**78**) and guvacine (**79**), two reasonably potent GAT inhibitors. These conformationally restricted small amino acids display almost the same inhibitory potency as the natural substrate GABA (**71**) at the four different GABA transporters mGAT1-mGAT4. However, they do not show any subtype selectivity except for mGAT2 which is not as efficiently inhibited as the remaining GATs, mGAT1, mGAT3 and mGAT4. Among the two enantiomers of nipecotic acid (**78**), the (*R*)-enantiomer

(*R*)-**78** exhibits significantly higher inhibitory potencies at all four GATs as compared to the (*S*)-enantiomer (*S*)-**78**.^{58b,73}

Table 1 Low molecular weight GAT inhibitors and their inhibitory potencies (pIC₅₀).

GABA uptake inhibition (pIC ₅₀ ± SEM) ^a				
compound	mGAT1	mGAT2	mGAT3	mGAT4
 GABA (71)				
 muscimol (76)				
 THPO (77)				
 (<i>R,S</i>)-nipecotic acid (78)				
 (<i>R</i>)-nipecotic acid [(<i>R</i>)- 78]				
 (<i>S</i>)-nipecotic acid [(<i>S</i>)- 78]				
 guvacine (79)				
GABA (71)	5.14 ± 0.09	4.56 ± 0.06	4.94 ± 0.09	5.18 ± 0.13
(<i>R,S</i>)-(78) ^b	4.88 ± 0.10	3.10 ± 0.09	4.64 ± 0.07	4.70 ± 0.07
(<i>R</i>)-(78) ^b	5.19 ± 0.03	3.39 ± 0.05	4.76 ± 0.05	4.95 ± 0.05
(<i>S</i>)-(78) ^b	4.24 ± 0.05	3.13 ± 0.14	3.83 ± 0.04	3.63 ± 0.06
guvacine (79) ^b	4.87 ± 0.06	3.31 ± 0.03	4.59 ± 0.05	1.1 0.05

(a) pIC₅₀ ± SEM have been determined in [³H]GABA uptake assays in our group and are the result of three individual experiments each performed in triplicate. (b) Reference literature⁷³.

The above-mentioned small GAT inhibitors are all highly polar and exist either in a cationic or in a zwitterionic state at physiological pH thus making them unable to pass the blood brain barrier (BBB). To improve their therapeutic potential and turn them into systemically active compounds, lipophilic aromatic side chains have been linked to them, especially to the cyclic amino acids **78**, (*R*)-**78**, (*S*)-**78** and **79**. With this modification not only an increased permeation of the BBB but also improved inhibitory potencies and subtype selectivity came along in many cases.^{58b} The lipophilic side chains usually constituted of di-, tri- or biaryl units and were connected to the amino nitrogen atom of the cyclic amino acids via a flexible linker of varying composition.⁷⁴ Examples for GAT inhibitors of such a structure and their inhibitory potencies are shown in Table 2.

The most prominent GAT inhibitor is Tiagabine (**75**) (Gabitril®), used for the treatment of epileptic seizures and the only inhibitor approved as therapeutic drug

so far.^{58,63b} It is a selective inhibitor of mGAT1 and displays a pIC_{50} value of 6.88 ± 0.12 at this GABA transporter whereas the other GATs are virtually unaffected.⁷⁵ By modeling studies, it was shown that Tiagabine (**75**) occupies the substrate binding site of mGAT1 with its nipecotic acid subunit while the lipophilic aromatic residue is accommodated in a hydrophobic pocket (S2) in the vestibule facing towards the extracellular space. With the known importance of this hydrophobic pocket (S2) for the binding of other lipophilic inhibitors in homology models of mGAT1 and the evidence from the described modeling studies a similar binding mode of the mGAT1 inhibitors NO-711 (**80**) and DDPM-2571 (**81**) can be assumed.⁷⁶ Deviating from Tiagabine (**75**) these two substances employ guvacine (**79**) as amino acid subunit, which is linked to the aromatic residues via an oxime function.

Table 2 Inhibitory potencies of GAT inhibitors with a lipophilic side chain.

Compound	GABA uptake inhibition ($pIC_{50} \pm SEM$) ^a			
	mGAT1	mGAT2	mGAT3	mGAT4
Tiagabine (75) ^b	6.88 ± 0.12	52%	64%	73%
NO-711 (80) ^b	6.83 ± 0.06	3.20 ± 0.09	3.62 ± 0.04	3.07 ± 0.05
DDPM-2571 (81) ^c	8.27 ± 0.03	4.31	4.35	4.07
NCC05-2090 (82) ^d	4.72 ^e	5.85 ^e	4.39 ^e	4.82 ^e
(S)-SNAP-5114 (83) ^b	4.07 ± 0.09	56%	5.29 ± 0.04	5.81 ± 0.10

(a) $pIC_{50} \pm SEM$ have been determined in [³H]GABA uptake assays in our group and are the result of three individual experiments each performed in triplicate. Percent values indicate remaining [³H]GABA uptake in presence of 100 μ M test compound. (b) Reference literature ⁷⁵. (c) Reference literature ⁷⁷. (d) Reference literature ⁷⁸. (e) pK_i values.

Within NO-711 (**80**) similar to Tiagabine (**75**) the lipophilic domain is formed by a diaryl residue whereas in DDPM-2571 (**81**) it is described by a biaryl moiety. The inhibitory potency of NO-711 (**80**, $pIC_{50} = 6.83 \pm 0.06$) at mGAT1 is comparable to

Tiagabine (**75**) yet DDPM-2571 (**81**) is significantly more potent and displays the highest known inhibitory potency to date with a pIC_{50} value of 8.27 ± 0.03 at this target.^{75,77}

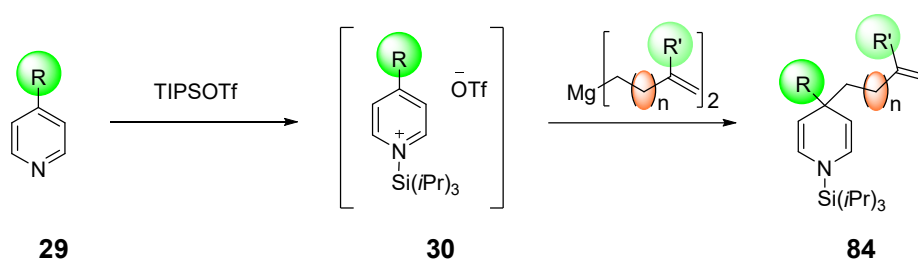
So far, good subtype selectivity in combination with a high inhibitory potency has only been achieved for mGAT1 selective GAT inhibitors such as the substances described above. Compounds selectively targeting the remaining GATs, mGAT2-mGAT4, therefore are of high demand to clarify the physiological role of these.^{63b} Examples showing at least decent subtype selectivity or inhibitory potency for these targets are the GAT2 selective inhibitor NNC05-2090 (**82**) developed by Thomsen et al.⁷⁸ and the compound (*S*)-SNAP-5114 (**83**) which was developed by Dhar et al.⁷⁹ NNC05-2090 (**82**) exhibits at least a tenfold selectivity over mGAT1, mGAT3 and mGAT4 but it is only moderately potent and does not incorporate a carboxylic acid function thus setting it apart from most other GAT inhibitors. The nipecotic acid derivative (*S*)-SNAP-5114 (**83**) is one of the most potent mGAT4 inhibitors and constitutes of (*S*)-nipecotic acid linked to a triaryl methyl moiety via an ethyleneoxy linker. However (*S*)-SNAP-5114 (**83**) demonstrates also moderate inhibitory potency at mGAT3 and therefore can be considered a mixed mGAT3/mGAT4 inhibitor. Unlike with unsubstituted nipecotic acid, for (*S*)-SNAP-5114 (**83**) the (*S*)-enantiomer is significantly more potent than the (*R*)-enantiomer.

Despite the progress made so far in the development of GAT inhibitors there is still a demand for further development of substances with improved properties. By that for instance the adverse side effects of Tiagabine (**75**) might be overcome^{58a} and highly selective and potent inhibitors of mGAT2-mGAT4 could be obtained. In addition, this would allow to study the physiological role of these three GAT inhibitors in more detail and help to estimate the potential of mGAT4 as possible target for the treatment of neuronal diseases.

2 Aims and Scope

The importance and utility of 1,4-dihydropyridines, the 2-azabicyclo[2.2.2]octane scaffold and GAT inhibitors in chemistry and medicine is well known. Hence, in this study we aimed at the development of methods for the construction of 2-azabicyclo[2.2.2]octane derivatives from 4,4-disubstituted 1,4-dihydropyridines and their use as lipophilic domains in potential GABA uptake inhibitors. In doing so we intended to emphasize and link the synthetic value of the individual components and study their performance as part of GAT inhibitors in addressing the GATs as potential targets for the treatment of neurological diseases.

First, the synthesis of 1,4-dihydropyridines with an ω -alkenyl substituent in 4-position was aimed for. The known methods for the preparation of such molecules yet displayed several disadvantages as poor regioselectivities, elaborate reagent preparation or the need for specially tailored pyridines.⁸⁰ Hence, based on the method for the synthesis of 4,4-disubstituted 1,4-dihydropyridines developed by Bräckow in our group,¹³ dihydropyridines of the same kind displaying an ω -alkenyl moiety in 4-position should be synthesized. As previous attempts for the synthesis of the desired structures with the procedure described only led to low amounts of products,¹³⁻¹⁵ the method should be optimized in respect to the obtained yields. Starting from 4-substituted pyridine derivatives the introduction of ω -alkenyl residues of varying chain length by means of bisorganomagnesium compounds into intermediately generated pyridinium ions was planned.

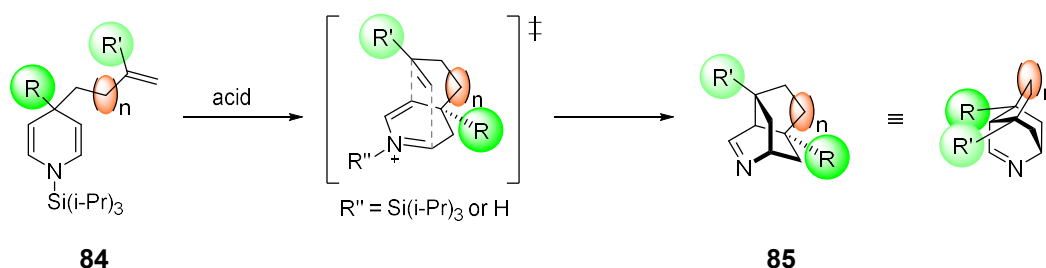


Scheme 16 General approach for the synthesis of 4,4-disubstituted 1,4-dihydropyridines bearing an ω -alkenyl residue in 4-position following the method of Bräckow.¹³

Besides plain ω -alkenyl moieties also substituted ω -alkenyl moieties carrying another rest at the internal alkene carbon center should be used, allowing a further variation of the final products. Moreover, the regioselectivity of the nucleophilic

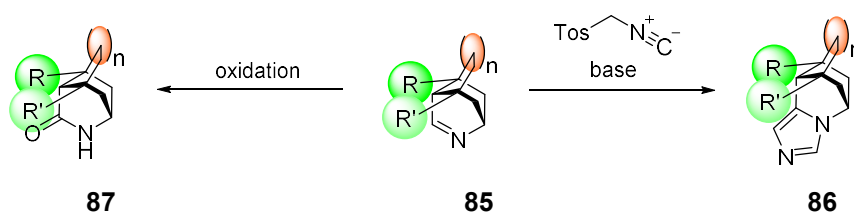
addition in the course of this reaction should be studied to explore the capability of the new method, also in comparison to literature known methods.

In a previous study carried out by Schmaunz in our group the applicability of 4-allyl substituted 1,4-dihydropyridines as starting materials to access polycyclic cage compounds containing a 2-azabicyclo[2.2.2]octane scaffold was demonstrated with few examples.^{15a} The above aspired 1,4-dihydropyridines **84** likewise should be further converted to get access to a multitude of differently substituted tricycles **85** inheriting a 2-azabicyclo[2.2.2]octane skeleton, ideally also by means of an acid catalyzed intramolecular hetero-Diels Alder reaction. In doing so, a uniform method should be employed in order to achieve a broad applicability.



Scheme 17 Planned construction of tricycles containing a 2-azabicyclo[2.2.2]octane scaffold via an intramolecular hetero-Diels-Alder reaction of 1,4-dihydropyridines **84**.

As the polycyclic imines **85** can be considered as valuable building blocks for drug development, their potential should be broadened. To expand the versatility of these compounds the C=N subunit should be used for further chemical manipulation and consequently diversification. The annelation of an imidazole ring by application of the van Leusen imidazole synthesis (\rightarrow **86**) as well as an oxidation to the corresponding lactams **87** was intended.



Scheme 18 Synthesis of 1,5-ringfused imidazoles **86** and lactams **87** from cyclic imines **85**.

Finally, the new tricyclic compounds should be employed in the construction of novel GAT inhibitors to overcome existing problems of known GAT inhibitors like unsatisfactory inhibitory potency, poor subtype selectivity or unfavorable side effects. A modification of the, as lipophilic domain commonly used, polyaryl residues towards polycyclic cage structures should also be implemented due to the often advantageous pharmacokinetic and pharmacodynamic properties of the latter and the possibility to achieve a well-defined orientation of attached residues. Hence, GAT inhibitors **88** exhibiting the tricyclic scaffold of imines **85** after reduction to amines as lipophilic residue should be synthesized (Figure 9). With the structural diversity of the previously obtained tricyclic imines **85**, the introduced scaffolds should be varied with regard to the bridge sizes used and the residues attached. Additionally, the plain alky-chain linker, by which the polycycles were intended to be connected to nipecotic acid, should display a variable length. The obtained structures would enable to obtain first structure activity relationships (SAR) for this new kind of GAT inhibitors.

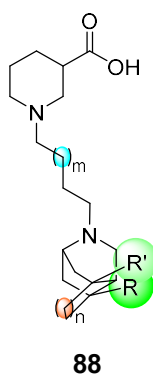


Figure 9 General structure of the aspired GAT inhibitors **88** and overview of the planned structural modifications.

3 Summary of Manuscripts and Published Results

3.1 First publication: “Accessing Tricyclic Imines Comprising a 2-Azabicyclo[2.2.2]octane Scaffold by Intramolecular Hetero-Diels–Alder Reaction of 4-Alkenyl-Substituted *N*-Silyl-1,4-dihydropyridines”

Although the 1,4-dihydropyridine (1,4-DHP) scaffold is frequently found in nature and medicine, the knowledge about 1,4-DHPs with an alkenyl moiety in 4-position is limited. Yet, by means of a cyclization reaction, 1,4-DHPs of such kind provide the opportunity of easy access to molecules with an isoquinuclidine {2-azabicyclo[2.2.2]octane} ring system, that can be found in alkaloids. Therefore, the development of a method which would give access to a multitude of 4,4-disubstituted 1,4-DHPs carrying an ω -alkenyl residue in 4-position was aimed at. A subsequent intramolecular cyclization should then provide polycycles comprising a 2-azabicyclo[2.2.2]octane skeleton .

The construction of the desired 1,4-DHPs was carried out following a method of Bräckow, starting with the activation of 4-substituted pyridines with triisopropylsilyl triflate to give intermediate pyridinium salts, which were trapped with bisorganomagnesium compounds.¹³ In an effort to increase the yields obtained so far, initially the reaction conditions were studied and optimized for a model system comprising the structurally simple pyridine derivative 4-methylpyridine and bis(homoallyl)magnesium. In doing so, the course of the reaction was analyzed at varying concentrations of bisorganomagnesium reagent, temperatures or reaction times. This led to the identification of reaction conditions allowing the formation of significantly improved amounts of product. Next the optimized reaction conditions were applied to other pyridines with 4-substituents such as phenyl, benzyl, 4-methoxyphenyl or 4-methoxybenzyl. To further expand the scope of this method, besides homoallyl also ω -alkenyl substituents of differing chain length, i.e. allyl and pent-4-en-1-yl residues, were added to the pyridinium ions of the aforementioned pyridine derivatives thereby employing the corresponding organomagnesium compounds. That way a broad range of differently 4,4-disubstituted 1,4-DHPs with a ω -alkenyl residue of varying chain length as one of the 4-substituents was produced.

During the reaction optimization and the synthesis of the various 1,4-DHPs, the regioselectivity for the addition of the ω -alkenyl substituents to the pyridinium ions

was studied continuously by ^1H NMR spectroscopy. For the addition of the long-chained homoallyl and pent-4-en-1-yl residues good regioselectivities with a preferred 4-addition leading to the formation of the desired 1,4-DHPs were observed. However, the regioselectivity decreased with increasing steric demand of the 4-substituent of the pyridine derivative used as starting material. When bisallylmagnesium was used as nucleophile the allyl residue added preferentially to the 2-position leading to large amounts of the undesired 1,2-DHPs. However, compared to literature known syntheses, considerable improvements in regioselectivity in favor of the 1,4-DHPs were achieved.

The subsequent cyclization of some 1,4-DHPs equipped with different alkenyl residues based on a method developed by Schmaunz in our group,^{15a} provided only access to some of the desired tricyclic imines with a 2-azabicyclo[2.2.2]octane scaffold. In order to get access to all tricyclic imines via an acid catalyzed intramolecular hetero-Diels-Alder reaction, diverse acids and solvents were tested. Thereby, reaction conditions were found which enabled the cyclization of all of the previously synthesized 1,4-DHPs. The new cyclization method proved to be broadly applicable, quick and highly efficient. By this means access to various substituted tricyclic imines all containing a 2-azabicyclo[2.2.2]octane skeleton with an additional bridge of variable length was granted.

Declaration of contributions: The synthesis of the 4,4-disubstituted 1,4-DHPs, the tricyclic imines and their precursor molecules was done by myself, including the evaluation of the analytical data. I carried out all experiments necessary for the development of the described synthetic methods. I wrote the manuscript of the publication and generated all schemes, tables and graphics supported by Prof. Dr. Klaus T. Wanner. The manuscript was corrected by Prof. Dr. Klaus T. Wanner.

3.2 Second Publication: “Synthesis of 1,5-Ring-Fused Imidazoles from Cyclic Imines and TosMIC – Identification of in situ Generated *N*-Methyleneformamide as a Catalyst in the van Leusen Imidazole Synthesis”

To expand the synthetic value and the potential use of the 2-azabicyclo[2.2.2]octane derivatives, the synthesis of which has been described before,⁸¹ these compounds should be transformed into 1,5-ring-fused imidazole derivatives.

One tricyclic imine was chosen as model compound to identify reaction conditions that would allow an efficient access to the 1,5-ring-fused imidazoles via the van Leusen imidazole synthesis. First concentrations of the reagent *p*-toluenesulfonylmethyl isocyanide (TosMIC), the base *tert*-butylamine and reaction times were varied. In doing so, by serendipity a decomposition product of the reagent TosMIC, namely *N*-(tosylmethyl)formamide, was found to significantly improve the yield of the 1,5-ring-fused imidazole. When the reaction conditions were further adapted, i.e. *N*-(tosylmethyl)formamide was added as a catalyst, an excellent yield of the reaction product could be achieved.

Subsequent ¹H NMR experiments revealed that the addition of *N*-(tosylmethyl)formamide not only significantly improved the yield of the 1,5-ring-fused imidazole but also accelerated the overall reaction. In additional ¹H NMR experiments a similar promoting effect of *N*-(tosylmethyl)formamide was identified for the transformation of all other tricyclic imines included in this study into 1,5-ring-fused imidazole derivatives. This effect was furthermore observed, when 3,4-dihydroisoquinoline was employed as starting material.

To elucidate the mode of action of *N*-(tosylmethyl)formamide the reaction course was monitored by ¹H NMR spectroscopy. It turned out that *N*-(tosylmethyl)formamide decomposes in the presence of the base *tert*-butylamine to *p*-toluenesulfinate. According to literature the decomposition of *N*-(tosylmethyl)formamide with Cs₂CO₃ not only leads to *p*-toluenesulfinate but also to *N*-methyleneformamide.⁸² Hence, *N*-methyleneformamide was assumed to be generated under the conditions employed by us, as well. In addition to the results of mass spectrometric experiments the isolation of a 1,3,5,7-tetraazazoctane ring system, formed from two molecules of the employed tricyclic imine and two molecules of methyleneformamide provided clear evidence for the formation of

methyleneformamide in our experiments. These findings allowed us to develop the following rationale for the promoting effect of *N*-(tosylmethyl)formamide on the van Leusen imidazole synthesis. *N*-(tosylmethyl)formamide serves as a pre-catalyst that in the presence of base is decomposed to *p*-toluenesulfinate and *N*-methyleneformamide. By adding to the latter acting as Michael acceptor the tricyclic imine is transformed into the corresponding iminium ion and thus activated for the attack of TosMIC. In the next step of the reaction, that is thus accelerated, *N*-methyleneformamide is released and can again act as organocatalyst whereas the newly formed imine-TosMIC adduct reacts to the desired 1,5-ring-fused imidazole derivative.

Declaration of contributions: The synthesis of the 1,5-ringfused imidazoles and their precursor molecules was done by myself, including the evaluation of the analytical data. I carried out all experiments necessary for the development of the described synthetic method and for the elucidation of the reaction mechanism. One symmetrical tricyclic imine was synthesized by Simone Heitsch during her bachelor thesis "Synthese neuartiger GAT-Inhibitoren mit symmetrischem lipophilen Rest" which was supervised by me. The ¹H NMR experiments aiming at the evaluation of the promoting effect of *N*-(tosylmethyl)formamide were performed together with Dr. Lars Allmendinger and Claudia Glas. X-ray crystal structures were determined by Dr. Peter Mayer. The manuscript of the publication was written and all schemes, tables and graphics were generated by myself supported by Prof. Dr. Klaus T. Wanner. The manuscript was revised by Prof. Dr. Klaus T. Wanner.

3.3 Third Publication: “Synthesis and biological evaluation of novel *N*-substituted nipecotic acid derivatives with tricyclic cage structures in the lipophilic domain as GABA uptake inhibitors”

The GABA transporters constitute highly interesting pharmacological targets, for instance for the treatment of neurological diseases. In consequence a multitude of structurally diverse GAT inhibitors have been designed many of them exhibiting polyaromatic lipophilic side chains. However, inhibitors with polycyclic cage structures serving as lipophilic domain are scarce although cage structures often display beneficial pharmacokinetic and pharmacodynamic properties. As a result, a systematic study aiming at the development and evaluation of GAT inhibitors with such a subunit was carried out to assess the potential of the latter.

In this study polycyclic cage compounds based on a 2-azabicyclo[2.2.2]octane scaffold should be connected via a plain hydrocarbon linker originating from the nitrogen atom of the polycycle with the amino nitrogen atom of nipecotic acid. For this purpose, symmetric tricyclic imines, of which the synthesis had been described before,⁸³ comprising the aforementioned polycyclic scaffold were used, as these structures allowed a variation of the substituents attached to the polycyclic cage as well as a variation of the size of one of the bridges in the polycycle. Thus, not only the size of the tricyclic scaffold but also the spatial orientation of the attached residues could be altered possibly giving insight on the impact of these structural modifications on the biological activity. Furthermore, by a variation of the length of the used hydrocarbon spacer additional information should be gained regarding the structure activity relationship.

For the synthesis of the test compounds initially nipecotic acid ester derivatives equipped with an *N*-alkyl substituent with a terminal acetal function were prepared serving as precursors for a subsequent reductive amination reaction. Upon acetal cleavage nipecotic acid ester derivatives with an *N*-alkyl substituent displaying a terminal aldehyde function were obtained and subjected to reductive amination with amines that were generated by reduction of the respective symmetric tricyclic imines. The obtained *N*-substituted nipecotic acid ester derivatives exhibiting a tricyclic amine as lipophilic domain were then finally hydrolyzed to the corresponding nipecotic acids and evaluated together with the esters for their biological activity at all four mGAT subtypes.

The results of the biological evaluation revealed upon comparison of the compounds among each other, that there was no general correlation between the inhibitory potency and the length of the hydrocarbon linker or the size of the bridge in the lipophilic domain for the nipecotic acid derivatives with a free carboxylic acid or ester function. However, the substituents attached to the polycyclic cage affected the biological activity, at least in the case of the nipecotic acid ester derivatives as for them almost exclusively higher inhibitory potencies at mGAT1-mGAT4 were observed when phenyl instead of methyl residues were present. Interestingly, these at the cage subunit phenyl substituted nipecotic acid ester derivatives exhibited also higher inhibitory potencies as compared to their corresponding carboxylic acids, whereas such an effect could not be observed for the methyl substituted nipecotic acid ester derivatives thus highlighting the importance of the ester function and the phenyl residues for the biological activity. The phenyl substituted nipecotic acid ester derivatives usually displayed equally moderate inhibitory activity at all four GATs, yet also in some cases moderate subtype selectivity at mGAT3 and mGAT4 was observed.

Declaration of contributions: The syntheses of all *N*-substituted nipecotic acid derivatives and their precursor molecules were done by myself, including the evaluation of the analytical data. I carried out all experiments necessary for the development of the described synthetic methods. Two *N*-substituted nipecotic acid ester derivatives were synthesized by Simone Heitsch during her bachelor thesis “Synthese neuartiger GAT-Inhibitoren mit symmetrischem lipophilen Rest” which was supervised by me. Biological testing was performed by the technical assistants of the group under supervision of Dr. Georg Höfner. I wrote the manuscript and generated all schemes, tables and graphics supported by Prof. Dr. Klaus T. Wanner. The manuscript was revised by Prof. Dr. Klaus T. Wanner.

4 Further Experiments

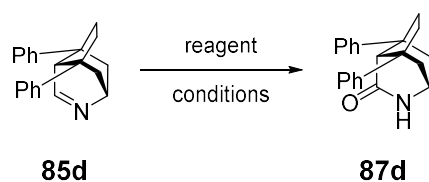
The following section contains results unpublished in one of the formerly presented papers.

4.1 Synthesis of polycyclic lactams

To further broaden the synthetic value of the tricyclic imines **85** and thus expand the potential uses of these valuable building blocks for medicinal chemistry their transformation to the corresponding lactams **87** was aimed at. For instance, such lactams **87** could offer an interesting alternative to the tricyclic amines that were employed as lipophilic domain in GAT inhibitors **88** and are derived from the imines **85**. In contrast to these tricyclic amines the lactams **87** will not show any significant basicity. Accordingly they will not display any charge at physiological pH which will make them even better suited for an application in the lipophilic domain of GAT inhibitors.

To access the lactams **87** first appropriate reaction conditions had to be sought. Jørgensen et al. had introduced a straightforward oxidation method employing potassium permanganate in an acetonitrile/ water solution to synthesize amides from acyclic imines that carried sterically demanding residues on either side of the carbon-nitrogen double bond.⁸⁴ As the imine function in the tricyclic imines **85** was also carrying sterically demanding substituents and in some cases shielded to some extent,⁸³ these conditions seemed promising for the desired transformation. However, when employing the reaction conditions to the tricyclic imine **85d** (Table 3, entry 1), which was chosen as model compound to study the synthesis of the lactams **87**, no reaction occurred and imine **85d** was left unchanged.

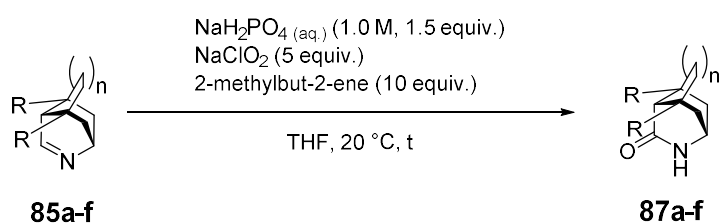
Reaction conditions that had proved to be suitable for the transformation of a cyclic imine to a lactam have been presented by Tomioka et al.⁸⁵ Although they had only oxidized sterically less shielded 3,4-dihydroisoquinoline to 3,4-dihydroisoquinolin-1-one using Pinnick oxidation conditions, it seemed worth trying to apply their method for the oxidation of the tricyclic imines **85** since only few oxidations of cyclic imines to lactams have been described in literature so far. When imine **85d** was treated with sodium chlorite and 2-methylbut-2-ene in a mixture of 1.0 M aqueous sodium dihydrogen phosphate solution and tetrahydrofuran, the desired lactam **87d** could be obtained in a good yield of 68% after 48 h (Table 3, entry 2).

Table 3 Reaction conditions applied for the oxidation of imine **85d**.

Entry	reagent ^a	conditions ^a	result/ yield 87d
1	KMnO ₄ (2 equiv.)	MeCN/ H ₂ O (2:1), 50 °C, 64 h	no reaction
2	NaH ₂ PO ₄ (aq.) (1.0 M, 1.5 equiv.) NaClO ₂ (5 equiv.) 2-Methylbut-2-ene (10 equiv.)	THF, 20 °C, 48 h	68%
3	NaH ₂ PO ₄ (aq.) (1.0 M, 1.5 equiv.) NaClO ₂ (5 equiv.)	THF, 20 °C, 4 h	68%

^a Reactions according to literature.⁸⁴⁻⁸⁵

Interestingly, the reaction was found to proceed much faster when the radical scavenger 2-methylbut-2-ene was omitted (Table 3, entry 3). However, as the yield was unchanged and undesired side reactions of the hypochlorous acid which is formed as side product should be excluded, the original reaction conditions were chosen for the transformation of the remaining tricyclic imines **85a-c** and **85e-f** to the lactams **87a-c** and **87e-f** despite the longer reaction time.

Table 4 Synthesis of the lactams **87a-f**.

Entry	R	n	Imine	t [h]	Lactam	Yield [%]
1	Me	0	85a	18	87a	28
2	Ph	0	85b	48	87b	59
3	Me	1	85c	48	87c	48
4	Ph	1	85d	48	87d	68 ^a
5	Me	2	85e	4	87e	46
6	Ph	2	85f	3.5	87f	35

^a Identical to Table 3, entry 2.

With the afore tested reaction conditions in addition to imine **85d** the tricyclic imines **85a-c** and **85e-f** could be successfully oxidized to the corresponding lactams **87a-c** and **87e-f**. Though some of the obtained yields were rather low (28%-35%; Table 4, entries 1,6), most of the lactams were accessed in moderate yields (46%-68%; Table 4, entries 2-5) proofing the applied reaction conditions to be generally suitable to access the lactams **87a-f**.

Experimental data

All solvents were distilled prior to use and all purchased chemicals were used without further purification. TLC was performed with plates from Merck KGaA (silica gel 60 F254 on aluminum sheets). For purification via flash chromatography (FC) silica gel 60 (40–63 μm mesh size) from Merck KGaA was employed. All melting points were determined with a BÜCHI 510 melting point apparatus and are uncorrected. Infrared spectra were recorded with a Perkin Elmer Paragon 1000 and a Jasco FT/IR-410. Solid substances were measured as KBr pellets and oils as film on NaCl. HRMS were obtained with a Finnigan LTQ FT (ESI). ^1H and ^{13}C NMR spectra were acquired with a Avance III HD Bruker BioSpin (400 or 500 MHz), referenced to the solvent residual peak as internal standard and analyzed with MestReNova (Version 12.0.0–20080; Mestrelab Research S.L.; released 26.09.2017). Nonequivalent protons attached to the same carbon center were differentiated by superscript a and b (e.g. NCH_2^{a} , NCH_2^{b}).

General procedure for the synthesis of symmetric tricyclic lactams

To a solution of 2-methylbut-2-ene (5.0 equiv.) and NaClO_2 (10 equiv.) in THF (3.90 mL/mmol_{imine}) an aqueous solution of NaH_2PO_4 (1.0 M, 1.5 equiv.) was added. Subsequently a solution of the imine (1.0 equiv.) in THF (0.5 M) was added dropwise to this mixture at 20 °C via a syringe within 5-10 min. The syringe was washed twice with THF (0.5 mL/mmol_{imine}) and the washings were added to the reaction mixture. The reaction was stirred vigorously until disappearance of the starting material was confirmed by MS analysis. Then the reaction mixture was diluted with EtOAc (30 mL/mmol_{imine}) and washed with water, aqueous $\text{Na}_2\text{S}_2\text{O}_3$ solution (10%) and brine (each 10 mL/mmol_{imine}). The organic layer was dried

(Na₂SO₄), filtered and concentrated under vacuum. The resulting crude was purified by FC.

1,7-Dimethyl-4-azatricyclo[3.3.1.0^{2,7}]nonan-3-one **87a**

Synthesis according to the general procedure described above from imine **85a** (0.10 g, 0.67 mmol), 2-methylbut-2-ene (0.47 g, 6.7 mmol, 0.72 mL), NaClO₂ (0.30 g, 3.4 mmol) and an aqueous solution of NaH₂PO₄ (1.0 M, 1.0 mL). The reaction was stopped after 18 h. Purification by FC (SiO₂, EtOAc/NEt₃ 98:2 → EtOAc/MeOH/NEt₃ 88/10/2).

87a: 31 mg (28%). Colorless amorphous solid. IR (KBr): $\tilde{\nu}$ = 3176, 2949, 2860, 1672, 1446, 1404, 1313, 1277, 1142, 791, 769, 515, 424 cm⁻¹. ¹H NMR (500 MHz, CD₂Cl₂, 25 °C): δ = 1.06 (s, 6 H, CH₃), 1.35–1.46 (m, 3 H, CCH₂^aC, CCH₂^aCH), 1.70–1.82 (m, 3 H, CCH₂^bC, CCH₂^bCH), 2.24 (d, J = 2.0 Hz, 1 H, CCHC), 3.72 (dp, J = 5.3/2.6 Hz, 1 H, NHCH), 7.49 (br s, 1 H, NH) ppm. ¹³C NMR (125 MHz, CD₂Cl₂, 25 °C): δ = 26.6 (CH₃), 37.5 (CCH₃), 42.5 (CH₂CH), 48.4 (NHCH), 50.0 (CCH₂C), 55.1 (CHCO), 173.7 (CO) ppm. M (C₁₀H₁₅NO) = 165.24. HRMS (ESI): [M+H⁺] calcd. for C₁₀H₁₆NO 166.1226; found 166.1226.

1,7-Diphenyl-4-azatricyclo[3.3.1.0^{2,7}]nonan-3-one **87b**

Synthesis according to the general procedure described above from imine **85b** (0.10 g, 0.37 mmol), 2-methylbut-2-ene (0.26 g, 3.7 mmol, 0.39 mL), NaClO₂ (0.17 g, 1.8 mmol) and an aqueous solution of NaH₂PO₄ (1.0 M, 0.55 mL). The reaction was stopped after 48 h. Purification by FC (SiO₂, EtOAc/NEt₃ 98:2).

87b: 62 mg (59%). Colorless amorphous solid. IR (KBr): $\tilde{\nu}$ = 3182, 3026, 2937, 1672, 1495, 1444, 1350, 1290, 1119, 760, 700 cm⁻¹. ¹H NMR (400 MHz, CD₂Cl₂, 25 °C): δ = 1.83–1.95 (m, 2 H, CCH₂^aCH), 2.22–2.35 (m, 3 H, CCH₂^aC, CCH₂^bCH), 2.70 (dt, J = 9.1/2.1 Hz, 1 H, CCH₂^aC), 3.19 (d, J = 2.0 Hz, 1 H, CCHC), 3.99 (dp, J = 5.1/2.6 Hz, 1 H, NHCH), 7.13–7.24 (m, 6 H, CCHCH, CCHCHCH), 7.26–7.35 (m, 4 H, CCHCH), 7.88 (d, J = 3.6 Hz, 1 H, NH) ppm. ¹³C NMR (100 MHz, CD₂Cl₂, 25 °C): δ = 44.2 (CCH₂), 44.7 (CH₂CH), 47.2 (CCH₂C), 48.2 (NHCH), 53.3 (CHCO), 125.4 (CCHCH), 126.8 (CCHCHCH), 129.1 (CCHCH), 147.9 (CCHCH), 173.3 (CO)

ppm. $M(C_{20}H_{19}NO) = 289.38$. HRMS (ESI): $[M+H^+]$ calcd. for $C_{20}H_{20}NO$ 290.1539; found 290.1540.

3,6-Dimethyl-9-azatricyclo[4.3.1.0^{3,7}]decan-8-one **87c**

Synthesis according to the general procedure described above from imine **85c** (0.10 g, 0.61 mmol), 2-methylbut-2-ene (0.43 g, 6.1 mmol, 0.66 mL), $NaClO_2$ (0.28 g, 3.1 mmol) and an aqueous solution of NaH_2PO_4 (1.0 M, 0.92 mL). The reaction was stopped after 48 h. Purification by FC (SiO_2 , EtOAc/ NEt_3 98:2 \rightarrow EtOAc/MeOH/ NEt_3 88/10/2).

87c: 53 mg (48%). Colorless amorphous solid. IR (KBr): $\tilde{\nu} = 3188, 3086, 2947, 2866, 1670, 1454, 1400, 1335, 1167, 1124, 779, 584, 500\text{ cm}^{-1}$. 1H NMR (400 MHz, CD_2Cl_2 , 25 °C): $\delta = 1.09$ (s, 6 H, CH_3), 1.45–1.59 (m, 4 H, $CH(CH_2)_2$), 1.59–1.70 (m, 4 H, CCH_2CH_2C), 1.85 (d, $J = 1.8$ Hz, 1 H, $CHCO$), 3.44 (dp, $J = 5.5/2.7$ Hz, 1 H, $NHCH$), 7.43 (br s, 1 H, NH) ppm. ^{13}C NMR (100 MHz, CD_2Cl_2 , 25 °C): $\delta = 28.2$ (CH_3), 40.4 (CH_2CH_2), 43.1 (CCH_3), 46.2 ($CH(CH_2)_2$), 46.9 ($NHCH$), 62.6 ($CHCO$), 176.3 (CO) ppm. $M(C_{11}H_{17}NO) = 179.26$. HRMS (ESI): $[M+H^+]$ calcd. for $C_{11}H_{18}NO$ 180.1383; found 180.1383.

3,6-Diphenyl-9-azatricyclo[4.3.1.0^{3,7}]decan-8-one **87d**

Synthesis according to the general procedure described above from imine **85d** (0.10 g, 0.35 mmol), 2-methylbut-2-ene (0.25 g, 3.5 mmol, 0.37 mL), $NaClO_2$ (0.15 g, 1.7 mmol) and an aqueous solution of NaH_2PO_4 (1.0 M, 0.52 mL). The reaction was stopped after 48 h. Purification by FC (SiO_2 , EtOAc/ NEt_3 98:2).

87c: 72 mg (68%). Colorless amorphous solid. IR (KBr): $\tilde{\nu} = 3180, 3026, 2951, 1678, 1496, 1444, 1400, 1336, 1172, 1018, 766, 704, 509, 459\text{ cm}^{-1}$. 1H NMR (400 MHz, CD_2Cl_2 , 25 °C): $\delta = 1.95$ –2.16 (m, 6 H, $CH(CH_2^a)_2$, CCH_2CH_2C), 2.17–2.25 (m, 2 H, $CH(CH_2^b)_2$), 3.34 (d, $J = 1.9$ Hz, 1 H, $CHCO$), 3.54 (dp, $J = 5.6/2.8$ Hz, 1 H, $NHCH$), 7.15–7.21 (m, 2 H, $CCHCHCH$), 7.27–7.34 (m, 5 H, $CCHCH$, NH), 7.39–7.45 (m, 4 H, $CCHCH$) ppm. ^{13}C NMR (100 MHz, CD_2Cl_2 , 25 °C): $\delta = 41.6$ (CH_2CH_2), 47.0 ($NHCH$), 48.2 ($CH(CH_2)_2$), 50.5 (CCH_2), 55.3 ($CHCO$), 125.9 ($CCHCH$), 126.4 ($CCHCHCH$), 129.0 ($CCHCH$), 150.2 ($CCHCH$), 176.0 (CO) ppm.

M (C₂₁H₂₁NO) = 303.41. HRMS (ESI): [M+H⁺] calcd. for C₂₁H₂₂NO 304.1696; found 304.1695.

3,7-Dimethyl-10-azatricyclo[5.3.1.0^{3,8}]undecan-9-one 87e

Synthesis according to the general procedure described above from imine **85e** (30 mg, 0.17 mmol), 2-methylbut-2-ene (0.12 g, 1.7 mmol, 0.18 mL), NaClO₂ (77 mg, 0.85 mmol) and an aqueous solution of NaH₂PO₄ (1.0 M, 0.25 mL). The reaction was stopped after 4 h. Purification by FC (SiO₂, EtOAc/NEt₃ 98:2 → EtOAc/MeOH/NEt₃ 88/10/2).

87e: 15 mg (46%). Yellow solid. Mp.: 137 °C. IR (KBr): $\tilde{\nu}$ = 3199, 3082, 2954, 2926, 1670, 1439, 1375, 1327, 1153, 1076, 980, 754, 592, 486 cm⁻¹. ¹H NMR (500 MHz, CD₂Cl₂, 25 °C): δ = 0.96 (s, 6 H, CH₃), 1.04–1.12 (m, 2 H, CCH₂^aCH₂), 1.32–1.59 (m, 9 H, CCH₂^bCH₂, CCH₂CH₂, CHCO, CH(CH₂)₂), 3.50–3.58 (m, 1 H, NHCH), 6.56 (br s, 1 H, NH) ppm. ¹³C NMR (125 MHz, CD₂Cl₂, 25 °C): δ = 19.4 (CCH₂CH₂), 31.9 (CH₃), 33.1 (CCH₃), 37.8 (CCH₂CH₂), 39.2 (CH(CH₂)₂), 48.2 (NHCH), 59.5 (CHCO), 176.9 (CO) ppm. M (C₁₂H₁₉NO) = 193.29. HRMS (ESI): [M+H⁺] calcd. for C₁₂H₂₀NO 194.1539; found 194.1539.

3,7-Diphenyl-10-azatricyclo[5.3.1.0^{3,8}]undecan-9-one 87f

Synthesis according to the general procedure described above from imine **85f** (30 mg, 0.10 mmol), 2-methylbut-2-ene (70 mg, 1.0 mmol, 0.11 mL), NaClO₂ (45 mg, 0.50 mmol) and an aqueous solution of NaH₂PO₄ (1.0 M, 0.15 mL). The reaction was stopped after 3.5 h. Purification by FC (SiO₂, EtOAc/NEt₃ 98:2).

87f: 11 mg (35%). Colorless solid. Mp.: 241 °C. IR (KBr): $\tilde{\nu}$ = 3172, 3051, 2927, 2845, 1687, 1497, 1354, 1126, 1030, 754, 696, 596, 540, 498 cm⁻¹. ¹H NMR (400 MHz, CD₂Cl₂, 25 °C): δ = 1.38–1.50 (m, 2 H, CCH₂^aCH₂), 1.67–1.92 (m, 4 H, CCH₂^bCH₂, CCH₂CH₂), 1.95–2.07 (m, 2 H, CH(CH₂^a)₂), 2.10–2.22 (m, 2 H, CH(CH₂^b)₂), 3.28 (d, *J* = 1.8 Hz, 1 H, CHCO), 3.54–3.63 (m, 1 H, NHCH), 6.52 (d, *J* = 4.2 Hz, 1 H, NH), 7.14–7.22 (m, 2 H, CCHCHCH), 7.27–7.36 (m, 4 H, CCHCH), 7.46–7.53 (m, 4 H, CCHCH) ppm. ¹³C NMR (100 MHz, CD₂Cl₂, 25 °C): δ = 20.2 (CCH₂CH₂), 40.7 (CH(CH₂)₂), 41.0 (CCH₂CH₂), 42.2 (CCH₂), 48.4 (NHCH), 51.3

(CHCO), 126.3 (CCHCHCH), 126.8 (CCHCH), 128.7 (CCHCH), 151.6 (CCHCH), 175.4 (CO) ppm. M (C₂₂H₂₃NO) = 317.43. HRMS (ESI): [M+H⁺] calcd. for C₂₂H₂₄NO 318.1852; found 318.1853.

5 Summary of the Thesis

The abundance of compounds comprising a 1,4-dihydropyridine or a 2-azabicyclo[2.2.2]octane scaffold in natural products, medicinal drugs or chemical compounds nicely highlights the importance of these substances for chemical research. Hence, the goal of this study was to provide methods that would give access to diverse polycycles incorporating the 2-azabicyclo[2.2.2]octane skeleton, which should be accomplished by employing 4,4-disubstituted 1,4-dihydropyridines as intermediates. With the respective methods not only a broad variety of different polycycles should be made available proofing the versatility and synthetic value of the compounds, but also lipophilic building blocks to be integrated in the side chain of GAT inhibitors, should be generated. Thus, GAT inhibitors with lipophilic domains of so far unprecedented structure should be accessed and studied for their structure activity relationship.

First, 4- ω -alkenyl substituted 1,4-dihydropyridines were synthesized, which should serve as starting materials for the construction of the aspired polycycles. In the synthetic method, developed for this purpose and optimized for their yields, initially 4-substituted pyridine derivatives with substituents such as methyl, phenyl, benzyl, 4-methoxyphenyl or 4-methoxybenzyl were activated to their corresponding *N*-silyl pyridinium salts with triisopropylsilyl triflate. These intermediates were trapped with bisorganomagnesium reagents to introduce the 4- ω -alkenyl residues into the 4-position of the former pyridine derivatives. Besides plain ω -alkenyl residues like allyl, homoallyl or pent-4-en-1-yl also ω -alkenyl residues carrying an additional residue at the internal alkenyl carbon center were added to the 4-position of the pyridinium salts leading to a broad range of differently 4,4-disubstituted 1,4-dihydropyridines with 4- ω -alkenyl residues of varying chain length. Alongside with the synthesis of the 1,4-dihydropyridines the regioselectivity of the addition of the ω -alkenyl residues to the pyridinium ions was studied revealing good regioselectivities with preferred 4-addition in most cases and considerable improvements in regioselectivity as compared to literature known methods.

With the 4- ω -alkenyl substituted 1,4-dihydropyridines at hand the transformation thereof into polycycles, i.e. tricyclic imines, incorporating a 2-azabicyclo[2.2.2]octane scaffold was attempted in an acid catalyzed intramolecular hetero-Diels-Alder reaction. As the literature known procedure for

this cyclization failed in some cases to yield the desired cyclization products when applied to the newly synthesized 1,4-dihydropyridines a new cyclization method was developed. This method proved to be broadly applicable, quick and highly efficient. The new method granted access to various tricyclic imines all including the desired 2-azabicyclo[2.2.2]octane skeleton with an additional bridge of varying size and either one or two substituents attached to the bridgehead atoms.

To further expand the potential uses of the obtained 2-azabicyclo[2.2.2]octane derivatives that are to be considered valuable building blocks for drug development the disubstituted tricyclic imines were oxidized under Pinnick oxidation conditions to the corresponding lactams. In addition, the same tricyclic imines were used as starting materials for the preparation of 1,5-ring-fused imidazole derivatives via the van Leusen imidazole synthesis. During optimization of the synthesis of the 1,5-ring-fused imidazoles, *N*-(tosylmethyl)formamide, a decomposition product of the reagent *p*-toluenesulfonylmethyl isocyanide (TosMIC), by serendipity was found to significantly improve the yield of the reaction. Furthermore, the addition of *N*-(tosylmethyl)formamide considerably reduced the reaction time, a beneficial effect that in combination with the improved yield could be observed for all syntheses of the 1,5-ring-fused imidazole derivatives starting from the tricyclic imines. Mechanistic investigations by ^1H NMR spectroscopy to elucidate the function of *N*-(tosylmethyl)formamide revealed a decomposition of *N*-(tosylmethyl)formamide to *N*-methyleneformamide and *p*-toluenesulfinate under the applied basic reaction conditions. The generated *N*-methyleneformamide is assumed to act as Michael acceptor when attacked by the tricyclic imines which are thus transformed into the corresponding iminium ions and thereby activated for the attack of TosMIC. After the nucleophilic addition the organocatalyst *N*-methyleneformamide is released again and the TosMIC-imine adducts reacts to the 1,5-ring-fused imidazole.

Finally, the polycycles were used for the construction of potential GAT inhibitors exhibiting these units as part of the *N*-substituent to study how such rigid and sterically demanding lipophilic residues effect the biological activity. To access the aspired structures, previously obtained symmetric tricycles containing a 2-azabicyclo[2.2.2]octane scaffold were linked to the amino nitrogen of nipecotic acid via a plain hydrocarbon linker originating from the nitrogen atom of the polycycle. This was accomplished by a reductive amination reaction of nipecotic

acid ester derivatives with *N*-alkyl substituents displaying a terminal aldehyde function and amines, which were synthesized by reduction of the symmetric tricyclic imines. The newly synthesized GAT inhibitors differed from each other either by variation of the substituents attached to the polycycle or by the size of one of the bridges in the polycycle. In addition, GAT inhibitors with hydrocarbon linkers of different lengths in between the nipecotic acid subunit and the polycycle were produced. Successive hydrolysis of the *N*-substituted nipecotic acid ester derivatives yielded the related nipecotic acid derivatives that were evaluated together with the esters for their biological activity at mGAT1-4. Unfortunately, the nipecotic acid derivatives with a free carboxylic acid function exhibited only weak inhibitory activities at all four mGAT subtypes. In contrast, phenyl-substituted nipecotic acid ester derivatives displayed moderate inhibitory potency at mGAT1-4 and showed even moderate subtype selectivity at mGAT3 and mGAT4 in some cases. As it turned out, phenyl residues attached to the polycycle and the ester function in the nipecotic acid subunit were essential for reasonable biological activity, whereas the length of the hydrocarbon linker or the size of the variable bridge in the polycycle did not seem to affect the latter.

In summary, efficient methods allowing the synthesis of a broad variety of 4,4-disubstituted 1,4-dihydropyridines with an ω -alkenyl residue in 4-position as well as diverse polycycles with a 2-azabicyclo[2.2.2]octane scaffold were developed. The prepared polycycles proved to be highly versatile and enabled to study the potential of GAT inhibitors with a bulky and rigid lipophilic domain in the side chain for the first time.

6 List of Abbreviations

1,4-DHP	1,4-dihydropyridine
AD	Alzheimer's disease
BBB	blood brain barrier
CNS	central nervous system
dDAT	dopamine transporter from <i>Drosophila melanogaster</i>
DNA	deoxyribonucleic acid
FDA	US Food and Drug Administration
GABA	γ -aminobutyric acid
GABA-T	GABA transaminase
GAD	glutamic acid decarboxylase
GAT	GABA transporter
GPCR	G-protein coupled receptor
hSERT	human serotonin transporter
HUGO	Human Genome Organization
LeuT _{Aa}	leucine transporter from <i>Aquifex aeolicus</i>
mGAT	mouse GABA transporter
NADH	nicotinamide adenine dinucleotide
NSS	neurotransmitter sodium symporter
PD	Parkinson's disease
SEM	standard error of mean
SLC 6	solute carrier family 6
TBDMSOTf	<i>tert</i> -butyldimethylsilyl triflate
THPO	4,5,6,7-tetrahydroisoxazolo[4,5-c]pyridin-3-ol

TIPSOTf	triisopropylsilyl triflate
TM	transmembrane helices
TosMIC	tosylmethyl isocyanide
VGAT	vesicular neurotransmitter transporter

7 Literature

- (1) (a) Sharma, V. K.; Singh, S. K. *RSC Adv.* **2017**, *7*, 2682-2732. (b) Silva, A.; Silva, E.; Varandas, P. *Synthesis* **2013**, *45*, 3053-3089. (c) Lavilla, R. *J. Chem. Soc., Perkin Trans. 1* **2002**, 1141-1156.
- (2) Belenky, P.; Bogan, K. L.; Brenner, C. *Trends Biochem. Sci.* **2007**, *32*, 12-19.
- (3) (a) Edraki, N.; Mehdipour, A. R.; Khoshneviszadeh, M.; Miri, R. *Drug Discovery Today* **2009**, *14*, 1058-1066. (b) Bossert, F.; Vater, W. *Med. Res. Rev.* **1989**, *9*, 291-324. (c) Bossert, F.; Vater, W. *Naturwissenschaften* **1971**, *58*, 578.
- (4) Goldmann, S. *Pharm. Unserer Zeit* **2005**, *5*, 366-373.
- (5) Hantzsch, A. *Justus Liebigs Ann. Chem.* **1882**, *215*, 1-82.
- (6) Bull, J. A.; Mousseau, J. J.; Pelletier, G.; Charette, A. B. *Chem. Rev.* **2012**, *112*, 2642-2713.
- (7) Sulzbach, R. A. *J. Organometal. Chem.* **1970**, *24*, 307-314.
- (8) (a) Tsuge, O.; Kanemasa, S.; Naritomi, T.; Tanaka, J. *Chemistry Lett.* **1984**, 1255-1258. (b) Tsuge, O.; Kanemasa, S.; Naritomi, T.; Tanaka, J. *Bull. Chem. Soc. Jpn.* **1987**, *60*, 1497-1504.
- (9) (a) Akiba, K.; Iseki, Y.; Wada, M. *Tetrahedron Lett.* **1982**, *23*, 3935-3936. (b) Akiba, K.; Iseki, Y.; Wada, M. *Bull. Chem. Soc. Jpn.* **1984**, *57*, 1994-1999.
- (10) Bennasar, M.-L.; Juan, C.; Bosch, J. *Tetrahedron Lett.* **1998**, *39*, 9275-9278.
- (11) Mani, N. S.; Chen, P.; Jones, T. K. *J. Org. Chem.* **1999**, *64*, 6911-6914.
- (12) Bräckow, J., PhD thesis, Ludwig-Maximilians-Universität München, 2006.
- (13) Bräckow, J.; Wanner, K. T. *Tetrahedron* **2006**, *62*, 2395-2404.
- (14) Sperger, C. A.; Wanner, K. T. *Tetrahedron* **2009**, *65*, 5824-5833.
- (15) (a) Schmaunz, C. E.; Mayer, P.; Wanner, K. T. *Synthesis* **2014**, *46*, 1630-1638. (b) Schmaunz, C. E.; Wanner, K. T. *Synthesis* **2011**, *20*, 3332-3342.
- (16) Rappenglück, S.; Niessen, K.; Seeger, T.; Worek, F.; Thiermann, H.; Wanner, K. *Synthesis* **2017**, *49*, 4055-4064.
- (17) Löffler, G.; Petrides, P. E.; Heinrich, P. C. *Biochemie und Pathobiochemie*; 8th ed.; Springer: Heidelberg, 2007.
- (18) Vitaku, E.; Smith, D. T.; Njardarson, J. T. *J. Med. Chem.* **2014**, *57*, 10257-10274.
- (19) (a) Wipf, P.; Skoda, E. M.; Mann, A. *The Practice of Medicinal Chemistry*; 4th ed.; Academic Press: London, San Diego, Waltham, Oxford, 2015. (b) Joubert, J.; Geldenhuys, W. J.; Van der Schyf, C. J.; Oliver, D. W.; Kruger, H. G.; Govender, T.; Malan, S. F. *ChemMedChem* **2012**, *7*, 375-384. (c) Zheng, Y.; Tice, C. M.; Singh, S. B. *Bioorg. Med. Chem. Lett.* **2014**, *24*, 3673-3682.
- (20) Brookes, K. B.; Hickmott, P. W.; Jutle, K. K.; Schreyer, C. A. *S. Afr. J. Chem.* **1992**, *45*, 8-11.

- (21) Stockdale, T. P.; Williams, C. M. *Chem. Soc. Rev.* **2015**, *44*, 7737-7763.
- (22) Khan, M. O. F.; Levi, M. S.; Clark, C. R.; Ablorderrey, S. Y.; Law, S.-J.; Wilson, N. H.; Borne, R. F. *Stud. Nat. Prod. Chem.* **2008**, *34*, 753-787.
- (23) Nagata, K.; Aistrup, G. L.; Honda, H.; Shono, T.; Narahashi, T. *Pestic. Biochem. Phys.* **1999**, *64*, 157-165.
- (24) Zubaran, C. *CNS Drug Reviews* **2000**, *6*, 219-240.
- (25) Wauters, I.; De Blicke, A.; Muylaert, K.; Heugebaert, T. S. A.; Stevens, C. V. *Eur. J. Org. Chem.* **2014**, 1296-1304.
- (26) Graham, P. M.; Delafuente, D. A.; Liu, W.; Myers, W. H.; Sabat, M.; Harman, W. D. *J. Am. Chem. Soc.* **2005**, *127*, 10568-10572.
- (27) (a) Okamura, H.; Nagaike, H.; Iwagawa, T.; Nakatani, M. *Tetrahedron Lett.* **2000**, *41*, 8317-8321. (b) Passarella, D.; Favia, R.; Giardini, A.; Lesma, G.; Martinelli, M.; Silvani, A.; Danieli, B.; Efange, S. M. N.; Mash, D. C. *Bioorg. Med. Chem.* **2003**, *11*, 1007-1014.
- (28) (a) Silva, E. M. P.; Rocha, D. H. A.; Silva, A. M. S. *Synthesis* **2018**, *50*, 1773-1782. (b) Martin, R. M.; Bergman, R. G.; Ellman, J. A. *Org. Lett.* **2013**, *15*, 444-447. (c) Khan, M. O. F.; Levi, M. S.; Tekwani, B. L.; Wilson, N. H.; Borne, R. F. *Bioorg. Med. Chem.* **2007**, *15*, 3919-3925.
- (29) (a) Hartman, G. D.; Halczenko, W.; Philipps, B. T. *J. Org. Chem.* **1985**, *50*, 2427-2431. (b) Hartman, G. D.; Halczenko, W.; Philipps, B. T. *J. Org. Chem.* **1986**, *51*, 142-148. (c) Hartman, G. D.; Philipps, B. T.; Halczenko, W. *J. Org. Chem.* **1987**, *52*, 1136-1139. (d) Hartman, G. D.; Philipps, B. T.; Halczenko, W.; Pitzenberger, S. M. *J. Org. Chem.* **1989**, *54*, 4137-4137.
- (30) Raucher, S.; Bray, B. L. *J. Org. Chem.* **1985**, *50*, 3236-3237.
- (31) (a) Kono, M.; Harada, S.; Nozaki, T.; Hashimoto, Y.; Murata, S.; Gröger, H.; Kuroda, Y.; Yamada, K.; Takasu, K.; Hamada, Y.; Nemoto, T. *Org. Lett.* **2019**, *21*, 3750-3754. (b) Moisan, L.; Thuéry, P.; Nicolas, M.; Doris, E.; Rousseau, B. *Angew. Chem. Int. Ed.* **2006**, *45*, 5334-5336.
- (32) Satoh, N.; Akiba, T.; Yokoshima, S.; Fukuyama, T. *Angew. Chem. Int. Ed.* **2007**, *46*, 5734-5736.
- (33) (a) Gaba, M.; Mohan, C. *Med. Chem. Res.* **2015**, *25*, 173-210. (b) Pozharskii, A. F.; Soldatenkov, A. T.; Katritzky, A. R. *Heterocycles in Life and Society: An Introduction to Heterocyclic Chemistry, Biochemistry and Applications*; John Wiley & Sons, 2011.
- (34) SciFinder® database query. scifinder.cas.org (retrieved 10.08.2020).
- (35) (a) Whitwam, J. G. *Brit. Med. J.* **1988**, *297*, 999-1000. (b) Whitwam, J. G.; Amrein, R. *Acta Anaesthesiol. Scand.* **1995**, *39*, 3-14. (c) Böhme, H.; Hartke, K.; Bracher, F. *Arzneibuch-Kommentar: Wissenschaftliche Erläuterungen zum Europäischen Arzneibuch und zum Deutschen Arzneibuch.*; 6.0/1326; Wiss. Verl.-Ges.: Stuttgart, 2017.
- (36) Bast Jr., R. C.; Croce, C. M.; Hait, W. N.; Hong, W. K.; Kufe, D. W.; Piccart-Gebhart, M.; Pollock, R. E.; Weichselbaum, R. R.; Wang, H.; Holland, J. F. *Holland-Frei Cancer Medicine*; 9 ed.; John Wiley & Sons: Hoboken, New Jersey, 2017.

- (37) (a) Pierre, F.; Regan, C. F.; Chevrel, M.-C.; Siddiqui-Jain, A.; Macalino, D.; Streiner, N.; Drygin, D.; Haddach, M.; O'Brien, S. E.; Rice, W. G.; Ryckman, D. M. *Bioorg. Med. Chem. Lett.* **2012**, *22*, 3327-3331. (b) Chen, B.-C.; Zhao, R.; Bednarz, M. S.; Wang, B.; Sundeen, J. E.; Barrish, J. C. *J. Org. Chem.* **2004**, *69*, 977-979.
- (38) Gracias, V.; Gasiiecki, A. F.; Djuric, S. W. *Org. Lett.* **2005**, *7*, 3183-3186.
- (39) Gracias, V.; Gasiiecki, A. F.; Djuric, S. W. *Tetrahedron Lett.* **2005**, *46*, 9049-9052.
- (40) (a) Beebe, X.; Gracias, V.; Djuric, S. W. *Tetrahedron Lett.* **2006**, *47*, 3225-3228. (b) Gracias, V.; Darczak, D.; Gasiiecki, A. F.; Djuric, S. W. *Tetrahedron Lett.* **2005**, *46*, 9053-9056.
- (41) Pelletier, G.; Charette, A. B. *Org. Lett.* **2013**, *15*, 2290-2293.
- (42) Sandeep, M.; Dushyant, P. S.; Sravani, B.; Reddy, K. R. *Eur. J. Org. Chem.* **2018**, 3036-3047.
- (43) (a) *Houben-Weyl Methoden der Organischen Chemie*; 4 ed.; Georg Thieme Verlag: Stuttgart 1994; Vol. E 8 c. (b) van Leusen, A. M.; Wildeman, J.; Oldenziel, O. H. *J. Org. Chem.* **1977**, *42*, 1153-1159.
- (44) Zheng, X.; Ma, Z.; Zhang, D. *Pharmaceuticals* **2020**, *13*.
- (45) Muruges, V.; Harish, B.; Adishesu, M.; Babu Nanubolu, J.; Suresh, S. *Adv. Synth. Catal.* **2016**, *358*, 1309-1321.
- (46) Satyam, K.; Muruges, V.; Suresh, S. *Org. Biomol. Chem.* **2019**, *17*, 5234-5238.
- (47) (a) Zheng, P.; Zhang, J.; Ma, H.; Yuan, X.; Chen, P.; Zhou, J.; Zhang, H. *Bioorg. Med. Chem.* **2019**, *27*, 1391-1404. (b) Huang, Y.; Zhang, J.; Yu, Z.; Zhang, H.; Wang, Y.; Lingel, A.; Qi, W.; Gu, J.; Zhao, K.; Shultz, M. D.; Wang, L.; Fu, X.; Sun, Y.; Zhang, Q.; Jiang, X.; Zhang, J.; Zhang, C.; Li, L.; Zeng, J.; Feng, L.; Zhang, C.; Liu, Y.; Zhang, M.; Zhang, L.; Zhao, M.; Gao, Z.; Liu, X.; Fang, D.; Guo, H.; Mi, Y.; Gabriel, T.; Dillon, M. P.; Atadja, P.; Oyang, C. *J. Med. Chem.* **2017**, *60*, 2215-2226.
- (48) Lüllmann, H.; Mohr, K.; Hein, L. *Pharmakologie und Toxikologie*; 17th Ed. ed.; Georg Thieme Verlag: Stuttgart, 2010.
- (49) (a) Guzmán, B. C.-F.; Vinnakota, C.; Govindpani, K.; Waldvogel, H. J.; Faull, R. L. M.; Kwakowsky, A. *J. Neurochem.* **2018**, *146*, 649-669. (b) Lanctot, K. L.; Herrmann, N.; Mazzotta, P.; Khan, L. R.; Ingber, N. *Can. J. Psychiatry* **2004**, *49*, 439-453.
- (50) (a) Błaszczyk, J. W. *Front. Neurosci.* **2016**, *10*. (b) Firbank, M. J.; Parikh, J.; Murphy, N.; Killen, A.; Allan, C. L.; Collerton, D.; Blamire, A. M.; Taylor, J.-P. *Neurology* **2018**, *91*, 675-685. (c) van Nuland, A. J. M.; den Ouden, H. E. M.; Zach, H.; Dirkx, M. F. M.; van Asten, J. J. A.; Scheenen, T. W. J.; Toni, I.; Cools, R.; Helmich, R. C. *Hum. Brain Mapp.* **2020**, *41*, 1017-1029.
- (51) Kalueff, A. V.; Nutt, D. J. *Depression and Anxiety* **2007**, *24*, 495-517.
- (52) (a) Kleppner, S. R.; Tobin, A. J. *Expert Opin. Ther. Targets* **2001**, *5*, 219-239. (b) Treimann, D. M. *Epilepsia* **2001**, *42*, 8-12.

- (53) (a) Fact Sheet Epilepsy. www.who.int/news-room/fact-sheets/detail/epilepsy (retrieved 15.08.2020). (b) Brodie, M. J.; Besag, F.; Ettinger, A. B.; Mula, M.; Gobbi, G.; Comai, S.; Aldenkamp, A. P.; Steinhoff, B. J. *Pharmacol. Rev.* **2016**, *68*, 563-602.
- (54) Kriegstein, A. R.; Owens, D. F. *Nat. Rev. Neurosci.* **2002**, *3*, 715-727.
- (55) (a) Roth, F. C.; Draguhn, A. *Neural Plast.*, *2012*, 805-830. (b) Bowery, N. G.; Smart, T. G. *Brit. J. Pharmacol.* **2006**, *147*, 109-119.
- (56) Schousboe, A.; Madsen, K. K.; Barker-Haliski, M. L.; White, H. S. *Neurochem. Res.* **2014**, *39*, 1980-1987.
- (57) Nutt, D. J.; Malizia, A. L. *Brit. J. Psych.* **2001**, *179*, 390-396.
- (58) (a) Leppik, I. E.; Gram, L.; Deaton, R.; Sommerville, K. W. *Epilepsy Res.* **1999**, *33*, 235-246. (b) Madsen, K. K.; White, H. S.; Schousboe, A. *Pharmacol. Ther.* **2010**, *125*, 394-401.
- (59) Madsen, K. K.; Clausen, R. P.; Larsson, O. M.; Krogsgaard-Larsen, P.; Schousboe, A.; White, H. S. *J. Neurochem.* **2009**, *109*, 139-144.
- (60) (a) Borden, L. A. *Neurochem. Int.* **1996**, *29*, 335-356. (b) Christiansen, B.; Meinild, A.-K.; Jensen, A. A.; Bräuner-Osborne, H. *J. Biol. Chem.* **2007**, *282*, 19331-19341. (c) Conti, F.; Minelli, A.; Melone, M. *Brain Res. Rev.* **2004**, *45*, 196-212. (d) Liu, Q.-R.; López-Corcuera, B.; Mandiyan, S.; Nelson, H.; Nelson, N. *J. Biol. Chem.* **1993**, *268*, 2106-2112.
- (61) (a) Zhou, Y.; Holmseth, S.; Guo, C.; Hassel, B.; Höfner, G.; Huitfeldt, H. S.; Wanner, K. T.; Danbolt, N. C. *J. Biol. Chem.* **2012**, *287*, 35733-35746. (b) Zhou, Y.; Holmseth, S.; Hua, R.; Lehre, A. C.; Olofsson, A. M.; Poblete-Naredo, I.; Kempson, S. A.; Danbolt, N. C. *Am. J. Physiol. Renal. Physiol.* **2012**, *302*, 316-328. (c) Palacín, M.; Estévez, R.; Bertran, J.; Zorzano, A. *Physiol. Rev.* **1998**, *78*, 969-1054.
- (62) (a) Jin, X.-T.; Galvan, A.; Wichmann, T.; Smith, Y. *Front. Syst. Neurosci.* **2011**, *5*. (b) Minelli, A.; DeBiasi, S.; Brecha, N. C.; Zuccarello, L. V.; Conti, F. *J. Neurosci.* **1996**, *16*, 6255-6264.
- (63) (a) Brøer, S. G., U. *Br. J. Pharmacol.* **2012**, *164*, 256-278. (b) Kristensen, A. S.; Andersen, J.; Jørgensen, T. N.; Sørensen, L.; Eriksen, J.; Loland, C. J.; Strømgaard, K.; Gether, U. *Pharmacol. Rev.* **2011**, *63*, 585-640.
- (64) Willford, S. L.; Anderson, C. M.; Spencer, S. R.; Eskandari, S. *J. Membrane Biol.* **2015**, *248*, 795-810.
- (65) (a) Guastella, J.; Nelson, N.; Nelson, H.; Czyzyk, L.; Keynan, S.; Miedel, M. C.; Davidson, N.; Lester, H. A.; Kanner, B. I. *Science* **1990**, *249*, 1303-1306. (b) Radian, R.; Kanner, B. I. *J. Biol. Chem.* **1985**, *260*, 11859-11865.
- (66) (a) Beuming, T.; Shi, L.; Javitch, J. A.; Weinstein, H. *Mol. Pharmacol.* **2006**, *70*, 1630-1642. (b) Yamashita, A.; Singh, S. K.; Kawate, T.; Jin, Y.; Gouaux, E. *Nature* **2005**, *437*, 215-223.
- (67) (a) Penmatsa, A.; Wang, K. H.; Gouaux, E. *Nat. Struct. Mol. Biol.* **2015**, *22*, 506-509. (b) Penmatsa, A.; Wang, K. H.; Gouaux, E. *Nature* **2013**, *503*, 85-91. (c) Coleman, J. A.; Green, E. M.; Gouaux, E. *Nature* **2016**, *532*, 334-339.
- (68) (a) Krishnamurthy, H.; Gouaux, E. *Nature* **2012**, *481*, 469-474. (b) Krishnamurthy, H.; Piscitelli, C. L.; Gouaux, E. *Nature* **2009**, *459*, 347-355.

- (c) Singh, S. K.; Piscitelli, C. L.; Yamashita, A.; Gouaux, E. *Science* **2008**, *322*, 1655-1661.
- (69) Jardetzky, O. *Nature* **1966**, *211*, 969-970.
- (70) Shi, L.; Quick, M.; Zhao, Y.; Weinstein, H.; Javitch, J. A. *Mol. Cell* **2008**, *30*, 667-677.
- (71) (a) Singh, S. K.; Yamashita, A.; Gouaux, E. *Nature* **2007**, *448*, 952-956. (b) Wang, H.; Elferich, J.; Gouaux, E. *Nat. Struct. Mol. Biol.* **2012**, *19*, 212-219. (c) Zhen, J.; Reith, M. E. A. *J. Neurochem.* **2016**, *138*, 694-699. (d) Zhao, Y.; Terry, D. S.; Shi, L.; Quick, M.; Weinstein, H.; Blanchard, S. C.; Javitch, J. A. *Nature* **2011**, *474*, 109-113. (e) Piscitelli, C. L.; Krishnamurthy, H.; Gouaux, E. *Nature* **2010**, *468*, 1129-1132.
- (72) Zhou, Z. Z., J.; Karpowich, N. K.; Goetz, R. M.; Law, C. J.; Reith, M. A. E.; Wang, D.-N. *Science* **2007**, *317*, 1390-1393.
- (73) (a) Andreß, J. C.; Böck, M. C.; Höfner, G.; Wanner, K. T. *Med. Chem. Res.* **2020**, *29*, 1321-1340. (b) Hellenbrand, T.; Höfner, G.; Wein, T.; Wanner, K. T. *Bioorg. Med. Chem.* **2016**, *24*, 2072-2096.
- (74) (a) Andersen, K. E.; Lau, J.; Lundt, B. F.; Petersen, H.; Huusfeldt, P. O.; Suzdak, P. D.; Swedberg, M. D. B. *Bioorg. Med. Chem.* **2001**, *9*, 2773-2785. (b) Böck, M. C.; Höfner, G.; Wanner, K. T. *ChemMedChem* **2020**, *15*, 1-17. (c) Knutsen, L. J. S.; Andersen, K. E.; Lau, J.; Lundt, B. F.; Henry, R. F.; Morton, H. E.; Nærum, L.; Petersen, H.; Stephensen, H.; Suzdak, P. D.; Swedberg, M. D. B.; Thomsen, C.; Sørensen, P. O. *J. Med. Chem.* **1999**, *42*, 3447-3462. (d) Schaarschmidt, M.; Höfner, G.; Wanner, K. T. *ChemMedChem* **2019**, *14*, 1135-1151. (e) Tóth, K.; Höfner, G.; Wanner, K. T. *Bioorg. Med. Chem.* **2018**, *26*, 3668-3687.
- (75) Kragler, A.; Höfner, G.; Wanner, K. T. *Eur. J. Med. Chem.* **2008**, *43*, 2404-2411.
- (76) (a) Skovstrup, S.; Taboureau, O.; Bräuner-Osborne, H.; Jørgenson, F. S. *ChemMedChem* **2010**, *5*, 986-1000. (b) Wein, T.; Petrera, M.; Allmendinger, L.; Höfner, G.; Pabel, J.; Wanner, K. T. *ChemMedChem* **2016**, *11*, 509-518. (c) Zafar, S.; Jabeen, I. *Front. Chem.* **2018**, *6*.
- (77) Kern, F. T.; Wanner, K. T. *ChemMedChem* **2015**, *10*, 396-410.
- (78) Thomsen, C.; Sørensen, P. O.; Egebjerg, J. *Br. J. Pharmacol.* **1997**, *120*, 983-985.
- (79) Dhar, T. G. M.; Borden, L. A.; Tyagarajan, S.; Smith, K. E.; Branchek, T. A.; Weinshank, R. L.; Gluchowski, C. *J. Med. Chem.* **1994**, *37*, 2334-2342.
- (80) (a) Jochmann, P.; Dols, T. S.; Spaniol, T. P.; Perrin, L.; Maron, L.; Okuda, J. *Angew. Chem. Int. Ed.* **2010**, *49*, 7795-7798. (b) Yamaguchi, R.; Moriyasu, M.; Yoshioka, M.; Kawanisi, M. *J. Org. Chem.* **1985**, *50*, 287-288. (c) Corey, E. J.; Tian, Y. *Org. Lett.* **2005**, *7*, 5535-5537. (d) Charette, A. B.; Mathieu, S.; Martel, J. *Org. Lett.* **2005**, *7*, 5401-5404. (e) Schultz, A. G.; Flood, L.; Springer, J. P. *J. Org. Chem.* **1986**, *51*, 838-841. (f) Bannasar, M.-L.; Juan, C.; Bosch, J. *Tetrahedron Lett.* **2001**, *42*, 585-588. (g) Courtois, G.; Al-Arnaout, A.; Miginiac, L. *Tetrahedron Lett.* **1985**, *26*, 1027-1030. (h) Yamada, S.; Inoue, M. *Org. Lett.* **2007**, *9*, 1477-1480. (i) Cámpora, J.; Pérez, C. M.;

- Rodríguez-Delgado, A.; Naz, A. M.; Palma, P.; Álvarez, E. *Organometallics* **2007**, *26*, 1104-1107.
- (81) Rudy, H.-K. A.; Wanner, K. T. *Synthesis* **2019**, *51*, 4296-4310.
- (82) Chen, J.; Guo, W.; Wang, Z.; Hu, L.; Chen, F.; Xia, Y. *J. Org. Chem.* **2016**, *81*, 5504-5512.
- (83) Rudy, H.-K. A.; Mayer, P.; Wanner, K. T.; *Eur. J. Org. Chem.* **2020**, 3599-3612.
- (84) Larsen, J.; Jørgensen, K. A.; Christensen, D. *J. Chem. Soc. Perkin Trans. I* **1991**, 1187-1190.
- (85) Mohamed, M. A.; Yamada, K.; Tomioka, K. *Tetrahedron Lett.* **2009**, *50*, 3436-3438.

8 Publications and Manuscripts

First publication:

Heinrich-Karl A. Rudy, and Klaus T. Wanner, *Synthesis* **2019**, *51*, 4296–4310.

“Accessing Tricyclic Imines Comprising a 2-Azabicyclo[2.2.2]octane Scaffold by Intramolecular Hetero-Diels–Alder Reaction of 4-Alkenyl-Substituted *N*-Silyl-1,4-dihydropyridines”

Second publication:

Heinrich-Karl A. Rudy, Peter Mayer, and Klaus T. Wanner, *Eur. J. Org. Chem.* **2020**, 3599–3612.

“Synthesis of 1,5-Ring-Fused Imidazoles from Cyclic Imines and TosMIC – Identification of in situ Generated *N*-Methyleneformamide as a Catalyst in the van Leusen Imidazole Synthesis”

Manuscript of the third publication:

Heinrich-Karl A. Rudy, Georg Höfner, and Klaus T. Wanner, *Chem. Med. Res.* **2020**, accepted.

“Synthesis and biological evaluation of novel *N*-substituted nipecotic acid derivatives with tricyclic cage structures in the lipophilic domain as GABA uptake inhibitors”

Reprinted with permission. Copyright of the publications belong to the publishers.

8.1 First publication

4296

Synthesis

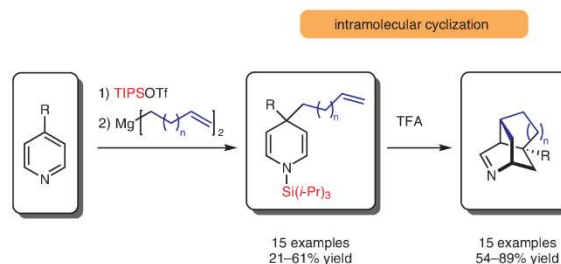
H.-K. A. Rudy, K. T. Wanner

Paper

Accessing Tricyclic Imines Comprising a 2-Azabicyclo[2.2.2]octane Scaffold by Intramolecular Hetero-Diels–Alder Reaction of 4-Alkenyl-Substituted *N*-Silyl-1,4-dihydropyridines

Heinrich-Karl A. Rudy
Klaus T. Wanner*

Ludwig-Maximilians-Universität München, Department für Pharmazie –
Zentrum für Pharmaforschung, Butenandstr. 5-13, Haus C,
81377 Munich, Germany
klaus.wanner@cup.uni-muenchen.de



Received: 04.07.2019
Accepted after revision: 07.08.2019
Published online: 05.09.2019
DOI: 10.1055/s-0039-1690619; Art ID: ss-2019-z0378-op

Abstract Tricyclic imines inheriting a 2-azabicyclo[2.2.2]octane (isoquinuclidine) scaffold were provided with high regioselectivity in moderate to very good yields by a smooth, broadly applicable intramolecular hetero-Diels–Alder reaction of various 4- ω -alkenyl-substituted 1,4-dihydropyridines (DHPs) under trifluoroacetic acid catalysis. The required 4,4-disubstituted 1,4-DHPs were obtained by introduction of ω -alkenyl moieties of varying chain length via diorganomagnesium reagents into the 4-position of diversely 4-substituted pyridines after prior *N*-activation with triisopropylsilyltriflate.

Key words intramolecular hetero-Diels–Alder reaction, 2-azabicyclo[2.2.2]octane, polycycles, 1,4-dihydropyridines, diorganomagnesium reagents, heterocycles

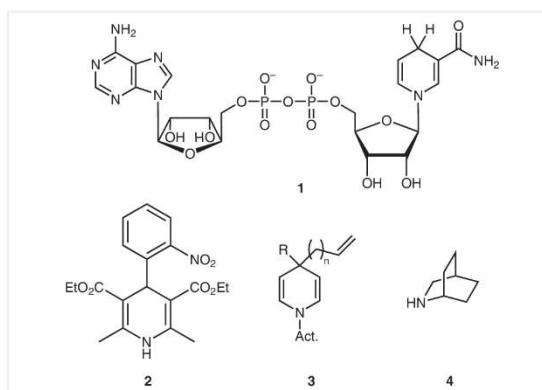


Figure 1 Structures of NADH (1), nifedipine (2), general structure of a 4- ω -alkenyl-substituted 1,4-DHP 3 and 2-azabicyclo[2.2.2]octane (4)

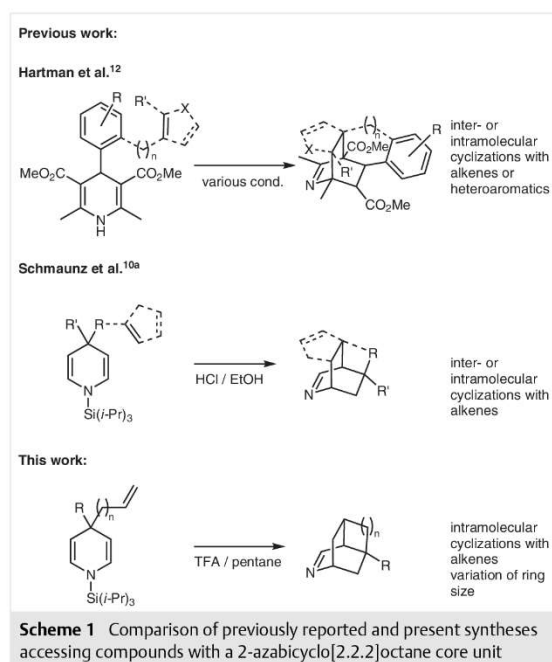
The 1,4-dihydropyridine (1,4-DHP) moiety is a common scaffold frequently found in compounds of synthetic or natural origin with important biological activities. Prominent examples to be mentioned are nicotinamide adenine dinucleotide (NADH (1), Figure 1), which is an ubiquitous coenzyme for redox reactions in cells, or nifedipine (2), which is listed by the WHO for healthcare systems as an essential drug for the treatment of hypertension.¹ Throughout the years, many different concepts for the synthesis of 1,4-DHPs have been published which are commonly either based on Hantzsch-type condensation reactions or 1,4-addition of nucleophiles to pyridinium salts, mostly *N*-acylpyridinium and *N*-alkylpyridinium salts.^{1a,c,2}

Whereas a large variety of either 4-mono- or 4,4-disubstituted 1,4-DHPs with alkyl or aryl residues in the 4-position have been synthesized, only limited examples of 1,4-DHPs 3 with a 4- ω -alkenyl substituent are known. Thereby, the most prevalent 4- ω -alkenyl moiety is the allyl residue. Known 4-allyl-mono-substituted 1,4-DHPs have almost exclusively been generated by addition of organometallic

derivatives such as allylcalcium,³ allylstannane,⁴ allylmagnesium reagents,⁵ or allylcuprates⁶ to either *N*-acyl^{4a,7} and *N*-alkylpyridinium ions^{5b,6} or pyridines lacking prior activation.^{3,8}

All these methods suffer from severe drawbacks such as a poor regioselectivity for competing 1,4- and 1,2-addition reactions, high toxicity, and laborious methods for the preparation of the required organometallic reagents or the need for pyridine rings equipped with residues for neighboring-group assistance. Syntheses of 4-mono-substituted 1,4-DHPs with as compared to the allyl unit extended ω -alkenyl chains in 4-position are, however, scarce. Few such compounds were obtained either only as side products in syntheses by Krow et al. and Comins et al. aiming at the construction of 2- ω -alkenyl-substituted 1,2-DHPs or by Rudler et al. by employing silyl ketene acetals, derived from pent-4-enoic and hex-5-enoic acid, in addition reactions to pyridinium ions.⁹

Even less explored are the syntheses of 4,4-disubstituted 1,4-DHPs with one of the two 4-substituents being an ω -alkenyl moiety. So far such compounds have only been isolated by Wanner et al., Krow et al., and Okuda et al., though they provide a highly useful synthetic access to isoquinuclidine derivatives.^{3a,9a,10} The isoquinuclidine ring system **4** (2-azabicyclo[2.2.2]octane) is found in many alkaloids, e.g., in ibogaine, and has also been used as intermediate in the synthesis of oseltamivir.¹¹ Examples demonstrating the accessibility of compounds with an 2-azabicyclo[2.2.2]octane skeleton as core unit by employing 4-monosubstituted 1,4-DHPs, obtained by Hantzsch dihydropyridine syntheses, in inter- or intramolecular cyclization reactions have been published by Hartman et al. (Scheme 1).^{10a,12} The use of 4,4-disubstituted *N*-silyl 1,4-DHPs obtained from trapping reactions of *N*-dihydropyridinium ions with nucleophiles in inter- or intramolecular hetero-Diels–Alder reactions under acidic conditions has been demonstrated by us.^{10a,12}



This had also included the preparation of 4-allyl-substituted *N*-silyl-1,4-DHP and their intramolecular cyclization to give the corresponding 2-azabicyclo[2.2.2]octane derivatives. With the present study we intended to develop a method giving for the first time access to a broad range of 4,4-disubstituted *N*-silyl-1,4-DHP with one of the 4-substituents in the 4-position being an ω -alkenyl residue of varying chain length which should finally be used for intramo-

lecular cyclization reactions to give the corresponding tricyclic imines with a 2-azabicyclo[2.2.2]octane core structure.^{10,13}

To study the feasibility of the introduction of ω -alkenyl moieties (other than allyl groups) into the 4-position of 4-substituted pyridine derivatives, as the first step of the overall sequence for the preparation of isoquinuclidine derivatives, 4-methylpyridine **5a** was chosen as model system, because the methyl group gives neither rise to large steric nor electronic effects. Furthermore, based on the knowledge from previous experiments that aimed at the synthesis of 4,4-disubstituted 1,4-dihydropyridines, only diorganomagnesium reagents should be used, at least for initial experiments, because these had proven superior reactivity as compared to Grignard reagents.^{10b,13a,b}

For the first experiments, a but-4-en-1-yl residue was chosen for the addition reactions to 4-methylpyridine (**5a**). When 4-methylpyridine (**5a**) was treated with TIPSOTf (1.1 equiv) in CH_2Cl_2 at 20 °C for 15 min to generate the pyridinium ion **6a** and subsequently with di(*tert*-but-3-en-1-yl)magnesium (2 equiv in THF/ Et_2O , 1:1) at –78 °C followed by slowly warming the reaction mixture to –50 °C (Table 1, entry 1), the desired 1,4-dihydropyridine **7a** could be obtained in a yield of 22%. Similar low yields had been observed before for the addition of allyl residues to 4-substituted pyridines after prior *N*-silylation.¹⁰ However, to our delight with a ratio of 81:19 in favor of the 1,4-dihydropyridine **7a** as compared to the 1,2-dihydropyridine **8a**, the regioselectivity was quite satisfying.

In subsequent reactions, the crude reaction products obtained after aqueous workup were analyzed with regard to their composition by ^1H NMR spectroscopy using 2,4,6-collidine as internal standard for quantification. That way the amount of formed 1,4-dihydropyridine **7a** could be directly determined ('NMR' yield). In addition, at the same time also the amount of formed 1,2-dihydropyridine **8a** could be directly specified, which was otherwise strongly impeded as 1,2-dihydropyridines are generally higher susceptible to oxidation typically resulting in the formation of the corresponding aromatic systems.

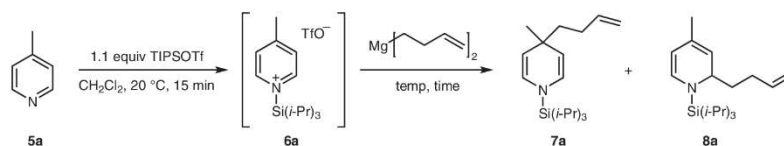
Though in case of the addition of a *tert*-butyl moiety to a *N*-silylpyridinium ion lowering the temperature from –78 °C to –85 °C had been found beneficial with regard to the yield of the 1,4-addition product,^{13a} the opposite was true in the present case employing di(*tert*-but-3-en-1-yl)magnesium as nucleophile. When the addition of di(*tert*-but-3-en-1-yl)magnesium to **6a** was performed at –85 °C, only a diminished yield of 8% was obtained (Table 1, entry 2 vs. entry 1).^{13a} Hence, in further experiments pyridinium ion **6a** was treated with di(*tert*-but-3-en-1-yl)magnesium at –60 °C, –40 °C, and –30 °C, respectively (Table 1, entries 3–5). Thereby, the yield for the 4-addition product **7a** rose from 29% (Table 1, entry 3) to 33% (Table 1, entry 4), and finally to 41% (Table 1, entry 5). Additionally, in all three experiments an improved regioselectivity of 92:8 independent from the

4298

Synthesis

H.-K. A. Rudy, K. T. Wanner

Paper

Table 1 Optimization of the Addition of Di(but-3-en-1-yl)magnesium to *N*-TIPS 4-Methylpyridinium Triflate **6a**

Entry	R ₂ Mg (equiv)	Temp (°C)	Time (h)	NMR yield (%) ^a		Total	NMR ratio of 7a/8a ^a	Isolated yield of 7a (%)
				7a	8a			
1	2.0	-78 to -50	2	– ^b	– ^b	–	81:19 ^c	22
2	2.0	-85	2	6	– ^d	6	– ^d	8
3	2.0	-60	2	29	2	31	92:8	29
4	2.0	-40	2	34	3	37	92:8	33
5	2.0	-30	2	43	4	47	92:8	41
6	2.0	0	2	45	4	49	92:8	– ^e
7	1.1	-30	2	41	4	45	92:8	42
8	0.55	-30	2	44	4	48	91:9	44
9	1.1	-30	18	44	2	46	96:4	44

^a The yield of **7a** and **8a** in the crude product and the product ratio were determined by ¹H NMR spectroscopy with 2,4,6-collidine as internal standard. Upward deviations of the isolated yield from the NMR yield are within the expected accuracy of measurement.¹⁴

^bNot determined.

^c Determined using ¹H NMR spectroscopy without internal standard.

^dNot determinable due to low signal intensity.

^eNot determinable due to the formation of inseparable side products.

reaction temperature was observed (Table 1, entries 3–5). A further increase of the temperature to 0 °C led only to a minor improvement of the NMR yield (compare Table 1, entries 5 and 6) with the regioselectivity being unchanged. However, due to extensive formation of inseparable side products, this result could not be confirmed as no pure product could be isolated. Hence, a temperature of -30 °C was considered best for performing trapping reactions of intermediate pyridinium ions such as **6a** and was therefore applied for further experiments.

In order to render the trapping reactions of the pyridinium ions more economic, it was intended to reduce the equivalents of the diorganomagnesium species employed. Accordingly, in the next experiments only 1.1 or 0.55 equivalents, respectively, of di(but-3-en-1-yl)magnesium have been applied. In both cases, the yield of the main regioisomer **7a**, the 4-addition product, as well as the ratio of regioisomers (**7a/8a**) remained largely unchanged in comparison to the reaction performed under identical conditions, but with 2.0 equivalents of di(but-3-en-1-yl)magnesium (Table 1, entries 5, 7, and 8). Also the extension of the reaction time from 2 h to 18 h for the trapping of the intermediate *N*-silylpyridinium ion **6a** with 1.1 equivalents of the diorganomagnesium species (at -30 °C) did not markedly alter the outcome of the reaction (Table 1, entry 9 vs. entry 7), the yield and the regioselectivity being only slightly increased (yield 44%, **7a/8a** = 96:4; Table 1, entry 9),

indicating that the reaction is mostly complete within 2 h. Though the application of 0.55 equivalents of the diorganomagnesium species for the trapping reaction had actually led to a slightly better product yield (44% vs. 42%), future reactions were intended to be performed with 1.1 equivalents of the diorganomagnesium species as this was thought to be more reliable, whereas 0.55 equivalents should only be used when the organometallic species is tedious to prepare.

Next, the so far developed standard reaction conditions were utilized to perform addition reactions with a set of differently 4-substituted pyridine derivatives including **5a**, i.e., **5a–e**, employing diorganomagnesium species exhibiting either allyl, homoallyl, or pent-4-en-1-yl residues as nucleophiles. When the pyridine derivatives **5b–e** after activation with 1.1 equivalents of TIPSOTf in CH₂Cl₂ were treated with 1.1 equivalents of di(but-3-en-1-yl)magnesium at -30 °C for 18 h according to the aforementioned standard procedure, the addition products **7b–e** and **8b–e** were obtained in fair to good overall yields (Table 2, entries 2–5: total NMR yields 40–80%; **7b–e** 35–54%). In any case, the desired 1,4-addition products **7b–e** were clearly predominating though the regioselectivity observed for the addition of di(but-3-en-1-yl)magnesium to pyridine **5a** of 96:4 (**7a/8a** = 96:4, Table 2, entry 1 identical to Table 1, entry 9) had dropped to 76:24 to 88:12 (Table 2, entries 2–5). This reduction of regioselectivity is likely to be attributed to the

4299

Synthesis

H.-K. A. Rudy, K. T. Wanner

Paper

Table 2 Trapping of Various 4-Substituted *N*-TIPS-Pyridinium Ions with Di(ω -alkenyl)magnesium Reagents

Entry	Starting material		n	Time (h)	Products		NMR yield (%) ^a			NMR ratio of A/B ^b	Isolated yield of A (%)
	R	R			A	B	A	B	Total		
1	5a	Me	1	18	7a	8a	44	2 ^b	46 ^b	96:4 ^b	44 ^b
2	5b	Ph	1	18	7b	8b	62	18	80	78:22	54
3	5c	Bn	1	18	7c	8c	35	5	40	88:12	35
4	5d	4-MeOC ₆ H ₄	1	18	7d	8d	45	12	57	79:21	40
5	5e	4-MeOC ₆ H ₄ CH ₂	1	18	7e	8e	40	12	52	76:24	39
6	5a	Me	2	18	9a	10a	44	1	45	98:2	43
7	5b	Ph	2	2	9b	10b	62	7	69	90:10	59
8	5c	Bn	2	18	9c	10c	38	5	43	88:12	37
9	5d	4-MeOC ₆ H ₄	2	18	9d	10d	62	17	79	78:22	61
10	5e	4-MeOC ₆ H ₄ CH ₂	2	18	9e	10e	45	12	57	79:21	41
11	5a	Me	0	2	11a	12a	33	25	58	57:43	35
12	5b	Ph	0	2	11b	12a	35	44	79	44:56	33
13	5c	Bn	0	2	11c	12b	21	47	68	31:69	21
14	5d	4-MeOC ₆ H ₄	0	2	11d	12d	24	40	60	37:63	23
15	5e	4-MeOC ₆ H ₄ CH ₂	0	2	11e	12e	22	57	79	28:72	23

^aThe yield of **A** and **B** in the crude product and the product ratio were determined using ¹H NMR spectroscopy with 2,4,6-collidine as internal standard. Upward deviations of the isolated yield from the NMR yield are within the expected accuracy of measurement. ¹⁴

^bIdentical to Table 1, entry 9.

increased steric demand of the 4-substituents in **5b–e** as compared to that of the 4-methyl group in **5a** hampering the addition of the nucleophiles to the 4-position of the *N*-silylpyridinium ions **6b–e**. 1,4-Dihydropyridines **7b–e** could be easily separated from 1,2-dihydropyridines **8b–e** despite their physicochemical similarities. This was accomplished in a two-step sequence by first exposing the crude reaction mixture to air for oxidation, to which the 1,2-dihydropyridines were far more susceptible than the corresponding 1,4-dihydropyridines, the latter of which could then easily be isolated by column chromatography.

The optimized conditions proved also well suited for the addition of a pent-4-en-1-yl moiety to the *N*-silylpyridinium ions **6a–e**. When the *N*-silylpyridinium salts **6a–e** were reacted with di(pent-4-en-1-yl)magnesium, the 1,4- and 1,2-addition products **9a–e** and **10a–e** were obtained in good overall yield. Thereby, the obtained results closely reflect the outcome of the but-4-en-1-yl addition reactions, not only in regard of the overall yield (Table 2, entries 6–10:

total NMR yields 43–79%; **9a–e** 37–61%), but also of the regioselectivity (from 78:22 up to 98:2; see Table 2, entries 6–10). Only for the addition of the pent-4-en-1-yl residue to activated pyridinium derivative **5d** an exception was found. In that case, the yields for **9d/10d** and pure **9d** were distinctly higher than the yields observed for the addition of di(but-3-en-1-yl)magnesium to this pyridinium salt (Table 2, entry 9 vs. entry 4).

Finally, the optimized reaction conditions were applied to the addition of an allyl moiety to the 4-substituted pyridine derivatives **5a–e** via their iminium salts **6a–e** in order to construct the corresponding 4-allyl-substituted 1,4-dihydropyridines (Table 2, entries 11–15). This had previously proved to be quite challenging since the desired 4-allyl-substituted 1,4-dihydropyridines could be isolated^{10,13b} in low yields only, either due to the formation of complex reaction mixtures or due to the preferred 2-addition of the allyl residue.

4300

Synthesis

H.-K. A. Rudy, K. T. Wanner

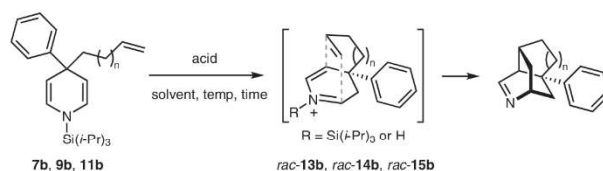
Paper

Although the yields for the 1,4-dihydropyridines **11a–e** (Table 2, entries 11–15) were still in a low range, and the regioselectivity was predominantly on the side of the 2-addition product, significant improvements could be achieved. For the synthesis of the known 4-phenylpyridine-derived 1,4-dihydropyridine **11b** (Table 2, entry 12) the yield rose to 33% (lit.^{10b} 20%) and the regioselectivity of 44:56 (lit.^{10b} 20:78) was notably shifted towards the formation of the 4-addition product. A raise in yield to 21% (lit.^{10b} 12%) and a shift in regioselectivity to 31:69 (lit.^{10b} 21:70) could also be observed for the synthesis of the 4-benzyl-substituted 1,4-dihydropyridine **11c** (Table 2, entry 13), albeit to a lesser extent. The differences regarding yield and regioselectivity are likely to be due to the distinctly higher reaction temperature compared to the one applied in the reactions described in literature leading to a, in our case advantageous, less 2-selective addition reaction.^{10b,13b} For the addition of an allyl moiety to the 4-methylpyridine (**5a**) derived iminium salt **6a** even a preference for the 1,4-dihydropyridine **11a** could be observed, the ratio of isomers amounting to 57:43 (Table 2, entry 11), which is presumably to be assigned to the lower steric hindrance of the methyl group in iminium salt **6a** as compared to that of the 4-residues in **6b–e**. Within this row, also the syntheses of 1,4-dihydropyridines **11d–e** from the corresponding iminium salts **6d** and **6e** proceeded successfully with yields of 23% and with a ratio of isomers of 37:63 (for **11d**) and 28:72 (for **11e**), respectively.

With the 4- ω -alkenyl-substituted 1,4-dihydropyridines **7a–e**, **9a–e**, and **11a–e** in hand the intramolecular hetero-Diels–Alder reactions of these compounds were studied. Here, as in literature the term hetero-Diels–Alder reaction is used to denote [4+2] cycloaddition reactions independent of whether these reactions proceed via a concerted or stepwise reaction mechanism, an issue not yet clarified for the present and closely related transformation reactions.^{10a,12,15}

Intramolecular cycloaddition reactions of 4,4-disubstituted 1,4-dihydropyridines displaying, e.g., an allyl residue in the 4-position of an *N*-silyl-1,4-dihydropyridine under acid-catalyzed reaction conditions have already been reported before by us (see example from literature; Table 3, entry 1).^{10a} Thereby, the respective *N*-silyl-1,4-dihydropyridines were treated with hydrogen chloride in ethanol at 80 °C for 1 h. When these conditions were applied to 1,4-dihydropyridine **7b** exhibiting in addition to a phenyl residue a but-3-en-1-yl moiety in 4-position and therefore being structurally closely related to dihydropyridine **11b** after a reaction time of 60 min, the desired 3-phenyl-9-azatricyclo[4.3.1.0^{3,7}]dec-8-en (*rac*-**14b**) was obtained in good yield of 78% (Table 3, entry 2). As a control of the reaction progress by TLC had indicated that the reaction had gone to completion quite rapidly, i.e., within a few minutes, it appeared appropriate to test milder reaction conditions. Hence, the reaction temperature was reduced from 80 °C to 30 °C.

Table 3 Cyclization of 4-Alkenyl-Substituted 1,4-Dihydropyridines under Varying Conditions



Entry	Dihydropyridine	n	Acid (equiv)	Solvent	Temp (°C)	Time (min)	Product	Yield (%)
1	11b	0	HCl (10)	EtOH	80	60	<i>rac</i> - 13b	63 ^a
2	7b	1	HCl (10)	EtOH	80	60	<i>rac</i> - 14b	78 ^b
3	7b	1	HCl (10)	EtOH	30	15	<i>rac</i> - 14b	94
4	9b	2	HCl (10)	EtOH	30	15	<i>rac</i> - 15b	decomp.
5	9b	2	AcOH (10)	CH ₂ Cl ₂	20	15	<i>rac</i> - 15b	decomp.
6	9b	2	TfOH (10)	CH ₂ Cl ₂	20	15	<i>rac</i> - 15b	traces
7	9b	2	TFA (10)	CH ₂ Cl ₂	20	15	<i>rac</i> - 15b	21
8	9b	2	TFA (5)	MeOH	20	15	<i>rac</i> - 15b	decomp.
9	9b	2	TFA (15)	pentane	20	15	<i>rac</i> - 15b	74

^a Data obtained from the literature.^{10a}

^b Conditions adopted from the literature.^{10a}

4301

Synthesis

H.-K. A. Rudy, K. T. Wanner

Paper

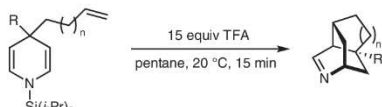
This led to an excellent yield of 94% whereby a reaction time of 15 min was fully sufficient (Table 3, entry 3). As reported for the cycloaddition for related reaction systems, also in the present case no regioisomers of *rac*-**14b** could be detected.^{10a} Surprisingly, attempts to cyclize 1,4-dihydropyridine **9b** exhibiting a pent-4-en-1-yl moiety in 4-position under the same conditions at 30 °C gave rise to decomposition products only (Table 3, entry 4). Therefore, in a series of experiments, 1,4-dihydropyridine **9b** was subjected to varying reaction conditions, in order to identify those that might affect the desired cycloaddition reaction to *rac*-**15b** and possibly be suitable for this type of transformation in general.

In the next experiments, EtOH was replaced by CH₂Cl₂ as solvent and instead of HCl (10 equiv) acetic acid (10 equiv) and trifluoromethanesulfonic acid (10 equiv), respectively, were used. In the case of acetic acid again only decomposition products could be observed after a reaction time of 15 min though the reaction temperature had been further lowered to 20 °C, whereas with trifluoromethanesulfonic acid traces of the product could be identified in the crude reaction product by ¹H NMR spectroscopy. Indicating that a less strong acid might be necessary, the cyclization was carried out with trifluoroacetic acid under otherwise identical reaction conditions yielding 21% of the desired cyclization product *rac*-**15b** (Table 3, entry 7). When CH₂Cl₂ was again replaced by MeOH, a cyclization attempt carried out with trifluoroacetic acid (Table 3, entry 8) as before, except that the acid equivalents were reduced from 10 to 5 equivalents, led to decomposition products only. Hence as a consequence, a far less polar solvent, i.e., pentane, should be tested as reaction solvent. Indeed, when the cyclization of dihydropyridine **9b** was attempted in pentane with trifluoroacetic acid (15 equiv) at 20 °C, the desired tricyclic imine *rac*-**15b** could be obtained in a good yield, i.e., 74% (Table 3, entry 9). Application of fewer equivalents of trifluoroacetic acid (i.e., 5 or 10 equiv) led to a reduced conversion and increased side-product formation as was determined by ¹H NMR spectroscopic analysis of the crude reaction products.

The reaction conditions so far developed for the cyclization of dihydropyridine **9b** were then applied to the 1,4-dihydropyridines **9a** and **9c–e** analogous to **9b**, but differing from the latter with regard to the second non-pent-4-en-1-yl substituent in 4-position (**9a**: R = Me, **9c**: R = Bn, **9d**: R = 4-MeOC₆H₄, **9e**: R = 4-MeOC₆H₄CH₂, Table 4). When the 1,4-dihydropyridines **9a** and **9c–e** (see Table 2) were subjected to the aforementioned standard conditions, i.e., trifluoroacetic acid (15 equiv) in pentane at 20 °C for 15 min, the intramolecular cyclization afforded *rac*-**15a** and *rac*-**15c–e** in moderate to very good yields (Table 4, entries 1–4, 54–89%). Next, to check whether the newly found reaction conditions are suitable for the intramolecular hetero-Diels–Alder reaction in general, the latter was also carried out with the 1,4-dihydropyridines **7a–e** bear-

ing a but-3-en-1-yl residue (Table 4, entries 5–9) and **11a–e** (Table 4, entries 10–14) exhibiting an allyl moiety. The formation of the desired tricyclic imines *rac*-**14a–e** from the 4-homoallyl-substituted 1,4-dihydropyridines **7a–e** proceeded successfully in very good yields (79–89%, Table 4, entries 5–9) with the new standard method.

Table 4 Synthesis of Various Tricyclic Imines



Entry	1,4-Dihydropyridine		Product	Yield (%)
	R	n		
1	9a Me	2	<i>rac</i> - 15a	77
2	9c Bn	2	<i>rac</i> - 15c	74
3	9d 4-MeOC ₆ H ₄	2	<i>rac</i> - 15d	54
4	9e 4-MeOC ₆ H ₄ CH ₂	2	<i>rac</i> - 15e	89
5	7a Me	1	<i>rac</i> - 14a	79
6	7b Ph	1	<i>rac</i> - 14b	84
7	7c Bn	1	<i>rac</i> - 14c	86
8	7d 4-MeOC ₆ H ₄	1	<i>rac</i> - 14d	89
9	7e 4-MeOC ₆ H ₄ CH ₂	1	<i>rac</i> - 14e	85
10	11a Me	0	<i>rac</i> - 13a	84
11	11b Ph	0	<i>rac</i> - 13b	85
12	11c Bn	0	<i>rac</i> - 13c	83
13	11d 4-MeOC ₆ H ₄	0	<i>rac</i> - 13d	85 ^a
14	11e 4-MeOC ₆ H ₄ CH ₂	0	<i>rac</i> - 13e	67 ^a

^aPentane/EtOH, 4:1 was used as the solvent system.

Comparing the cyclization of 1,4-dihydropyridine **7b** under the former already published^{10a} (EtOH, HCl, see Table 3, entries 2 and 3) and the newly developed cyclization conditions (see Table 4, entry 6) revealed that with the new standard method (TFA, pentane) an increase in yield (84% vs. 78%) was achieved in comparison to the literature known method^{10a} (Table 4, entry 6 vs. Table 3, entry 2). Though the previously achieved excellent yield of 94% for the tricyclic imine *rac*-**14b**, obtained under the adapted literature method^{10a} (see Table 3, entry 3), could not be reached with the new standard method. The decrease in yield to 84% was acceptable considering the broader applicability of the new method, which was proven by the successful cyclization of the 4-allyl-substituted 1,4-dihydropyridines **11a–e**. Good to very good yields (67–85%) were obtained for the formation of the tricyclic imines *rac*-**13a–e**. The syntheses of the known 4-azatricyclo-[3.3.1.0^{2,7}]non-3-enes *rac*-**13b** and *rac*-**13c** (Table 4, entries 11 and 12) resulted in yields of 85% (lit.^{10a} 63%) and

83% (lit.^{10a} 92%), respectively, showing a significant improvement in the first case and only a marginally worse result in the second one compared to our previously described cyclization method.^{10a}

In conclusion, we have successfully synthesized a series of 4- ω -alkenyl-substituted 1,4-DHP that were employed in subsequent cyclization reactions yielding the corresponding tricyclic imines. The approach introduced is the first one to focus on the addition of ω -alkenyl-moieties of varying chain length to the 4-position of already 4-substituted pyridine derivatives in order to provide 4,4-disubstituted 1,4-DHP. To the current state of knowledge, the obtained yields and regioselectivities for the C-4 addition products are superior to all literature methods. The intermediate ω -alkenyl-substituted 1,4-DHP derivatives proved to be excellent precursors for a smooth intramolecular hetero-Diels-Alder reaction which provided various tricyclic imines with high yield. The therefore newly developed cyclization method is easy, fast, and broadly applicable to the synthesis of miscellaneous tricyclic ring systems with a 2-azabicyclo[2.2.2]octane scaffold.

All anhydrous reactions were performed under an argon atmosphere in oven-dried glassware. Solvents were distilled prior to use and THF, Et₂O, 1,4-dioxane, and CH₂Cl₂ were dried according to standard procedures under a nitrogen atmosphere.¹⁶ All chemicals were used as purchased from the supplier without further purification. TLC plates purchased from Merck KGaA (silica gel 60 F254 or aluminum oxide 60 F254 on aluminum sheets, neutral) were employed as the stationary phase. Flash chromatography was conducted with silica gel 60 (40–63 μ m mesh size) from Merck KGaA or with activated basic alumina Brockmann I (150 μ m mesh size) from Sigma-Aldrich, which was adjusted to Brockmann III activity grade prior to use.¹⁷ For the determination of melting points a BÜCHI 510 melting point apparatus was used. All melting points are uncorrected. Infrared spectra of solid substances were measured as KBr pellets and oils as film with a Perkin Elmer Paragon 1000 and a Jasco FT/IR-410. HRMS was carried out with a Finnigan LTQ FT (ESI) and a Finnigan MAT 95 (EI). ¹H NMR and ¹³C NMR spectra were recorded with an Avance III HD Bruker BioSpin (400 or 500 MHz) and referenced to the solvent residual peak as internal standard and analyzed with MestReNova (Version 12.0.0–20080; Mestrelab Research S.L.; released 26.09.2017).¹⁸ 4-(4-Methoxybenzyl)pyridine (**5e**) was synthesized according to literature.¹⁹

Procedures

Preparation of Diorganomagnesium Solutions

Commercially available allylmagnesium chloride (2 m in THF) was diluted to a concentration of 1 m with THF and converted into di(allyl)magnesium with 1,4-dioxane according to the procedure mentioned below.

Magnesium turnings (1.5 equiv) were covered with THF (0.13 mL/mmol), and a solution of the organic halide (1.0 equiv) in THF (0.8 mL/mmol) was added dropwise to keep the reaction mixture boiling mildly. After complete addition stirring was continued for 1 h at 20 °C followed by addition of 1,4-dioxane (1.1 equiv) and further stirring

for 1 h at 20 °C. The resulting suspension was centrifuged (30 min, 3000 g), the supernatant was separated, and the remaining slurry was suspended in Et₂O to retrieve the same volume as before. Centrifugation was repeated (30 min, 3000 g), and the supernatants were combined. The concentration of the diorganomagnesium solution was determined according to Yong et al.²⁰

Synthesis of 4,4-Disubstituted 1-*N*-Triisopropylsilyl-1,4-dihydropyridines; General Procedure (GP1)

To a solution of the 4-substituted pyridine derivative in CH₂Cl₂ (0.86 mL/mmol) was added TIPSOTf (1.1 equiv). After stirring for 15 min at r.t., the resulting mixture was cooled to –30 °C and the corresponding R₂Mg solution (1.1 equiv) was added dropwise. The reaction was quenched after the time indicated by the addition of water (10 mL/mmol), and the aqueous layer was extracted with CH₂Cl₂ (3 \times 10 mL/mmol). The organic layers were combined, dried over MgSO₄, and concentrated under vacuum. Quantification of the dihydropyridines in the crude product was done by ¹H NMR spectroscopy using 2,4,6-collidine as internal standard. The crude material was stirred under air for the period specified to oxidize side products and then purified by flash chromatography (FC).

Synthesis of Tricyclic Imines; General Procedure (GP2)

TFA (15 equiv) was added to a solution of the 4,4-disubstituted 1-*N*-triisopropylsilyl-1,4-dihydropyridine (1.0 equiv) in pentane (10 mL/mmol) in one portion, and the resulting mixture was stirred for 15 min at 20 °C. The reaction was quenched by the addition of K₂CO₃ (8 equiv), and a 1:1 mixture of 2 M HCl_{aq} and EtOH (40 mL/mmol) was added. The solution was washed with pentane (6 \times 20 mL/mmol) and adjusted to pH = 9 with K₂CO₃. The aqueous layer was extracted with CH₂Cl₂ (4 \times 20 mL/mmol), the organic layers were combined, dried over Na₂SO₄, and the solvent was removed under vacuum. The crude product was purified by FC.

4-(4-Methoxyphenyl)pyridine (**5d**)

Pyridine (1.45 g, 18.3 mmol, 1.47 mL) was dissolved in CH₂Cl₂ (22 mL) at 20 °C, and TIPSOTf (6.35 g, 20.1 mmol, 5.57 mL) was added. The solution was stirred for 15 min, cooled to –78 °C, and a solution of di(4-methoxyphenyl)magnesium (0.46 M in THF/Et₂O, 1:1, 20.1 mmol, 44 mL) was added dropwise. Stirring was continued for 12 h within the reaction mixture was slowly warmed to –50 °C. The reaction was stopped by the addition of H₂O (100 mL) and subsequently extraction with CH₂Cl₂ (4 \times 100 mL) followed. The organic phases were combined, dried (MgSO₄), and the solvent was removed under vacuum. The neat intermediate product was stirred under air at 20 °C for 96 h, dissolved in CH₂Cl₂ (50 mL), and extracted with 2M HCl (5 \times 80 mL). The combined aqueous phases were washed with Et₂O (2 \times 80 mL), the pH was adjusted to 9 with K₂CO₃, and the aqueous layer was extracted with CH₂Cl₂ (4 \times 80 mL). Combination of the CH₂Cl₂ phases following drying with MgSO₄ and removal of the solvent under vacuum provided the product which was purified by FC (SiO₂; EtOAc/MeOH, 97:3).

Yield: 2.25 g (66%); colorless solid; mp 93 °C; *R*_f = 0.45 (SiO₂, EtOAc/MeOH, 97:3).

IR (film): 3084, 2968, 2937, 2841, 1606, 1523, 1487, 1286, 1255, 1227, 1188, 1036, 1016, 810, 569, 499 cm^{–1}.

¹H NMR (500 MHz, CD₂Cl₂): δ = 3.85 (s, 3 H, OCH₃), 6.99–7.04 (m, 2 H, CHCHCOCH₃), 7.46–7.50 (m, 2 H, NCHCH), 7.61–7.65 (m, 2 H, CHCHCOCH₃), 8.56–8.60 (m, 2 H, NCHCH).

^{13}C NMR (125 MHz, CD_2Cl_2): δ = 55.9 (CH_3), 115.0 (CHCHCOCH_3), 121.4 (NCHCH), 128.6 (CHCHCOCH_3), 130.8 (CCHCHCOCH_3), 148.1 (NCHCHC), 150.8 (NCHCH), 161.2 (COCH_3).

HRMS (EI): m/z [M^+] calcd for $\text{C}_{12}\text{H}_{11}\text{NO}$: 185.0835; found: 185.0833.

The analytical data accord with the literature.²¹

4-(But-3-en-1-yl)-4-methyl-1-trisopropylsilyl-1,4-dihydropyridine (7a)

Synthesis according to GP1 from 4-methylpyridine (**5a**, 93 mg, 1.00 mmol, 97 μL), TIPSOTf (337 mg, 1.00 mmol, 296 μL), and di(*but-3-en-1-yl*)magnesium (0.23 m in THF/ Et_2O , 1:1, 1.10 mmol, 4.78 mL). The reaction was stopped after 18 h. Quantitative determination indicated 135 mg (44%) of dihydropyridine **7a** followed by stirring under air for 1 d. Purification by FC (Al_2O_3 -basic, activity III, pentane) afforded **7a**.

Yield: 134 mg (44%); colorless oil; R_f = 0.97 (Al_2O_3 ; pentane).

IR (film): 3076, 3039, 2945, 2868, 1668, 1639, 1601, 1464, 1286, 1074, 974, 883, 733, 669 cm^{-1} .

^1H NMR (400 MHz, CDCl_3): δ = 1.02 (s, 3 H, CH_3), 1.08 (d, J = 7.2 Hz, 18 H, $\text{CH}(\text{CH}_3)_2$), 1.18–1.29 (m, 5 H, $\text{CH}_2\text{CH}_2\text{CH}$, $\text{CH}(\text{CH}_3)_2$), 2.00–2.09 (m, 2 H, $\text{CH}_2\text{CH}_2\text{CH}$), 4.15–4.20 (m, 2 H, NCHCH), 4.88 (ddt, J = 10.2, 2.3, 1.3 Hz, 1 H, $\text{CH}_2\text{CH}_2\text{CHCH}_2^a$), 4.94–5.01 (m, 1 H, $\text{CH}_2\text{CH}_2\text{CHCH}_2^b$), 5.88 (ddt, J = 16.8, 10.2, 6.6 Hz, 1 H, CH_2CHCH_2), 5.96–6.01 (m, 2 H, NCHCH).

^{13}C NMR (100 MHz, CDCl_3): δ = 11.6 ($\text{CH}(\text{CH}_3)_2$), 18.0 ($\text{CH}(\text{CH}_3)_2$), 31.0 ($\text{CH}_2\text{CH}_2\text{CH}$), 33.8 (CH_3), 33.9 (CCH_3), 45.1 ($\text{CH}_2\text{CH}_2\text{CH}$), 107.8 (NCHCH), 113.4 ($\text{CH}_2\text{CH}_2\text{CHCH}_2$), 128.3 (NCHCH), 140.5 (CH_2CHCH_2).

HRMS (ESI): m/z [$\text{M} + \text{H}$]⁺ calcd for $\text{C}_{19}\text{H}_{36}\text{NSi}$: 306.2612; found: 306.2610.

4-(But-3-en-1-yl)-4-phenyl-1-trisopropylsilyl-1,4-dihydropyridine (7b)

Synthesis according to GP1 from 4-phenylpyridine (**5b**, 686 mg, 4.42 mmol), TIPSOTf (1.48 g, 4.86 mmol, 1.31 mL), and di(*but-3-en-1-yl*)magnesium (0.27 m in THF/ Et_2O , 1:1, 4.86 mmol, 18.0 mL). The reaction was stopped after 18 h. Quantitative determination indicated 1.00 g (62%) of dihydropyridine **7b** followed by stirring under air for 2 d. Purification by FC (Al_2O_3 -basic, activity III, pentane) afforded **7b**.

Yield: 882 mg (54%); orange solid; mp 46 °C; R_f = 0.57 (Al_2O_3 ; pentane).

IR (KBr): 3076, 3053, 2945, 2866, 1666, 1460, 1286, 1076, 1053, 972, 906, 885, 690, 521 cm^{-1} .

^1H NMR (400 MHz, CDCl_3): δ = 1.11 (d, J = 7.3 Hz, 18 H, $\text{CH}(\text{CH}_3)_2$), 1.22–1.34 (m, 3 H, $\text{CH}(\text{CH}_3)_2$), 1.71–1.79 (m, 2 H, $\text{CH}_2\text{CH}_2\text{CH}$), 2.10–2.19 (m, 2 H, $\text{CH}_2\text{CH}_2\text{CH}$), 4.40 (d, J = 7.4 Hz, 2 H, NCHCH), 4.94 (ddd, J = 10.2, 1.9, 1.0 Hz, 1 H, $\text{CH}_2\text{CH}_2\text{CHCH}_2^a$), 5.00–5.08 (m, 1 H, $\text{CH}_2\text{CH}_2\text{CHCH}_2^b$), 5.95 (ddt, J = 16.8, 10.2, 6.5 Hz, 1 H, CH_2CHCH_2), 6.14 (d, J = 7.5 Hz, 2 H, NCHCH), 7.15 (t, J = 7.3 Hz, 1 H, CCHCHCH), 7.33 (t, J = 7.5 Hz, 2 H, CCHCHCH), 7.42 (d, J = 8.3 Hz, 2 H, CCHCHCH).

^{13}C NMR (100 MHz, CDCl_3): δ = 11.6 ($\text{CH}(\text{CH}_3)_2$), 18.0 ($\text{CH}(\text{CH}_3)_2$), 30.9 ($\text{CH}_2\text{CH}_2\text{CH}$), 41.7 (CCH_2CH_2), 42.3 ($\text{CH}_2\text{CH}_2\text{CH}$), 106.3 (NCHCH), 113.8 ($\text{CH}_2\text{CH}_2\text{CHCH}_2$), 125.4 (CCHCHCH), 126.8 (CCHCHCH), 128.2 (CCHCHCH), 128.3 (NCHCH), 140.1 (CH_2CHCH_2), 152.5 (CCHCHCH).

HRMS (ESI): m/z [$\text{M} + \text{H}$]⁺ calcd for $\text{C}_{24}\text{H}_{38}\text{NSi}$: 368.2768; found: 368.2766.

4-(But-3-en-1-yl)-4-benzyl-1-trisopropylsilyl-1,4-dihydropyridine (7c)

Synthesis according to GP1 from 4-benzylpyridine (**5c**, 748 mg, 4.42 mmol, 0.71 mL), TIPSOTf (1.48 g, 4.86 mmol, 1.31 mL), and di(*but-3-en-1-yl*)magnesium (0.27 m in THF/ Et_2O , 1:1, 4.86 mmol, 18.0 mL). The reaction was stopped after 18 h. Quantitative determination indicated 590 mg (35%) of dihydropyridine **7c** followed by stirring under air for 1 d. Purification by FC (Al_2O_3 -basic, activity III, pentane) afforded **7c**.

Yield: 557 mg (33%); colorless solid; mp 39 °C; R_f = 0.88 (Al_2O_3 ; pentane).

IR (KBr): 3061, 3028, 2943, 2866, 1670, 1462, 1288, 1063, 972, 881, 746, 698, 661, 499 cm^{-1} .

^1H NMR (400 MHz, CDCl_3): δ = 0.98 (d, J = 7.3 Hz, 18 H, $\text{CH}(\text{CH}_3)_2$), 1.09–1.21 (m, 3 H, $\text{CH}(\text{CH}_3)_2$), 1.27–1.34 (m, 2 H, $\text{CH}_2\text{CH}_2\text{CH}$), 2.03–2.13 (m, 2 H, $\text{CH}_2\text{CH}_2\text{CH}$), 2.54 (s, 2 H, CCH_2C), 4.07–4.13 (m, 2 H, NCHCH), 4.90 (ddt, J = 10.2, 2.3, 1.2 Hz, 1 H, $\text{CH}_2\text{CH}_2\text{CHCH}_2^a$), 4.96–5.03 (m, 1 H, $\text{CH}_2\text{CH}_2\text{CHCH}_2^b$), 5.90 (ddt, J = 17.1, 10.3, 6.6 Hz, 1 H, CH_2CHCH_2), 5.92–5.97 (m, 2 H, NCHCH), 7.10–7.15 (m, 3 H, CCHCHCH , CCHCHCH), 7.17–7.23 (m, 2 H, CCHCHCH).

^{13}C NMR (100 MHz, CDCl_3): δ = 11.5 ($\text{CH}(\text{CH}_3)_2$), 17.9 ($\text{CH}(\text{CH}_3)_2$), 31.4 ($\text{CH}_2\text{CH}_2\text{CH}$), 39.8 (CCH_2CH_2), 43.4 ($\text{CH}_2\text{CH}_2\text{CH}$), 52.3 (CCH_2C), 105.9 (NCHCH), 113.5 ($\text{CH}_2\text{CH}_2\text{CHCH}_2$), 125.6 (CCHCHCH), 127.4 (CCHCHCH), 129.3 (NCHCH), 131.1 (CCHCHCH), 139.2 (CCHCHCH), 140.4 (CH_2CHCH_2).

HRMS (ESI): m/z [$\text{M} + \text{H}$]⁺ calcd for $\text{C}_{25}\text{H}_{40}\text{NSi}$: 382.2925; found: 382.2922.

4-(But-3-en-1-yl)-4-(4-methoxyphenyl)-1-trisopropylsilyl-1,4-dihydropyridine (7d)

Synthesis according to GP1 from 4-(4-methoxyphenyl)pyridine (**5d**, 648 mg, 3.50 mmol), TIPSOTf (1.18 g, 3.85 mmol, 1.03 mL), and di(*but-3-en-1-yl*)magnesium (0.27 m in THF/ Et_2O , 1:1, 3.85 mmol, 14.3 mL). The reaction was stopped after 18 h. Quantitative determination indicated 626 mg (45%) of dihydropyridine **7d** followed by stirring under air for 2 d. Purification by FC (Al_2O_3 -basic, activity III, pentane) afforded **7d**.

Yield: 559 mg (40%); colorless solid; mp 54 °C; R_f = 0.13 (Al_2O_3 ; pentane).

IR (KBr): 3076, 3051, 2951, 2868, 1668, 1508, 1290, 1254, 1176, 1059, 976, 833, 692, 665, 501 cm^{-1} .

^1H NMR (500 MHz, CDCl_3): δ = 1.11 (d, J = 7.4 Hz, 18 H, $\text{CH}(\text{CH}_3)_2$), 1.28 (sept, J = 7.4 Hz, 3 H, $\text{CH}(\text{CH}_3)_2$), 1.69–1.75 (m, 2 H, $\text{CH}_2\text{CH}_2\text{CH}$), 2.10–2.18 (m, 2 H, $\text{CH}_2\text{CH}_2\text{CH}$), 3.80 (s, 3 H, OCH_3), 4.33–4.38 (m, 2 H, NCHCH), 4.94 (ddt, J = 10.2, 2.2, 1.1 Hz, 1 H, $\text{CH}_2\text{CH}_2\text{CHCH}_2^a$), 5.00–5.08 (m, 1 H, $\text{CH}_2\text{CH}_2\text{CHCH}_2^b$), 5.95 (ddt, J = 16.8, 10.2, 6.6 Hz, 1 H, CH_2CHCH_2), 6.10–6.15 (m, 2 H, NCHCH), 6.85–6.90 (m, 2 H, $\text{CH}(\text{OCH}_3)$), 7.30–7.36 (m, 2 H, $\text{CHCH}(\text{OMe})$).

^{13}C NMR (125 MHz, CDCl_3): δ = 11.6 ($\text{CH}(\text{CH}_3)_2$), 18.0 ($\text{CH}(\text{CH}_3)_2$), 31.0 ($\text{CH}_2\text{CH}_2\text{CH}$), 41.0 (CCH_2CH_2), 42.2 ($\text{CH}_2\text{CH}_2\text{CH}$), 55.4 (CH_3), 106.6 (NCHCH), 113.5 ($\text{CH}(\text{OCH}_3)$), 113.7 ($\text{CH}_2\text{CH}_2\text{CHCH}_2$), 127.8 ($\text{CHCH}(\text{OCH}_3)$), 128.1 (NCHCH), 140.2 (CH_2CHCH_2), 145.1 ($\text{CCHCH}(\text{OCH}_3)$), 157.3 (COCH_3).

HRMS (ESI): m/z [$\text{M} + \text{H}$]⁺ calcd for $\text{C}_{25}\text{H}_{40}\text{NOSi}$: 398.2874; found: 398.2872.

4304

Synthesis

H.-K. A. Rudy, K. T. Wanner

Paper

4-(But-3-en-1-yl)-4-(4-methoxybenzyl)-1-triisopropylsilyl-1,4-dihydropyridine (7e)

Synthesis according to GP1 from 4-(4-methoxybenzyl)pyridine (**5e**, 598 mg, 3.00 mmol), TIPSOTf (1.01 g, 3.30 mmol, 0.89 mL), and di(but-3-en-1-yl)magnesium (0.26 m in THF/Et₂O, 1:1, 3.30 mmol, 12.7 mL). The reaction was stopped after 18 h. Quantitative determination indicated 494 mg (40%) of dihydropyridine **7e** followed by stirring under air for 2 d. Purification by FC (Al₂O₃-basic, activity III, pentane) afforded **7e**.

Yield: 483 mg (39%); colorless solid; mp 45 °C; *R*_f = 0.18 (Al₂O₃; pentane).

IR (KBr): 3084, 3037, 2949, 2864, 2360, 1670, 1510, 1286, 1240, 1063, 972, 881, 768, 690, 662, 499 cm⁻¹.

¹H NMR (400 MHz, CDCl₃): δ = 0.98 (d, *J* = 7.4 Hz, 18 H, CH(CH₃)₂), 1.10–1.20 (m, 3 H, CH(CH₃)₂), 1.25–1.32 (m, 2 H, CH₂CH₂CH), 2.03–2.12 (m, 2 H, CH₂CH₂CH), 2.47 (s, 2 H, CCH₂C), 3.76 (s, 3 H, CH₃), 4.05–4.10 (m, 2 H, NCHCH), 4.90 (ddt, *J* = 10.2, 2.3, 1.2 Hz, 1 H, CH₂CH₂CHCH₂^a), 4.96–5.03 (m, 1 H, CH₂CH₂CHCH₂^b), 5.89 (ddt, *J* = 17.1, 10.3, 6.6 Hz, 1 H, CH₂CHCH₂), 5.92–5.96 (m, 2 H, NCHCH), 6.73–6.79 (m, 2 H, CHC(OCH₃)), 7.01–7.06 (m, 2 H, CHCHC(OMe)).

¹³C NMR (100 MHz, CDCl₃): δ = 11.5 (CH(CH₃)₂), 17.9 (CH(CH₃)₂), 31.4 (CH₂CH₂CH), 39.8 (CCH₂CH₂), 43.3 (CH₂CH₂CH), 51.3 (CCH₂C), 55.3 (OCH₃), 105.9 (NCHCH), 112.9 (CHC(OCH₃)), 113.5 (CH₂CH₂CHCH₂), 129.3 (NCHCH), 131.4 (CCHCHC(OCH₃)), 131.9 (CHCHC(OCH₃)), 140.5 (CH₂CHCH₂), 157.8 (COCH₃).

HRMS (ESI): *m/z* [M + H]⁺ calcd for C₂₆H₄₂NOSi: 412.3030; found: 412.3028.

4-Methyl-4-(pent-4-en-1-yl)-1-triisopropylsilyl-1,4-dihydropyridine (9a)

Synthesis according to GP1 from 4-methylpyridine (**5a**, 279 mg, 3.00 mmol, 290 μL), TIPSOTf (1.01 g, 3.30 mmol, 0.89 mL), and di(pent-4-en-1-yl)magnesium (0.23 m in THF/Et₂O, 1:1, 3.30 mmol, 14.5 mL). The reaction was stopped after 18 h. Quantitative determination indicated 422 mg (44%) of dihydropyridine **9a** followed by stirring under air for 1 d. Purification by FC (Al₂O₃-basic, activity III, pentane) afforded **9a**.

Yield: 414 mg (43%); colorless oil; *R*_f = 0.90 (Al₂O₃; pentane).

IR (film): 3078, 3039, 2945, 2868, 1668, 1462, 1286, 1076, 370, 883, 731, 665 cm⁻¹.

¹H NMR (400 MHz, CDCl₃): δ = 1.00 (s, 3 H, CH₃), 1.08 (d, *J* = 7.2 Hz, 18 H, CH(CH₃)₂), 1.10–1.17 (m, 2 H, CH₂CH₂CH₂CH), 1.18–1.28 (m, 3 H, CH(CH₃)₂), 1.35–1.44 (m, 2 H, CH₂CH₂CH), 1.99–2.08 (m, 2 H, CH₂CH₂CH), 4.14–4.20 (m, 2 H, NCHCH), 4.91 (ddt, *J* = 10.2, 2.3, 1.3 Hz, 1 H, CH₂CH₂CHCH₂^a), 4.94–5.01 (m, 1 H, CH₂CH₂CHCH₂^b), 5.81 (ddt, *J* = 16.8, 10.2, 6.6 Hz, 1 H, CH₂CHCH₂), 5.94–6.00 (m, 2 H, NCHCH).

¹³C NMR (100 MHz, CDCl₃): δ = 11.6 (CH(CH₃)₂), 18.1 (CH(CH₃)₂), 25.6 (CH₂CH₂CH₂), 33.8 (CCH₃), 33.8 (CCH₃), 34.5 (CH₂CH₂CH), 45.5 (CH₂CH₂CH₂CH), 108.2 (NCHCH), 113.9 (CH₂CH₂CHCH₂), 128.0 (NCHCH), 139.7 (CH₂CHCH₂).

HRMS (ESI): *m/z* [M + H]⁺ calcd for C₂₀H₃₈NSi: 320.2768; found: 320.2767.

4-(Pent-4-en-1-yl)-4-phenyl-1-triisopropylsilyl-1,4-dihydropyridine (9b)

Synthesis according to GP1 from 4-phenylpyridine (**5b**, 310 mg, 2.00 mmol), TIPSOTf (674 mg, 2.20 mmol, 590 μL), and di(pent-4-en-1-yl)magnesium (0.28 m in THF/Et₂O, 1:1, 2.20 mmol, 7.9 mL). The reaction

was stopped after 2 h. Quantitative determination indicated 473 mg (62%) of dihydropyridine **9b** followed by stirring under air for 1 d. Purification by FC (Al₂O₃-basic, activity III, pentane) afforded **9b**. Yield: 451 mg (59%); orange solid; mp 53 °C; *R*_f = 0.65 (Al₂O₃; pentane).

IR (KBr): 3080, 3051, 2947, 2866, 2362, 1668, 1599, 1464, 1288, 1078, 978, 881, 746, 696, 667, 627, 499 cm⁻¹.

¹H NMR (500 MHz, CDCl₃): δ = 1.11 (d, *J* = 7.5 Hz, 18 H, CH(CH₃)₂), 1.28 (sept, *J* = 7.5 Hz, 3 H, CH(CH₃)₂), 1.45–1.54 (m, 2 H, CH₂CH₂CH), 1.64–1.71 (m, 2 H, CH₂CH₂CH₂CH), 2.09–2.16 (m, 2 H, CH₂CH₂CH), 4.40 (d, *J* = 8.2 Hz, 2 H, NCHCH), 4.92–4.97 (m, 1 H, CH₂CH₂CHCH₂^a), 4.98–5.05 (m, 1 H, CH₂CH₂CHCH₂^b), 5.80–5.90 (m, 1 H, CH₂CHCH₂), 6.13 (d, *J* = 8.2 Hz, 2 H, NCHCH), 7.12–7.17 (m, 1 H, CCHCHCH), 7.30–7.36 (m, 2 H, CCHCHCH), 7.39–7.44 (m, 2 H, CCHCHCH).

¹³C NMR (125 MHz, CDCl₃): δ = 11.6 (CH(CH₃)₂), 18.0 (CH(CH₃)₂), 25.5 (CH₂CH₂CH), 34.4 (CH₂CH₂CH), 41.8 (CCH₂), 42.7 (CCH₂), 106.6 (NCHCH), 114.2 (CH₂CH₂CHCH₂), 125.3 (CCHCHCH), 126.8 (CCHCHCH), 128.1 (CCHCHCH), 128.2 (NCHCH), 139.5 (CH₂CHCH₂), 152.7 (CCCH₂).

HRMS (EI): *m/z* [M]⁺ calcd for C₂₅H₃₉NSi: 381.2846; found: 381.2854.

4-Benzyl-4-(pent-4-en-1-yl)-1-triisopropylsilyl-1,4-dihydropyridine (9c)

Synthesis according to GP1 from 4-benzylpyridine (**5c**, 508 mg, 3.00 mmol, 480 μL), TIPSOTf (1.01 g, 3.30 mmol, 0.89 mL), and di(pent-4-en-1-yl)magnesium (0.23 m in THF/Et₂O, 1:1, 3.30 mmol, 14.5 mL). The reaction was stopped after 18 h. Quantitative determination indicated 451 mg (38%) of dihydropyridine **9c** followed by stirring under air for 1 d. Purification by FC (Al₂O₃-basic, activity III, pentane) afforded **9c**.

Yield: 439 mg (37%); colorless solid; mp 39 °C; *R*_f = 0.70 (Al₂O₃; pentane).

IR (KBr): 3062, 3028, 2947, 2864, 2360, 1670, 1462, 1288, 1061, 972, 908, 881, 698, 661, 619 cm⁻¹.

¹H NMR (500 MHz, CDCl₃): δ = 0.98 (d, *J* = 7.4 Hz, 18 H, CH(CH₃)₂), 1.15 (sept, *J* = 7.5 Hz, 3 H, CH(CH₃)₂), 1.20–1.26 (m, 2 H, CH₂CH₂CH), 1.40–1.49 (m, 2 H, CCH₂CH₂), 2.06 (q, *J* = 7.1 Hz, 2 H, CH₂CH₂CH), 2.52 (s, 2 H, CCH₂C), 4.07–4.12 (m, 2 H, NCHCH), 4.92 (ddt, *J* = 10.2, 2.2, 1.1 Hz, 1 H, CH₂CH₂CHCH₂^a), 4.96–5.02 (m, 1 H, CH₂CH₂CHCH₂^b), 5.83 (ddt, *J* = 16.9, 10.2, 6.6 Hz, 1 H, CH₂CHCH₂), 5.90–5.95 (m, 2 H, NCHCH), 7.09–7.15 (m, 3 H, CCHCHCH, CCHCHCH), 7.17–7.23 (m, 2 H, CCHCHCH).

¹³C NMR (125 MHz, CDCl₃): δ = 11.5 (CH(CH₃)₂), 17.9 (CH(CH₃)₂), 25.9 (CH₂CH₂CH), 34.5 (CH₂CH₂CH), 39.8 (CCH₂CH₂), 43.8 (CCH₂CH₂), 52.2 (CCH₂C), 106.2 (NCHCH), 114.0 (CH₂CH₂CHCH₂), 125.5 (CCHCHCH), 127.4 (CCHCHCH), 129.0 (NCHCH), 131.1 (CCHCHCH), 139.3 (CCHCHCH), 139.7 (CH₂CHCH₂).

HRMS (ESI): *m/z* [M + H]⁺ calcd for C₂₆H₄₂NSi: 396.3081; found: 396.3079.

4-(4-Methoxyphenyl)-4-(pent-4-en-1-yl)-1-triisopropylsilyl-1,4-dihydropyridine (9d)

Synthesis according to GP1 from 4-(4-methoxyphenyl)pyridine (**5d**, 741 mg, 4.00 mmol), TIPSOTf (1.35 g, 4.40 mmol, 1.18 mL), and di(pent-4-en-1-yl)magnesium (0.28 m in THF/Et₂O, 1:1, 4.40 mmol, 15.5 mL). The reaction was stopped after 18 h. Quantitative determination indicated 1.02 g (62%) of dihydropyridine **9d** followed by stirring under air for 2 d. Purification by FC (Al₂O₃-basic, activity III, pentane) afforded **9d**.

Yield: 1.01 g (61%); colorless solid; mp 64 °C; R_f = 0.17 (Al₂O₃; pentane).

IR (KBr): 3080, 2999, 2945, 2867, 1664, 1606, 1506, 1288, 1244, 1188, 1059, 970, 746, 665, 511 cm⁻¹.

¹H NMR (400 MHz, CDCl₃): δ = 1.10 (d, J = 7.4 Hz, 18 H, CH(CH₃)₂), 1.28 (sept, J = 7.6 Hz, 3 H, CH(CH₃)₂), 1.43–1.53 (m, 2 H, CH₂CH₂CH), 1.60–1.68 (m, 2 H, CCH₂), 2.12 (q, J = 7.1 Hz, 2 H, CH₂CH₂CH₂CH), 3.79 (s, 3 H, CH₃), 4.35 (d, J = 8.2 Hz, 2 H, NCHCH), 4.90–4.96 (m, 1 H, CH₂CH₂CHCH₂), 4.97–5.05 (m, 1 H, CH₂CH₂CHCH₂), 5.84 (ddt, J = 16.8, 10.2, 6.5 Hz, 1 H, CH₂CHCH₂), 6.10 (d, J = 8.2 Hz, 2 H, NCHCH), 6.84–6.90 (m, 2 H, CHC(OCH₃)), 7.29–7.35 (m, 2 H, CHCHC(OCH₃)).

¹³C NMR (100 MHz, CDCl₃): δ = 11.6 (CH(CH₃)₂), 18.0 (CH(CH₃)₂), 25.5 (CH₂CH₂CH), 34.4 (CH₂CH₂CH), 41.0 (CCH₂), 42.7 (CCH₂), 55.4 (OCH₃), 106.9 (NCHCH), 113.5 (CHC(OCH₃)), 114.1 (CH₂CH₂CHCH₂), 127.8 (CHCHC(OCH₃)), 127.9 (NCHCH), 139.6 (CH₂CHCH₂), 145.4 (CCHCHC(OCH₃)), 157.3 (COCH₃).

HRMS (ESI): m/z [M + H]⁺ calcd for C₂₆H₄₂NOSi: 412.3030; found: 412.3026.

4-(4-Methoxybenzyl)-4-(pent-4-en-1-yl)-1-triisopropylsilyl-1,4-dihydropyridine (9e)

Synthesis according to GP1 from 4-(4-methoxybenzyl)pyridine (5e, 598 mg, 3.00 mmol), TIPSOTf (1.01 g, 3.30 mmol, 0.89 mL), and di(pent-4-en-1-yl)magnesium (0.28 m in THF/Et₂O, 1:1, 3.30 mmol, 11.6 mL). The reaction was stopped after 18 h. Quantitative determination indicated 577 mg (45%) of dihydropyridine **9e** followed by stirring under air for 2 d. Purification by FC (Al₂O₃-basic, activity III, pentane) afforded **9e**.

Yield: 529 mg (41%); colorless oil; R_f = 0.19 (Al₂O₃; pentane).

IR (film): 2945, 2866, 1670, 1610, 1510, 1464, 1286, 1244, 1176, 1099, 1063, 970, 908, 883 cm⁻¹.

¹H NMR (400 MHz, CDCl₃): δ = 0.97 (d, J = 7.3 Hz, 18 H, CH(CH₃)₂), 1.08–1.19 (m, 3 H, CH(CH₃)₂), 1.19–1.25 (m, 2 H, CCH₂CH₂), 1.38–1.49 (m, 2 H, CCH₂CH₂), 2.01–2.11 (m, 2 H, CH₂CH₂CH₂CH), 2.45 (s, 2 H, CCH₂C), 3.76 (s, 3 H, CH₃), 4.04–4.10 (m, 2 H, NCHCH), 4.92 (ddt, J = 10.2, 2.3, 1.2 Hz, 1 H, CH₂CH₂CHCH₂), 4.95–5.03 (m, 1 H, CH₂CH₂CHCH₂), 5.83 (ddt, J = 16.9, 10.2, 6.6 Hz, 1 H, CH₂CHCH₂), 5.89–5.95 (m, 2 H, NCHCH), 6.73–6.78 (m, 2 H, CHC(OCH₃)), 7.00–7.06 (m, 2 H, CHCHC(OCH₃)).

¹³C NMR (100 MHz, CDCl₃): δ = 11.5 (CH(CH₃)₂), 17.9 (CH(CH₃)₂), 25.9 (CCH₂CH₂), 34.5 (CH₂CH₂CH), 39.8 (CCH₂CH₂), 43.8 (CCH₂CH₂), 51.2 (CCH₂C), 55.3 (OCH₃), 106.2 (NCHCH), 112.9 (CHC(OCH₃)), 114.0 (CH₂CH₂CHCH₂), 129.0 (NCHCH), 131.6 (CCHCHC(OCH₃)), 131.9 (CHCHC(OCH₃)), 139.8 (CH₂CHCH₂), 157.7 (COCH₃).

HRMS (ESI): m/z [M + H]⁺ calcd for C₂₇H₄₄NOSi: 426.3187; found: 426.3182.

4-Allyl-4-methyl-1-triisopropylsilyl-1,4-dihydropyridine (11a)

Synthesis according to GP1 from 4-methylpyridine (5a, 889 mg, 9.55 mmol, 0.93 mL), TIPSOTf (3.22 g, 10.5 mmol, 2.82 mL), and di(allyl)magnesium (0.36 m in THF/Et₂O, 1:1, 10.5 mmol, 29.5 mL). The reaction was stopped after 2 h. Quantitative determination indicated 919 mg (33%) of dihydropyridine **11a** followed by stirring under air for 3 d. Purification by FC (Al₂O₃-basic, activity III, pentane) afforded **11a**.

Yield: 977 mg (35%); colorless oil; R_f = 0.95 (Al₂O₃; pentane).

IR (film): 3074, 3043, 2947, 2868, 1670, 1600, 1464, 1286, 1076, 1053, 976, 883, 731, 687 cm⁻¹.

¹H NMR (400 MHz, CDCl₃): δ = 1.04 (s, 3 H, CCH₃), 1.08 (d, J = 7.2 Hz, 18 H, CH(CH₃)₂), 1.18–1.30 (m, 3 H, CH(CH₃)₂), 1.99 (dt, J = 7.2, 1.2 Hz, 2 H, CCH₂CH), 4.21–4.28 (m, 2 H, NCHCH), 4.92–5.01 (m, 2 H, CCH₂CHCH₂), 5.85 (ddt, J = 17.0, 10.3, 7.2 Hz, 1 H, CH₂CHCH₂), 5.94–6.00 (m, 2 H, NCHCH).

¹³C NMR (100 MHz, CDCl₃): δ = 11.6 (CH(CH₃)₂), 18.0 (CH(CH₃)₂), 32.6 (CCH₃), 33.9 (CCH₃), 50.8 (CCH₂), 108.1 (NCHCH), 115.9 (CCH₂CHCH₂), 128.0 (NCHCH), 136.7 (CH₂CHCH₂).

HRMS (EI): m/z [M]⁺ calcd for C₁₈H₃₃NSi: 291.2377; found: 291.2375.

4-Allyl-4-phenyl-1-triisopropylsilyl-1,4-dihydropyridine (11b)

Synthesis according to GP1 from 4-phenylpyridine (5b, 1.48 g, 9.55 mmol), TIPSOTf (3.22 g, 10.5 mmol, 2.82 mL), and di(allyl)magnesium (0.36 m in THF/Et₂O, 1:1, 10.5 mmol, 29.5 mL). The reaction was stopped after 2 h. Quantitative determination indicated 1.18 g (35%) of dihydropyridine **11b** followed by stirring under air for 4 d. Purification by FC (Al₂O₃-basic, activity III, pentane) afforded **11b**.

Yield: 1.11 g (35%); yellow solid; mp 33 °C; R_f = 0.90 (Al₂O₃; pentane).

IR (KBr): 3049, 2947, 2866, 1666, 1597, 1462, 1288, 1099, 1076, 1043, 978, 881, 762, 690, 663, 519 cm⁻¹.

¹H NMR (400 MHz, CDCl₃): δ = 1.10 (d, J = 7.4 Hz, 18 H, CH(CH₃)₂), 1.27 (sept, J = 7.4 Hz, 3 H, CH(CH₃)₂), 2.52 (dt, J = 7.0, 1.2 Hz, 2 H, CCH₂CH), 4.42–4.48 (m, 2 H, NCHCH), 5.00–5.08 (m, 2 H, CCH₂CHCH₂), 5.83 (ddt, J = 17.4, 10.4, 7.0 Hz, 1 H, CH₂CHCH₂), 6.08–6.13 (m, 2 H, NCHCH), 7.15 (tt, 1 H, J = 7.5, 1.2 Hz, CCHCHCH), 7.30–7.36 (m, 2 H, CCHCHCH), 7.39–7.43 (m, 2 H, CCHCHCH).

¹³C NMR (100 MHz, CDCl₃): δ = 11.6 (CH(CH₃)₂), 18.0 (CH(CH₃)₂), 41.6 (CCH₂), 48.2 (CCH₂), 106.5 (NCHCH), 116.4 (CCH₂CHCH₂), 125.4 (CCHCHCH), 126.8 (CCHCHCH), 128.1 (NCHCH), 128.2 (CCHCHCH), 136.5 (CH₂CHCH₂), 151.7 (CCCH₂).

HRMS (EI): m/z [M]⁺ calcd for C₂₃H₃₅NSi: 353.2533; found: 353.2519.

4-Allyl-4-benzyl-1-triisopropylsilyl-1,4-dihydropyridine (11c)

Synthesis according to GP1 from 4-benzylpyridine (5c, 1.62 g, 9.55 mmol, 1.52 mL), TIPSOTf (3.22 g, 10.5 mmol, 2.82 mL), and di(allyl)magnesium (0.36 m in THF/Et₂O, 1:1, 10.5 mmol, 29.5 mL). The reaction was stopped after 2 h. Quantitative determination indicated 737 mg (21%) of dihydropyridine **11c** followed by stirring under air for 4 d. Purification by FC (Al₂O₃-basic, activity III, pentane) afforded **11c**.

Yield: 722 mg (21%); colorless oil; R_f = 0.63 (Al₂O₃; pentane).

IR (film): 3082, 3026, 2945, 2866, 1670, 1462, 1284, 1059, 1045, 1016, 991, 972, 920, 883, 743, 689, 662, 623, 511 cm⁻¹.

¹H NMR (500 MHz, CDCl₃): δ = 0.98 (d, J = 7.4 Hz, 18 H, CH(CH₃)₂), 1.10–1.19 (m, 3 H, CH(CH₃)₂), 2.09 (d, J = 7.1 Hz, 2 H, CCH₂CH), 2.57 (s, 2 H, CCH₂C), 4.14–4.19 (m, 2 H, NCHCH), 4.97–5.05 (m, 2 H, CCH₂CHCH₂), 5.87–5.97 (m, 3 H, CH₂CHCH₂, NCHCH), 7.10–7.16 (m, 3 H, CCHCHCH, CCHCHCH), 7.18–7.24 (m, 2 H, CCHCHCH).

¹³C NMR (125 MHz, CDCl₃): δ = 11.5 (CH(CH₃)₂), 17.9 (CH(CH₃)₂), 39.5 (CCH₂CH), 49.2 (CCH₂CH), 51.1 (CCH₂C), 106.1 (NCHCH), 116.0 (CCH₂CHCH₂), 125.6 (CCHCHCH), 127.5 (CCHCHCH), 129.0 (NCHCH), 131.1 (CCHCHCH), 136.9 (CH₂CHCH₂), 139.2 (CCHCHCH).

HRMS (EI): m/z [M]⁺ calcd for C₂₄H₃₇NSi: 367.2690; found: 367.2699.

4306

Synthesis

H.-K. A. Rudy, K. T. Wanner

Paper

4-Allyl-4-(4-methoxyphenyl)-1-triisopropylsilyl-1,4-dihydropyridine (11d)

Synthesis according to GP1 from 4-(4-methoxyphenyl)pyridine (**5d**, 1.76 g, 9.55 mmol), TIPSOTf (3.22 g, 10.5 mmol, 2.82 mL), and di(allyl)magnesium (0.30 m in THF/Et₂O, 1:1, 10.5 mmol, 35.2 mL). The reaction was stopped after 2 h. Quantitative determination indicated 879 mg (24%) of dihydropyridine **11d** followed by stirring under air for 4 d. Purification by FC (Al₂O₃-basic, activity III, pentane) afforded **11d**.

Yield: 840 mg (21%); colorless solid; mp 47 °C; *R*_f = 0.39 (Al₂O₃; pentane).

IR (KBr): 3072, 2999, 2951, 2864, 1666, 1601, 1506, 1464, 1290, 1244, 1092, 1051, 982, 881, 829, 760, 690, 669, 516 cm⁻¹.

¹H NMR (500 MHz, CDCl₃): δ = 1.10 (d, *J* = 7.4 Hz, 18 H, CH(CH₃)₂), 1.27 (sept, *J* = 7.5 Hz, 3 H, CH(CH₃)₂), 2.50 (dt, *J* = 7.0, 1.2 Hz, 2 H, CCH₂CH), 3.80 (s, 3 H, OCH₃), 4.39–4.44 (m, 2 H, NCHCH), 4.99–5.06 (m, 2 H, CCH₂CHCH₂), 5.83 (ddt, *J* = 17.4, 10.4, 7.0 Hz, 1 H, CH₂CHCH₂), 6.07–6.12 (m, 2 H, NCHCH), 6.85–6.91 (m, 2 H, CHCO), 7.30–7.36 (m, 2 H, CHCHCO).

¹³C NMR (125 MHz, CDCl₃): δ = 11.6 (CH(CH₃)₂), 18.0 (CH(CH₃)₂), 40.9 (CCH₂), 48.2 (CCH₂), 55.4 (OCH₃), 106.8 (NCHCH), 113.6 (CHCO), 116.3 (CCH₂CHCH₂), 127.8 (CHCHCO; NCHCH), 136.6 (CH₂CHCH₂), 144.4 (CCCH₂), 157.3 (COCH₃).

HRMS (EI): *m/z* [M]⁺ calcd for C₂₄H₃₇NOSi; 383.2639; found: 383.2657.

4-Allyl-4-(4-methoxybenzyl)-1-triisopropylsilyl-1,4-dihydropyridine (11e)

Synthesis according to GP1 from 4-(4-methoxybenzyl)pyridine (**5e**, 1.60 g, 8.03 mmol), TIPSOTf (2.71 g, 8.83 mmol, 2.37 mL), and di(allyl)magnesium (0.30 m in THF/Et₂O, 1:1, 8.83 mmol, 29.6 mL). The reaction was stopped after 2 h. Quantitative determination indicated 703 mg (22%) of dihydropyridine **11e** followed by stirring under air for 4 d. Purification by FC (Al₂O₃-basic, activity III, pentane) afforded **11e**.

Yield: 741 mg (23%); colorless oil; *R*_f = 0.50 (Al₂O₃; pentane).

IR (film): 3083, 3027, 2945, 2866, 2360, 1670, 1581, 1463, 1288, 1103, 1059, 1014, 993, 971, 914, 883, 688 cm⁻¹.

¹H NMR (500 MHz, CDCl₃): δ = 0.98 (d, *J* = 7.5 Hz, 18 H, CH(CH₃)₂), 1.10–1.20 (m, 3 H, CH(CH₃)₂), 2.08 (d, *J* = 7.2 Hz, 2 H, CCH₂CH), 2.51 (s, 2 H, CCH₂C), 3.77 (s, 3 H, OCH₃), 4.14 (d, *J* = 8.0 Hz, 2 H, NCHCH), 4.95–5.07 (m, 2 H, CCH₂CHCH₂), 5.86–5.98 (m, 3 H, CH₂CHCH₂, NCHCH), 6.74–6.79 (m, 2 H, CHCO), 7.02–7.08 (m, 2 H, CHCHCO).

¹³C NMR (125 MHz, CDCl₃): δ = 11.5 (CH(CH₃)₂), 17.9 (CH(CH₃)₂), 39.6 (CCH₂CH), 49.1 (CCH₂CH), 50.1 (CCH₂C), 55.3 (OCH₃), 106.1 (NCHCH), 113.0 (CHCO), 115.9 (CCH₂CHCH₂), 129.0 (NCHCH), 131.4 (CCHCHCO), 131.9 (CHCHCO), 136.9 (CH₂CHCH₂), 157.8 (COCH₃).

HRMS (EI): *m/z* [M]⁺ calcd for C₂₅H₃₉NOSi; 397.2795; found: 397.2819.

rac-1-Methyl-4-azatricyclo[3.3.1.0^{2,7}]non-3-en (rac-13a)

Synthesis according to GP2 from dihydropyridine **11a** (450 mg, 1.54 mmol) and TFA (2.65 g, 23.2 mmol, 1.78 mL) in pentane (15.4 mL). Purification by FC (Al₂O₃-basic, activity III, pentane/CH₂Cl₂/MeOH, 88:10:2) afforded **rac-13a**.

Yield: 174 mg (84%); yellow oil; *R*_f = 0.15 (Al₂O₃; pentane/CH₂Cl₂/MeOH, 88:10:2).

IR (film): 2949, 2858, 1614, 1452, 1375, 1350, 1333, 1269, 1160, 985, 916, 858, 829, 688 cm⁻¹.

¹H NMR (400 MHz, CDCl₃): δ = 0.83 (dq, *J* = 12.4, 2.2 Hz, 1 H, NCHCH₂C), 0.92 (s, 3 H, CH₃), 1.01 (ddq, *J* = 12.6, 6.4, 1.9 Hz, 1 H, NCHCH₂CH), 1.17 (d, *J* = 9.1 Hz, 1 H, CCH₂^aCHCH), 1.60 (dd, *J* = 12.5, 3.2 Hz, 1 H, NCHCH₂^bCH), 1.68 (dd, *J* = 12.4, 3.1 Hz, 1 H, NCHCH₂^bC), 1.99 (ddt, *J* = 8.7, 6.6, 2.0 Hz, 1 H, CCH₂^bCHCH), 2.07 (q, *J* = 6.2 Hz, 1 H, NCHCHCH), 2.84–2.90 (m, 1 H, NCHCH), 4.48–4.53 (m, 1 H, NCHCH₂), 8.08 (d, *J* = 3.7 Hz, 1 H, NCHCH).

¹³C NMR (100 MHz, CDCl₃): δ = 26.9 (CH₃), 27.6 (NCHCH₂CH), 30.7 (NCHCH₂CH), 38.7 (CCH₃), 38.9 (NCHCH₂C), 43.3 (CCH₂CHCH), 44.3 (NCHCH), 56.1 (NCHCH₂), 167.2 (NCHCH).

HRMS (EI): *m/z* [M – H]⁺ calcd for C₉H₁₂N; 134.0964; found: 134.0962.

rac-1-Phenyl-4-azatricyclo[3.3.1.0^{2,7}]non-3-en (rac-13b)

Synthesis according to GP2 from dihydropyridine **11b** (1.08 g, 3.05 mmol) and TFA (5.22 g, 45.8 mmol, 3.50 mL) in pentane (30.5 mL). Purification by FC (Al₂O₃-basic, activity III, pentane/CH₂Cl₂/MeOH, 88:10:2) afforded **rac-13b**.

Yield: 509 mg (85%); yellow oil; *R*_f = 0.66 (Al₂O₃; pentane/CH₂Cl₂/MeOH, 88:10:2).

IR (KBr): 3024, 2995, 2935, 2860, 1676, 1610, 1493, 1446, 1333, 1288, 1077, 766, 750, 702, 687, 540 cm⁻¹.

¹H NMR (500 MHz, CDCl₃): δ = 1.17 (ddq, *J* = 12.6, 6.2, 1.8 Hz, 1 H, NCHCH₂CH), 1.25 (dq, *J* = 12.7, 2.3 Hz, 1 H, NCHCH₂C), 1.60 (d, *J* = 9.2 Hz, 1 H, CCH₂^aCHCH), 1.79 (dd, *J* = 12.7, 3.2 Hz, 1 H, NCHCH₂^bCH), 2.02 (dd, *J* = 12.7, 3.0 Hz, 1 H, NCHCH₂^bC), 2.22 (q, *J* = 6.4 Hz, 1 H, NCHCHCH), 2.53 (ddt, *J* = 9.0, 6.8, 2.0 Hz, 1 H, CCH₂^bCHCH), 3.26–3.32 (m, 1 H, NCHCH), 4.63–4.68 (m, 1 H, NCHCH₂), 6.96–7.02 (m, 2 H, CCHCHCH), 7.14–7.19 (m, 1 H, CCHCHCH), 7.24–7.31 (m, 2 H, CCHCHCH), 8.34 (d, *J* = 3.7 Hz, 1 H, NCHCH).

¹³C NMR (125 MHz, CDCl₃): δ = 27.6 (NCHCH₂CH), 30.9 (NCHCH₂CH), 41.0 (NCHCH₂C), 41.3 (CCH₂CHCH), 43.3 (NCHCH), 45.8 (CCH₂), 56.0 (NCH(CH₂)), 124.9 (CCHCHCH), 126.0 (CCHCHCH), 128.4 (CCHCHCH), 147.8 (CCCH₂) 166.9 (NCHCH).

HRMS (EI): *m/z* [M]⁺ calcd for C₁₄H₁₅N; 197.1199; found: 197.1196.

rac-1-Benzyl-4-azatricyclo[3.3.1.0^{2,7}]non-3-en (rac-13c)

Synthesis according to GP2 from dihydropyridine **11c** (690 mg, 1.88 mmol) and TFA (3.22 g, 28.2 mmol, 2.16 mL) in pentane (18.8 mL). Purification by FC (Al₂O₃-basic, activity III, pentane/CH₂Cl₂/MeOH, 88:10:2) afforded **rac-13c**.

Yield: 331 mg (83%); beige solid; mp 88 °C; *R*_f = 0.27 (Al₂O₃; pentane/CH₂Cl₂/MeOH, 88:10:2).

IR (KBr): 3021, 2993, 2945, 2922, 2854, 1605, 1493, 1454, 1435, 1329, 1263, 1151, 771, 752, 704, 646, 484 cm⁻¹.

¹H NMR (500 MHz, CDCl₃): δ = 0.99 (dq, *J* = 12.4, 2.3 Hz, 1 H, NCHCH₂C), 1.03 (ddq, *J* = 12.6, 6.7, 2.0 Hz, 1 H, NCHCH₂CH), 1.16 (d, *J* = 9.1 Hz, 1 H, CCH₂^aCHCH), 1.60 (ddd, *J* = 15.2, 12.5, 3.1 Hz, 2 H, NCHCH₂^bC; NCHCH₂^bCH), 2.07 (q, *J* = 5.8 Hz, 1 H, NCHCH₂CH), 2.12 (ddt, *J* = 9.0, 6.8, 2.0 Hz, 1 H, CCH₂^bCHCH), 2.47 (d, *J* = 13.3 Hz, 1 H, CCH₂^aC), 2.55 (d, *J* = 13.4 Hz, 1 H, CCH₂^bC), 2.96–3.02 (m, 1 H, NCHCH), 4.48–4.53 (m, 1 H, NCHCH₂), 7.02–7.06 (m, 2 H, CCHCHCH), 7.17–7.23 (m, 1 H, CCHCHCH), 7.23–7.29 (m, 2 H, CCHCHCH), 8.04 (d, *J* = 3.7 Hz, 1 H, NCHCH).

¹³C NMR (125 MHz, CDCl₃): δ = 27.8 (NCHCH₂CH), 31.3 (NCHCH₂CH), 37.0 (NCHCH₂C), 41.3 (CCH₂CHCH), 42.4 (NCHCH), 43.2 (NCHCHC), 46.5 (CCH₂C), 55.9 (NCHCH₂), 126.3 (CCHCHCH), 128.3 (CCHCHCH), 129.7 (CCHCHCH) 138.2 (CCHCHCH), 166.9 (NCHCH).

HRMS (EI): m/z [M]⁺ calcd for C₁₅H₁₇N: 211.1356; found: 211.1354.

rac-1-(4-Methoxyphenyl)-4-azatricyclo[3.3.1.0^{2,7}]non-3-en (rac-13d)

Synthesis according to GP2 from dihydropyridine **11d** (840 mg, 2.19 mmol) and TFA (3.74 g, 32.8 mmol, 2.51 mL) in pentane/EtOH, 4:1 (22.0 mL). Purification by FC (Al₂O₃-basic, activity III, pentane/CH₂Cl₂/MeOH, 88:10:2) afforded **rac-13d**.

Yield: 421 mg (85%); yellow oil; R_f = 0.48 (Al₂O₃; pentane/CH₂Cl₂/MeOH, 89:10:1).

IR (film): 2997, 2933, 2858, 2833, 1610, 1514, 1462, 1443, 1346, 1250, 1178, 1034, 827, 810, 675 cm⁻¹.

¹H NMR (500 MHz, CDCl₃): δ = 1.16 (ddq, J = 12.6, 6.2, 1.9 Hz, 1 H, NCHCH₂CH), 1.23 (dq, J = 12.7, 2.3 Hz, 1 H, NCHCH₂C), 1.56 (d, J = 9.2 Hz, 1 H, CCH₂^aCHCH), 1.77 (dd, J = 12.6, 3.2 Hz, 1 H, NCHCH₂^bCH), 1.98 (dd, J = 12.7, 3.0 Hz, 1 H, NCHCH₂^bC), 2.20 (q, J = 6.3 Hz, 1 H, NCHCHCH), 2.50 (ddt, J = 9.1, 6.8, 2.0 Hz, 1 H, CCH₂^bCHCH), 3.22–3.27 (m, 1 H, NCHCH), 3.77 (s, 3 H, OCH₃), 4.61–4.66 (m, 1 H, NCH(CH₂)₂), 6.79–6.83 (m, 2 H, CHCOCH₃), 6.89–6.93 (m, 2 H, CHCHCO), 8.32 (d, J = 3.7 Hz, 1 H, NCHCH).

¹³C NMR (125 MHz, CDCl₃): δ = 27.6 (NCHCH₂CH), 30.9 (NCHCH₂CH), 40.9 (NCHCH₂C), 41.5 (CCH₂CHCH), 43.6 (NCHCH), 45.2 (CCH₂), 55.4 (OCH₃), 56.0 (NCHCH₂), 113.9 (CHCO), 126.0 (CHCHCO), 140.1 (CCH₂), 157.9 (COCH₃), 167.0 (NCHCH).

HRMS (ESI): m/z [M + H]⁺ calcd for C₁₅H₁₈NO: 228.1383; found: 228.1382.

rac-1-(4-Methoxybenzyl)-4-azatricyclo[3.3.1.0^{2,7}]non-3-en (rac-13e)

Synthesis according to GP2 from dihydropyridine **11e** (700 mg, 1.76 mmol) and TFA (3.01 g, 28.2 mmol, 2.02 mL) in pentane/EtOH, 4:1 (17.6 mL). Purification by FC (Al₂O₃-basic, activity III, pentane/CH₂Cl₂/MeOH, 88:10:2) afforded **rac-13e**.

Yield: 284 mg (67%); yellow oil; R_f = 0.42 (Al₂O₃; pentane/CH₂Cl₂/MeOH, 88:10:2).

IR (KBr): 2995, 2933, 2852, 1684, 1610, 1512, 1464, 1441, 1351, 1333, 1302, 1244, 1178, 1036, 829, 681 cm⁻¹.

¹H NMR (500 MHz, CDCl₃): δ = 0.97 (dq, J = 12.4, 2.2 Hz, 1 H, NCHCH₂^aC), 1.03 (ddq, J = 12.5, 6.3, 1.9 Hz, 1 H, NCHCH₂^aCH), 1.14 (d, J = 8.9 Hz, 1 H, CCH₂^aCHCH), 1.57 (dd, J = 12.5, 3.0 Hz, 1 H, NCHCH₂^bC), 1.61 (dd, J = 12.6, 3.2 Hz, 1 H, NCHCH₂^bCH), 2.03–2.12 (m, 2 H, NCHCH₂CH, CCH₂^bCHCH), 2.41 (d, J = 13.5 Hz, 1 H, CCH₂^aC), 2.48 (d, J = 13.6 Hz, 1 H, CCH₂^bC), 2.94–2.98 (m, 1 H, NCHCH), 3.78 (s, 3 H, OCH₃), 4.47–4.51 (m, 1 H, NCHCH₂), 6.78–6.82 (m, 2 H, CHCO), 6.93–6.97 (m, 2 H, CHCHCO), 8.03 (d, J = 3.7 Hz, 1 H, NCHCH).

¹³C NMR (125 MHz, CDCl₃): δ = 27.8 (NCHCH₂CH), 31.3 (NCHCH₂CH), 36.9 (NCHCH₂C), 41.3 (CCH₂CHCH), 42.4 (NCHCH), 43.4 (NCHCHC), 45.6 (CCH₂C), 55.3 (OCH₃), 55.9 (NCHCH₂), 113.7 (CHCO), 130.3 (CCHCHCO), 130.5 (CHCHCO), 158.2 (COCH₃), 167.0 (NCHCH).

HRMS (ESI): m/z [M + H]⁺ calcd for C₁₆H₂₀NO: 242.1539; found: 242.1538.

rac-3-Methyl-9-azatricyclo[4.3.1.0^{3,7}]dec-8-en (rac-14a)

Synthesis according to GP2 from dihydropyridine **7a** (380 mg, 1.24 mmol) and TFA (2.13 g, 18.7 mmol, 1.43 mL) in pentane (12.4 mL). Purification by FC (Al₂O₃-basic, activity III, pentane/CH₂Cl₂/MeOH, 88:10:2) afforded **rac-14a**.

Yield: 146 mg (79%); colorless oil; R_f = 0.21 (Al₂O₃; pentane/CH₂Cl₂/MeOH, 88:10:2).

IR (film): 3215, 2937, 2866, 1616, 1450, 1340, 1190, 1149, 1061, 985, 943, 874, 714 cm⁻¹.

¹H NMR (500 MHz, CDCl₃): δ = 0.96 (s, 3 H, CH₃), 1.13–1.19 (m, 1 H, CHCH₂^aCH), 1.23 (ddt, J = 13.2, 3.1, 1.1 Hz, 1 H, CHCH₂^aC), 1.37–1.45 (m, 2 H, CHCH₂^bC, CCH₂^aCH₂), 1.46–1.54 (m, 1 H, CHCH₂^bCH), 1.54–1.63 (m, 2 H, CCH₂^bCH₂), 1.91–2.03 (m, 2 H, CCH₂^bCH₂, CHCHCH₂), 2.33 (t, J = 4.2 Hz, 1 H, CHCHCH), 4.14 (p, J = 2.6 Hz, 1 H, NCHCH₂), 8.24 (d, J = 4.1 Hz, 1 H, NCHCH).

¹³C NMR (125 MHz, CDCl₃): δ = 28.2 (CH₃), 32.0 (CHCH₂CH₂), 34.1 (CHCH₂CH₂), 36.4 (CHCH₂CH), 39.8 (CHCH₂CH₂), 41.7 (CH₂CCH₂), 42.6 (CCH₂CH), 50.1 (NCHCH), 54.0 (NCHCH₂), 171.2 (NCHCH).

HRMS (ESI): m/z [M + H]⁺ calcd for C₁₀H₁₆N: 150.1277; found: 150.1276.

rac-3-Phenyl-9-azatricyclo[4.3.1.0^{3,7}]dec-8-en (rac-14b)

Synthesis according to GP2 from dihydropyridine **7b** (870 mg, 2.37 mmol) and TFA (4.05 g, 35.5 mmol, 2.72 mL) in pentane (23.7 mL). Purification by FC (Al₂O₃-basic, activity III, pentane/CH₂Cl₂/MeOH, 88.5:10:1.5) afforded **rac-14b**.

Yield: 420 mg (84%); colorless oil; R_f = 0.48 (Al₂O₃; pentane/CH₂Cl₂/MeOH, 88.5:10:1.5).

IR (film): 3055, 3022, 2997, 2945, 2868, 1618, 1495, 1444, 1340, 1188, 1034, 987, 760, 700 cm⁻¹.

¹H NMR (500 MHz, CDCl₃): δ = 1.32 (dt, J = 13.3, 2.0 Hz, 1 H, CHCH₂^aCH), 1.54–1.62 (m, 1 H, CHCH₂^aCH₂), 1.65 (ddt, J = 13.2, 10.3, 2.9 Hz, 1 H, CHCH₂^bCH), 1.73 (ddt, J = 13.3, 3.0, 0.9 Hz, 1 H, CCH₂^aCH), 1.87 (dd, J = 13.3, 2.5 Hz, 1 H, CCH₂^bCH), 1.97–2.16 (m, 4 H, CHCH₂^bCH₂, CHCH₂CH₂, CHCH₂CH₂), 3.02 (t, J = 4.3 Hz, 1 H, CHCHCH), 4.24 (p, J = 2.6 Hz, 1 H, NCHCH₂), 7.11–7.16 (m, 1 H, CCHCHCH), 7.16–7.21 (m, 2 H, CCHCHCH), 7.23–7.29 (m, 2 H, CCHCHCH), 8.48 (d, J = 4.0 Hz, 1 H, NCHCH).

¹³C NMR (125 MHz, CDCl₃): δ = 31.5 (CHCH₂CH₂), 34.0 (CHCH₂CH₂), 36.3 (CHCH₂CH), 41.1 (CHCH₂CH₂), 44.9 (CCH₂CH), 46.7 (NCHCH), 50.2 (CCH₂CH₂), 53.9 (NCHCH₂), 125.8 (CCHCHCH), 125.9 (CCHCHCH), 128.5 (CCHCHCH), 149.9 (CCCH₂), 170.5 (NCHCH).

HRMS (ESI): m/z [M + H]⁺ calcd for C₁₅H₁₈N: 212.1434; found: 212.1432.

rac-3-Benzyl-9-azatricyclo[4.3.1.0^{3,7}]dec-8-en (rac-14c)

Synthesis according to GP2 from dihydropyridine **7c** (540 mg, 1.41 mmol) and TFA (2.42 g, 21.2 mmol, 1.62 mL) in pentane (14.1 mL). Purification by FC (Al₂O₃-basic, activity III, pentane/CH₂Cl₂/MeOH, 88.5:10:1.5) afforded **rac-14c**.

Yield: 274 mg (86%); yellow oil; R_f = 0.40 (Al₂O₃; pentane/CH₂Cl₂/MeOH, 88.5:10:1.5).

IR (film): 3084, 3059, 3026, 2945, 2868, 1616, 1495, 1452, 1342, 762, 731, 704 cm⁻¹.

¹H NMR (500 MHz, CDCl₃): δ = 1.17 (dd, J = 13.4, 2.4 Hz, 1 H, CHCH₂^aCH), 1.31 (dd, J = 13.2, 2.1 Hz, 1 H, CCH₂^aCH), 1.35–1.43 (m, 1 H, CHCH₂^aCH₂), 1.45–1.54 (m, 3 H, CHCH₂^bCH, CCH₂^bCH, CHCH₂CH₂^a), 1.72–1.80 (m, 1 H, CHCH₂CH₂^b), 1.84–1.94 (m, 2 H, CHCH₂CH₂^b, CHCH₂^bCH₂), 2.42 (t, J = 4.2 Hz, 1 H, CHCHCH), 2.52 (s, 2 H, CCH₂C), 4.16 (p, J = 2.6 Hz, 1 H, NCHCH₂), 7.11–7.15 (m, 2 H, CCHCHCH), 7.18–7.23 (m, 1 H, CCHCHCH), 7.24–7.29 (m, 2 H, CCHCHCH), 8.25 (d, J = 4.1 Hz, 1 H, NCHCH).

^{13}C NMR (125 MHz, CDCl_3): δ = 31.6 (CHCH_2CH_2), 33.2 (CHCHCH_2), 36.5 (CHCH_2CH_2), 36.9 (CHCH_2CH), 40.7 (CCH_2CH), 46.6 (CHCCH_2), 47.1 (CCH_2C), 47.8 (NCHCH), 53.7 (NCHCH_2), 126.3 (CCHCHCH), 128.1 (CCHCHCH), 130.3 (CCHCHCH), 138.8 (CCHCHCH), 171.0 (NCHCH).

HRMS (ESI): m/z [$\text{M} + \text{H}$] $^+$ calcd for $\text{C}_{16}\text{H}_{20}\text{N}$: 226.1590; found: 226.1589.

rac-3-(4-Methoxyphenyl)-9-azatricyclo[4.3.1.0^{3,7}]dec-8-en (rac-14d)

Synthesis according to GP2 from dihydropyridine **7d** (545 mg, 1.37 mmol) and TFA (2.35 g, 20.6 mmol, 1.58 mL) in pentane (13.7 mL). Purification by FC (Al_2O_3 -basic, activity III, pentane/ CH_2Cl_2 /MeOH, 88:10:2) afforded **rac-14d**.

Yield: 295 mg (89%); colorless solid; mp 97 °C; R_f = 0.17 (Al_2O_3 ; pentane/ CH_2Cl_2 /MeOH, 88:10:2).

IR (KBr): 2999, 2939, 2868, 2835, 1614, 1512, 1335, 1306, 1259, 1238, 1180, 1036, 827, 555 cm^{-1} .

^1H NMR (500 MHz, CDCl_3): δ = 1.31 (d, J = 13.2 Hz, 1 H, CHCH_2^aCH), 1.53–1.60 (m, 1 H, $\text{CHCH}_2^a\text{CH}_2$), 1.64 (ddt, J = 13.1, 10.3, 2.8 Hz, 1 H, CHCH_2^bCH), 1.71 (dt, J = 13.3, 2.8 Hz, 1 H, CCH_2^aCH), 1.83 (dd, J = 13.3, 2.4 Hz, 1 H, CCH_2^bCH), 2.00–2.13 (m, 4 H, $\text{CHCH}_2^b\text{CH}_2$, CHCH_2CH_2 , CHCH_2CH_2), 2.97 (t, J = 4.3 Hz, 1 H, CHCHCH), 3.77 (s, 3 H, CH_3), 4.23 (p, J = 2.6 Hz, 1 H, NCHCH_2), 6.77–6.83 (m, 2 H, CHCO), 7.08–7.13 (m, 2 H, CHCHCO), 8.46 (d, J = 4.0 Hz, 1 H, NCHCH).

^{13}C NMR (125 MHz, CDCl_3): δ = 31.5 (CHCH_2CH_2), 34.0 (CHCH_2CH_2), 36.4 (CHCH_2CH), 41.1 (CHCH_2CH_2), 44.9 (CCH_2CH), 47.1 (NCHCH), 49.5 (CCH_2CH_2), 53.9 (NCHCH_2), 55.4 (CH_3), 113.8 (CHCO), 126.9 (CHCHCO), 142.2 (CCHCHCO), 157.6 (CO), 170.6 (NCHCH).

HRMS (ESI): m/z [$\text{M} + \text{H}$] $^+$ calcd for $\text{C}_{16}\text{H}_{20}\text{NO}$: 242.1539; found: 242.1538.

rac-3-(4-Methoxybenzyl)-9-azatricyclo[4.3.1.0^{3,7}]dec-8-en (rac-14e)

Synthesis according to GP2 from dihydropyridine **7e** (465 mg, 1.13 mmol) and TFA (1.93 g, 16.9 mmol, 1.29 mL) in pentane (11.3 mL). Purification by FC (Al_2O_3 -basic, activity III, pentane/ CH_2Cl_2 /MeOH, 88:10:2) afforded **rac-14e**.

Yield: 244 mg (85%); yellow oil; R_f = 0.19 (Al_2O_3 ; pentane/ CH_2Cl_2 /MeOH, 88:10:2).

IR (film): 2995, 2945, 2868, 1614, 1512, 1464, 1441, 1342, 1302, 1248, 1178, 1036, 833, 820, 758 cm^{-1} .

^1H NMR (500 MHz, CDCl_3): δ = 1.17 (dd, J = 12.9, 2.0 Hz, 1 H, CHCH_2^aCH), 1.30 (dd, J = 13.3, 2.3 Hz, 1 H, CCH_2^aCH), 1.35–1.43 (m, 1 H, $\text{CHCH}_2^a\text{CH}_2$), 1.44–1.54 (m, 3 H, CHCH_2^bCH , CCH_2^bCH , $\text{CHCH}_2\text{CH}_2^a$), 1.70–1.79 (m, 1 H, $\text{CHCH}_2\text{CH}_2^b$), 1.84–1.94 (m, 2 H, CHCHCH_2 , $\text{CHCH}_2^b\text{CH}_2$), 2.40 (t, J = 4.3 Hz, 1 H, CHCHCH), 2.46 (s, 2 H, CCH_2C), 3.78 (s, 3 H, CH_3), 4.16 (p, J = 2.6 Hz, 1 H, NCHCH_2), 6.79–6.84 (m, 2 H, CHCO), 7.02–7.07 (m, 2 H, CHCHCO), 8.24 (d, J = 4.1 Hz, 1 H, NCHCH).

^{13}C NMR (125 MHz, CDCl_3): δ = 31.7 (CHCH_2CH_2), 33.3 (CHCHCH_2), 36.5 (CHCH_2CH_2), 36.9 (CHCH_2CH), 40.7 (CCH_2CH), 46.2 (CCH_2C), 46.7 (CHCCH_2), 47.8 (NCHCH), 53.8 (NCHCH_2), 55.3 (CH_3), 113.5 (CHCO), 130.9 (CCHCHCO), 131.2 (CHCHCO), 158.2 (CO), 171.0 (NCHCH).

HRMS (ESI): m/z [$\text{M} + \text{H}$] $^+$ calcd for $\text{C}_{17}\text{H}_{22}\text{N}$: 256.1696; found: 256.1695.

rac-3-Methyl-10-azatricyclo[5.3.1.0^{3,8}]undec-9-en (rac-15a)

Synthesis according to GP2 from dihydropyridine **9a** (410 mg, 1.28 mmol) and TFA (2.19 g, 19.2 mmol, 1.47 mL) in pentane (12.8 mL). Purification by FC (Al_2O_3 -basic, activity III, pentane/ CH_2Cl_2 /MeOH, 88:10:2) afforded **rac-15a**.

Yield: 160 mg (77%); yellow oil; R_f = 0.21 (Al_2O_3 ; pentane/ CH_2Cl_2 /MeOH, 88:10:2).

IR (film): 3404, 2993, 2922, 2862, 1614, 1469, 1454, 1338, 1134, 1001, 922, 892, 681, 642 cm^{-1} .

^1H NMR (400 MHz, CDCl_3): δ = 0.80 (s, 3 H, CH_3), 1.05–1.19 (m, 3 H, $\text{CCH}_2^a\text{CH}_2$, NCHCH_2^aC , $\text{NCHCH}_2^b\text{CH}$), 1.26–1.39 (m, 2 H, $\text{CCH}_2^b\text{CH}_2$, $\text{CHCH}_2^a\text{CH}_2$), 1.39–1.60 (m, 5 H, $\text{CH}_2\text{CH}_2\text{CH}_2$, $\text{CHCH}_2^b\text{CH}_2$, NCHCH_2^bC , $\text{NCHCH}_2^b\text{CH}$), 1.70 (dp, J = 11.6, 3.4 Hz, 1 H, CHCH_2CH_2), 1.99 (t, J = 3.7 Hz, 1 H, NCHCH), 4.17–4.21 (m, 1 H, NCHCH_2), 8.37 (d, J = 4.2 Hz, 1 H, NCHCH).

^{13}C NMR (100 MHz, CDCl_3): δ = 17.1 ($\text{CH}_2\text{CH}_2\text{CH}_2$), 27.3 (CHCH_2CH_2), 28.4 (CHCH_2CH_2), 28.6 (CHCH_2CH), 32.0 (CCH_3), 32.3 (CH_3), 36.6 (NCHCH_2C), 37.8 (CCH_2CH_2), 46.3 (NCHCH), 54.8 (NCHCH_2), 174.8 (NCHCH).

HRMS (EI): m/z [M] $^+$ calcd for $\text{C}_{11}\text{H}_{17}\text{N}$: 163.1356; found: 163.1365.

rac-3-Phenyl-10-azatricyclo[5.3.1.0^{3,8}]undec-9-en (rac-15b)

Synthesis according to GP2 from dihydropyridine **9b** (200 mg, 0.52 mmol) and TFA (896 mg, 7.86 mmol, 0.60 mL) in pentane (5.2 mL). Purification by FC (Al_2O_3 -basic, activity III, pentane/ CH_2Cl_2 /MeOH, 88:10:2) afforded **rac-15b**.

Yield: 87 mg (74%); yellow oil; R_f = 0.26 (Al_2O_3 ; pentane/ CH_2Cl_2 /MeOH, 84:14:2).

IR (film): 3055, 3024, 2925, 2858, 1616, 1495, 1469, 1444, 1338, 1030, 955, 893, 760, 702 cm^{-1} .

^1H NMR (400 MHz, CDCl_3): δ = 1.32–1.48 (m, 3 H, CHCH_2^aCH , $\text{CCH}_2^a\text{CH}_2$, $\text{CHCH}_2^b\text{CH}_2$), 1.54–1.68 (m, 3 H, $\text{CH}_2\text{CH}_2^a\text{CH}_2$, CHCH_2^bCH , $\text{CHCH}_2^b\text{CH}_2$), 1.69–1.83 (m, 2 H, $\text{CCH}_2^b\text{CH}_2$, $\text{CH}_2\text{CH}_2^b\text{CH}_2$), 1.88–2.01 (m, 3 H, NCHCH_2C , CHCH_2CH_2), 2.89 (t, J = 3.7 Hz, 1 H, NCHCH), 4.28 (p, J = 2.8 Hz, 1 H, NCHCH_2), 7.10–7.16 (m, 1 H, CCHCHCH), 7.22–7.30 (m, 4 H, CCHCHCH , CCHCHCH), 8.43 (d, J = 4.0 Hz, 1 H, NCHCH).

^{13}C NMR (100 MHz, CDCl_3): δ = 17.3 ($\text{CH}_2\text{CH}_2\text{CH}_2$), 27.2 (CHCH_2CH_2), 28.3 (CHCH_2CH_2), 29.4 (CHCH_2CH), 37.3 (NCHCH_2C), 40.5 (CCH_2CH_2), 40.7 (CCH_2), 42.1 (NCHCH), 54.2 (NCHCH_2), 125.7 (CCHCHCH), 126.1 (CCHCHCH), 128.4 (CCHCHCH), 152.6 (CCCH_2), 173.9 (NCHCH).

HRMS (EI): m/z [M] $^+$ calcd for $\text{C}_{16}\text{H}_{19}\text{N}$: 225.1512; found: 225.1506.

rac-3-Benzyl-10-azatricyclo[5.3.1.0^{3,8}]undec-9-en (rac-15c)

Synthesis according to GP2 from dihydropyridine **9c** (420 mg, 1.06 mmol) and TFA (1.81 g, 15.9 mmol, 1.22 mL) in pentane (10.6 mL). Purification by FC (Al_2O_3 -basic, activity III, pentane/ CH_2Cl_2 /MeOH, 88:10:2) afforded **rac-15c**.

Yield: 188 mg (74%); colorless oil; R_f = 0.22 (Al_2O_3 ; pentane/ CH_2Cl_2 /MeOH, 88:10:2).

IR (film): 3084, 3057, 2926, 2848, 1014, 1495, 1469, 1450, 1340, 1120, 1068, 1025, 974, 758, 706 cm^{-1} .

^1H NMR (500 MHz, CDCl_3): δ = 1.12–1.24 (m, 3 H, $\text{CCH}_2^a\text{CH}_2$, $\text{CHCH}_2^a\text{CH}_2$, CHCH_2^aCH), 1.32–1.58 (m, 7 H, $\text{CCH}_2^b\text{CH}_2$, $\text{CHCH}_2^b\text{CH}_2$, CHCH_2^bCH , $\text{CH}_2\text{CH}_2\text{CH}_2$, NCHCH_2C), 1.70 (dp, J = 10.2, 3.4 Hz, 1 H, CHCH_2CH_2), 2.09 (t, J = 3.7 Hz, 1 H, NCHCH), 2.35 (d, J = 13.2 Hz, 1 H, CCH_2^aC), 2.44 (d, J = 13.2 Hz, 1 H, CCH_2^bC), 4.23–4.29 (m, 1 H,

4309

Synthesis

H.-K. A. Rudy, K. T. Wanner

Paper

NCHCH₂), 7.09–7.13 (m, 2 H, CCHCHCH), 7.19–7.24 (m, 1 H, CCHCHCH), 7.25–7.30 (m, 2 H, CCHCHCH), 8.51 (d, *J* = 4.1 Hz, 1 H, NCHCH).

¹³C NMR (125 MHz, CDCl₃): δ = 16.7 (CH₂CH₂CH₂), 27.2 (CHCH₂CH₂), 28.1 (CHCH₂CH₂), 29.2 (CHCH₂CH), 33.9 (CCH₂CH₂), 35.3 (NCHCH₂C), 36.4 (CCH₂CH₂), 43.3 (NCHCH), 50.6 (CCH₂C), 54.6 (NCHCH₂), 126.3 (CCHCHCH), 128.0 (CCHCHCH), 130.9 (CCHCHCH), 137.9 (CCHCHCH), 174.7 (NCHCH).

HRMS (ESI): *m/z* [M+H]⁺ calcd for C₁₇H₂₂N: 240.1747; found: 240.1745.

rac-3-(4-Methoxyphenyl)-10-azatricyclo[5.3.1.0^{3,8}]undec-9-en (rac-15d)

Synthesis according to GP2 from dihydropyridine **9d** (900 mg, 2.19 mmol) and TFA (3.74 g, 32.8 mmol, 2.51 mL) in pentane (21.9 mL). Purification by FC (Al₂O₃-basic, activity III, pentane/CH₂Cl₂/MeOH, 88:10:2) afforded **rac-15d**.

Yield: 301 mg (54%); colorless solid; mp 75 °C; *R*_f = 0.18 (Al₂O₃; pentane/CH₂Cl₂/MeOH, 88:10:2).

IR (KBr): 2989, 2929, 2843, 1612, 1514, 1441, 1284, 1252, 1180, 1111, 1030, 893, 820, 690, 553 cm⁻¹.

¹H NMR (500 MHz, CDCl₃): δ = 1.30–1.44 (m, 3 H, CHCH₂^aCH, CCH₂^aCH₂, CHCH₂^aCH₂), 1.52–1.64 (m, 3 H, CH₂CH₂^aCH₂, CHCH₂^bCH, CHCH₂^bCH₂), 1.66–1.75 (m, 2 H, CCH₂^bCH₂, CH₂CH₂^bCH₂), 1.85–1.96 (m, 3 H, NCHCH₂C, CHCH₂CH₂), 2.81 (t, *J* = 3.7 Hz, 1 H, NCHCH), 3.76 (s, 3 H, OCH₃), 4.24–4.28 (m, 1 H, NCHCH₂), 6.77–6.82 (m, 2 H, CHCO), 7.13–7.18 (m, 2 H, CHCHCO), 8.39 (d, *J* = 3.9 Hz, 1 H, NCHCH).

¹³C NMR (125 MHz, CDCl₃): δ = 17.4 (CH₂CH₂CH₂), 27.3 (CHCH₂CH₂), 28.3 (CHCH₂CH₂), 29.4 (CHCH₂CH), 37.2 (NCHCH₂C), 39.9 (CCH₂), 40.5 (CCH₂CH₂), 42.5 (NCHCH), 54.3 (NCHCH₂), 55.4 (OCH₃), 113.8 (CHCO), 127.1 (CHCHCO), 144.8 (CCH₂), 157.4 (COCH₃), 174.0 (NCHCH).

HRMS (ESI): *m/z* [M + H]⁺ calcd for C₁₇H₂₂NO: 256.1696; found: 256.1694.

rac-3-(4-Methoxybenzyl)-10-azatricyclo[5.3.1.0^{3,8}]undec-9-en (rac-15e)

Synthesis according to GP2 from dihydropyridine **9e** (430 mg, 1.01 mmol) and TFA (1.73 g, 15.2 mmol, 1.16 mL) in pentane (10.1 mL). Purification by FC (Al₂O₃-basic, activity III, pentane/CH₂Cl₂/MeOH, 88:10:2) afforded **rac-15e**.

Yield: 241 mg (89%); yellow oil; *R*_f = 0.20 (Al₂O₃; pentane/CH₂Cl₂/MeOH, 88:10:2).

IR (film): 2993, 2925, 2848, 2062, 1882, 1612, 1512, 1468, 1442, 1248, 1178, 1122, 1036, 822, 758, 729, 700 cm⁻¹.

¹H NMR (400 MHz, CDCl₃): δ = 1.10–1.23 (m, 3 H, CCH₂^aCH₂, CHCH₂^aCH₂, CHCH₂^aCH), 1.28–1.36 (m, 2 H, CCH₂^bCH₂, NCHCH₂^aC), 1.39 (dd, *J* = 13.6, 2.0 Hz, 1 H, NCHCH₂^bC), 1.41–1.58 (m, 4 H, CHCH₂^bCH₂, CHCH₂^bCH, CH₂CH₂CH₂), 1.69 (dp, *J* = 10.0, 3.3 Hz, 1 H, CHCH₂CH₂), 2.07 (t, *J* = 3.8 Hz, 1 H, NCHCH), 2.28 (d, *J* = 13.2 Hz, 1 H, CCH₂^aC), 2.37 (d, *J* = 13.2 Hz, 1 H, CCH₂^bC), 3.79 (s, 3 H, OCH₃), 4.22–4.27 (m, 1 H, NCHCH₂), 6.78–6.84 (m, 2 H, CHCO), 6.98–7.05 (m, 2 H, CHCHCO), 8.49 (d, *J* = 4.2 Hz, 1 H, NCHCH).

¹³C NMR (100 MHz, CDCl₃): δ = 16.7 (CH₂CH₂CH₂), 27.2 (CHCH₂CH₂), 28.2 (CHCH₂CH₂), 29.2 (CHCH₂CH), 33.9 (CCH₂CH₂), 35.2 (NCHCH₂C), 36.4 (CCH₂CH₂), 43.3 (NCHCH), 49.7 (CCH₂C), 54.6 (NCHCH₂), 55.3 (OCH₃), 113.4 (CHCO), 130.0 (CCHCHCO), 131.7 (CHCHCO), 158.2 (COCH₃), 174.7 (NCHCH).

HRMS (ESI): *m/z* [M + H]⁺ calcd for C₁₈H₂₄NO: 270.1852; found: 270.1851.

Supporting Information

Supporting information for this article is available online at <https://doi.org/10.1055/s-0039-1690619>.

References

- (1) (a) Sharma, V. K.; Singh, S. K. *RSC Adv.* **2017**, *7*, 2682. (b) Silva, A.; Silva, E.; Varandas, P. *Synthesis* **2013**, *45*, 3053. (c) Lavilla, R. *J. Chem. Soc., Perkin Trans. 1* **2002**, 1141. (d) Belenky, P.; Bogan, K. L.; Brenner, C. *Trends Biochem. Sci.* **2007**, *32*, 12. (e) World Health Organization (WHO) *Model List of Essential Medicines* **2017**, 1–58.
- (2) (a) Eisner, U.; Kuthan, J. *Chem. Rev.* **1972**, *72*, 1. (b) Stout, D. M.; Meyers, A. I. *Chem. Rev.* **1982**, *82*, 223. (c) Bull, J. A.; Mousseau, J. J.; Pelletier, G.; Charette, A. B. *Chem. Rev.* **2012**, *112*, 2642.
- (3) (a) Jochmann, P.; Dols, T. S.; Spaniol, T. P.; Perrin, L.; Maron, L.; Okuda, J. *Angew. Chem. Int. Ed.* **2010**, *49*, 7795. (b) Lichtenberg, C.; Spaniol, T. P.; Perrin, L.; Maron, L.; Okuda, J. *Chem. Eur. J.* **2012**, *18*, 6448.
- (4) (a) Yamaguchi, R.; Moriyasu, M.; Yoshioka, M.; Kawanisi, M. *J. Org. Chem.* **1985**, *50*, 287. (b) Corey, E. J.; Tian, Y. *Org. Lett.* **2005**, *7*, 5535.
- (5) (a) Charette, A. B.; Mathieu, S.; Martel, J. *Org. Lett.* **2005**, *7*, 5401. (b) Schultz, A. G.; Flood, L.; Springer, J. P. *J. Org. Chem.* **1986**, *51*, 838.
- (6) Bennasar, M.-L.; Juan, C.; Bosch, J. *Tetrahedron Lett.* **2001**, *42*, 585.
- (7) (a) Yamada, S.; Inoue, M. *Org. Lett.* **2007**, *9*, 1477. (b) Courtois, G.; Al-Arnaout, A.; Miginiac, L. *Tetrahedron Lett.* **1985**, *26*, 1027.
- (8) (a) Sandoval, J. J.; Palma, P.; Alvarez, E.; Rodríguez-Delgado, A.; Cámpora, J. *Chem. Commun.* **2013**, *49*, 6791. (b) Cámpora, J.; Pérez, C. M.; Rodríguez-Delgado, A.; Naz, A. M.; Palma, P.; Álvarez, E. *Organometallics* **2007**, *26*, 1104. (c) Sandoval, J. J.; Melero, C.; Palma, P.; Álvarez, E.; Rodríguez-Delgado, A.; Cámpora, J. *Organometallics* **2016**, *35*, 3336.
- (9) (a) Krow, G. R.; Lee, Y. B.; Raghavachari, R.; Szczepanski, S. W.; Alston, P. V. *Tetrahedron* **1991**, *47*, 8499. (b) Comins, D. L.; Mantlo, N. B. *Tetrahedron Lett.* **1987**, *28*, 759. (c) Rudler, H.; Denise, B.; Xu, Y.; Parlier, A.; Vaissermann, J. *Eur. J. Org. Chem.* **2005**, *3724*.
- (10) (a) Schmaunz, C. E.; Mayer, P.; Wanner, K. T. *Synthesis* **2014**, *46*, 1630. (b) Bräckow, J.; Wanner, K. T. *Tetrahedron* **2006**, *62*, 2395.
- (11) (a) Satoh, N.; Akiba, T.; Yokoshima, S.; Fukuyama, T. *Angew. Chem. Int. Ed.* **2007**, *46*, 5734. (b) Khan, M. O. F.; Levi, M. S.; Clark, C. R.; Ablorderrey, S. Y.; Law, S.-J.; Wilson, N. H.; Borne, R. F. *Stud. Nat. Prod. Chem.* **2008**, *34*, 753.
- (12) (a) Hartman, G. D.; Halczenko, W.; Philipps, B. T. *J. Org. Chem.* **1985**, *50*, 2427. (b) Hartman, G. D.; Halczenko, W.; Philipps, B. T. *J. Org. Chem.* **1986**, *51*, 142. (c) Hartman, G. D.; Philipps, B. T.; Halczenko, W. *J. Org. Chem.* **1987**, *52*, 1136. (d) Hartman, G. D.; Philipps, B. T.; Halczenko, W.; Pitzemberger, S. M. *J. Org. Chem.* **1989**, *54*, 4137.
- (13) (a) Rappenglück, S.; Niessen, K.; Seeger, T.; Worek, F.; Thiermann, H.; Wanner, K. *Synthesis* **2017**, *49*, 4055. (b) Sperger, C. A.; Wanner, K. T. *Tetrahedron* **2009**, *65*, 5824. (c) Schmaunz, C. *Dissertation*; Ludwig-Maximilians Universität München: Germany, **2012**.

4310

Synthesis

H.-K. A. Rudy, K. T. Wanner

Paper

- (14) Claridge, T. D. W. *High-Resolution NMR Techniques in Organic Chemistry*, 2 ed., Vol. 27; Elsevier: Amsterdam, **2009**.
- (15) Jørgensen, K. A. *Angew. Chem. Int. Ed.* **2000**, 39, 3558.
- (16) Perrin, D. D.; Armarego, W. L. F. *Purification of Laboratory Chemicals*; Pergamon Press: New York, **1988**.
- (17) Hünig, S.; Kreitmeier, P.; Märkl, G.; Sauer, J. *Arbeitsmethoden in der Organischen Chemie*; Lehmanns: Berlin, **2006**.
- (18) Gottlieb, H. E.; Kotlyar, V.; Nudelman, A. J. *Org. Chem.* **1997**, 62, 7512.
- (19) Schmaunz, C.; Pabel, J.; Wanner, K. T. *Synthesis* **2010**, 13, 2147.
- (20) Yong, K. H.; Taylor, N. J.; Chong, J. M. *Org. Lett.* **2002**, 4, 3553.
- (21) (a) Núñez, A.; Sánchez, A.; Burgos, C.; Alvarez-Builla, J. *Tetrahedron* **2004**, 60, 6217. (b) Zhang, X.; McNally, A. *Angew. Chem.* **2017**, 56, 9833.

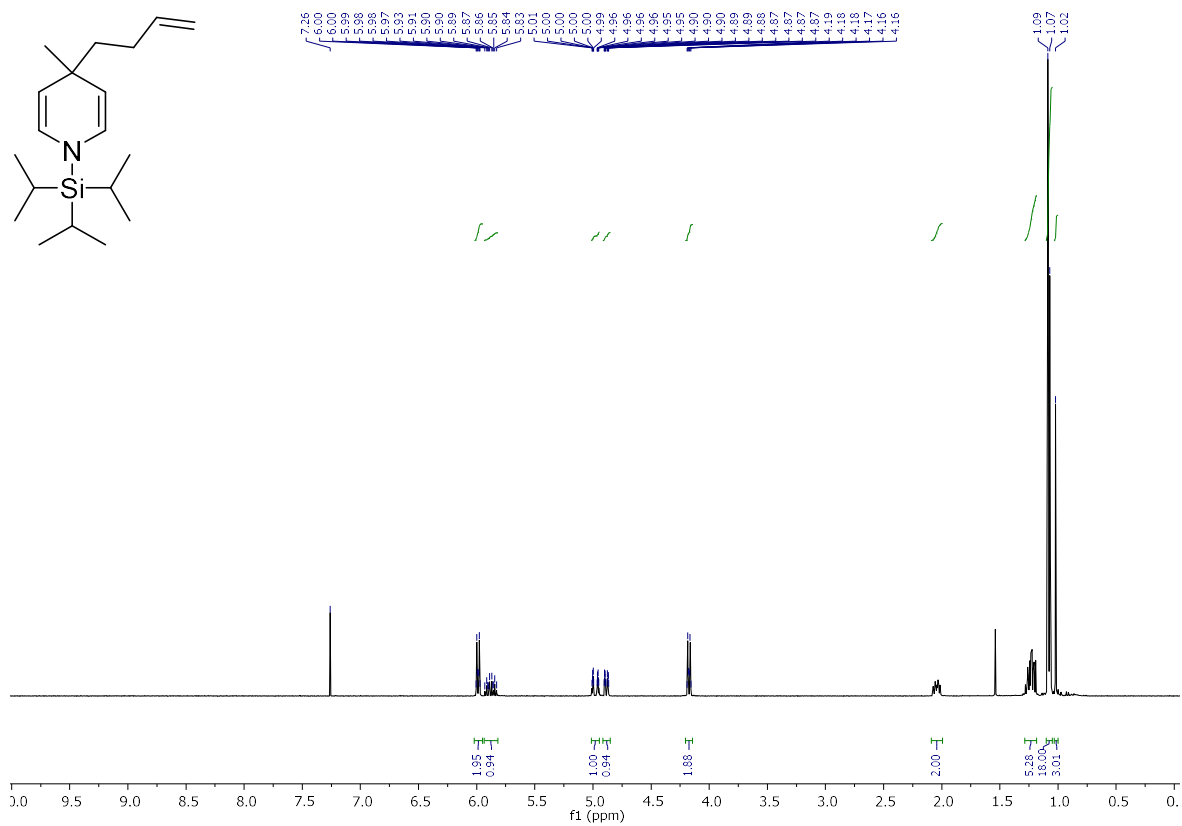
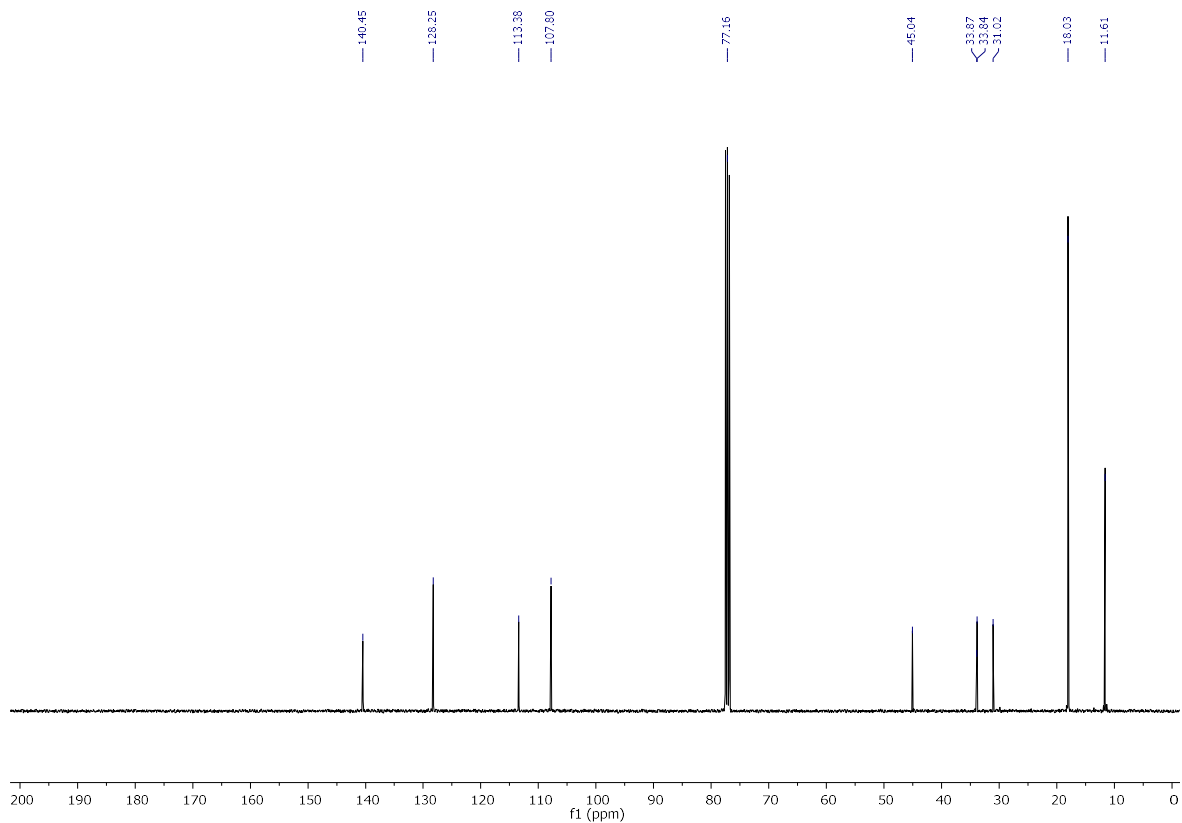


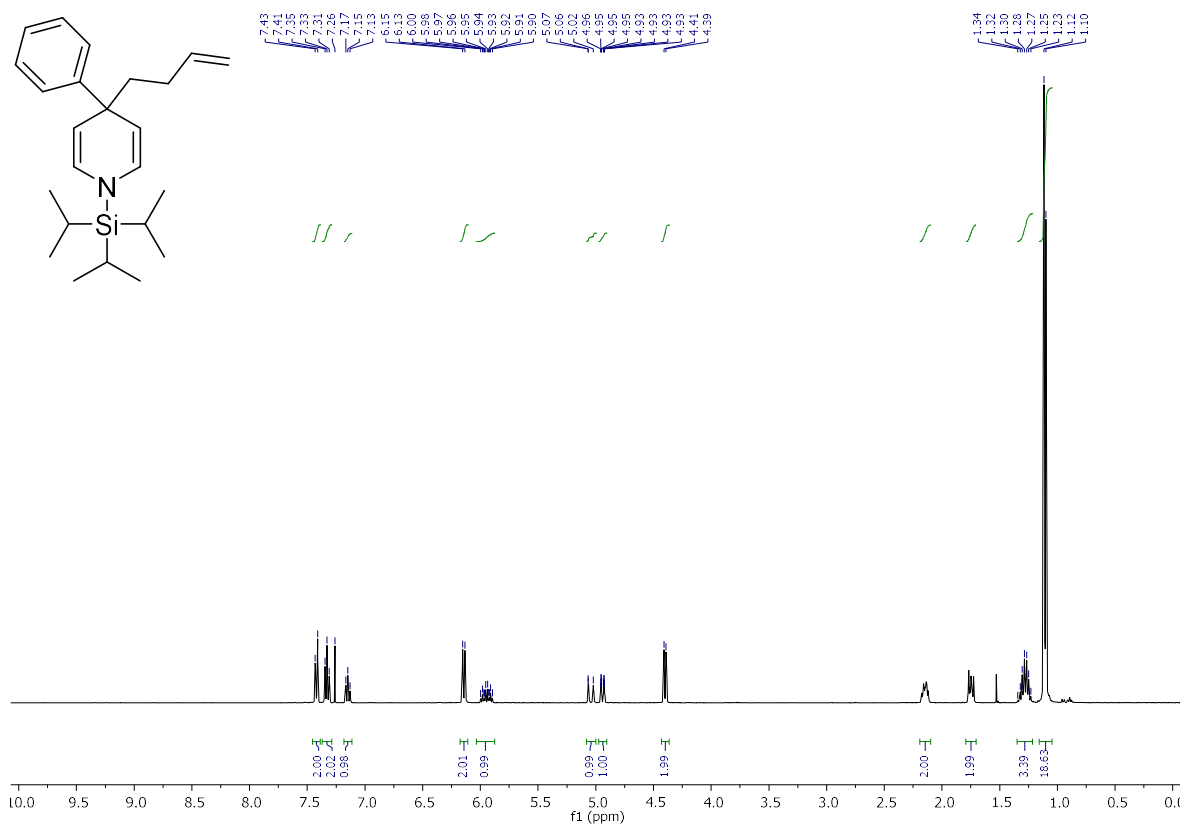
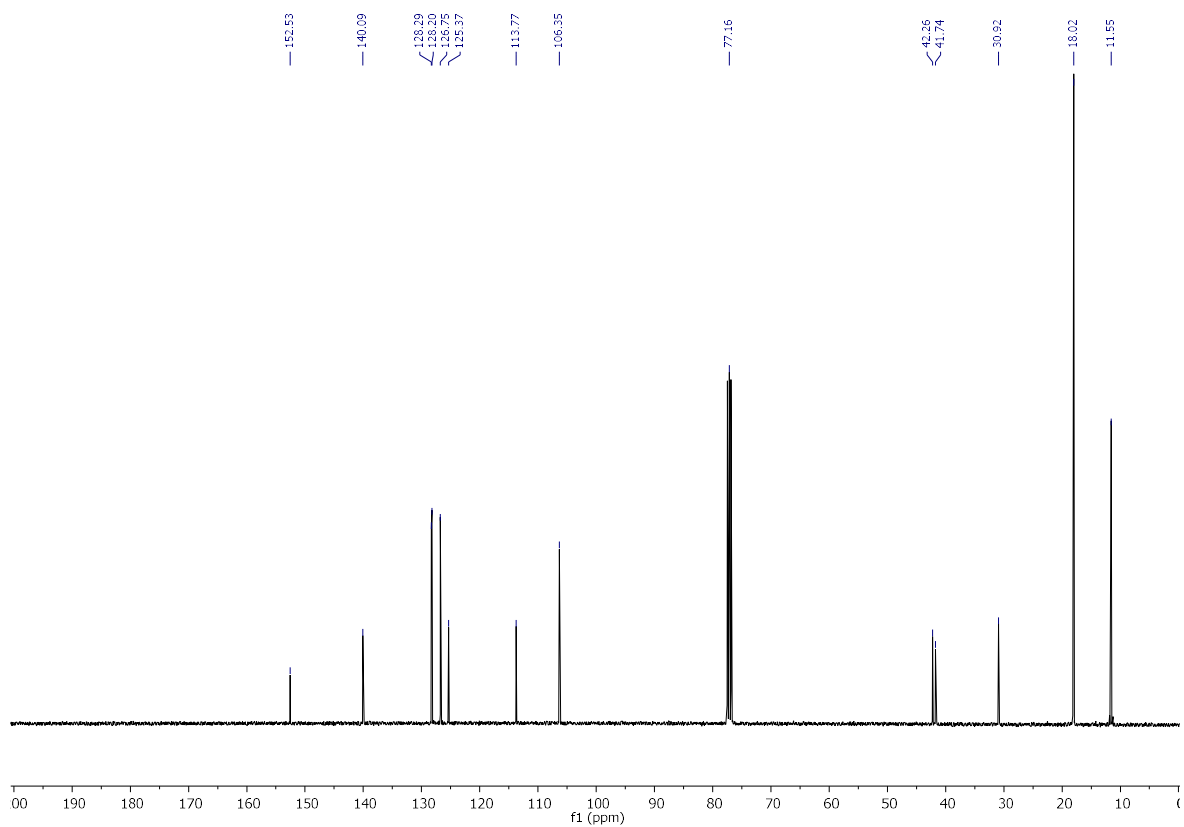
Supporting Information

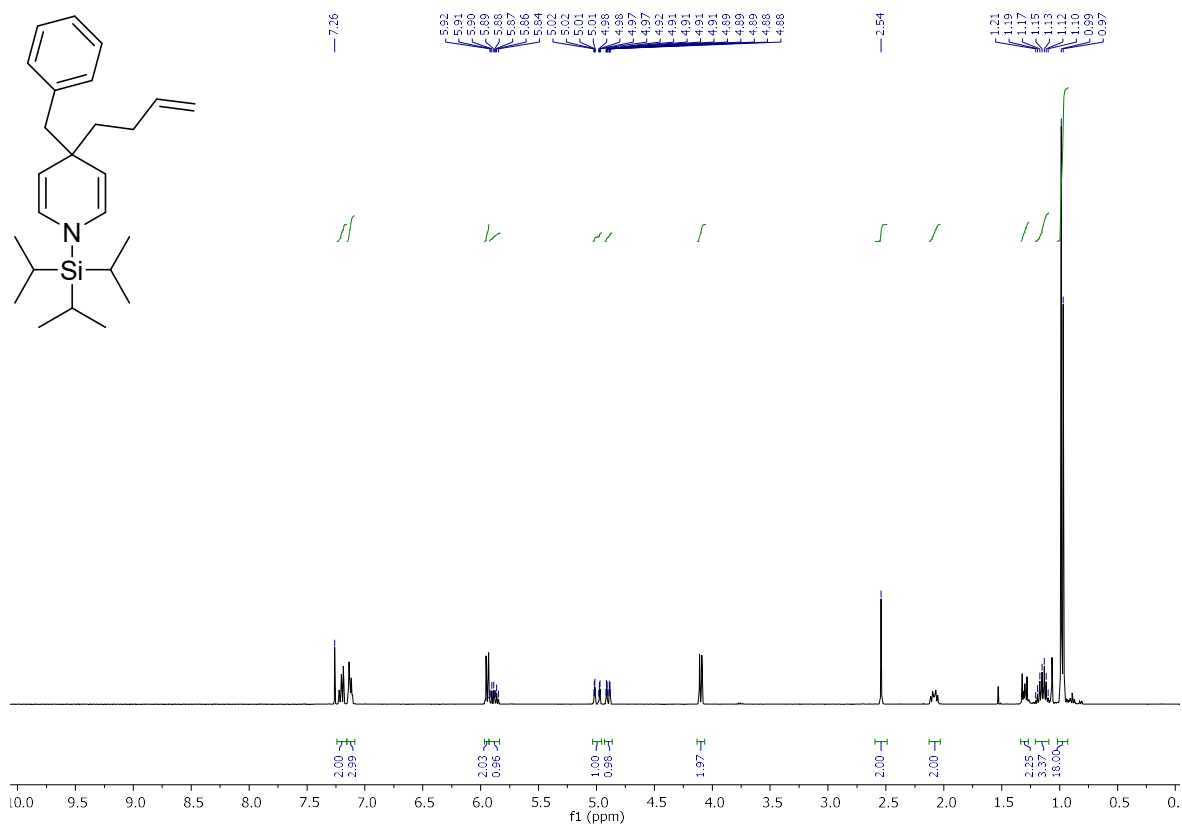
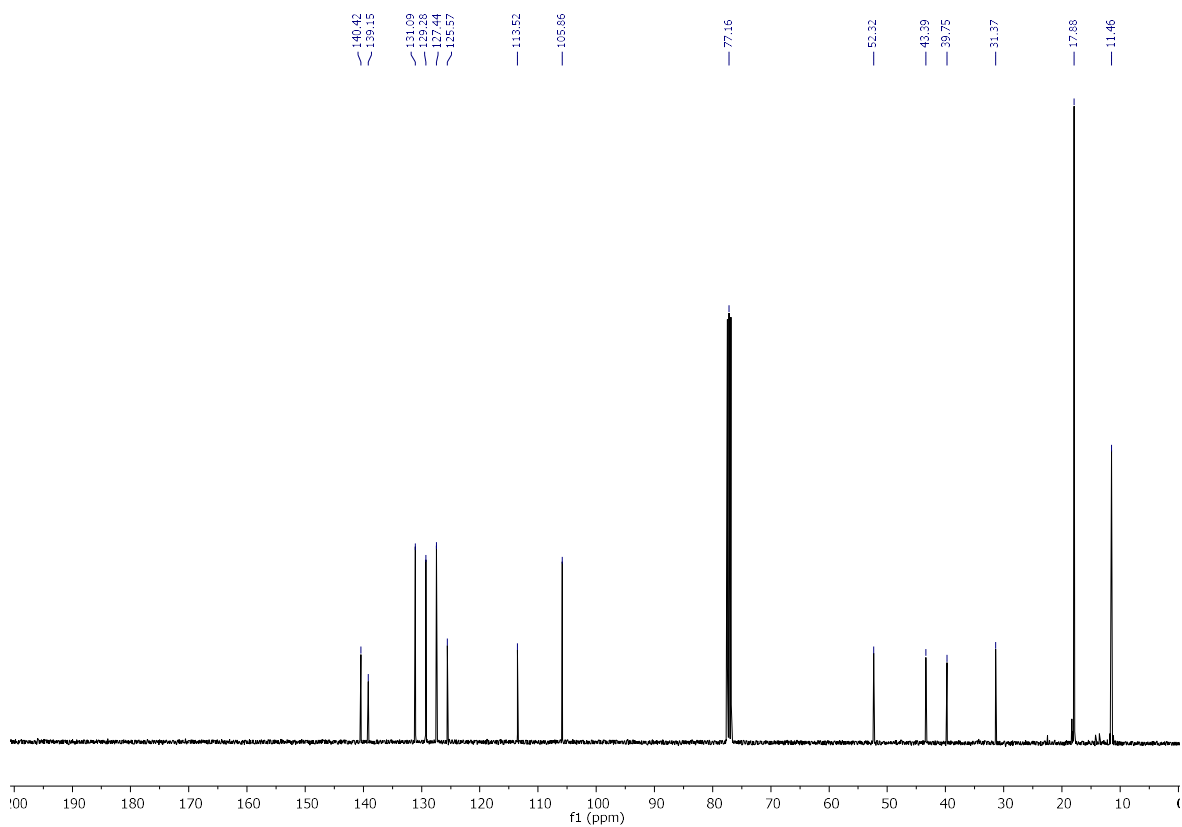
Accessing Tricyclic Imines Comprising an 2-Azabicyclo[2.2.2]octane Scaffold by Intramolecular Hetero-Diels-Alder Reactions of 4-Alkenyl Substituted *N*-Silyl-1,4-dihydropyridines

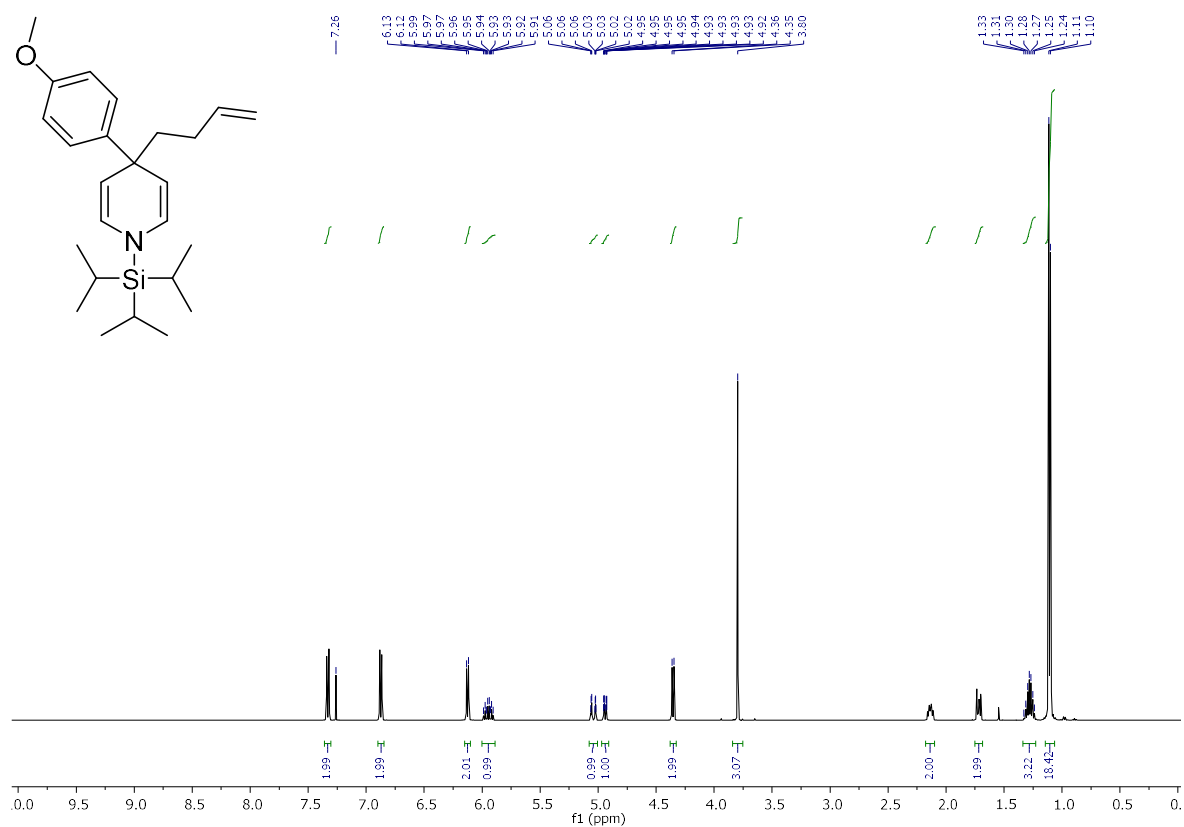
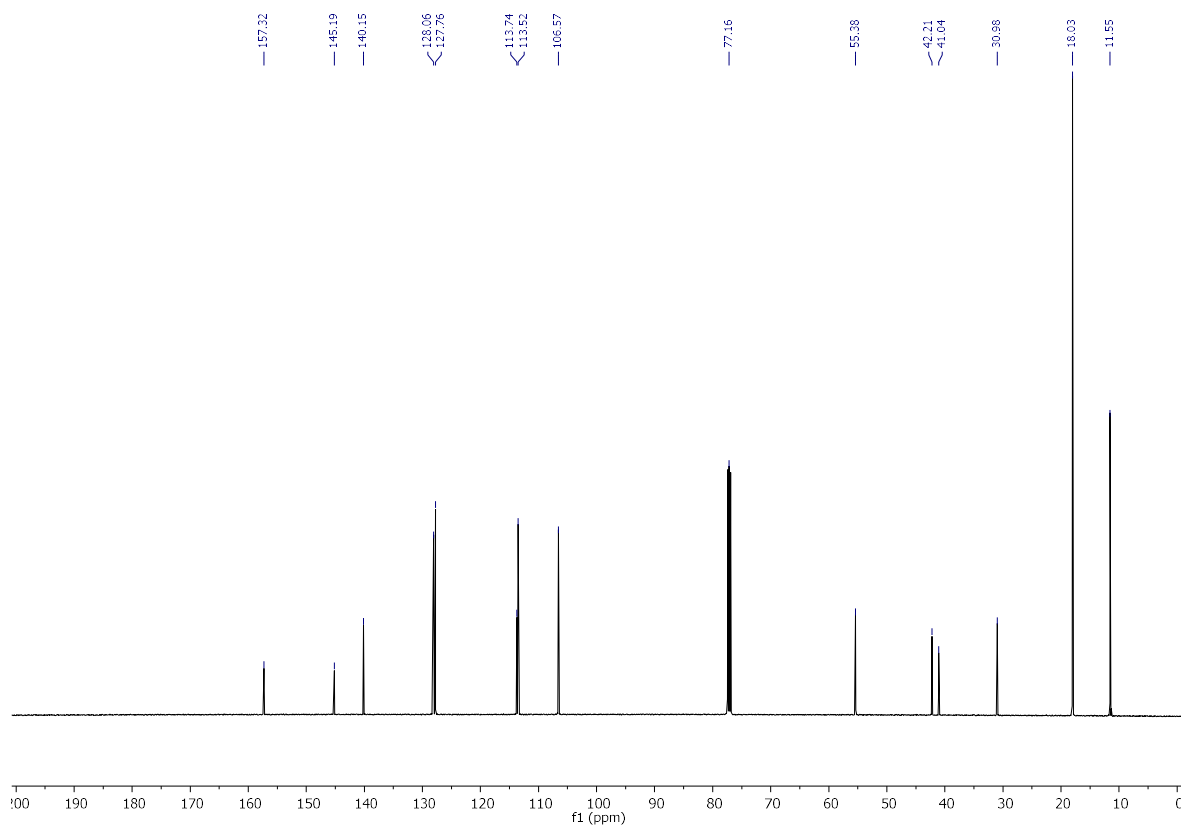
Heinrich-Karl A. Rudy,^a Klaus T. Wanner^{a*}

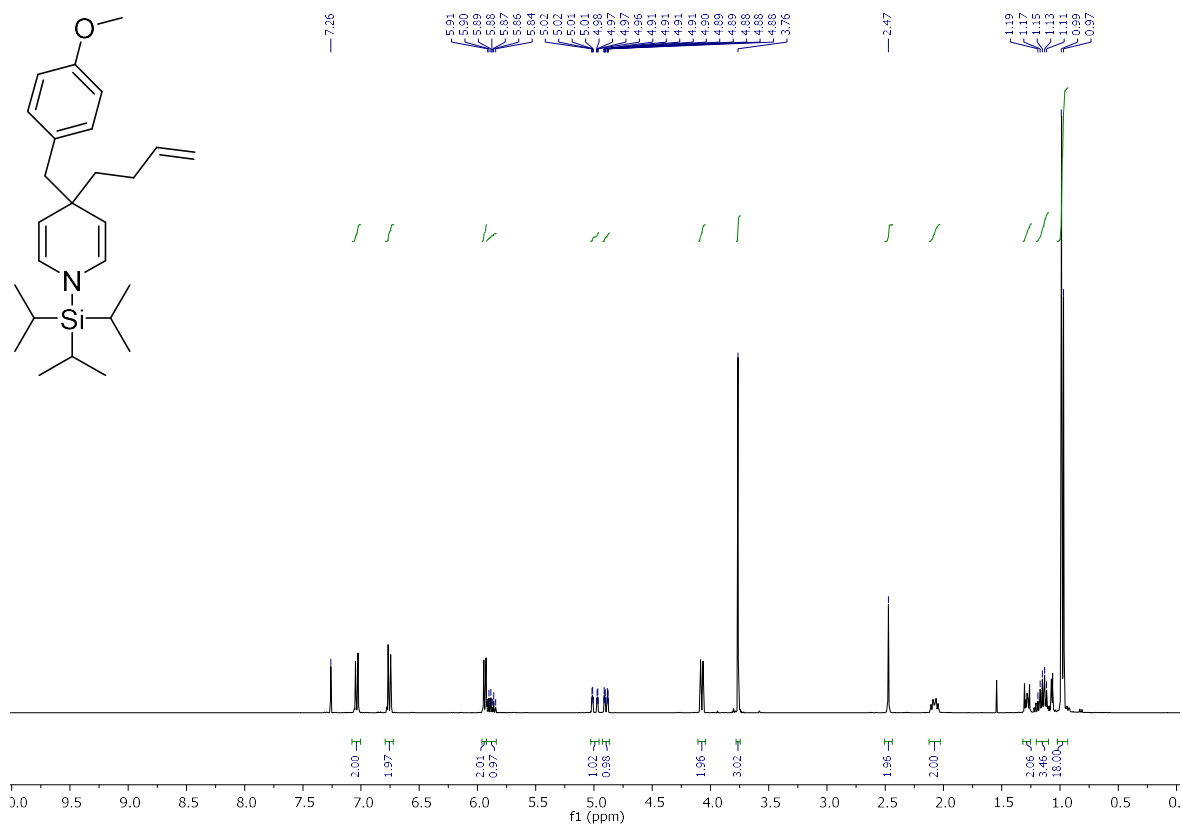
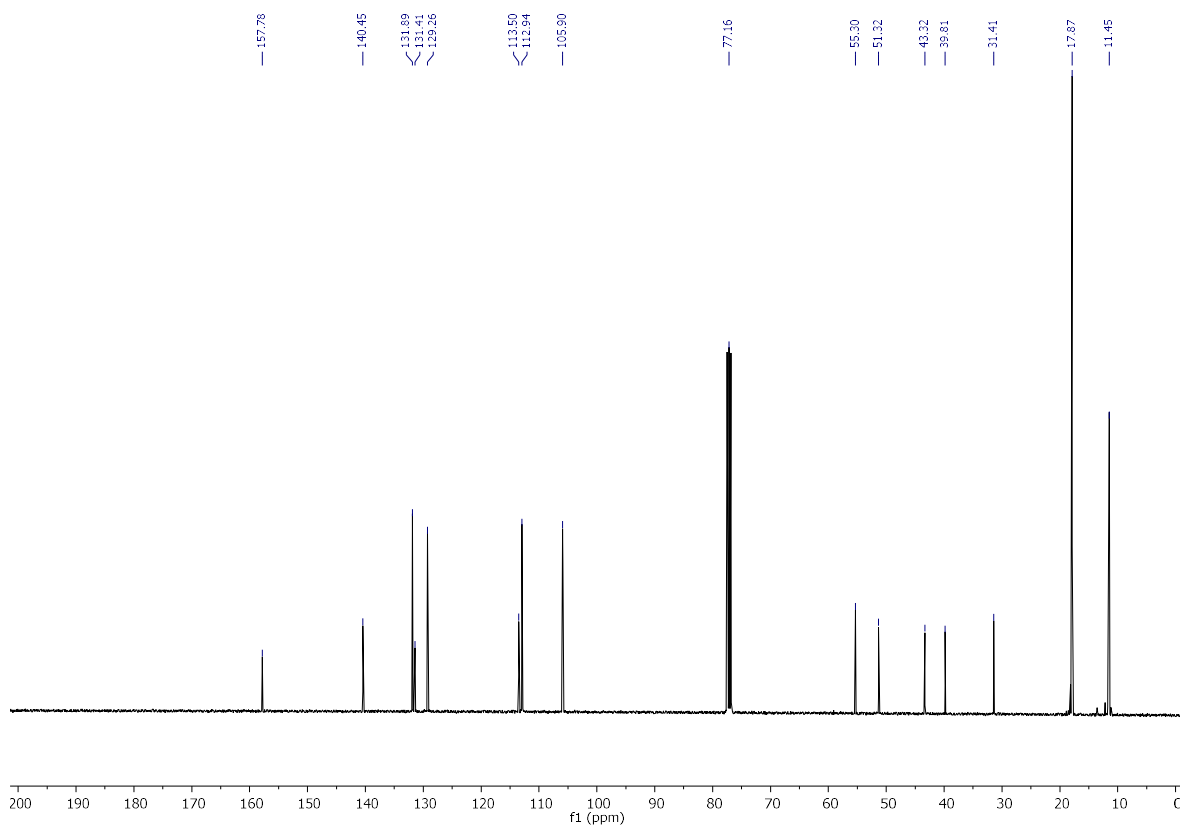
^a Ludwig-Maximilians-Universität München, Department für Pharmazie – Zentrum
für Pharmaforschung, Butenandtstr. 5-13, Haus C, 81377 Munich, Germany
klaus.wanner@cup.uni-muenchen.de

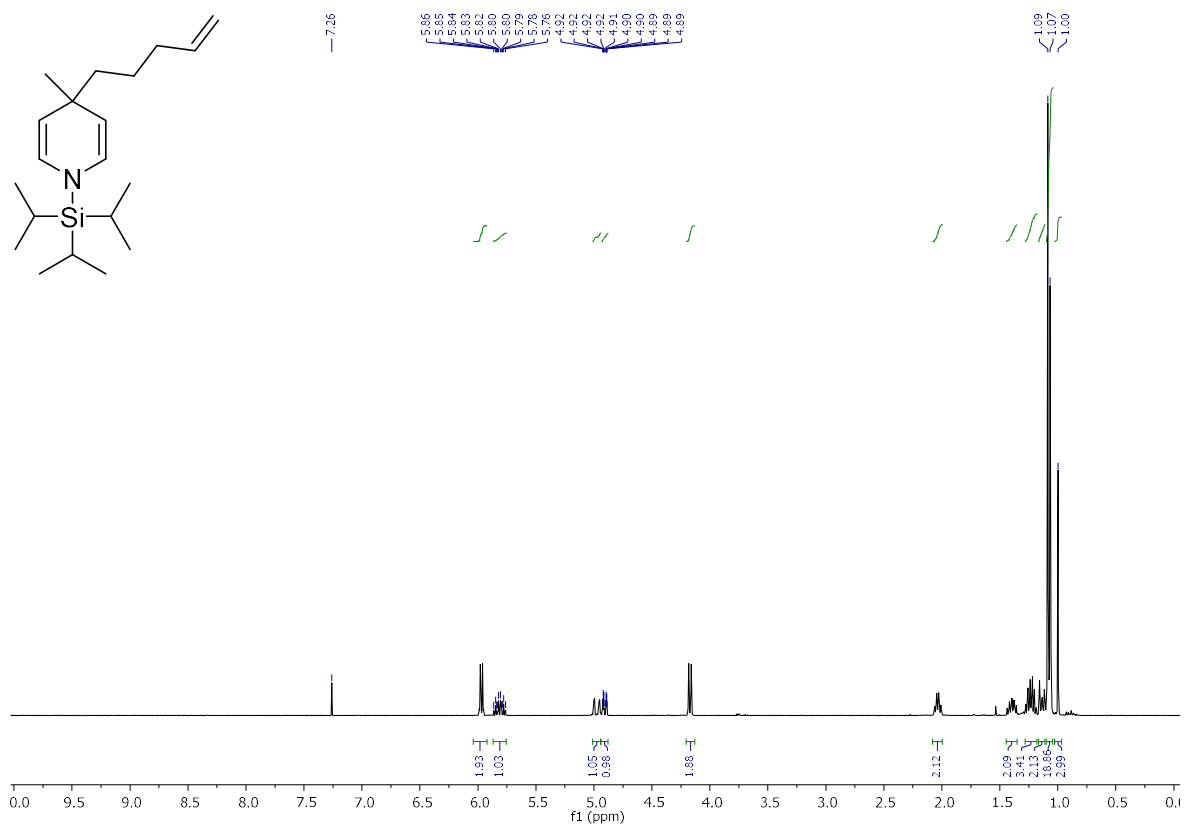
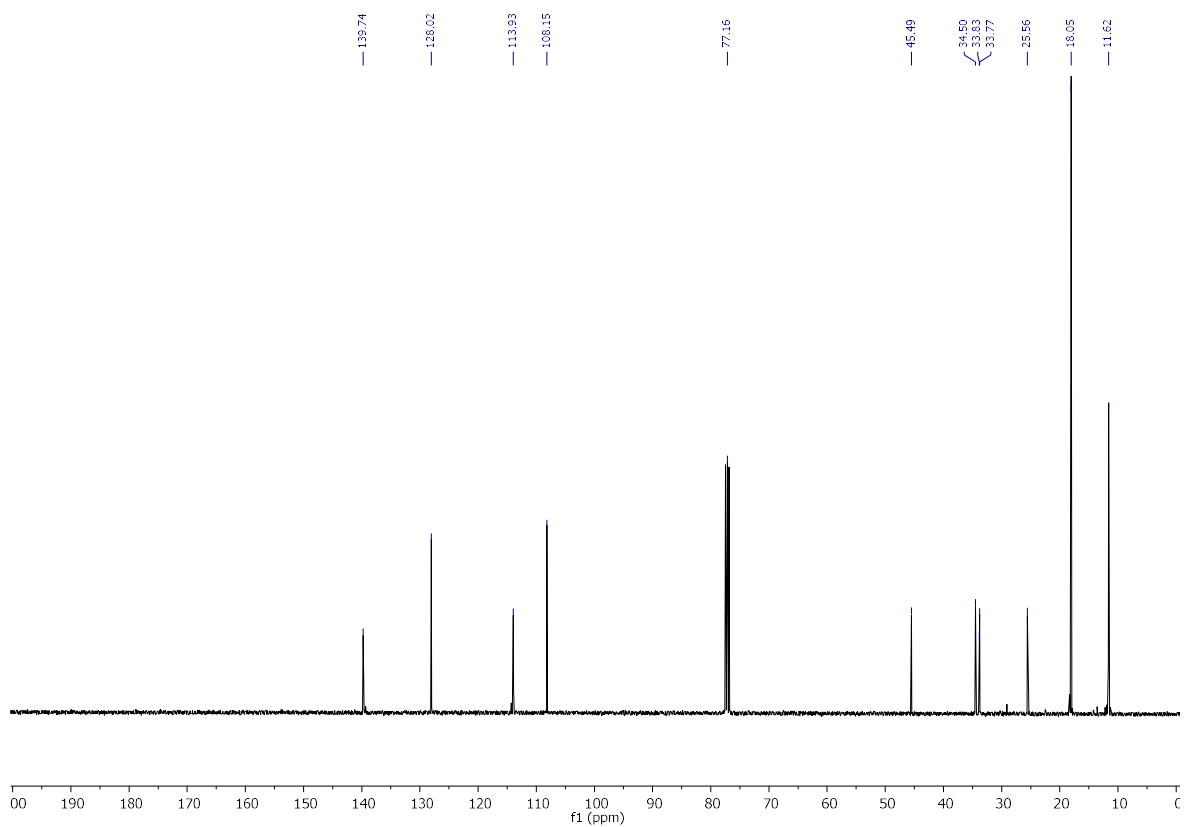
^1H and ^{13}C NMR spectra**7a (^1H):****7a (^{13}C):**

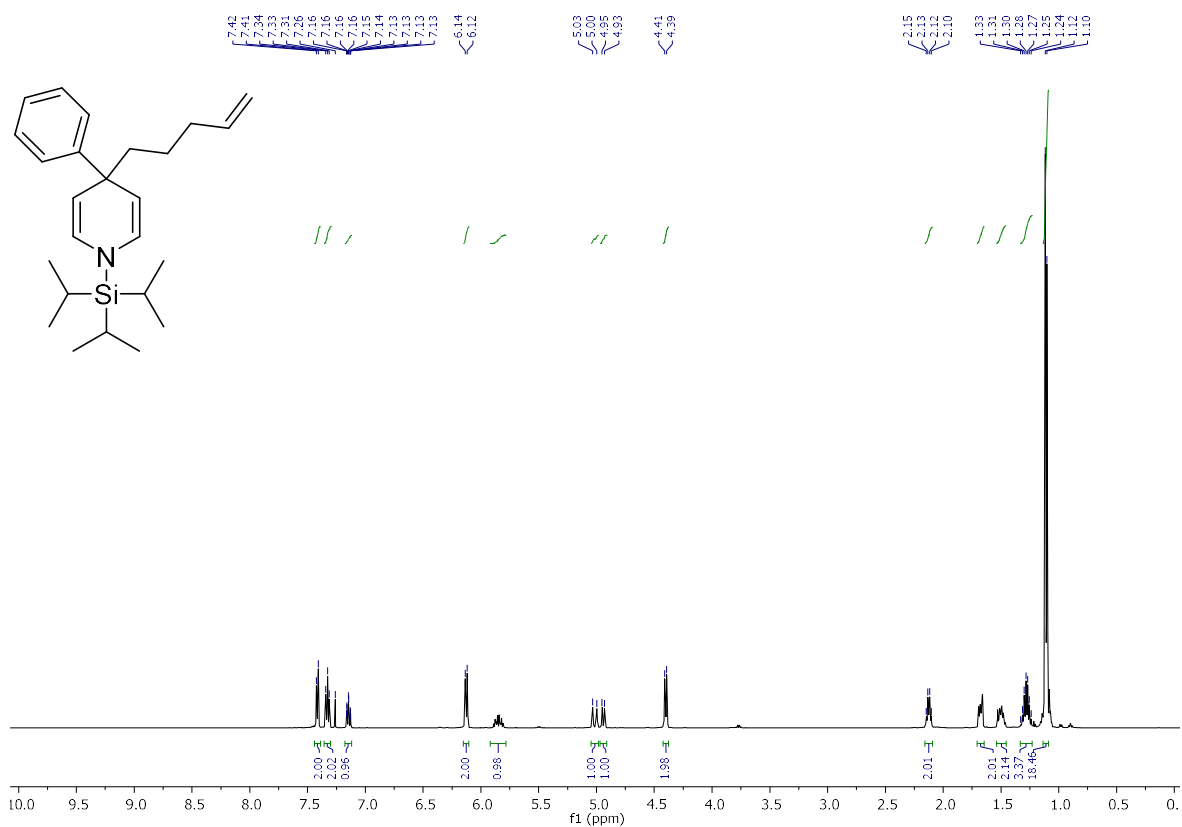
7b (^1H):**7b** (^{13}C):

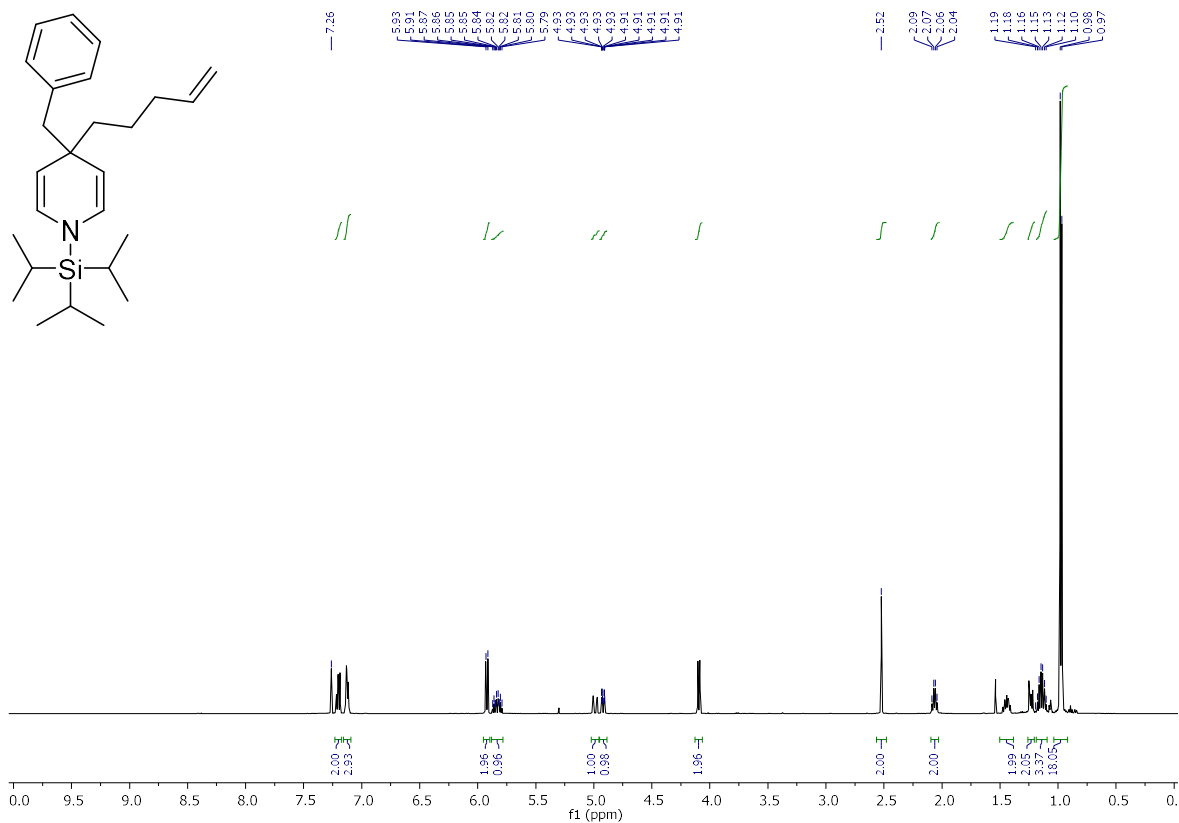
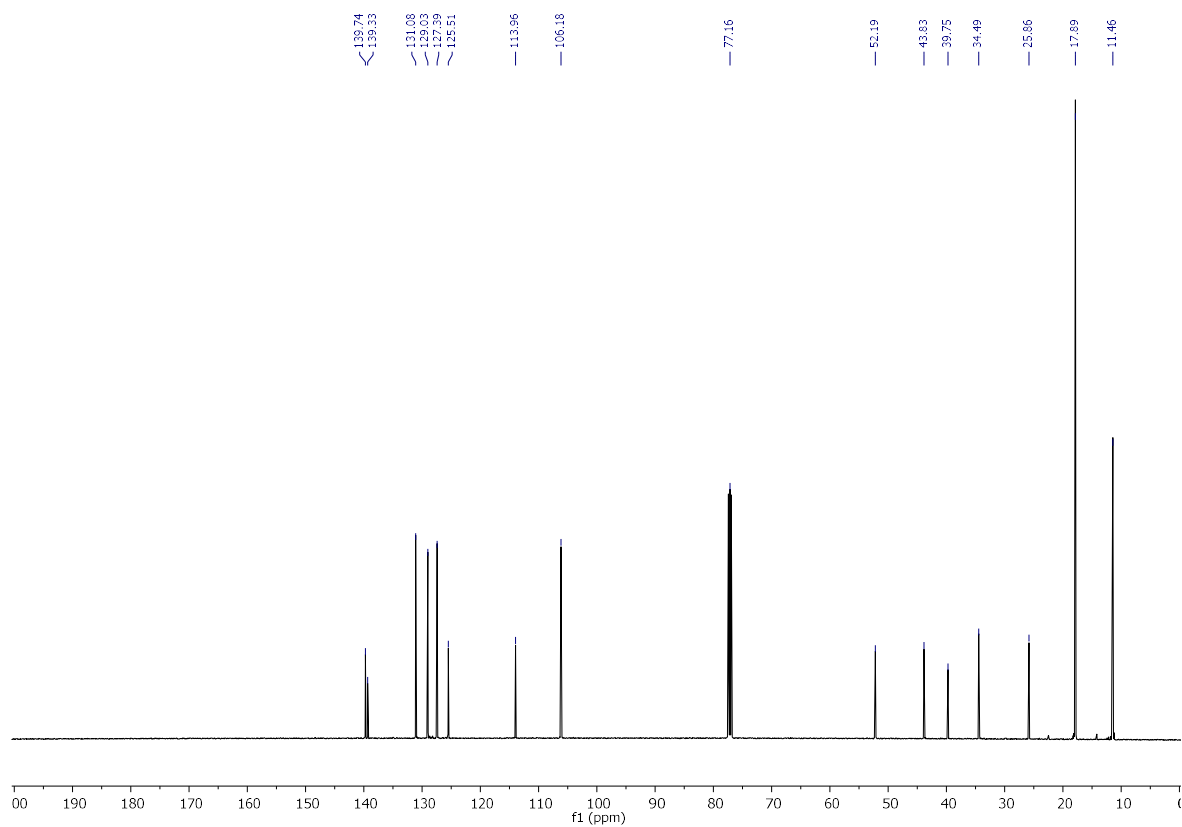
7c (^1H):**7c** (^{13}C):

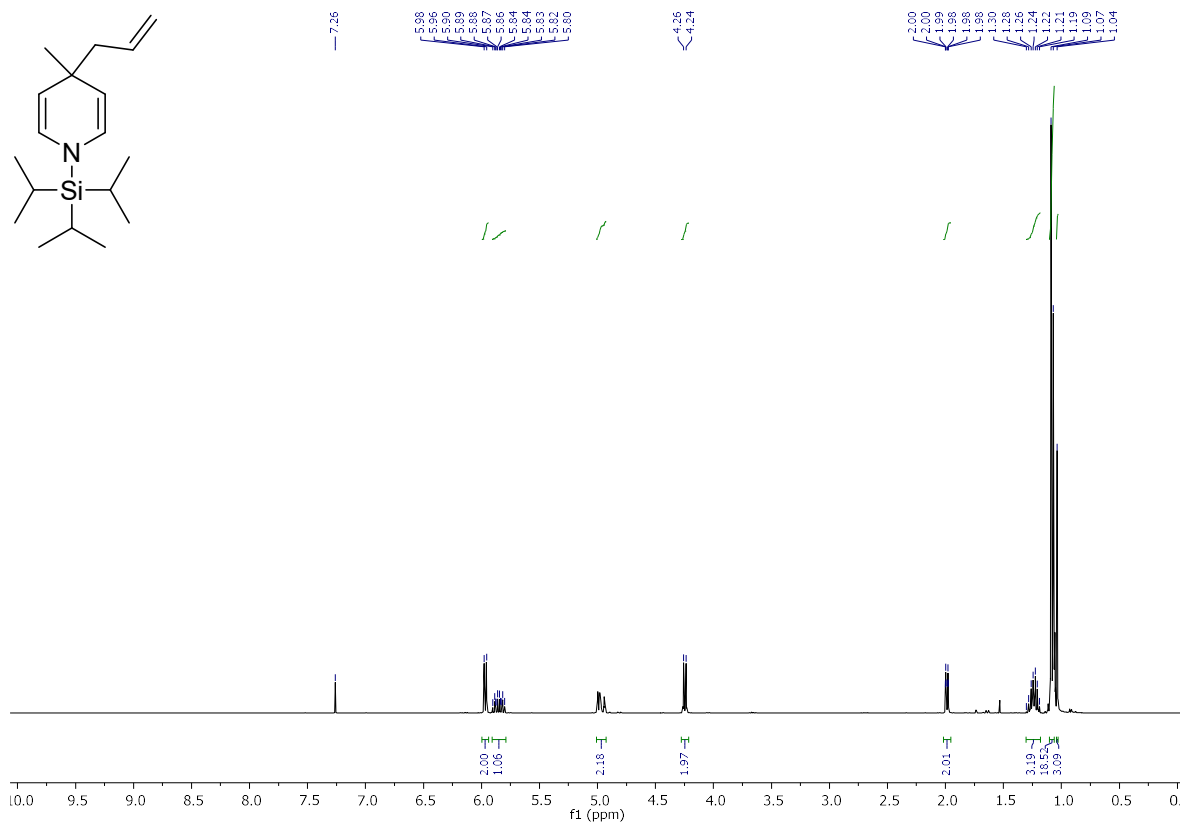
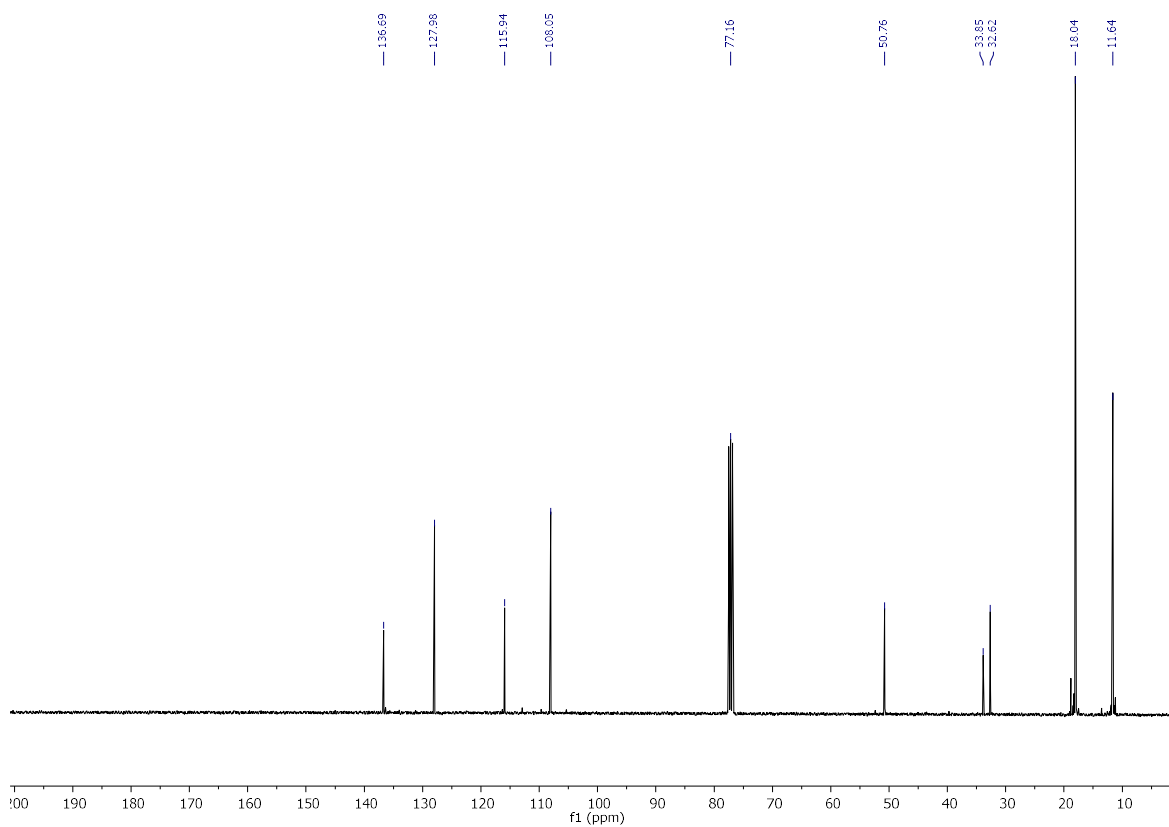
7d (¹H):**7d (¹³C):**

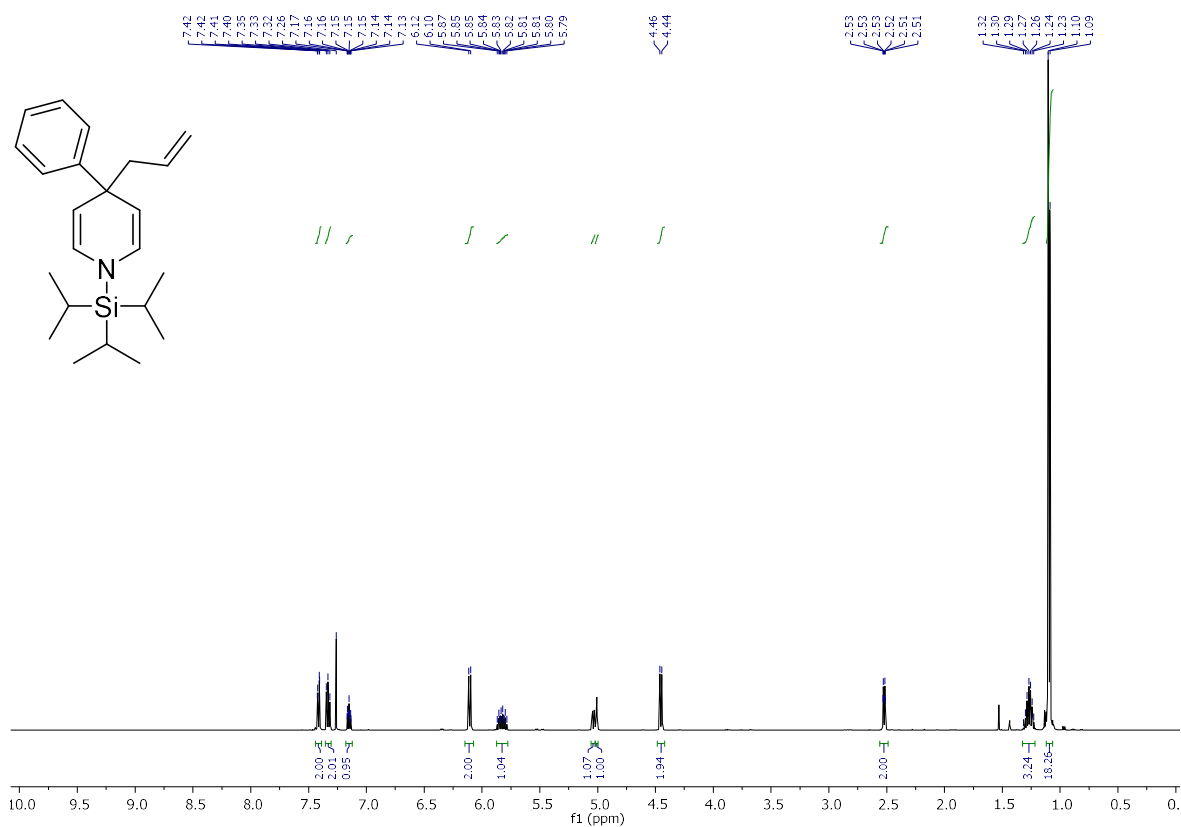
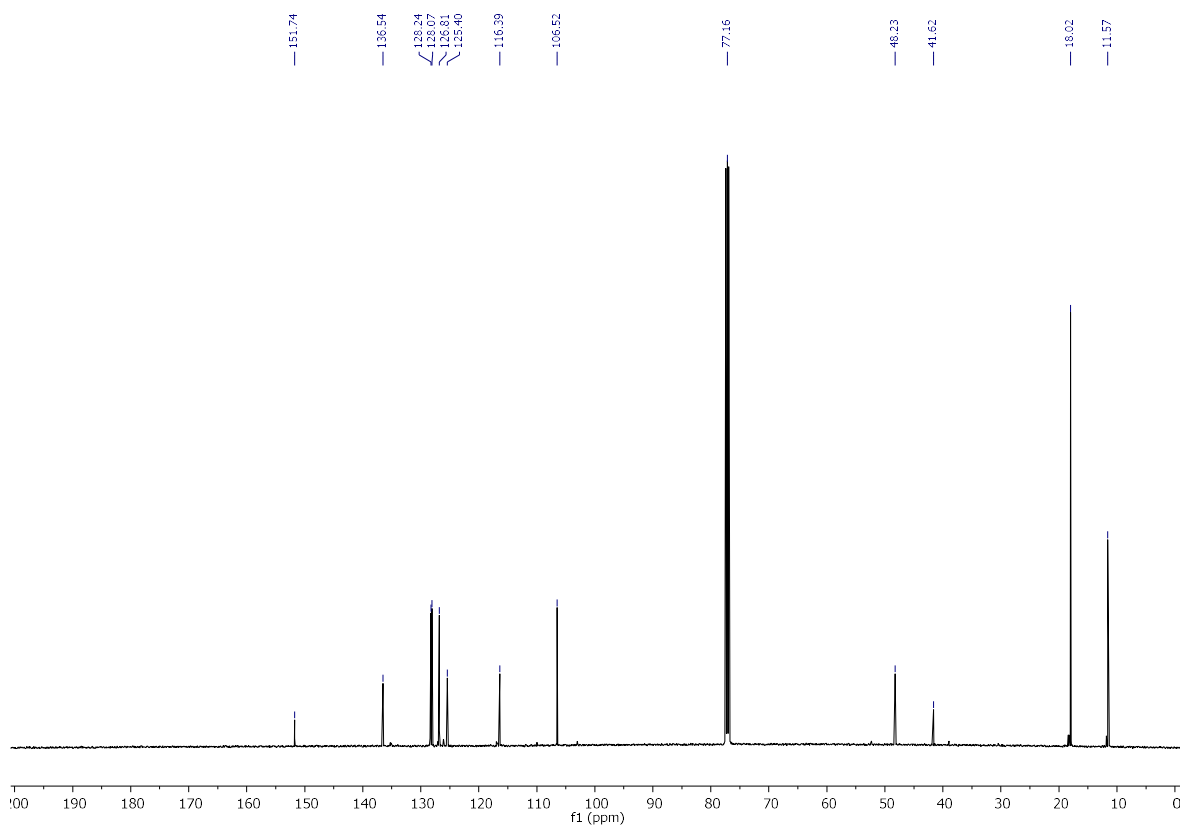
7e (^1H):**7e** (^{13}C):

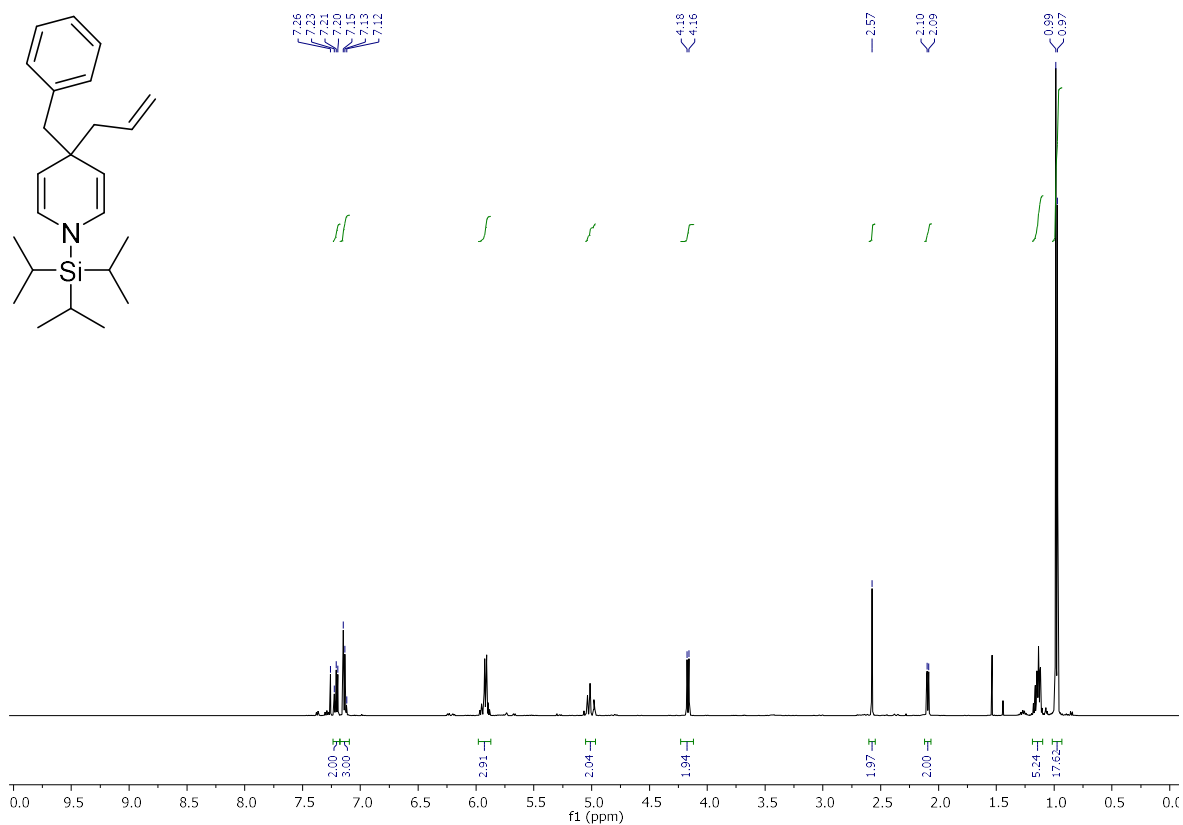
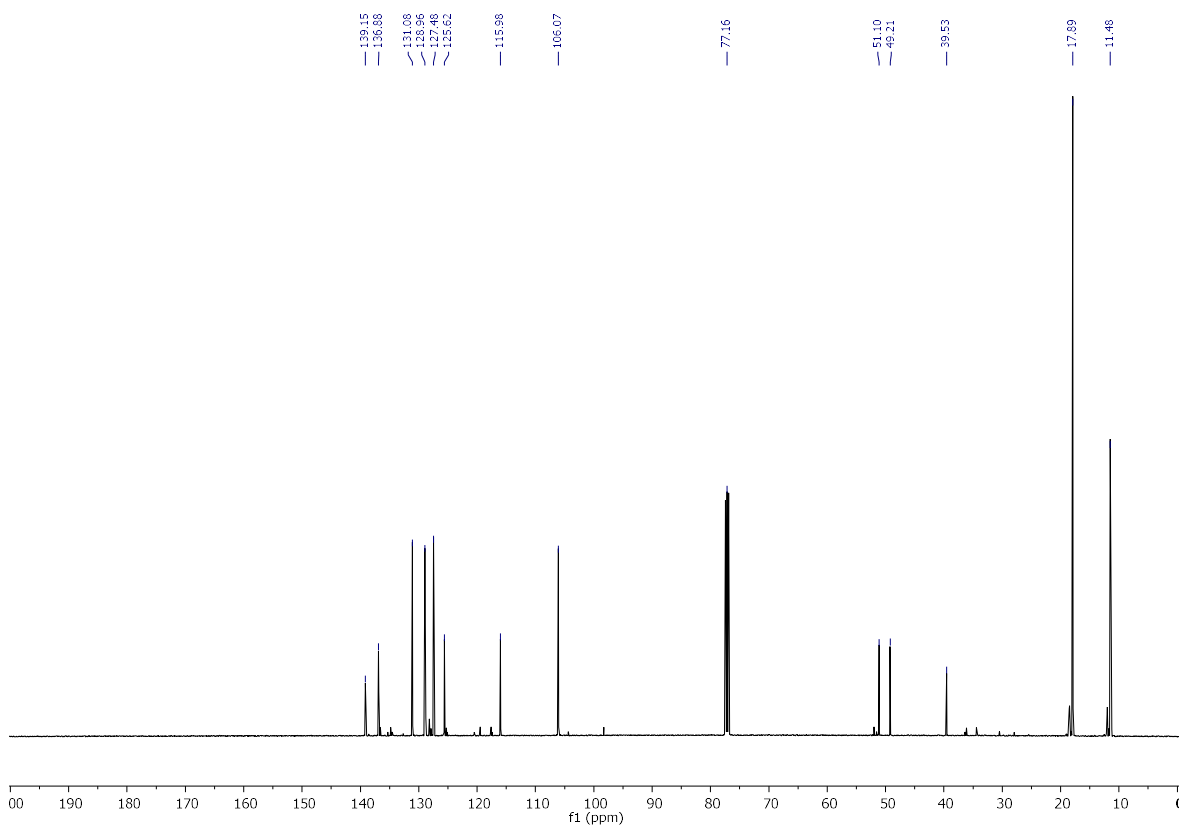
9a (^1H):**9a** (^{13}C):

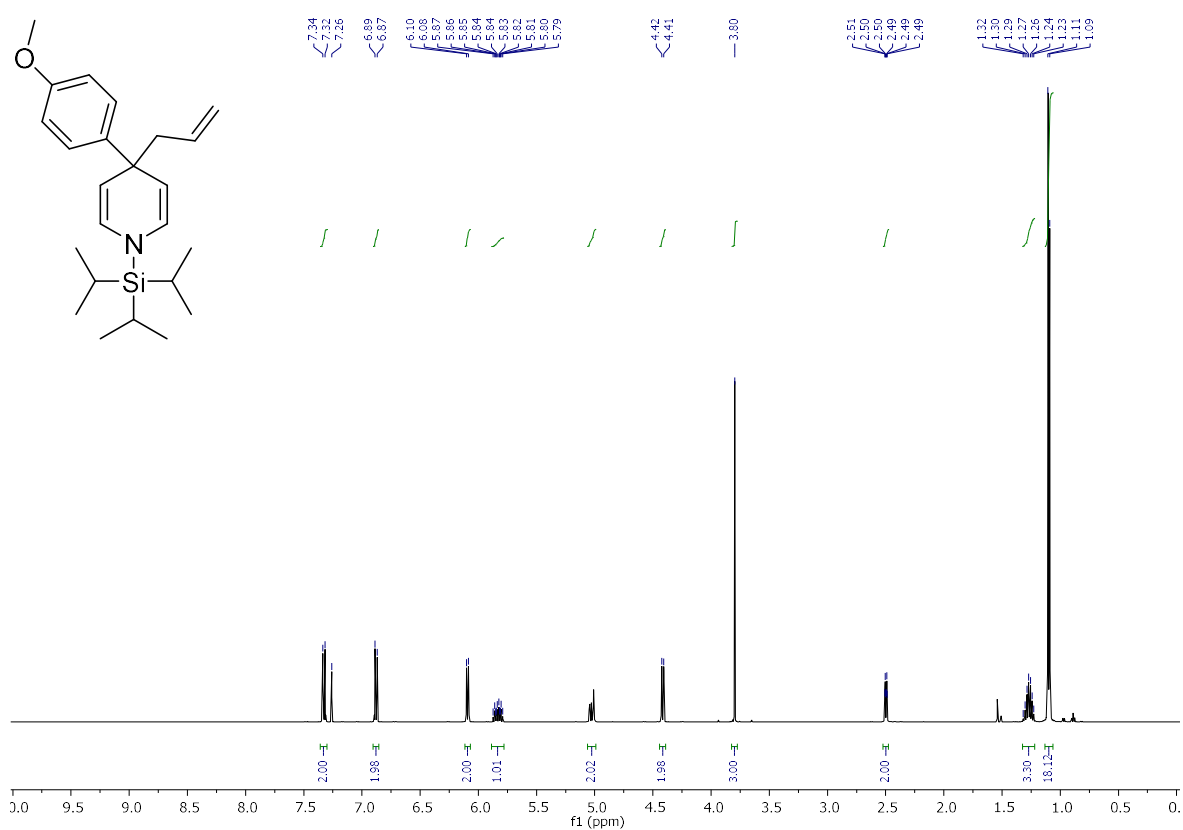
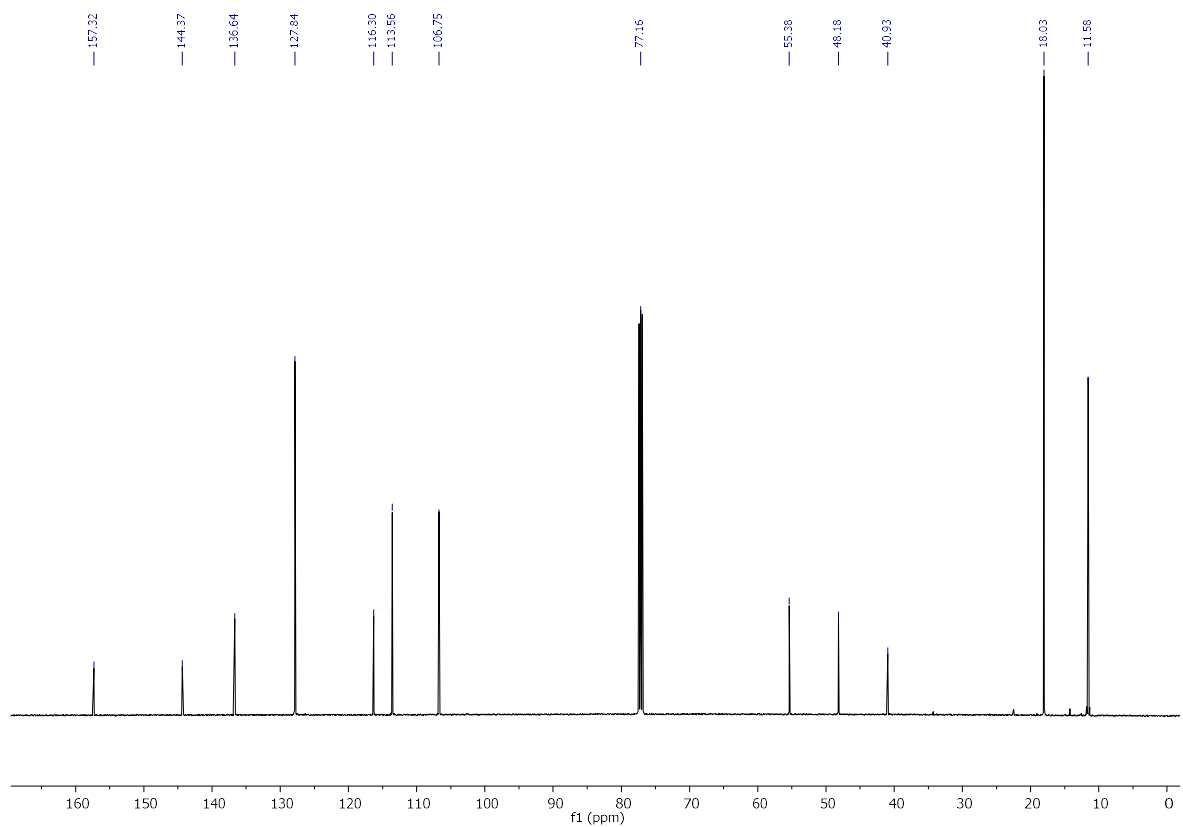
9b (^1H):

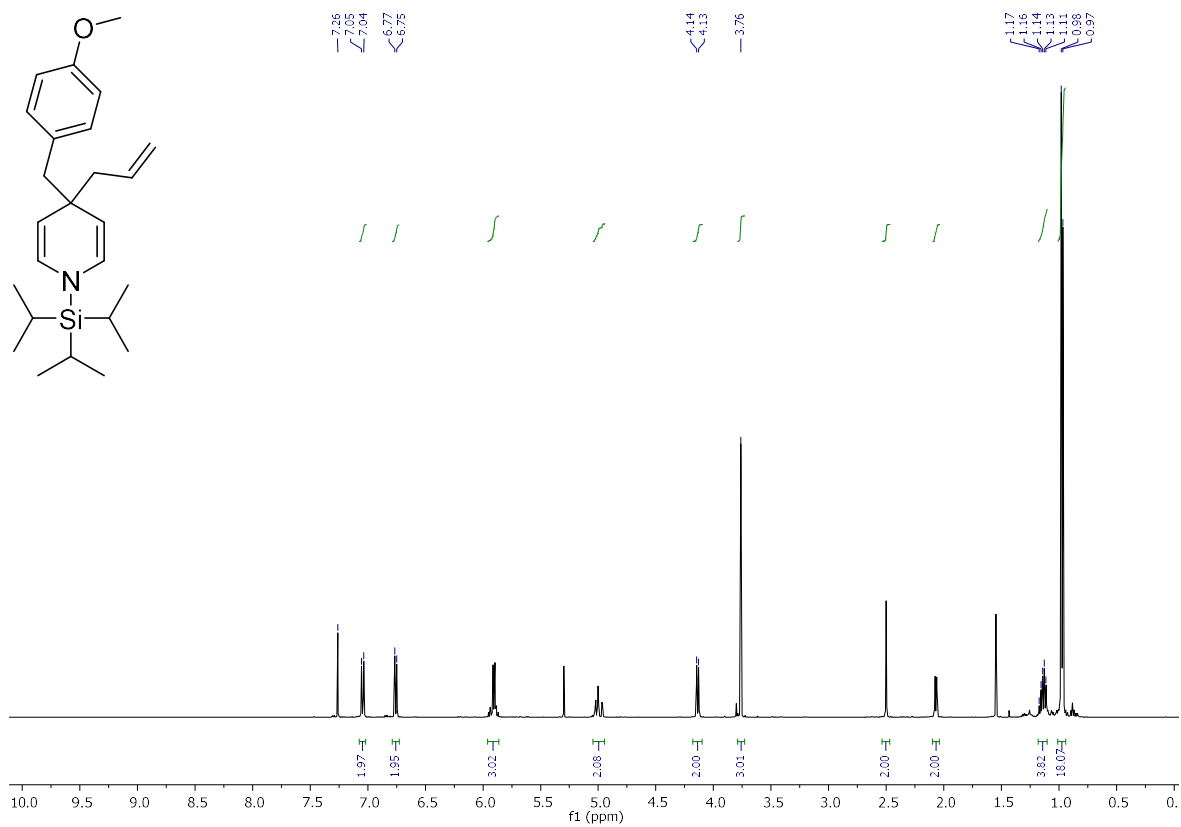
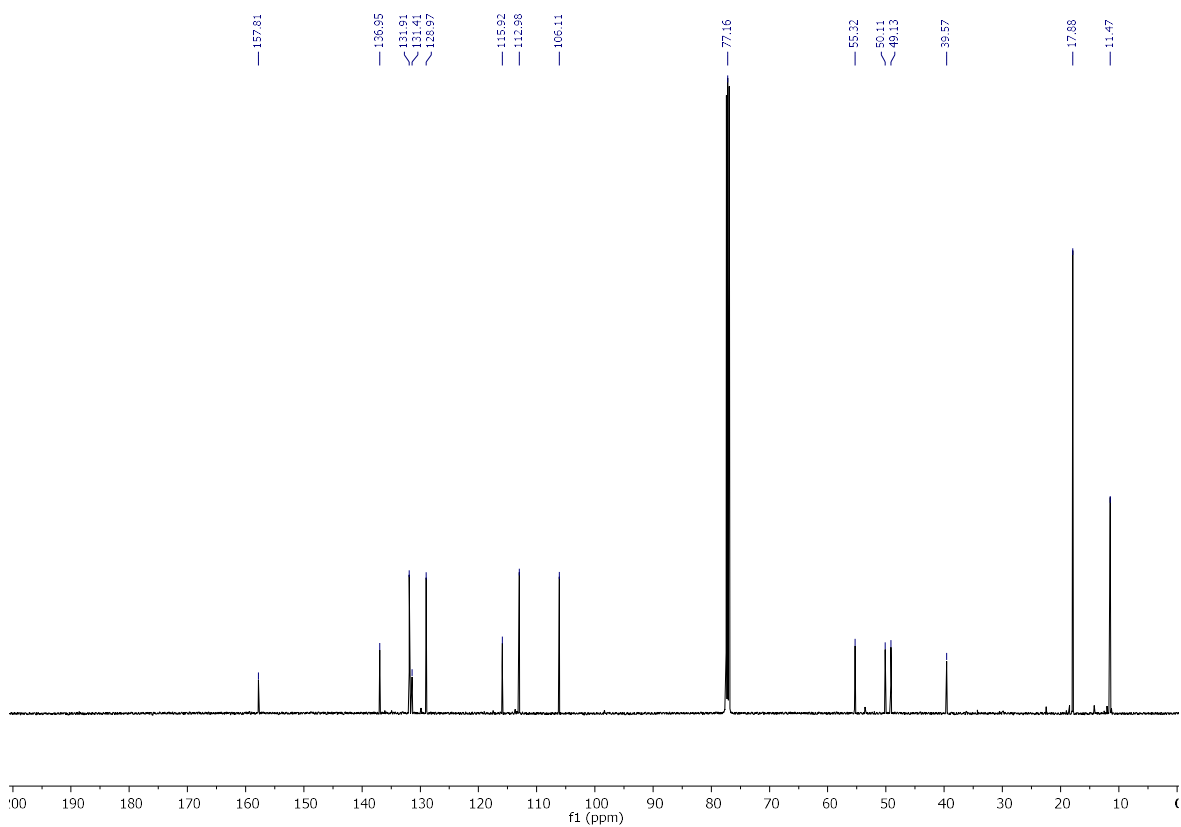
9c (^1H):**9c** (^{13}C):

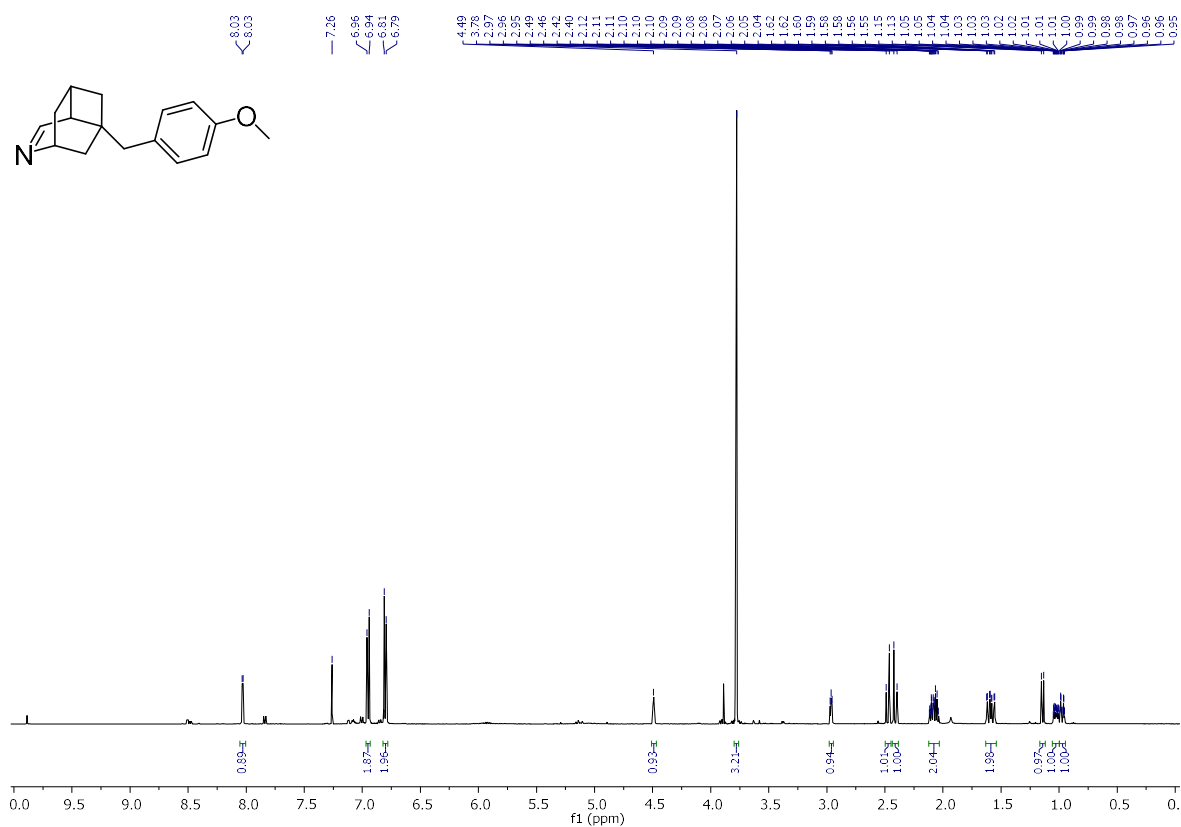
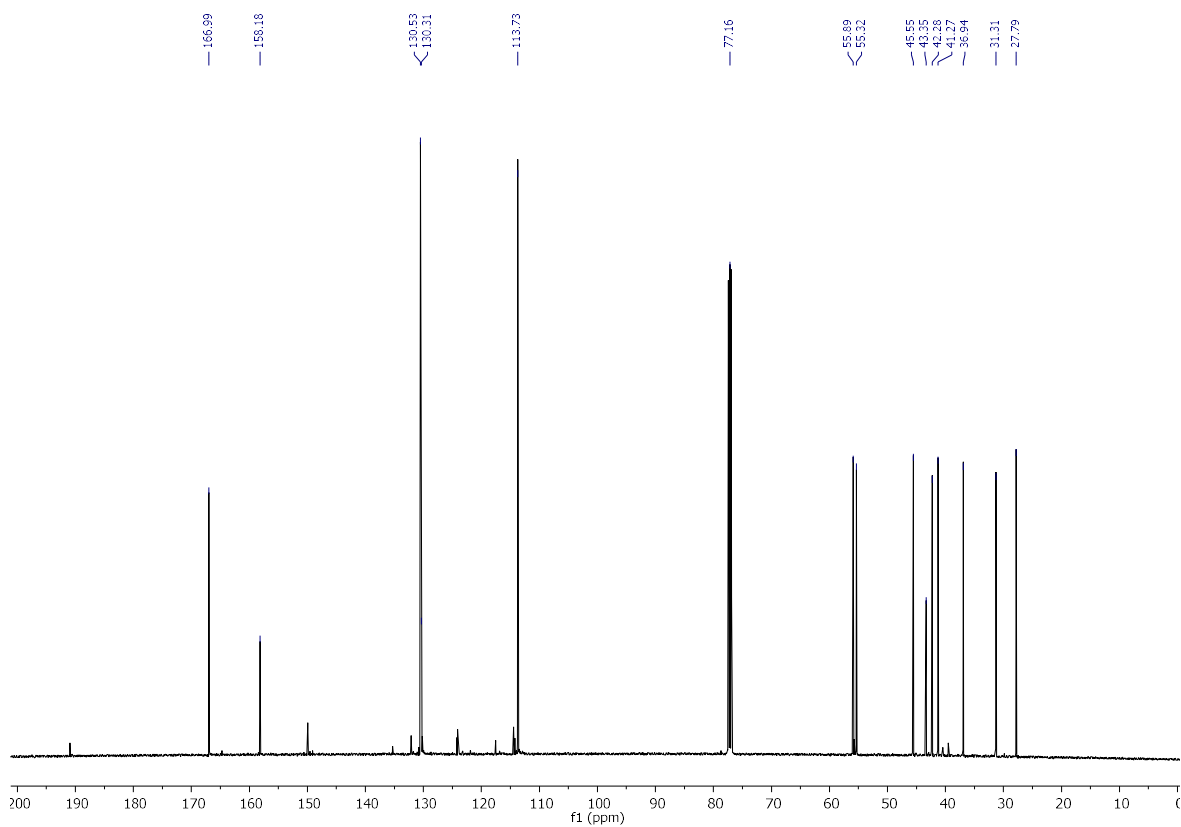
11a (^1H):**11a** (^{13}C):

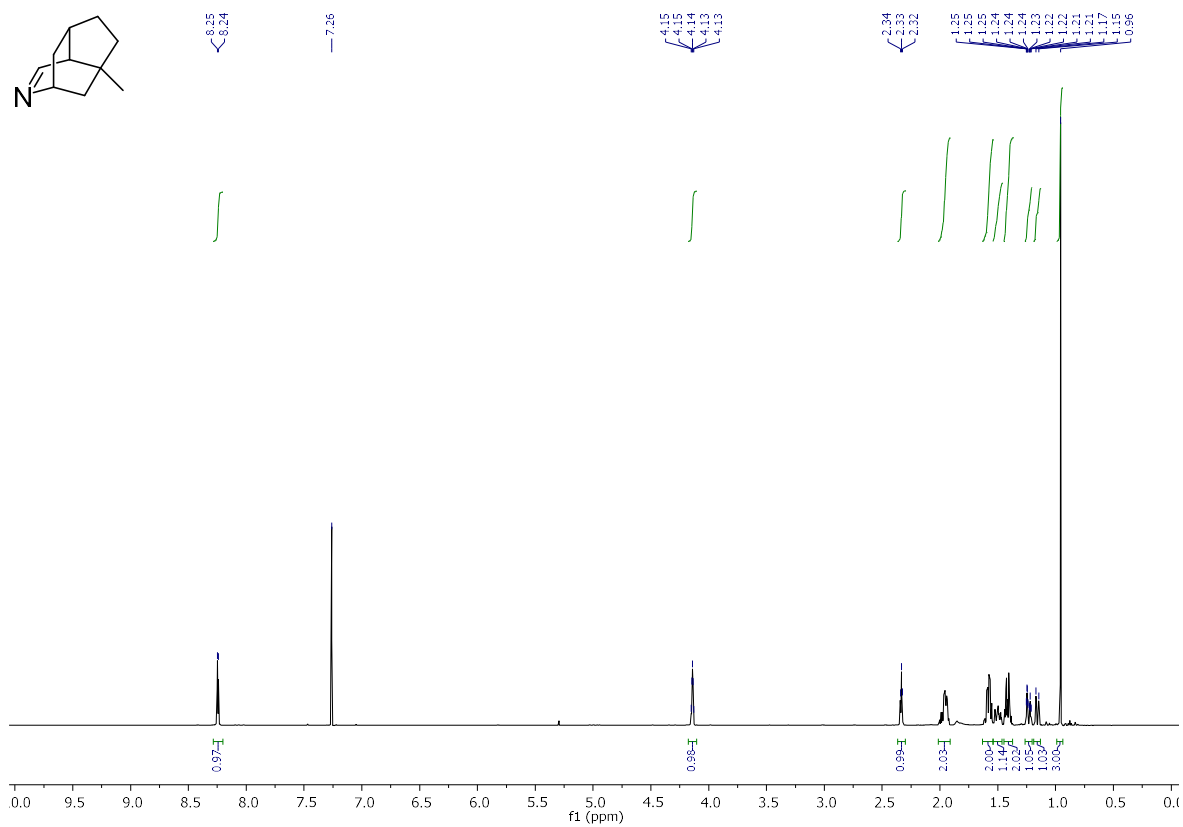
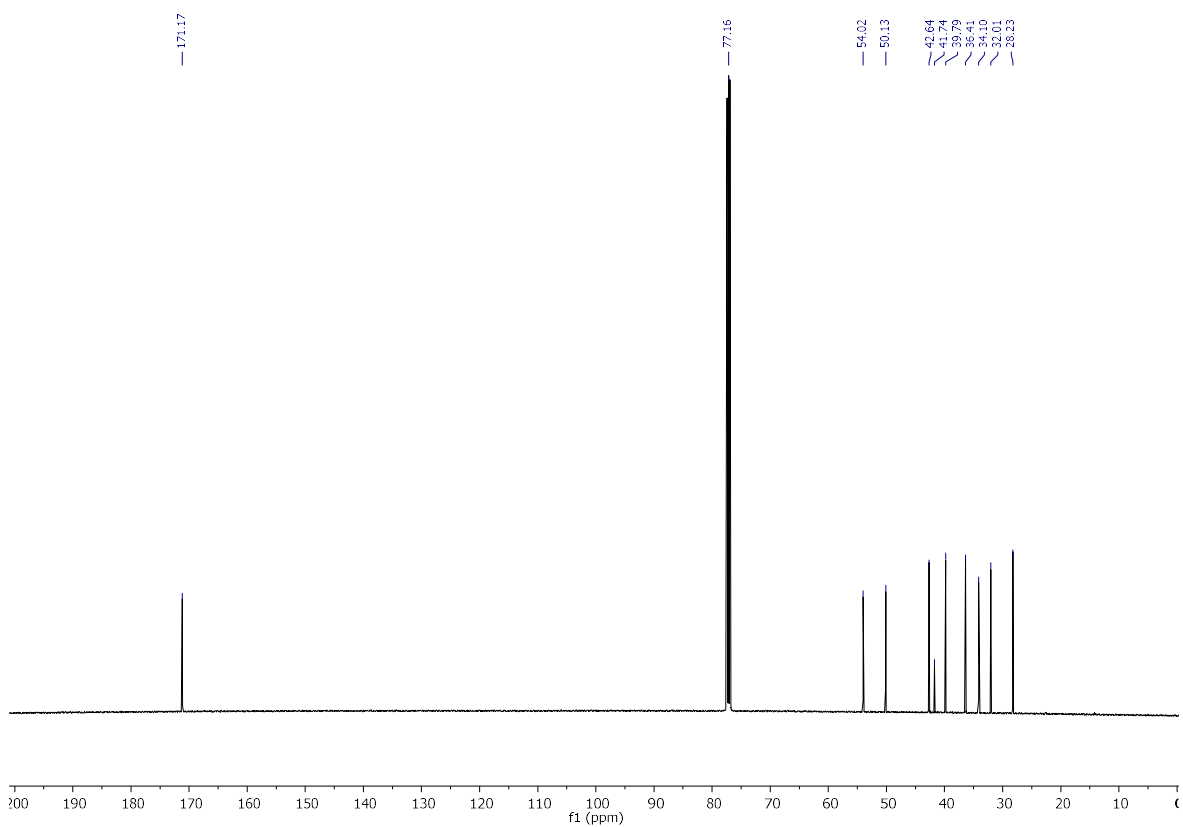
11b (¹H):**11b (¹³C):**

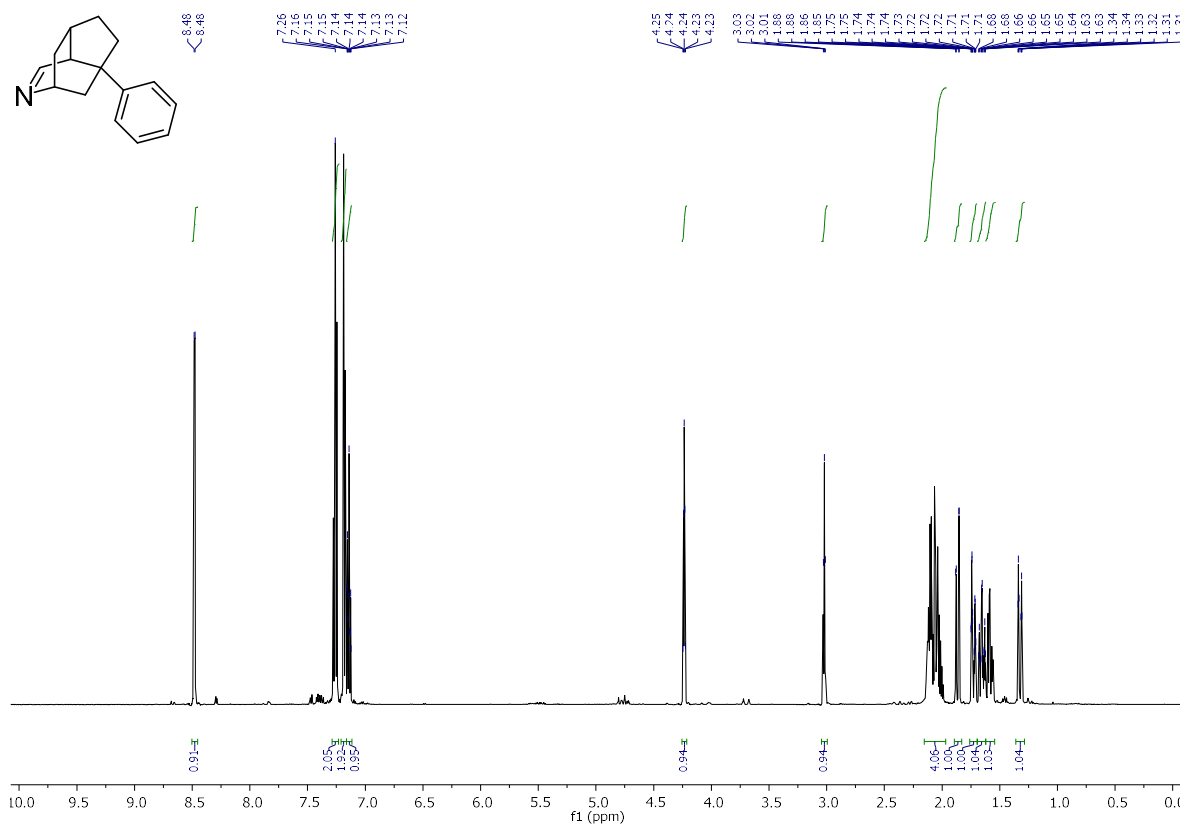
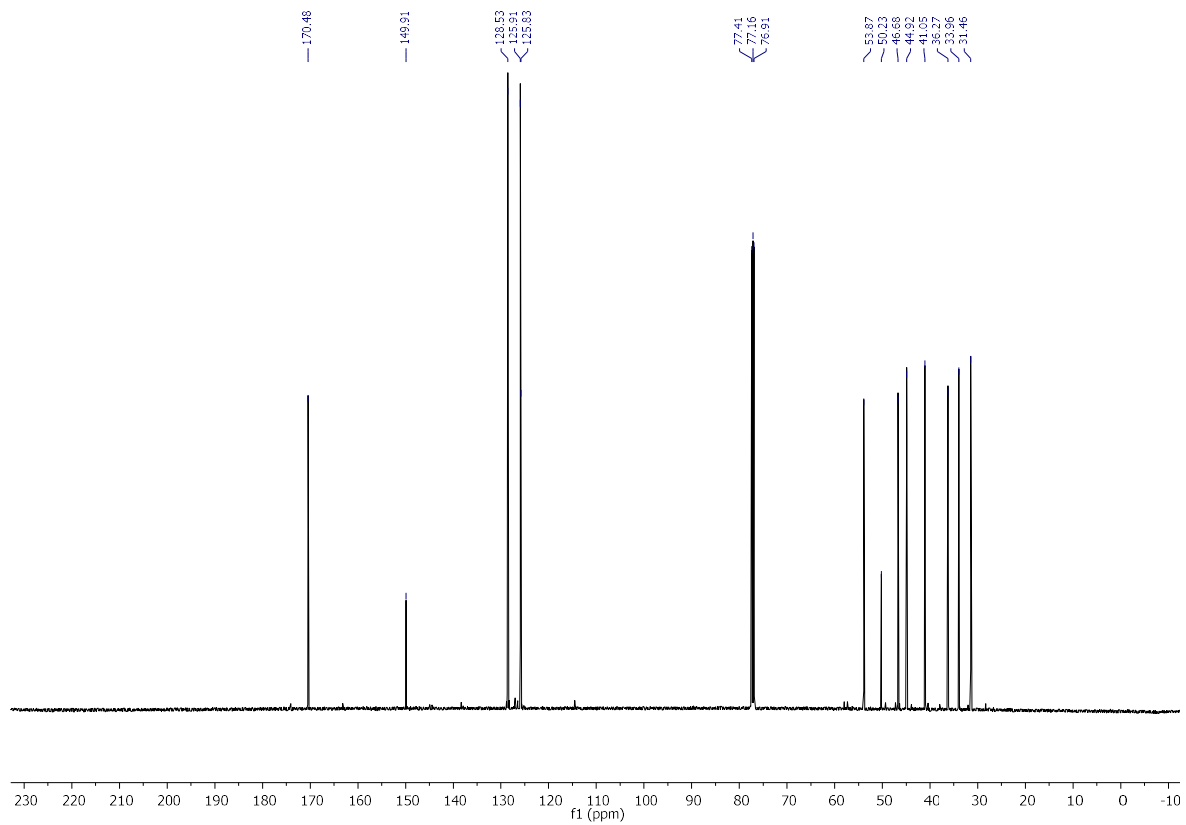
11c (¹H):**11c (¹³C):**

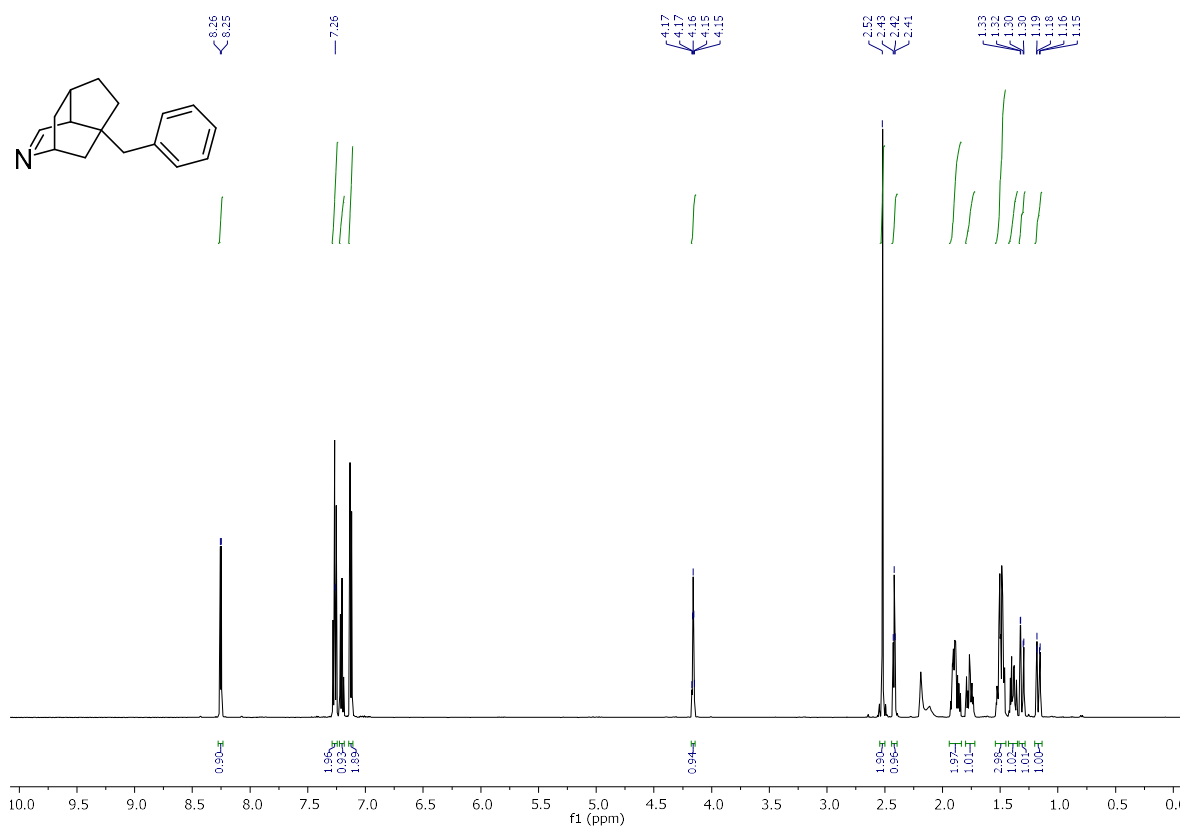
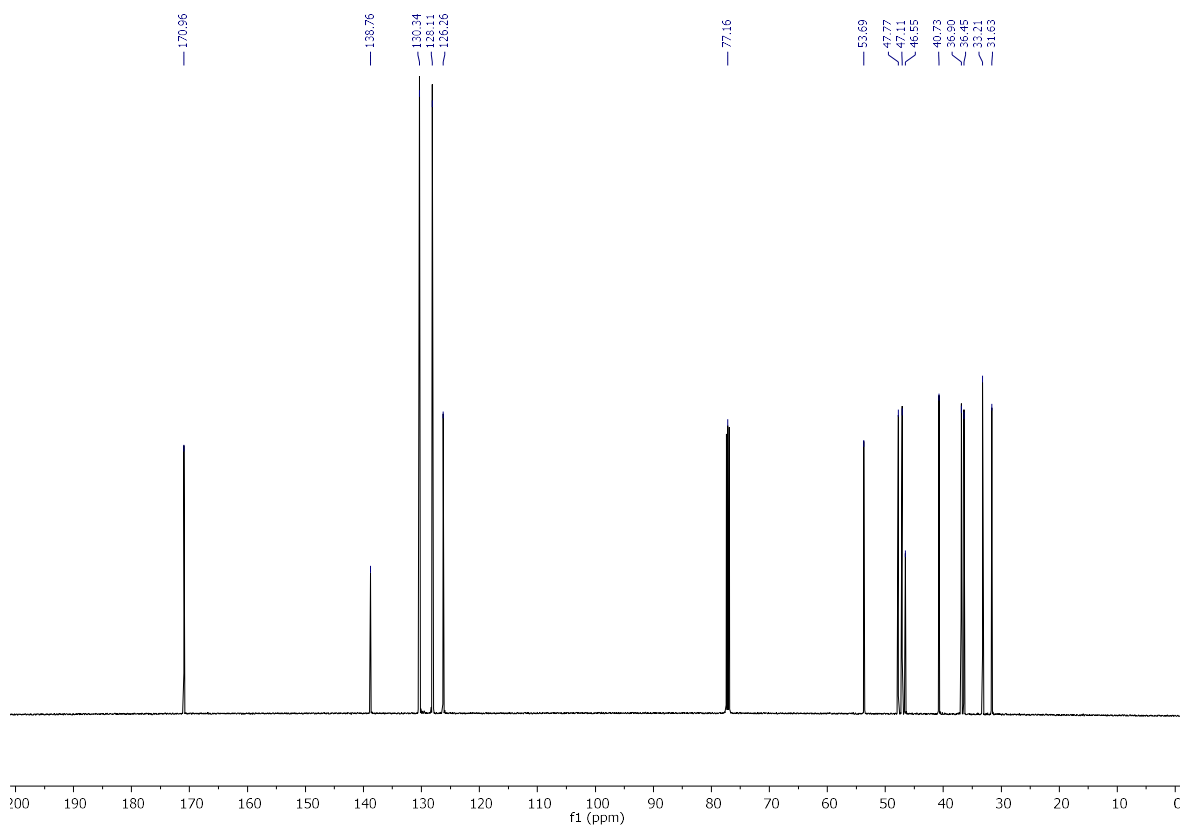
11d (¹H):**11d (¹³C):**

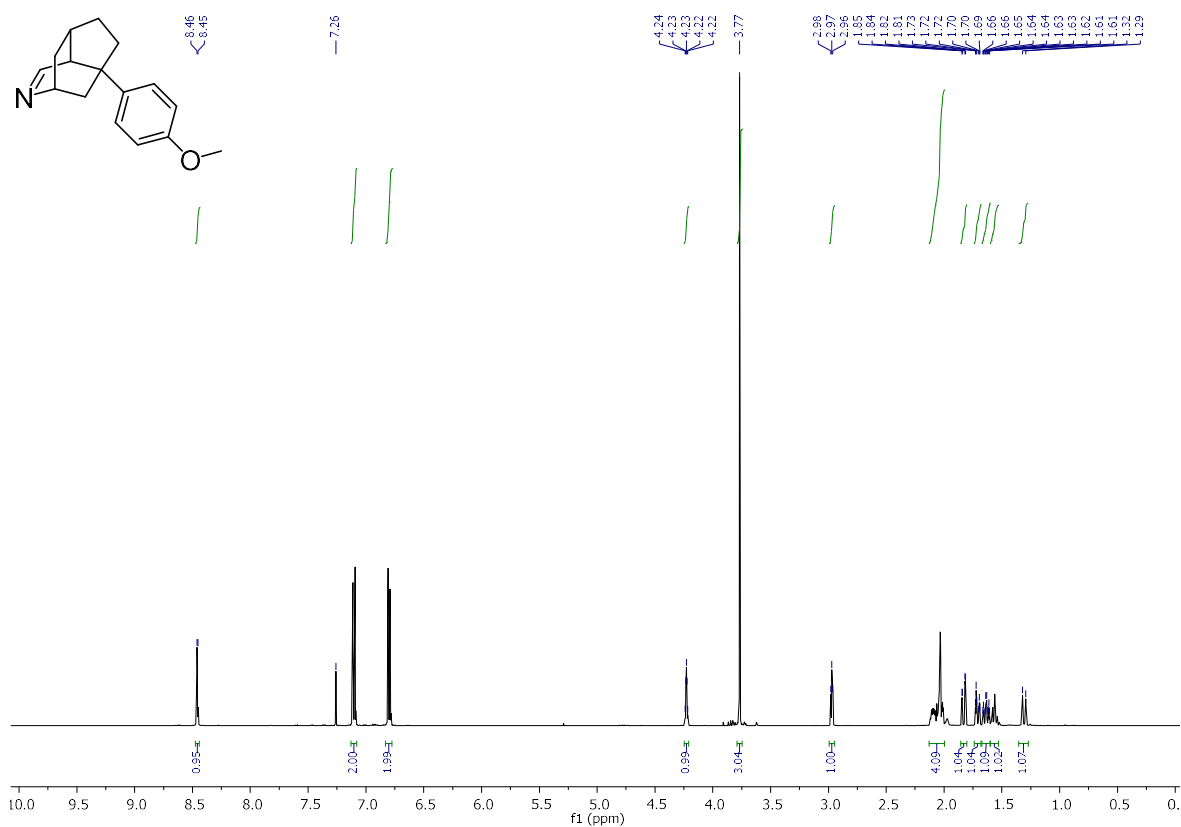
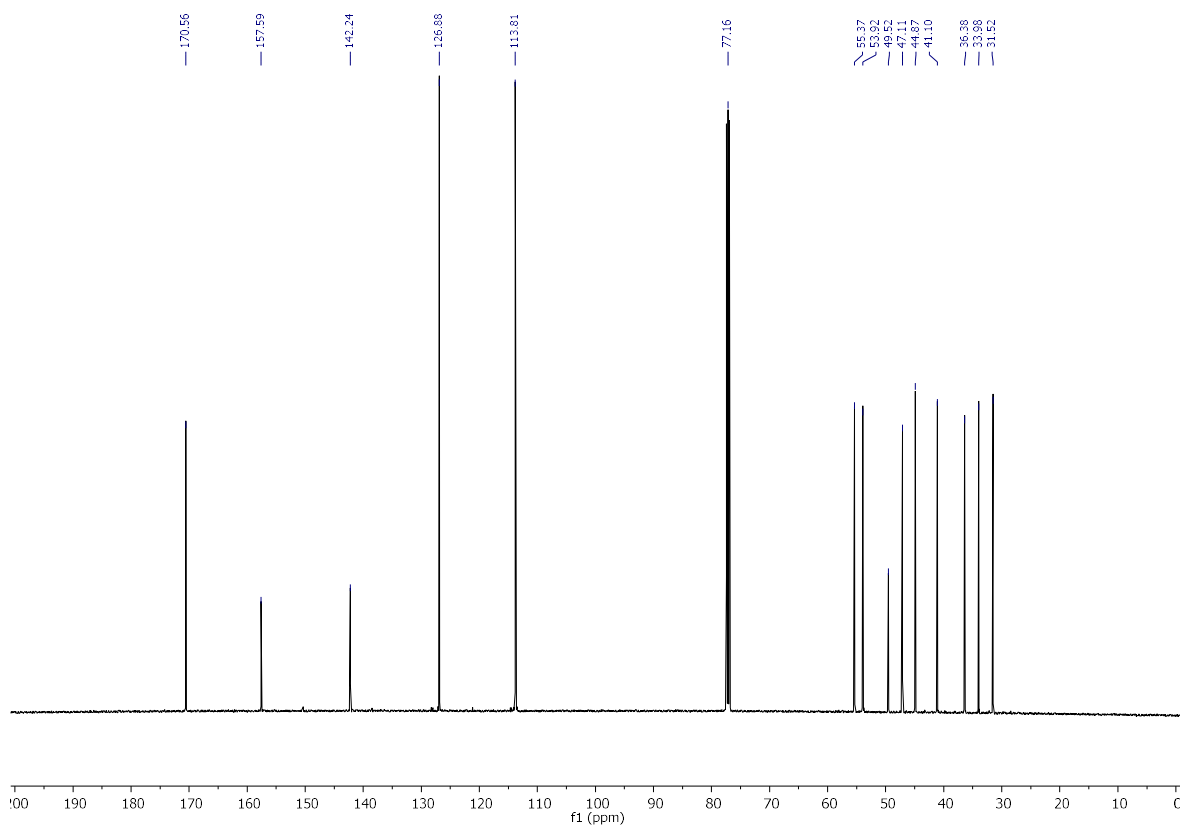
11e (^1H):**11e** (^{13}C):

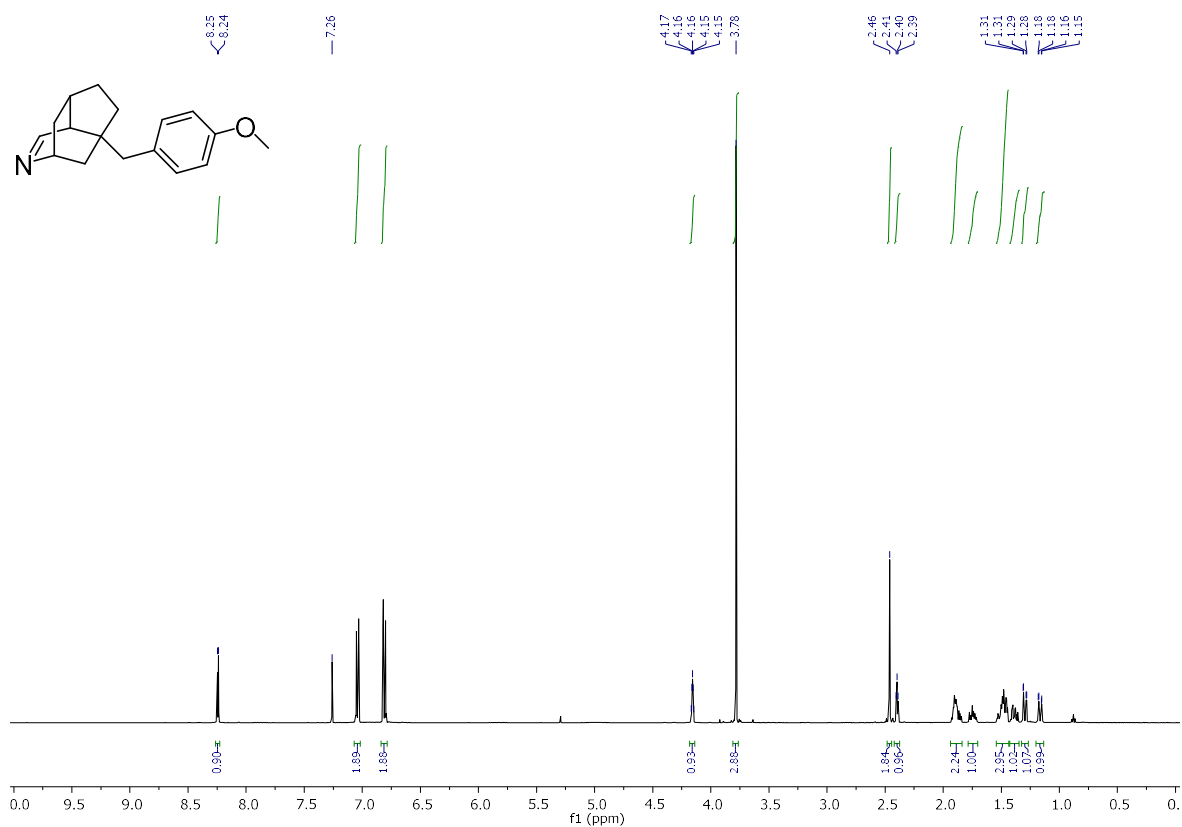
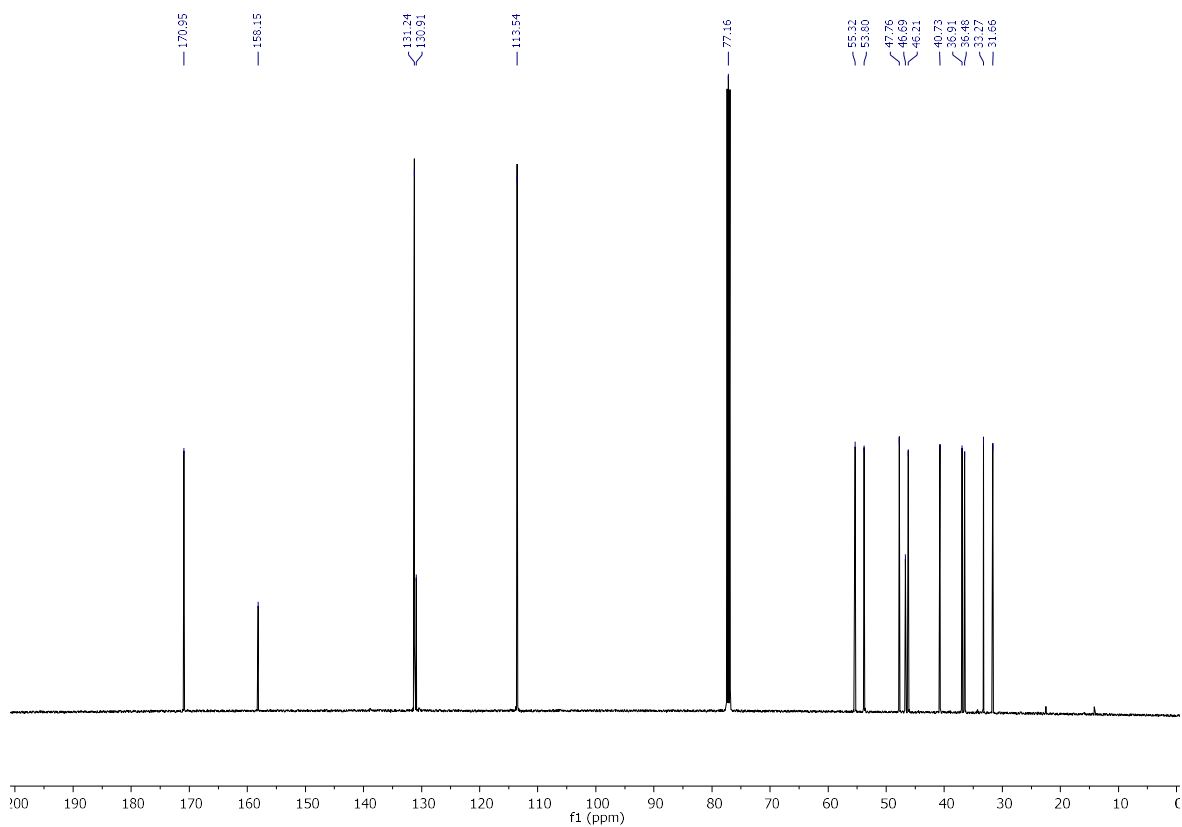
13e (¹H):**13e (¹³C):**

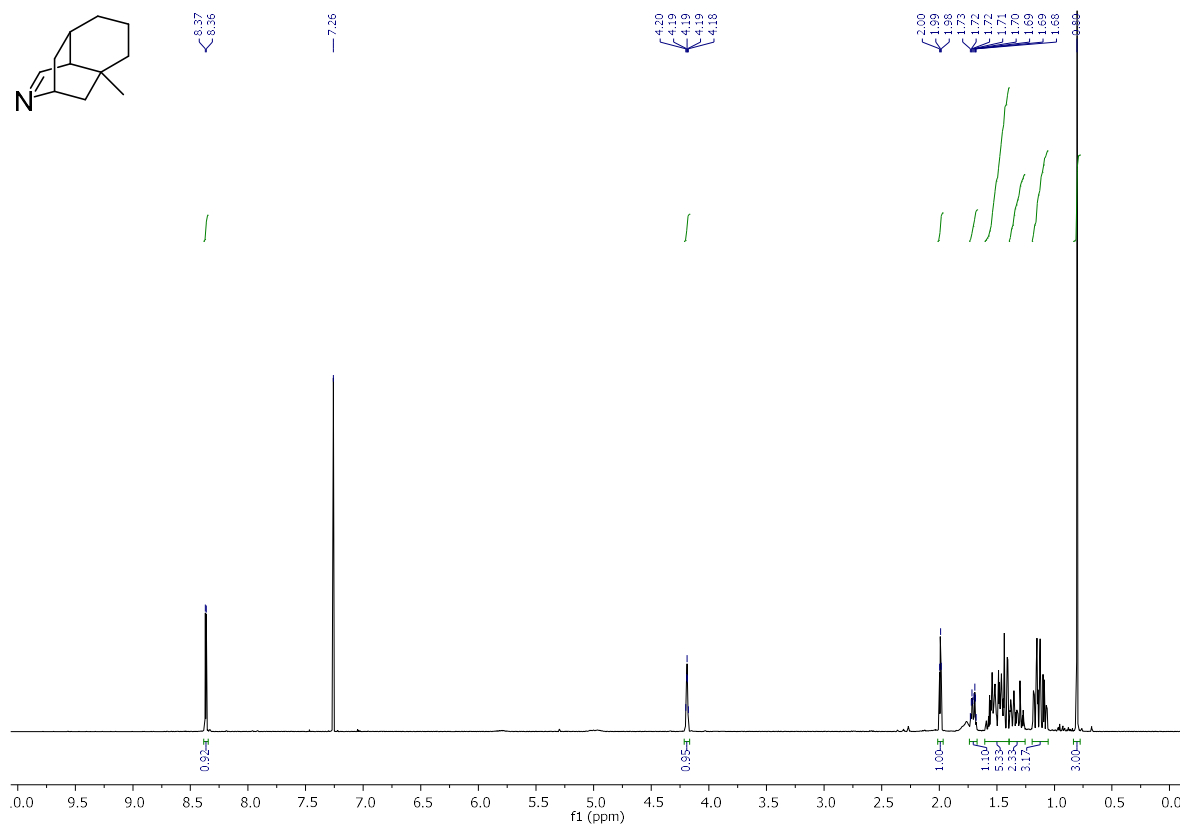
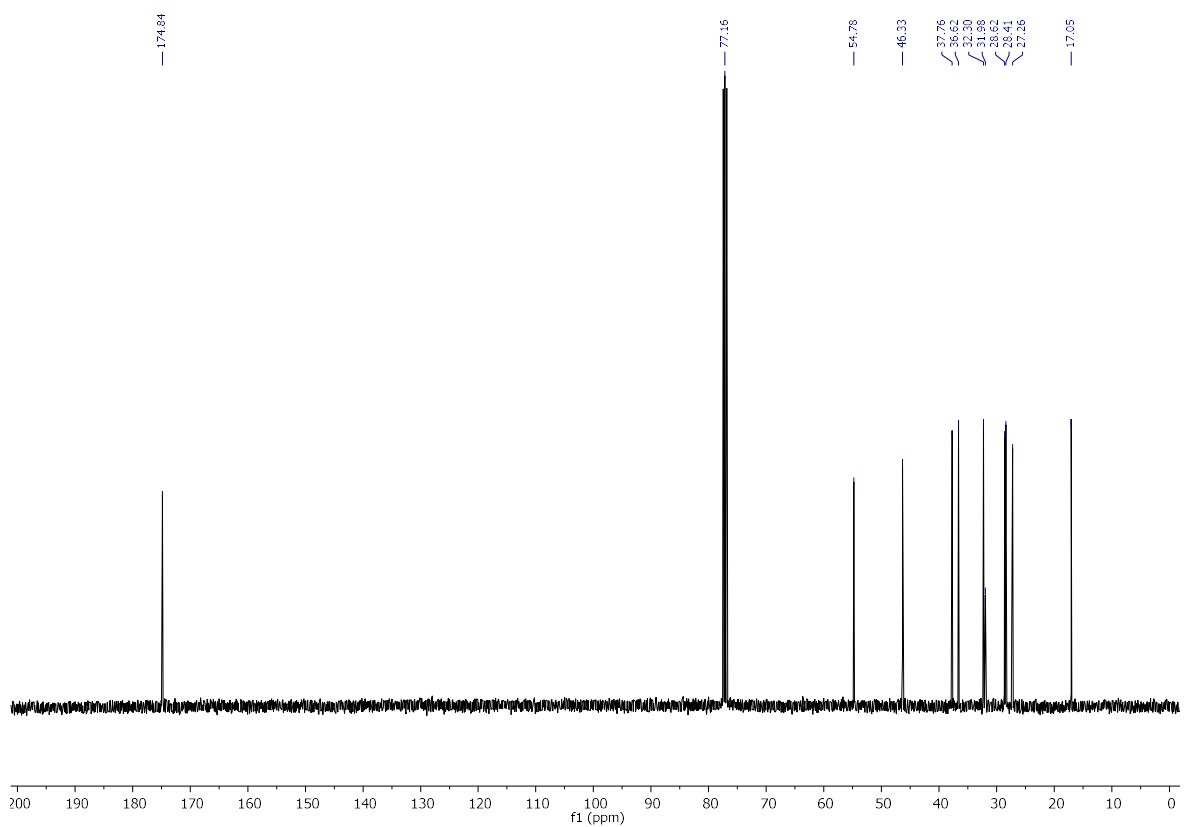
14a (¹H):**14a (¹³C):**

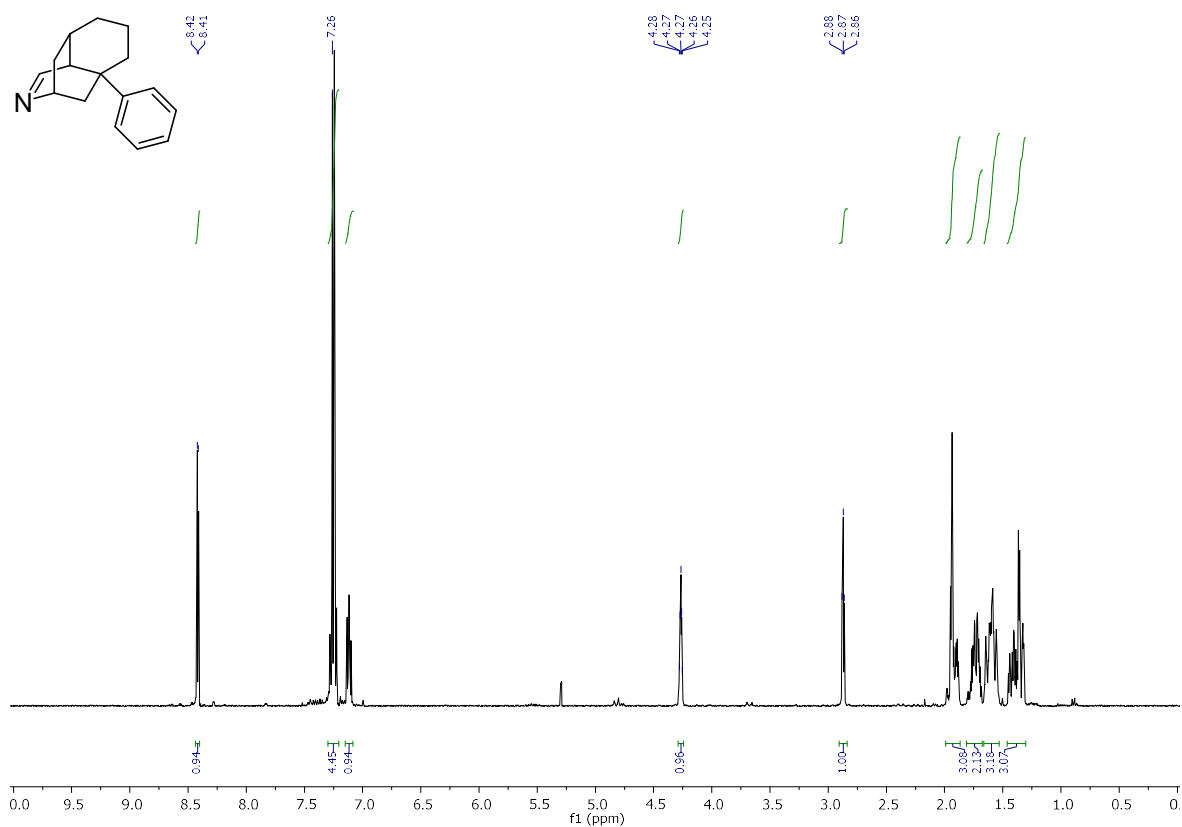
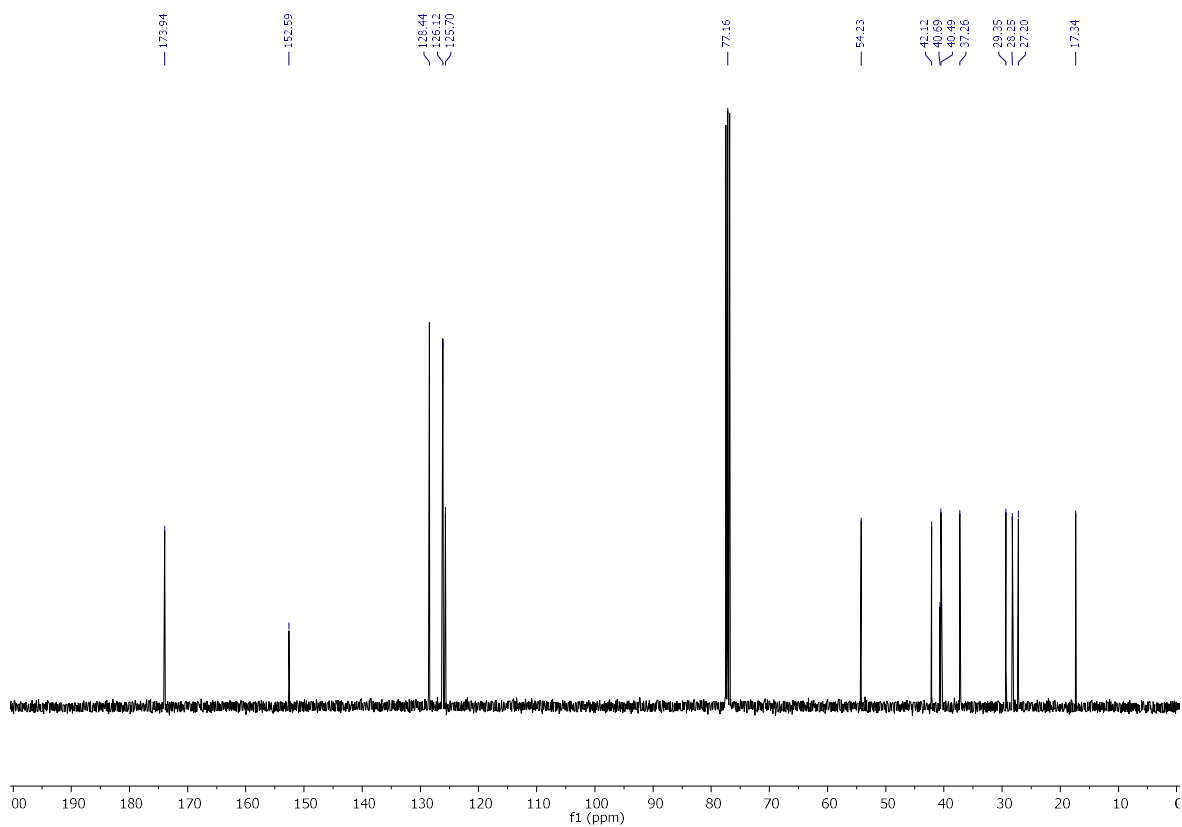
14b (¹H):**14b (¹³C):**

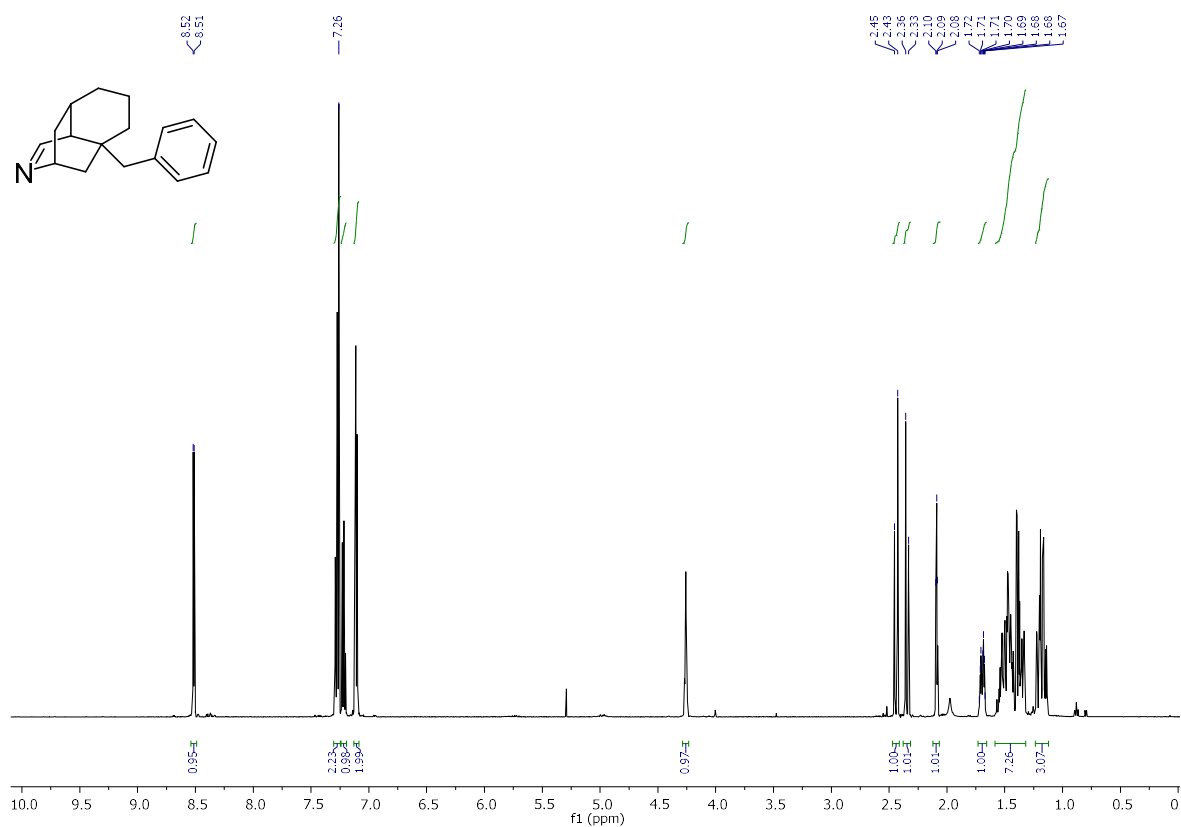
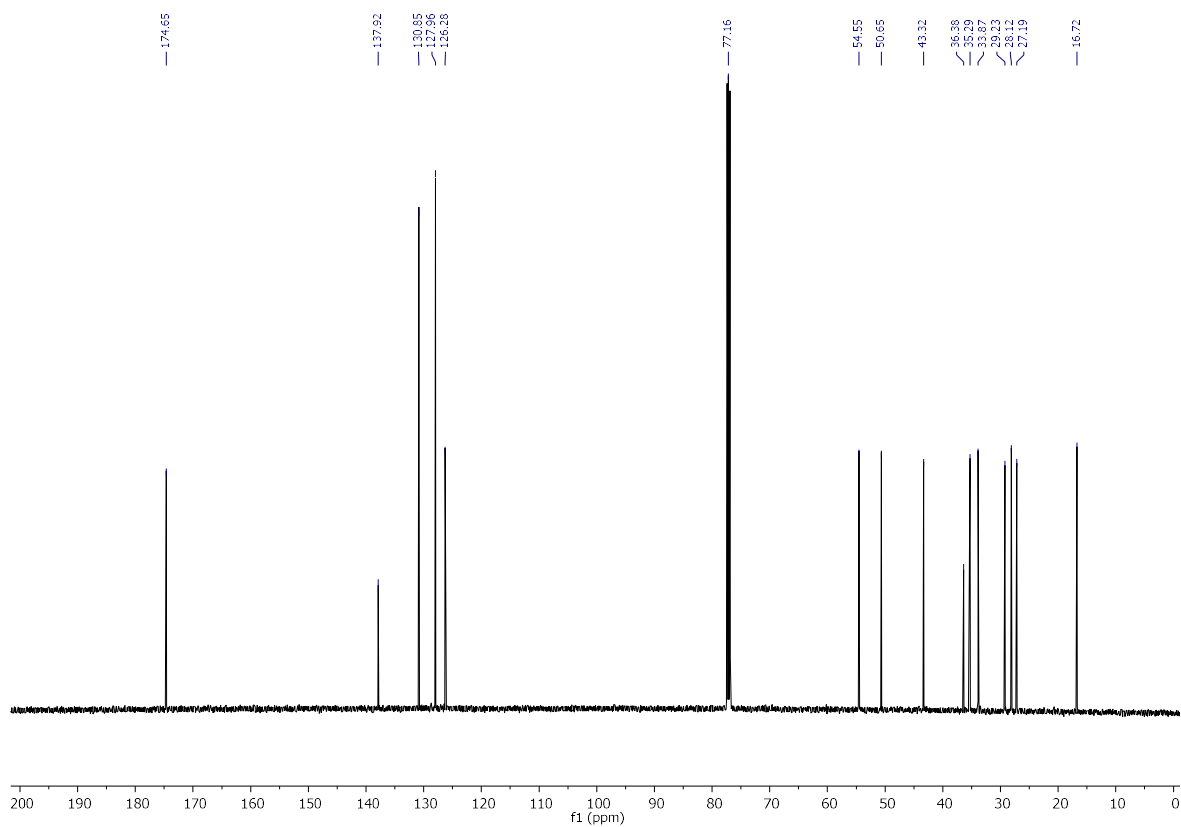
14c (¹H):**14c (¹³C):**

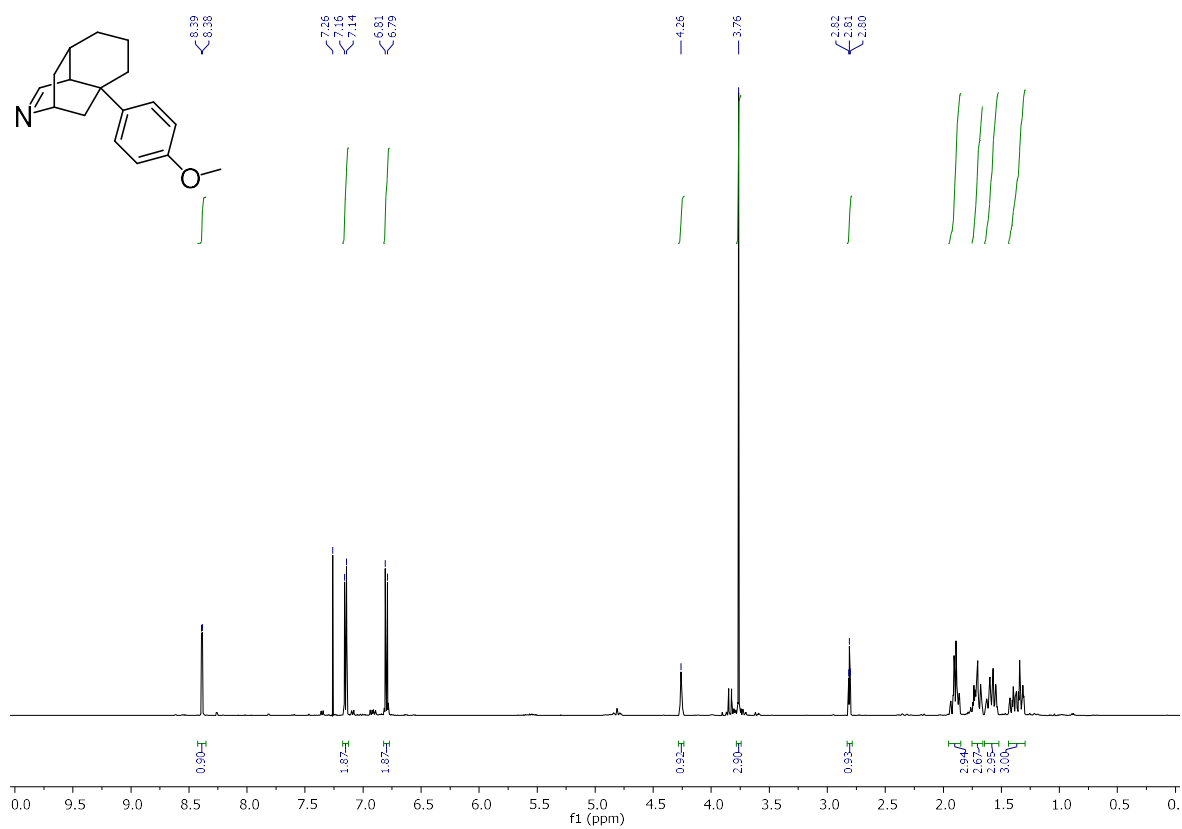
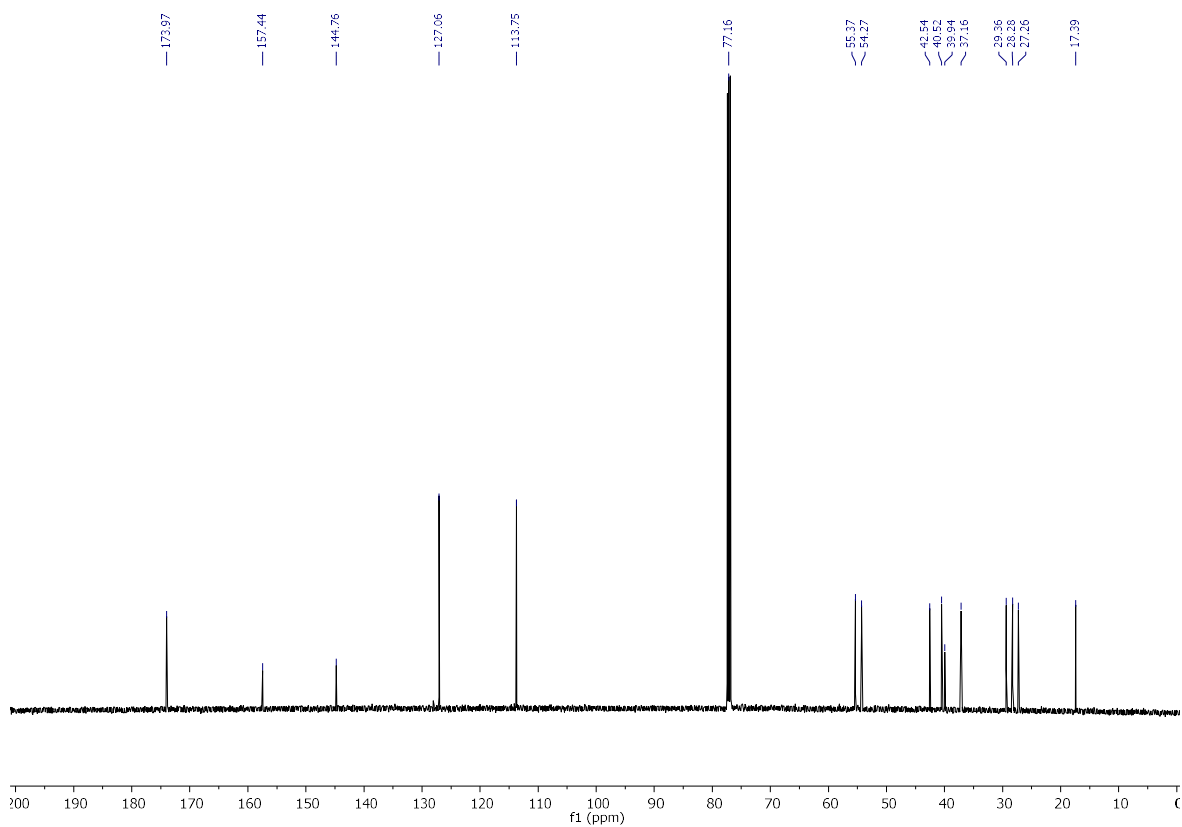
14d (¹H):**14d (¹³C):**

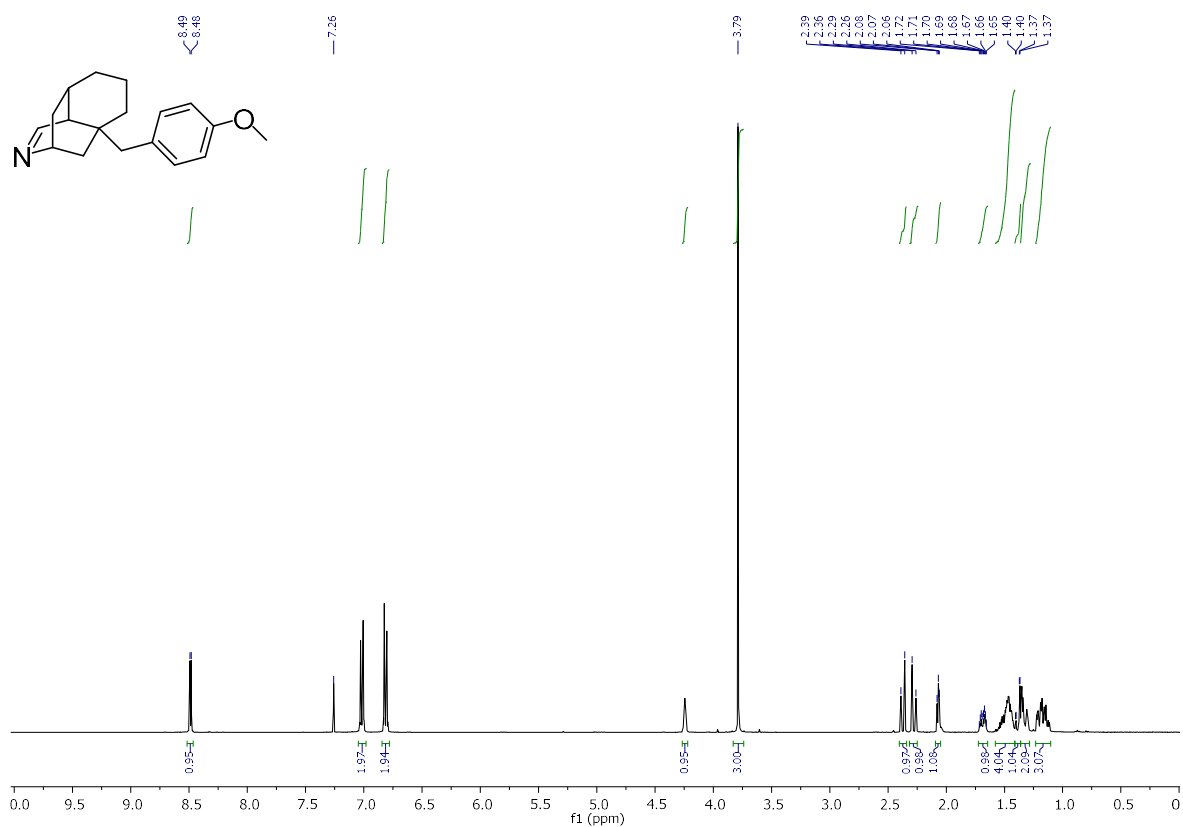
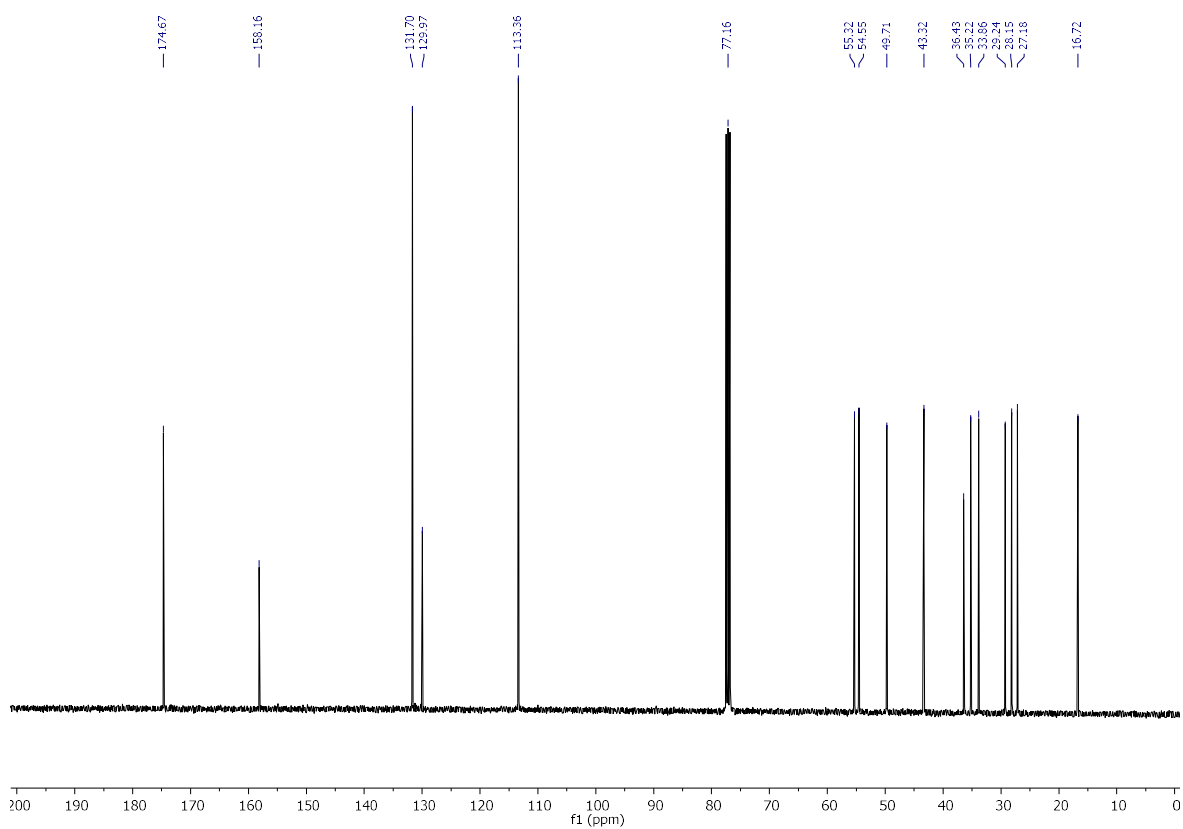
14e (^1H):**14e (^{13}C):**

15a (¹H):**15a (¹³C):**

15b (¹H):**15b (¹³C):**

15c (¹H):**15c (¹³C):**

15d (¹H):**15d (¹³C):**

15e (¹H):**15e (¹³C):**

8.2 Second publication

Organocatalysis

Synthesis of 1,5-Ring-Fused Imidazoles from Cyclic Imines and TosMIC – Identification of in situ Generated *N*-Methyleneformamide as a Catalyst in the van Leusen Imidazole Synthesis

Heinrich-Karl A. Rudy,^[a] Peter Mayer,^[b] and Klaus T. Wanner*^[a]

In memory of Prof. Rolf Huisgen

Abstract: Imidazoles fused with a cyclic system in 1,5-position were synthesized via the van Leusen imidazole synthesis employing saturated aliphatic tricycles including an imine function in the base catalyzed cycloaddition reaction with *p*-toluenesulfonyl-methyl isocyanide (TosMIC). Thereby, *N*-(tosylmethyl)formamide, a decomposition product of TosMIC, was found to act as a promoter of this reaction leading to considerably reduced reaction times and improved yields. Mechanistic studies revealed that *N*-(tosylmethyl)formamide is transformed

into *N*-methyleneformamide acting as a catalyst in this reaction under the applied basic conditions. Being a Michael acceptor, the employed imines add to this compound, thus being transformed into iminium ions. The so formed intermediates facilitate the first step of the van Leusen imidazole synthesis, which is the addition of deprotonated TosMIC to the iminium subunit. *N*-methyleneformamide is finally reformed during the overall reaction and can thus be considered as an organocatalyst of the studied cycloaddition reaction.

Introduction

Imidazole rings are a common structural motif present in many natural products, medicinal drugs, and chemical compounds.^[1] Thus, imidazole rings are found for example in numerous anticancer, antibacterial, antiparasitic, antihistaminic, antihypertensive, antineuropathic, and antifungal drugs.^[2] Crop protection agents containing an imidazole heterocycle, for instance Prochloraz (1) or Imazalil (2) (Figure 1), are widely applied to maintain crop quality and quantity.^[1a,3]

Since the first imidazole syntheses by Debus and Radziszewski in the 19th century, a multitude of synthetic methods for the preparation of imidazoles has evolved.^[4] A common approach for the preparation of imidazoles is the van Leusen imidazole synthesis which is based on the 1,3-cycloaddition of tosylmethyl isocyanide (TosMIC) with imines under basic conditions.^[4c,5] By this method, a large variety of either 1,5-di-, or

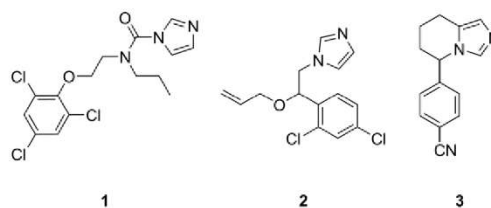


Figure 1. Structures of Prochloraz (1), Imazalil (2) and Fadrozole (3).

1,4,5-tri-substituted imidazoles employing acyclic imines as starting materials has been synthesized.^[5,6] In contrast, examples in which the van Leusen imidazole synthesis has been applied to the construction of imidazoles displaying a fused ring system originating from 1,5-position are less common which is likely due to the fact that cyclic imines are less abundant than their acyclic counterparts.

Exhibiting an imine subunit, pyrazine-2(1*H*)one derivatives have been employed in cycloaddition reactions with TosMIC yielding the corresponding ring fused systems that served as intermediates for the development of anticancer agents.^[7] Further examples for the construction of 1,5-ring-fused imidazoles by means of TosMIC are found in syntheses of imidazobenzodiazepine and imidazo β -carboline derivatives.^[8–10] Furthermore, also nitrogen containing heteroaromatic compounds like quinolone, isoquinoline, and quinoxaline formally displaying a C=N subunit have successfully been employed in the synthesis of the corresponding *N*-fused imidazo heterocycles employing TosMIC (Figure 2).^[11]

[a] H.-K. A. Rudy, Prof. Dr. K. T. Wanner
Department für Pharmazie – Zentrum für Pharmaforschung,
Ludwig-Maximilians-Universität München
Butenandstr. 5-13, 81377 München, Germany
E-mail: klaus.wanner@cup.uni-muenchen.de

[b] Dr. P. Mayer
Department für Chemie, Ludwig-Maximilians-Universität München,
Butenandstr. 5-13, 81377 München, Germany

Supporting information and ORCID(s) from the author(s) for this article are available on the WWW under <https://doi.org/10.1002/ejoc.202000280>.

© 2020 The Authors. Published by Wiley-VCH Verlag GmbH & Co. KGaA. This is an open access article under the terms of the Creative Commons Attribution License, which permits use, distribution and reproduction in any medium, provided the original work is properly cited.

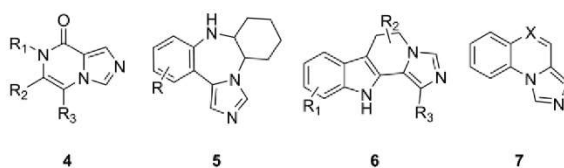


Figure 2. Structures of 1,5-ring-fused imidazoles synthesized from TosMIC and pyrazine-2(1*H*)ones (**4**);^[7] benzodiazepines (**5**);^[9] β -carboline derivatives (**6**)^[10] and nitrogen containing heteroaromatics (**7**).^[11]

Though, *N*-fused imidazoles with a saturated aliphatic cycle in 1,5-position are of great interest as for example Fadrozole (**3**), a non-steroidal aromatase inhibitor used for the treatment of breast cancer,^[12] cycloaddition reactions of basic cyclic imines devoid of any additional functionalities have not been explored in the van Leusen imidazole synthesis, except for a cycloaddition reaction with 4-azahomoadamant-4-ene.^[13]

It is likely to be attributed to the limited availability of appropriate cyclic imines which are devoid of any additional unsaturation that cycloaddition reactions of this type of compounds with TosMIC for the preparation of the respective *N*-fused imidazoles have hardly been explored so far. We have repeatedly reported on the synthesis of this kind of alicyclic imines by acid catalyzed intramolecular cycloaddition reactions of 4,4-disubstituted 1,4-dihydropyridines (1,4-DHPs) with one of the 4-substituents serving as dienophile.^[14] The tricyclic imines resulting from these reactions exhibiting a highly defined geometry are to be considered as valuable building blocks for the construction of drug like compounds, as they represent scaffolds of high

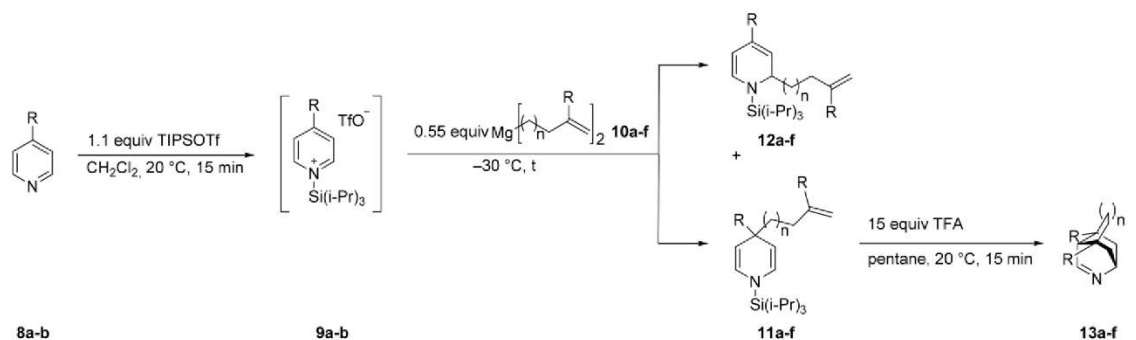
rigidity encompassing well defined trajectories for individual substituents. To further improve the versatility of these building blocks, we now intended to utilize the imine function for the annellation of an imidazole ring by the van Leusen imidazole synthesis to introduce a polar subdomain in this otherwise apolar compounds.

Results and Discussion

As starting material for the annellation of an imidazole ring, we intended to use tricyclic imines which are symmetric, possess substituents *R* at bridge heads of different size (CH_3 , C_6H_5), and vary with regard of the length of the “upper bridge” ($n = 0-2$). Therefore, compounds **13a–13f** should be employed for this purpose. For the synthesis of these compounds, **13a–13f**, the synthetic procedure developed for the construction of related, but non-symmetrically substituted tricyclic imines should be followed.^[14a] Accordingly, in the first step appropriately 4,4-disubstituted 1,4-dihydropyridines should be prepared via reaction of *N*-silylpyridinium ions with bisorganomagnesium compounds. An acid catalyzed intramolecular hetero-Diels-Alder reaction of these 4,4-disubstituted 1,4-dihydropyridines – with one 4-substituent exhibiting a double bond serving as dienophile – should finally furnish the respective tricyclic imines.

Hence, for the synthesis of the required 1,4-DHPs **11a–11f**, following a published procedure, 4-methylpyridine **8a** or 4-phenylpyridine **8b** were treated with TIPSOTf (1.1 equiv., in CH_2Cl_2 at 20 °C for 15 min) to generate the corresponding pyridinium ions **9a–9b** which were then trapped by addition of

Table 1. Synthesis of symmetric tricyclic imines **13a–f**.



Entry	Starting material		Reagent				Products		NMR yield (%) ^[a]		Isol. yield (%)	
		R	n	R	t (h)	11	12	11	12	11a-f	13a-f	
1	8a	Me	10a	0	Me	16	11a	12a	59	17	55	76
2	8b	Ph	10b	0	Ph	16	11b	12b	26	16	19	94
3	8a	Me	10c	1	Me	16	11c	12c	40	– ^[b]	37	62
4	8b	Ph	10d	1	Ph	16	11d	12d	66	20	52	95
5	8a	Me	10e	2	Me	18	11e	12e	49	– ^[b]	50	78
6	8b	Ph	10f	2	Ph	48	11f	12f	– ^[c]	– ^[c]	55	74

[a] The yield of **11** and **12** in the crude product and the product ratio were determined using ^1H NMR spectroscopy with 2,4,6-collidine as internal standard. Isol. yields surpassing the NMR-yield are within error deviations.^[16] [b] Not determinable due to low signal intensity. [c] Not determined.

the respective bisorganomagnesium species **10a–10f** (–30 °C). However, for economic reasons here only 0.55 equivalents instead of 1.1 equiv. of the organometallic reagents were used in contrast to the literature procedure.^[14a] As in related cases,^[14,15] these reactions resulted in mixtures of the regioisomeric 1,2- and 1,4-addition products, i.e. of **11a–11f** and **12a–12f**. In these mixtures according to ¹H NMR quantification based on the use of an internal standard, the desired 1,4-addition products **11a–11e** clearly prevailed in each case over the respective 1,2-addition products **12a–12e**. Thus, the ¹H NMR yields for **11a–11e** amounted to 26–66 % whereas for **12a–12e**, they ranged from values partly too low for an accurate determination (<1 %) to up to 20 %. In line with these results, **11a–11e** could finally be isolated in yields from 19–55 %. Dihydropyridine **11f**, for which the crude product had not been analyzed by ¹H NMR, was isolated in a yield of 55 %, indicating that also this addition reaction had proceeded in favor of the 1,4-addition product.

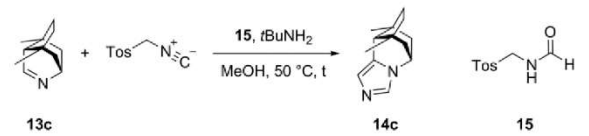
The successive intramolecular hetero-Diels-Alder reaction of **11a–11f** could finally be accomplished by subjecting the obtained 4,4-disubstituted 1,4-dihydropyridines **11a–11f** to TFA (15 equiv.) in pentane (at 20 °C for 15 min), i.e. reaction conditions published for related cycloaddition reactions before.^[14a] That way the desired tricyclic imines **13a–13f** were obtained in good to excellent yields (Table 1, entries 1–6: 62–95 %).

Next, we focused on the anellation of an imidazole ring to the imine function of the synthesized tricyclic imines **13a–13f** to generate the desired condensation products, imidazole derivatives **14**. This we intended to perform as already mentioned afore according to the so called van Leusen imidazole synthesis, in which imines are reacted with TosMIC in the presence of a base to give the corresponding imidazole derivative.^[5]

When imine **13c**, chosen as a model compound, was treated with TosMIC (1.5 equiv.) in MeOH and subsequently with *t*BuNH₂ (2.0 equiv., 20 °C) and stirred for 14 h at 50 °C (Table 2 entry 1), the desired imidazole **14c** could be obtained, yet only in a yield of 29 %. Upon extension of the reaction time to 96 h, the yield rose to moderate 49 % (Table 2, entry 2). Assuming

that an increased amount of deprotonated TosMIC might raise the reaction rate thus reducing the required reaction time, in a next attempt 6 equivalents of the base were employed under otherwise identical reaction conditions (50 °C, 14 h). However, the amount of formed product **14c** dropped to 19 % (Table 2, entry 3) indicating that a higher concentration of the base had an adverse effect. Therefore, the original ratio of TosMIC to *t*BuNH₂ of 1.5:2 was restored and the amount of TosMIC and *t*BuNH₂ relative to imine **13c** was doubled (Table 2, entry 4). This led to an improved, but still mediocre yield of 37 % (Table 2, entry 4). To our surprise, when the reaction was carried out with another batch of TosMIC under the initial reaction conditions (1.5 equiv. TosMIC, 2 equiv. *t*BuNH₂, 14 h), the yield improved from 29 % to 40 % (Table 2, compare entries 5 and 1). Careful analysis of the batch of TosMIC employed in this reaction revealed that about 2/3 of the reagent had undergone conversion into *N*-(tosylmethyl)formamide (**15**) by addition of water and only 1/3 of the reagent had remained unchanged. This result suggested that *N*-(tosylmethyl)formamide (**15**) has a positive effect on the imidazole formation given the fact that the actual quantity of TosMIC utilized was only about 1/3 of the calculated 1.5 equiv. whereas the yield of imidazole **14c** was still higher than that for the reaction with pure TosMIC (Table 2, compare entries 5 and 1). Accordingly, at next an experiment was performed which was identical with the first reaction (Table 2, entry 1) with pure TosMIC (1.5 equiv.) except that in addition 3 equiv. of *N*-(tosylmethyl)formamide (**15**) were added prior to heating to 50 °C for 14 h (Table 2, entry 6). In this case, a yield of 44 % was reached for imidazole **14c** which was significantly better than the result of the original reaction without *N*-(tosylmethyl)formamide (**15**), (Table 2, entry 1) and similar to that performed with the impure TosMIC sample (Table 2, entry 5). Although the amount of TosMIC and *N*-(tosylmethyl)formamide (**15**) had notably been raised as compared to the formerly conducted experiment (Table 2, compare entries 5 and 6), the yield remained roughly unchanged. Hence, it seemed reasonable that the effect mediated by *N*-(tosylmethyl)formamide (**15**) might also depend on the amount of the base

Table 2. Optimization of the synthesis of imidazole **14c**.



Entry	TosMIC [equiv.]	base [equiv.]	15 [equiv.]	t [h]	Isol. Yield [%]
1	1.5	<i>t</i> BuNH ₂ (2)	0	14	29
2	1.5	<i>t</i> BuNH ₂ (2)	0	96	49
3	1.5	<i>t</i> BuNH ₂ (6)	0	14	19
4	3.0	<i>t</i> BuNH ₂ (4)	0	14	37
5	n.d. ^[a]	<i>t</i> BuNH ₂ (2)	n.d. ^[a]	14	40
6	1.5	<i>t</i> BuNH ₂ (2)	3	14	44
7	1.5	<i>t</i> BuNH ₂ (6)	3	14	91
8	1.5	<i>n</i> BuNH ₂ (6)	3	14	48
9	1.5	DBU (6)	3	14	84

[a] The exact amount of TosMIC and **15** employed is unknown as a partially decomposed sample of TosMIC (the amount formally corresponding to 1.5 equiv.) containing also **15** was used. ¹H NMR spectroscopy indicated the amount of TosMIC in the mixture to be ca. 1/3 that of **15** ca. 2/3.

present. Therefore, the last reaction (Table 2, entry 6) was repeated with 6 instead of 3 equivalents of $t\text{BuNH}_2$ with the other reaction conditions remaining unchanged. In that case (1.5 equiv. TosMIC, 3 equiv. formamide **15**, 6 equiv. $t\text{BuNH}_2$), imidazole **14c** was isolated in an excellent yield of 91 %, suggesting that for the positive effect of formamide **15** on the imidazole formation indeed a sufficient amount of the base is required. Thus, in this reaction, the base $t\text{BuNH}_2$ might not only be required for the deprotonation of the cycloaddition reagent TosMIC, but also for a so far unknown activation of formamide **15**.

To verify whether other bases also might be suitable for this reaction, $t\text{BuNH}_2$ was substituted by *n*-butylamine or by 1,8-diazabicyclo(5.4.0)undec-7-ene (DBU) (Table 2, entries 8–9). With *n*BuNH₂, the yield significantly decreased to only 48 %, whereas DBU proved to be a suitable base as well and a very good yield (84 %) was achieved. However, as it is known that TosMIC does not decompose in the presence of $t\text{BuNH}_2$ ^[5] and the best yield in our experiments was obtained with this base, $t\text{BuNH}_2$ was chosen as base for all future experiments. Next, for the so far developed reaction conditions, ¹H NMR experiments were performed in the presence of 1,3,5-trimethoxybenzene as internal standard over a period of 20.5 h (Figure 3, solid line) to get an estimate in what quantity the starting material **13c** is consumed and the product **14c** is formed.

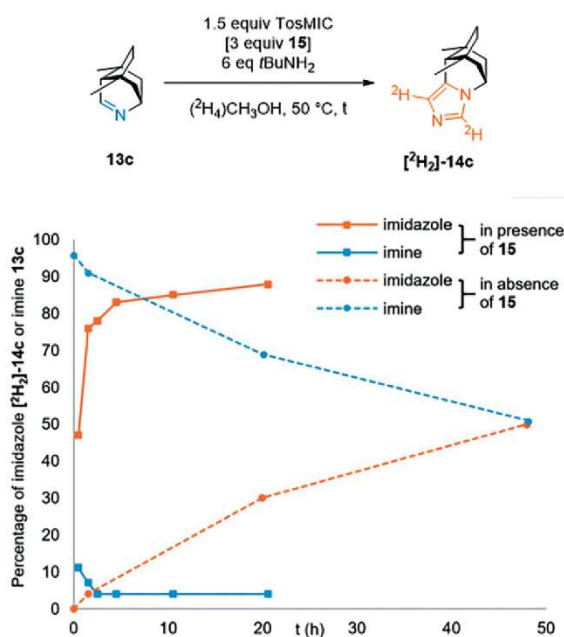


Figure 3. Time course of the imidazole formation in the absence and in the presence of *N*-(tosylmethyl)formamide (**15**). The percentage of **13c** and **[²H₂]-14c** in the reaction mixture was determined by ¹H NMR spectroscopy applying 1,3,5-trimethoxybenzene as internal standard.

Because of the need of (²H₄)CH₃OH as a deuterated solvent, these ¹H NMR experiments, however, did not reflect the signals of TosMIC, but of its deuterated analogue [²H₂]-TosMIC (exchange of protons of CH₂ group) and finally also those of the

double deuterated form of the final product, [²H₂]-**14c**. In case of the reaction of **13c** with TosMIC in the presence of *N*-(tosylmethyl)formamide (**15**), the percentage of the product [²H₂]-**14c** was fast-growing. An amount of 47 % and 76 % had been reached after 0.5 h and 1.5 h, respectively thereafter it took 19 h to further raise to 88 % (after 20.5 h). Interestingly, the share of remaining imine **13c** had dropped within 0.5 h to a value as low as 11 %. Thereafter, it lowered to 4 % within a reaction time of 2.5 h from whereon no further significant change could be observed. Due to the fact that a good ¹H NMR yield for imidazole [²H₂]-**14c** could already be observed after a reaction time of 1.5 h, this reaction time was considered sufficient for any further reaction to be performed.

In contrast, the reaction of imine **13c** with [²H₂]-TosMIC to give imidazole [²H₂]-**14c** performed in the absence of formamide **15** (Figure 3, dashed line) proceeded much slower. After 1.5 h, just 4 % of imidazole [²H₂]-**14c** had formed. This amount rose slowly to 51 % within 48 h, which equals the quantity that had been reached within only 0.5 h in the prior experiment with formamide **15**, clearly demonstrating the promoting effect of this compound (**15**). Intriguingly, in case of the cycloaddition reaction of **14c** with TosMIC executed in the presence of formamide **15**, a large gap between the amount of remaining starting material **13c** and formed product [²H₂]-**14c** exists, the sum of the share of both compounds being distinctly below 100 %. This phenomenon was most pronounced at the beginning of the reaction and became continuously less with increasing reaction time. In the absence of formamide **15**, no such discrepancy could be observed (see Figure 3). This clearly points to the formation of some intermediate during the reaction performed in the presence of *N*-(tosylmethyl)formamide (**15**), though at this point due to the complexity of the ¹H NMR spectra no such compound could be identified.

Next, the reaction conditions established for the cycloaddition of **13c** with TosMIC in the presence of *N*-(tosylmethyl)formamide (**15**) were applied to the tricyclic imines **13a–13b** and **13d–13f**. In order to get insight in the promoting effect of *N*-(tosylmethyl)formamide (**15**), these reactions were also performed in the absence of *N*-(tosylmethyl)formamide (**15**).

In both cases, the consumption of imine and formation of imidazole was quantified directly by ¹H NMR at the time point given. For this reason, the reactions were carried out in (²H₄)CH₃OH again. When imine **13a** was treated with TosMIC (1.5 equiv.) in the presence of formamide **15** (3 equiv.) and $t\text{BuNH}_2$ (6 equiv.) for 1.5 h at 50 °C, the desired imidazole [²H₂]-**14a** was formed to 51 % with no imine **13a** remaining (Table 3, entry 1). When in the same reaction formamide **15** was omitted, the ¹H NMR yield of imidazole [²H₂]-**14a** dropped to 25 %, and 45 % of the starting material **13a** was found to be still present. The results obtained for the reactions of imines **13b–13d** with TosMIC leading to [²H₂]-**14b–14d** (for the sake of completeness data of the formation of [²H₂]-**14c** described above have been included here, too) highlight the positive effect of *N*-(tosylmethyl)formamide (**15**) even better. Thus, the yields for imidazoles [²H₂]-**14b–14d** amounted to 46–76 % when formamide **15** was present, whereas only negligible amounts were identified when **15** was absent and large amounts of starting materials,

Table 3. Synthesis of various imidazoles.

Entry	Imine		Imidazole		t (h)	Percentage according to ¹ H NMR (%) ^[a]			
	struct.		struct.			in absence of 15		in presence of 15	
	R	no.	R	no.		Imine 13	Imidazole 14	Imine 13	Imidazole 14
1	Me	13a	Me	[²H₂]-14a	1.5	45	25	0	51 (63) ^[b]
					3	–	–	0	53
2	Ph	13b	Ph	[²H₂]-14b	1.5	98	traces	8	46 (59) ^[b]
					3	–	–	6	46
3	Me	13c	Me	[²H₂]-14c	1.5	91 ^[b]	4 ^[b]	7 ^[b]	76 ^[c] (91) ^[b,c]
					3	–	–	30	53
4	Ph	13d	Ph	[²H₂]-14d	1.5	90	traces	32	48 / 59 ^[d] (56) ^[b]
					3	–	–	30	53
5	Me	13e	Me	[²H₂]-14e	6 d	92	2	78	14 ^[e]
					6	82	2	83	12 ^[e]
7		13g		[²H₂]-14g	1.5	0	41	0	21 ^[e]
						25	66	0	83
8		13h		[²H₂]-14h	1.5	72 ^[f]	23 ^[f]	0 ^[f]	86 ^[f]

[a] The amount of **13** and **14** in the crude reaction mixture was determined using ¹H NMR spectroscopy with 1,3,5-trimethoxybenzene as internal standard.

[b] Isolated yield after purification (given in parentheses). The experiment was carried out in non-deuterated methanol leading to a non-deuterated imidazole.

[c] Identical to data given in Figure 3; isolated yield identical to data given in Table 2. [d] Yield determined after aqueous workup (addition of 1,3,5-trimethoxybenzene as internal standard to the crude reaction mixture, evaporation of (²H₄)CH₃OH, redissolving in CH₂Cl₂ and twofold washing with brine) using ¹H NMR spectroscopy. [e] In consequence of the low yields obtained, only analysis by ¹H NMR and ESI-HRMS was conducted for these products.

[f] Reaction at 25 °C.

imines **13b–d**, remained unchanged (Table 3, entries 2–4). To ensure that the moderate ^1H NMR yields for the syntheses of imidazoles $[\text{}^2\text{H}_2]\text{-14a–14b,d}$ in the presence of **15** were not due to an insufficient reaction time, these were repeated, setting the reaction time to 3 h. Yet, the quantities for unreacted imines **13a–13b,d** and formed imidazoles $[\text{}^2\text{H}_2]\text{-14a–14b,d}$ remained virtually unchanged (Table 3, entries 1, 2 and 4) which is in line with what had been observed when studying the time course of the transformation of **13c** into $[\text{}^2\text{H}_2]\text{-14c}$ (Figure 3). Similar to this transformation described in Figure 3, also the sum of the quantities of unreacted imine and formed imidazole was distinctly lower than 100 %, in particular for the transformations of imines **13a–13b** into imidazoles $[\text{}^2\text{H}_2]\text{-14a–14b}$. Remarkably, when the synthesis of imidazoles **14a–14d** was carried out in non-deuterated methanol (in the presence of **15**), the yields achieved after purification for the, in consequence non-deuterated imidazoles **14a–14d** were higher (56–91 % vs. 46–76 %; see Table 3, entries 1–4) than those observed in the ^1H NMR experiments [in $(^2\text{H}_4)\text{CH}_3\text{OH}$] afore. This is likely to be attributed to a so far unknown precursor of **14a–14d** which upon workup is at least partially transformed in the respective imidazole derivative. This was exemplarily verified by subjecting the ^1H NMR experiment with imidazole $[\text{}^2\text{H}_2]\text{-14d}$ (reaction time 1.5 h) to an aqueous workup. Thereupon, the yield for $[\text{}^2\text{H}_2]\text{-14d}$ determined by ^1H NMR out of the crude reaction

product rose from 48 % to 59 %, now being in good accord with the isolated yield of 56 % (Table 3, entry 4). By crystallization and subsequent X-ray crystallography of the non-deuterated imidazole **14d** the unique structure of these imidazoles was corroborated (Figure 4).

In contrast to the results described above, the yields obtained in the syntheses of imidazoles $[\text{}^2\text{H}_2]\text{-14e–f}$ from imines **13e–13f** were quite disappointing. Monitoring the reactions by TLC revealed that within 1.5 h no detectable amount of product had formed independent of the absence or presence of formamide **15**. When the reaction time was extended to 6 d for the formation without *N*-(tosylmethyl)formamide (**15**), still only minute amounts of imidazole derivatives $[\text{}^2\text{H}_2]\text{-14e–14f}$ could be detected (ca. 2 %, Table 3, entries 5–6). In contrast, the yield for these compounds was distinctly higher when formamide **15** was present in the reaction mixture, though still low with values of 14 % and 12 % for $[\text{}^2\text{H}_2]\text{-14e}$ and $[\text{}^2\text{H}_2]\text{-14f}$, respectively. Hence, despite the poor outcome of these reactions, the positive effect of formamide **15** was still clearly evident.

The poor yields obtained for the cycloaddition reaction performed with the cyclic imines **13e–13f** appear quite astonishing, considering the close structural similarity of these compounds with the imines **13a–13d**, for which the yields for the cycloaddition products, the imidazole derivatives $[\text{}^2\text{H}_2]\text{-14a–14d}$ had been quite satisfying. Clearly, this phenomenon must

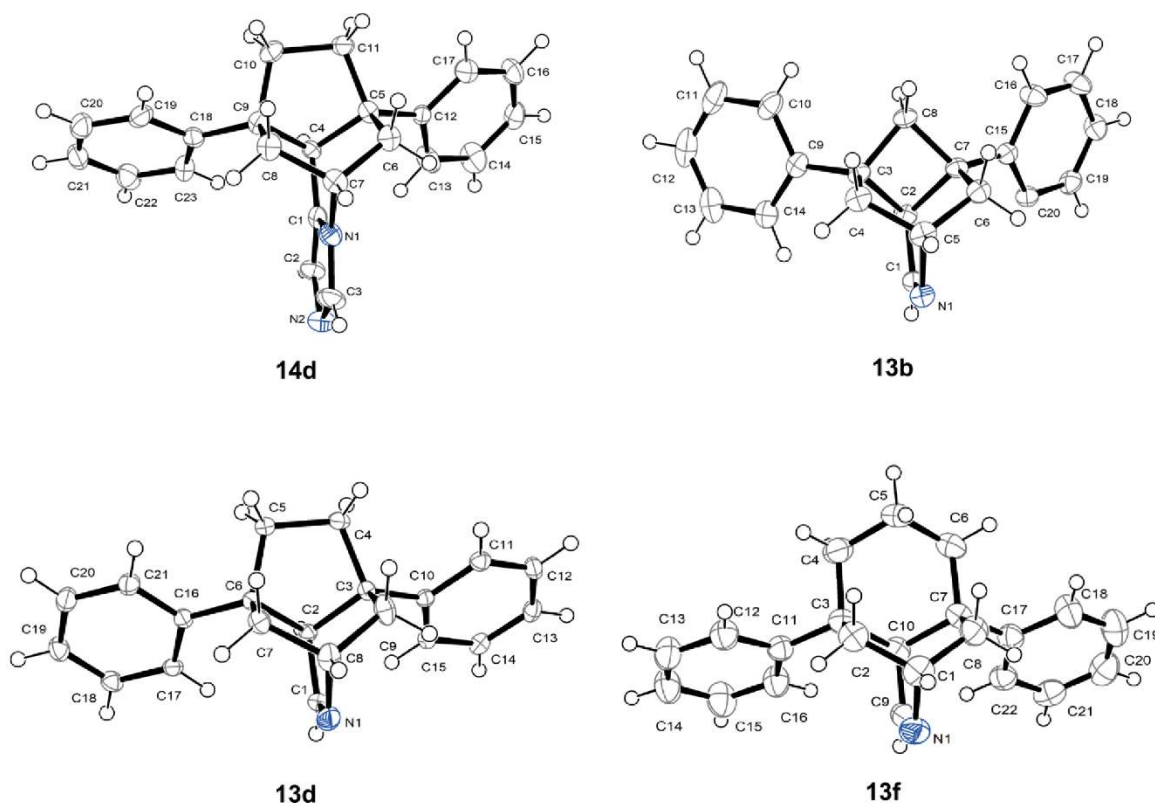


Figure 4. X-ray crystal structures of imidazole **14d** and tricyclic imines **13b**, **13d** and **13f**.^[17]

be associated with the continuous enlargement of the "upper bridge", from a CH₂, to a CH₂CH₂, and finally a CH₂CH₂CH₂ unit upon the transition from **13a–13b** to **13c–13d** and finally to **13e–13f**. As a result of the increasing size of this bridge, the adjacent bridgehead substituents should be pushed towards the imine function, thus increasing the shielding and associated with that reducing the reactivity of the latter. The assumed change of the orientation of the aforementioned bridgehead substituents could be verified by X-ray structures obtained for the phenyl-substituted imines **13b**, **13d**, and **13f**. These clearly show that with the increasing size of the "upper bridge" the bridgehead substituents are getting closer to the imine function.

Finally, the effect of *N*-(tosylmethyl)formamide (**15**) on the cycloaddition reaction of imines **13a–13f** with TosMIC should exemplarily also be studied for some imines structurally different from **13a–13f**. As such 2,3,4,5-tetrahydropyridine (**13g**) and 3,4-dihydroisoquinoline (**13h**) were selected. In case of the reaction with imine **13g**, the starting material was fully consumed within 1.5 h, independent of whether formamide **15** was present or not. However, this time the yield of the cycloaddition product [²H₂]-**14g** was higher when **15** was absent (41 %) than when it was present (21 %). Possibly, formamide **15** mediates decomposition reactions in this case as a multitude of side products was detected by ¹H NMR, which might be associated with the dynamic character of imine **13g** existing in mono- and trimeric form.^[18] However, the positive effect of *N*-(tosylmethyl)formamide (**15**) in the cycloaddition reaction with TosMIC became again evident when 3,4-dihydroisoquinoline (**13h**) was used as starting material. Employing the standard conditions, the ¹H NMR yield for the product [²H₂]-**14h** amounted to 83 % when formamide **15** was present and to 66 % when it was absent. Thereby, according to the ¹H NMR data in the first case the starting material had been completely consumed (0 %, **13h**) and in the latter 25 % remained unchanged (reaction time 1.5 h). The positive effect of *N*-(tosylmethyl)formamide (**15**) became even more apparent, when the conversion of imine **13h** into [²H₂]-**14h** was performed at a reduced temperature of 25 °C instead of 50 °C. Then, after the same reaction time (1.5 h) only 23 % of the imine **13h** had been transformed into product [²H₂]-**14h** when **15** was absent, but 86 % in its presence (¹H NMR yields, Table 3, entry 8).

Next, to shed some light on the fate and possibly on the function of *N*-(tosylmethyl)formamide **15** in the above described cycloaddition reaction, a series of control experiments was performed. First, formamide **15** dissolved in (²H₄)CH₃OH was kept for 1.5 h at 50 °C in the absence of any additive and further in the presence of TosMIC (0.5 equiv.), tricyclic imine **13c** (0.33 equiv.), or *t*BuNH₂ (2.0 equiv.) (Table 4, entries 1–4). According to the subsequently performed ¹H NMR analysis of the respective reactive mixtures, formamide **15** remained completely unchanged when no additive or TosMIC was present, or was accompanied with minute amounts of the decomposition product **16** (ca. 1 %; **16** was identified in a subsequent reaction) when tricyclic imine **13c** was present. However, when *tert*-butylamine was added (Table 4, entry 4) only minor amounts of **15** (4 %) remained unchanged after 1.5 h and new species had

formed. One of these could be identified as *p*-toluenesulfonic acid **16**, the share of which amounted to 96 %. Thereby, the base-induced decomposition of formamide **15** proceeds rather fast, as about 35 % of this compound had been converted into *p*-toluenesulfonic acid **16** even at the lower temperature of 25 °C within 7 min (Table 4, entry 5).

Table 4. Reactions of *N*-(tosylmethyl)formamide **15** under varying conditions.

Entry	Additive (equiv)	T [°C]	t (min)	¹ H NMR ratio 15 : 16
1	none	50	90	100:0
2	TosMIC (0.5)	50	90	100:0
3	13c (0.33)	50	90	99:1
4	<i>t</i> BuNH ₂ (2)	50	90	4:96
5	<i>t</i> BuNH ₂ (2)	25	7	65:35
6	TosMIC (0.5) <i>t</i> BuNH ₂ (2)	50	90	6:94
7	13c (0.33) <i>t</i> BuNH ₂ (2)	50	90	2:98
8	Cs ₂ CO ₃ (1)	25	20	2:98

To check whether TosMIC or imine **13c** might influence the *t*BuNH₂ induced decomposition of formamide **15**, control experiments were performed, in which in addition to *t*BuNH₂ either TosMIC or imine **13c** was present (Table 4, entries 6–7). The decay of formamide **15** turned out to be largely independent from these additives. However, new signals appeared in the ¹H NMR spectra (as compared to the reactions without these additives) indicating that from **15** derived decomposition products might have reacted with TosMIC and tricyclic imine **13c**, respectively. Yet, attempts to identify the newly formed species remained unsuccessful due to the high complexity of the ¹H NMR spectra and the low amounts of the respective compounds present.

According to Xia et al.,^[19] *N*-(tosylmethyl)formamide (**15**) upon treatment with Cs₂CO₃ (in toluene, at 70 °C) undergoes a decomposition reaction yielding *p*-toluenesulfinate **16** and *N*-methyleneformamide (**17**). Thereby the formation of the latter had only become evident from a by-product that had formed via its participation in a Michael addition reaction. Hence, it seemed reasonable to assume that also upon treatment of formamide **15** with *t*BuNH₂ (as it is e.g. the case in the reaction listed in Table 4, entry 4) besides *p*-toluenesulfinate (**16**) also *N*-methyleneformamide (**17**) is generated, though also as a rather short-lived intermediate.

A first hint that *N*-methyleneformamide **17** may also have formed under the reaction conditions used for the cycloaddition of imines **13** with TosMIC, i.e. when *t*BuNH₂ in (²H₄)CH₃OH is applied as a base, came from an MS analysis (ESI-HRMS, see SI). A reaction product obtained by treatment of imine **13c** with formamide **15** and *t*BuNH₂ (Table 4, entry 7) showed a MS signal attributable to an adduct consisting of imine **13c** and *N*-methyleneformamide **17**.

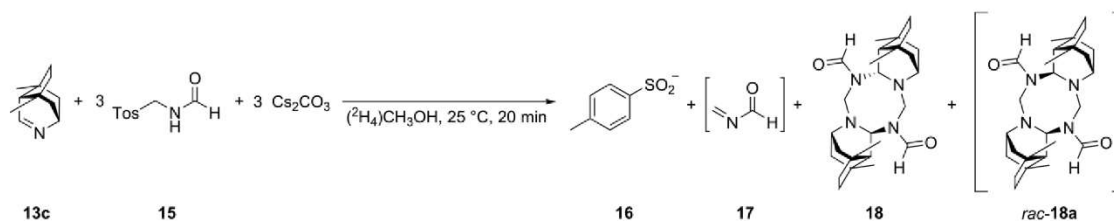
Next, $t\text{BuNH}_2$ should be substituted by Cs_2CO_3 in the cycloaddition reactions of imine **13c** with TosMIC. That way, so our hope, consecutive reactions of *N*-methyleneformamide (**17**) might be shifted towards intermediates important for the cycloaddition reaction with TosMIC, as no competing reactions with $t\text{BuNH}_2$ as nucleophile could take place.

A control experiment performed in this context, in which *N*-(tosylmethyl)formamide **15** was treated with Cs_2CO_3 in $(^2\text{H}_4)\text{CH}_3\text{OH}$ at 25 °C, revealed that also under these reaction conditions and within 20 min, **15** is almost quantitatively transformed in *p*-toluenesulfonic acid salt **16** (Table 4, entry 8). Though still no evidence for the formation of *N*-methyleneformamide (**17**) was found. However, when the decomposition experiment of *N*-(tosylmethyl)formamide **15** by Cs_2CO_3 in $(^2\text{H}_4)\text{CH}_3\text{OH}$ at 25 °C was performed in the presence of imine **13c** (Scheme 1), a new compound could be detected and isolated. This compound could be identified as the dimer **18**^[20] the structure of which comprising a unique 1,3,5,7-tetraazocane ring could be unequivocally established by X-ray crystallography (Figure 5). As can be seen from the structure of dimer **18**, this compound is the result of the combination of two molecules of the tricyclic imine **13c** with two molecules of *N*-methyleneformamide **17**. Accordingly, upon decomposition of formamide **15** besides *p*-toluenesulfonic acid **16** (compare to Table 4, entry 8), *N*-methyleneformamide **17** must have formed. Still, the existence of *N*-methyleneformamide **17** itself could not be corroborated, which might indicate that it is prone to rapid consecutive reactions under the reaction conditions given.

Interestingly, later on dimer **18** (and what is thought to be its racemic diastereomer *rac*-**18a**) could also be identified in the ^1H NMR spectra of experiments performed before (see support-

ing information). In particular, these were the control experiment when the decomposition of formamide **15** by $t\text{BuNH}_2$ had been studied in presence of imine **13c** (Table 4, entry 7) as well as the experiments in which the reactions time course under the original reaction conditions had been monitored by ^1H NMR (Figure 3, reaction with *N*-(tosylmethyl)formamide **15**; NMR taken after 0.5 h). Obviously also $t\text{BuNH}_2$ similar to Cs_2CO_3 appears to lead to the formation of *N*-methyleneformamide **17** upon fragmentation of *N*-(tosylmethyl)formamide (**15**).

Based on the above described results, the following mechanism for the catalytic effect of *N*-(tosylmethyl)formamide **15** on the synthesis of imidazoles seems plausible (Scheme 2). In the first step, *N*-(tosylmethyl)formamide (**15**) is cleaved by *tert*-butylamine to give *p*-toluenesulfonic acid **16** besides *N*-methyleneformamide **17**. By acting as a Michael acceptor methyleneformamide **17** reacts with imine **13c** to the iminium ion **19**, which exists in a reversible equilibrium with the isolated dimer **18** (and *rac*-**18a**) which has been isolated. Then TosMIC adds to this derivative, the thus activated intermediate iminium ion **19** – which possibly exists in an equilibrium with a cyclic oxadiazene species – to give the addition product **20**. Retro-Michael addition releases *N*-methyleneformamide **17** which is now available for a new reaction cycle. The nitrogen centered anion **21** that has been liberated by the retro-Michael addition should then successively react to imidazole **14c**, as it has been proposed by van Leusen et al. for the formation of imidazoles from imines and TosMIC, where a species analogous to **21** has been postulated as primary addition product.^[5] According to this rationale, *N*-methyleneformamide **17** acts as a catalyst for the activation of the imine function thus accelerating the imidazole synthesis.



Scheme 1. Cs_2CO_3 -induced decomposition of *N*-(tosylmethyl)formamide **15** in presence of imine **13c**.

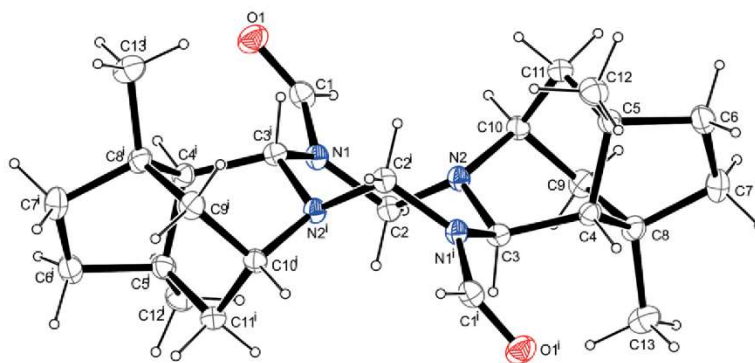
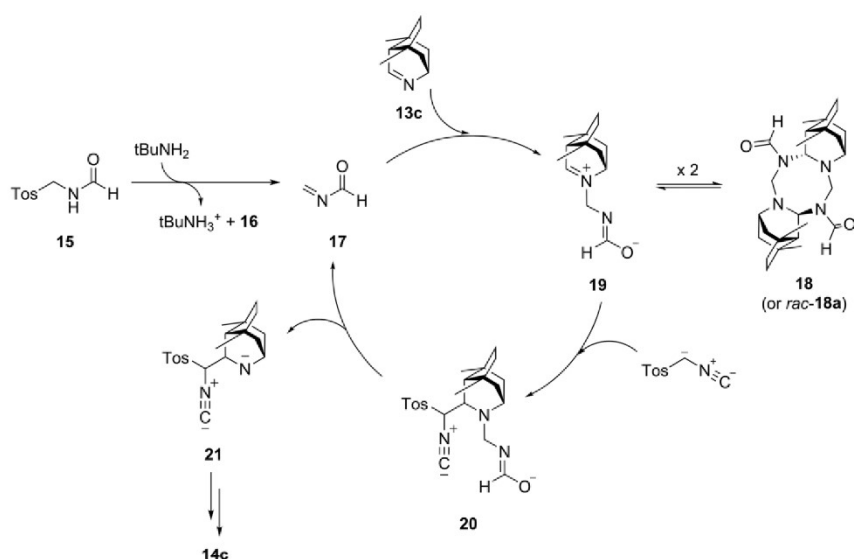


Figure 5. X-ray crystal structure of dimer **18**.^[17]



Scheme 2. Rationale for the promoting effect of *N*-(tosylmethyl)formamide (**15**).

Finally, to ensure the promoting effect for the imidazole syntheses arises from *N*-methyleneformamide **17** and not from another decomposition product of *N*-(tosylmethyl)formamide **15**, *p*-toluenesulfonic acid **16** and the most obvious hydrolysis products of *N*-methyleneformamide (**17**), i.e. formaldehyde and formamide, were studied for their effects on the formation of imidazole **14c** under the standard conditions (Table 5, entries 1–3). None of the tested compounds led to a reasonable effect and the starting imine **13c** remained largely unchanged. Interestingly, also the attempt to mimic the function of *N*-methyleneformamide **17** with acrolein in the course of the imidazole synthesis proved to be unsuccessful (Table 5, entry 4). As it seems, acrolein, due to its high reactivity, is prone to extensive side reactions leading to consumption of starting material **13c** and of TosMIC, that way interfering with the formation of the desired imidazole **14c**. This highlights nicely the unique function of *N*-methyleneformamide **17** as a catalyst that activates the imine function in the van Leusen imidazole synthesis.

Table 5. Control experiments to affirm *N*-methyleneformamide (**17**) as catalyst.

Entry	additive	Percentage according to ¹ H NMR (%) ^[a]	
		13c	[²H₂]-14c
1	16 (Na ⁺ salt)	93	4
2	formaldehyde	82	8
3	formamide	88	3
4	acrolein	68	4

[a] The amount of **13c** and **[²H₂]-14c** in the crude reaction mixture was determined using ¹H NMR spectroscopy with 1,3,5-trimethoxybenzene as internal standard.

Conclusion

In summary, a small set of imidazoles fused with a cyclic system in 1- and 5-position, starting from saturated aliphatic tricycles incorporating an imine functional group and TosMIC has been synthesized. By serendipity, *N*-(tosylmethyl)formamide was identified as a pre-catalyst for the imidazole synthesis, leading to significantly increased yields and shortened reaction times. Mechanistic studies suggest that by a *tert*-butylamine induced decomposition of *N*-(tosylmethyl)formamide, *N*-methyleneformamide is generated. Being a Michael acceptor, *N*-methyleneformamide (**17**) acts as an organocatalyst of these reactions by reacting with the imines, thus forming the corresponding iminium ions **19**, that are activated for the nucleophilic attack by TosMIC. This appears to be the first time an activation of imines for imidazole synthesis via cycloaddition with TosMIC is described which is likely to possess great potential for the employment of less reactive imines for the construction of 1,5-disubstituted imidazoles via the van Leusen imidazole synthesis. Accordingly, further studies exploring the scope of this method, the use of methyleneformamide (**17**) as an organocatalyst on an expanded set of acyclic and cyclic imines in the van Leusen imidazole synthesis can be expected to become a rewarding endeavor.

Experimental Section

Anhydrous reactions were performed under an argon atmosphere in vacuo-dried glassware. All solvents were distilled prior to use and dry THF, Et₂O, 1,4-dioxane and CH₂Cl₂ were prepared under a nitrogen atmosphere according to standard procedures.^[21] All purchased chemicals were used without further purification. TLC was performed with plates from Merck KGaA (silica gel 60 F₂₅₄ or aluminum oxide 60 F₂₅₄ on aluminum sheets, neutral). For purification via flash chromatography (FC) silica gel 60 (40–63 μm mesh size) from Merck KGaA or activated basic alumina Brockmann I (150 μm

mesh size) from Sigma-Aldrich adjusted to Brockmann III activity grade^[22] prior to use were employed. Melting points were determined with a BÜCHI 510 melting point apparatus. All melting points are uncorrected. Infrared spectra were recorded with a Perkin Elmer Paragon 1000 and a Jasco FT/IR-410. Solid substances were measured as KBr pellets and oils as film on NaCl. HRMS were obtained with a Finnigan MAT 95 (EI) and a Finnigan LTQ FT (ESI). ¹H and ¹³C NMR spectra were acquired with a Avance III HD Bruker BioSpin (400 or 500 MHz), referenced to the solvent residual peak as internal standard and analyzed with MestReNova (Version 12.0.0–20080; Mestrelab Research S.L.; released 26.09.2017).^[23]

2,3,4,5-Tetrahydropyridine **13g**^[24] and *N*-(tosylmethyl)formamide **15**^[19] were synthesized according to the literature.

Synthesis of 4,4-disubstituted *N*-triisopropylsilyl-1,4-dihydropyridines (general procedure/ GP1)

The 4-substituted pyridine derivatives were dissolved in CH₂Cl₂ (0.86 mL/mmol) and TIPSOTf (1.1 equiv.) was added. Prior to cooling to –30 °C and subsequent dropwise addition of the R₂Mg solution (0.55 equiv.) the solution was stirred at r.t. for 15 min. After the time given the reaction was quenched by addition of water (10 mL/mmol) followed by extraction of the aqueous layer with CH₂Cl₂ (3 × 10 mL/mmol). The combined organic layers were dried with MgSO₄ and the solvent was removed under vacuum. Quantitative determination of the dihydropyridines in the crude product was achieved by ¹H NMR spectroscopy using 2,4,6-collidine as internal standard. The oxidation of side products was realized by stirring of the crude product under air for the specified period of time, followed by purification by FC.

Synthesis of symmetric tricyclic imines (general procedure / GP2)

The symmetric tricyclic imines were prepared in analogy to the literature.^[14a]

TFA (15 equiv.) was added to a solution of the 4,4-disubstituted *N*-triisopropylsilyl-1,4-dihydropyridine (1.0 equiv.) in pentane (10 mL/mmol) in one portion and the resulting mixture was stirred for 15 min at 20 °C. The reaction was quenched by the addition of K₂CO₃ (8 equiv.) and a 1:1 mixture of 2 M HCl_{aq} and EtOH (40 mL/mmol) was added. The solution was washed with pentane (6 × 20 mL/mmol) and adjusted to pH = 9 with K₂CO₃. The aqueous layer was extracted with CH₂Cl₂ (4 × 20 mL/mmol), the organic layers were combined, dried with Na₂SO₄, and the solvent was removed under vacuum. The crude product was purified by FC.

Synthesis of symmetric tricyclic imidazoles (general procedure / GP3)

To a solution of TosMIC (1.5 equiv.) in methanol (6.7 mL/mmol) the imine (1.0 equiv.) and subsequently *N*-(tosylmethyl)formamide (3 equiv.) was added at 20 °C. The resulting mixture was treated with *t*BuNH₂ (6 equiv.), stirred for 1.5 h at 50 °C and then allowed to reach 20 °C. The solvent was removed under vacuum, the residue was dissolved in CH₂Cl₂ (20 mL/mmol) and washed with saturated aqueous NaCl solution (20 mL/mmol) twice. The organic layer was dried with MgSO₄, the solvent removed under vacuum and the crude product was purified by FC.

NMR experiments

The ¹H NMR experiments to study the formation of the imidazoles (Figure 3; Table 3, Table 5) and to explore the function of *N*-(tosylmethyl)formamide **15** (Table 4; Scheme 1) were carried out on the basis of GP3 in (CD₃)₂CO. The concentrations of the reagents used were identical to those described in GP3 and as follows: Imines **13a–13h** (0.1 mmol/mL), TosMIC (0.15 mmol/mL), *N*-(tosyl-

methyl)formamide **15** (0.3 mmol/mL), *t*BuNH₂ (0.6 mmol/mL). After the reaction time indicated the crude reaction mixtures were cooled to 20 °C and analyzed by ¹H NMR spectroscopy. Quantification of the imines **13a–13h** and the imidazoles **14a–14h** in the crude reaction mixture was achieved by ¹H NMR spectroscopy with 1,3,5-trimethoxybenzene as internal standard. Assignment of the imine and imidazole protons was accomplished by means of reference spectra given in this publication or in literature.

Preparation of bis(organo)magnesium solutions 10c–f

The bis(organo)magnesium solutions employed in the synthesis of the 4,4-disubstituted *N*-triisopropylsilyl-1,4-dihydropyridines were prepared according to our previously published procedure.^[14a] The utilized organic halides (3-bromoprop-1-en-2-yl)benzene,^[25] 4-bromo-2-methylbut-1-ene,^[26] 1-bromo-3-phenylbut-3-ene^[27] (synthesis via 3-phenylbut-3-en-1-ol^[28]), 5-bromo-2-methylpent-1-ene^[29] and (5-chloropent-1-en-2-yl)benzene^[30] were synthesized according to literature. 3-Bromo-2-methyl-1-propene was purchased.

Magnesium turnings (1.5 equiv.) were covered with THF (0.13 mL/mmol) and a solution of the organic halide (1.0 equiv.) in THF (0.8 mL/mmol) was added dropwise to keep the reaction mixture boiling mildly. After complete addition stirring was continued for 1 h at 20 °C followed by addition of 1,4-dioxane (1.1 equiv.) and further stirring for 1 h at 20 °C. The resulting suspension was centrifuged (30 min, 3000 g), the supernatant was separated and the remaining slurry was suspended in Et₂O to retrieve the same volume as before. Centrifugation was repeated (30 min, 3000 g) and the supernatants were combined. The concentrations of the bis-(organo)magnesium solutions were determined according to a procedure of Chong et al.^[31]

Deviating from this, bis(2-methylallyl)magnesium **10a** and bis(2-phenylallyl)magnesium **10b** were synthesized as reported below.

Bis(2-methylallyl)magnesium 10a

3-Bromo-2-methylpropene (1.0 equiv., 2 M in THF) was added to magnesium powder (1.2 equiv., 3 M in THF) over a period of 2 h at 0 °C. The reaction mixture was kept at 0 °C for 2 h, subsequently stirred at 20 °C for 12 h followed by addition of 1,4-dioxane (1.1 equiv.) and further stirring for 1 h at 20 °C. The resulting suspension was centrifuged (30 min, 3000 g), the supernatant was separated and the remaining slurry was suspended in Et₂O to retrieve the same volume as before. Centrifugation was repeated (30 min, 3000 g) and the supernatants were combined.

Bis(2-phenylallyl)magnesium 10b

To a suspension of Rieke magnesium (preparation in analogy to literature,^[32] 0.57 M in THF; 1 equiv.) was added (3-bromoprop-1-en-2-yl)benzene (0.40 equiv.) dropwise. The mixture was kept at 20 °C for 1 h followed by addition of 1,4-dioxane (0.55 equiv.) and further stirring for 1 h at 20 °C. The resulting suspension was centrifuged (30 min, 3000 g) and the supernatant was separated.

4-Methyl-4-(2-methylallyl)-1-triisopropylsilyl-1,4-dihydropyridine 11a

Synthesis according to GP1 from 4-picoline (305 mg, 3.27 mmol, 318 μL), TIPSOTf (1.10 g, 3.59 mmol, 0.97 mL) and bis(2-methylallyl)magnesium **10a** (0.09 M in THF/Et₂O 1:1, 1.80 mmol, 20.0 mL). The reaction was stopped after 16 h. Quantitative determination indicated 590 mg (59 %) of dihydropyridine **11a** followed by stirring under air for 2 d. Purification by FC (Al₂O₃-basic, activity III, pentane) afforded **11a**.

Colorless oil (552 mg, 55 %); *R*_f = 0.95 (Al₂O₃; pentane); ¹H NMR (400 MHz, CDCl₃): δ = 5.93 (d, *J* = 8.2 Hz, 2 H, 2 × NCHCH),

4.76 (dq, $J = 2.9/1.5$ Hz, 1 H, $CCH_2CCH_2^b$), 4.66–4.61 (m, 1 H, $CCH_2CCH_2^a$), 4.29 (d, $J = 8.2$ Hz, 2 H, $2 \times NCHCH$), 1.97 (d, $J = 0.7$ Hz, 2 H, CCH_2C), 1.77 (dd, $J = 1.4/0.8$ Hz, 3 H, CH_2CCH_3), 1.30–1.18 (m, 3 H, $3 \times CH(CH_3)_2$), 1.07 (d, $J = 7.2$ Hz, 18H, $3 \times CH(CH_3)_2$), 1.05 (s, 3 H, $CHCCCH_3$); ^{13}C NMR (100 MHz, $CDCl_3$): $\delta = 144.6$ ($CHCCH_2C$), 127.5 (NCH), 113.1 (CCH_2CCH_2), 108.6 (NCHCH), 53.9 ($CHCCH_2$), 34.4 (CHC), 34.2 ($CHCCH_3$), 25.0 ($CHCCH_2CCH_3$), 18.0 ($3 \times CH(CH_3)_2$), 11.6 ($3 \times CH(CH_3)_2$); IR (film): $\tilde{\nu} = 3072, 3043, 2945, 2868, 1670, 1601, 1464, 1369, 1288, 1088, 1065, 1016, 970, 883, 733, 689, 660$ cm^{-1} ; HRMS (EI): m/z [M] $^+$ calcd. for $C_{19}H_{35}NSi$: 305.2533, found 305.2583.

4-Phenyl-4-(2-phenylallyl)-1-triisopropylsilyl-1,4-dihydropyridine 11b

Synthesis according to GP1 from 4-phenylpyridine (1.38 g, 8.89 mmol), TIPSOTf (3.00 g, 9.78 mmol, 2.6 mL) and bis(2-phenylallyl)magnesium **10b** (0.10 m in THF, 4.89 mmol, 50.0 mL). The reaction was stopped after 16 h. Quantitative determination indicated 996 mg (26 %) of dihydropyridine **11b** followed by stirring under air for 2 d. Purification by FC (Al_2O_3 -basic, activity III, pentane) afforded **11b**.

Orange solid (723 mg, 19 %); $R_f = 0.41$ (Al_2O_3 ; pentane); m.p. 59 °C; 1H NMR (400 MHz, $CDCl_3$): $\delta = 7.43$ – 7.38 (m, 2 H, $2 \times CHCCCHCHCH$), 7.35– 7.28 (m, 4 H, $2 \times CHCCCHCHCH$, $2 \times C_{alkene}CCH$), 7.25– 7.16 (m, 3 H, $2 \times C_{alkene}CCHCH$, $C_{alkene}CCHCHCH$), 7.13 (tt, $J = 7.3/1.2$ Hz, 1 H, $CHCCCHCHCH$), 5.89 (d, $J = 8.2$ Hz, 2 H, $2 \times NCH$), 5.28 (d, $J = 1.9$ Hz, 1 H, $CCH_2CCH_2^b$), 5.03– 4.98 (m, 1 H, $CCH_2CCH_2^a$), 4.35 (d, $J = 8.3$ Hz, 2 H, $2 \times NCHCH$), 2.99 (s, 2 H, CCH_2C), 1.27– 1.13 (m, 3 H, $3 \times CH(CH_3)_2$), 1.05 (d, $J = 7.2$ Hz, 18H, $3 \times CH(CH_3)_2$); ^{13}C NMR (100 MHz, $CDCl_3$): $\delta = 152.5$ ($CHCCCHCHCH$), 147.0 ($C_{alkene}CCH$), 144.0 ($C_{alkene}CCH$), 128.2 ($CHCCCHCHCH$), 127.9 ($C_{alkene}CCHCH$), 127.7 (NCH), 127.1 ($C_{alkene}CCH$), 126.7 ($C_{alkene}CCHCHCH$), 126.6 ($CHCCCHCHCH$), 125.3 ($CHCCCHCHCH$), 116.7 (CCH_2CCH_2), 106.7 (NCHCH), 49.0 (CCH_2CCH_2), 42.8 (CCH_2CCH_2), 18.0 ($3 \times CH(CH_3)_2$), 11.5 ($3 \times CH(CH_3)_2$); IR (film): $\tilde{\nu} = 3643, 3325, 3271, 3055, 3022, 2927, 2864, 1946, 1871, 1803, 1599, 1495, 1444, 1032, 758, 700$ cm^{-1} ; HRMS (ESI): m/z [M + H] $^+$ calcd. for $C_{29}H_{46}NSi$ 430.2925, found 430.2926.

4-Methyl-4-(3-methylbut-3-en-1-yl)-1-triisopropylsilyl-1,4-dihydropyridine 11c

Synthesis according to GP1 from 4-picoline (1.14 g, 12.3 mmol, 1.2 mL), TIPSOTf (4.14 g, 13.5 mmol, 3.6 mL) and bis(3-methylbut-3-en-1-yl)magnesium **10c** (0.25 m in THF/ Et_2O 1:1, 6.77 mmol, 27.0 mL). The reaction was stopped after 16 h. Quantitative determination indicated 1.57 g (40 %) of dihydropyridine **11c**. Purification by FC (Al_2O_3 -basic, activity III, pentane) afforded **11c**.

Colorless solid (1.45 g, 37 %); $R_f = 0.97$ (Al_2O_3 ; pentane); m.p. 33 °C; 1H NMR (400 MHz, $CDCl_3$): $\delta = 6.03$ – 5.96 (m, 2 H, $2 \times NCH$), 4.65 (q, $J = 1.1$ Hz, 2 H, $CH_2CH_2CCH_2$), 4.21– 4.15 (m, 2 H, $2 \times NCHCH$), 2.04– 1.94 (m, 2 H, $CHCCH_2CH_2$), 1.72 (t, $J = 1.0$ Hz, 3 H, $C_{alkene}CH_3$), 1.29– 1.18 (m, 5 H, $3 \times CH(CH_3)_2$, $CHCCH_2$), 1.08 (d, $J = 7.2$ Hz, 18H, $3 \times CH(CH_3)_2$), 1.03 (s, 3 H, $CHCCH_3$); ^{13}C NMR (100 MHz, $CDCl_3$): $\delta = 147.8$ ($CH_2CH_2CCH_2$), 128.3 (NCH), 108.6 ($CH_2CH_2CCH_2$), 107.8 (NCHCH), 44.0 ($CHCCH_2$), 34.9 ($CH_2CH_2CCH_2$), 33.8 ($CHCCH_3$, CHC), 23.2 ($CHC(CH_2)_2CCH_3$), 18.0 ($3 \times CH(CH_3)_2$), 11.6 ($3 \times CH(CH_3)_2$); IR (KBr): $\tilde{\nu} = 3091, 3041, 2945, 2866, 1668, 1647, 1599, 1464, 1377, 1286, 1109, 1078, 1045, 1016, 972, 881, 746, 733, 689, 663, 619, 513$ cm^{-1} ; HRMS (EI): m/z [M] $^+$ calcd. for $C_{20}H_{37}NSi$ 319.2690, found 319.2692.

4-Phenyl-4-(3-phenylbut-3-en-1-yl)-1-triisopropylsilyl-1,4-dihydropyridine 11d

Synthesis according to GP1 from 4-phenylpyridine (534 mg, 3.44 mmol), TIPSOTf (1.16 g, 3.78 mmol, 1.05 mL) and bis(3-phenyl-

but-3-en-1-yl)magnesium **10d** (0.20 m in THF/ Et_2O 1:1, 1.89 mmol, 9.6 mL). The reaction was stopped after 16 h. Quantitative determination indicated 1.01 g (66 %) of dihydropyridine **11d** followed by stirring under air for 4 d. Purification by FC (Al_2O_3 -basic, activity III, pentane) afforded **11d**.

Yellow solid (788 mg, 52 %); $R_f = 0.52$ (Al_2O_3 ; pentane); m.p. 54 °C; 1H NMR (500 MHz, $CDCl_3$): $\delta = 7.46$ – 7.42 (m, 2 H, $2 \times C_{alkene}CCH$), 7.41– 7.38 (m, 2 H, $2 \times CHCCCHCHCH$), 7.34– 7.29 (m, 4 H, $4 \times CCCHCHCH$), 7.27– 7.23 (m, 1 H, $C_{alkene}CCHCHCH$), 7.14 (tt, $J = 7.3/1.3$ Hz, 1 H, $CHCCCHCHCH$), 6.19 (d, $J = 8.3$ Hz, 2 H, $2 \times NCH$), 5.31 (d, $J = 1.4$ Hz, 1 H, $CH_2CH_2CCH_2^b$), 5.11 (d, $J = 1.4$ Hz, 1 H, $CH_2CH_2CCH_2^a$), 4.44 (d, $J = 8.3$ Hz, 2 H, $2 \times NCHCH$), 2.66– 2.57 (m, 2 H, $CH_2CH_2CCH_2$), 1.86– 1.78 (m, 2 H, $CH_2CH_2CCH_2$), 1.30 (sep, $J = 7.5$ Hz, 3 H, $3 \times CH(CH_3)_2$), 1.12 (d, $J = 7.4$ Hz, 18H, $3 \times CH(CH_3)_2$); ^{13}C NMR (125 MHz, $CDCl_3$): $\delta = 152.4$ ($CHCCCHCHCH$), 149.5 ($C_{alkene}CCH$), 141.6 ($C_{alkene}CCH$), 128.5 (NCH), 128.3 ($CCCHCHCH$), 128.2 ($CCCHCHCH$), 127.3 ($C_{alkene}CCHCHCH$), 126.8 ($CHCCCHCHCH$), 126.2 ($C_{alkene}CCH$), 125.4 ($CHCCCHCHCH$), 111.6 ($CH_2CH_2CCH_2$), 106.2 (NCHCH), 41.9 ($CCH_2CH_2CCH_2$), 41.8 ($CH_2CH_2CCH_2$), 32.4 ($CH_2CH_2CCH_2$), 18.1 ($3 \times CH(CH_3)_2$), 11.6 ($3 \times CH(CH_3)_2$). Signals indicated by * cannot be assigned unambiguously and are interchangeable; IR (KBr): $\tilde{\nu} = 3082, 3051, 2949, 2866, 1664, 1597, 1464, 1444, 1288, 1076, 1047, 976, 881, 777, 740, 692, 665, 632, 523, 498$ cm^{-1} ; HRMS (ESI): m/z [M + H] $^+$ calcd. for $C_{30}H_{42}NSi$ 444.3081, found 444.3088.

4-Methyl-4-(4-methylpent-4-en-1-yl)-1-triisopropylsilyl-1,4-dihydropyridine 11e

Synthesis according to GP1 from 4-picoline (521 mg, 5.59 mmol, 0.54 mL), TIPSOTf (1.88 g, 6.15 mmol, 1.7 mL) and bis(4-methylpent-4-en-1-yl)magnesium **10e** (0.21 m in THF/ Et_2O 1:1, 3.07 mmol, 15.0 mL). The reaction was stopped after 18 h. Quantitative determination indicated 907 mg (49 %) of dihydropyridine **11e**. Purification by FC (Al_2O_3 -basic, activity III, pentane) afforded **11e**.

Colorless oil (935 mg, 50 %); $R_f = 0.93$ (Al_2O_3 ; pentane); 1H NMR (500 MHz, $CDCl_3$): $\delta = 6.00$ – 5.95 (m, 2 H, $2 \times NCH$), 4.68– 4.61 (m, 2 H, $CH_2CH_2CCH_2$), 4.20– 4.13 (m, 2 H, $2 \times NCHCH$), 1.99 (t, $J = 7.6$ Hz, 2 H, $CH_2CH_2CCH_2$), 1.69 (s, 3 H, $C_{alkene}CH_3$), 1.48– 1.39 (m, 2 H, $CH_2CH_2CCH_2$), 1.28– 1.18 (m, 3 H, $3 \times CH(CH_3)_2$), 1.14– 1.03 (m, 2 H, $CHCCH_2$), 1.08 (d, $J = 7.4$ Hz, 18 H, $3 \times CH(CH_3)_2$), 1.00 (s, 3 H, $CHCCH_3$); ^{13}C NMR (125 MHz, $CDCl_3$): $\delta = 146.8$ ($CH_2CH_2CCH_2$), 128.0 (NCH), 109.5 ($CH_2CH_2CCH_2$), 108.1 (NCHCH), 45.6 ($CHCCH_2$), 38.5 ($CH_2CH_2CCH_2$), 33.8 ($CHCCH_3$, CHC), 24.3 ($CH_2CH_2CCH_2$), 22.6 ($C_{alkene}CH_3$), 18.0 ($3 \times CH(CH_3)_2$), 11.6 ($3 \times CH(CH_3)_2$); IR (film): $\tilde{\nu} = 3072, 3039, 2945, 2895, 2868, 1668, 1606, 1462, 1383, 1286, 1076, 1016, 970, 883, 731, 688, 665$ cm^{-1} ; HRMS (EI): m/z [M – CH_3] $^+$ calcd. for $C_{20}H_{36}NSi$ 318.2612, found 318.2603.

4-Phenyl-4-(4-phenylpent-4-en-1-yl)-1-triisopropylsilyl-1,4-dihydropyridine 11f

Synthesis according to GP1 from 4-phenylpyridine (818 mg, 5.27 mmol), TIPSOTf (1.78 g, 5.80 mmol, 1.56 mL) and bis(3-phenylbut-3-en-1-yl)magnesium **10f** (0.19 m in THF/ Et_2O 1:1, 2.90 mmol, 15.5 mL). The reaction was stopped after 48 h. Quantitative determination was omitted followed by stirring under air for 2 d. Purification by FC (Al_2O_3 -basic, activity III, pentane) afforded **11f**.

Yellow solid (1.31 g, 55 %); $R_f = 0.63$ (Al_2O_3 ; pentane); m.p. 61 °C; 1H NMR (500 MHz, $CDCl_3$): $\delta = 7.41$ – 7.35 (m, 4 H, $2 \times CHCCCHCHCH$, $2 \times C_{alkene}CCH$), 7.33– 7.28 (m, 4 H, $4 \times CCCHCHCH$), 7.26– 7.20 (m, 1 H, $C_{alkene}CCHCHCH$), 7.12 (tt, $J = 7.3/1.3$ Hz, 1 H, $CHCCCHCHCH$), 6.09– 6.02 (m, 2 H, $2 \times NCH$), 5.25 (d, $J = 1.5$ Hz, 1 H, $CH_2CH_2CCH_2^b$), 5.06 (dt, $J = 1.4/1.3$ Hz, 1 H, $CH_2CH_2CCH_2^a$), 4.35– 4.30 (m, 2 H, $2 \times NCHCH$), 2.55 (t, $J = 7.4$ Hz, 2 H, $CH_2CCH_2CH_2$), 1.73– 1.65 (m,

2 H, CH₂CCH₂CH₂CH₂), 1.61–1.54 (m, 2 H, CH₂CH₂CH₂), 1.28–1.18 (m, 3 H, 3 × CH(CH₃)₂), 1.06 (d, *J* = 7.4 Hz, 18 H, 3 × CH(CH₃)₂); ¹³C NMR (125 MHz, CDCl₃): δ = 152.7 (CHCCCHCHCH), 149.1 (C_{alkene}C), 141.9 (C_{alkene}C), 128.3 (CCCHCHCH)*, 128.1 (CCCHCHCH)*, 128.1 (NCH), 127.3 (C_{alkene}CCHCHCH), 126.8 (CHCCCHCHCH), 126.3 (C_{alkene}CCH), 125.3 (CHCCCHCHCH), 112.0 (CH₂CH₂CCH₂), 106.5 (NCHCH), 41.8 (NCHCHC), 35.9 (CH₂CH₂CCH₂), 24.8 (CH₂CH₂CH₂), 18.0 (3 × CH(CH₃)₂), 11.5 (3 × CH(CH₃)₂). Signals indicated by * cannot be assigned unambiguously and are interchangeable; IR (KBr): ν̄ = 3049, 2949, 2864, 1666, 1626, 1601, 1491, 1460, 1387, 1288, 1078, 1057, 976, 883, 766, 744, 694, 665, 631 cm⁻¹; HRMS (EI): *m/z* [M]⁺ calcd. for C₃₁H₄₃NSi 457.3160, found 457.3170.

1,7-Dimethyl-4-azatricyclo[3.3.1.0^{2,7}]non-3-ene 13a

Synthesis according to GP2 from dihydropyridine **11a** (622 mg, 2.04 mmol) and TFA (3.48 g, 30.5 mmol, 2.34 mL) in pentane (20 mL). Purification by FC (Al₂O₃-basic, activity III, pentane/CH₂Cl₂/MeOH 88.5:10:1.5) afforded imine **13a**.

Yellow oil (230 mg, 76 %); *R*_f = 0.35 (Al₂O₃; pentane/CH₂Cl₂/MeOH 88.5:10:1.5); ¹H NMR (400 MHz, CDCl₃): δ = 8.08 (d, *J* = 3.8 Hz, 1 H, NCHCH), 4.46 (tt, *J* = 3.1/1.9 Hz, 1 H, NCH(CH₂)₂), 2.48 (d, *J* = 3.7 Hz, 1 H, NCHCH), 1.71 (dt, *J* = 9.0/2.3 Hz, 1 H, CCH₂^bC), 1.58 (dd, *J* = 12.6/2.1 Hz, 2 H, 2 × NCHCH₂^b), 1.29 (d, *J* = 9.0 Hz, 1 H, CCH₂^aC), 0.94 (s, 6 H, 2 × CH₃), 0.82–0.75 (m, 2 H, 2 × NCHCH₂^a); ¹³C NMR (100 MHz, CDCl₃): δ = 167.1 (NCHCH), 56.5 (NCH(CH₂)₂), 50.9 (NCHCH), 49.3 (CCH₂C), 37.8 (NCH(CH₂)₂), 34.9 (CCH₂), 26.6 (CH₃); IR (film): ν̄ = 3388, 2997, 2947, 2920, 2860, 1672, 1610, 1450, 1375, 1342, 1282, 1151, 1016, 719 cm⁻¹; HRMS (EI): *m/z* [M]⁺ calcd. for C₁₀H₁₅N 149.1199, found 149.1203.

1,7-Diphenyl-4-azatricyclo[3.3.1.0^{2,7}]non-3-ene 13b

Synthesis according to GP2 from dihydropyridine **11b** (700 mg, 1.63 mmol) and TFA (2.81 g, 24.4 mmol, 1.89 mL) in pentane (16 mL). Purification by FC (Al₂O₃-basic, activity III, pentane/CH₂Cl₂/MeOH 87:10:3) afforded imine **13b**.

Colorless solid (417 mg, 94 %); *R*_f = 0.34 (Al₂O₃; pentane/CH₂Cl₂/MeOH 87:10:3); m.p. 95 °C; ¹H NMR (500 MHz, CDCl₃): δ = 8.57 (d, *J* = 3.7 Hz, 1 H, NCHCH), 7.33–7.26 (m, 4 H, CCCHCHCH), 7.21–7.15 (m, 2 H, CCCHCHCH), 7.08–7.01 (m, 4 H, CCCHCHCH), 4.76–4.69 (m, 1 H, NCH(CH₂)₂), 3.34 (d, *J* = 3.6 Hz, 1 H, NCHCH), 2.78 (dt, *J* = 9.0/2.2 Hz, 1 H, CCH₂^bC), 2.15–2.06 (m, 3 H, 2 × NCHCH₂^b, CCH₂^aC), 1.35 (d, *J* = 13.5 Hz, 2 H, 2 × NCHCH₂^a); ¹³C NMR (125 MHz, CDCl₃): δ = 166.7 (NCHCH), 147.1 (CCCH₂), 128.6 (CCHCHCH), 126.3 (CCHCHCH), 125.1 (CCHCHCH), 56.6 (NCH(CH₂)₂), 48.9 (NCHCH), 45.6 (CCH₂C), 42.4 (CH₂C), 40.2 (NCH(CH₂)₂); IR (KBr): ν̄ = 3051, 3020, 2960, 2926, 2846, 1610, 1599, 1495, 1444, 1340, 1205, 1070, 752, 700, 540, 482 cm⁻¹; HRMS (EI): *m/z* [M]⁺ calcd. for C₂₀H₁₉N 273.1512, found 273.1514.

3,6-Dimethyl-9-azatricyclo[4.3.1.0^{3,7}]dec-8-ene 13c

Synthesis according to GP2 from dihydropyridine **11c** (2.32 g, 7.26 mmol) and TFA (20.7 g, 109 mmol, 13.9 mL) in pentane (72 mL). Purification by FC (Al₂O₃-basic, activity III, pentane/CH₂Cl₂/MeOH 88:10:2) afforded imine **13c**.

Yellow oil (735 mg (62 %); *R*_f = 0.58 (Al₂O₃; pentane/CH₂Cl₂/MeOH 88:10:2); ¹H NMR (500 MHz, CDCl₃): δ = 8.20 (d, *J* = 4.1 Hz, 1 H, NCHCH), 4.14 (p, *J* = 2.6 Hz, 1 H, NCH(CH₂)₂), 2.11 (d, *J* = 4.1 Hz, 1 H, NCHCH), 1.67–1.60 (m, 2 H, 2 × CCH₂^bCH₂), 1.57–1.50 (m, 2 H, 2 × CCH₂^aCH₂), 1.43–1.37 (m, 2 H, 2 × NCHCH₂^b), 1.21–1.15 (m, 2 H, 2 × NCHCH₂^a), 0.94 (s, 6 H, 2 × CH₃); ¹³C NMR (125 MHz, CDCl₃): δ = 171.2 (NCHCH), 56.9 (NCHCH), 55.2 (NCH(CH₂)₂), 42.7 (NCH(CH₂)₂), 42.2 (CH₂C), 39.8 (CH₂CH₂), 28.7 (CH₃); IR (film): ν̄ = 2997, 2947, 2866, 2360, 1616, 1454, 1375, 1340, 1304, 1172, 1097, 997 cm⁻¹; HRMS (EI): *m/z* [M]⁺ calcd. for C₁₁H₁₇N 163.1356, found 163.1365.

3,6-Diphenyl-9-azatricyclo[4.3.1.0^{3,7}]dec-8-ene 13d

Synthesis according to GP2 from dihydropyridine **11d** (3.11 g, 7.00 mmol) and TFA (12.0 g, 105 mmol, 8.0 mL) in pentane (70 mL). Purification by FC (Al₂O₃-basic, activity III, pentane/CH₂Cl₂/MeOH 88.5:10:1.5) afforded imine **13d**.

Beige solid (1.92 g, 95 %); *R*_f = 0.42 (Al₂O₃; pentane/CH₂Cl₂/MeOH 88.5:10:1.5); m.p. 140 °C; ¹H NMR (400 MHz, CD₂Cl₂): δ = 8.62 (d, *J* = 3.8 Hz, 1 H, NCHCH), 7.36–7.25 (m, 8 H, CCHCHCH, CCHCHCH), 7.22–7.16 (m, 2 H, CCHCHCH), 4.30 (p, *J* = 2.7 Hz, 1 H, NCH(CH₂)₂), 3.50 (d, *J* = 3.8 Hz, 1 H, NCHCH), 2.25–2.12 (m, 4 H, CH₂CH₂), 2.08–2.00 (m, 2 H, 2 × NCHCH₂^b), 1.80–1.72 (m, 2 H, 2 × NCHCH₂^a); ¹³C NMR (100 MHz, CD₂Cl₂): δ = 169.9 (NCHCH), 150.6 (CCCH₂), 129.0 (CCHCHCH), 126.3 (CCHCHCH), 126.2 (CCHCHCH), 55.4 (NCH(CH₂)₂), 50.7 (CH₂C), 50.1 (NCHCH), 45.2 (NCH(CH₂)₂), 40.9 (CH₂CH₂); IR (KBr): ν̄ = 3080, 3053, 2999, 2943, 2929, 2864, 1618, 1601, 1579, 1493, 1446, 1338, 1302, 1080, 906, 764, 712, 700, 546 cm⁻¹; HRMS (EI): *m/z* [M]⁺ calcd. for C₂₁H₂₁N 287.1669, found 287.1676.

3,7-Dimethyl-10-azatricyclo[5.3.1.0^{3,8}]undec-9-ene 13e

Synthesis according to GP2 from dihydropyridine **11e** (850 mg, 2.55 mmol) and TFA (4.40 g, 38.2 mmol, 2.95 mL) in pentane (26 mL). Purification by FC (Al₂O₃-basic, activity III, pentane/CH₂Cl₂/MeOH 88:10:2) afforded imine **13e**.

Yellow oil (353 mg, 78 %); *R*_f = 0.30 (Al₂O₃; pentane/CH₂Cl₂/MeOH 88:10:2); ¹H NMR (400 MHz, CDCl₃): δ = 8.38 (d, *J* = 4.2 Hz, 1 H, NCHCH), 4.22–4.16 (m, 1 H, NCH(CH₂)₂), 1.74 (d, *J* = 4.2 Hz, 1 H, NCHCH), 1.54–1.44 (m, 2 H, CH₂CH₂CH₂), 1.40–1.30 (m, 4 H, 2 × NCHCH₂^b, 2 × CCH₂^bCH₂), 1.12–1.00 (m, 4 H, 2 × NCHCH₂^a, 2 × CCH₂^aCH₂), 0.81 (s, 6 H, 2 × CH₃); ¹³C NMR (100 MHz, CDCl₃): δ = 175.5 (NCHCH), 55.9 (NCH(CH₂)₂), 53.1 (NCHCH), 37.7 (CH₂CH₂CH₂), 35.7 (NCH(CH₂)₂), 32.9 (CH₂C), 32.1 (CH₃), 19.1 (CH₂CH₂CH₂); IR (film): ν̄ = 3049, 2997, 2924, 2864, 2843, 1614, 1456, 1375, 1336, 1309, 1178, 1076, 1014, 984, 895, 708 cm⁻¹; HRMS (ESI): *m/z* [M + H]⁺ calcd. for C₁₂H₂₀N 178.1590, found 178.1590.

3,7-Diphenyl-10-azatricyclo[5.3.1.0^{3,8}]undec-9-ene 13f

Synthesis according to GP2 from dihydropyridine **11f** (600 mg, 1.31 mmol) and TFA (2.26 g, 19.7 mmol, 1.5 mL) in pentane (13 mL). Purification by FC (Al₂O₃-basic, activity III, pentane/CH₂Cl₂/MeOH 88:10:2) afforded imine **13f**.

Colorless solid (293 mg, 74 %); *R*_f = 0.20 (Al₂O₃; pentane/CH₂Cl₂/MeOH 88:10:2); m.p. 193 °C; ¹H NMR (400 MHz, CDCl₃): δ = 8.40 (d, *J* = 3.7 Hz, 1 H, NCHCH), 7.40–7.34 (m, 4 H, CCHCHCH), 7.34–7.27 (m, 4 H, CCHCHCH), 7.16 (tt, *J* = 7.2/1.4 Hz, 2 H, CCHCHCH), 4.41–4.33 (m, 1 H, NCH(CH₂)₂), 3.47 (d, *J* = 3.7 Hz, 1 H, NCHCH), 2.11–1.98 (m, 4 H, NCH(CH₂)₂), 1.90 (qt, *J* = 13.6/3.7 Hz, 1 H, CH₂CH₂^bCH₂), 1.84–1.69 (m, 3 H, 2 × CCH₂^bCH₂, CH₂CH₂^aCH₂), 1.49 (dt, *J* = 13.3/4.0 Hz, 2 H, 2 × CCH₂^aCH₂); ¹³C NMR (100 MHz, CDCl₃): δ = 173.8 (NCHCH), 151.8 (CCCH₂), 128.5 (CCHCHCH), 126.3 (CCHCHCH), 125.9 (CCHCHCH), 54.6 (NCH(CH₂)₂), 45.1 (NCHCH), 41.4 (CCH₂), 40.1 (CH₂CH₂CH₂), 36.8 (NCH(CH₂)₂), 19.9 (CH₂CH₂CH₂); IR (KBr): ν̄ = 3055, 3022, 2939, 2918, 2846, 1610, 1495, 1442, 1354, 1286, 1082, 1026, 901, 756, 702, 548 cm⁻¹; HRMS (ESI): *m/z* [M + H]⁺ calcd. for C₂₂H₂₄N 302.1903, found 302.1902.

3,5-Dimethyl-7(1,5)imidazolotricyclo[3.2.1.0^{3,6}]octaphan 14a

Synthesis according to GP3 from imine **13a** (37 mg, 0.25 mmol), TosMIC (72 mg, 0.37 mmol), *N*-(tosylmethyl)formamide (157 mg, 0.736 mmol) and *t*BuNH₂ (109 mg, 1.47 mmol, 0.16 mL) in methanol (2.5 mL). Purification by FC (SiO₂, EtOAc/MeOH/NEt₃ 93:5:2) afforded imidazole **14a**.

Colorless oil (29 mg, 63 %); *R*_f = 0.23 (SiO₂, EtOAc/MeOH/NEt₃ 93:5:2); ¹H NMR (500 MHz, CDCl₃): δ = 7.48 (s, 1 H, NCHN), 6.80 (s,

1 H, CCHN), 4.62 (br s, 1 H, NCH(CH₂)₂), 2.75 (s, 1 H, CCHC), 1.90 (dd, *J* = 12.8/2.7 Hz, 2 H, NCH(CH₂^b)₂), 1.74 (dt, *J* = 9.3/2.1 Hz, 1 H, CCH₂^c), 1.46 (d, *J* = 9.3 Hz, 1 H, CCH₂^c), 1.29–1.21 (m, 2 H, NCH(CH₂^a)₂), 0.97 (s, 6 H, 2 × CH₃); ¹³C NMR (125 MHz, CDCl₃): δ = 130.6 (NCHN), 129.9 (CCHN), 122.6 (CCHN), 50.7 (NCH(CH₂)₂), 49.1 (CCH₂C), 45.1 (CCHC), 41.9 (NCH(CH₂)₂), 40.0 (CCH₃), 25.3 (CH₃); IR (film): ν̄ = 3374, 2944, 2860, 1671, 1479, 1455, 1397, 1374, 1333, 1275, 1234, 1193, 1109, 1091, 953, 936, 799, 658 cm⁻¹; HRMS (ESI): *m/z* [M + H]⁺ calcd. for C₁₂H₁₇N₂ 189.1386, found 189.1385.

3,5-Diphenyl-7(1,5)imidazolotricyclo[3.2.1.0^{3,6}]octaphan 14b

Synthesis according to GP3 from imine **13b** (200 mg, 0.732 mmol), TosMIC (214 mg, 1.10 mmol), *N*-(tosylmethyl)formamide (468 mg, 2.19 mmol) and *t*BuNH₂ (324 mg, 4.39 mmol, 0.46 mL) in methanol (7.5 mL). Purification by FC (SiO₂, EtOAc/MeOH/NEt₃ 93:5:2) afforded imidazole **14b**.

Colorless solid (134 mg, 59%); *R*_f = 0.31 (SiO₂, EtOAc/MeOH/NEt₃ 93:5:2); m.p. 162 °C; ¹H NMR (400 MHz, CD₂Cl₂): δ = 7.63 (s, 1 H, NCHN), 7.29–7.22 (m, 4 H, CCHCH), 7.16 (tt, *J* = 7.4/1.3 Hz, 2 H, CCHCHCH), 7.11–7.05 (m, 4 H, CCHCH), 7.00 (s, 1 H, CCHN), 4.90 (br s, 1 H, NCH(CH₂)₂), 3.74 (s, 1 H, CCHC), 2.76 (dt, *J* = 9.2/2.2 Hz, 1 H, CCH₂^c), 2.41 (dd, *J* = 13.2/3.2 Hz, 2 H, NCH(CH₂^b)₂), 2.28 (d, *J* = 9.2 Hz, 1 H, CCH₂^a), 1.81–1.73 (m, 2 H, NCH(CH₂^a)₂); ¹³C NMR (125 MHz, CD₂Cl₂): δ = 147.8 (CCHCH), 131.7 (NCHN), 130.5 (CCHN), 128.9 (CCHCH), 126.8 (CCHCHCH), 125.5 (CCHCH), 122.5 (CCHN), 51.3 (NCH(CH₂)₂), 46.6 (CCH₂), 45.5 (CCH₂C), 45.1 (CCHC), 44.6 (NCH(CH₂)₂); IR (KBr): ν̄ = 3103, 3024, 2937, 1676, 1603, 1493, 1479, 1444, 1398, 1327, 1288, 1230, 1209, 1092, 943, 756, 698, 660, 528 cm⁻¹; HRMS (ESI): *m/z* [M + H]⁺ calcd. for C₂₂H₂₁N₂ 313.1699, found 313.1697.

3,6-Dimethyl-8(1,5)imidazolotricyclo[4.2.1.0^{3,7}]nonaphan 14c

Synthesis according to GP3 from imine **13c** (200 mg, 1.23 mmol), TosMIC (359 mg, 1.84 mmol), *N*-(tosylmethyl)formamide (784 mg, 3.68 mmol) and *t*BuNH₂ (543 mg, 7.35 mmol, 0.78 mL) in methanol (12.5 mL). Purification by FC (SiO₂, EtOAc/MeOH/NEt₃ 93:5:2) afforded imidazole **14c**.

Colorless solid (226 mg, 91%); *R*_f = 0.28 (SiO₂, EtOAc/MeOH/NEt₃ 93:5:2); m.p. 99 °C; ¹H NMR (400 MHz, CDCl₃): δ = 7.44 (s, 1 H, NCHN), 6.89 (s, 1 H, CCHN), 4.35 (p, *J* = 2.7 Hz, 1 H, NCH(CH₂)₂), 2.37 (s, 1 H, CCHC), 1.74–1.63 (m, 6 H, NCH(CH₂^b)₂, CCH₂CH₂C), 1.46–1.38 (m, 2 H, NCH(CH₂^a)₂), 0.88 (s, 6 H, 2 × CH₃); ¹³C NMR (100 MHz, CDCl₃): δ = 130.3 (NCHN), 129.9 (CCHN), 124.4 (CCHN), 51.6 (CCHC), 49.4 (NCH(CH₂)₂), 46.1 (NCH(CH₂)₂), 43.6 (CCH₃), 39.5 (CCH₂CH₂C), 27.3 (CH₃); IR (KBr): ν̄ = 3086, 2950, 2922, 2867, 1693, 1484, 1469, 1448, 1394, 1236, 1203, 1085, 942, 850, 803, 661 cm⁻¹; HRMS (ESI): *m/z* [M + H]⁺ calcd. for C₁₃H₁₉N₂ 203.1543, found 203.1541.

3,6-Diphenyl-8(1,5)imidazolotricyclo[4.2.1.0^{3,7}]nonaphan 14d

Synthesis according to GP3 from imine **13d** (600 mg, 2.09 mmol), TosMIC (611 mg, 3.13 mmol), *N*-(tosylmethyl)formamide (1.34 g, 6.26 mmol) and *t*BuNH₂ (925 mg, 12.5 mmol, 1.32 mL) in methanol (21 mL). Purification by FC (SiO₂, EtOAc/MeOH/NEt₃ 93:5:2) afforded imidazole **14d**.

Colorless solid (380 mg, 56%); *R*_f = 0.32 (SiO₂, EtOAc/MeOH/NEt₃ 93:5:2); m.p. 160 °C; ¹H NMR (400 MHz, CD₂Cl₂): δ = 7.42 (s, 1 H, NCHN), 7.30–7.20 (m, 8 H, CCHCH, CCHCH), 7.18–7.10 (m, 2 H, CCHCHCH), 6.95 (t, *J* = 0.6 Hz, 1 H, CCHN), 4.62 (p, *J* = 2.7 Hz, 1 H, NCH(CH₂)₂), 3.94 (s, 1 H, CCHC), 2.39–2.32 (m, 2 H, NCH(CH₂^b)₂), 2.30–2.21 (m, 4 H, CCH₂CH₂C), 2.17–2.10 (m, 2 H, NCH(CH₂^a)₂); ¹³C NMR (100 MHz, CD₂Cl₂): δ = 149.4 (CCHCH), 130.9 (NCHN), 130.4 (CCHN), 128.9 (CCHCH), 126.4 (CCHCHCH), 126.1 (CCHCH), 124.6 (CCHN), 50.8 (CCH₂), 49.9 (NCH(CH₂)₂), 48.3 (NCH(CH₂)₂), 45.9

(CCHC), 40.8 (CCH₂CH₂C); IR (KBr): ν̄ = 3020, 2947, 2868, 1682, 1599, 1495, 1481, 1466, 1444, 1396, 1342, 1273, 1228, 1092, 1026, 945, 760, 729, 700, 656, 540 cm⁻¹; HRMS (ESI): *m/z* [M + H]⁺ calcd. for C₂₃H₂₃N₂ 327.1856, found 327.1854.

3,7-Dimethyl-9(1,5-²H₂)imidazolotricyclo[5.2.1.0^{3,8}]decaphan 14e

Synthesis according to GP3 from imine **13e** (22 mg, 0.12 mmol), TosMIC (36 mg, 0.18 mmol), *N*-(tosylmethyl)formamide (78 mg, 0.37 mmol) and *t*BuNH₂ (54 mg, 0.73 mmol, 78 μL) in (²H₄)CH₃OH (1.25 mL). Purification by FC (SiO₂, EtOAc/MeOH/NEt₃ 93:5:2) afforded imidazole **14e**.

Colorless oil (NMR-Yield 4 mg, 14%); *R*_f = 0.18 (SiO₂, EtOAc/MeOH/NEt₃ 93:5:2); ¹H NMR (500 MHz, CD₃OD): δ = 4.62–4.57 (m, 1 H, NCH(CH₂)₂), 2.19 (s, 1 H, CCHC), 1.79–1.55 (m, 6 H, 3 × CH₂), 1.32–1.21 (m, 4 H, 2 × CH₂), 0.69 (s, 6 H, 2 × CH₃); HRMS (ESI): *m/z* [M + H]⁺ calcd. for C₁₄H₁₉D₂N₂ 219.1825, found 219.1824.

3,7-Diphenyl-9(1,5-²H₂)imidazolotricyclo[5.2.1.0^{3,8}]decaphan 14f

Synthesis according to GP3 from imine **13f** (18 mg, 61 μmol), TosMIC (18 mg, 92 μmol), *N*-(tosylmethyl)formamide (39 mg, 0.18 mmol) and *t*BuNH₂ (27 mg, 0.37 mmol, 39 μL) in (²H₄)CH₃OH (0.63 mL). Purification by FC (SiO₂, EtOAc/MeOH/NEt₃ 93:5:2) afforded imidazole **14f**.

Colorless oil (NMR-Yield 2 mg, 12%); *R*_f = 0.18 (SiO₂, EtOAc/MeOH/NEt₃ 93:5:2); ¹H NMR (400 MHz, CD₃OD): δ = 7.31–7.25 (m, 4 H, CCHCHCH), 7.24–7.17 (m, 4 H, CCHCHCH), 7.07 (tt, *J* = 7.3/1.3 Hz, 2 H, CCHCHCH), 4.88–4.85 (m, 1 H, NCH(CH₂)₂), 3.88 (s, 1 H, CCHC), 2.47–2.37 (m, 2 H, CH₂), 2.35–2.27 (m, 2 H, CH₂), 2.16–2.02 (m, 1 H, CH₂^b), 1.93–1.86 (m, 2 H, CH₂), 1.86–1.78 (m, 1 H, CH₂^a), 1.77–1.66 (m, 2 H, CH₂); HRMS (ESI): *m/z* [M + H]⁺ calcd. for C₂₄H₂₃D₂N₂ 343.2138, found 343.2138.

5,6,7,8-Tetrahydro(1,3-²H₂)imidazo[1,5-*a*]pyridine 14g

Synthesis according to GP3 from imine **13g** (20 mg, 0.25 mmol), TosMIC (72 mg, 0.37 mmol), *N*-(tosylmethyl)formamide (157 mg, 0.736 mmol) and *t*BuNH₂ (109 mg, 1.47 mmol, 0.16 mL) in (²H₄)CH₃OH (2.5 mL) at 25 °C. Purification by FC (SiO₂, EtOAc/MeOH/NEt₃ 93:5:2) afforded imidazole **14g**.

Yellow oil (NMR-Yield 6 mg, 21%); *R*_f = 0.24 (SiO₂, EtOAc/MeOH/NEt₃ 93:5:2); ¹H NMR (500 MHz, CDCl₃): δ = 3.96 (t, *J* = 6.1 Hz, 2 H, NCH₂), 2.75 (t, *J* = 6.4 Hz, 2 H, CCH₂), 1.96–1.89 (m, 2 H, CH₂), 1.84–1.77 (m, 2 H, CH₂); Due to rapid proton deuterium exchange of the starting imine **13g** in course of the imine enamine equilibrium unplanned deuterium incorporation into the tetrahydropyridine core occurred and led to a decreased signal intensity at 2.75 ppm. HRMS (ESI): *m/z* [M + H]⁺ calcd. for C₇H₉D₂N₂ 125.1042, found 125.1043.

5,6-Dihydro(1,3-²H₂)imidazo[5,1-*a*]isoquinoline 14h

Synthesis according to GP3 from imine **13h** (32 mg, 0.25 mmol), TosMIC (72 mg, 0.37 mmol), *N*-(tosylmethyl)formamide (157 mg, 0.736 mmol) and *t*BuNH₂ (109 mg, 1.47 mmol, 0.16 mL) in (²H₄)CH₃OH (2.5 mL) at 25 °C. Purification by FC (SiO₂, EtOAc/MeOH/NEt₃ 93:5:2) afforded imidazole **14h**.

Yellow oil (36 mg, 86%); *R*_f = 0.21 (SiO₂, EtOAc/MeOH/NEt₃ 93:5:2); ¹H NMR (400 MHz, CD₃OD): δ = 7.59–7.54 (m, 1 H, NCCCCH), 7.29–7.22 (m, 2 H, CH₂CCH, NCCCCH), 7.22–7.16 (m, 1 H, CH₂CCHCH), 4.19 (t, *J* = 6.6 Hz, 2 H, NCH₂), 3.06 (t, *J* = 6.6 Hz, 2 H, CCH₂); ¹³C NMR (100 MHz, CD₃OD): δ = 137.2 (t, NCDN), 132.7 (CH₂C), 130.5 (NCC), 129.4 (NCCCCH), 128.4 (CH₂CCH, CH₂CCHCH), 127.9 (NCC), 124.2 (NCCCCH), 123.2 (t, NCCD), 43.0 (NCH₂), 29.9 (CCH₂); IR (KBr): ν̄ = 3375, 2971, 2893, 2630, 1692, 1608, 1547, 1482, 1458, 1426,

1322, 1212, 1025, 947, 816, 766, 737, 717 cm^{-1} ; HRMS (ESI): m/z [M + H]⁺ calcd. for $\text{C}_{11}\text{H}_9\text{D}_2\text{N}_2$ 173.1042, found 173.1042.

Dimer 18

Imine **13c** (30 mg, 0.18 mmol), *N*-(tosylmethyl)formamide (118 mg, 0.55 mmol) and Cs_2CO_3 (180 mg, 0.553 mmol) were dissolved in ($^2\text{H}_4$) CH_3OH (1.88 mL) and stirred for 20 min at 25 °C. Subsequent ^1H NMR analysis indicated the formation of dimer **18** to an extent of 65 % (determined by NMR ratio relative to the methyl group of Tos⁻). Purification by twofold preparative TLC (SiO_2 , $\text{CH}_2\text{Cl}_2/\text{MeOH}$ 9:1) afforded dimer **18** (admixed with a substance (ratio 80:20) that is most likely a diastereomer of dimer **18**).

Colorless crystals (1.8 mg, 4 %); R_f = 0.70 (SiO_2 , $\text{CH}_2\text{Cl}_2/\text{MeOH}$ 9:1); m.p. 156 °C; ^1H NMR (500 MHz, CD_3OD): δ = 8.13 (s, 2 H, NCHO), 4.53 (d, J = 13.1 Hz, 2 H, $2 \times \text{NCH}_2^{\text{b}}\text{N}$), 4.31 (d, J = 2.9 Hz, 2 H, $2 \times \text{NCHCH}$), 3.99 (d, J = 13.1 Hz, 2 H, $2 \times \text{NCH}_2^{\text{a}}\text{N}$), 2.87 (p, J = 2.8 Hz, 2 H, $2 \times \text{NCHCH}_2$), 1.81 (dt, J = 12.7/2.8 Hz, 2 H, $2 \times \text{NCHCH}_2^{\text{a}}$), 1.74 (dt, J = 13.5/2.9 Hz, 2 H, $2 \times \text{NCHCH}_2^{\text{b}}$), 1.58–1.37 (m, 12 H, $2 \times \text{NCHCH}_2^{\text{b}}$, $4 \times \text{CH}_3\text{CCH}_2$, $2 \times \text{NCHCH}$), 1.28–1.19 (m, 8 H, $2 \times \text{CH}_3$, $2 \times \text{NCHCH}_2^{\text{a}}$), 1.09 (s, 6 H, $2 \times \text{CH}_3$); ^{13}C NMR (125 MHz, CD_3OD): δ = 164.3 ($2 \times \text{NCHO}$), 92.8 ($2 \times \text{NCHCH}$), 56.6 ($2 \times \text{NCH}_2\text{N}$), 51.5 ($2 \times \text{NCHCH}_2$), 50.8 ($2 \times \text{NCHCH}$), 47.9 ($2 \times \text{NCHCH}_2$), 42.4 ($2 \times \text{CH}_3\text{CCH}_2$), 41.4 ($2 \times \text{CH}_3\text{CCH}_2$), 41.3 ($2 \times \text{CCH}_3$), 41.2 ($2 \times \text{NCHCH}_2$), 39.8 ($2 \times \text{CCH}_3$), 29.1 ($2 \times \text{CH}_3$), 26.7 ($2 \times \text{CH}_3$); IR (KBr): $\tilde{\nu}$ = 2941, 2924, 2866, 1657, 1365, 1313, 1261, 1238, 1174, 1146, 1120, 986, 970, 733 cm^{-1} ; HRMS (ESI): m/z [M + H]⁺ calcd. for $\text{C}_{26}\text{H}_{41}\text{O}_2\text{N}_4$ 441.3224, found 441.3222.

Keywords: Cyclic Imine · Cycloaddition · Nitrogen heterocycles · Organocatalysis · TosMIC

- [1] a) A. F. Pozharskii, A. T. Soldatenkov, A. R. Katritzky in *Heterocycles in Life and Society: An Introduction to Heterocyclic Chemistry, Biochemistry and Applications*, 2nd Ed. John Wiley & Sons, New York, **2011**; b) G. Dodson, A. Wlodawer, *Trends Biochem. Sci.* **1998**, *23*, 347–352.
- [2] a) M. Gaba, C. Mohan, *Med. Chem. Res.* **2015**, *25*, 173–210; b) L. Zhang, X. M. Peng, G. L. Damu, R. X. Geng, C. H. Zhou, *Med. Res. Rev.* **2014**, *34*, 340–437.
- [3] a) R. P. Pohanish in *Sittig's Handbook of Pesticides and Agricultural Chemicals*, Elsevier, Norwich, NY, USA, **2014**, p. 483 & 679; b) S. Khay, A. M. Abd El-Aty, J.-H. Choi, J.-H. Shim, *Toxicol. Res.* **2008**, *24*, 87–91; c) A. Uclés, A. V. García, M. D. Gil García, A. M. Aguilera del Real, A. R. Fernández-Alba, *Anal. Methods* **2015**, *7*, 9158–9165.
- [4] a) H. Debus, *Ann. Chem. Pharm.* **1858**, *107*, 199–208; b) B. Radziszewski, *Ber. Dtsch. Chem. Ges.* **1882**, *15*, 2706–2708; c) E. Schaumann in *Houben-Weyl Methoden der Organischen Chemie, Vol. E8c* (Eds.: K. H. Büchel, J. Falbe, H. Hagemann, M. Hanack, D. Klamann, R. Kreher, H. Kropf, M. Regitz, E. Schaumann) 4th Ed. Georg Thieme Verlag, Stuttgart, **1994**.
- [5] A. M. van Leusen, J. Wildeman, O. H. Oldenziel, *J. Org. Chem.* **1977**, *42*, 1153–1159.
- [6] a) D. van Leusen, A. M. van Leusen, *Org. React.* **2004**, *57*, 417–666; b) M. R. Grimmett in *Science of Synthesis, Vol. 12* (Eds.: R. Neier, D. Bellus), Georg Thieme Verlag, Stuttgart, **2002**, p. 325–528.
- [7] a) L. Zhao, Y. Yang, Y. Guo, L. Yang, J. Zhang, J. Zhou, H. Zhang, *Bioorg. Med. Chem.* **2017**, *25*, 2482–2490; b) P. Zheng, J. Zhang, H. Ma, X. Yuan, P. Chen, J. Zhou, H. Zhang, *Bioorg. Med. Chem.* **2019**, *27*, 1391–1404; c) Y. Huang, J. Zhang, Z. Yu, H. Zhang, Y. Wang, A. Lingel, W. Qi, J. Gu, K. Zhao, M. D. Shultz, L. Wang, X. Fu, Y. Sun, Q. Zhang, X. Jiang, J. Zhang, C. Zhang, L. Li, J. Zeng, L. Feng, C. Zhang, Y. Liu, M. Zhang, L. Zhang, M. Zhao, Z. Gao, X. Liu, D. Fang, H. Guo, Y. Mi, T. Gabriel, M. P. Dillon, P. Atadja, C. Oyang, *J. Med. Chem.* **2017**, *60*, 2215–2226; d) Y. Yang, P. Chen, L. Zhao, F. Zhang, B. Zhang, C. Xu, H. Zhang, J. Zhou, *Bioorg. Chem.* **2019**, *90*, 103044; e) X. Liu, Z. Wu, J. Tian, X. Yuan, L. Zhao, P. Chen, H. Zhang, J. Zhou, *Med. Chem. Res.* **2018**, *27*, 2089–2099; f) H. Mukaiyama, T. Nishimura, S. Kobayashi, T. Ozawa, N. Kamada, Y. Komatsu, S. Kikuchi, H. Oonota, H. Kusama, *Bioorg. Med. Chem.* **2007**, *15*, 868–885; g) P. Chen, J. C. Barrish, E. Iwanowicz, J. Lin, M. S. Bednarz, B.-C. Chen, *Tetrahedron Lett.* **2001**, *42*, 4293–4295; h) R. Saijo, H. Sekiya, E. Tamai, K. Kurihara, J. Maki, H. Sakagami, M. Kawase, *Chem. Pharm. Bull.* **2017**, *65*, 365–372.
- [8] J. González, C. del Pozo, A. Macías, E. Alonso, *Synthesis* **2004**, *2004*, 2697–2703.
- [9] V. Murugesu, B. Harish, M. Adishesu, J. Babu Nanubolu, S. Suresh, *Adv. Synth. Catal.* **2016**, *358*, 1309–1321.
- [10] K. Satyam, V. Murugesu, S. Suresh, *Org. Biomol. Chem.* **2019**, *17*, 5234–5238.
- [11] S. P. J. M. van Nipsen, C. Mensink, A. M. van Leusen, *Tetrahedron Lett.* **1980**, *21*, 3723–3726.
- [12] a) R. C. Bast Jr., C. M. Croce, W. N. Hait, W. K. Hong, D. W. Kufe, M. Piccart-Gebhart, R. E. Pollock, R. R. Weichselbaum, H. Wang, J. F. Holland in *Holland-Frei Cancer Medicine*, 9th Ed. John Wiley & Sons, Hoboken, New Jersey, **2017**, p. 722–723; b) C. Schumacher, W. Fuhrer, R. E. Steele, *PCT Int. Appl. WO* **2018/078049** **2018**; c) R. E. Steele, C. Schumacher, *PCT Int. Appl. WO* **2019/211394** **2019**.
- [13] T. Sasaki, S. Eguchi, N. Toi, *J. Org. Chem.* **1979**, *44*, 3711–3715.
- [14] a) H.-K. A. Rudy, K. T. Wanner, *Synthesis* **2019**, *51*, 4296–4310; b) C. E. Schmaunz, P. Mayer, K. T. Wanner, *Synthesis* **2014**, *46*, 1630–1638.
- [15] a) J. Bräckow, K. T. Wanner, *Tetrahedron* **2006**, *62*, 2395–2404; b) C. A. Sperger, K. T. Wanner, *Tetrahedron* **2009**, *65*, 5824–5833.
- [16] T. D. W. Claridge in *Tetrahedron Organic Chemistry*, vol. 27, *High-Resolution NMR Techniques in Org. Chemistry*, 2nd Ed. Elsevier, Amsterdam, **2009**.
- [17] Deposition Number(s) 1987516 (for imine **13d**), 1987517 (for imine **13b**), 1987518 (for imine **13f**), 1995913 (for imidazole **14d**) and 1987519 (for dimer **18**) contain(s) the supplementary crystallographic data for this paper. These data are provided free of charge by the joint Cambridge Crystallographic Data Centre and Fachinformationszentrum Karlsruhe Access Structures service www.ccdc.cam.ac.uk/structures. ORTEP (Burnett, M. N.; Johnson, C. K. *ORTEP-III: Oak Ridge Thermal Ellipsoid Plot Program for Crystal Structure Illustrations*, Oak Ridge National Laboratory Report ORNL-6895, **1996**); Windows version (Farrugia, L. J., Univ. Glasgow) used.
- [18] G. P. Claxton, L. Allen, J. M. Grisar, *Org. Synth.* **1977**, *56*, 118.
- [19] J. Chen, W. Guo, Z. Wang, L. Hu, F. Chen, Y. Xia, *J. Org. Chem.* **2016**, *81*, 5504–5512.
- [20] In the NMR spectra a second set of signals, albeit with a low intensity of ca. 20 %, was observed which is likely to be attributed to the racemic diastereomer of **18**, *rac-18a*, though this could not be verified.
- [21] D. D. Perrin, W. L. F. Armarego in *Purification of Laboratory Chemicals* 4th Ed. Pergamon, New York, **1996**, p. 15–16.
- [22] S. Hünig, P. Kreitmeier, G. Märkl, J. Sauer in *Arbeitsmethoden in der Organischen Chemie*, Lehmanns, Berlin, **2006**, p. 179–180.
- [23] G. R. Fulmer, A. J. M. Miller, N. H. Sherden, H. E. Gottlieb, A. Nudelman, B. M. Stoltz, J. E. Bercaw, K. I. Goldberg, *Organometallics* **2010**, *29*, 2176–2179.
- [24] M. R. Monaco, P. Renzi, D. M. S. Schietroma, M. Bella, *Org. Lett.* **2011**, *13*, 4546–4549.
- [25] C. B. Tripathi, S. Mukherjee, *Angew. Chem. Int. Ed.* **2013**, *52*, 8450–8453.
- [26] W. F. Berkowitz, Y. Wu, *J. Org. Chem.* **1997**, *62*, 1536–1539.
- [27] J. Y. See, H. Yang, Y. Zhao, M. W. Wong, Z. Ke, Y.-Y. Yeung, *ACS Catal.* **2018**, *8*, 850–858.
- [28] S. Sultana, S. Bondalapati, K. Indukuri, P. Gogoi, P. Saha, A. K. Saikia, *Tetrahedron Lett.* **2013**, *54*, 1576–1578.
- [29] C. Fuganti, P. Grasselli, S. Servi, *J. Chem. Soc., Perkin Trans. 1* **1983**, 241–244.
- [30] C. Y. Huang, A. G. Doyle, *J. Am. Chem. Soc.* **2015**, *137*, 5638–5641.
- [31] K. H. Yong, N. J. Taylor, J. M. Chong, *Org. Lett.* **2002**, *4*, 3553–3556.
- [32] R. D. Rieke, S. E. Bales, *J. Am. Chem. Soc.* **1974**, *96*, 1775–1781.

Received: March 4, 2020



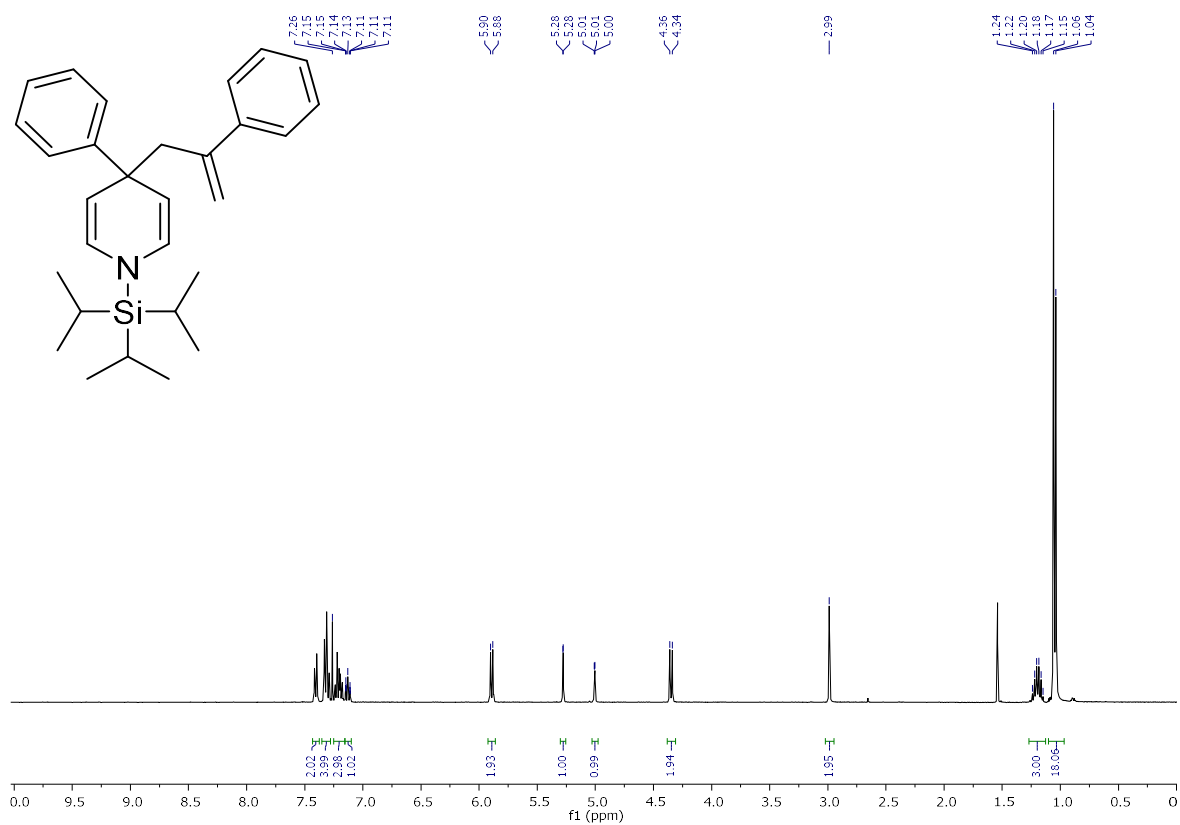
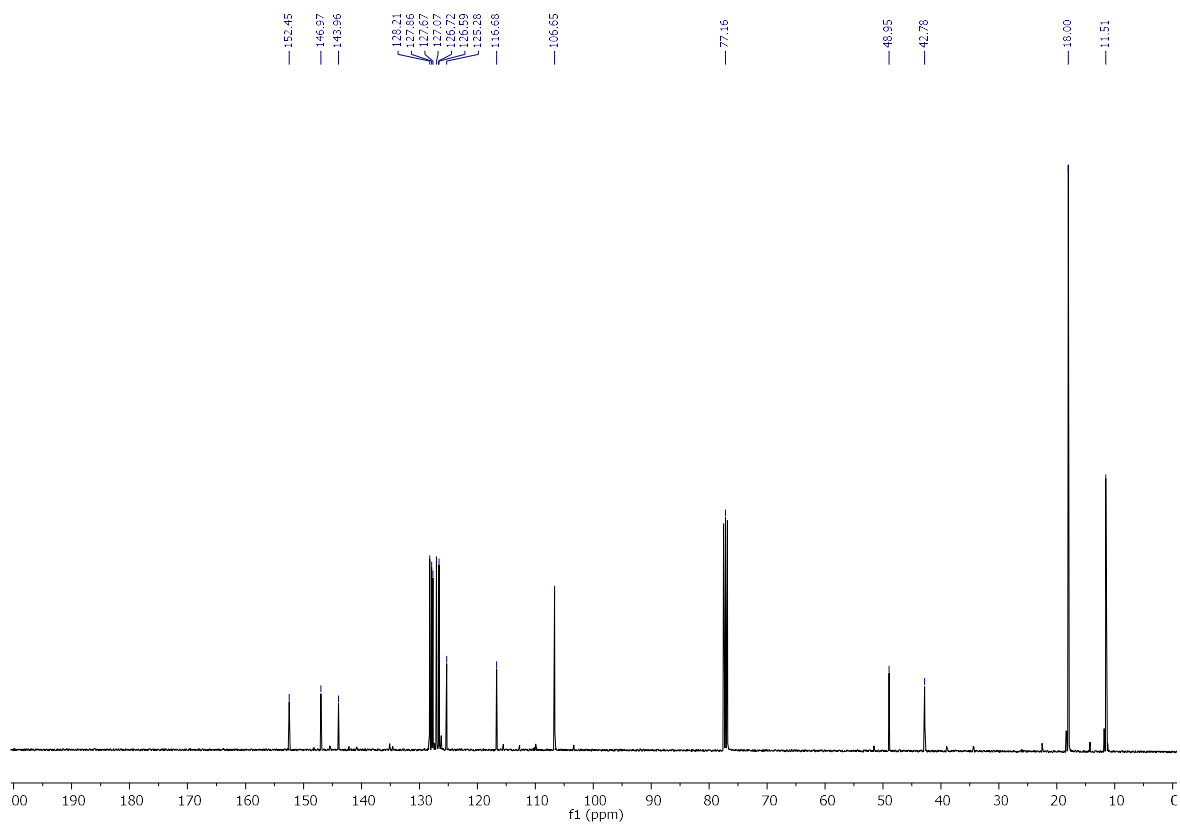
Supporting Information

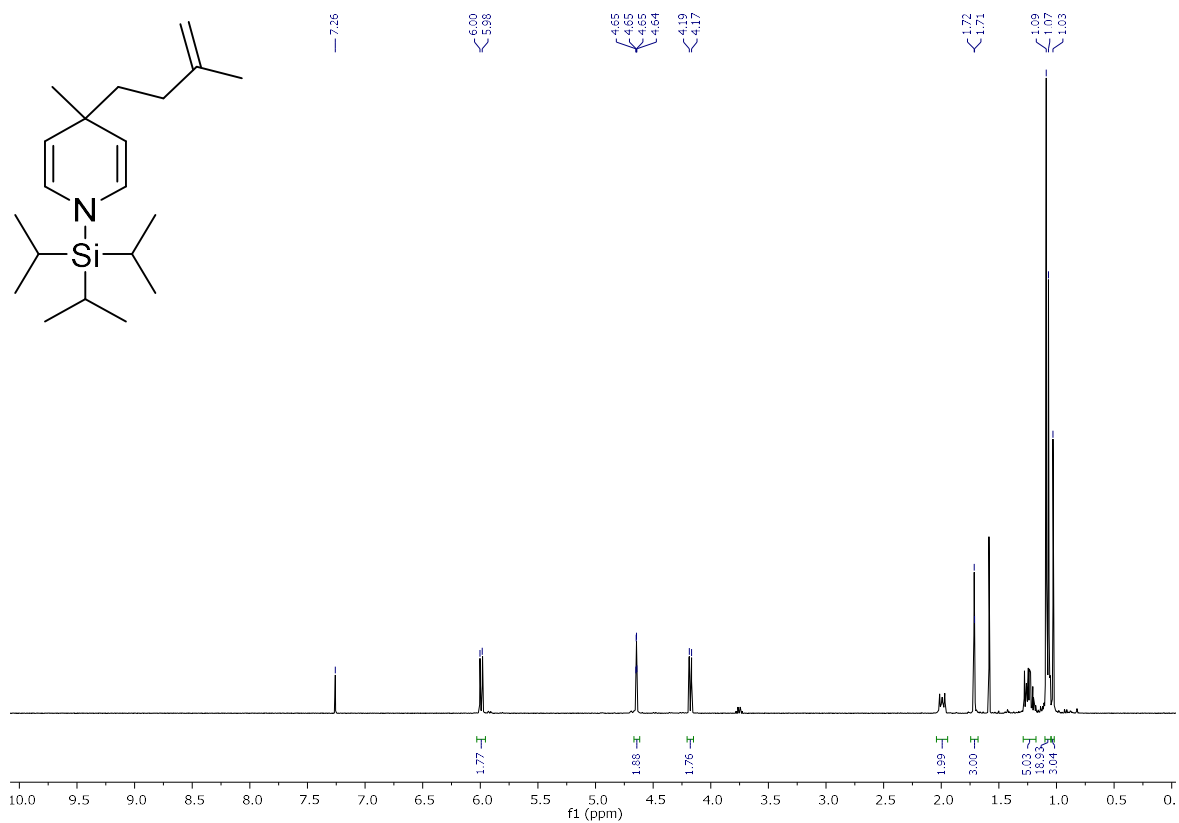
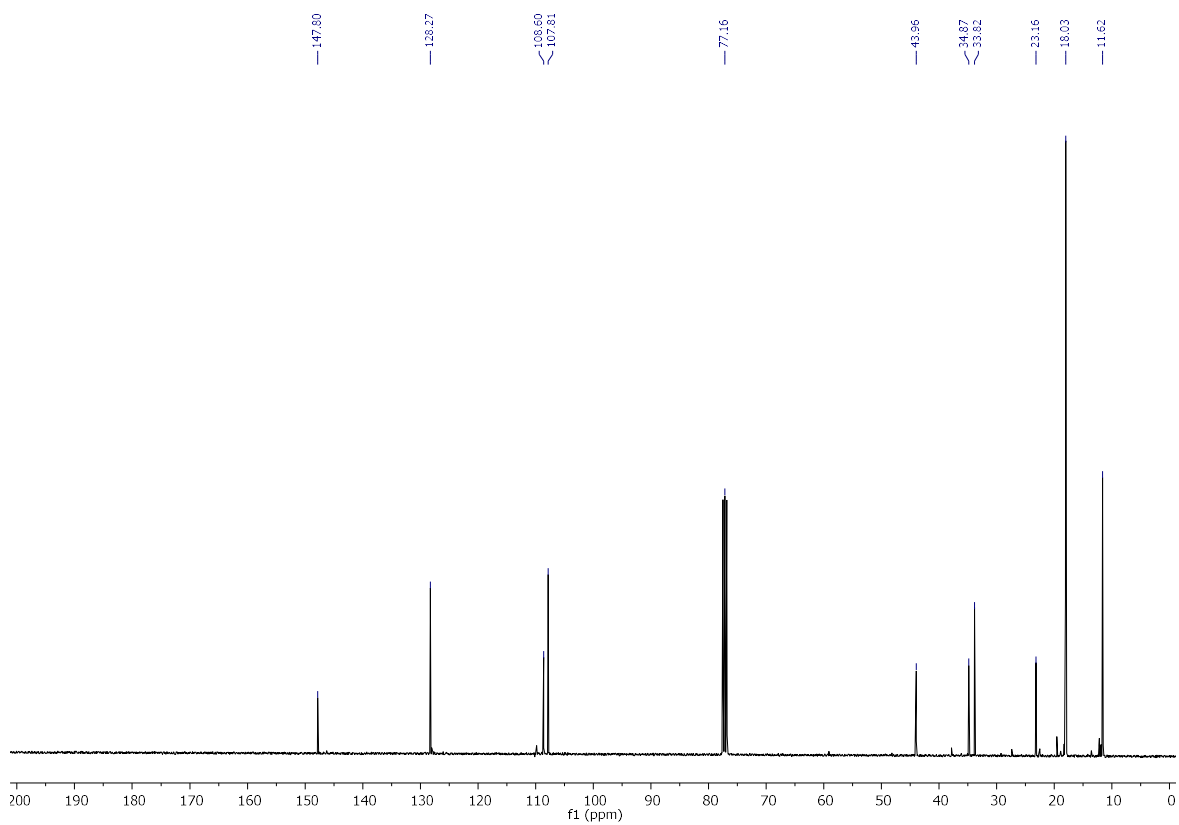
Synthesis of 1,5-Ring-Fused Imidazoles from Cyclic Imines and TosMIC – Identification of in situ Generated *N*-Methyleneformamide as a Catalyst in the van Leusen Imidazole Synthesis

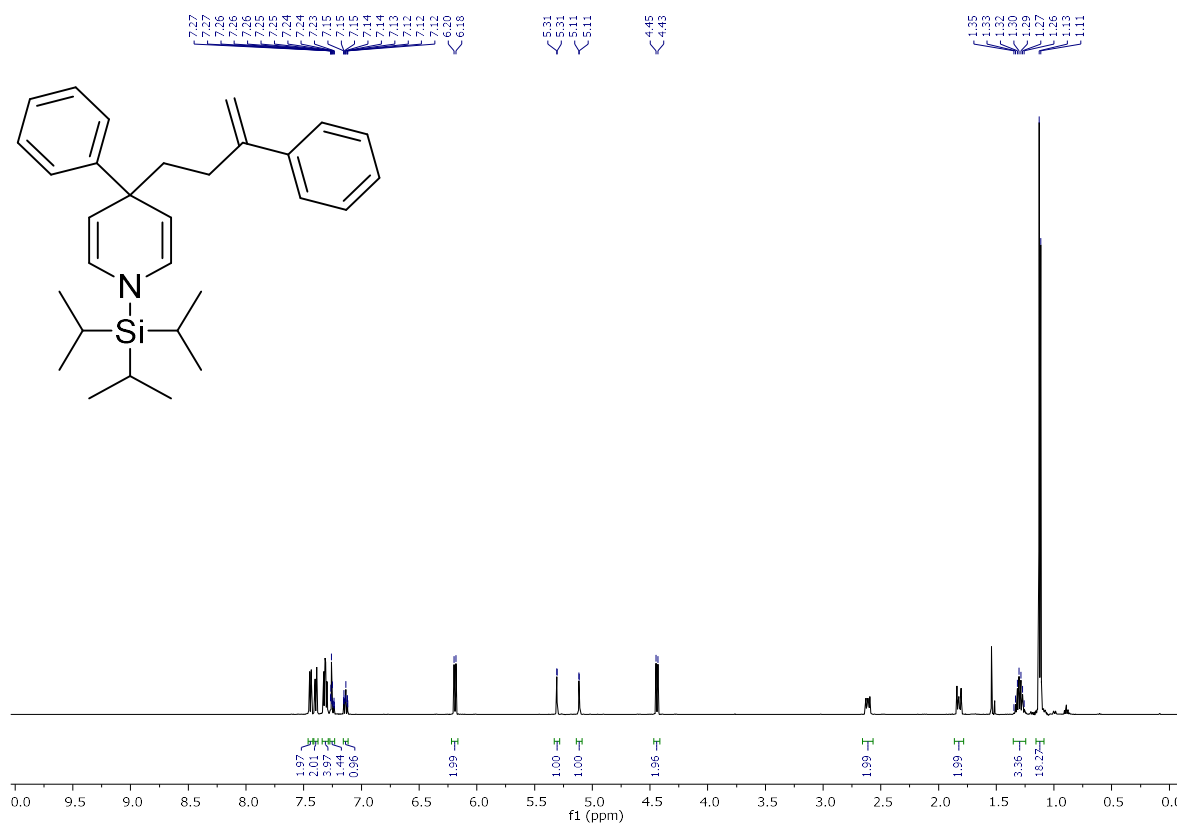
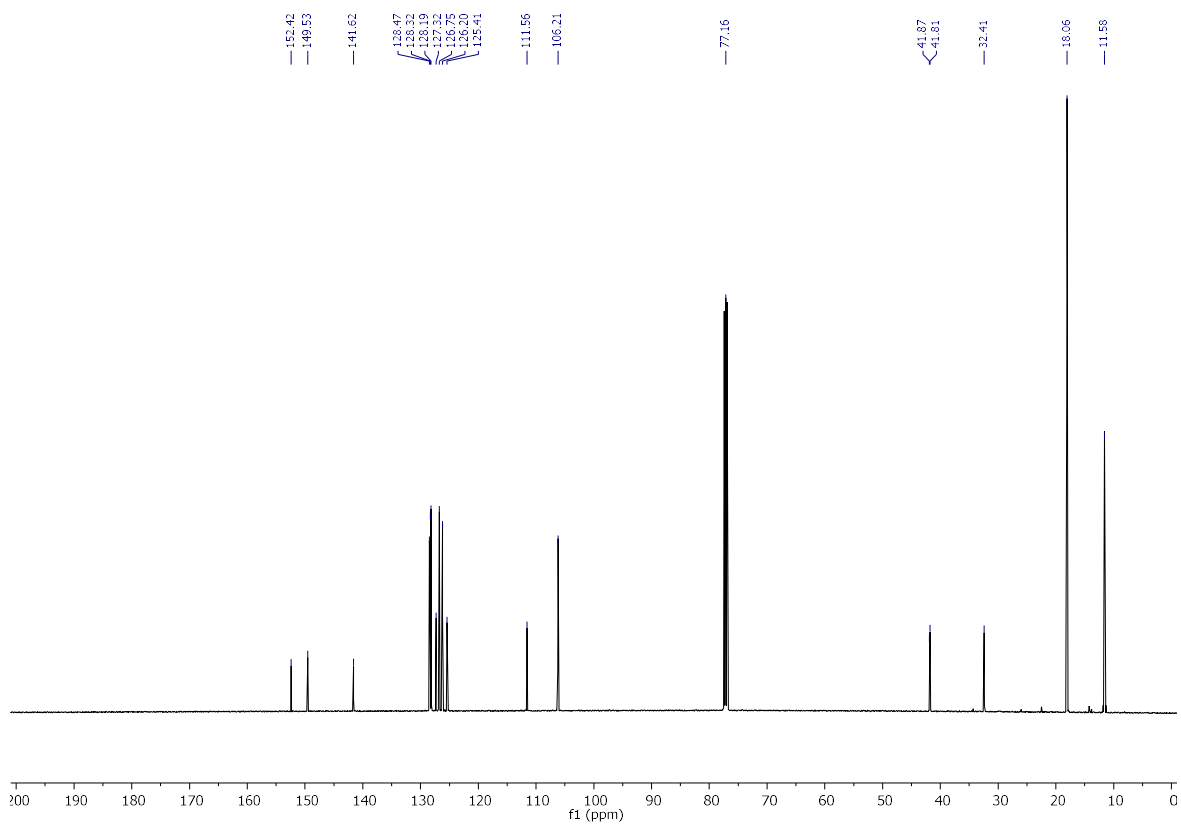
Heinrich-Karl A. Rudy, Peter Mayer, and Klaus T. Wanner*

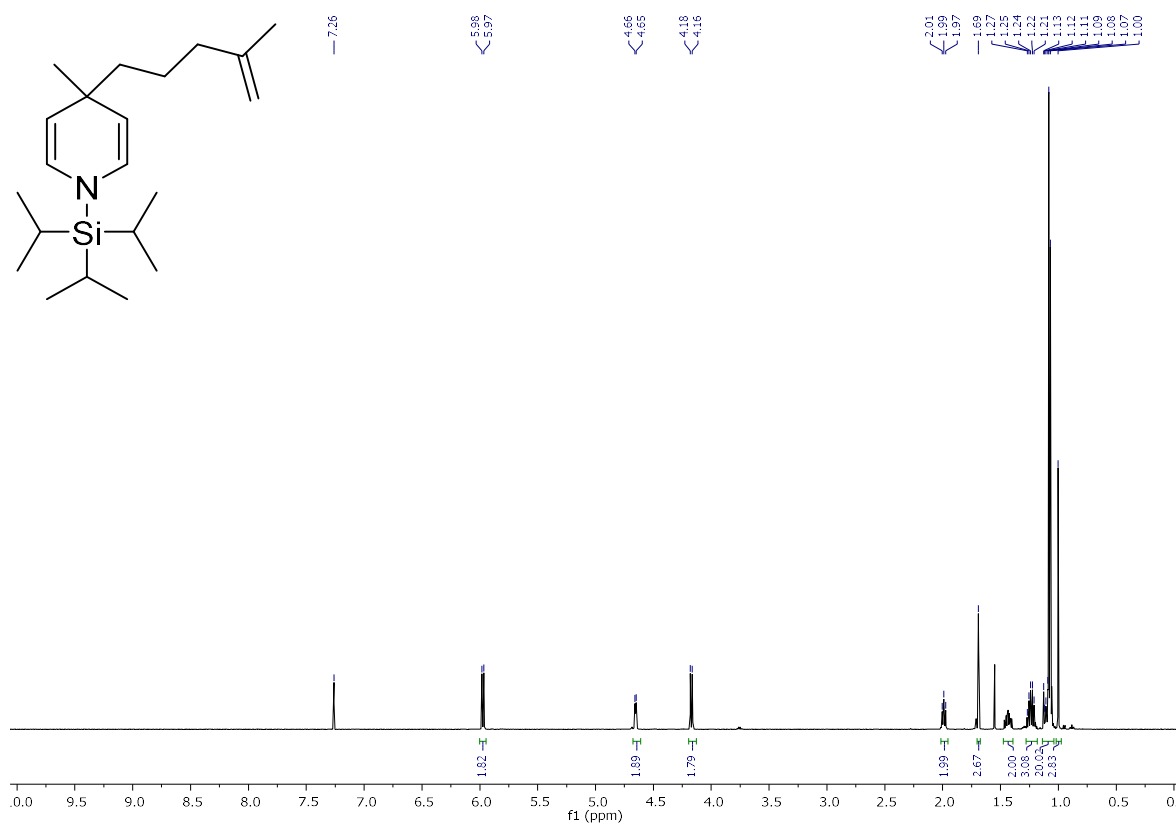
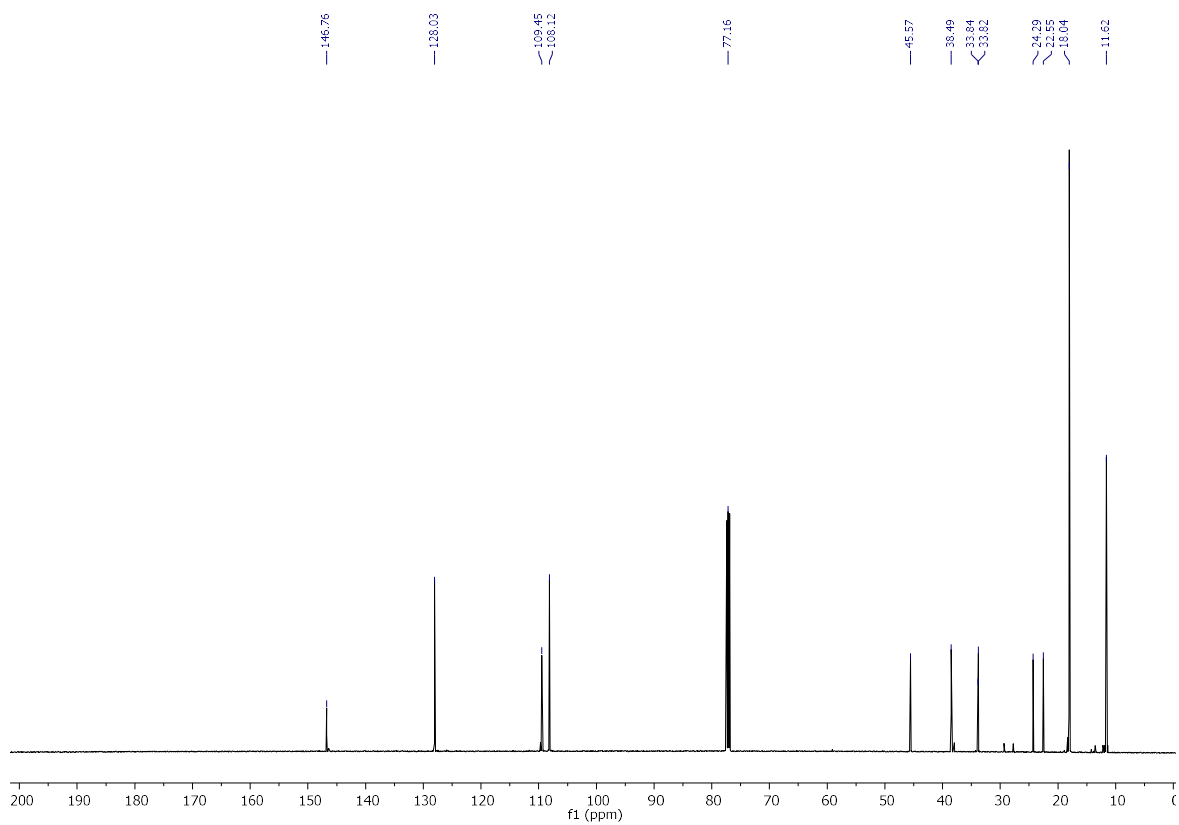
Table of Contents

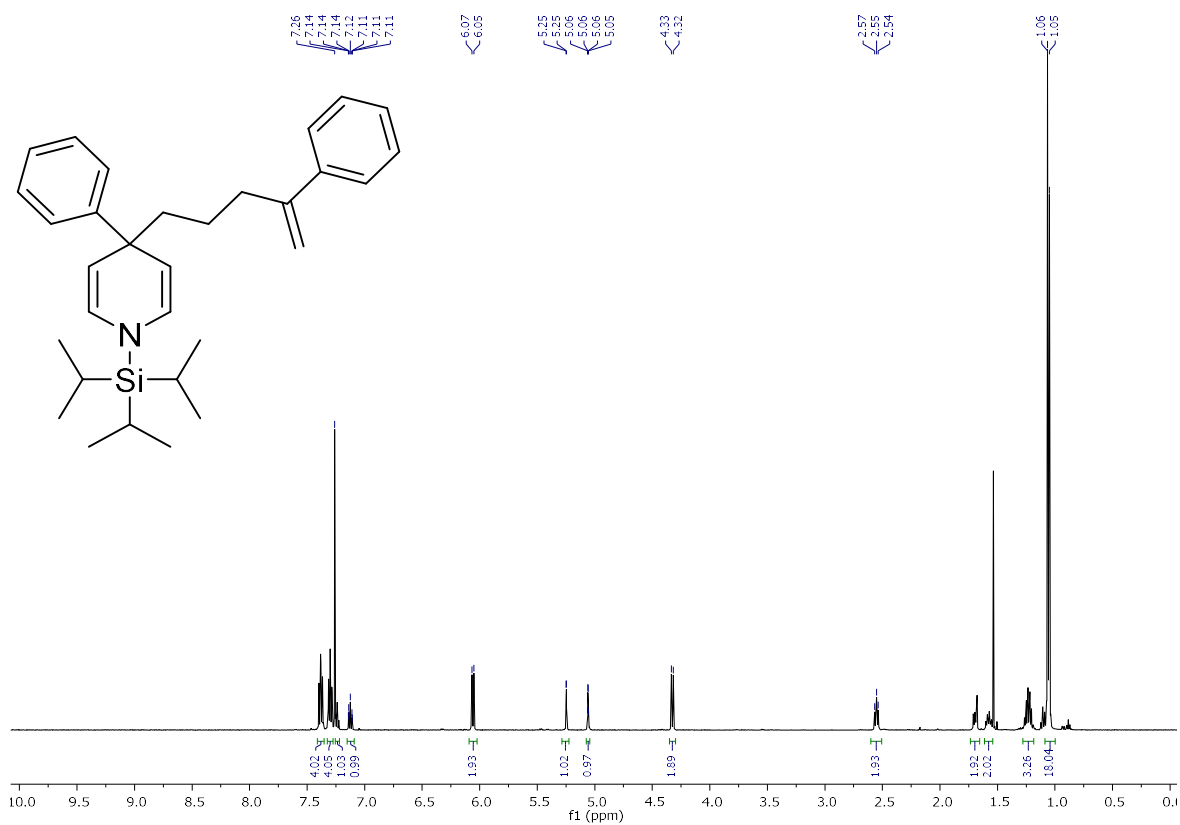
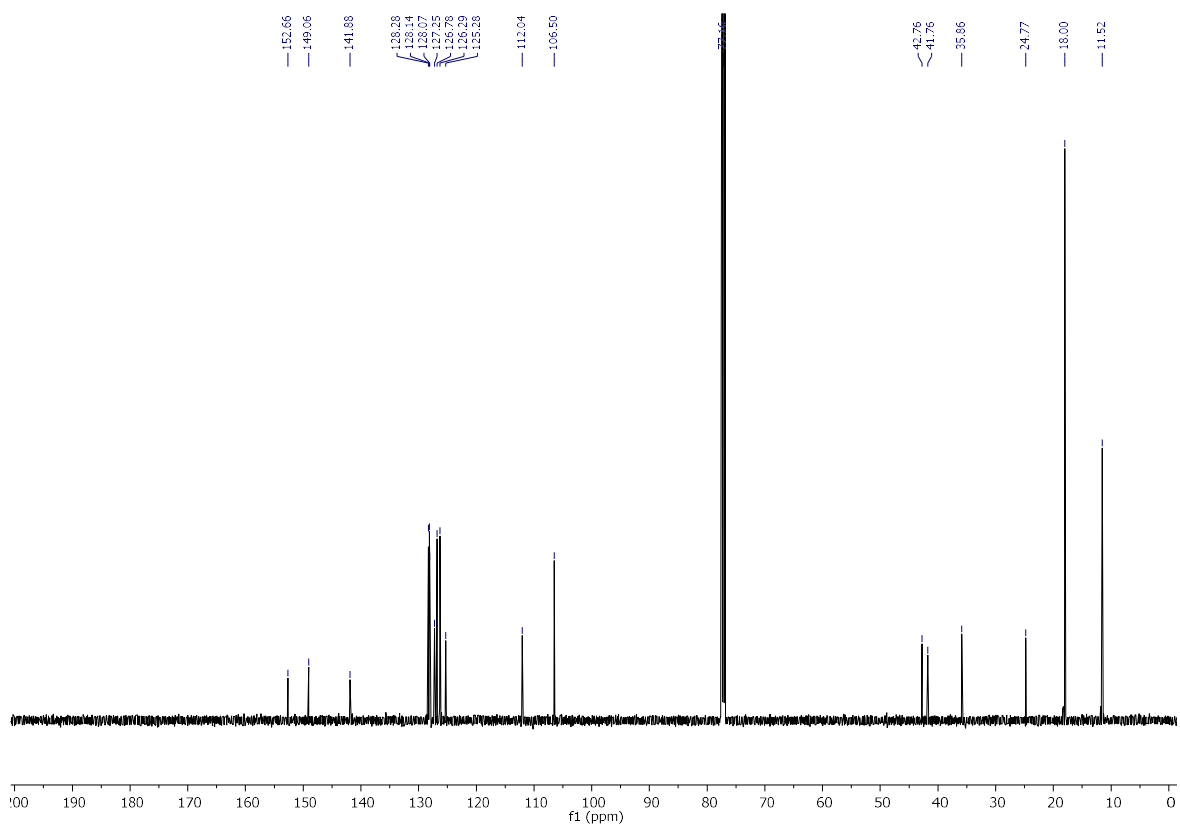
1.	^1H and ^{13}C NMR spectra for compounds 11a-f , 13a-f , 14a-d,h , 18	2-20
2.	NMR experiments	
2.1	^1H NMR and HRMS spectra for compounds 14e-g	21-23
2.2	^1H NMR spectra of reactions of <i>N</i> -(tosylmethyl)formamide 15 under varying conditions (Table 4)	24
2.3	HRMS spectrum of adduct of imine 13c and <i>N</i> -methyleneformamide 17	25
2.4	Identification of Dimer 18 in other ^1H NMR spectra	26-27
2.5	^1H and ^{13}C NMR spectra confirming the proton deuterium exchange of TosMIC leading to [$^2\text{H}_2$]-TosMIC	28-30

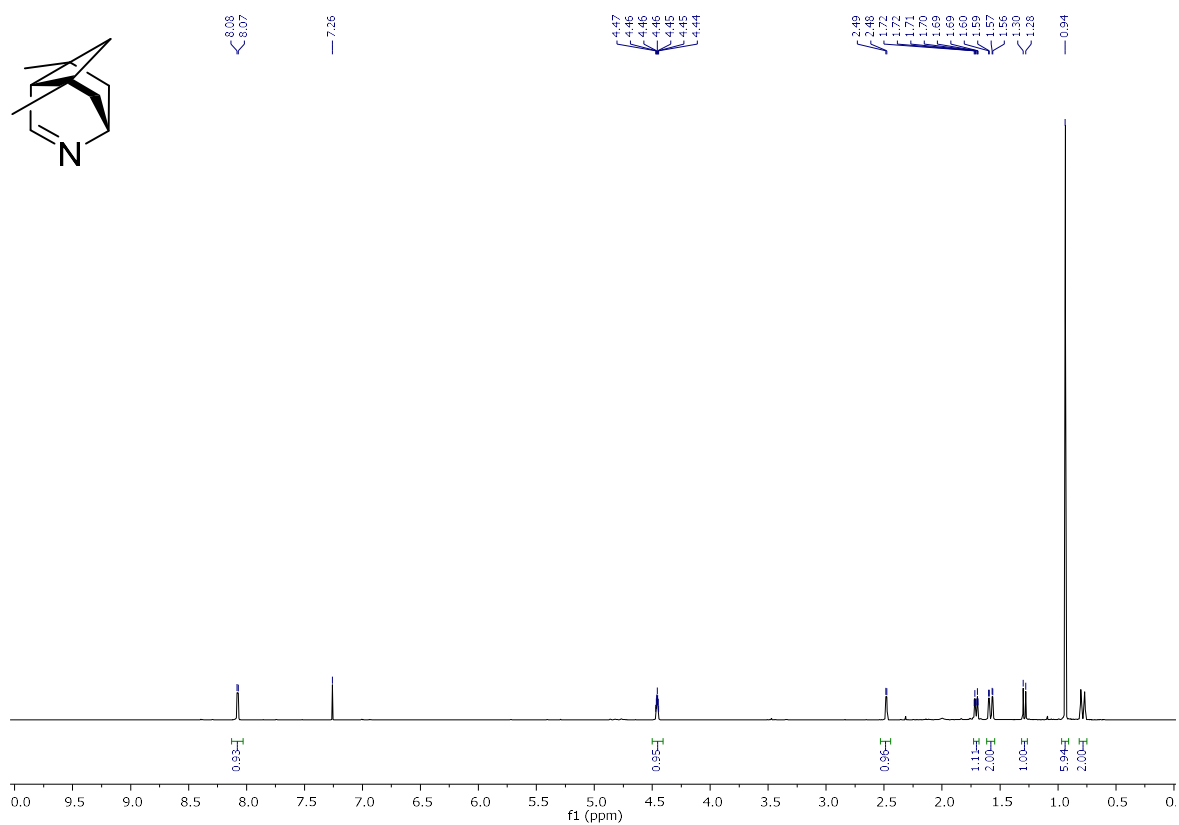
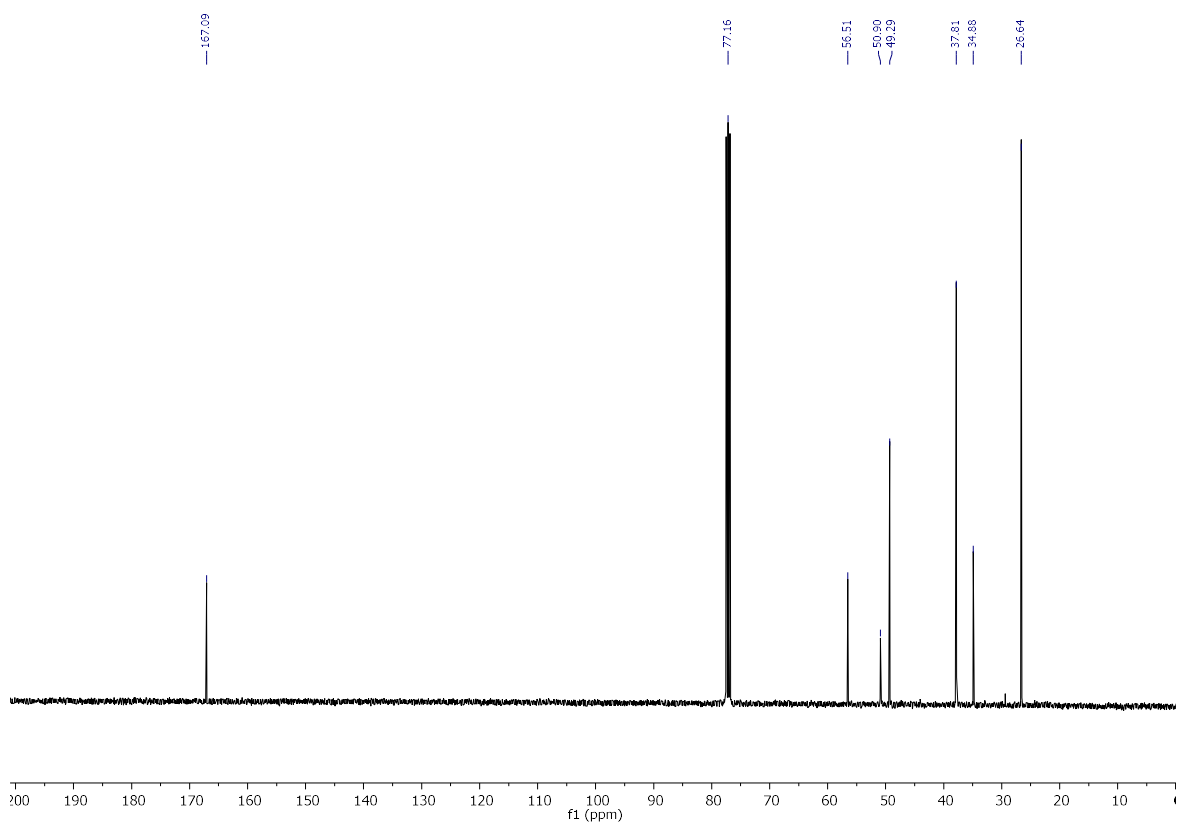
11b (¹H):**11b (¹³C):**

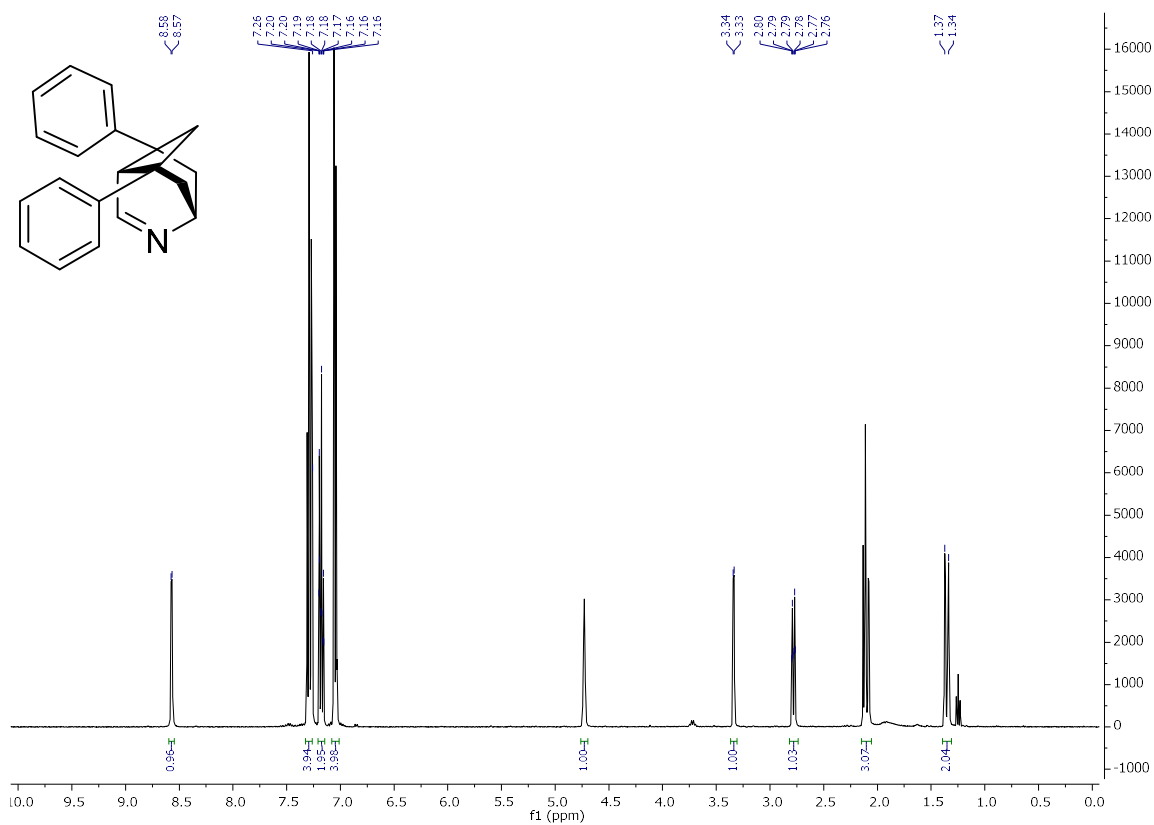
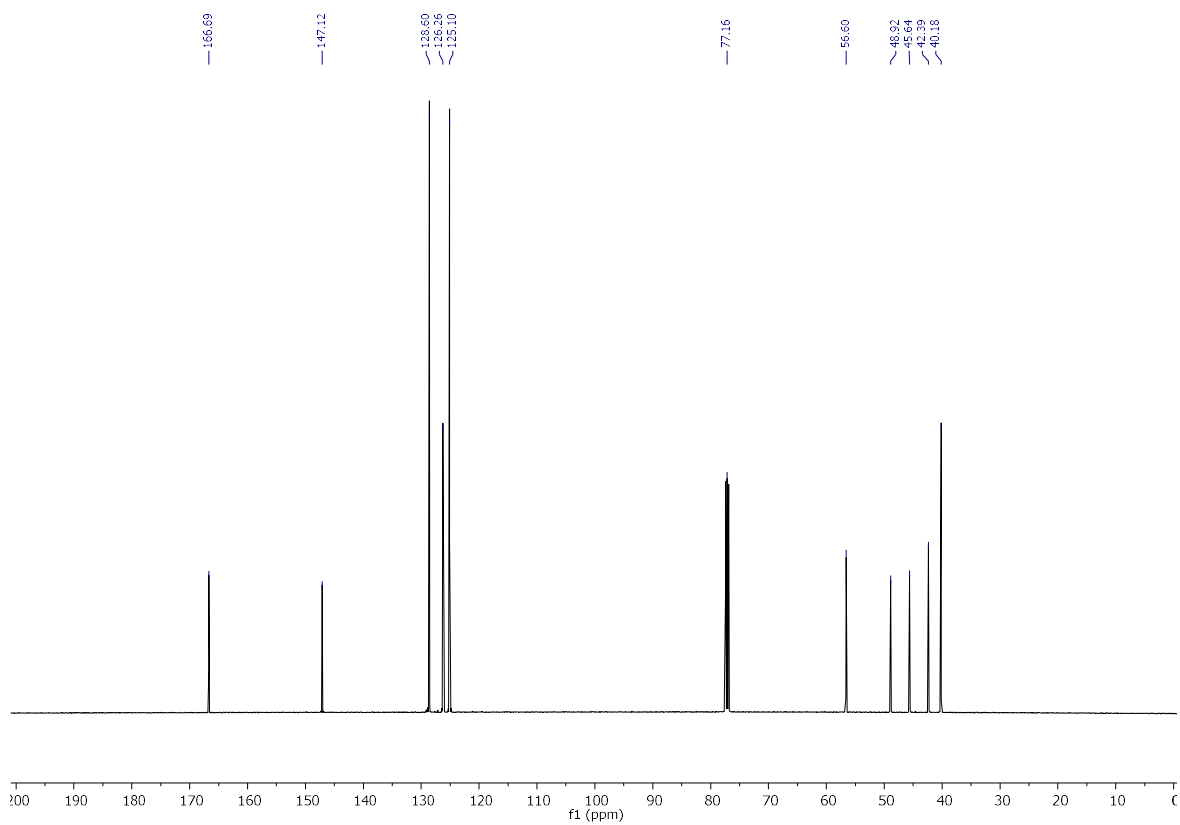
11c (^1H):**11c** (^{13}C):

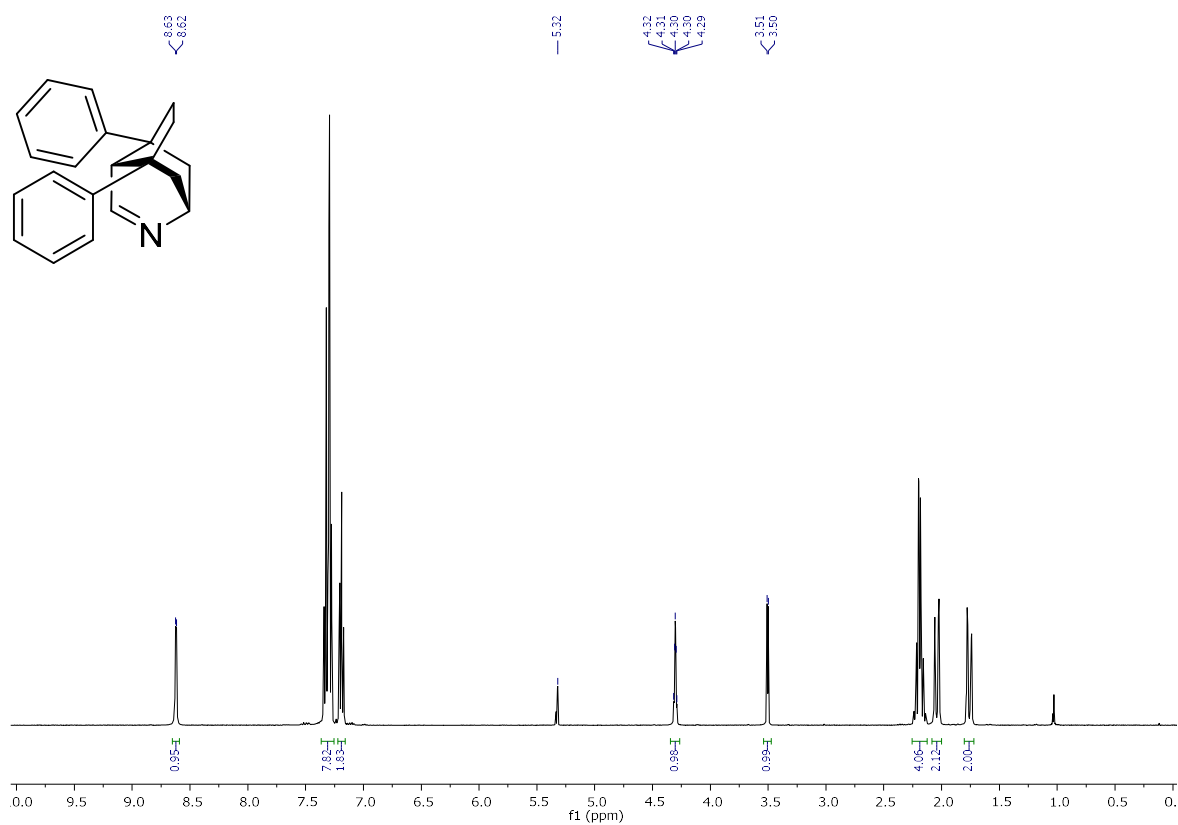
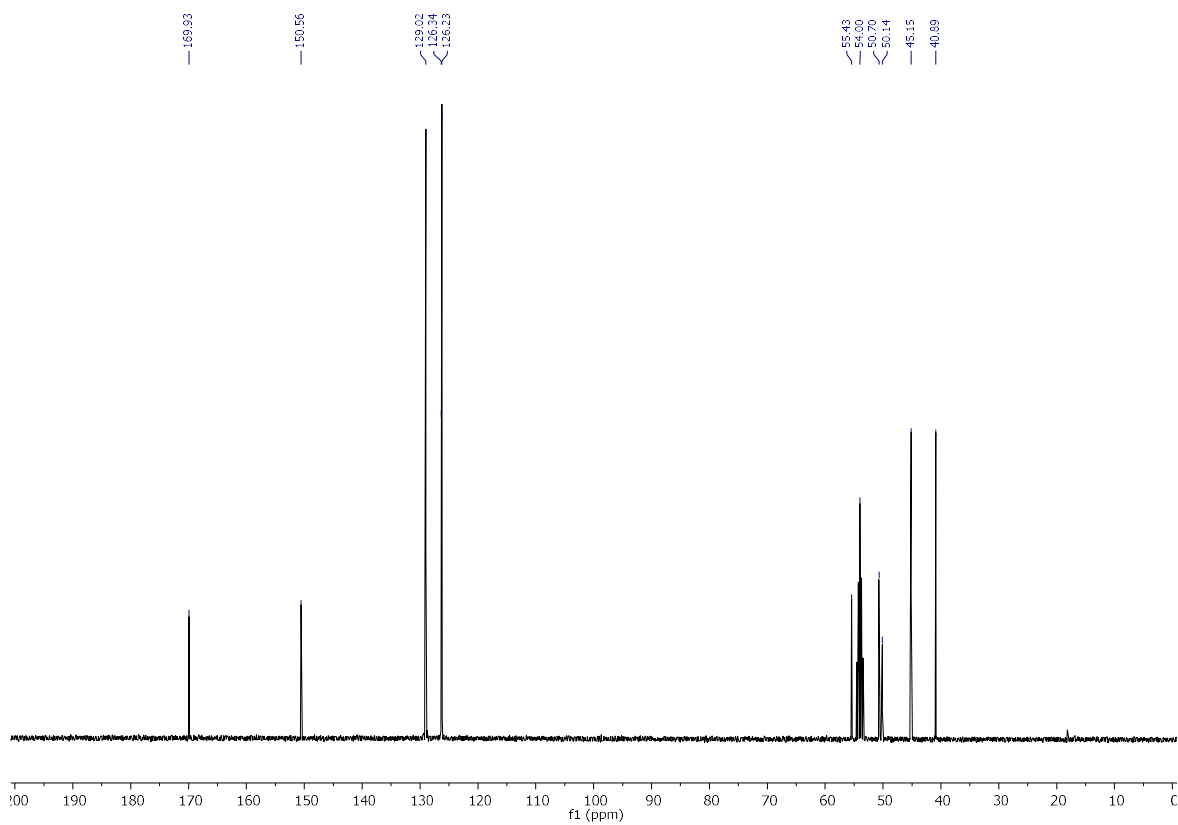
11d (¹H):**11d (¹³C):**

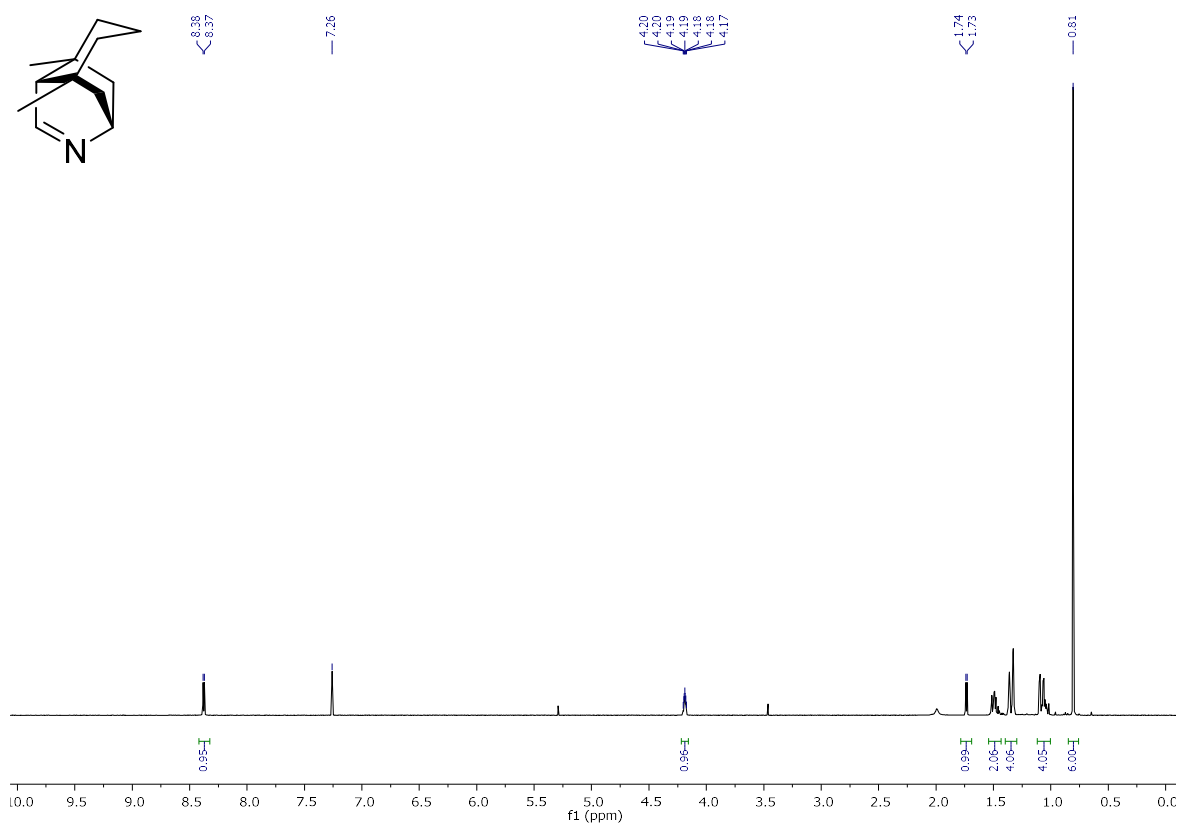
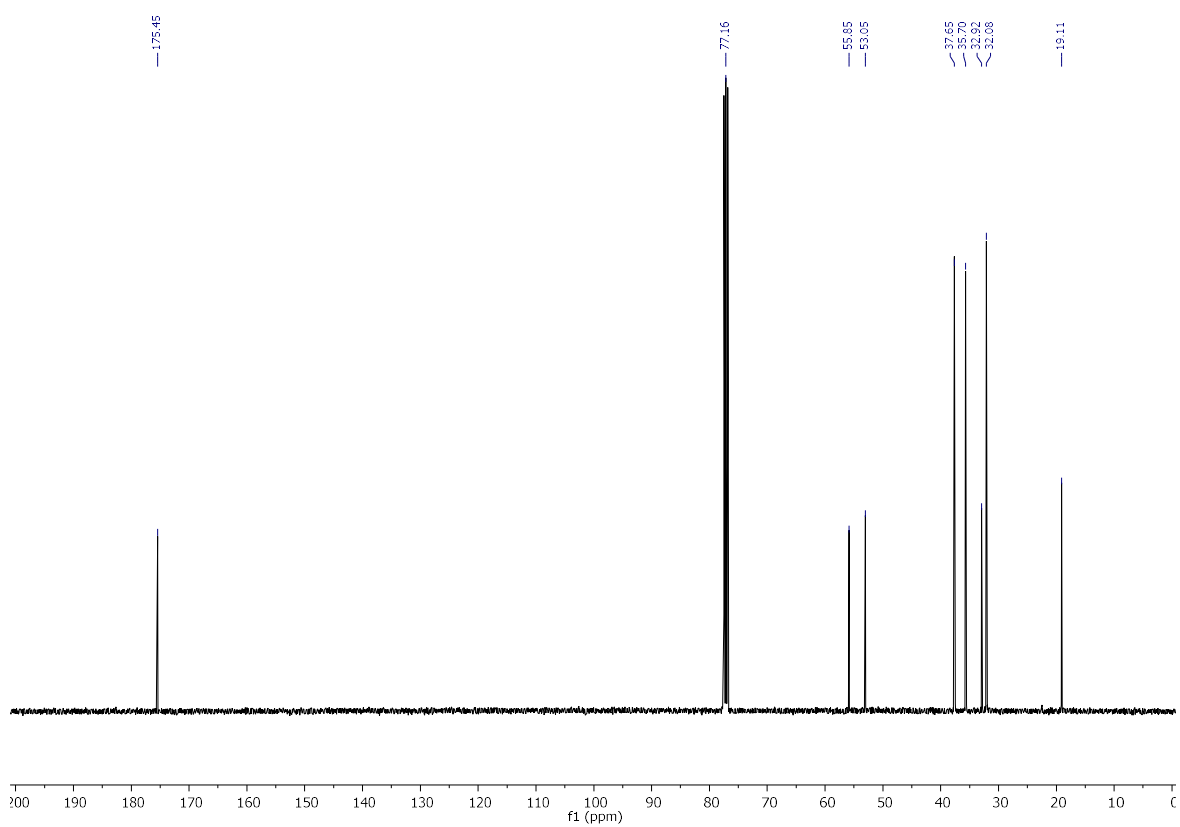
11e (^1H):**11e** (^{13}C):

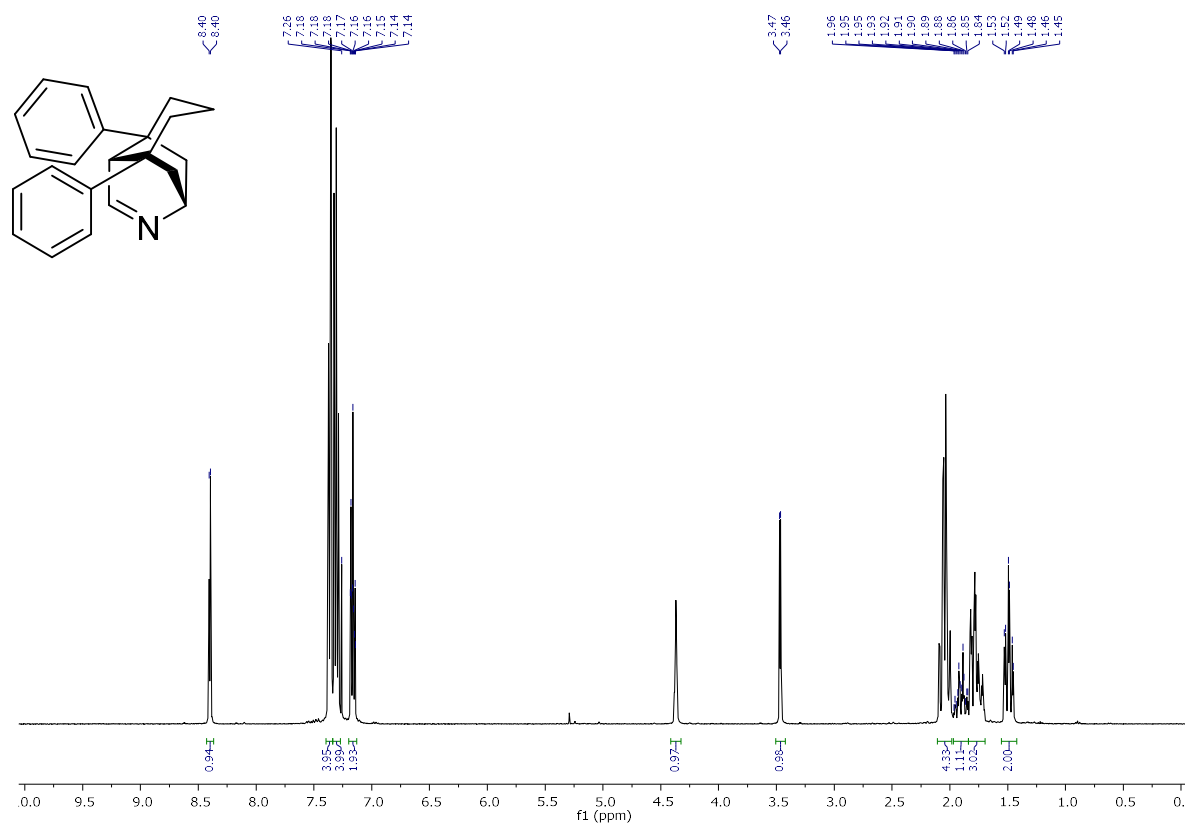
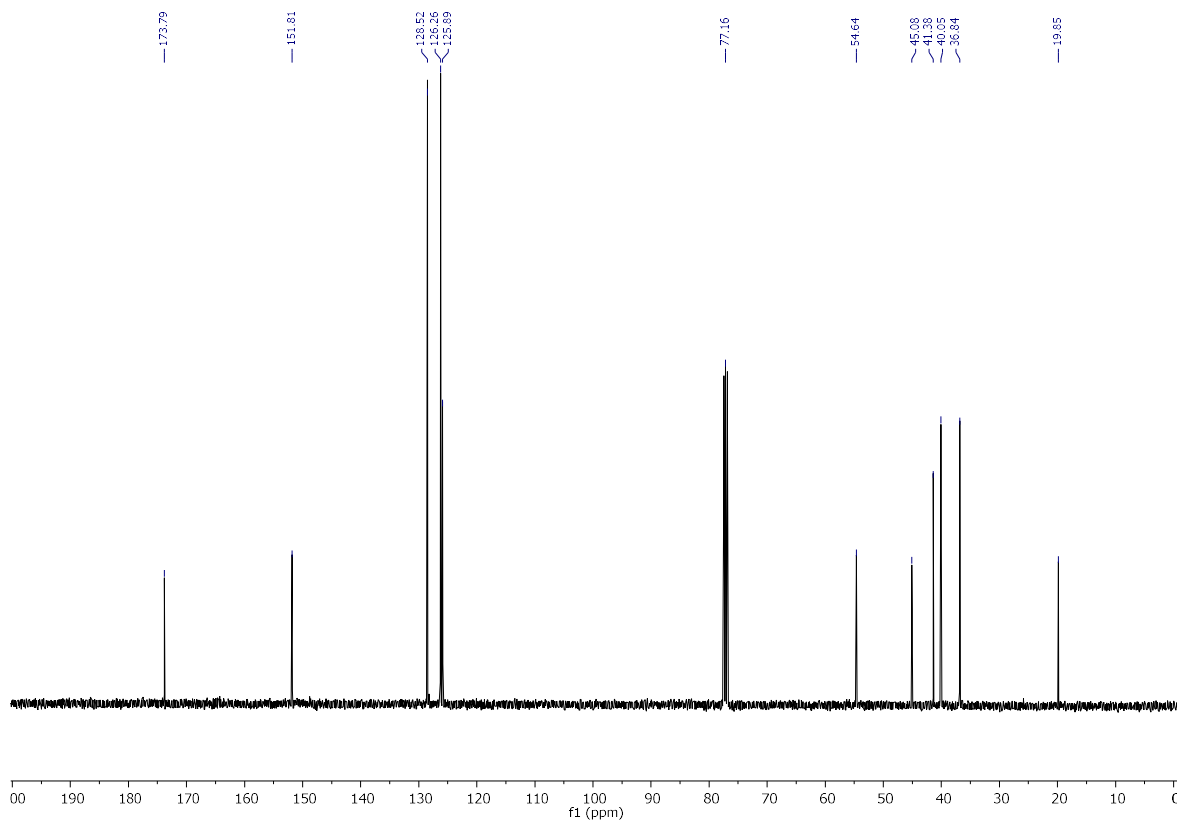
11f (^1H):**11f** (^{13}C):

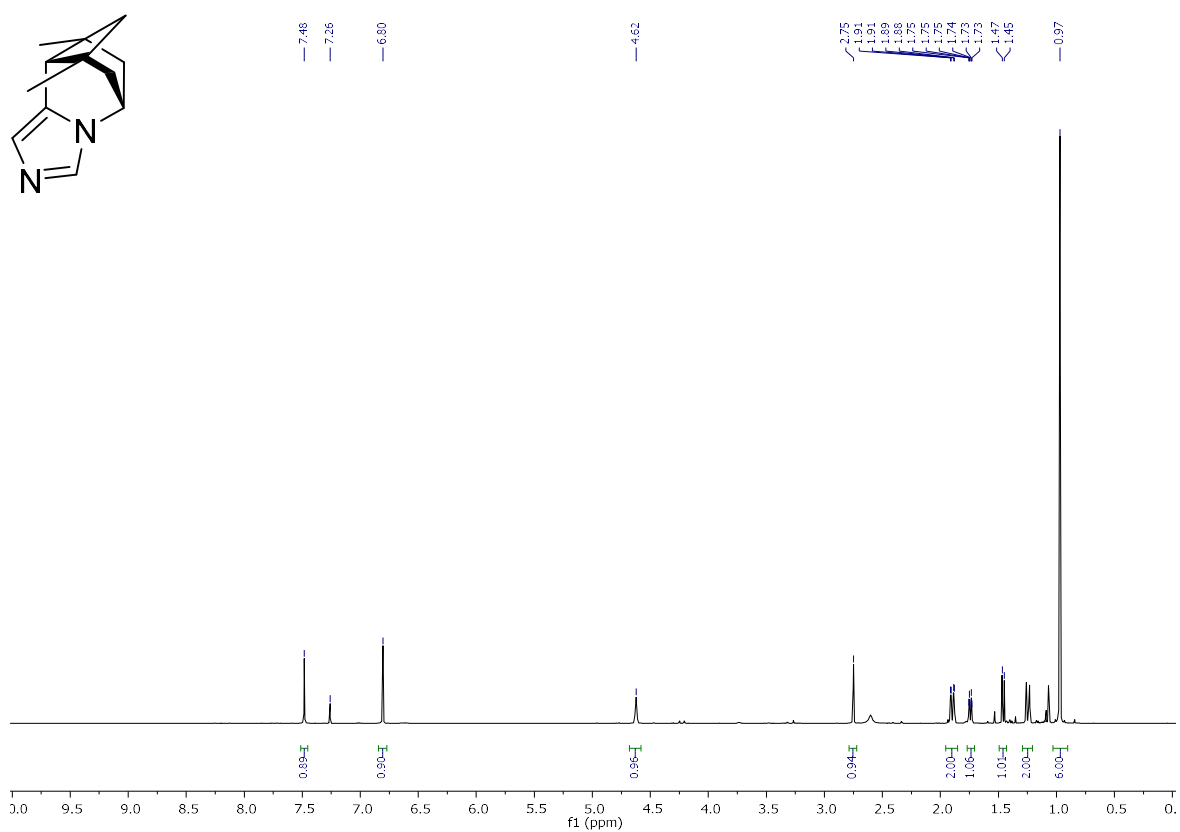
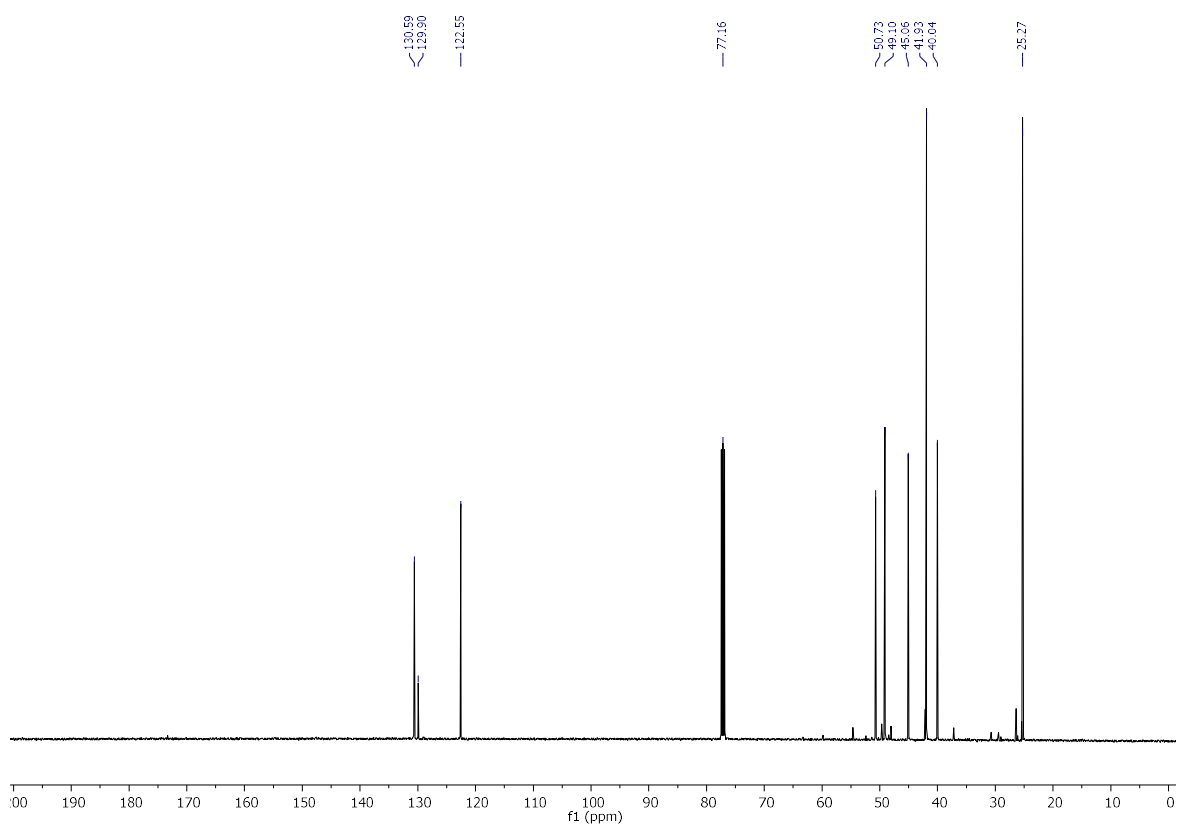
13a (^1H):**13a** (^{13}C):

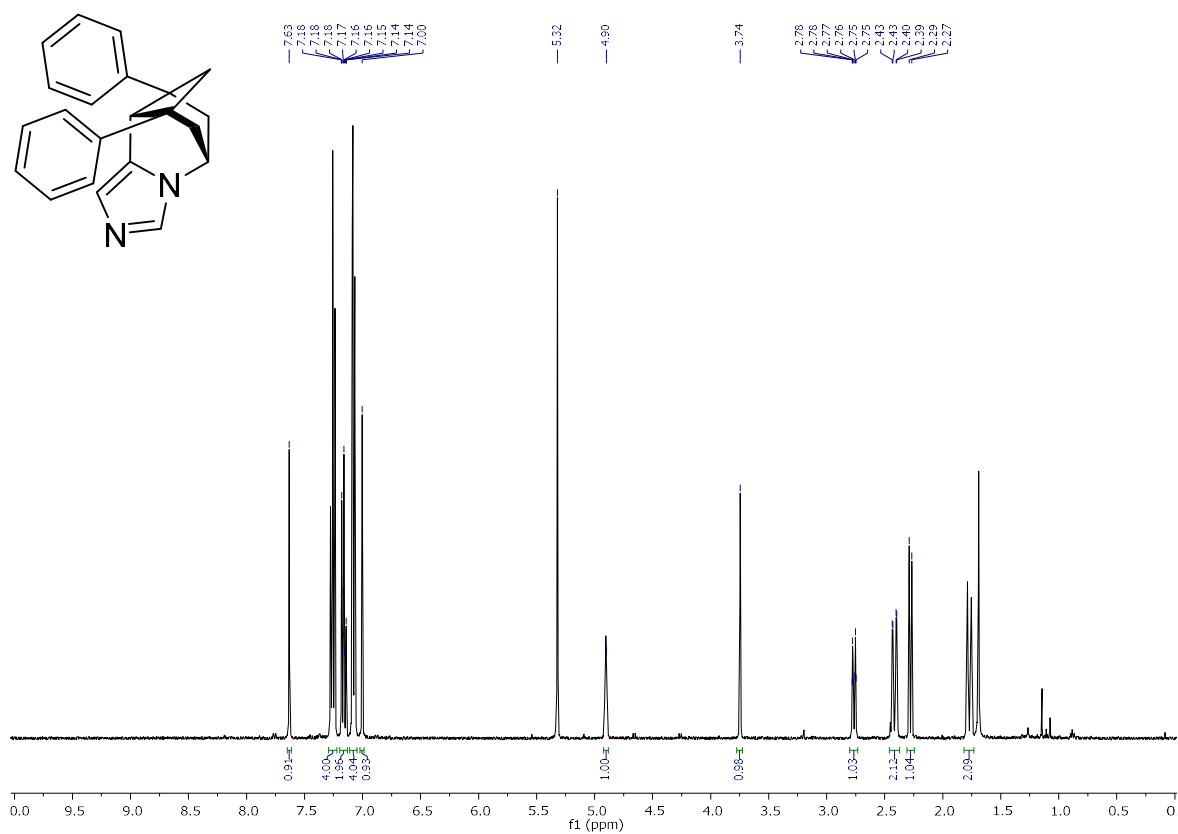
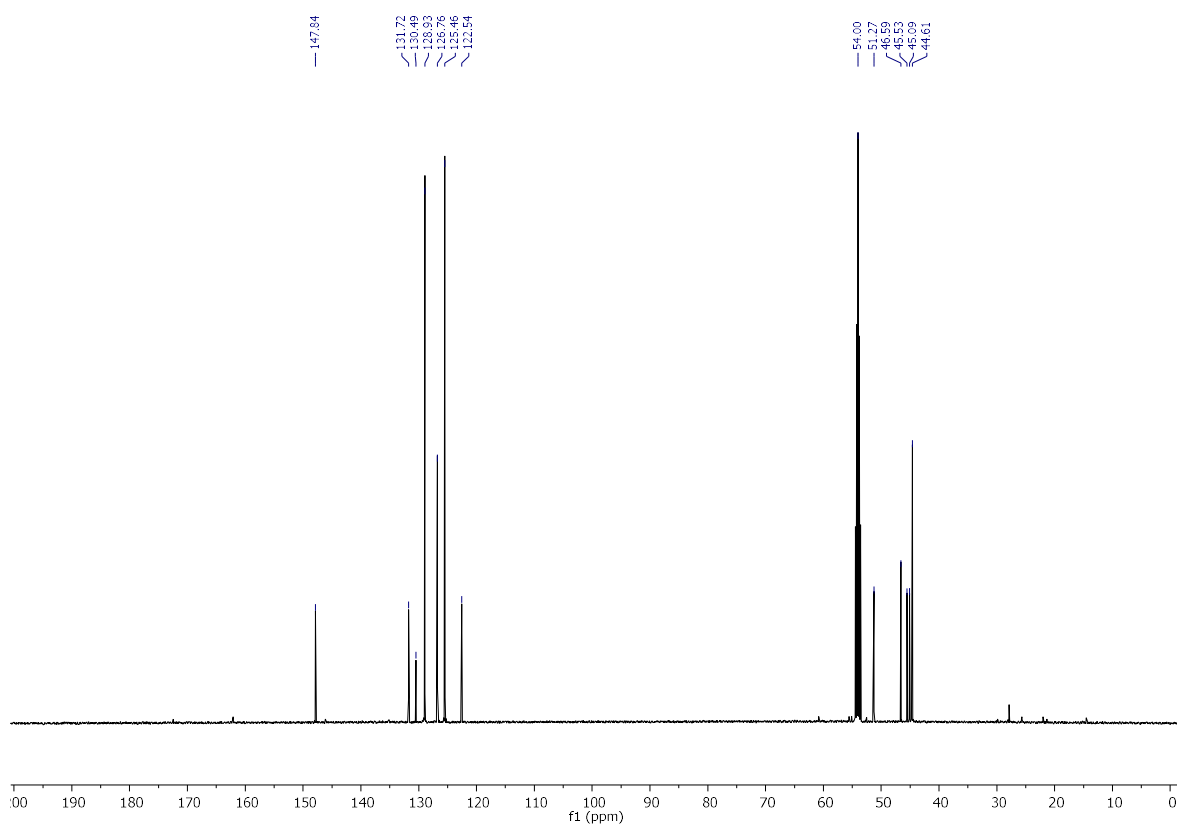
13b (¹H):**13b (¹³C):**

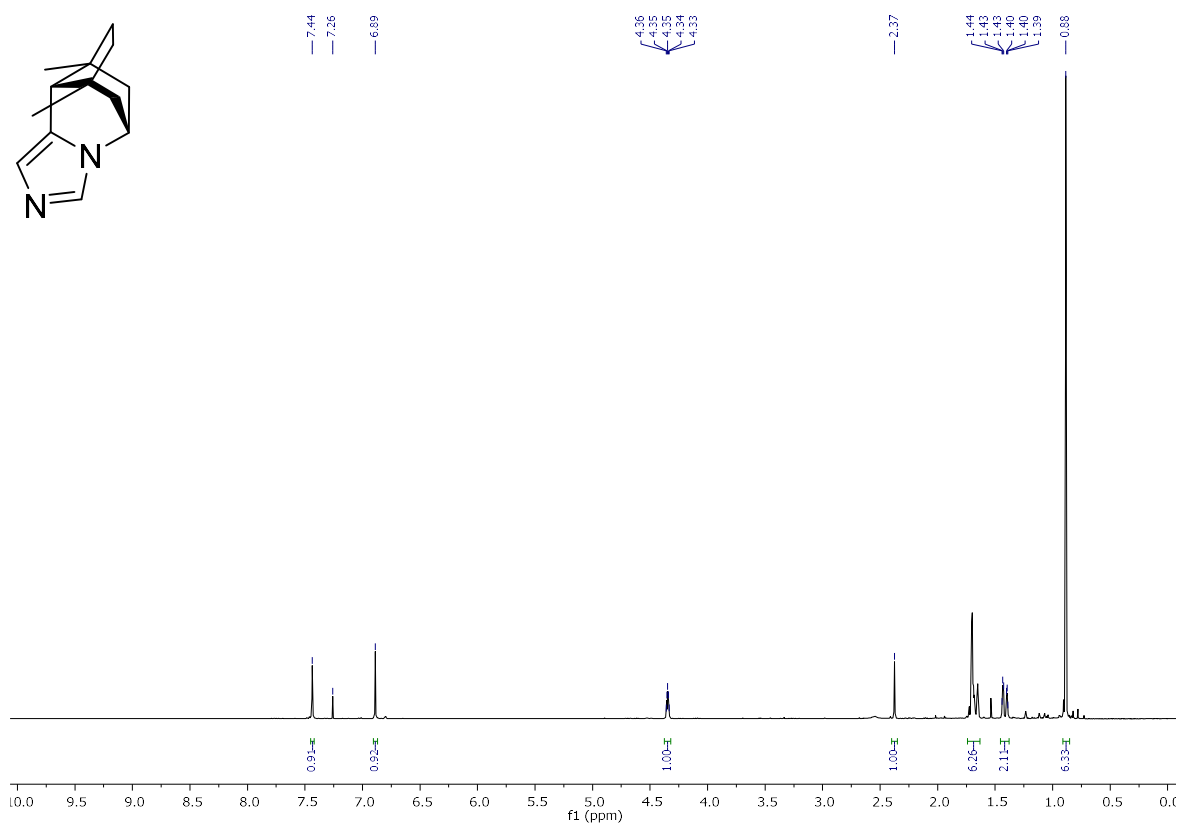
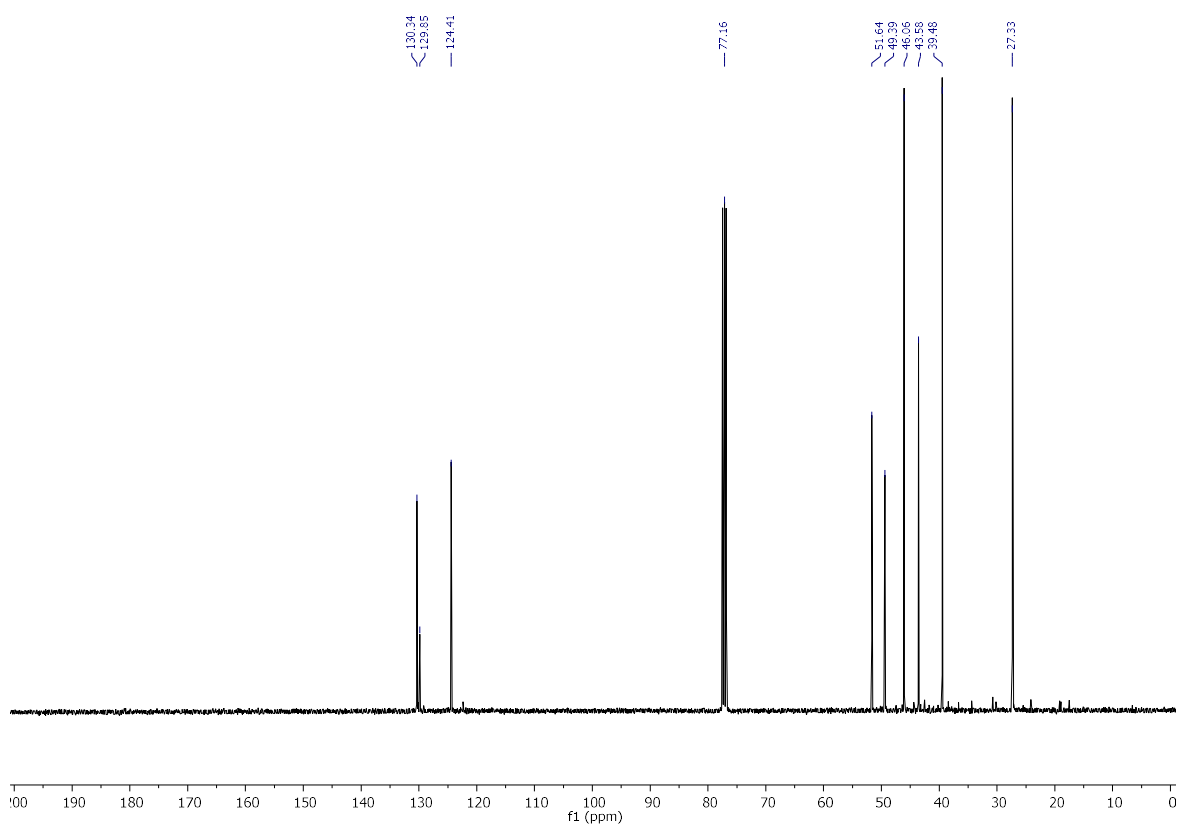
13d (¹H):**13d (¹³C):**

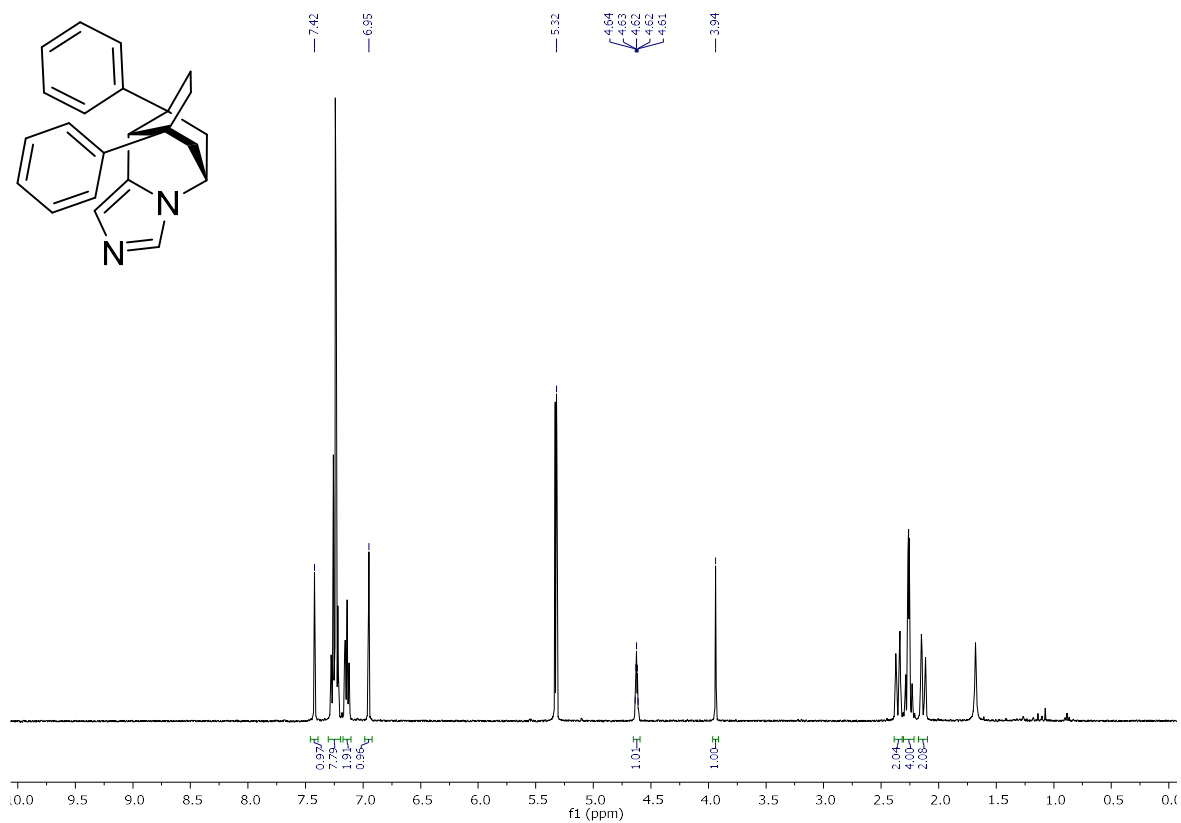
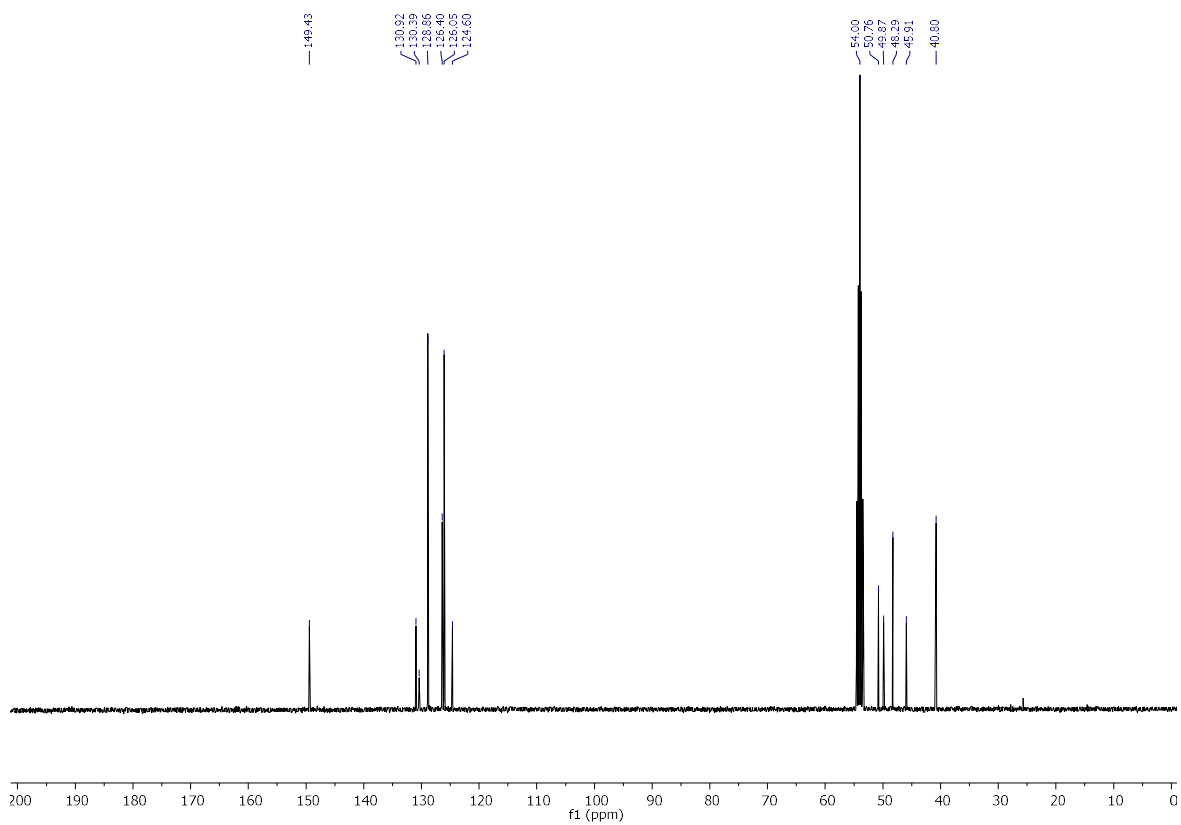
13e (^1H):**13e** (^{13}C):

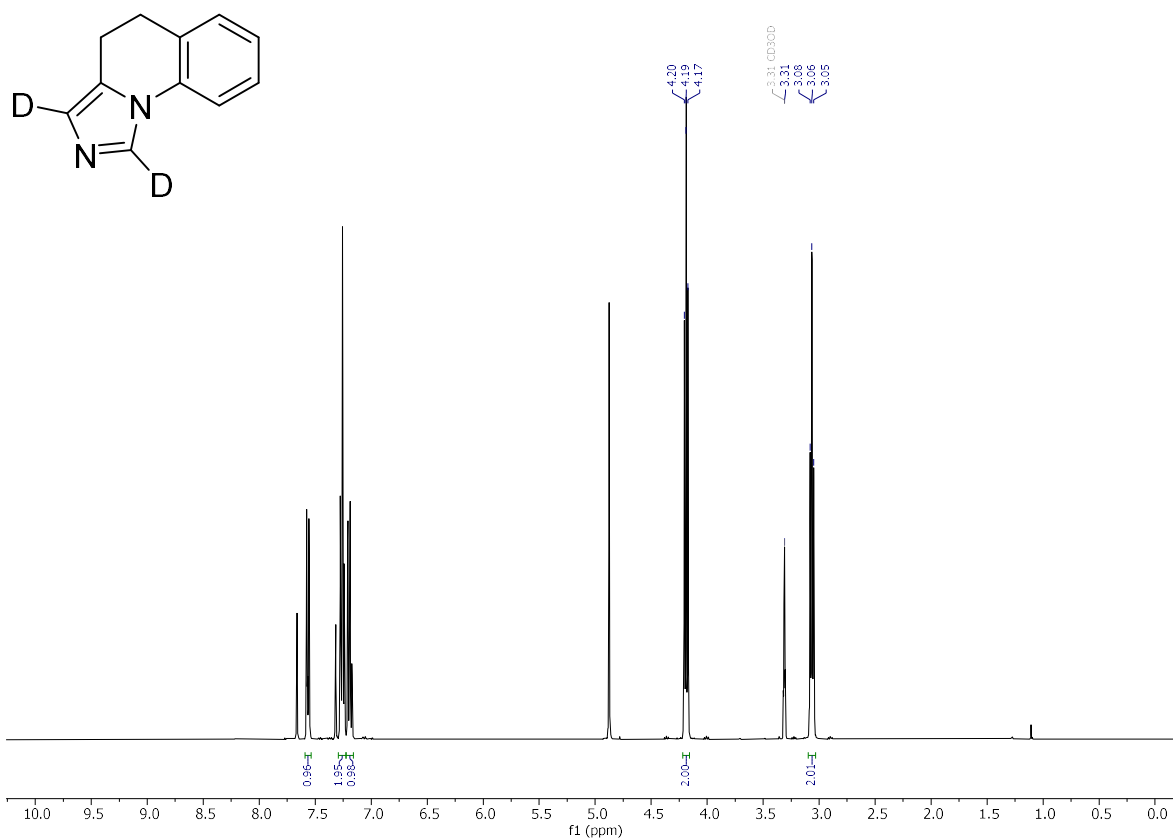
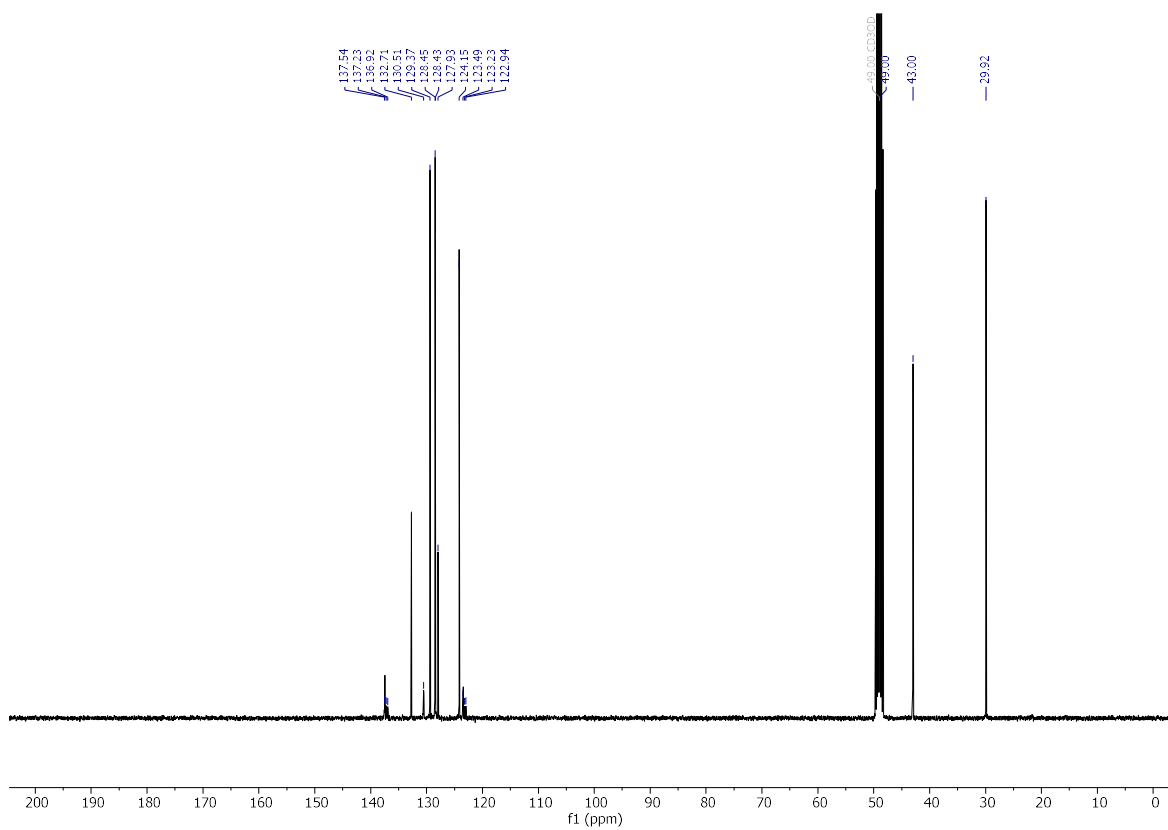
13f (^1H):**13f** (^{13}C):

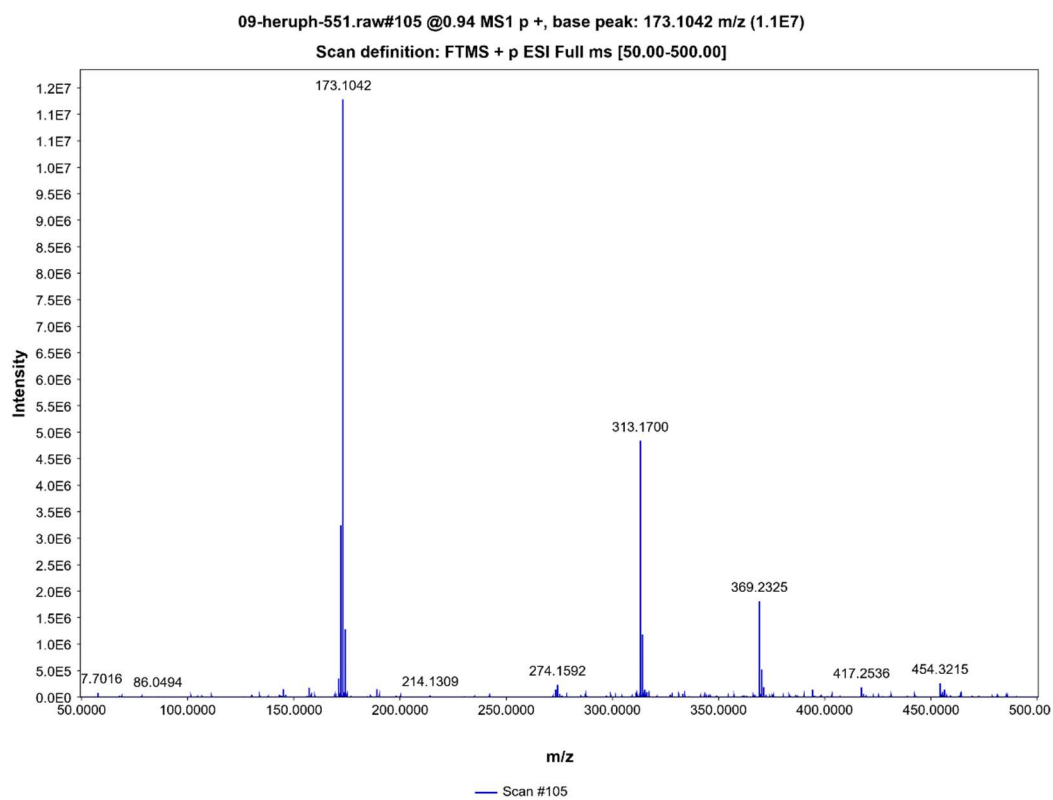
14a (^1H):**14a** (^{13}C):

14b (¹H):**14b (¹³C):**

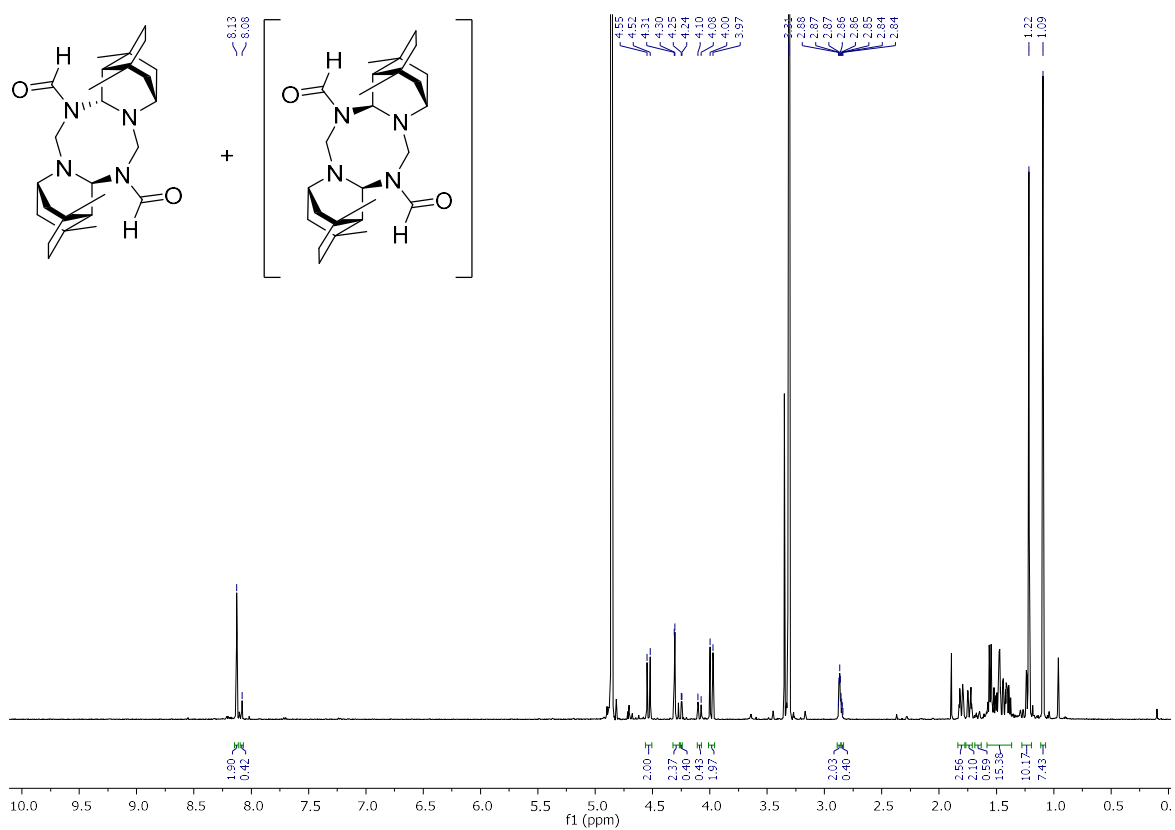
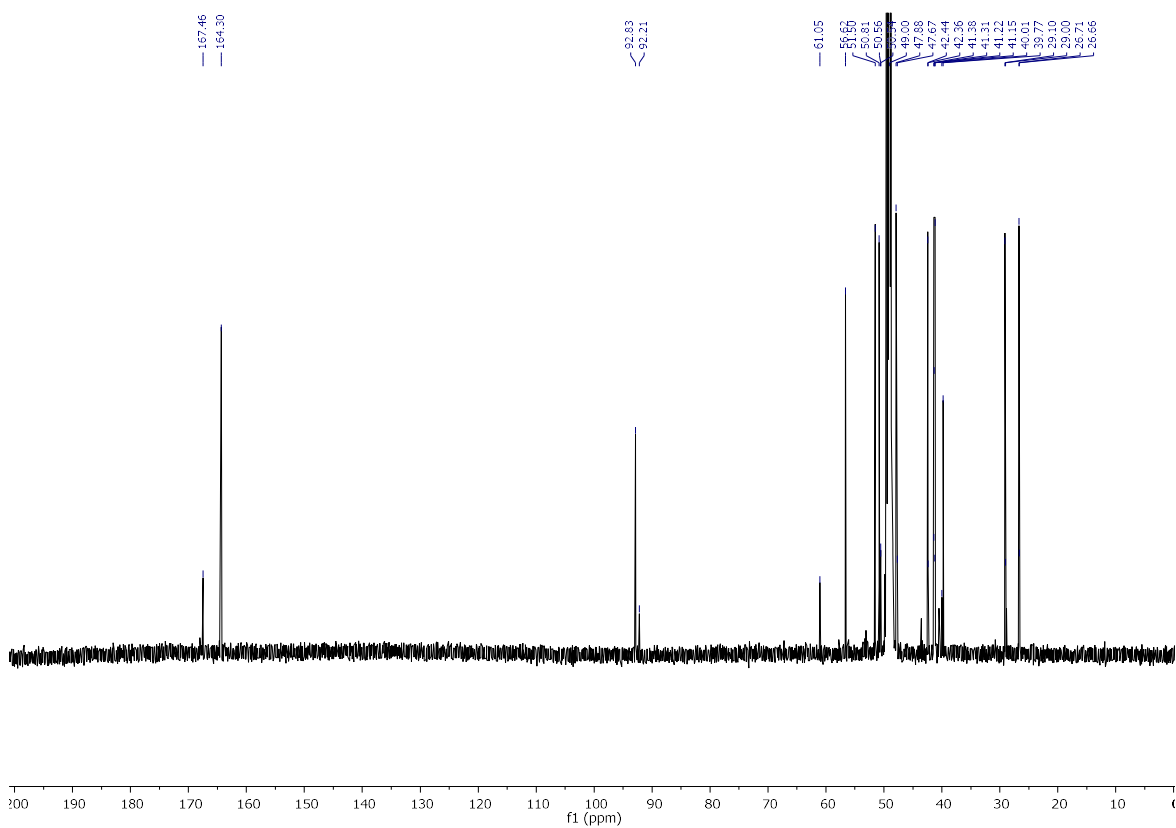
14c (^1H):**14c** (^{13}C):

14d (¹H):**14d (¹³C):**

14h (¹H):**14h (¹³C):**

HRMS spectrum for **14h**:

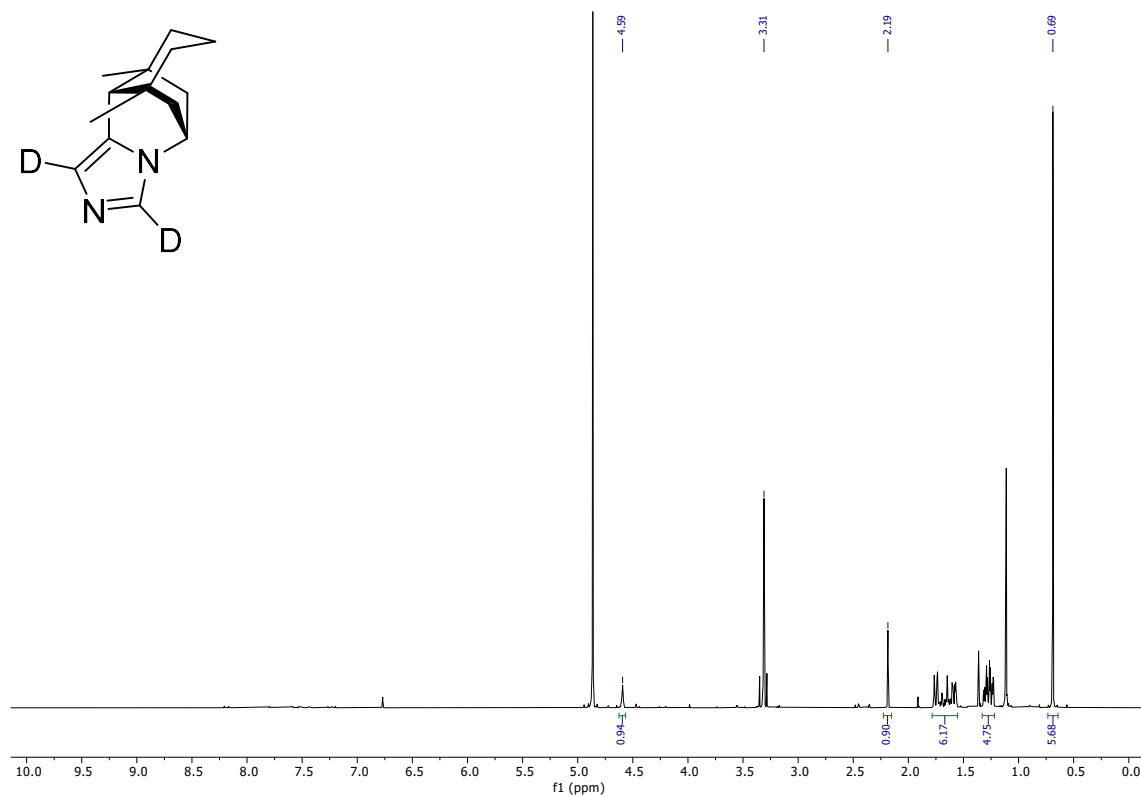
HRMS (ESI): m/z $[M+H]^+$ calcd for $C_{11}H_9D_2N_2$ 173.1042; found 173.1042.

18 (¹H):**18 (¹³C):**

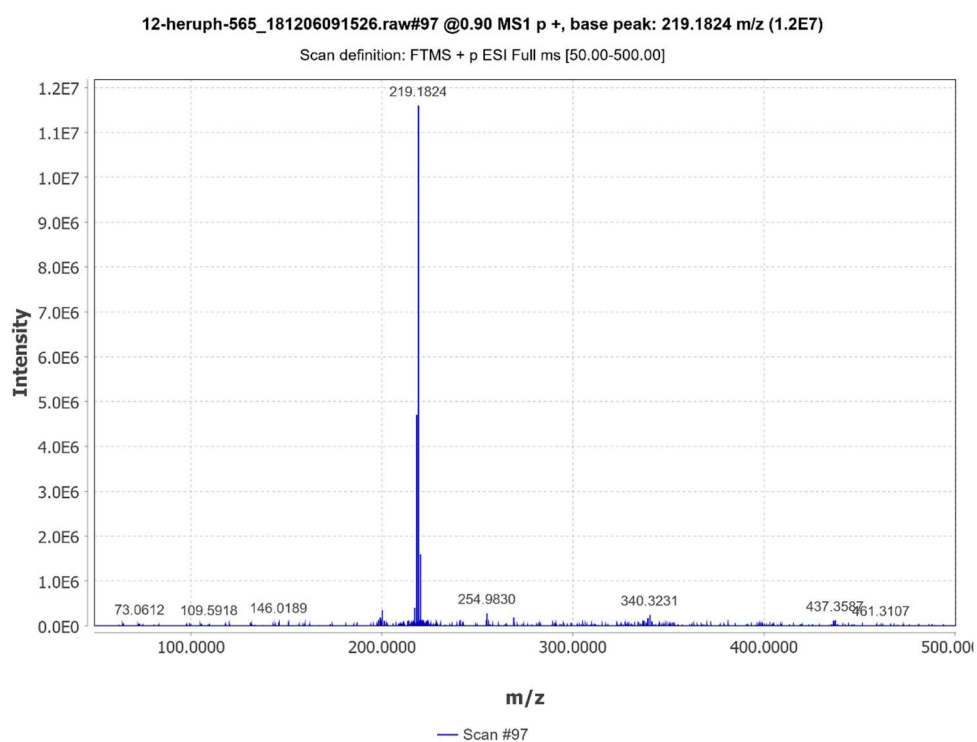
2. NMR experiments

2.1 ^1H NMR and HRMS spectra for compounds 14e-g

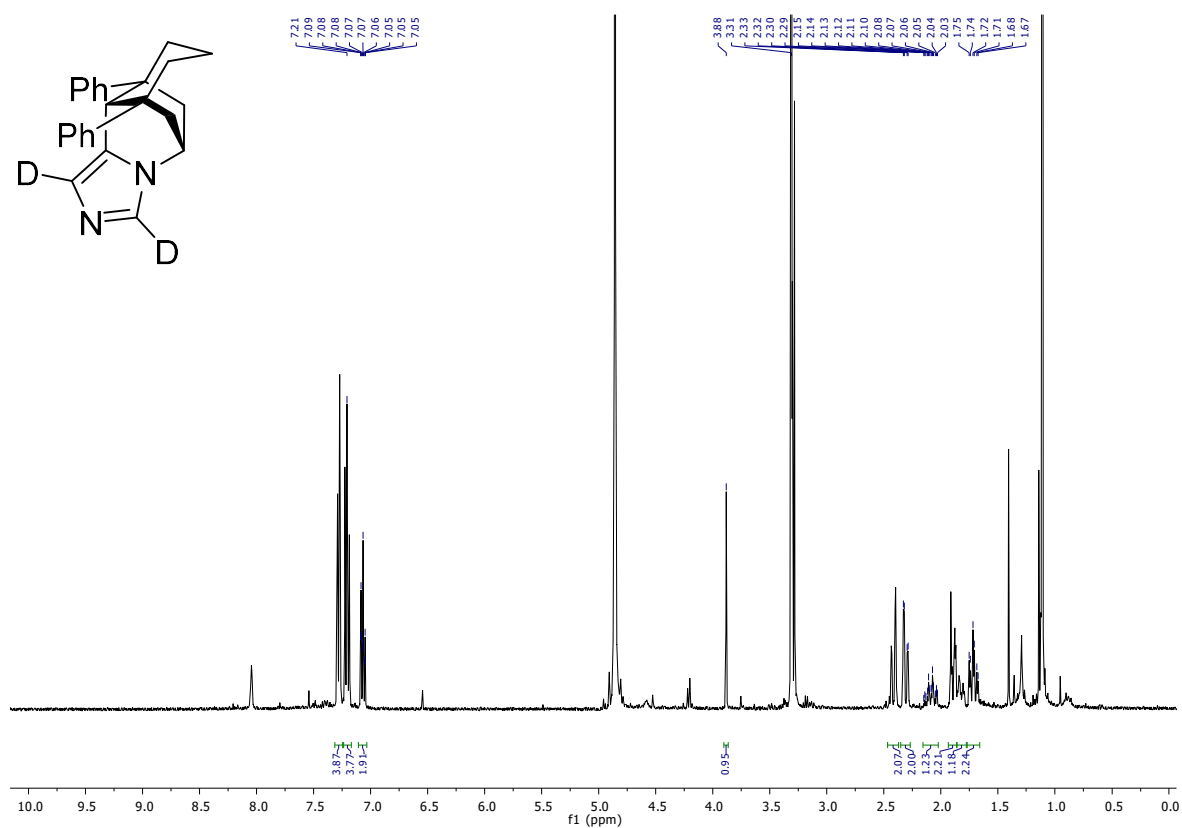
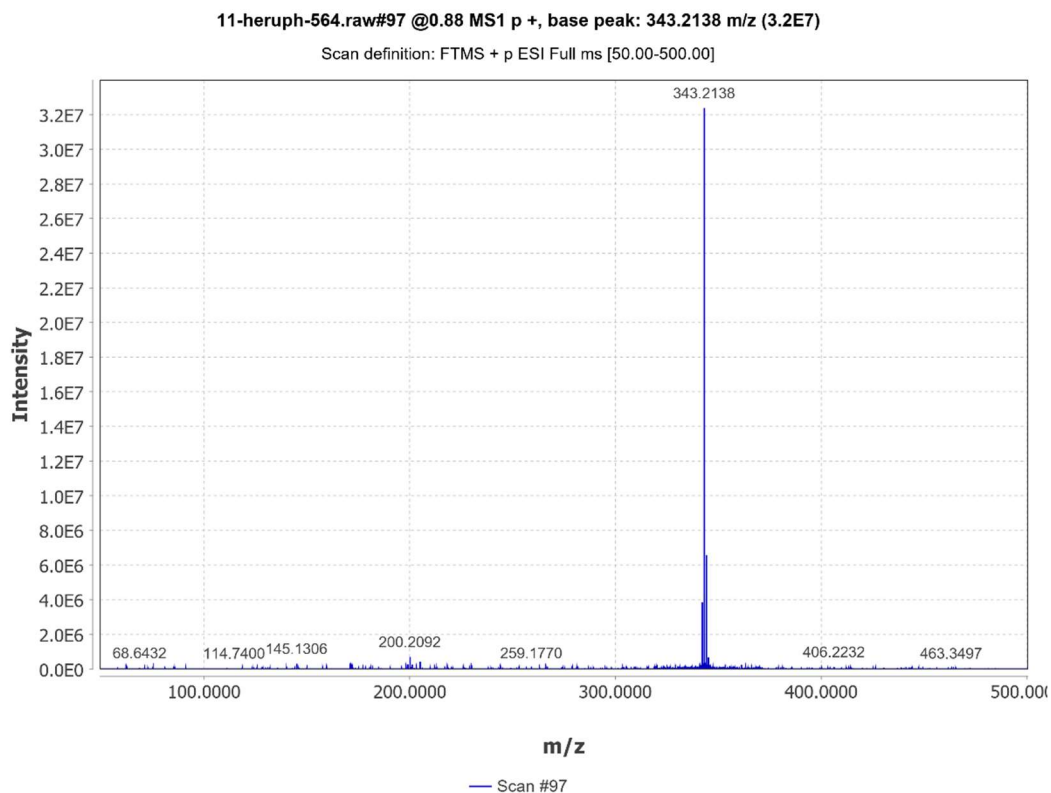
Reference spectrum for **14e** (^1H):



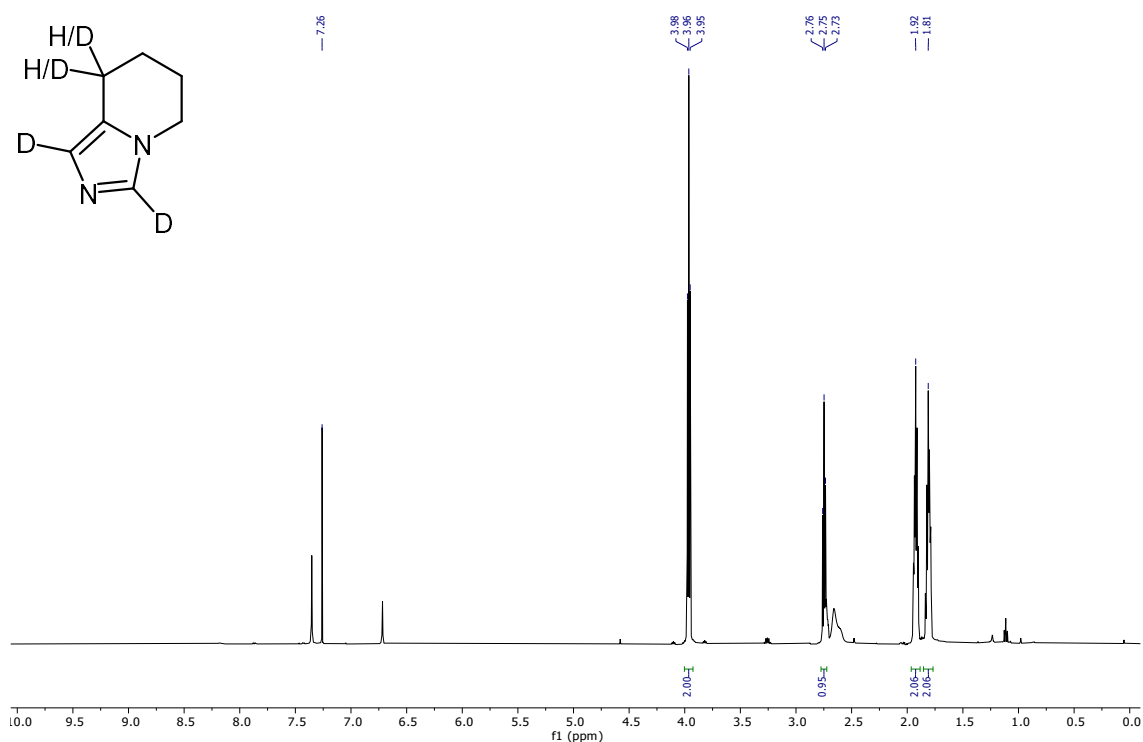
HRMS spectrum for **14e**:



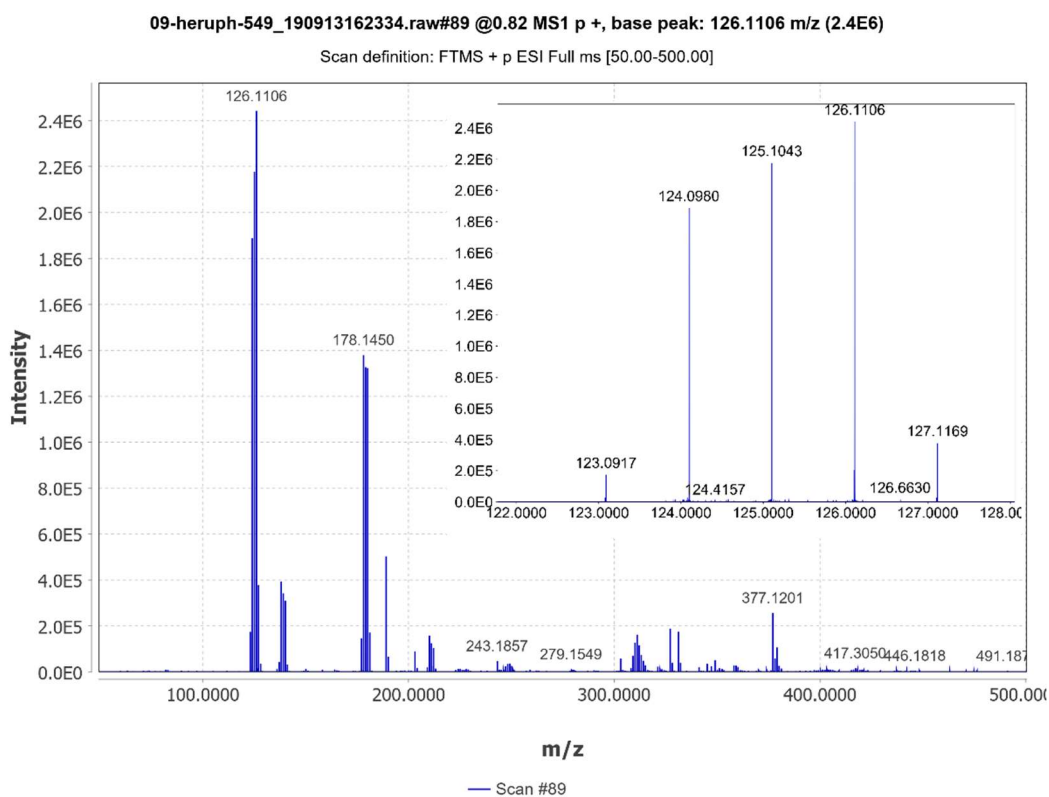
HRMS (ESI): m/z $[\text{M}+\text{H}]^+$ calcd for $\text{C}_{14}\text{H}_{19}\text{D}_2\text{N}_2$ 219.1825; found 219.1824.

Reference spectrum for **14f** (^1H):HRMS spectrum for **14f**:HRMS (ESI): m/z $[\text{M}+\text{H}]^+$ calcd for $\text{C}_{24}\text{H}_{23}\text{D}_2\text{N}_2$ 343.2138; found 343.2138.

Reference spectrum for **14g** (^1H):

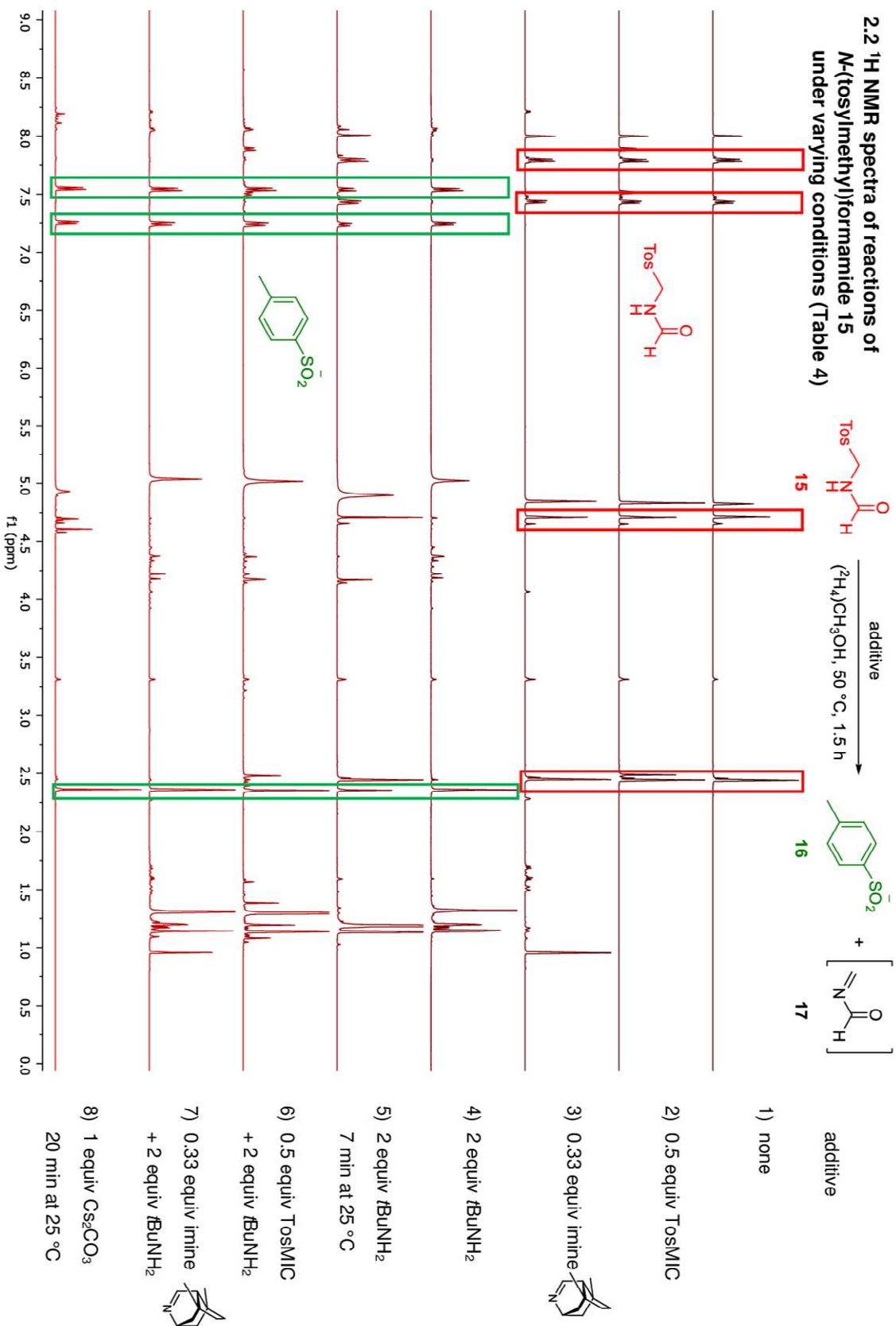


HRMS spectrum for **14g**:



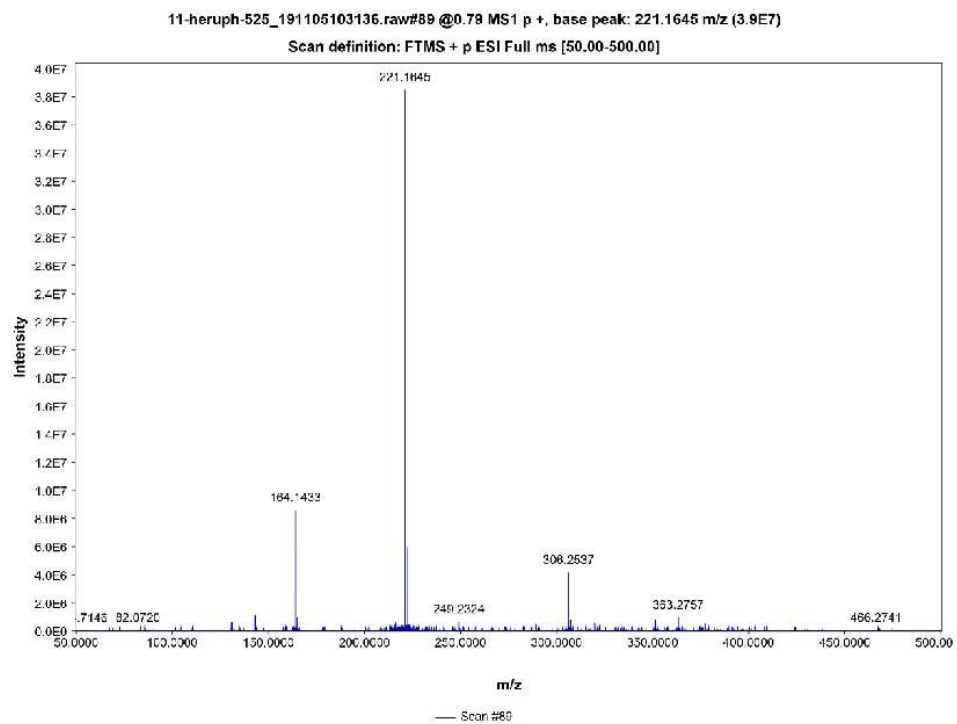
HRMS (ESI): m/z $[\text{M}+\text{H}]^+$ calcd for $\text{C}_7\text{H}_9\text{D}_2\text{N}_2$ 125.1042; found 125.1043.

2.2 ^1H NMR spectra of reactions of *N*-(tosylmethyl)formamide **15 under varying conditions (Table 4)**



Due to the occurrence of an amide rotamer of *N*-(tosylmethyl)formamide **15** a second set of signals can be observed in the ^1H NMR spectra (entries 1-3).

2.3 HRMS spectrum for adduct of imine 13c and *N*-methyleneformamide 17 (Table 4, entry 7)



HRMS (ESI): m/z $[M+H]^+$ calcd for $C_{13}H_{21}ON_2$ 221.1648; found 221.1645.

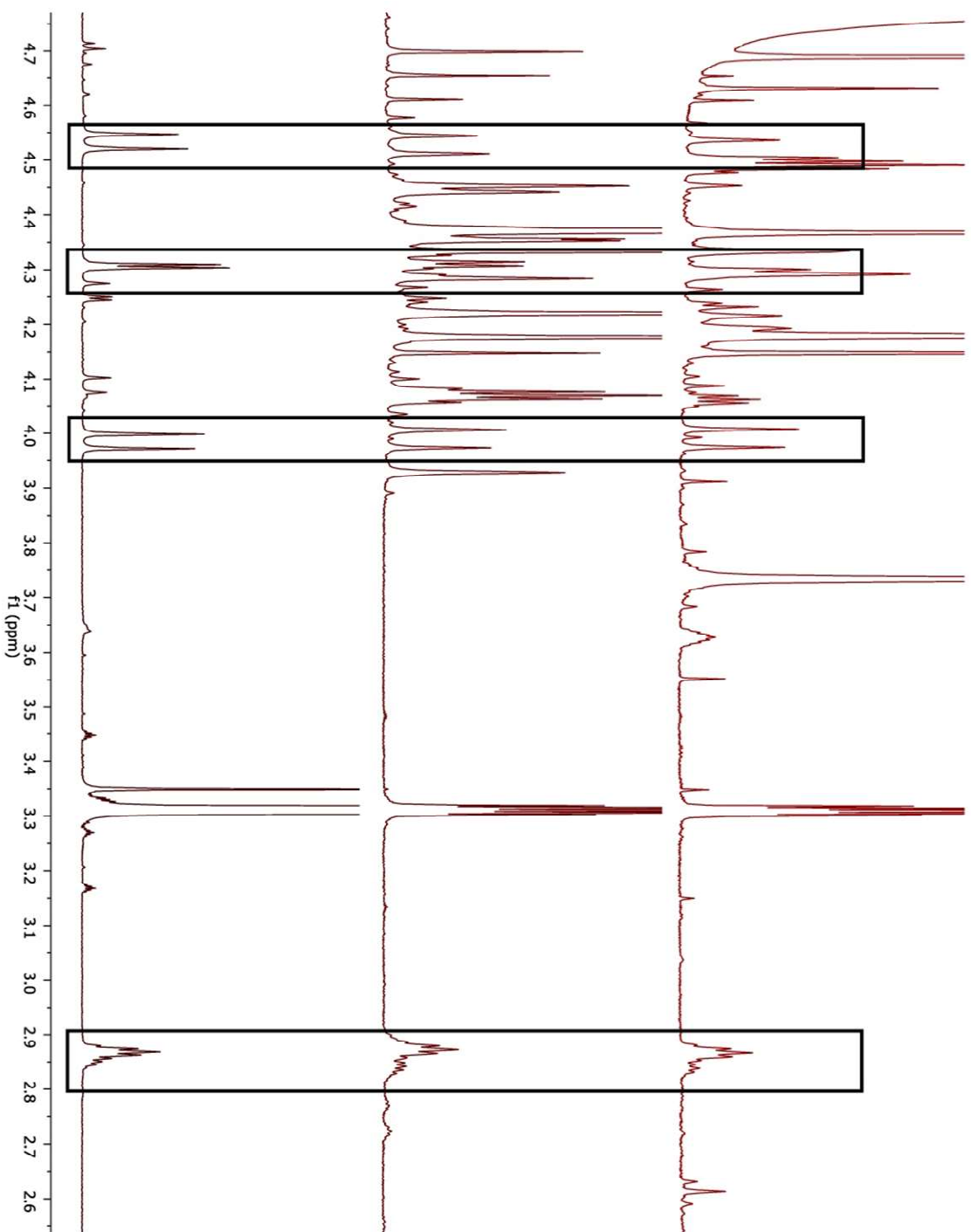
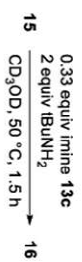
2.4 Identification of Dimer 18 in other ^1H NMR spectra

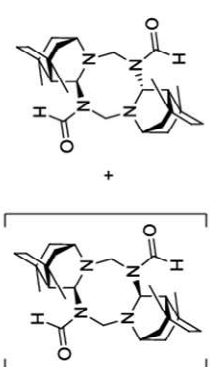
Figure 3 Progression of imidazole formation



Table 4, entry 7



Dimer 18



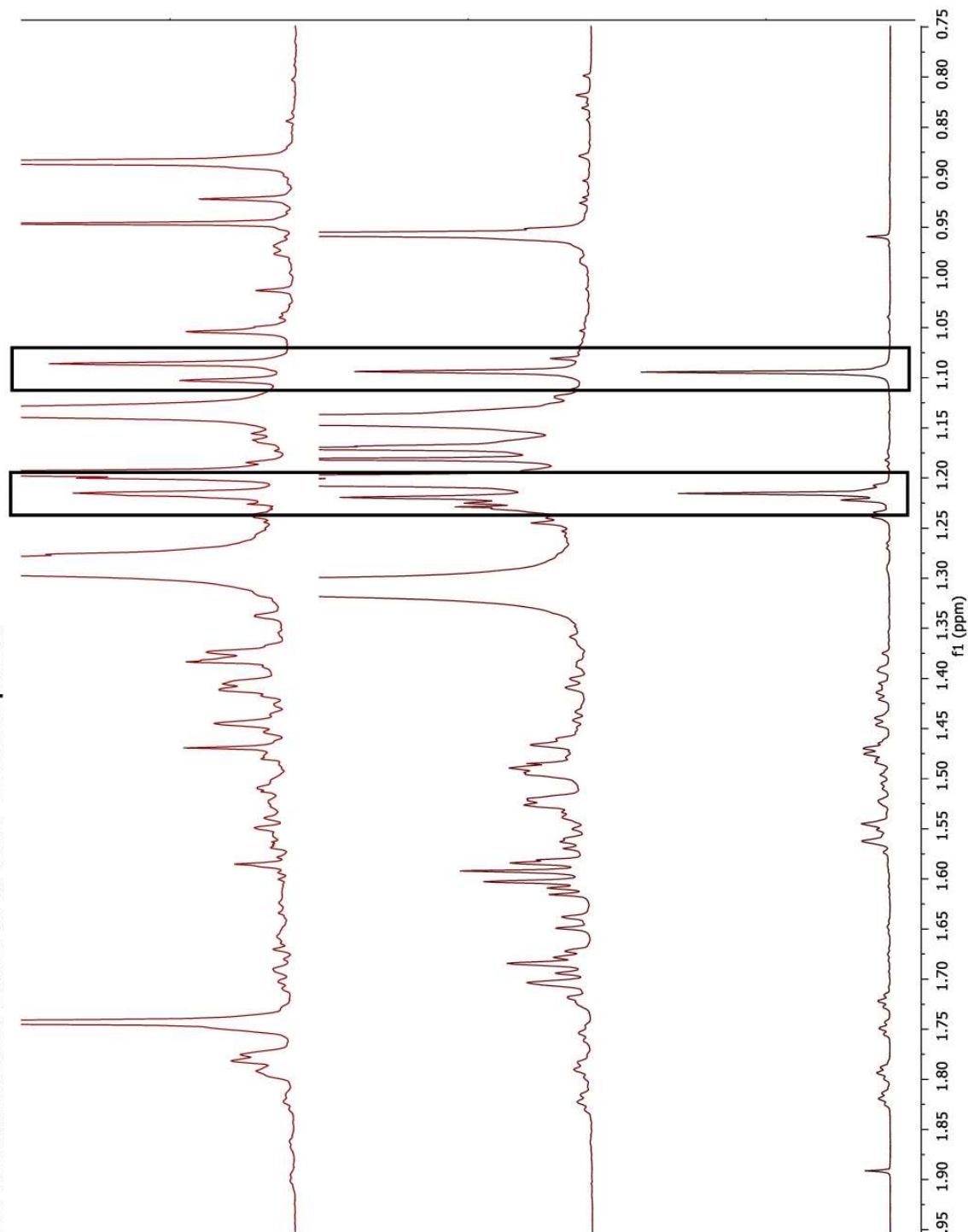
2.4 Identification of Dimer 18 in other ^1H NMR spectra

Figure 3 Progression of imidazole formation

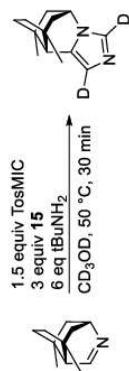
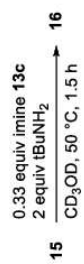
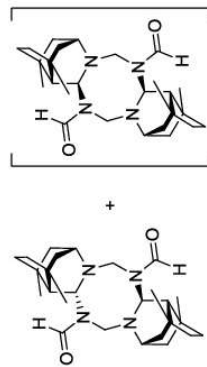
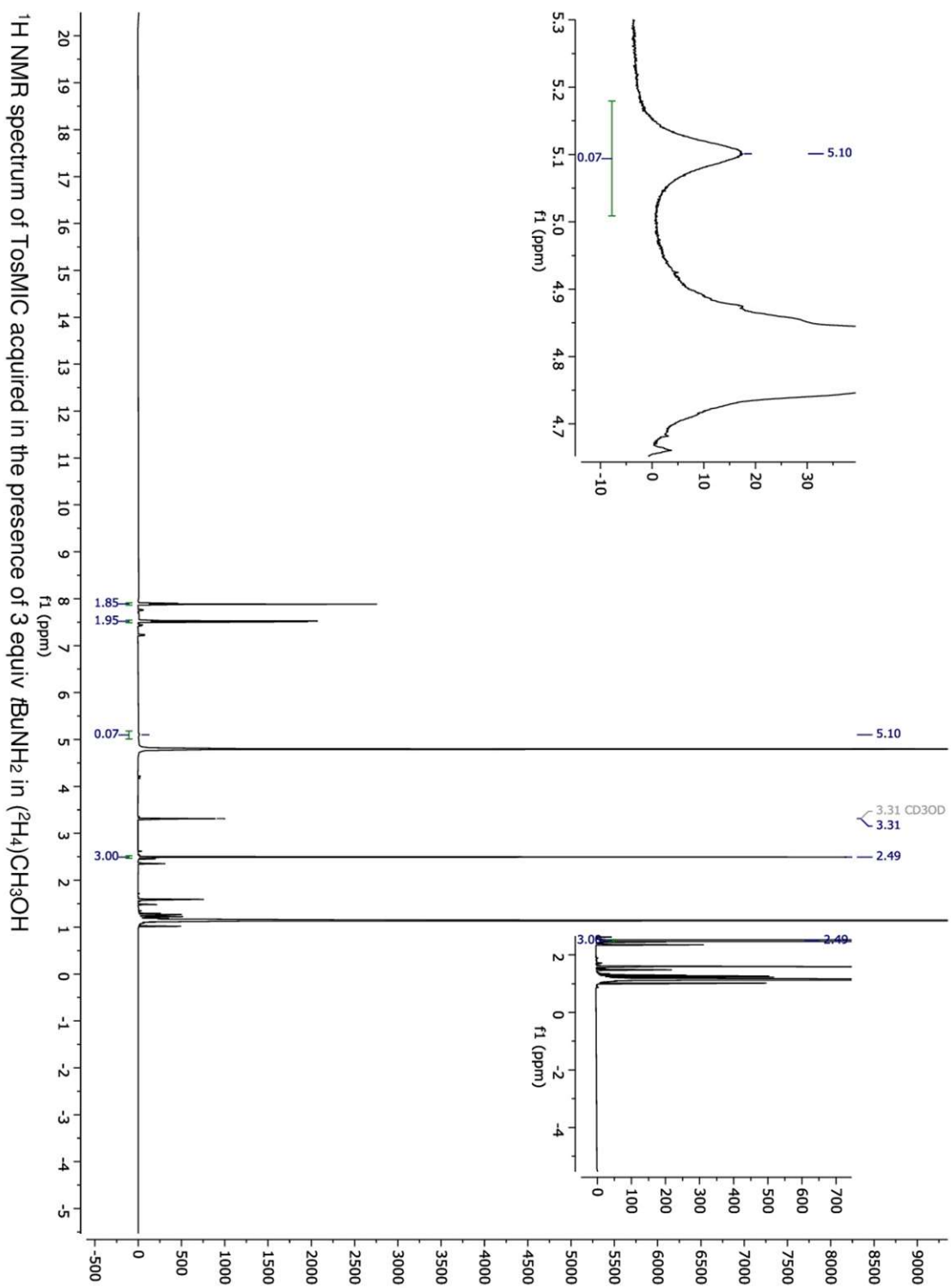


Table 4, entry 7

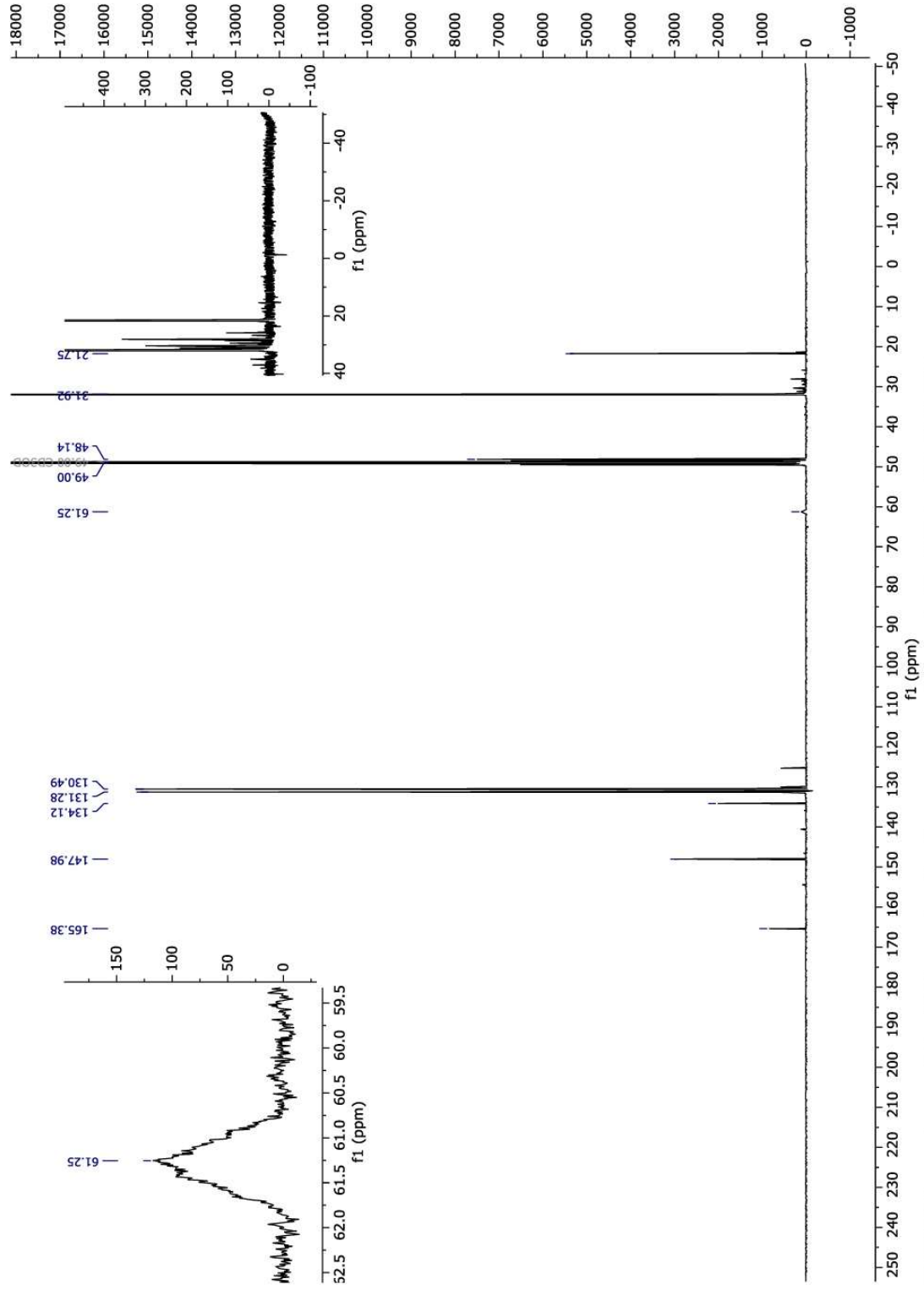


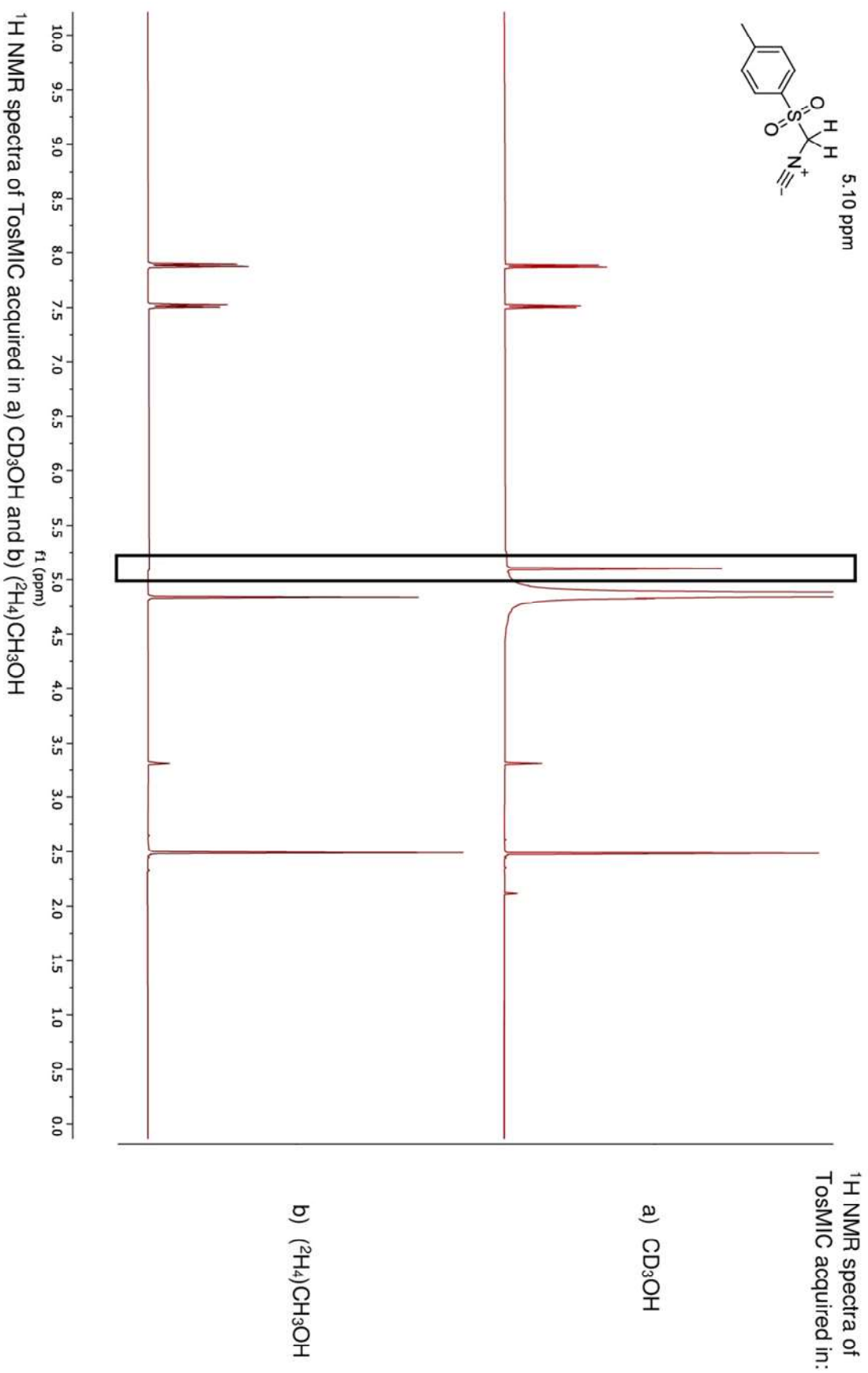
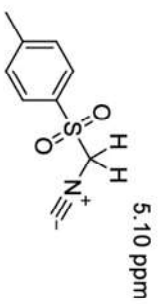
Dimer 18



2.5 ^1H and ^{13}C NMR spectra confirming the proton deuterium exchange of TosMIC leading to $[\text{2H}_2]$ -TosMIC

2.5 ^1H and ^{13}C NMR spectra confirming the proton deuterium exchange of TosMIC leading to $[\text{t}^2\text{H}_2]\text{-TosMIC}$



2.5 ^1H and ^{13}C NMR spectra confirming the proton deuterium exchange of TosMIC leading to $[\text{2H}_2]$ -TosMIC

8.3 Manuscript of the third publication

Synthesis and biological evaluation of novel *N*-substituted nipecotic acid derivatives with tricyclic cage structures in the lipophilic domain as GABA uptake inhibitors

Heinrich-Karl A. Rudy, Georg Höfner, Klaus T. Wanner

Ludwig-Maximilians-Universität München, Department of Pharmacy – Center for Drug Research, Butenandtstraße 5-13, Haus C, 81377 Munich, Germany

✉ Klaus T. Wanner

klaus.wanner@cup.uni-muenchen.de

Abstract

A new class of GABA reuptake inhibitors with sterically demanding, highly rigid tricyclic cage structures as the lipophilic domain was synthesized and investigated in regard to their biological activity at the murine GABA transporters (mGAT1-mGAT4). The construction of these compounds, consisting of nipecotic acid, a symmetric tricyclic amine and a plain hydrocarbon linker connecting the two subunits via their amino nitrogens, was accomplished via reductive amination of a nipecotic acid derivative with an *N*-alkyl substituent displaying a terminal aldehyde function with tricyclic secondary amines. The target compounds varied with regard to spacer length, the bridge size of one of the bridges and the substituents of the tricyclic skeleton to study the impact of these changes on their potency. Among the tested compounds nipecotic acid ethyl ester derivatives with phenyl residues attached to the cage subunit showed reasonable inhibitory potency and subtype selectivity in favor of mGAT3 and mGAT4, respectively.

Key words

GABA transporters, GABA uptake inhibitor, nipecotic acid, polycycles, cage structures

Introduction

A balanced interplay between excitatory and inhibitory neurotransmission represents the fundamental basis for proper functioning of the central nervous system (CNS) in mammals. A disruption of this interplay due to, for example, an insufficient signaling of GABAergic neurons can lead to or intensify neurological disorders like Alzheimer's disease (AD) (Lanctot et al. 2004, Guzmán et al. 2018), depression (Kalueff and Nutt 2007), epilepsy (Kleppner and Tobin 2001, Treimann 2001) or Parkinson's disease (PD) (Błaszczuk 2016, Firbank et al. 2018, van Nuland et al. 2020). One approach to influence the GABAergic neurotransmission and thus to treat the aforementioned diseases is to increase the release and the concentration of γ -aminobutyric acid **1** (GABA), representing the predominant inhibitory neurotransmitter in the CNS (Krogsgaard-Larsen 1988, Scheschonka et al. 2007, Lüllmann et al. 2010), in the synaptic cleft. As GABA is quickly removed from the synaptic cleft by reuptake into the presynaptic neurons and surrounding glia cells this may be achieved by inhibition of the GABA-transporters (GATs) in charge of this process (Borden 1996, Sałat et al. 2015, Schousboe et al. 2014).

GATs are membrane-bound transport proteins of the solute carrier family 6 (SLC6). They consist of twelve transmembrane helices and translocate their substrate GABA through the cell membrane by cotransport of sodium and chloride ions (Gether et al. 2006, Kristensen et al. 2011). Latest findings suggest a stoichiometry of 3:1:1 ($\text{Na}^+:\text{Cl}^-:\text{GABA}$) for sodium and chloride ions and GABA in this transport process (Willford et al. 2015). For the GABA transporters four different subtypes are known, which are denominated differently depending on the species they were cloned from (Borden 1996, Conti et al. 2004). When originating from mouse tissue they are termed mGAT1-mGAT4 (Liu et al. 1993, Conti et al. 2004, Madsen et al. 2009). For all other species including human, dog or rat they are denominated as GAT-1 (\equiv mGAT1), BGT-1 (\equiv mGAT2), GAT-2 (\equiv mGAT3) and GAT-3 (\equiv mGAT4) whereby the individual transporter name is provided with a prefix such as h for human to indicate the individual species. This nomenclature has also been adopted by the Gene Nomenclature Committee of the Human Genome Organization (HUGO) but without any prefix as which it has also found use as a species independent nomenclature system (Conti et al. 2004, Christiansen et al. 2007, Madsen et al. 2009). As the biological test system applied in this study is based on GATs originating from mice, for the sake of consistency the corresponding nomenclature mGAT1-mGAT4 will be used throughout this paper.

Although they are structurally closely related, mGAT1-mGAT4 are expressed very differently. The predominating transporter subtype in the CNS is mGAT1, which is primarily located on the plasma membrane of presynaptic GABAergic neurons (Borden 1996, Palacín et al. 1998, Conti et al. 2004). mGAT4 represents the second most abundant GABA transporter in the brain, albeit with distinctly lower concentration than mGAT1, where it is responsible for the transport of GABA into glia cells which are neighboring the GABAergic neurons (Minelli et al. 1996, Palacín et al. 1998, Christiansen et al. 2007, Jin et al. 2011). In contrast mGAT2 and mGAT3 are only weakly expressed in the brain and occur mainly in kidney and liver. As the level of mGAT2 and mGAT3 in the brain is too low for having a reasonable effect on the termination of GABAergic neurotransmission, mGAT1 and mGAT4 are the most promising targets amongst these proteins to be addressed for the treatment of above mentioned diseases (Palacín et al. 1998, Zhou, Holmseth, Guo, et al. 2012, Zhou, Holmseth, Hua, et al. 2012).

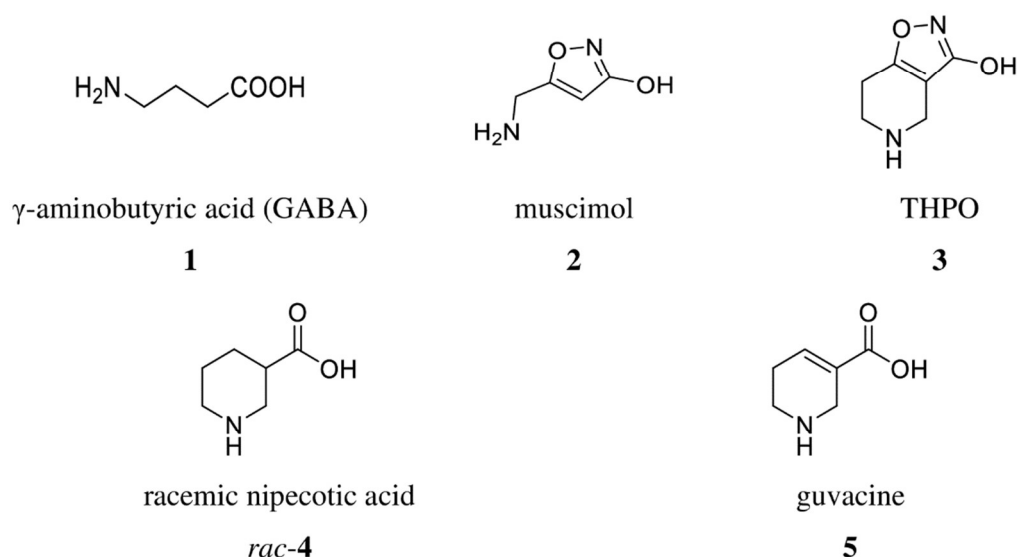
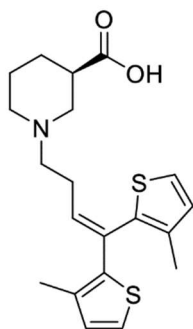


Figure 1: Structures of GABA and some low molecular weight GAT inhibitors.

Muscimol (**2**) and THPO (**3**) which are structurally related to GABA, the natural substrate of GATs, were identified to be weak inhibitors at GATs. Structural alterations of the isoxazolone function of THPO (**3**) led to racemic nipecotic acid (*rac*-**4**) and guvacine (**5**) as the first reasonably potent inhibitors of the GABA transporters. However, because of their zwitterionic character at physiological pH and their high polarity these compounds are not able to pass the blood brain barrier (BBB). In order to increase lipophilicity and BBB permeation di- and triaryl residues were added via a linker to the amino nitrogen of the parent compounds. GAT inhibitors of this general structure have been synthesized in large numbers and broad structural diversity

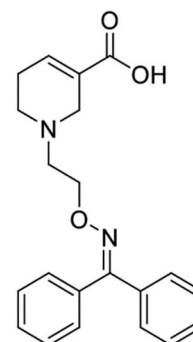
(Andersen et al. 1999, Knutsen et al. 1999, Andersen, Lau, et al. 2001, Tóth et al. 2018, Tóth et al. 2018, Schaarschmidt et al. 2019, Böck et al. 2020). This includes the most prominent GAT inhibitor Tiagabine **6**, a mGAT1 selective inhibitor, which is used in the treatment of epileptic seizures (Andersen et al. 1993, Madsen et al. 2010). The *N*-linked lipophilic aryl-alkyl side chain does not only improve the permeation of the BBB but often also mediates a substantial increase in potency and subtype selectivity of the GAT inhibitors. Modeling studies revealed the putative binding pose for mGAT1 inhibitors such as Tiagabine (**6**). According to that the amino acid subunit binds in the substrate binding pocket (S1) whereas the lipophilic residue is accommodated in a binding site (S2) equipped with aliphatic residues and located in the vestibule oriented towards the extracellular space (Skovstrup et al. 2010, Wein et al. 2016, Zafar and Jabeen 2018). NO711 (**7**) and (*S*)-SNAP-5114 (**8**) represent two further well known GAT inhibitors of which the former, **7**, like Tiagabine (**6**) is highly selective for mGAT1 and can be considered like **6** as prototype for compounds exhibiting this subtype selectivity. A major difference of (*S*)-SNAP-5114 (**8**) as compared to these compounds is to be attributed to the lipophilic domain, which by comprising a triarylmethyl unit is distinctly larger than that of **6** and **7**. It is this large steric demand of the lipophilic triaryl methyl subunit together with the (*S*)-configuration of nipecotic acid that is thought to mediate the subtype selectivity for mGAT4 of (*S*)-SNAP-5114 (**8**) (Dhar et al. 1994, Kristensen et al. 2011).

Tiagabine (**6**)

$pIC_{50} = 6.88 \pm 0.12$ (mGAT1)

$pIC_{50} = 73\%$ (mGAT4)

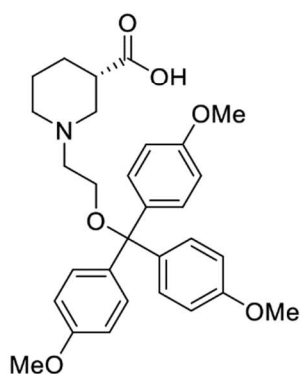
(Kragler et al. 2008)

NO711 (**7**)

$pIC_{50} = 6.83 \pm 0.06$ (mGAT1)

$pIC_{50} = 3.07 \pm 0.05$ (mGAT4)

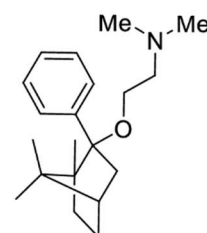
(Kragler et al. 2008)

*(S)*-SNAP-5114 (**8**)

$pIC_{50} = 4.07 \pm 0.09$ (mGAT1)

$pIC_{50} = 5.71 \pm 0.07$ (mGAT4)

(Pabel et al. 2012)

Deramciclane (*rac*-**9**)

$pIC_{50} = 4.59$ (mGAT1)^a

$pIC_{50} = 4.34$ (mGAT4)^a

(Dhar et al. 1994)

Figure 2: Structures of important GAT inhibitors. The inhibitory potencies for mGAT1 and mGAT4 are given as $pIC_{50} \pm SEM$ (if determined), that have been obtained in [³H]GABA uptake assays and reported literature. Percentage values represent the remaining [³H]GABA uptake at a concentration of 100 μM test compound. [a] The values refer to the human GAT subtypes hGAT1 and hGAT3.

Tiagabine (**6**) suffers from a series of adverse side effects and (*S*)-SNAP-5114 (**8**), though among the most potent mGAT4 inhibitors, of moderate potency (Dhar et al. 1994, Leppik

1999). Thus there is still a great need for GAT inhibitors with less adverse effects and higher potency. Structural changes to the aforementioned prototypic structures led to compounds with partially rigidized lipophilic domains at the terminal position of alkyl or heteroalkyl chains originating from the amino nitrogen of the polar subunit (Andersen, Sørensen, et al. 2001, Kerscher-Hack et al. 2016). That way aryl groups present in the lipophilic domain were forced to adopt specific spatial orientations. Another option to achieve a well-defined orientation of substituents in the lipophilic domain is to use compounds with a polycyclic cage structure as central unit. The high rigidity of cage structure allows to reduce the flexibility of attached substituents and may lower the conformational entropy penalty resulting from target binding (Zheng et al. 2014, Wipf et al. 2015). In addition, the high lipophilicity of cage derived hydrocarbon rich structures may positively affect the pharmacokinetic and pharmacodynamic properties of drugs as it can facilitate the crossing of the BBB and the binding to lipophilic domains (Joubert et al. 2012, Stockdale and Williams 2015). As a result of their inherent stability and steric bulk, polycyclic cage compounds also can slow down metabolic degradation (Brookes et al. 1992, Joubert et al. 2012, Stockdale and Williams 2015). Currently drugs with polycyclic cage structures are in use for the treatment of neurodegenerative diseases like AD and PD (Stockdale and Williams 2015). The drug Deramciclone (*rac-9*) is a rare example for a GAT inhibitor albeit with moderate inhibitory activity at all four GAT subtypes in which a polycyclic cage serving as lipophilic residue is present (Kovács et al. 1989). Since no systematic study aiming at the development of GAT inhibitors with a polycyclic cage subunit as lipophilic domain has been presented so far, though this appears to be quite rewarding, we intended to carry out such a study.

To this end, polycyclic cage structures based on a 2-azabicyclo[2.2.2]octane scaffold should be used, as they are easily available by an efficient and straightforward synthesis recently reported by us (Schmaunz et al. 2014, Rudy and Wanner 2019). For the present study the symmetric tricyclic imines **10** should be used (for general structure see Figure 3). Though these polycyclic imines **10** display the same 2-azabicyclo[2.2.2]octane skeleton, the size of the bridge between the two substituted bridgehead atoms and thus the size of the tricyclic scaffold but also the orientation of the bridgehead substituents may be varied (Rudy et al. 2020), thus allowing to study the impact of these two parameters on the inhibitory potency of the target compounds. As bridgehead substituents initially exclusively methyl and phenyl residues should be used as the synthesis of the respective symmetric tricyclic imines is known (Rudy et al. 2020). For the connection of these tricyclic cage units via their amino nitrogen, resulting from reduction of the imine function, with the amino nitrogen of racemic nipecotic acid (*rac-4*) a plain alky chain

linker of varying length should be used. That way, the influence of the linker length on the biological activity should be explored as well.

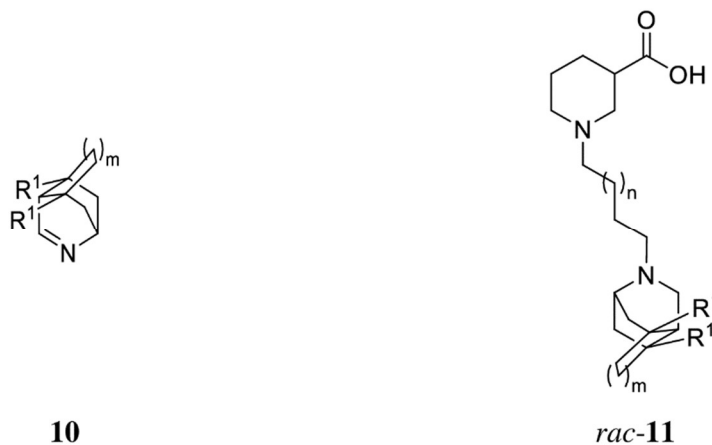


Figure 3: General structure of the polycycles **10** to be used as starting material for the construction of the desired GAT inhibitors *rac-11*.

Materials and Methods

Anhydrous reactions were performed under an argon atmosphere in vacuum-dried glassware. All solvents were distilled prior to use and dry 1,4-dioxane and CH₂Cl₂ were prepared under a nitrogen atmosphere according to standard procedures (Perrin and Armarego 1988). The CH₂Cl₂ employed as solvent in reactions was stabilized with amylene, the CH₂Cl₂ used for workups was stabilized with ethanol. All purchased chemicals were used without further purification. TLC was performed with plates from Merck KGaA (silica gel 60 F₂₅₄). For purification via flash chromatography (FC) silica gel 60 (40–63 μm mesh size) from Merck KGaA was employed. Purification by preparative RP-MPLC was performed using an Büchi instrument (C-605 binary pump system, C-630 UV detector at 254 nm and C-660 fraction collector) and a Sepacore glass column B-685 (26×230 mm) equipped with YMC Gel Triart Prep C18-S (12 nm, 5–20 μm). Melting points were determined with a BÜCHI 510 melting point apparatus and are uncorrected. Infrared spectra were recorded with a Perkin Elmer Paragon 1000 and a Jasco FT/IR-410. Solid substances were measured as KBr pellets and oils as film on NaCl. HRMS were obtained with a Finnigan MAT 95 (EI) and a Finnigan LTQ FT (ESI). ¹H and ¹³C NMR spectra were acquired with a Avance III HD Bruker BioSpin (400 or 500 MHz), referenced to the solvent residual peak as internal standard (Fulmer et al. 2010) and analyzed with MestReNova (Version 12.0.0 – 20080; Mestrelab Research S.L.; released 26.09.2017). Nonequivalent protons attached to the same carbon center were differentiated by

superscript a and b (e.g. NCH₂^a, NCH₂^b). The purity of the biologically tested compounds was determined by quantitative ¹H NMR (qH NMR) according to a method described by Pauli et al. with internal calibration (Pauli et al. 2014). The qH NMR measurements were carried out under conditions allowing complete relaxation to assure the exact determination of peak area ratios. Used internal standards were benzyl benzoate (LOT# BCBN 6347V; purity 99.43%) and 1,3,5-trimethoxy benzene (LOT# BCBW 3670; purity 99.96%) in CDCl₃, CD₂Cl₂, CD₃OD or CD₃OD + 1M NaOD in D₂O (6:1). All tested esters had a purity >95%. The tested carboxylic acids contained varying amounts of water which was not considered an impurity as the acids were dissolved in aqueous media later on to perform the assays. The amount of water was identified by qH NMR and calculated from the change of the peak area ratio of the exchangeable protons (water peak) to the solvent residual protons compared to the same peak area ratio determined for pure solvent. In due consideration of the amount of water contained, the purity of all carboxylic acids was >95% with exception of the biologically inactive acids *rac*-**18b** and *rac*-**11m**, for which no purity was determined.

General Procedures

Synthesis of Ethyl nipecotate precursors *rac*-15a-15f (general procedure/ GP1)

Potassium carbonate and sodium iodide were added to a solution of racemic ethyl nipecotate *rac*-**16** (1.0 equiv) in the solvent stated. The organic halide was added to this mixture that was stirred for the time period and at the temperature indicated in the respective experiment. The mixture was concentrated under vacuum, dissolved in ethyl acetate and washed with water. Drying of the organic phase (Na₂SO₄) and removal of the solvent under vacuum afforded the crude product which was purified by FC.

Deprotection and reductive amination of the dimethoxy protected aldehydes *rac*-15e-15f with tricyclic imines 10a-10d (general procedure/ GP2)

Part A: The tricyclic imine was dissolved in CH₂Cl₂ (15 mL/mmol) and sodium triacetoxyborohydride (2.5 equiv) and acetic acid (2.1 equiv) were added. The solution was stirred at 20 °C for 45 min.

Part B: In the meantime, the dimethoxy acetal (2.0 equiv) was dissolved in CH₂Cl₂ (16 mL/mmol), and FeCl₃ · 6 H₂O was added. The acetal/ salt suspension was rotated on a rotary evaporator at 45 °C (no vacuum) for 20 min. In doing so, the total volume was

maintained by regular solvent addition. The suspension was quenched with concentrated aqueous NaHCO_3 , extracted with CH_2Cl_2 (stabilized with amylene) for three times, dried (Na_2SO_4) and concentrated under vacuum. The remaining crude aldehyde was dissolved in CH_2Cl_2 (6.25 mL/mmol_{Acetal}), added to the imine/ triacetoxyborohydride solution and stirred for the time period and at the temperature stated in the experiment. The reaction was quenched with potassium carbonate solution (1 mol/L), extracted with CH_2Cl_2 for three times, dried (Na_2SO_4) and concentrated under vacuum to afford the crude product which was finally purified by FC (SiO_2 , EtOAc/MeOH/ NEt_3 88:10:2) and, if denoted, by RP-MPLC (DCM/MeOH 1:1).

Deprotection and reductive amination of the dimethoxy protected aldehydes *rac*-15e-15f with tricyclic imines 10e-10f (general procedure/ GP3)

Part A: The tricyclic imine was dissolved in MeOH (13.3 mL/mmol) and sodium cyanoborohydride (5 equiv) and hydrochloric acid (1 mol/L in Et_2O , 10 equiv) were added. The solution was stirred at 20 °C for 3 h. The reaction was quenched with water, adjusted to pH = 11 with K_2CO_3 and the crude amine was extracted with CH_2Cl_2 for three times. After drying (Na_2SO_4) and removal of the solvent under vacuum the crude amine was dissolved in CH_2Cl_2 (15 mL/mmol) again and sodium triacetoxyborohydride (2.5 equiv) and acetic acid (2.1 equiv) were added.

Part B: Identical with **Part B** from GP2.

Hydrolysis of the *N*-substituted nipecotic acid ethyl esters (general procedure/ GP4)

The ester (1 equiv) was dissolved in MeOH (23 mL/ mmol) and successively H_2O (5.7 mL/ mmol) and $\text{Ba}(\text{OH})_2 \cdot 8 \text{H}_2\text{O}$ (4 equiv) were added. The mixture was stirred at 20 °C for 16 h. Then CO_2 was bubbled through the solution until all barium carbonate had precipitated and pH = 8 was reached. The suspension was diluted with MeOH (28.7 mL/ mmol) and for all experiments with ≥ 0.1 mmol nipecotic acid ethyl ester the suspension was centrifuged (20 min, 3000 g) and the clear supernatant filtered via a syringe filter (PTFE, 0.2 μm pore size). For experiments carried out with ≤ 0.1 mmol nipecotic acid ethyl ester the centrifugation step was

omitted. The solvent was removed under vacuum and the crude *N*-substituted nipecotic acid was purified by RP-MPLC (MeOH).

***rac*-1-[3-(1,7-Dimethyl-4-azatricyclo[3.3.1.0^{2,7}]nonan-4-yl)propyl]piperidine-3-carboxylic acid *rac*-11a**

According to **GP4**: Ester *rac*-**19a** (10 mg, 29 μ mol, 1.0 equiv) and Ba(OH)₂ · 8 H₂O (36 mg, 0.12 mmol, 4 equiv). The product was obtained as colorless oil (8 mg, 87%). IR (film) $\tilde{\nu}$ = 3398, 2937, 2858, 2800, 1587, 1450, 1398, 1375, 1217, 1151, 1126, 1099 cm⁻¹; ¹H NMR (500 MHz, CD₃OD): δ = 3.52 (s, 1 H, CHN), 3.25 (dd, *J* = 13.3/ 2.3 Hz, 1 H, CHNCH₂^aCH), 3.21–3.11 (m, 3 H, CHNCH₂CH₂, CHNCH₂^bCH), 3.11–3.01 (m, 1 H, OCCHCH₂^aN), 2.91–2.83 (m, 1 H, CHCH₂CH₂CH₂^a), 2.70–2.59 (m, 2 H, CHN(CH₂)₂CH₂), 2.45–2.33 (m, 2 H, OCCHCH₂^bN, OCCH), 2.33–2.21 (m, 1 H, CHCH₂CH₂CH₂^b), 1.97–1.74 (m, 8 H, CHNCH₂CH₂, NCH(CH₂)₂, CHCH₂^aCH₂, CHCH₂CH₂^a), 1.71–1.64 (m, 2 H, CCH₂^aC, CHNCH₂CH), 1.64–1.52 (m, 2 H, CHCH₂^bCH₂, CHCH₂CH₂^b), 1.50 (d, *J* = 9.1 Hz, 1 H, CCH₂^bC), 1.10 (s, 3 H, CH₃), 1.09 (s, 3 H, CH₃) ppm; ¹³C NMR (125 MHz, CD₃OD) δ = 181.6 (CO), 58.3 (CHN(CH₂)₂CH₂), 58.0 (OCCHCH₂N), 57.4 (CHNCH₂CH₂), 56.0 (NCH), 55.4 (CHCH₂CH₂CH₂), 50.7 (CCH₂C), 47.9 (CHNCH₂CH), 45.8 (OCCH), 43.7 (CHNCH₂CH), 37.5 (NCHCH₂), 37.2 (NCHCH₂), 36.5 (CCH₃), 36.3 (CCH₃), 28.6 (CHCH₂CH₂), 25.7 (CHCH₂CH₂), 24.9 (CH₃), 24.9 (CH₃), 22.0 (CHNCH₂CH₂) ppm; HRESIMS *m/z* (pos): 321.2534 C₁₉H₃₃N₂O₂ (calcd. 321.2537).

***rac*-1-[3-(1,7-Diphenyl-4-azatricyclo[3.3.1.0^{2,7}]nonan-4-yl)propyl]piperidine-3-carboxylic acid *rac*-11b**

According to **GP4**: Ester *rac*-**19b** (14 mg, 30 μ mol, 1.0 equiv) and Ba(OH)₂ · 8 H₂O (37 mg, 0.12 mmol, 4 equiv). The product was obtained as colorless viscous oil (12 mg, 91%). IR (film) $\tilde{\nu}$ = 3456, 3057, 3024, 2927, 2854, 2804, 1574, 1495, 1446, 1402, 1333, 1155, 1030, 758, 698 cm⁻¹; ¹H NMR (500 MHz, CD₃OD): δ = 7.37–7.29 (m, 4 H, CCHCH), 7.29–7.24 (m, 4 H, CCHCH), 7.18 (t, *J* = 7.1 Hz, 2 H, CCHCHCH), 3.29 (d, *J* = 2.3 Hz, 2 H, CHNCH₂CH), 3.24 (br s, 1 H, CHN), 3.17 (d, *J* = 10.4 Hz, 1 H, NCH₂^aCHCO), 2.98 (d, *J* = 11.5 Hz, 1 H, CHCH₂CH₂CH₂^a), 2.85–2.70 (m, 2 H, CHNCH₂CH₂), 2.70–2.54 (m, 3 H, CHNCH₂CH, CHN(CH₂)₂CH₂), 2.45 (tt, *J* = 10.3/ 3.5 Hz, 1 H, CHCO), 2.42–2.28 (m, 4 H, CCH₂^aC, NCH(CH₂^a)₂, NCH₂^bCHCO), 2.28–2.11 (m, 4 H, CCH₂^bC, NCH(CH₂^b)₂, CHCH₂CH₂CH₂^b), 2.01–1.90 (m, 1 H, CHCH₂^aCH₂), 1.85 (p, *J* = 7.4 Hz, 2 H, CHNCH₂CH₂), 1.76 (dp, *J* = 13.7/

3.7 Hz, 1 H, CHCH₂CH₂^a), 1.67–1.54 (m, 1 H, CHCH₂CH₂^b), 1.54–1.41 (m, 1 H, CHCH₂^bCH₂) ppm; ¹³C NMR (125 MHz, CD₃OD) δ = 181.8 (CO), 149.5 (CCHCH), 129.6 (CCHCH), 127.1 (CCHCHCH), 125.9 (CCHCH), 58.0 (CHN(CH₂)₂CH₂), 57.9 (OCCHCH₂N), 56.3 (CHNCH₂CH₂), 54.9 (CHCH₂CH₂CH₂), 54.6 (NCH), 50.3 (CHNCH₂CH), 50.0 (CCH₂C), 45.5 (OCCH), 43.9 (CHNCH₂CH), 43.1 (CCH₂C), 40.4 (NCHCH₂), 40.3 (NCHCH₂), 28.8 (CHCH₂CH₂), 25.3 (CHCH₂CH₂), 24.8 (CHNCH₂CH₂) ppm; HRESIMS *m/z* (pos): 445.2852 C₂₉H₃₇N₂O₂ (calcd. 445.2850).

***rac*-1-[3-(3,6-Dimethyl-9-azatricyclo[4.3.1.0^{3,7}]decan-9-yl)propyl]piperidine-3-carboxylic acid *rac*-11c**

According to **GP4**: Ester *rac*-**19c** (20 mg, 55 μ mol, 1.0 equiv) and Ba(OH)₂ · 8 H₂O (70 mg, 0.22 mmol, 4 equiv). The product was obtained as yellow oil (13 mg, 70%). IR (film) $\tilde{\nu}$ = 3398, 2943, 2864, 2806, 1574, 1471, 1452, 1396, 1184, 1155, 1095, 951 cm⁻¹; ¹H NMR (500 MHz, CD₃OD): δ = 3.23–3.05 (m, 4 H, NCH, CHNCH₂CH, OCCHCH₂^aN) 2.98 (t, *J* = 7.2 Hz, 2 H, CHNCH₂CH₂), 2.90 (d, *J* = 11.3 Hz, 1 H, CHCH₂CH₂CH₂^a), 2.66–2.50 (m, 2 H, CHN(CH₂)₂CH₂), 2.41 (t, *J* = 10.4/ 3.7 Hz, 1 H, OCCH), 2.27 (t, *J* = 9.7 Hz, 1 H, OCCHCH₂^bN), 2.23–2.13 (m, 1 H, CHCH₂CH₂CH₂^b), 2.00–1.88 (m, 3 H, NCH(CH₂^a)₂, CHCH₂^aCH₂), 1.86 (p, *J* = 7.2 Hz, 2 H, CHNCH₂CH₂), 1.80–1.73 (m, 1 H, CHCH₂CH₂^a), 1.72–1.44 (m, 8 H, NCH(CH₂^b)₂, CHCH₂^bCH₂, CHCH₂CH₂^b, CCH₂CH₂C), 1.18 (d, *J* = 1.8 Hz, 6 H, CH₃), 1.14 (s, 1 H, CHNCH₂CH) ppm; ¹³C NMR (125 MHz, CD₃OD) δ = 181.9 (CO), 57.9 (CHN(CH₂)₂CH₂), 57.9 (OCCHCH₂N), 55.9 (CHNCH₂CH₂), 55.2 (CHCH₂CH₂CH₂), 53.9 (NCH), 48.8 (CHNCH₂CH), 46.3 (CHNCH₂CH), 45.9 (OCCH), 41.1 (CCH₂CH₂C), 40.5 (NCHC^bH₂), 40.4 (NCHC^aH₂), 39.8 (CCH₃), 28.9 (CHCH₂CH₂), 26.2 (CH₃), 25.7 (CHCH₂CH₂), 22.8 (CHNCH₂CH₂) ppm; HRESIMS *m/z* (pos): 335.2694 C₂₀H₃₅N₂O₂ (calcd. 335.2693).

***rac*-1-[3-(3,6-Diphenyl-9-azatricyclo[4.3.1.0^{3,7}]decan-9-yl)propyl]piperidine-3-carboxylic acid *rac*-11d**

According to **GP4**: Ester *rac*-**19d** (19 mg, 39 μ mol, 1.0 equiv) and Ba(OH)₂ · 8 H₂O (49 mg, 0.16 mmol, 4 equiv). The product was obtained as colorless oil (15 mg, 84%). IR (film) $\tilde{\nu}$ = 3452, 3055, 2945, 2868, 2810, 1579, 1495, 1444, 1396, 1153, 1105, 1030, 760, 700 cm⁻¹; ¹H NMR (500 MHz, CD₃OD): δ = 7.50–7.44 (m, 4 H, CCHCH), 7.42–7.36 (m, 4 H, CCHCH), 7.25–7.20 (m, 2 H, CCHCHCH), 3.24 (s, 1 H, NCH), 3.14–3.02 (m, 3 H, CHNCH₂CH, OCCHCH₂^aN), 2.95 (s, 1 H, CHNCH₂CH), 2.93–2.86 (m, 1 H, CHCH₂CH₂CH₂^a), 2.80–2.65

(m, 4 H, $\text{CHNCH}_2\text{CH}_2$, $\text{CHN}(\text{CH}_2)_2\text{CH}_2$), 2.59 (dd, $J = 14.4/2.4$ Hz, 2 H, $\text{NCH}(\text{CH}_2^a)_2$), 2.47 (br s, 1 H, $\text{OCCHCH}_2^b\text{N}$), 2.29 (br s, 1 H, $\text{CHCH}_2\text{CH}_2\text{CH}_2^b$), 2.24–2.09 (m, 3 H, $\text{NCH}(\text{CH}_2^b)_2$, OCCH), 2.05–1.86 (m, 4 H, $\text{CCH}_2\text{CH}_2\text{C}$), 1.72 (p, $J = 6.5$ Hz, 2 H, $\text{CHNCH}_2\text{CH}_2$), 1.70–1.65 (m, 1 H, $\text{CHCH}_2^a\text{CH}_2$), 1.57–1.47 (m, 1 H, $\text{CHCH}_2\text{CH}_2^a$), 1.47–1.36 (m, 1 H, $\text{CHCH}_2^b\text{CH}_2$), 1.13–0.98 (m, 1 H, $\text{CHCH}_2\text{CH}_2^b$) ppm; ^{13}C NMR (125 MHz, CD_3OD) $\delta = 180.4$ (CO), 149.3 (CCHCH), 129.9 (CCHC^aH), 129.8 (CCHC^bH), 127.2 (CCHCHCH), 126.8 (CC^aHCH), 126.8 (CC^bHCH), 58.5 ($\text{CHN}(\text{CH}_2)_2\text{CH}_2$), 57.5 (OCCHCH_2N), 56.5 ($\text{CHNCH}_2\text{CH}_2$), 54.5 ($\text{CHCH}_2\text{CH}_2\text{CH}_2$), 53.6 (NCH), 47.5 (CHNCH_2CH), 47.3 (C^aCH₂), 47.3 (C^bCH₂), 44.4 (CCH₂CH₂C), 44.3 (OCCH), 42.3 (CHNCH_2CH), 42.0 (NCHC^bH₂), 41.7 (NCHC^aH₂), 27.7 ($\text{CH}_2\text{CH}_2\text{CH}$), 24.1 (CHCH_2CH_2), 21.9 ($\text{CHNCH}_2\text{CH}_2$) ppm; HRESIMS m/z (pos): 459.3002 $\text{C}_{30}\text{H}_{39}\text{N}_2\text{O}_2$ (calcd. 459.3006).

***rac*-1-[3-(3,7-Dimethyl-10-azatricyclo[5.3.1.0^{3,8}]undecan-10-yl)propyl]piperidine-3-carboxylic acid *rac*-11e**

According to **GP4**: Ester *rac*-**19e** (20 mg, 53 μmol , 1.0 equiv) and $\text{Ba}(\text{OH})_2 \cdot 8 \text{H}_2\text{O}$ (67 mg, 0.21 mmol, 4 equiv). The product was obtained as yellow oil (15 mg, 81%). IR (film) $\tilde{\nu} = 3419$, 2922, 1709, 1574, 1452, 1400, 1223, 1157, 1095, 953 cm^{-1} ; ^1H NMR (500 MHz, CD_3OD): $\delta = 3.31$ – 3.29 (m, 2 H, CHNCH_2CH), 3.27 (s, 1 H, CHN), 3.11 (d, $J = 10.9$ Hz, 1 H, $\text{OCCHCH}_2^a\text{N}$), 3.04 (t, $J = 7.3$ Hz, 2 H, $\text{CHNCH}_2\text{CH}_2$), 2.90 (d, $J = 11.4$ Hz, 1 H, $\text{CHCH}_2\text{CH}_2\text{CH}_2^a$), 2.63– 2.50 (m, 2 H, $\text{CHN}(\text{CH}_2)_2\text{CH}_2$), 2.41 (tt, $J = 10.6/3.7$ Hz, 1 H, OCCH), 2.24 (t, $J = 10.4$ Hz, 1 H, $\text{OCCHCH}_2^b\text{N}$), 2.17 (t, $J = 10.4$ Hz, 1 H, $\text{CHCH}_2\text{CH}_2\text{CH}_2^b$), 2.00– 1.91 (m, 1 H, $\text{CHCH}_2^a\text{CH}_2$), 1.88 (p, $J = 7.3$ Hz, 2 H, $\text{CHNCH}_2\text{CH}_2$), 1.81– 1.69 (m, 3 H, $\text{NCH}(\text{CH}_2^a)_2$, $\text{CHCH}_2\text{CH}_2^a$), 1.67– 1.43 (m, 6 H, $\text{NCH}(\text{CH}_2^b)_2$, CCH_2CH_2 , $\text{CHCH}_2^b\text{CH}_2$, $\text{CHCH}_2\text{CH}_2^b$), 1.43– 1.35 (m, 2 H, $\text{CCH}_2^a\text{CH}_2\text{CH}_2^a\text{C}$), 1.21 (ddd, $J = 13.4/13.4/4.6$ Hz, 2 H, $\text{CCH}_2^b\text{CH}_2\text{CH}_2^b\text{C}$), 1.13 (s, 6 H, CH_3), 0.97 (s, 1 H, CHNCH_2CH) ppm; ^{13}C NMR (125 MHz, CD_3OD) $\delta = 182.0$ (CO), 57.8 (OCCHCH_2N), 57.7 ($\text{CHN}(\text{CH}_2)_2\text{CH}_2$), 55.7 ($\text{CHNCH}_2\text{CH}_2$), 55.3 ($\text{CHCH}_2\text{CH}_2\text{CH}_2$), 54.9 (NCH), 48.1 (CHNCH_2CH), 45.8 (OCCH), 45.4 (CHNCH_2CH), 41.0 (CCH₂CH₂CH₂C), 34.8 ($\text{NCH}(\text{CH}_2)_2$), 31.2 (CCH₃), 30.4 (CH₃), 29.0 (CHCH_2CH_2), 25.7 (CHCH_2CH_2), 23.1 ($\text{CHNCH}_2\text{CH}_2$), 19.7 (CCH₂CH₂) ppm; HRESIMS m/z (pos): 349.2851 $\text{C}_{21}\text{H}_{37}\text{N}_2\text{O}_2$ (calcd. 349.2850).

***rac*-1-[3-(3,7-Diphenyl-10-azatricyclo[5.3.1.0^{3,8}]undecan-10-yl)propyl]piperidine-3-carboxylic acid *rac*-11f**

According to **GP4**: Ester *rac*-**19f** (13 mg, 26 μ mol, 1.0 equiv) and Ba(OH)₂ · 8 H₂O (33 mg, 0.10 mmol, 4 equiv). The product was obtained as colorless oil (9 mg, 73%). IR (film) $\tilde{\nu}$ = 3398, 2926, 2848, 2360, 2341, 1578, 1497, 1444, 1396, 1155, 1082, 1032, 758, 700 cm⁻¹; ¹H NMR (500 MHz, CD₃OD): δ = 7.60–7.51 (m, 4 H, CCHCH), 7.45–7.37 (m, 4 H, CCHCH), 7.27–7.20 (m, 2 H, CCHCHCH), 3.43 (s, 1 H, NCH), 3.12–2.90 (m, 4 H, CHCH₂NCH, CHNCH₂CH, OCCHCH₂^aN), 2.80 (d, J = 11.6 Hz, 1 H, CHCH₂CH₂CH₂^a), 2.76–2.50 (m, 6 H, CHN(CH₂)₂CH₂, CHNCH₂CH₂, NCH(CH₂^a)₂), 2.32–2.12 (m, 3 H, NCH(CH₂^b)₂, OCCHCH₂^bN), 2.06–1.84 (m, 3 H, CCH₂CH₂^a, CHCH₂CH₂CH₂^b, OCCH), 1.71–1.42 (m, 8 H, CCH₂CH₂CH₂C, CCH₂CH₂^b, CHCH₂^aCH₂, CHNCH₂CH₂), 1.37–1.26 (m, 2 H, CHCH₂^bCH₂, CHCH₂CH₂^a), 0.74–0.53 (m, 1 H, CHCH₂CH₂^b) ppm; ¹³C NMR (125 MHz, CD₃OD) δ = 180.7 (CO), 151.1 (CH₂CC^a), 150.9 (CH₂CC^b), 130.0 (CCHC^aH), 129.9 (CCHC^bH), 127.3(CCHCHCH), 127.2 (CC^aHCH), 127.2 (CC^bHCH), 59.1 (CHN(CH₂)₂CH₂), 58.4 (CHNCH₂CH₂), 58.1 (OCCHCH₂N), 54.6 (NCH), 54.3 (CHCH₂CH₂CH₂), 50.0 (CHNCH₂CH), 45.0 (CC^aH₂CH₂), 45.0 (CC^bH₂CH₂), 44.9 (OCCH), 40.1 (C^aCH₂), 40.1 (C^bCH₂), 36.9 (CHNCH₂CH), 35.9 (NCHC^aH₂), 34.5 (NCHC^bH₂), 28.0 (CH₂CH₂CH), 24.3 (CHCH₂CH₂), 21.2 (CHNCH₂CH₂), 21.0 (CCH₂CH₂) ppm; HRESIMS m/z (pos): 473.3157 C₃₁H₄₁N₂O₂ (calcd. 473.3163).

***rac*-1-[4-(1,7-Dimethyl-4-azatricyclo[3.3.1.0^{2,7}]nonan-4-yl)butyl]piperidine-3-carboxylic acid *rac*-11g**

According to **GP4**: Ester *rac*-**19g** (28 mg, 77 μ mol, 1.0 equiv) and Ba(OH)₂ · 8 H₂O (97 mg, 0.31 mmol, 4 equiv). The product was obtained as yellow oil (20 mg, 77%). IR (film) $\tilde{\nu}$ = 3408, 2927, 2860, 2800, 1589, 1454, 1379, 1155, 1095, 1025, 939, 731 cm⁻¹; ¹H NMR (500 MHz, CD₃OD): δ = 3.19–3.09 (m, 1 H, OCCHCH₂^aN), 2.96–2.83 (m, 2 H, CHCH₂CH₂CH₂^a, CHN), 2.73 (d, J = 2.4 Hz, 2 H, CHNCH₂CH), 2.63–2.47 (m, 2 H, CHNCH₂CH₂), 2.46–2.29 (m, 3 H, CHN(CH₂)₃CH₂, OCCH), 2.09–1.96 (m, 2 H, CHCH₂^aCH₂, OCCHCH₂^bN), 1.92 (ddd, J = 11.8/11.8/2.5 Hz, 1 H, CHCH₂CH₂CH₂^b), 1.83 (d, J = 13.3 Hz, 2 H, NCH(CH₂^a)₂), 1.75–1.67 (m, 1 H, CHCH₂CH₂^a), 1.67–1.44 (m, 8 H, CHCH₂CH₂^b, NCH₂CH₂CH₂CH₂N, CCH₂^aC, NCH(CH₂^b)₂), 1.41 (s, 1 H, CHNCH₂CH), 1.40–1.31 (m, 2 H, CCH₂^bC, CHCH₂^bCH₂), 1.01 (s, 6 H, CH₃) ppm; ¹³C NMR (125 MHz, CD₂Cl₂) δ = 182.6 (CO), 60.1 (CHN(CH₂)₃CH₂), 58.2 (OCCHCH₂N), 57.8 (CHNCH₂CH₂), 55.0 (CHCH₂CH₂CH₂), 53.8 (NCH), 51.8 (CCH₂C), 48.1 (CHNCH₂CH), 46.3 (OCCH), 45.8 (CHNCH₂CH), 39.1 (NCH(CH₂)₂), 36.6 (CCH₃), 29.5 (CHCH₂CH₂), 26.9 (CHNCH₂CH₂CH₂), 26.0 (CHCH₂CH₂), 25.5 (CHNCH₂CH₂, CH₃) ppm; HRESIMS m/z (pos): 335.2695 C₂₀H₃₅N₂O₂ (calcd. 335.2693).

***rac*-1-[4-(1,7-Diphenyl-4-azatricyclo[3.3.1.0^{2,7}]nonan-4-yl)butyl]piperidine-3-carboxylic acid *rac*-11h**

According to **GP4**: Ester *rac*-**19h** (14 mg, 29 μ mol, 1.0 equiv) and Ba(OH)₂ · 8 H₂O (36 mg, 0.12 mmol, 4 equiv). The product was obtained as colorless viscous oil (13 mg, 98%). IR (KBr) $\tilde{\nu}$ = 3419, 3057, 3024, 2933, 2858, 2800, 1601, 1495, 1446, 1387, 1155, 1030, 760, 700, 536 cm⁻¹; ¹H NMR (500 MHz, CD₃OD): δ = 7.36–7.31 (m, 4 H, CCHCH), 7.31–7.25 (m, 4 H, CCHCH), 7.23–7.17 (m, 2 H, CCHCHCH), 3.45 (br s, 1 H, CHN), 3.42 (d, *J* = 2.2 Hz, 2 H, CHNCH₂CH), 3.11 (d, *J* = 10.5 Hz, 1 H, NCH₂^aCHCO), 3.08–2.78 (m, 7 H, NCH₂CH₂CH₂CH₂N, CHCH₂CH₂CH₂, NCH₂^bCHCO), 2.75 (s, 1 H, CHNCH₂CH), 2.60–2.52 (m, 1 H, CHCO), 2.44–2.33 (m, 3 H, CCH₂^aC, NCH(CH₂^a)₂), 2.29 (dd, *J* = 14.0/ 3.2 Hz, 2 H, NCH(CH₂^b)₂), 2.23 (d, *J* = 8.9 Hz, 1 H, CCH₂^bC), 1.93–1.81 (m, 2 H, CHCH₂CH₂^a, CHCH₂^aCH₂), 1.81–1.64 (m, 6 H, CHCH₂^bCH₂, CHCH₂CH₂^b, NCH₂CH₂CH₂CH₂N) ppm; ¹³C NMR (125 MHz, CD₃OD) δ = 180.4 (CO), 148.8 (CCHCH), 129.7 (CCHCH), 127.4 (CCHCHCH), 125.9 (CCHCH), 58.2 (CHN(CH₂)₃CH₂), 57.0 (CHNCH₂CH₂), 56.2 (OCCHCH₂N), 55.0 (NCH), 54.8 (CHCH₂CH₂CH₂), 50.3 (CHNCH₂CH), 50.0 (CCH₂C), 43.2 (OCCH), 43.0 (CHNCH₂CH), 42.9 (CCH₂C), 39.5 (NCH(CH₂)₂), 27.4 (CHCH₂CH₂), 25.1 (CHNCH₂CH₂CH₂)*, 23.5 (CHNCH₂CH₂)*, 23.5 (CHCH₂CH₂) ppm; Signals indicated by * cannot be assigned unambiguously and are interchangeable. HRESIMS *m/z* (pos): 459.3008 C₃₀H₃₉N₂O₂ (calcd. 459.3006).

***rac*-1-[4-(3,6-Dimethyl-9-azatricyclo[4.3.1.0^{3,7}]decan-9-yl)butyl]piperidine-3-carboxylic acid *rac*-11j**

According to **GP4**: Ester *rac*-**19j** (20 mg, 53 μ mol, 1.0 equiv) and Ba(OH)₂ · 8 H₂O (67 mg, 0.21 mmol, 4 equiv). The product was obtained as yellow oil (18 mg, 97%). IR (film) $\tilde{\nu}$ = 3398, 2943, 2866, 2800, 1579, 1471, 1450, 1396, 1180, 1155, 1093 cm⁻¹; ¹H NMR (400 MHz, CD₂Cl₂): δ = 10.77 (br s, 1 H, COOH), 3.06–2.87 (m, 4 H, NCH, CHNCH₂CH, OCCHCH₂^aN), 2.78–2.63 (m, 3 H, CHNCH₂CH₂, CHCH₂CH₂CH₂^a), 2.47–2.31 (m, 3 H, CHN(CH₂)₃CH₂, OCCH), 2.26–2.07 (m, 2 H, CHCH₂CH₂CH₂^b, OCCHCH₂^bN), 1.97–1.81 (m, 3 H, NCH(CH₂^a)₂, CHCH₂^aCH₂), 1.75–1.65 (m, 1 H, CHCH₂CH₂^a), 1.65–1.39 (m, 10 H, CHCH₂^bCH₂, CHCH₂CH₂^b, NCH₂CH₂CH₂CH₂N, CCH₂CH₂C), 1.34 (dd, *J* = 13.9/ 1.9 Hz, 2 H, NCH(CH₂^b)₂), 1.13 (s, 6 H, CH₃), 1.00 (s, 1 H, CHNCH₂CH) ppm; ¹³C NMR (100 MHz, CD₂Cl₂) δ = 178.8 (CO), 58.3 (CHN(CH₂)₃CH₂), 56.7 (CHNCH₂CH₂), 54.9 (OCCHCH₂N), 54.3 (CHCH₂CH₂CH₂), 51.4 (NCH), 48.5 (CHNCH₂CH), 44.7 (CHNCH₂CH), 43.4 (OCCH),

40.6 (CCH₂CH₂C), 40.0 (NCH(CH₂)₂), 39.2 (CCH₃), 28.1 (CHCH₂CH₂), 26.1 (CH₃), 24.8 (CHCH₂CH₂), 24.2 (CHNCH₂CH₂), 24.0 (CHN(CH₂)₂CH₂) ppm; HRESIMS *m/z* (pos): 349.2850 C₂₁H₃₇N₂O₂ (calcd. 349.2850).

***rac*-1-[4-(3,6-Diphenyl-9-azatricyclo[4.3.1.0^{3,7}]decan-9-yl)butyl]piperidine-3-carboxylic acid *rac*-11k**

According to **GP4**: Ester *rac*-**19k** (13 mg, 26 μmol, 1.0 equiv) and Ba(OH)₂ · 8 H₂O (33 mg, 0.10 mmol, 4 equiv). The product was obtained as colorless viscous oil (8 mg, 65%). IR (film) $\tilde{\nu}$ = 3398, 3054, 2943, 2866, 2802, 1651, 1587, 1495, 1444, 1394, 1153, 1105, 1032, 760, 702 cm⁻¹; ¹H NMR (500 MHz, CD₃OD): δ = 7.49–7.43 (m, 4 H, CCHCH), 7.39–7.33 (m, 4 H, CCHCH), 7.23–7.17 (m, 2 H, CCHCHCH), 3.02 (d, *J* = 9.1 Hz, 1 H, OCCHCH₂^aN), 2.98 (s, 1 H, NCH), 2.96–2.88 (m, 2 H, CHNCH₂CH), 2.85–2.77 (m, 2 H, CHCH₂CH₂CH₂^a, CHNCH₂CH), 2.56 (dt, *J* = 13.9/ 2.6 Hz, 2 H, NCH(CH₂^a)₂), 2.53–2.44 (m, 2 H, CHN(CH₂)₃CH₂), 2.44–2.30 (m, 4 H, OCCHCH₂^bN, OCCH, CHNCH₂CH₂), 2.25–2.16 (m, 1 H, CHCH₂CH₂CH₂^b), 2.08 (dt, *J* = 13.9/ 2.6 Hz, 2 H, NCH(CH₂^b)₂), 2.01–1.84 (m, 5 H, CHCH₂^aCH₂, CCH₂CH₂C), 1.73–1.65 (m, 1 H, CHCH₂CH₂^a), 1.58–1.38 (m, 6 H, CHCH₂^bCH₂, NCH₂CH₂CH₂CH₂N, CHCH₂CH₂^b) ppm; ¹³C NMR (125 MHz, CD₃OD) δ = 181.5 (CO), 150.1 (CCHCH), 129.6 (CCHCH), 126.8 (CCHCH), 126.8 (CCHCHCH), 59.0 (CHN(CH₂)₃CH₂), 57.1 (OCCHCH₂N), 56.3 (CHNCH₂CH₂), 54.8 (CHCH₂CH₂CH₂), 52.4 (NCH), 47.6 (C^aCH₂), 47.5 (C^bCH₂), 47.4 (CHNCH₂CH), 44.8 (OCCH), 44.3 (CCH₂CH₂C), 43.0 (CHNCH₂CH), 42.3 (NCHC^aH₂), 42.2 (NCHC^bH₂), 28.5 (CH₂CH₂CH), 25.6 (CHNCH₂CH₂), 24.7 (CHNCH₂CH₂CH₂), 24.5 (CHCH₂CH₂) ppm; HRESIMS *m/z* (pos): 473.3164 C₃₁H₄₁N₂O₂ (calcd. 473.3163).

***rac*-1-[4-(3,7-Dimethyl-10-azatricyclo[5.3.1.0^{3,8}]undecan-10-yl)butyl]piperidine-3-carboxylic acid *rac*-11l**

According to **GP4**: Ester *rac*-**19l** (17 mg, 44 μmol, 1.0 equiv) and Ba(OH)₂ · 8 H₂O (55 mg, 0.17 mmol, 4 equiv). The product was obtained as colorless viscous oil (15 mg, 96%). IR (film) $\tilde{\nu}$ = 3398, 2924, 2800, 1583, 1454, 1390, 1157, 1097, 1026, 953, 770 cm⁻¹; ¹H NMR (400 MHz, CD₂Cl₂): δ = 9.02 (br s, 1 H, COOH), 3.26–3.08 (m, 3 H, CHN, CHNCH₂CH), 2.97 (d, *J* = 10.2 Hz, 1 H, OCCHCH₂^aN), 2.89–2.76 (m, 2 H, CHNCH₂CH₂), 2.76–2.64 (m, 1 H, CHCH₂CH₂CH₂^a), 2.48–2.31 (m, 3 H, OCCH, CHN(CH₂)₃CH₂), 2.27–2.03 (m, 2 H, CHCH₂CH₂CH₂^b, OCCHCH₂^bN), 1.94–1.83 (m, 1 H, CHCH₂^aCH₂), 1.75 (dd, *J* = 13.9/ 2.7 Hz, 2 H, NCH(CH₂^a)₂), 1.72–1.31 (m, 13 H, NCH(CH₂^b)₂, CCH₂^aCH₂CH₂^aC, CHCH₂^bCH₂,

CHCH₂CH₂, NCH₂CH₂CH₂CH₂N, CCH₂CH₂), 1.14 (ddd, $J = 13.1/ 13.1/ 5.5$ Hz, 2 H, CCH₂^bCH₂CH₂^bC), 1.09 (s, 6 H, CH₃), 0.84 (s, 1 H, CHNCH₂CH) ppm; ¹³C NMR (100 MHz, CD₂Cl₂) $\delta = 179.0$ (CO), 58.2 (CHN(CH₂)₃CH₂), 56.7 (OCCHCH₂N), 54.9 (CHNCH₂CH₂), 54.4 (CHCH₂CH₂CH₂), 52.4 (NCH), 46.3 (CHNCH₂CH), 44.9 (CHNCH₂CH), 43.5 (OCCH), 40.4 (CCH₂CH₂CH₂C), 34.0 (NCH(CH₂)₂), 30.6 (CCH₃), 30.1 (CH₃), 28.2 (CHCH₂CH₂), 24.9 (CHCH₂CH₂), 24.2 (CHN(CH₂)₂CH₂)*, 23.9 (CHNCH₂CH₂)*, 19.2 (CCH₂CH₂) ppm; Signals indicated by * cannot be assigned unambiguously and are interchangeable; HRESIMS m/z (pos): 363.3006 C₂₂H₃₉N₂O₂ (calcd. 363.3006).

***rac*-1-[4-(3,7-Diphenyl-10-azatricyclo[5.3.1.0^{3,8}]undecan-10-yl)butyl]piperidine-3-carboxylic acid *rac*-11m**

According to **GP4**: Ester *rac*-**19m** (12 mg, 23 μ mol, 1.0 equiv) and Ba(OH)₂ · 8 H₂O (29 mg, 92 μ mol, 4 equiv). The product was obtained as colorless oil (6 mg, 53%). IR (film) $\tilde{\nu} = 3390, 3055, 2926, 2852, 2800, 1595, 1495, 1444, 1402, 1155, 1099, 1032, 756, 700$ cm⁻¹; ¹H NMR (500 MHz, CD₃OD): $\delta = 7.54$ (d, $J = 8.3$ Hz, 4 H, CCHCH), 7.44–7.34 (m, 4 H, CCHCH), 7.21 (t, $J = 7.3$ Hz, 2 H, CCHCHCH), 3.23 (s, 1 H, NCH), 2.95 (d, $J = 8.4$ Hz, 1 H, OCCHCH₂^aN), 2.92–2.84 (m, 2 H, CHNCH₂CH), 2.82 (s, 1 H, CHCH₂NCH), 2.78–2.73 (m, 1 H, CHCH₂CH₂CH₂^a), 2.73–2.64 (m, 2 H, NCH(CH₂^a)₂), 2.52–2.28 (m, 6 H, OCCHCH₂^bN, CHN(CH₂)₃CH₂, CHNCH₂CH₂, OCCH), 2.28–2.18 (m, 1 H, CHCH₂CH₂CH₂^b), 2.14 (ddd, $J = 14.6/ 5.6/ 2.3$ Hz, 2 H, NCH(CH₂^b)₂), 1.99–1.90 (m, 1 H, CCH₂CH₂^a), 1.89–1.82 (m, 1 H, CHCH₂^aCH₂), 1.72–1.59 (m, 4 H, CHCH₂CH₂^a, CCH₂CH₂^b, CCH₂^aCH₂CH₂^aC), 1.56–1.33 (m, 8 H, CHCH₂^bCH₂, CHCH₂CH₂^b, CHNCH₂CH₂, CHN(CH₂)₂CH₂, CCH₂^bCH₂CH₂^bC) ppm; ¹³C NMR (125 MHz, CD₃OD) $\delta = 181.3$ (CO), 151.5 (CH₂CC), 129.7 (CCHCH), 127.2 (CCHCH), 127.0 (CCHCHCH), 58.4 (CHN(CH₂)₃CH₂), 56.9 (OCCHCH₂N), 56.5 (CHNCH₂CH₂), 54.7 (CHCH₂CH₂CH₂), 53.0 (NCH), 50.0 (CHNCH₂CH), 45.0 (CCH₂CH₂CH₂C), 44.5 (OCCH), 40.3 (CCH₂), 37.5 (CHNCH₂CH), 35.3 (NCHC^aH₂), 35.1 (NCHC^bH₂), 28.3 (CH₂CH₂CH), 24.9 (CHNCH₂CH₂), 24.5 (CHCH₂CH₂), 24.1 (CHN(CH₂)₂CH₂), 21.1 (CCH₂CH₂) ppm; HRESIMS m/z (pos): 487.3315 C₃₂H₄₃N₂O₂ (calcd. 487.3319).

***rac*-Ethyl 1-(3-hydroxypropyl)piperidine-3-carboxylate *rac*-15a**

Synthesis according to literature (Dhar et al. 1994).

***rac*-Ethyl 1-(4-hydroxybutyl)piperidine-3-carboxylate *rac*-15b**

According to **GPI**: Reaction under exclusion of oxygen and light with potassium carbonate (4.15 g, 30.0 mmol, 3.0 equiv), sodium iodide (19 mg, 0.13 mmol, 0.01 equiv), ethyl nipecotate *rac*-**16** (1.57 g, 10.0 mmol, 1.6 mL, 1.0 equiv) and 4-bromobutan-1-ol (2.30 g, 15.0 mmol, 1.5 equiv) (no solvent used; the mixture was cooled to 0 °C prior to the halide addition). The temperature was kept at 0 °C for 6 h, then at 20 °C for 42 h. FC (SiO₂, CH₂Cl₂/ MeOH/ NEt₃ 93:5:2). The product was obtained as colorless oil (2.18 g, 95%). IR (film): $\tilde{\nu}$ = 3390, 2939, 2868, 2810, 2775, 1732, 1470, 1446, 1371, 1311, 1182, 1151, 1032, 862 cm⁻¹; ¹H NMR (400 MHz, CDCl₃): δ = 4.11 (dq, J = 7.2/ 0.5 Hz, 2 H, CH₂CH₃), 3.59–3.50 (m, 2 H, CH₂OH), 3.08 (d, J = 11.3 Hz, 1 H, NCH₂^aCH), 2.86 (d, J = 11.3 Hz, 1 H, CHCH₂CH₂CH₂^a), 2.59 (tt, J = 11.1/ 3.9 Hz, 1 H, CHCO), 2.43–2.34 (m, 2 H, NCH₂(CH₂)₃OH), 2.13 (t, J = 11.1 Hz, 1 H, NCH₂^bCH), 2.03–1.92 (m, 2 H, NCH₂CHCH₂^a, CHCH₂CH₂CH₂^b), 1.77–1.54 (m, 6 H, CHCH₂CH₂, CH₂CH₂CH₂OH), 1.40 (dq, J = 12.0/ 4.3 Hz, 1 H, NCH₂CHCH₂^b), 1.23 (t, J = 7.2 Hz, 3 H, CH₃) ppm; ¹³C NMR (100 MHz, CDCl₃): δ = 173.9 (CO), 62.8 (CH₂OH), 60.6 (CH₂CH₃), 59.0 (CH₂(CH₂)₃OH), 55.3 (CHCH₂N), 53.7 (CHCH₂CH₂CH₂), 41.5 (CHCO), 32.7 (CH₂CH₂OH), 27.1 (CHCH₂CH₂), 25.6 (CH₂CH₂CH₂OH), 24.4 (CHCH₂CH₂), 14.3 (CH₃) ppm; HREIMS m/z [M]⁺: 229.1692 C₁₂H₂₃NO₃ (calcd. 229.1672).

***rac*-Ethyl 1-[2-(1,3-dioxolan-2-yl)ethyl]piperidine-3-carboxylate *rac*-15c**

According to **GPI**: Potassium carbonate (9.12 g, 66.0 mmol, 3.3 equiv), sodium iodide (41 mg, 0.28 mmol, 0.01 equiv), ethyl nipecotate *rac*-**16** (3.14 g, 20.0 mmol, 3.1 mL, 1.0 equiv) and 2-(2-bromoethyl)-1,3-dioxolane (3.98 g, 22.0 mmol, 2.6 mL, 1.1 equiv) (no solvent used; the mixture was cooled to 0 °C prior to the halide addition). The temperature was kept at 0 °C for 3 h, then at 20 °C for 48 h. FC (SiO₂, CH₂Cl₂/ MeOH/ NEt₃ 93:5:2). The product was obtained as yellow oil (4.79 g, 93%). IR (film) $\tilde{\nu}$ = 2943, 2885, 2773, 1730, 1470, 1373, 1309, 1180, 1140, 1032, 945, 912, 800 cm⁻¹; ¹H NMR (400 MHz, CDCl₃): δ = 4.91 (t, J = 4.9 Hz, 1 H, OCH), 4.11 (q, J = 7.1 Hz, 2 H, CH₂CH₃), 4.00–3.76 (m, 4 H, OCH₂CH₂O), 3.03–2.91 (m, 1 H,

$\text{NCH}_2^{\text{a}}\text{CH}$), 2.76 (dt, $J = 11.2/ 3.6$ Hz, 1 H, $\text{NCH}_2^{\text{a}}\text{CH}_2\text{CH}_2$), 2.59–2.45 (m, 3 H, NCH_2CH , $\text{OCHCH}_2\text{CH}_2$), 2.14 (t, $J = 10.7$ Hz, 1 H, $\text{NCH}_2^{\text{b}}\text{CH}$), 2.04–1.80 (m, 4 H, OCHCH_2 , $\text{NCH}_2^{\text{b}}\text{CH}_2\text{CH}_2$, $\text{NCH}_2\text{CHCH}_2^{\text{a}}$), 1.76–1.65 (m, 1 H, $\text{NCH}_2\text{CH}_2^{\text{a}}\text{CH}_2$), 1.61–1.49 (m, 1 H, $\text{NCH}_2\text{CH}_2^{\text{b}}\text{CH}_2$), 1.42 (dq, $J = 11.9/ 3.9$ Hz, 1 H, $\text{NCH}_2\text{CHCH}_2^{\text{b}}$), 1.24 (t, $J = 7.1$ Hz, 3 H, CH_3) ppm; ^{13}C NMR (100 MHz, CDCl_3): $\delta = 174.3$ (CO), 103.5 (OCH), 65.0 ($\text{OCH}_2\text{CH}_2\text{O}$), 60.4 (CH_2CH_3), 55.6 (NCH_2CH), 53.9 ($\text{NCH}_2\text{CH}_2\text{CH}_2$), 53.7 ($\text{OCHCH}_2\text{CH}_2$), 42.1 (NCH_2CH), 31.5 (OCHCH_2), 27.1 ($\text{NCH}_2\text{CHCH}_2$), 24.7 ($\text{NCH}_2\text{CH}_2\text{CH}_2$), 14.4 (CH_3) ppm; HREIMS m/z $[\text{M}]^+$: 257.1611 $\text{C}_{13}\text{H}_{23}\text{NO}_4$ (calcd. 257.1622).

***rac*-Ethyl 1-[3-(1,3-dioxolan-2-yl)propyl]piperidine-3-carboxylate *rac*-15d**

According to **GPI**: Potassium carbonate (4.15 g, 30.0 mmol, 3.0 equiv), sodium iodide (19 mg, 0.13 mmol, 0.01 equiv), ethyl nipecotate *rac*-**16** (1.57 g, 10.0 mmol, 1.6 mL, 1.0 equiv) and 2-(3-chloropropyl)-1,3-dioxolane (1.66 g, 11.0 mmol, 1.45 mL, 1.1 equiv) in 1,4-dioxane (10 mL). The temperature was kept at 100 °C for 82 h. FC (SiO_2 , $\text{CH}_2\text{Cl}_2/\text{MeOH}/\text{NEt}_3$ 93:5:2). The product was obtained as yellow oil (2.15 g, 79%). IR (film) $\tilde{\nu} = 2945, 2877, 2806, 2769, 1730, 1470, 1446, 1371, 1309, 1209, 1180, 1151, 1034, 943, 862, 733$ cm^{-1} ; ^1H NMR (400 MHz, CDCl_3): $\delta = 4.87$ (dt, $J = 4.4/ 0.8$ Hz, 1 H, OCH), 4.11 (dq, $J = 7.1/ 0.6$ Hz, 2 H, CH_2CH_3), 4.01–3.77 (m, 4 H, $\text{OCH}_2\text{CH}_2\text{O}$), 2.98 (d, $J = 11.0$ Hz, 1 H, $\text{NCH}_2^{\text{a}}\text{CH}$), 2.75 (d, $J = 11.2$ Hz, 1 H, $\text{NCH}_2^{\text{a}}\text{CH}_2\text{CH}_2$), 2.59–2.47 (m, 1 H, NCH_2CH), 2.44–2.31 (m, 2 H, $\text{OCHCH}_2\text{CH}_2\text{CH}_2$), 2.12 (t, $J = 10.7$ Hz, 1 H, $\text{NCH}_2^{\text{b}}\text{CH}$), 2.02–1.86 (m, 2 H, $\text{NCH}_2^{\text{b}}\text{CH}_2\text{CH}_2$, $\text{NCH}_2\text{CHCH}_2^{\text{a}}$), 1.75–1.49 (m, 6 H, $\text{NCH}_2\text{CH}_2\text{CH}_2$, OCHCH_2 , $\text{OCHCH}_2\text{CH}_2$), 1.42 (dq, $J = 11.9/ 4.1$ Hz, 1 H, $\text{NCH}_2\text{CHCH}_2^{\text{b}}$), 1.24 (dt, $J = 7.1/0.9$ Hz, 3 H, CH_3) ppm; ^{13}C NMR (100 MHz, CDCl_3): $\delta = 174.4$ (CO), 104.6 (OCH), 65.0 ($\text{OCH}_2\text{CH}_2\text{O}$), 60.4 (CH_2CH_3), 58.7 ($\text{OCHCH}_2\text{CH}_2\text{CH}_2$), 55.7 (NCH_2CH), 53.8 ($\text{NCH}_2\text{CH}_2\text{CH}_2$), 42.1 (NCH_2CH), 31.9 ($\text{OCHCH}_2\text{CH}_2$), 27.2 ($\text{NCH}_2\text{CHCH}_2$), 24.8 ($\text{NCH}_2\text{CH}_2\text{CH}_2$), 21.4 (OCHCH_2), 14.4 (CH_3) ppm; HREIMS m/z $[\text{M}]^+$: 271.1745 $\text{C}_{14}\text{H}_{25}\text{NO}_4$ (calcd. 271.1778).

***rac*-Ethyl 1-(3,3-dimethoxypropyl)piperidine-3-carboxylate *rac*-15e**

According to **GPI**: Potassium carbonate (5.12 g, 37.0 mmol, 3.0 equiv), ethyl nipecotate *rac*-**16** (1.93 g, 12.3 mmol, 1.9 mL, 1.0 equiv) and 3-bromo-1,1-dimethoxypropane (2.49 g, 13.6 mmol, 1.9 mL, 1.1 equiv) in acetone (12 mL) (no sodium iodide was used). The temperature was kept at 70 °C for 18 h. FC (SiO_2 , $\text{CH}_2\text{Cl}_2/\text{MeOH}/\text{NEt}_3$ 93:5:2). The product

was obtained as yellow oil (2.17 g, 68%). IR (film) $\tilde{\nu}$ = 2943, 2827, 2775, 1732, 1470, 1446, 1371, 1311, 1180, 1126, 1057, 964, 912, 862 cm^{-1} ; ^1H NMR (400 MHz, CDCl_3): δ = 4.43 (t, J = 5.7 Hz, 1 H, OCH), 4.12 (q, J = 7.1 Hz, 2 H, CH_2CH_3), 3.31 (s, 6 H, OCH_3), 2.96 (d, J = 11.2 Hz, 1 H, $\text{NCH}_2^{\text{a}}\text{CH}$), 2.74 (d, J = 11.0 Hz, 1 H, $\text{NCH}_2^{\text{a}}\text{CH}_2\text{CH}_2$), 2.60–2.49 (m, 1 H, NCH_2CH), 2.44–2.35 (m, 2 H, $\text{OCHCH}_2\text{CH}_2$), 2.15 (t, J = 10.6 Hz, 1 H, $\text{NCH}_2^{\text{b}}\text{CH}$), 1.99 (dd, J = 11.0/ 2.7 Hz, 1 H, $\text{NCH}_2^{\text{b}}\text{CH}_2\text{CH}_2$), 1.95–1.87 (m, 1 H, $\text{NCH}_2\text{CHCH}_2^{\text{a}}$), 1.83–1.76 (m, 2 H, OCHCH_2), 1.76–1.67 (m, 1 H, $\text{NCH}_2\text{CH}_2^{\text{a}}\text{CH}_2$), 1.62–1.49 (m, 1 H, $\text{NCH}_2\text{CH}_2^{\text{b}}\text{CH}_2$), 1.49–1.37 (m, 1 H, $\text{NCH}_2\text{CHCH}_2^{\text{b}}$), 1.24 (t, J = 7.1 Hz, 3 H, CH_2CH_3) ppm; ^{13}C NMR (100 MHz, CDCl_3): δ = 174.3 (CO), 103.5 (OCH), 60.4 (CH_2CH_3), 55.7 (NCH_2CH), 54.2 ($\text{OCHCH}_2\text{CH}_2$), 54.0 ($\text{NCH}_2\text{CH}_2\text{CH}_2$), 53.0 (OCH_3), 42.1 (NCH_2CH), 30.2 (OCHCH_2), 27.1 ($\text{NCH}_2\text{CHCH}_2$), 24.8 ($\text{NCH}_2\text{CH}_2\text{CH}_2$), 14.4 (CH_3) ppm; HRESIMS m/z (pos): 260.1856 $\text{C}_{13}\text{H}_{26}\text{NO}_4$ (calcd. 260.1856).

***rac*-Ethyl 1-(4,4-dimethoxybutyl)piperidine-3-carboxylate *rac*-15f**

According to **GPI**: Potassium carbonate (4.15 g, 30.0 mmol, 3.0 equiv), sodium iodide (450 mg, 3.00 mmol, 0.3 equiv), ethyl nipecotate *rac*-**16** (1.57 g, 10.0 mmol, 1.6 mL, 1.0 equiv) and 4-chloro-1,1-dimethoxybutane (1.68 g, 11.0 mmol, 1.6 mL, 1.1 equiv) in acetone (10 mL). The temperature was kept at 70 °C for 62 h. FC (SiO_2 , $\text{CH}_2\text{Cl}_2/\text{MeOH}/\text{NEt}_3$ 94:5:1). The product was obtained as yellow oil (2.02 g, 74%). IR (film) $\tilde{\nu}$ = 2943, 2827, 2808, 2775, 1732, 1471, 1448, 1371, 1309, 1180, 1128, 1074, 1034, 962, 862, 794, 735 cm^{-1} ; ^1H NMR (500 MHz, CDCl_3): δ = 4.36 (t, J = 5.5 Hz, 1 H, OCH), 4.11 (q, J = 7.1 Hz, 2 H, CH_2CH_3), 3.30 (s, 6 H, OCH_3), 2.97 (d, J = 10.7 Hz, 1 H, $\text{NCH}_2^{\text{a}}\text{CH}$), 2.75 (d, J = 11.1 Hz, 1 H, $\text{CCHCH}_2\text{CH}_2\text{CH}_2^{\text{a}}$), 2.53 (tt, J = 10.7/ 3.8 Hz, 1 H, NCH_2CH), 2.36–2.30 (m, 2 H, $\text{OCHCH}_2\text{CH}_2\text{CH}_2$), 2.11 (t, J = 10.7 Hz, 1 H, $\text{NCH}_2^{\text{b}}\text{CH}$), 1.99–1.88 (m, 2 H, $\text{CCHCH}_2\text{CH}_2\text{CH}_2^{\text{b}}$, $\text{NCH}_2\text{CHCH}_2^{\text{a}}$), 1.74–1.67 (m, 1 H, $\text{NCH}_2\text{CHCH}_2\text{CH}_2^{\text{a}}$), 1.62–1.48 (m, 5 H, $\text{NCH}_2\text{CHCH}_2\text{CH}_2^{\text{b}}$, OCHCH_2 , $\text{OCHCH}_2\text{CH}_2$), 1.42 (dq, J = 13.3/ 3.8 Hz, 1 H, $\text{NCH}_2\text{CHCH}_2^{\text{b}}$), 1.24 (t, J = 7.1 Hz, 3 H, CH_2CH_3) ppm; ^{13}C NMR (125 MHz, CDCl_3): δ = 174.4 (CO), 104.6 (OCH), 60.4 (CH_2CH_3), 58.7 ($\text{OCHCH}_2\text{CH}_2\text{CH}_2$), 55.6 (NCH_2CH), 53.9 ($\text{CCHCH}_2\text{CH}_2\text{CH}_2$), 52.8 (OCH_3), 42.1 (NCH_2CH), 30.6 (OCHCH_2), 27.2 ($\text{NCH}_2\text{CHCH}_2$),

24.8 (NCH₂CHCH₂CH₂), 22.1 (OCHCH₂CH₂), 14.4 (CH₃) ppm; HREIMS m/z [M]⁺: 273.1956 C₁₄H₂₇NO₄ (calcd. 273.1935).

***rac*-1-(3-Hydroxypropyl)piperidine-3-carboxylic acid *rac*-18a**

According to **GP4**: Ester *rac*-**15a** (150 mg, 0.697 mmol, 1.0 equiv) and Ba(OH)₂ · 8 H₂O (880 mg, 2.79 mmol, 4 equiv). The product was obtained as colorless viscous oil (109 mg, 84%). IR (KBr) $\tilde{\nu}$ = 3394, 2951, 2871, 1589, 1450, 1392, 1068, 935, 773 cm⁻¹; ¹H NMR (400 MHz, CD₃OD/ 1 M NaOD in D₂O 6:1): δ = 3.60 (t, J = 6.3 Hz, 2 H, CH₂OH), 3.16–3.05 (m, 1 H, NCH₂^aCH), 2.91 (d, J = 11.0 Hz, 1 H, CHCH₂CH₂CH₂^a), 2.50–2.41 (m, 2 H, NCH₂(CH₂)₂OH), 2.36 (tt, J = 11.8/ 3.7 Hz, 1 H, CHCO), 2.06–1.87 (m, 3 H, CHCH₂^aCH₂, CHCH₂CH₂CH₂^b, NCH₂^bCH), 1.83–1.65 (m, 3 H, CHCH₂CH₂^a, CH₂CH₂OH), 1.57 (tq, J = 12.9/ 3.8 Hz, 1 H, CHCH₂CH₂^b), 1.34 (dq, J = 12.7/ 4.0 Hz, 1 H, CHCH₂^bCH₂) ppm; ¹³C NMR (100 MHz, CD₃OD/ 1 M NaOD in D₂O 6:1): δ = 183.0 (CO), 61.8 (CH₂OH), 58.0 (CHCH₂N), 57.1 (CH₂(CH₂)₂OH), 54.8 (CHCH₂CH₂CH₂), 46.3 (CHCO), 29.9 (CH₂CH₂OH), 29.3 (CHCH₂CH₂), 25.8 (CHCH₂CH₂) ppm; HRESIMS m/z (pos): 188.1279 C₉H₁₈NO₃ (calcd. 188.1281).

***rac*-1-(4-Hydroxybutyl)piperidine-3-carboxylic acid *rac*-18b**

According to **GP4**: Ester *rac*-**15b** (80 mg, 0.35 mmol, 1.0 equiv) and Ba(OH)₂ · 8 H₂O (442 mg, 1.40 mmol, 4 equiv). The product was obtained as yellow viscous oil (50 mg, 71%). IR (film) $\tilde{\nu}$ = 3348, 2940, 2868, 1714, 1589, 1448, 1392, 1061, 1026, 771 cm⁻¹; ¹H NMR (400 MHz, CD₃OD/ 1 M NaOD in D₂O 6:1): δ = 3.56 (t, J = 6.0 Hz, 2 H, CH₂OH), 3.17–3.08 (m, 1 H, NCH₂^aCH), 2.91 (d, J = 11.1 Hz, 1 H, CHCH₂CH₂CH₂^a), 2.43–2.30 (m, 3 H, CHCO, NCH₂(CH₂)₃OH), 2.05–1.86 (m, 3 H, CHCH₂^aCH₂, CHCH₂CH₂CH₂^b, NCH₂^bCH), 1.75–1.66 (m, 1 H, CHCH₂CH₂^a), 1.66–1.50 (m, 5 H, CHCH₂CH₂^b, CH₂CH₂CH₂OH), 1.34 (dq, J = 12.6/ 4.1 Hz, 1 H, CHCH₂^bCH₂) ppm; ¹³C NMR (100 MHz, CD₃OD/ 1 M NaOD in D₂O 6:1): δ = 182.9 (CO), 62.8 (CH₂OH), 59.9 (CH₂(CH₂)₃OH), 57.9 (CHCH₂N), 54.8 (CHCH₂CH₂CH₂), 46.2 (CHCO), 32.0 (CH₂CH₂OH), 29.4 (CHCH₂CH₂), 25.8 (CHCH₂CH₂), 24.3 (CH₂(CH₂)₂OH) ppm; HRESIMS m/z (pos): 202.1436 C₁₀H₂₀NO₃ (calcd. 202.1438).

***rac*-1-[2-(1,3-Dioxolan-2-yl)ethyl]piperidine-3-carboxylic acid *rac*-18c**

According to **GP4**: Ester *rac*-**15c** (150 mg, 0.583 mmol, 1.0 equiv) and Ba(OH)₂ · 8 H₂O (735 mg, 2.33 mmol, 4 equiv). The product was obtained as colorless viscous oil (118 mg,

88%). IR (KBr) $\tilde{\nu}$ = 3419, 2954, 2893, 1589, 1450, 1390, 1140, 1030, 651, 771 cm^{-1} ; ^1H NMR (400 MHz, $\text{CD}_3\text{OD}/1\text{ M NaOD}$ in D_2O 6:1): δ = 4.91–4.85 (m, 1 H, OCHO), 4.00–3.81 (m, 4 H, $\text{OCH}_2\text{CH}_2\text{O}$), 3.13–3.03 (m, 1 H, $\text{NCH}_2^{\text{a}}\text{CH}$), 2.88 (d, J = 11.0 Hz, 1 H, $\text{CHCH}_2\text{CH}_2\text{CH}_2^{\text{a}}$), 2.54–2.41 (m, 2 H, $\text{CH}_2\text{CH}_2\text{CHO}$), 2.36 (tt, J = 11.8/ 3.7 Hz, 1 H, CHCO), 2.06–1.81 (m, 5 H, $\text{CCHCH}_2^{\text{a}}\text{CH}_2$, $\text{CHCH}_2\text{CH}_2\text{CH}_2^{\text{b}}$, $\text{NCH}_2^{\text{b}}\text{CH}$, CH_2CHO), 1.75–1.66 (m, 1 H, $\text{CCHCH}_2\text{CH}_2^{\text{a}}$), 1.57 (tq, J = 12.9/ 3.8 Hz, 1 H, $\text{CCHCH}_2\text{CH}_2^{\text{b}}$), 1.33 (dq, J = 12.7/ 4.1 Hz, 1 H, $\text{CCHCH}_2^{\text{b}}\text{CH}_2$) ppm; ^{13}C NMR (100 MHz, $\text{CD}_3\text{OD}/1\text{ M NaOD}$ in D_2O 6:1): δ = 182.9 (CO), 104.3 (OCHO), 65.9 ($\text{OCH}_2\text{CH}_2\text{O}$), 57.9 (CHCH_2N), 54.7 ($\text{CHCH}_2\text{CH}_2\text{CH}_2$), 54.4 ($\text{CH}_2\text{CH}_2\text{CHO}$), 46.2 (CHCO), 31.6 ($\text{CH}_2\text{CH}_2\text{CHO}$), 29.3 (CHCH_2CH_2), 25.7 (CHCH_2CH_2) ppm; HRESIMS m/z (pos): 230.1385 $\text{C}_{11}\text{H}_{20}\text{NO}_4$ (calcd. 230.1387).

***rac*-1-[3-(1,3-Dioxolan-2-yl)propyl]piperidine-3-carboxylic acid *rac*-18d**

According to **GP4**: Ester *rac*-**15d** (150 mg, 0.553 mmol, 1.0 equiv) and $\text{Ba}(\text{OH})_2 \cdot 8\text{H}_2\text{O}$ (697 mg, 2.21 mmol, 4 equiv). The product was obtained as colorless solid (124 mg, 92%). Mp 132 °C; IR (KBr) $\tilde{\nu}$ = 3429, 2954, 2887, 1610, 1483, 1387, 1140, 1041, 962, 912, 822, 768, 700, 530 cm^{-1} ; ^1H NMR (400 MHz, $\text{CD}_3\text{OD}/1\text{ M NaOD}$ in D_2O 6:1): δ = 4.88–4.84 (m, 1 H, OCHO), 4.00–3.80 (m, 4 H, $\text{OCH}_2\text{CH}_2\text{O}$), 3.15–3.06 (m, 1 H, $\text{NCH}_2^{\text{a}}\text{CH}$), 2.89 (d, J = 11.1 Hz, 1 H, $\text{CCH}(\text{CH}_2)_2\text{CH}_2^{\text{a}}$), 2.44–2.31 (m, 3 H, $\text{CH}_2(\text{CH}_2)_2\text{CHO}$, CHCO), 2.05–1.94 (m, 2 H, $\text{CCHCH}_2^{\text{a}}\text{CH}_2$, $\text{NCH}_2^{\text{b}}\text{CH}$), 1.91 (ddd, J = 11.8/ 11.8/ 2.8 Hz, 1 H, $\text{CCH}(\text{CH}_2)_2\text{CH}_2^{\text{b}}$), 1.75–1.51 (m, 6 H, $\text{CCHCH}_2\text{CH}_2$, $\text{NCH}_2\text{CH}_2\text{CH}_2\text{CHO}$), 1.33 (dq, J = 12.6/ 4.1 Hz, 1 H, $\text{CCHCH}_2^{\text{b}}\text{CH}_2$) ppm; ^{13}C NMR (100 MHz, $\text{CD}_3\text{OD}/1\text{ M NaOD}$ in D_2O 6:1): δ = 183.0 (CO), 105.3 (OCHO), 65.9 ($\text{OCH}_2\text{CH}_2\text{O}$), 59.9 ($\text{CH}_2(\text{CH}_2)_2\text{CHO}$), 58.0 (CHCH_2N), 54.7 ($\text{CCH}(\text{CH}_2)_2\text{CH}_2$), 46.2 (CHCO), 32.8 ($\text{CH}_2\text{CH}_2\text{CHO}$), 29.4 ($\text{CCHCH}_2\text{CH}_2$), 25.8 ($\text{CCHCH}_2\text{CH}_2$), 21.7 (CH_2CHO) ppm; HRESIMS m/z (pos): 244.1541 $\text{C}_{12}\text{H}_{22}\text{NO}_4$ (calcd. 244.1543).

***rac*-1-(3,3-Dimethoxypropyl)piperidine-3-carboxylic acid *rac*-18e**

According to **GP4**: Ester *rac*-**15e** (150 mg, 0.578 mmol, 1.0 equiv) and $\text{Ba}(\text{OH})_2 \cdot 8\text{H}_2\text{O}$ (729 mg, 2.31 mmol, 4 equiv). The product was obtained as colorless solid (57 mg, 43%). Mp 124 °C; IR (KBr) $\tilde{\nu}$ = 3435, 2951, 2834, 1601, 1450, 1385, 1192, 1128, 1053, 997, 947, 770, 704, 525 cm^{-1} ; ^1H NMR (400 MHz, $\text{CD}_3\text{OD}/1\text{ M NaOD}$ in D_2O 6:1): δ = 4.44 (t, J = 5.6 Hz, 1 H, OCHO), 3.34 (s, 6 H, OCH_3), 3.12–3.04 (m, 1 H, $\text{NCH}_2^{\text{a}}\text{CH}$), 2.87 (d, J = 11.0 Hz, 1 H,

CHCH₂CH₂CH₂^a), 2.46–2.30 (m, 3 H, CHCO, CH₂CH₂CHO), 2.06–1.88 (m, 3 H, CCHCH₂^aCH₂, CHCH₂CH₂CH₂^b, NCH₂^bCH), 1.88–1.78 (m, 2 H, CH₂CHO), 1.75–1.66 (m, 1 H, CCHCH₂CH₂^a), 1.57 (tq, *J* = 12.9/ 3.8 Hz, 1 H, CCHCH₂CH₂^b), 1.33 (dq, *J* = 12.6/ 4.1 Hz, 1 H, CCHCH₂^bCH₂) ppm; ¹³C NMR (100 MHz, CD₃OD/ 1 M NaOD in D₂O 6:1): δ = 182.9 (CO), 105.0 (OCHO), 58.0 (CHCH₂N), 55.1 (CH₂CH₂CHO), 54.8 (CHCH₂CH₂CH₂), 53.7 (OCH₃), 46.2 (CHCO), 30.6 (CH₂CHO), 29.3 (CCHCH₂CH₂), 25.8 (CCHCH₂CH₂) ppm; HRESIMS *m/z* (pos): 232.1541 C₁₁H₂₂NO₄ (calcd. 232.1543).

***rac*-1-(4,4-Dimethoxybutyl)piperidine-3-carboxylic acid *rac*-18f**

According to **GP4**: Ester *rac*-**15f** (150 mg, 0.549 mmol, 1.0 equiv) and Ba(OH)₂ · 8 H₂O (691 mg, 2.19 mmol, 4 equiv). The product was obtained as colorless solid (85 mg, 63%). Mp 99 °C; IR (KBr) $\tilde{\nu}$ = 3433, 2945, 2831, 1601, 1456, 1385, 1126, 1072, 1049, 960, 768, 706 cm⁻¹; ¹H NMR (400 MHz, CD₃OD/ 1 M NaOD in D₂O 6:1): δ = 4.46–4.37 (m, 1 H, OCHO), 3.34 (s, 6 H, OCH₃), 3.14–3.05 (m, 1 H, NCH₂^aCH), 2.89 (d, *J* = 11.0 Hz, 1 H, CCH(CH₂)₂CH₂^a), 2.43–2.29 (m, 3 H, CHCO, CH₂CH₂CH₂CHO), 2.05–1.85 (m, 3 H, CCHCH₂^aCH₂, CCH(CH₂)₂CH₂^b, NCH₂^bCH), 1.75–1.65 (m, 1 H, CCHCH₂CH₂^a), 1.65–1.50 (m, 5 H, CCHCH₂CH₂^b, CH₂CH₂CHO), 1.33 (dq, *J* = 12.7/ 4.0 Hz, 1 H, CCHCH₂^bCH₂) ppm; ¹³C NMR (100 MHz, CD₃OD/ 1 M NaOD in D₂O 6:1): δ = 183.0 (CO), 106.1 (OCHO), 59.7 (CH₂(CH₂)₂CHO), 57.9 (CHCH₂N), 54.7 (CCH(CH₂)₂CH₂), 53.8 (OCH₃), 46.2 (CHCO), 31.7 (CH₂CHO), 29.3 (CCHCH₂CH₂), 25.7 (CCHCH₂CH₂), 22.3 (CH₂CH₂CHO) ppm; HRESIMS *m/z* (pos): 246.1698 C₁₂H₂₄NO₄ (calcd. 246.1700).

***rac*-Ethyl 1-[3-(1,7-dimethyl-4-azatricyclo[3.3.1.0^{2,7}]nonan-4-yl)propyl]piperidine-3-carboxylate *rac*-19a**

According to **GP2**: Tricyclic imine **10a** (30 mg, 0.20 mmol, 1 equiv), sodium triacetoxyborohydride (106 mg, 0.500 mmol, 2.5 equiv), acetic acid (25 mg, 0.42 mmol, 24 μ L, 2.1 equiv), ethyl 1-(3,3-dimethoxypropyl) piperidine-3-carboxylate *rac*-**15e** (104 mg, 0.400 mmol, 2 equiv) and FeCl₃ · 6H₂O (303 mg, 1.12 mmol, 5.6 equiv). The reaction was kept at 40 °C for 18 h. The crude product was purified by FC and RP-MPLC. The product was obtained as yellow oil (19 mg, 27%). IR (film) $\tilde{\nu}$ = 2939, 2858, 2800, 1734, 1450, 1373, 1309, 1223, 1205, 1178, 1151, 1099, 1032 cm⁻¹; ¹H NMR (400 MHz, CD₂Cl₂): δ = 4.08 (q, *J* = 7.1 Hz, 2 H, CH₂CH₃), 2.91 (d, *J* = 11.0 Hz, 1 H, OCCHCH₂^aN), 2.77–2.68 (m, 2 H,

CHCH₂CH₂CH₂^a, CHN), 2.67 (d, *J* = 2.5 Hz, 2 H, CHNCH₂CH), 2.49 (tt, *J* = 10.3/ 3.8 Hz, 1 H, OCCH), 2.45–2.38 (m, 2 H, CHNCH₂CH₂), 2.37–2.28 (m, 2 H, CHN(CH₂)₂CH₂), 2.11 (t, *J* = 10.4 Hz, 1 H, OCCHCH₂^bN), 1.95 (ddd, *J* = 10.8/ 10.8/ 2.6 Hz, 1 H, CHCH₂CH₂CH₂^b), 1.91–1.81 (m, 1 H, CHCH₂^aCH₂), 1.78–1.63 (m, 3 H, CHCH₂CH₂^a, NCH(CH₂^a)₂), 1.61–1.38 (m, 7 H, CHCH₂^bCH₂, CHCH₂CH₂^b, NCH₂CH₂CH₂N, CCH₂^aC, NCH(CH₂^b)₂), 1.36 (s, 1 H, CHNCH₂CH), 1.33 (d, *J* = 8.6 Hz, 1 H, CCH₂^bC), 1.23 (t, *J* = 7.1 Hz, 3 H, CH₂CH₃), 0.98 (s, 6 H, CCH₃) ppm; ¹³C NMR (100 MHz, CD₂Cl₂) δ = 174.5 (CO), 60.5 (CH₂CH₃), 57.3 (CHN(CH₂)₂CH₂), 56.1 (OCCHCH₂N), 55.5 (CHNCH₂CH₂), 54.3 (CHCH₂CH₂CH₂), 53.4 (NCH), 51.3 (CCH₂C), 47.7 (CHNCH₂CH), 45.6 (CHNCH₂CH), 42.4 (OCCH), 39.6 (NCH(CH₂)₂), 36.0 (CCH₃), 27.5 (CHCH₂CH₂), 26.5 (CHNCH₂CH₂), 25.5 (CCH₃), 25.1 (CHCH₂CH₂), 14.4 (CH₂CH₃) ppm; HRESIMS *m/z* (pos): 349.2848 C₂₁H₃₇N₂O₂ (calcd. 349.2850).

***rac*-Ethyl 1-[3-(1,7-diphenyl-4-azatricyclo[3.3.1.0^{2,7}]nonan-4-yl)propyl]piperidine-3-carboxylate *rac*-19b**

According to **GP2**: Tricyclic imine **10b** (27 mg, 0.10 mmol, 1 equiv), sodium triacetoxyborohydride (53 mg, 0.25 mmol, 2.5 equiv), acetic acid (13 mg, 0.21 mmol, 12 μ L, 2.1 equiv), ethyl 1-(3,3-dimethoxypropyl)piperidine-3-carboxylate *rac*-**15e** (52 mg, 0.20 mmol, 2 equiv) and FeCl₃ · 6H₂O (541 mg, 2.00 mmol, 20 equiv). The reaction was kept at 40 °C for 12 h. The crude product was purified by FC and RP-MPLC. The product was obtained as yellow oil (11 mg, 23%). IR (film) $\tilde{\nu}$ = 3056, 3024, 2935, 2854, 2804, 1730, 1603, 1495, 1444, 1367, 1309, 1178, 1151, 1030, 758, 698 cm⁻¹; ¹H NMR (500 MHz, CD₂Cl₂): δ = 7.34–7.29 (m, 4 H, CCHCH), 7.29–7.24 (m, 4 H, CCHCH), 7.18 (tt, *J* = 7.1/ 1.4 Hz, 2 H, CCHCHCH), 4.09 (q, *J* = 7.1 Hz, 2 H, CH₂CH₃), 3.17 (d, *J* = 2.4 Hz, 2 H, CHNCH₂CH), 3.02 (p, *J* = 1.6 Hz, 1 H, CHN), 2.95 (d, *J* = 10.5 Hz, 1 H, OCCHCH₂^aN), 2.73 (d, *J* = 10.9 Hz, 1 H, CHCH₂CH₂CH₂^a), 2.58 (dd, *J* = 7.3/ 7.3 Hz, 2 H, CHNCH₂CH₂), 2.55 (s, 1 H, CCHC), 2.51 (tt, *J* = 10.3/ 3.9 Hz, 1 H, OCCH), 2.44 (dt, *J* = 8.7/ 2.0 Hz, 1 H, CCH₂^aC), 2.41–2.36 (m, 2 H, CHN(CH₂)₂CH₂), 2.27 (d, *J* = 13.1 Hz, 2 H, NCH(CH₂^a)₂), 2.14 (t, *J* = 10.4 Hz, 1 H, OCCHCH₂^bN), 2.11–2.05 (m, 3 H, CCH₂^bC, NCH(CH₂^b)₂), 1.99 (ddd, *J* = 10.9/ 10.9/ 2.1 Hz, 1 H, CHCH₂CH₂CH₂^b), 1.92–1.85 (m, 1 H, CHCH₂^aCH₂), 1.74–1.67 (m, 1 H, CHCH₂CH₂^a), 1.65 (p, *J* = 7.3 Hz, 2 H, NCH₂CH₂CH₂N), 1.58–1.48 (m, 1 H, CHCH₂CH₂^b), 1.48–1.38 (m, 1 H, CHCH₂^bCH₂), 1.23 (t, *J* = 7.1 Hz, 3 H, CH₂CH₃) ppm; ¹³C NMR (125 MHz, CD₂Cl₂) δ = 174.5 (CO), 149.4 (CCHCH), 128.7 (CCHCH), 126.1 (CCHCHCH), 125.4 (CCHCH), 60.5 (CH₂CH₃), 57.2 (CHN(CH₂)₂CH₂), 56.1 (OCCHCH₂N), 55.6 (CHNCH₂CH₂), 54.3

(CHCH₂CH₂CH₂), 53.6 (NCH), 49.9 (CHNCH₂CH), 49.1 (CCH₂C), 44.1 (CHNCH₂CH), 42.5 (CCH₂C), 42.4 (OCCH), 40.8 (NCH(CH₂)₂), 27.5 (CHCH₂CH₂), 26.6 (NCH₂CH₂CH₂N), 25.1 (CHCH₂CH₂), 14.5 (CH₂CH₃) ppm; HRESIMS *m/z* (pos): 473.3165 C₃₁H₄₁N₂O₂ (calcd. 473.3163).

***rac*-Ethyl 1-[3-(3,6-dimethyl-9-azatricyclo[4.3.1.0^{3,7}]decan-9-yl)propyl]piperidine-3-carboxylate *rac*-19c**

According to **GP2**: Tricyclic imine **10c** (33 mg, 0.20 mmol, 1 equiv), sodium triacetoxyborohydride (106 mg, 0.500 mmol, 2.5 equiv), acetic acid (25 mg, 0.42 mmol, 24 μ L, 2.1 equiv), ethyl 1-(3,3-dimethoxypropyl)piperidine-3-carboxylate *rac*-**15e** (104 mg, 0.400 mmol, 2 equiv) and FeCl₃ · 6H₂O (303 mg, 1.12 mmol, 5.6 equiv). The reaction was kept at 20 °C for 12 h. The crude product was purified by FC. The product was obtained as yellow oil (19 mg, 26%). IR (film) $\tilde{\nu}$ = 2942, 2864, 2804, 1732, 1450, 1371, 1311, 1209, 1180, 1153, 1099, 1032 cm⁻¹; ¹H NMR (500 MHz, CD₂Cl₂): δ = 4.08 (q, *J* = 7.1 Hz, 2 H, OCH₂CH₃), 2.90 (d, *J* = 10.5 Hz, 1 H, OCCHCH₂^aN), 2.74 (s, 2 H, CHNCH₂CH), 2.70 (d, *J* = 10.9 Hz, 1 H, CHCH₂CH₂CH₂^a), 2.56–2.39 (m, 4 H, CHNCH₂CH₂, NCH, OCCH), 2.37–2.29 (m, 2 H, CHN(CH₂)₂CH₂), 2.13 (t, *J* = 10.3 Hz, 1 H, OCCHCH₂^bN), 1.97 (ddd, *J* = 10.6/ 10.6/ 2.2 Hz, 1 H, CHCH₂CH₂CH₂^b), 1.91–1.82 (m, 1 H, CHCH₂^aCH₂), 1.76 (d, *J* = 12.8 Hz, 2 H, NCH(CH₂^a)₂), 1.72–1.65 (m, 1 H, CHCH₂CH₂^a), 1.61 (p, *J* = 7.3 Hz, 2 H, NCH₂CH₂CH₂), 1.56–1.36 (m, 6 H, CHCH₂^bCH₂, CHCH₂CH₂^b, CCH₂CH₂C), 1.29–1.19 (m, 5 H, NCH(CH₂^b)₂, CH₂CH₃), 1.10 (s, 6 H, CCH₃), 0.88 (s, 1 H, CHNCH₂CH) ppm; ¹³C NMR (100 MHz, CD₂Cl₂) δ = 174.5 (CO), 60.5 (CH₂CH₃), 57.0 (CHN(CH₂)₂CH₂), 56.1 (OCCHCH₂N), 54.5 (CHNCH₂CH₂), 54.3 (CHCH₂CH₂CH₂), 52.0 (NCH), 49.6 (CHNCH₂CH), 46.1 (CHNCH₂CH), 42.6 (OCCH), 41.9 (NCH(CH₂)₂), 40.8 (CCH₂CH₂C), 39.6 (CCH₃), 27.8 (CCHCH₂CH₂), 26.6 (CCH₃), 25.7 (CHNCH₂CH₂), 25.1 (CHCH₂CH₂), 14.5 (CH₂CH₃) ppm; HRESIMS *m/z* (pos): 363.3006 C₂₂H₃₉N₂O₂ (calcd. 363.3006).

***rac*-Ethyl 1-[3-(3,6-diphenyl-9-azatricyclo[4.3.1.0^{3,7}]decan-9-yl)propyl]piperidine-3-carboxylate *rac*-19d**

According to **GP2**: Tricyclic imine **10d** (29 mg, 0.10 mmol, 1 equiv), sodium triacetoxyborohydride (53 mg, 0.25 mmol, 2.5 equiv), acetic acid (13 mg, 0.21 mmol, 12 μ L, 2.1 equiv), ethyl 1-(3,3-dimethoxypropyl)piperidine-3-carboxylate *rac*-**15e** (52 mg, 0.20 mmol, 2 equiv) and FeCl₃ · 6H₂O (151 mg, 0.560 mmol, 5.6 equiv). The reaction was kept at 20 °C for 12 h. The crude product was purified by FC and RP-MPLC. The product was

obtained as yellow oil (12 mg, 25%). IR (film) $\tilde{\nu}$ = 3055, 3022, 2943, 2868, 2804, 1730, 1601, 1495, 1470, 1444, 1369, 1309, 1178, 1151, 1032, 760, 700 cm^{-1} ; ^1H NMR (400 MHz, CD_2Cl_2): δ = 7.52–7.42 (m, 4 H, CCHCH), 7.40–7.30 (m, 4 H, CCHCH), 7.24–7.17 (m, 2 H, CCHCHCH), 4.07 (q, J = 7.1 Hz, 2 H, OCH_2), 2.87 (d, J = 11.3 Hz, 1 H, $\text{OCCHCH}_2^{\text{a}}\text{N}$), 2.82 (s, 1 H, NCH), 2.71 (d, J = 1.6 Hz, 2 H, CHNCH_2CH), 2.66 (d, J = 11.5 Hz, 1 H, $\text{CHCH}_2\text{CH}_2\text{CH}_2^{\text{a}}$), 2.53–2.38 (m, 4 H, CHCH_2NCH , OCCH , $\text{NCH}(\text{CH}_2^{\text{a}})_2$), 2.38–2.25 (m, 4 H, $\text{NCH}_2\text{CH}_2\text{CH}_2\text{N}$), 2.08 (t, J = 10.5 Hz, 1 H, $\text{OCCHCH}_2^{\text{b}}\text{N}$), 2.05–1.79 (m, 8 H, $\text{CHCH}_2^{\text{a}}\text{CH}_2$, $\text{CHCH}_2\text{CH}_2\text{CH}_2^{\text{b}}$, $\text{NCH}(\text{CH}_2^{\text{b}})_2$, $\text{CCH}_2\text{CH}_2\text{C}$), 1.70–1.61 (m, 1 H, $\text{CHCH}_2\text{CH}_2^{\text{a}}$), 1.58–1.33 (m, 4 H, $\text{CHCH}_2^{\text{b}}\text{CH}_2$, $\text{NCH}_2\text{CH}_2\text{CH}_2\text{N}$, $\text{CHCH}_2\text{CH}_2^{\text{b}}$), 1.21 (t, J = 7.1 Hz, 3 H, CH_3) ppm; ^{13}C NMR (100 MHz, CD_2Cl_2) δ = 174.5 (CO), 149.9 (CH_2CC), 128.6 (CCHCH), 126.5 (CCHCH), 125.8 (CCHCHCH), 60.5 (OCH_2), 57.2 ($\text{CHN}(\text{CH}_2)_2\text{CH}_2$), 56.1 (OCCHCH_2N), 54.3 ($\text{CHCH}_2\text{CH}_2\text{CH}_2$), 54.1 ($\text{CHNCH}_2\text{CH}_2$), 51.7 (NCH), 47.3 (CCH_2), 46.7 (CHNCH_2CH), 44.9 (CHNCH_2CH), 42.5 ($\text{CCH}_2\text{CH}_2\text{C}$), 42.4 (OCCH), 42.3 ($\text{NCH}(\text{CH}_2)_2$), 27.4 ($\text{CH}_2\text{CH}_2\text{CH}$), 26.0 ($\text{CHNCH}_2\text{CH}_2$), 25.1 (CHCH_2CH_2), 14.4 (CH_3) ppm; HRESIMS m/z (pos): 487.3318 $\text{C}_{32}\text{H}_{43}\text{N}_2\text{O}_2$ (calcd. 487.3319).

***rac*-Ethyl 1-[3-(3,7-dimethyl-10-azatricyclo[5.3.1.0^{3,8}]undecan-10-yl)propyl]piperidine-3-carboxylate *rac*-19e**

According to **GP3**: Tricyclic imine **10e** (36 mg, 0.20 mmol, 1 equiv), sodium cyanoborohydride (66 mg, 1.0 mmol, 5 equiv), hydrochloric acid (73 mg, 2.0 mmol, 2.0 mL, 10 equiv), sodium triacetoxymethylborohydride (106 mg, 0.500 mmol, 2.5 equiv), acetic acid (25 mg, 0.42 mmol, 24 μL , 2.1 equiv), ethyl 1-(3,3-dimethoxypropyl)piperidine-3-carboxylate *rac*-**15e** (104 mg, 0.400 mmol, 2 equiv) and $\text{FeCl}_3 \cdot 6\text{H}_2\text{O}$ (1.08 g, 4.00 mmol, 20 equiv). The reaction was stirred at 40 °C for 12 h. The crude product was purified by FC. The product was obtained as yellow oil (28 mg, 37%). IR (film) $\tilde{\nu}$ = 2922, 2802, 1732, 1497, 1471, 1446, 1373, 1306, 1180, 1151, 1103, 1034, 862 cm^{-1} ; ^1H NMR (500 MHz, CD_2Cl_2): δ = 4.08 (q, J = 7.1 Hz, 2 H, CH_2CH_3), 2.96–2.84 (m, 3 H, CHNCH_2CH , $\text{OCCHCH}_2^{\text{a}}\text{N}$), 2.71 (d, J = 11.2 Hz, 1 H, $\text{CHCH}_2\text{CH}_2\text{CH}_2^{\text{a}}$), 2.61 (br s, 1 H, CHN), 2.56–2.45 (m, 3 H, $\text{CHNCH}_2\text{CH}_2$, OCCH), 2.33 (dd, J = 7.4/ 7.4 Hz, 2 H, $\text{CHN}(\text{CH}_2)_2\text{CH}_2$), 2.11 (t, J = 10.5 Hz, 1 H, $\text{OCCHCH}_2^{\text{b}}\text{N}$), 1.96 (ddd, J = 10.9/ 10.9/ 2.4 Hz, $\text{CHCH}_2\text{CH}_2\text{CH}_2^{\text{b}}$), 1.90–1.82 (m, 1 H, $\text{CHCH}_2^{\text{a}}\text{CH}_2$), 1.73–1.65 (m, 1 H, $\text{CHCH}_2\text{CH}_2^{\text{a}}$), 1.64–1.47 (m, 6 H, $\text{CHCH}_2\text{CH}_2^{\text{b}}$, $\text{CHNCH}_2\text{CH}_2$, $\text{NCH}(\text{CH}_2^{\text{a}})_2$, $\text{CCH}_2\text{CH}_2^{\text{a}}$), 1.46–1.36 (m, 2 H, $\text{CHCH}_2^{\text{b}}\text{CH}_2$, $\text{CCH}_2\text{CH}_2^{\text{b}}$), 1.32–1.25 (m, 4 H, $\text{NCH}(\text{CH}_2^{\text{b}})_2$, $\text{CCH}_2^{\text{a}}\text{CH}_2\text{CH}_2^{\text{a}}\text{C}$), 1.23 (t, J = 7.1 Hz, 3 H, CH_2CH_3), 1.10 (dd, J = 13.5/ 4.6 Hz, 2 H, $\text{CCH}_2^{\text{b}}\text{CH}_2\text{CH}_2^{\text{b}}\text{C}$), 1.05 (s, 6 H, CCH_3), 0.68 (s, 1 H, CHNCH_2CH) ppm; ^{13}C NMR (125 MHz,

CD₂Cl₂) δ = 174.5 (CO), 60.5 (CH₂CH₃), 57.1 (CHN(CH₂)₂CH₂), 56.1 (OCCHCH₂N), 54.8 (CHNCH₂CH₂), 54.3 (CHCH₂CH₂CH₂), 52.9 (NCH), 47.6 (CHNCH₂CH), 46.3 (CHNCH₂CH), 42.5 (OCCH), 40.8 (CCH₂CH₂CH₂C), 36.8 (NCH(CH₂)₂), 31.0 (CCH₃, CCH₃), 27.5 (CCHCH₂CH₂), 26.4 (CHNCH₂CH₂), 25.1 (CHCH₂CH₂), 19.6 (CCH₂CH₂), 14.5 (CH₂CH₃) ppm; HRESIMS m/z (pos): 377.3164 C₂₃H₄₁N₂O₂ (calcd. 377.3163).

***rac*-Ethyl 1-[3-(3,7-diphenyl-10-azatricyclo[5.3.1.0^{3,8}]undecan-10-yl)propyl]piperidine-3-carboxylate *rac*-19f**

According to **GP3**: Tricyclic imine **10f** (30 mg, 0.10 mmol, 1 equiv), sodium cyanoborohydride (33 mg, 0.50 mmol, 5 equiv), hydrochloric acid (36 mg, 1.0 mmol, 1.0 mL, 10 equiv), sodium triacetoxyborohydride (53 mg, 0.25 mmol, 2.5 equiv), acetic acid (13 mg, 0.21 mmol, 12 μ L, 2.1 equiv), ethyl 1-(3,3-dimethoxypropyl)piperidine-3-carboxylate *rac*-**15e** (52 mg, 0.20 mmol, 2 equiv) and FeCl₃ · 6H₂O (541 mg, 2.00 mmol, 20 equiv). The reaction was stirred at 40 °C for 12 h. The crude product was purified by FC and RP-MPLC. The product was obtained as colorless viscous oil (17 mg, 34%). IR (film) $\tilde{\nu}$ = 3057, 2926, 2852, 2802, 1730, 1597, 1495, 1444, 1369, 1306, 1180, 1151, 1032, 758, 700 cm⁻¹; ¹H NMR (500 MHz, CD₂Cl₂): δ = 7.52–7.47 (m, 4 H, CCHCH), 7.37–7.31 (m, 4 H, CCHCH), 7.19 (t, J = 7.3 Hz, 2 H, CCHCHCH), 4.06 (q, J = 7.2 Hz, 2 H, OCH₂), 2.88 (s, 1 H, NCH), 2.81 (d, J = 11.0 Hz, 1 H, OCCHCH₂^aN), 2.63–2.53 (m, 3 H, NCH(CH₂^a)₂, CHCH₂CH₂CH₂^a), 2.50 (d, J = 2.1 Hz, 2 H, CHNCH₂CH), 2.39 (tt, J = 10.4/ 3.8 Hz, 1 H, OCCH), 2.35 (s, 1 H, CHCH₂NCH), 2.22–2.11 (m, 4 H, CHN(CH₂)₂CH₂, CHNCH₂CH₂), 1.99 (t, J = 10.4 Hz, 1 H, OCCHCH₂^bN), 1.94–1.79 (m, 5 H, CHCH₂^aCH₂, CHCH₂CH₂CH₂^b, NCH(CH₂^b)₂, CCH₂CH₂^a), 1.65–1.37 (m, 8 H, CHCH₂^bCH₂, CHCH₂CH₂, CCH₂CH₂^b, CCH₂CH₂CH₂C), 1.37–1.32 (m, 2 H, CHNCH₂CH₂), 1.21 (t, J = 7.2 Hz, 3 H, CH₃) ppm; ¹³C NMR (125 MHz, CD₂Cl₂) δ = 174.5 (CO), 151.9 (CH₂CC), 128.5 (CCHCH), 126.7 (CCHCH), 125.7 (CCHCHCH), 60.5 (OCH₂), 56.9 (CHN(CH₂)₂CH₂), 56.0 (OCCHCH₂N), 54.5 (CHNCH₂CH₂), 54.1 (CHCH₂CH₂CH₂), 51.5 (NCH), 49.3 (CHNCH₂CH), 43.7 (CCH₂CH₂CH₂C), 42.4 (OCCH), 40.2 (CCH₂), 39.1 (CHNCH₂CH), 36.0 (NCH(CH₂)₂), 27.4 (CH₂CH₂CH), 26.2 (CHNCH₂CH₂), 25.0 (CHCH₂CH₂), 20.6 (CCH₂CH₂), 14.4 (CH₃) ppm; HRESIMS m/z (pos): 501.3476 C₃₃H₄₅N₂O₂ (calcd. 501.3476).

***rac*-Ethyl 1-[4-(1,7-dimethyl-4-azatricyclo[3.3.1.0^{2,7}]nonan-4-yl)butyl]piperidine-3-carboxylate *rac*-19g**

According to **GP2**: Tricyclic imine **10a** (30 mg, 0.20 mmol, 1 equiv), sodium triacetoxymethylborohydride (106 mg, 0.500 mmol, 2.5 equiv), acetic acid (25 mg, 0.42 mmol, 24 μ L, 2.1 equiv), ethyl 1-(4,4-dimethoxybutyl)piperidine-3-carboxylate *rac*-**15f** (109 mg, 0.400 mmol, 2 equiv) and $\text{FeCl}_3 \cdot 6\text{H}_2\text{O}$ (303 mg, 1.12 mmol, 5.6 equiv). The reaction was kept at 40 °C for 20 h. The crude product was purified by FC. The product was obtained as viscous yellow oil (32 mg, 44%). IR (film) $\tilde{\nu}$ = 2937, 2858, 2802, 1732, 1660, 1450, 1373, 1309, 1180, 1151, 1093, 1032 cm^{-1} ; ^1H NMR (400 MHz, CD_2Cl_2): δ = 4.08 (q, J = 7.1 Hz, 2 H, CH_2CH_3), 2.95–2.83 (m, 2 H, $\text{OCCHCH}_2^{\text{a}}\text{N}$, CHN), 2.76 (d, J = 1.2 Hz, 2 H, CHNCH_2CH), 2.72–2.65 (m, 1 H, $\text{CHCH}_2\text{CH}_2\text{CH}_2^{\text{a}}$), 2.56–2.44 (m, 3 H, $\text{CHNCH}_2\text{CH}_2$, OCCH), 2.35–2.25 (m, 2 H, $\text{CHN}(\text{CH}_2)_3\text{CH}_2$), 2.10 (t, J = 10.6 Hz, 1 H, $\text{OCCHCH}_2^{\text{b}}\text{N}$), 1.95 (ddd, J = 10.8/ 10.8/ 2.6 Hz, 1 H, $\text{CHCH}_2\text{CH}_2\text{CH}_2^{\text{b}}$), 1.91–1.78 (m, 3 H, $\text{CHCH}_2^{\text{a}}\text{CH}_2$, $\text{NCH}(\text{CH}_2^{\text{a}})_2$), 1.72–1.64 (m, 1 H, $\text{CHCH}_2\text{CH}_2^{\text{a}}$), 1.59 (dd, J = 13.1/ 3.5 Hz, 2 H, $\text{NCH}(\text{CH}_2^{\text{b}})_2$), 1.56–1.37 (m, 8 H, $\text{CHCH}_2^{\text{b}}\text{CH}_2$, $\text{CHCH}_2\text{CH}_2^{\text{b}}$, $\text{NCH}_2\text{CH}_2\text{CH}_2\text{CH}_2\text{N}$, $\text{CCH}_2^{\text{a}}\text{C}$, CCHC), 1.35 (d, J = 8.7 Hz, 1 H, $\text{CCH}_2^{\text{b}}\text{C}$), 1.22 (t, J = 7.1 Hz, 3 H, CH_2CH_3), 1.00 (s, 6 H, CCH_3) ppm; ^{13}C NMR (100 MHz, CD_2Cl_2) δ = 174.5 (CO), 60.5 (CH_2CH_3), 58.9 ($\text{CHN}(\text{CH}_2)_3\text{CH}_2$), 56.9 ($\text{CHNCH}_2\text{CH}_2$), 56.0 (OCCHCH_2N), 54.2 ($\text{CHCH}_2\text{CH}_2\text{CH}_2$), 53.4 (NCH), 51.1 (CCH_2C), 47.5 (CHNCH_2CH), 45.1 (CHNCH_2CH), 42.4 (OCCH), 38.8 ($\text{NCH}(\text{CH}_2)_2$), 36.0 (CCH_3), 27.5 (CHCH_2CH_2), 26.1 ($\text{CHNCH}_2\text{CH}_2\text{CH}_2$), 25.4 (CCH_3), 25.1 (CHCH_2CH_2), 25.0 ($\text{CHNCH}_2\text{CH}_2$), 14.4 (CH_2CH_3) ppm; HRESIMS m/z (pos): 363.3006 $\text{C}_{22}\text{H}_{39}\text{N}_2\text{O}_2$ (calcd. 363.3006).

***rac*-Ethyl 1-[4-(1,7-diphenyl-4-azatricyclo[3.3.1.0^{2,7}]nonan-4-yl)butyl]piperidine-3-carboxylate *rac*-19h**

According to **GP2**: Tricyclic imine **10b** (27 mg, 0.10 mmol, 1 equiv), sodium triacetoxymethylborohydride (53 mg, 0.25 mmol, 2.5 equiv), acetic acid (13 mg, 0.21 mmol, 12 μ L, 2.1 equiv), ethyl 1-(4,4-dimethoxybutyl)piperidine-3-carboxylate *rac*-**15f** (55 mg, 0.20 mmol, 2 equiv) and $\text{FeCl}_3 \cdot 6\text{H}_2\text{O}$ (151 mg, 0.560 mmol, 5.6 equiv). The reaction was kept at 40 °C for 20 h. The crude product was purified by FC and RP-MPLC. The product was obtained as yellow oil (23 mg, 47%). IR (film) $\tilde{\nu}$ = 3057, 3026, 2935, 2856, 2802, 1730, 1603, 1495, 1446, 1367, 1309, 1178, 1153, 1030, 758, 700 cm^{-1} ; ^1H NMR (400 MHz, CD_2Cl_2): δ = 7.35–7.24 (m, 8 H, CCHCH, CCHCH), 7.22–7.16 (m, 2 H, CCHCHCH), 4.09 (q, J = 7.1 Hz, 2 H, CH_2CH_3), 3.19 (d, J = 1.8 Hz, 2 H, CHNCH_2CH), 3.07 (s, 1 H, CHN), 2.93 (d, J = 10.7 Hz, 1 H, $\text{OCCHCH}_2^{\text{a}}\text{N}$), 2.72 (d, J = 11.1 Hz, 1 H, $\text{CHCH}_2\text{CH}_2\text{CH}_2^{\text{a}}$), 2.60 (t, J = 3.1 Hz, 2 H, $\text{CHNCH}_2\text{CH}_2$), 2.56 (s, 1 H, CCHC), 2.51 (tt, J = 10.3/ 3.9 Hz, 1 H, OCCH), 2.45 (dt, J = 8.8/ 2.3 Hz, 1 H, $\text{CCH}_2^{\text{a}}\text{C}$), 2.38–2.25 (m, 4 H, $\text{CHN}(\text{CH}_2)_3\text{CH}_2$, $\text{NCH}(\text{CH}_2^{\text{a}})_2$), 2.17–2.05 (m, 4 H,

OCCHCH₂^bN, CCH₂^bC, NCH(CH₂^b)₂, 1.97 (ddd, $J = 10.8/ 10.8/ 2.6$ Hz, 1 H, CHCH₂CH₂CH₂^b), 1.92–1.85 (m, 1 H, CHCH₂^aCH₂), 1.74–1.65 (m, 1 H, CHCH₂CH₂^a), 1.60–1.37 (m, 6 H, CHCH₂^bCH₂, CHCH₂CH₂^b, NCH₂CH₂CH₂CH₂N), 1.23 (t, $J = 7.1$ Hz, 3 H, CH₂CH₃) ppm; ¹³C NMR (100 MHz, CD₂Cl₂) $\delta = 174.5$ (CO), 149.2 (CCHCH), 128.7 (CCHCH), 126.2 (CCHCHCH), 125.4 (CCHCH), 60.5 (CH₂CH₃), 59.1 (CHN(CH₂)₃CH₂), 57.3 (CHNCH₂CH₂), 56.0 (OCCHCH₂N), 54.2 (CHCH₂CH₂CH₂), 53.6 (NCH), 49.8 (CHNCH₂CH), 48.9 (CCH₂C), 44.0 (CHNCH₂CH), 42.5 (CCH₂C), 42.4 (OCCH), 40.6 (NCH(CH₂)₂), 27.5 (CHCH₂CH₂), 26.7 (CHNCH₂CH₂CH₂), 25.1 (CHCH₂CH₂), 25.0 (CHNCH₂CH₂), 14.4 (CH₂CH₃) ppm; HRESIMS m/z (pos): 487.3317 C₃₂H₄₃N₂O₂ (calcd. 487.3319).

***rac*-Ethyl 1-[4-(3,6-dimethyl-9-azatricyclo[4.3.1.0^{3,7}]decan-9-yl)butyl]piperidine-3-carboxylate *rac*-19j**

According to **GP2**: Tricyclic imine **10c** (50 mg, 0.31 mmol, 1 equiv), sodium triacetoxyborohydride (162 mg, 0.766 mmol, 2.5 equiv), acetic acid (39 mg, 0.64 mmol, 37 μ L, 2.1 equiv), ethyl 1-(4,4-dimethoxybutyl)piperidine-3-carboxylate *rac*-**15f** (167 mg, 0.613 mmol, 2 equiv) and FeCl₃ · 6H₂O (464 mg, 1.72 mmol, 5.6 equiv). The reaction was kept at 20 °C for 2 h. The crude product was purified by FC. The product was obtained as yellow oil (84 mg, 73%). IR (film) $\tilde{\nu} = 2941, 2864, 2802, 1734, 1468, 1452, 1371, 1311, 1178, 1153, 1101, 1034, 862$ cm⁻¹; ¹H NMR (500 MHz, CD₂Cl₂): $\delta = 4.08$ (q, $J = 7.2$ Hz, 2 H, OCH₂CH₃), 2.91 (d, $J = 10.3$ Hz, 1 H, OCCHCH₂^aN), 2.78–2.63 (m, 3 H, CHCH₂CH₂CH₂^a, CHNCH₂CH), 2.49 (tt, $J = 10.4/ 3.8$ Hz, 1 H, OCCH), 2.44 (br s, 1 H, NCH), 2.39 (t, $J = 7.2$ Hz, 2 H, CHNCH₂CH₂), 2.34–2.27 (m, 2 H, CHN(CH₂)₃CH₂), 2.09 (t, $J = 10.4$ Hz, 1 H, OCCHCH₂^bN), 1.95 (dt, $J = 10.9/ 2.4$ Hz, 1 H, CHCH₂CH₂CH₂^b), 1.91–1.83 (m, 1 H, CHCH₂^aCH₂), 1.78–1.64 (m, 3 H, CHCH₂CH₂^a, NCH(CH₂^a)₂), 1.58–1.33 (m, 10 H, CHCH₂^bCH₂, CHCH₂CH₂^b, NCH₂CH₂CH₂CH₂N, CCH₂CH₂C), 1.28–1.18 (m, 5 H, NCH(CH₂^b)₂, CH₂CH₃), 1.09 (s, 6 H, CCH₃), 0.85 (t, $J = 2.3$ Hz, 1 H, CHNCH₂CH) ppm; ¹³C NMR (125 MHz, CD₂Cl₂) $\delta = 174.6$ (CO), 60.5 (CH₂CH₃), 59.2 (CHN(CH₂)₃CH₂), 56.4 (CHNCH₂CH₂), 56.0 (OCCHCH₂N), 54.2 (CHCH₂CH₂CH₂), 51.8 (NCH), 49.9 (CHNCH₂CH), 46.2 (CHNCH₂CH), 42.4 (NCH(CH₂)₂, OCCH), 40.8 (CCH₂CH₂C), 39.7 (CCH₃), 27.5 (CCHCH₂CH₂), 26.7 (CCH₃), 26.6 (CHNCH₂CH₂CH₂), 25.1 (CHNCH₂CH₂, CHCH₂CH₂), 14.4 (CH₂CH₃) ppm; HRESIMS m/z (pos): 377.3161 C₂₃H₄₁N₂O₂ (calcd. 377.3163).

***rac*-Ethyl 1-[4-(3,6-diphenyl-9-azatricyclo[4.3.1.0^{3,7}]decan-9-yl)butyl]piperidine-3-carboxylate *rac*-19k**

According to **GP2**: Tricyclic imine **10d** (50 mg, 0.17 mmol, 1 equiv), sodium triacetoxyborohydride (92 mg, 0.44 mmol, 2.5 equiv), acetic acid (22 mg, 0.37 mmol, 21 μ L, 2.1 equiv), ethyl 1-(4,4-dimethoxybutyl)piperidine-3-carboxylate *rac*-**15f** (116 mg, 0.348 mmol, 2 equiv) and $\text{FeCl}_3 \cdot 6\text{H}_2\text{O}$ (263 mg, 0.974 mmol, 5.6 equiv). The reaction was kept at 20 °C for 2 h. The crude product was purified by FC. The product was obtained as brown oil (63 mg, 72%). IR (film) $\tilde{\nu}$ = 2939, 2804, 2360, 1730, 1601, 1495, 1444, 1369, 1309, 1178, 1151, 1032, 910, 760, 733, 700 cm^{-1} ; ^1H NMR (400 MHz, CDCl_3): δ = 7.50–7.40 (m, 4 H, CCHCH), 7.39–7.30 (m, 4 H, CCHCH), 7.21 (tt, J = 7.3/ 1.3 Hz, 2 H, CCHCHCH), 4.11 (q, J = 7.1 Hz, 2 H, OCH_2), 2.94 (d, J = 11.2 Hz, 1 H, $\text{OCCHCH}_2^{\text{a}}\text{N}$), 2.87 (s, 1 H, NCH), 2.75 (d, J = 2.3 Hz, 2 H, CHNCH_2CH), 2.71 (d, J = 11.1 Hz, 1 H, $\text{CHCH}_2\text{CH}_2\text{CH}_2^{\text{a}}$), 2.61–2.46 (m, 3 H, OCCH, NCH(CH_2^{a})₂), 2.41 (s, 1 H, CHCH_2NCH), 2.33 (t, J = 7.1 Hz, 2 H, $\text{CHNCH}_2\text{CH}_2$), 2.30–2.24 (m, 2 H, $\text{CHN}(\text{CH}_2)_3\text{CH}_2$), 2.14–2.00 (m, 3 H, $\text{OCCHCH}_2^{\text{b}}\text{N}$, $\text{CCH}_2^{\text{a}}\text{CH}_2^{\text{a}}\text{C}$), 2.00–1.80 (m, 6 H, $\text{CHCH}_2^{\text{a}}\text{CH}_2$, $\text{CHCH}_2\text{CH}_2\text{CH}_2^{\text{b}}$, $\text{NCH}(\text{CH}_2^{\text{b}})_2$, $\text{CCH}_2^{\text{b}}\text{CH}_2^{\text{b}}\text{C}$), 1.73–1.64 (m, 1 H, $\text{CHCH}_2\text{CH}_2^{\text{a}}$), 1.60–1.51 (m, 1 H, $\text{CHCH}_2\text{CH}_2^{\text{b}}$), 1.51–1.34 (m, 5 H, $\text{CHCH}_2^{\text{b}}\text{CH}_2$, $\text{NCH}_2\text{CH}_2\text{CH}_2\text{CH}_2\text{N}$), 1.23 (t, J = 7.1 Hz, 3 H, CH_3) ppm; ^{13}C NMR (100 MHz, CDCl_3) δ = 174.4 (CO), 149.0 (CH_2CC), 128.5 (CCHCH), 126.1 (CCHCH), 125.7 (CCHCHCH), 60.4 (OCH_2), 58.8 ($\text{CHN}(\text{CH}_2)_3\text{CH}_2$), 55.6 (OCCHCH_2N , $\text{CHNCH}_2\text{CH}_2$), 53.8 ($\text{CHCH}_2\text{CH}_2\text{CH}_2$), 51.4 (NCH), 46.9 (CCH₂), 46.2 (CHNCH_2CH), 44.6 (CHNCH_2CH), 42.2 (CCH₂CH₂C), 42.0 (OCCH), 41.8 (NCH(CH_2)₂), 27.2 ($\text{CH}_2\text{CH}_2\text{CH}$), 25.8 ($\text{CHN}(\text{CH}_2)_2\text{CH}_2$), 24.7 ($\text{CHNCH}_2\text{CH}_2$), 24.7 (CHCH_2CH_2), 14.3 (CH_3) ppm; HRESIMS m/z (pos): 501.3470 $\text{C}_{33}\text{H}_{45}\text{N}_2\text{O}_2$ (calcd. 501.3476).

***rac*-Ethyl 1-[4-(3,7-dimethyl-10-azatricyclo[5.3.1.0^{3,8}]undecan-10-yl)butyl]piperidine-3-carboxylate *rac*-19l**

According to **GP3**: Tricyclic imine **10e** (32 mg, 0.18 mmol, 1 equiv), sodium cyanoborohydride (30 mg, 0.45 mmol, 2.5 equiv), hydrochloric acid (33 mg, 0.90 mmol, 0.9 mL, 5 equiv), sodium triacetoxyborohydride (95 mg, 0.45 mmol, 2.5 equiv), acetic acid (23 mg, 0.38 mmol, 22 μ L, 2.1 equiv), ethyl 1-(4,4-dimethoxybutyl)piperidine-3-carboxylate *rac*-**15f** (98 mg, 0.36 mmol, 2 equiv) and $\text{FeCl}_3 \cdot 6\text{H}_2\text{O}$ (272 mg, 1.01 mmol, 5.6 equiv). Deviating from GP3 only 2.5 equiv NaCNBH_3 and 5 equiv HCl were used. The reaction was kept at 20 °C for 2 h. The crude product was purified by FC. The product was obtained as yellow oil (25 mg, 36%). IR (film) $\tilde{\nu}$ = 2924, 2800, 1734, 1497, 1452, 1373, 1304,

1178, 1151, 1103, 1034, 862 cm^{-1} ; ^1H NMR (400 MHz, CDCl_3): δ = 4.11 (q, J = 7.1 Hz, 2 H, CH_2CH_3), 2.97 (dd, J = 11.2/ 2.9 Hz, 1 H, $\text{OCCHCH}_2^{\text{a}}\text{N}$), 2.91 (d, J = 1.7 Hz, 2 H, CHNCH_2CH), 2.76 (d, J = 11.2 Hz, 1 H, $\text{CHCH}_2\text{CH}_2\text{CH}_2^{\text{a}}$), 2.69 (br s, 1 H, CHN), 2.58–2.48 (m, 3 H, $\text{CHNCH}_2\text{CH}_2$, OCCH), 2.37–2.28 (m, 2 H, $\text{CHN}(\text{CH}_2)_3\text{CH}_2$), 2.08 (t, J = 10.8 Hz, 1 H, $\text{OCCHCH}_2^{\text{b}}\text{N}$), 1.98–1.87 (m, 2 H, $\text{CHCH}_2^{\text{a}}\text{CH}_2$, $\text{CHCH}_2\text{CH}_2\text{CH}_2^{\text{b}}$), 1.70 (dp, J = 13.4/ 3.7 Hz, 1 H, $\text{CHCH}_2\text{CH}_2^{\text{a}}$), 1.64–1.35 (m, 10 H, $\text{CHCH}_2^{\text{b}}\text{CH}_2$, $\text{CHCH}_2\text{CH}_2^{\text{b}}$, $\text{NCH}_2(\text{CH}_2)_2\text{CH}_2\text{N}$, $\text{NCH}(\text{CH}_2^{\text{a}})_2$, CCH_2CH_2), 1.32–1.25 (m, 4 H, $\text{NCH}(\text{CH}_2^{\text{b}})_2$, $\text{CCH}_2^{\text{a}}\text{CH}_2\text{CH}_2^{\text{a}}\text{C}$), 1.23 (t, J = 7.1 Hz, 3 H, CH_2CH_3), 1.10 (dd, J = 13.4/ 4.7 Hz, 2 H, $\text{CCH}_2^{\text{b}}\text{CH}_2\text{CH}_2^{\text{b}}\text{C}$), 1.05 (s, 6 H, CCH_3), 0.68 (t, J = 2.3 Hz, 1 H, CHNCH_2CH) ppm; ^{13}C NMR (100 MHz, CDCl_3) δ = 174.4 (CO), 60.4 (CH_2CH_3), 58.9 ($\text{CHN}(\text{CH}_2)_3\text{CH}_2$), 56.2 ($\text{CHNCH}_2\text{CH}_2$), 55.6 (OCCHCH_2N), 53.9 ($\text{CHCH}_2\text{CH}_2\text{CH}_2$), 52.3 (NCH), 47.3 (CHNCH_2CH), 45.7 (CHNCH_2CH), 42.1 (OCCH), 40.5 ($\text{CCH}_2\text{CH}_2\text{CH}_2\text{C}$), 36.1 ($\text{NCH}(\text{CH}_2)_2$), 30.9 (CCH_3), 30.7 (CCH_3), 27.2 ($\text{CCHCH}_2\text{CH}_2$), 26.3 ($\text{CHNCH}_2\text{CH}_2$), 24.8 ($\text{CHN}(\text{CH}_2)_2\text{CH}_2$, CHCH_2CH_2), 19.2 (CCH_2CH_2), 14.3 (CH_2CH_3) ppm; HRESIMS m/z (pos): 391.3317 $\text{C}_{24}\text{H}_{43}\text{N}_2\text{O}_2$ (calcd. 391.3319).

***rac*-Ethyl 1-[4-(3,7-diphenyl-10-azatricyclo[5.3.1.0^{3,8}]undecan-10-yl)butyl]piperidine-3-carboxylate *rac*-19m**

According to **GP3**: Tricyclic imine **10f** (30 mg, 0.10 mmol, 1 equiv), sodium cyanoborohydride (33 mg, 0.50 mmol, 5 equiv), hydrochloric acid (36 mg, 1.0 mmol, 1.0 mL, 10 equiv), sodium triacetoxyborohydride (53 mg, 0.25 mmol, 2.5 equiv), acetic acid (13 mg, 0.21 mmol, 12 μL , 2.1 equiv), ethyl 1-(4,4-dimethoxybutyl)piperidine-3-carboxylate *rac*-**15f** (55 mg, 0.20 mmol, 2 equiv) and $\text{FeCl}_3 \cdot 6\text{H}_2\text{O}$ (151 mg, 0.560 mmol, 5.6 equiv). The reaction was stirred at 40 $^\circ\text{C}$ for 12 h. The crude product was purified by FC and RP-MPLC. The product was obtained as colorless oil (18 mg, 35%). IR (film) $\tilde{\nu}$ = 3055, 2933, 2854, 2802, 1730, 1597, 1495, 1444, 1369, 1304, 1178, 1151, 1031, 758, 700 cm^{-1} ; ^1H NMR (400 MHz, CD_2Cl_2): δ = 7.50 (d, J = 8.2 Hz, 4 H, CCHCH), 7.41–7.30 (m, 4 H, CCHCH), 7.19 (t, J = 7.3 Hz, 2 H, CCHCHCH), 4.07 (q, J = 7.1 Hz, 2 H, OCH_2), 2.89–2.85 (m, 1 H, NCH), 2.82 (d, J = 10.2 Hz, 1 H, $\text{OCCHCH}_2^{\text{a}}\text{N}$), 2.60 (d, J = 11.0 Hz, 1 H, $\text{CHCH}_2\text{CH}_2\text{CH}_2^{\text{a}}$), 2.56 (dd, J = 13.0/ 3.0 Hz, 2 H, $\text{NCH}(\text{CH}_2^{\text{a}})_2$), 2.49 (d, J = 2.4 Hz, 2 H, CHNCH_2CH), 2.44 (tt, J = 10.4/ 3.8 Hz, 1 H, OCCH), 2.35 (s, 1 H, CHCH_2NCH), 2.21–2.10 (m, 4 H, $\text{CHN}(\text{CH}_2)_3\text{CH}_2$, $\text{CHNCH}_2\text{CH}_2$), 2.01 (t, J = 10.3 Hz, 1 H, $\text{OCCHCH}_2^{\text{b}}\text{N}$), 1.93–1.78 (m, 5 H, $\text{CHCH}_2^{\text{a}}\text{CH}_2$, $\text{CHCH}_2\text{CH}_2\text{CH}_2^{\text{b}}$, $\text{NCH}(\text{CH}_2^{\text{b}})_2$, $\text{CCH}_2\text{CH}_2^{\text{a}}$), 1.67–1.33 (m, 8 H, $\text{CHCH}_2^{\text{b}}\text{CH}_2$, CHCH_2CH_2 , $\text{CCH}_2\text{CH}_2^{\text{b}}$, $\text{CCH}_2\text{CH}_2\text{CH}_2\text{C}$), 1.33–1.25 (m, 2 H, $\text{CHNCH}_2\text{CH}_2$), 1.25–1.12 (m, 5 H, CH_3 , $\text{CHN}(\text{CH}_2)_2\text{CH}_2$) ppm; ^{13}C NMR (100 MHz, CD_2Cl_2) δ = 174.5 (CO), 152.0 (CH_2CC), 128.5

(CCHCH), 126.7 (CCHCH), 125.6 (CCHCHCH), 60.5 (OCH₂), 59.0 (CHN(CH₂)₃CH₂), 56.3 (CHNCH₂CH₂), 56.0 (OCCHCH₂N), 54.1 (CHCH₂CH₂CH₂), 51.5 (NCH), 49.3 (CHNCH₂CH), 43.8 (CCH₂CH₂CH₂C), 42.4 (OCCH), 40.2 (CCH₂), 39.1 (CHNCH₂CH), 36.0 (NCH(CH₂)₂), 27.5 (CH₂CH₂CH), 26.8 (CHN(CH₂)₂CH₂), 25.1 (CHCH₂CH₂), 24.9 (CHNCH₂CH₂), 20.6 (CCH₂CH₂), 14.4 (CH₃) ppm; HRESIMS *m/z* (pos): 515.3632 C₃₄H₄₇N₂O₂ (calcd. 515.3632).

Biological evaluation

[³H]GABA uptake assays: The [³H]GABA uptake assays were performed as previously described with intact HEK293 cells stably expressing mGAT1, mGAT2, mGAT3, mGAT4 in a 96-well plate format (Kragler et al. 2008).

MS Binding Assays: For the MS binding assays mGAT1 membrane preparations, obtained from a stable HEK293 cell line, and NO711 as native MS marker were employed in competitive binding experiments as described earlier (Zepperitz et al. 2006).

Results and Discussion

Synthesis

As direct precursors for the preparation of the target compounds *rac*-**11** their carboxylic acid esters *rac*-**19** should be employed. Their synthesis should be accomplished by linking of the tricyclic amines **14** with suitable *N*-substituted nipecotic acid derivatives via reductive amination. Accordingly, besides the tricyclic amines **14**, which should be accessible from the tricyclic imines **10** by reduction, nipecotic acid derivatives carrying *N*-alkyl substituents with an aldehyde function at the terminal position of the *N*-alkyl chain were needed. These nipecotic acid derivatives with *N*-alkyl chains of different lengths between the amino nitrogen and the terminal aldehyde function, *rac*-**12** and *rac*-**13**, should be generated from suitable precursors, *rac*-**15**, in which the aldehyde function is present in masked form, for instance as alcohol or acetal group.

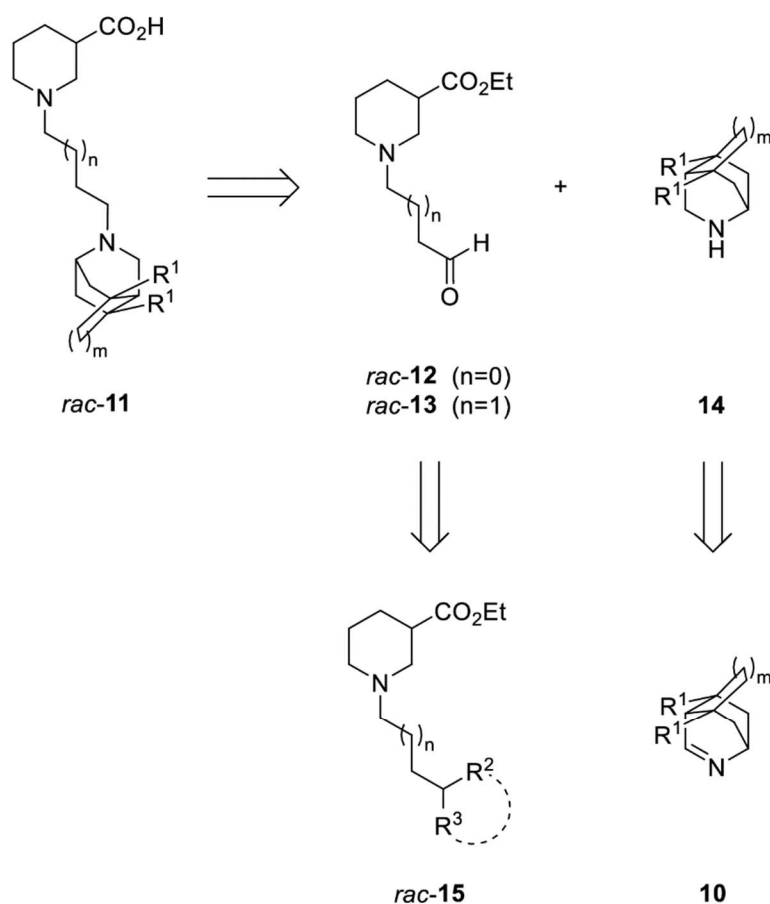


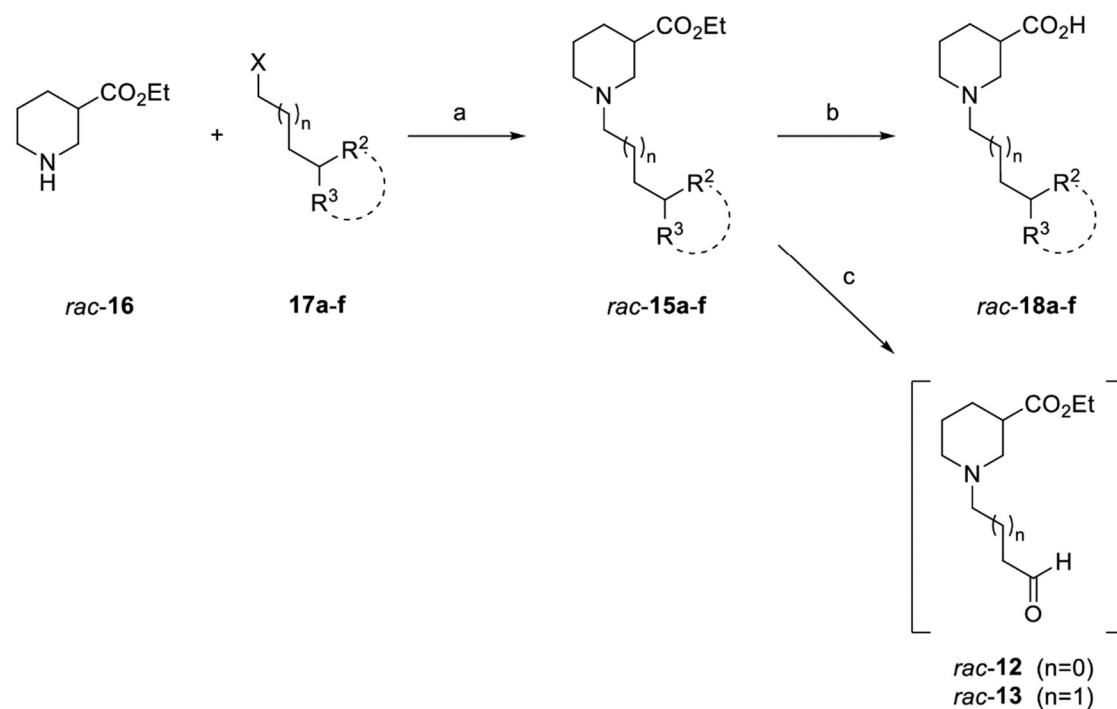
Figure 4: Retrosynthetic analysis of the targeted *N*-substituted nipecotic acid derivatives *rac-11*.

Preparation of the aldehyde precursors *rac-15a-f* and generation of the aldehydes *rac-12-13*

The required nipecotic acid derivatives with an *N*-alkyl residue with a terminal alcohol or acetal function, *rac-15a-f*, were obtained by *N*-alkylation of racemic ethyl nipecotate *rac-16* with ω -hydroxy and ω -dimethoxy substituted *n*-propyl- and *n*-butylhalides **17a-b** and **17e-f** and the ω -(1,3-dioxolane-2-yl) substituted ethyl- and *n*-propylhalides **17c-d**, respectively, in good to excellent yields (Table 1, entries 1-6). The synthesis of alcohol *rac-15a* was performed according to a procedure described by Dhar et al. (Dhar et al. 1994), which method was also used for the construction of *rac-15b-f*. As besides the aldehyde precursors *rac-15a-f* also the corresponding free carboxylic acids *rac-18a-f* should be evaluated for their inhibitory potency at mGAT1-mGAT4 the later were synthesized as well. This was accomplished by treating *rac-15a-f* with $Ba(OH)_2 \cdot 8 H_2O$ in analogy to a literature procedure (Böck et al. 2020), which led to *rac-18a-f* in moderate to excellent yields (43-92%, Table 1, entries 1-6).

With the aldehyde precursors *rac*-**15a-f** in hand, the synthesis of the aldehydes *rac*-**12-13** was studied. Attempts to access the aldehydes *rac*-**12-13** by oxidation of the alcohols *rac*-**15a-b** showed, that even using mild oxidation conditions, e.g. Swern-, Parikh-Doering or Dess-Martin periodinane oxidation, the desired aldehydes were not formed or only in traces. As, in addition, the starting material had been completely consumed and a multitude of side products appeared, this approach was dismissed. Instead attempts to deprotect the acetals *rac*-**15c-f** were undertaken. In this regard, only reaction conditions that should allow to deprotect the acetals without affecting the ester function were taken into account. Although several deprotection protocols were tested [I₂, acetone (Sun et al. 2004); TMSOTf, 2,6-lutidine, CH₂Cl₂ (Fujioka et al. 2004); pyridinium *p*-toluenesulfonate, THF/H₂O (Denmark and Gomez 2003); FeCl₃ · 6 H₂O, CH₂Cl₂ (Sen et al. 1997); HCl, MeCN/H₂O (Rancati et al. 2016)], the cyclic acetals *rac*-**15c-d** proved to be too stable and showed only marginal or no aldehyde formation. In contrast, the dimethyl acetals *rac*-**15e-f** were easily deprotected by treatment with FeCl₃ · 6 H₂O in CH₂Cl₂ according to a procedure of Sen et al. Analysis of the crude product from the cleavage reaction of dimethyl acetal *rac*-**15f** directly after aqueous workup by ¹H NMR spectroscopy showed predominant formation of aldehyde **13** (n = 1) and only low amounts of remaining dimethyl acetal *rac*-**15f**. However, the crude aldehyde *rac*-**13** was contaminated with unknown side products, resulting from decomposition most likely, which in addition to the dimethyl acetal *rac*-**15f** could not be separated from the desired compound *rac*-**13**. A similar situation was observed when the deprotection of dimethyl acetal *rac*-**15e** to aldehyde *rac*-**12** was attempted. In consequence, the crude aldehydes *rac*-**12-13** should be directly used for the subsequent reductive amination without prior chromatographic purification and without any delay.

Table 1: Synthesis of the nipecotic acid derived aldehyde precursors *rac-15a-f* and their hydrolysis to the carboxylic acids *rac-18a-f*.



Entry	Halide	X	n	R ²	R ³	Ester	Yield	Acid	Yield
1	17a	Br	0	OH	H	<i>rac-15a</i> ⁽¹⁾	95	<i>rac-18a</i>	84
2	17b	Br	1	OH	H	<i>rac-15b</i>	95	<i>rac-18b</i>	71
3	17c	Br	0	OCH ₂ CH ₂ O		<i>rac-15c</i>	93	<i>rac-18c</i>	88
4	17d	Cl	1	OCH ₂ CH ₂ O		<i>rac-15d</i>	79	<i>rac-18d</i>	92
5	17e	Br	0	OMe	OMe	<i>rac-15e</i>	68	<i>rac-18e</i>	63
6	17f	Cl	1	OMe	OMe	<i>rac-15f</i>	74	<i>rac-18f</i>	43

Reagents and conditions: (a) K₂CO₃, NaI, neat, acetone or 1,4-dioxane; (b) Ba(OH)₂ · 8 H₂O, MeOH/H₂O; (c) various conditions tested, for *rac-15e-f*: FeCl₃ · 6 H₂O, CH₂Cl₂. (1) Synthesis according to literature (Dhar et al. 1994).

Reduction of the imines **10a-f** and synthesis of the target compounds *rac-11a-m*

The amines **14a-f**, required for the reductive amination of *rac-12* and *rac-13*, were synthesized by reduction of the tricyclic imines **10a-f**. The use of NaBH₃CN under acidic conditions seemed well suited for this purpose as it had been successfully applied for the reduction of related tricyclic imines with an 2-azabicyclo[2.2.2]octane scaffold (Schmaunz et al. 2014). Indeed, when imines **10a-f** were treated with NaBH₃CN and HCl in methanol the corresponding amines **14a-f** were formed. Unfortunately, amines **14a-b** (bridge size m = 0) were found to be unstable and to decompose quickly, whereas amines **14c-f** did not show such a behavior. Hence,

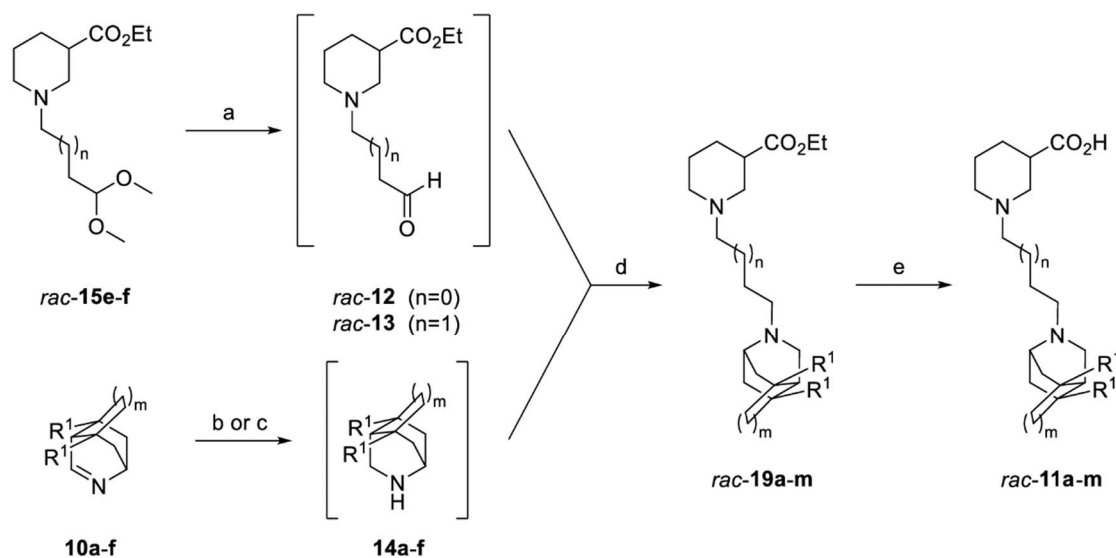
in addition to the aldehydes *rac*-**12-13**, it seemed best to use also amines **14a-f** directly after their formation without prior purification and isolation.

Considering that both, the aldehydes *rac*-**12-13** and amines **14a-f** had appeared to be labile to some extent, we intended to generate and directly subject them to the next reaction step, the reductive amination to give the respective esters *rac*-**19**. Thus, for the overall reaction sequence first acetals *rac*-**15e-f** should be cleaved by treatment with $\text{FeCl}_3 \cdot 6 \text{H}_2\text{O}$ in CH_2Cl_2 . Then the respective aldehyde should be added to a mixture of imine and reducing agent, which was premixed to mediate imine reduction and to allow subsequent reductive amination of the aldehyde function of *rac*-**12** or *rac*-**13** with the formed amine. When in a test reaction aldehyde **13** was added to a mixture of an imine, structurally similar to imine **10c** but with one of the methyl residues substituted by hydrogen (for a depiction of the structure see compound *rac*-14a in Rudy and Wanner, 2019), and NaBH_3CN , that had proven well suited for the reduction of the imines **10** to the corresponding amines **14**, besides the reductive amination product also the alcohol *rac*-**15b** resulting from the reduction of aldehyde *rac*-**13** was obtained. However, when the mild reducing agent $\text{NaBH}(\text{OAc})_3$ (Abdel-Magid et al. 1996, Abdel-Magid 2006) in combination with acetic acid was used instead of NaBH_3CN no such unfavorable reaction occurred. Thus, starting from dimethyl acetal *rac*-**15f** and the imines **10a-d** the esters *rac*-**19g-k** were obtained in moderate to good yields (Table 2, entries 7-10). This method could also successfully be applied to the reductive coupling of dimethyl acetal *rac*-**15e** – via the corresponding aldehyde *rac*-**12** – with the imines **10a-d** to give the desired esters *rac*-**19a-d**. However, in these cases the yields were poor (Table 2, entries 1-4), which is likely to be attributed to the instability of the intermediate aldehyde *rac*-**12** and its propensity to undergo a retro-Michael addition leading to further side reactions.

Unfortunately, reaction of imines **10e-f** with *in situ* generated aldehydes *rac*-**12** and *rac*-**13** did not lead to the desired products, the nipecotic acid esters *rac*-**19e-f** and *rac*-**19l-m** under the aforementioned reaction conditions. Actually, despite treatment with $\text{NaBH}(\text{OAc})_3$ imines **10e-f** remained unchanged, indicating that they are less reactive than compounds **10a-d**. This is likely to be due to a more severe shielding of the imine function by the adjacent R^1 groups as a result of the larger “upper” bridge ($m = 2$) in **10e-f** as it was claimed before in cycloaddition reactions performed with these compounds (Rudy et al. 2020). To overcome this problem the aforementioned procedure was changed as follows: Instead of $\text{NaBH}(\text{OAc})_3$ NaBH_3CN was employed for the reduction of imines **10e-f** to the amines **14e-f**. Then, when the conversion to the amines **14e-f** had gone to completion according to TLC, excess reducing agent was removed by basic-aqueous workup and the crude amines were reacted with $\text{NaBH}(\text{OAc})_3$ and the

aldehydes *rac-12-13* in analogy to the original procedure. That way, the remaining esters *rac-19e-f* and *rac-19l-m* could finally be obtained in yields of 34-37% (Table 2, entries 5-6 and 11-12). Basic hydrolysis of the esters *rac-19a-m* with $\text{Ba}(\text{OH})_2 \cdot 8 \text{H}_2\text{O}$ according to a literature procedure (Böck et al. 2020) provided finally the desired carboxylic acids *rac-11a-m* in moderate to excellent yields (53% - 98%).

Table 2: Synthesis of the target compounds *rac-11a-m* with tricyclic amines as lipophilic residues.



Entry	Imine	R^1	m	Acetal	n	Ester	Yield	Acid	Yield
1	10a	Me	0	<i>rac-15e</i>	0	<i>rac-19a</i>	27	<i>rac-11a</i>	87
2	10b	Ph	0	<i>rac-15e</i>	0	<i>rac-19b</i>	23	<i>rac-11b</i>	91
3	10c	Me	1	<i>rac-15e</i>	0	<i>rac-19c</i>	26	<i>rac-11c</i>	70
4	10d	Ph	1	<i>rac-15e</i>	0	<i>rac-19d</i>	25	<i>rac-11d</i>	84
5	10e	Me	2	<i>rac-15e</i>	0	<i>rac-19e</i>	37	<i>rac-11e</i>	81
6	10f	Ph	2	<i>rac-15e</i>	0	<i>rac-19f</i>	34	<i>rac-11f</i>	73
7	10a	Me	0	<i>rac-15f</i>	1	<i>rac-19g</i>	44	<i>rac-11g</i>	77
8	10b	Ph	0	<i>rac-15f</i>	1	<i>rac-19h</i>	47	<i>rac-11h</i>	98
9	10c	Me	1	<i>rac-15f</i>	1	<i>rac-19j</i>	73	<i>rac-11j</i>	97
10	10d	Ph	1	<i>rac-15f</i>	1	<i>rac-19k</i>	72	<i>rac-11k</i>	65
11	10e	Me	2	<i>rac-15f</i>	1	<i>rac-19l</i>	36	<i>rac-11l</i>	96
12	10f	Ph	2	<i>rac-15f</i>	1	<i>rac-19m</i>	35	<i>rac-11m</i>	53

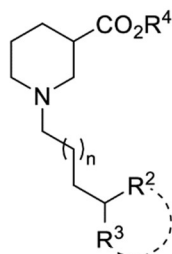
Reagents and conditions: (a) $\text{FeCl}_3 \cdot 6 \text{H}_2\text{O}$, CH_2Cl_2 ; (b) Reduction of **10a-d**: $\text{NaBH}(\text{OAc})_3$, AcOH, CH_2Cl_2 ; (c) Reduction of **10e-f**: NaBH_3CN , HCl, MeOH; (d) $\text{NaBH}(\text{OAc})_3$, AcOH, CH_2Cl_2 ; (e) $\text{Ba}(\text{OH})_2 \cdot 8 \text{H}_2\text{O}$, MeOH/ H_2O .

Biological Evaluation

For the evaluation of the inhibitory potencies of the nipecotic acid derivatives *rac-11a-m* exhibiting a free carboxylic acid function and a fully established lipophilic domain, as well as of *rac-18a-f* possessing only small *N*-substituents and their corresponding esters *rac-15a-f* and *rac-19a-m* at the different GAT subtypes mGAT1-mGAT4 a standardized [³H]GABA uptake assay was used (Kragler et al. 2008). HEK293 cell lines, each stably expressing one individual subtype of the GABA transporters, represent the basis of this assay. Additionally, with a MS Binding Assay the binding affinities towards mGAT1 were determined using NO711 as native MS marker. If the tested compounds did not reduce the [³H]GABA uptake or NO711 marker binding significantly below 50% in preliminary experiments at a concentration of 100 μM, which corresponds to a pIC₅₀ of ≤ 4.0 and a pK_i of ≤ 4.0 respectively, only percent values of the remaining [³H]GABA uptake or NO711 marker binding are given. In case of a significant reduction of the [³H]GABA uptake or NO711 marker binding below 50% at an inhibitor concentration of 100 μM, the inhibitory potency (pIC₅₀) and the binding affinity (pK_i), respectively, were determined in a single experiment performed in triplicates.

As Tiagabine (**6**), NO711 (**7**), (*S*)-SNAP-5114 (**8**) or Deramciclane (*rac-9*) represent prototypic GAT inhibitors, they provide important reference values for the estimation of the biological activities of the newly synthesized and tested compounds described in this paper, despite the marked differences in their chemical structures. When considering the values of these reference compounds (see Figure 2), it must be noted that these were partially obtained for enantiomerically pure [Tiagabine, (*S*)-SNAP-5114] or achiral (NO711) GAT inhibitors, whereas the substances displayed in this work are racemic mixtures.

Table 3: Binding affinities and inhibitory potencies of nipecotic acid derivatives *rac-15a-f* and *rac-18a-f*.



Entry	Compound	R ²	R ³	n	R ⁴	pIC ₅₀ [a]				
						pK _i [a]	mGAT1	mGAT2	mGAT3	mGAT4
1	<i>rac-15a</i>	OH	H	0	Et	91%	113%	89%	110%	99%
2	<i>rac-18a</i>	OH	H	0	H	82%	67%	82%	81%	87%
3	<i>rac-15b</i>	OH	H	1	Et	91%	111%	97%	103%	89%
4	<i>rac-18b</i>	OH	H	1	H	96%	87%	93%	80%	96%
5	<i>rac-15c</i>	OCH ₂ CH ₂ O		0	Et	82%	104%	72%	92%	96%
6	<i>rac-18c</i>	OCH ₂ CH ₂ O		0	H	104%	71%	76%	70%	83%
7	<i>rac-15d</i>	OCH ₂ CH ₂ O		1	Et	86%	95%	88%	103%	85%
8	<i>rac-18d</i>	OCH ₂ CH ₂ O		1	H	103%	87%	92%	81%	89%
9	<i>rac-15e</i>	OMe	OMe	0	Et	90%	93%	82%	106%	96%
10	<i>rac-18e</i>	OMe	OMe	0	H	98%	50%	89%	61%	69%
11	<i>rac-15f</i>	OMe	OMe	1	Et	87%	100%	89%	89%	100%
12	<i>rac-18f</i>	OMe	OMe	1	H	97%	46%	97%	74%	75%

[a] All values were determined in one experiment performed in triplicate. The results of the MS binding assay are given as pK_i, the results of the [³H]GABA uptake assay as pIC₅₀. Percent values indicate remaining specific NO711 binding or remaining [³H]GABA uptake, respectively, in presence of 100 μM test compound.

The initially tested nipecotic acid esters *rac-15a-f*, that had been synthesized to serve as synthetic intermediates for the introduction of the tricyclic cage unit, and the corresponding carboxylic acids *rac-18a-f* displayed only very weak to negligible inhibitory potency and affinity. Only the dimethoxy substituted nipecotic acid derivatives *rac-18e* and *rac-18f* showed weak inhibitory potency at mGAT1 the remaining [³H]GABA uptake amounting to 50% and 46%, respectively, at a test compound concentration of 100 μM. In addition, these compounds displayed inhibitory potency at mGAT3 and mGAT4, though this was even lower than that at

mGAT1 with values for the remaining [³H]GABA uptake in the range of 61% - 75% (Table 3, entries 10 and 12).

Due to their structural similarity it seemed appropriate to compare the test results for the synthesized carboxylic acids *rac-11a-m* and carboxylic acid esters *rac-19a-m* exhibiting a tricyclic residue as lipophilic domain among each other as this should provide insight on the influence of the spacer length (n), the bridge size (m) and the residues (R) on the biological activity. The comparison of test results of carboxylic acids of identical structure varying only in their spacer lengths (n = 0 or n = 1) among each other showed no significant impact of the spacer length on the biological activity for most structures. Only for the two nipecotic acid derivatives *rac-11g* and *rac-11k* with a butyl spacer improved inhibitory potencies were observed compared to their analogues with a propyl spacer *rac-11a* and *rac-11d*. For compound *rac-11g* a pIC₅₀ of 4.25 at mGAT1 was determined, whereas the structurally related carboxylic acid *rac-11a* with a propyl spacer could only reduce the [³H]GABA uptake to 66%. Even more pronounced was the effect for carboxylic acid *rac-11k* for which a pIC₅₀ of 4.40 at mGAT1 and a remaining [³H]GABA uptake of 45% at mGAT2 was found. The corresponding nipecotic acid derivate *rac-11d* with a propyl spacer merely reduced the [³H]GABA uptake to 66% at mGAT1 and to 79% at mGAT2.

A comparative analysis of the biological activity of carboxylic acid esters *rac-19a-m* among each other to study the influence of the spacer length led to diverging results. For some esters of otherwise identical structure the variation of the spacer length did not seem to affect the results of the biological testing (compare: *rac-19a* and *rac-19g*; *rac-19e* and *rac-19i*). However, most nipecotic acid ester derivatives showed differences in the biological activity at the different GAT subtypes when the spacer length was altered. The carboxylic ester *rac-19b* substituted with phenyl residues and equipped with a methylene bridge (m = 0) and a propyl spacer (n = 0) exhibited higher inhibitory potencies at mGAT2 and mGAT3 with pIC₅₀ values of 4.53 and 4.43, respectively, compared to its analogue *rac-19h* with a butyl spacer. Yet this analogue *rac-19h* displayed a higher inhibitory potency at mGAT4 with a pIC₅₀ value of 4.89, whereas the potencies at mGAT1 were almost identical. Nipecotic acid ester derivative *rac-19c* with a C₃-spacer reached lower remaining [³H]GABA uptake with values ranging from 50% - 60% at mGAT2-mGAT4 as compared to its structural analogue *rac-19j* with a C₄-spacer. For the phenyl substituted ester *rac-19k* with a butyl spacer (n = 1) and a C₂-bridge (m = 1) at mGAT1-mGAT3 inhibitory potencies with pIC₅₀ values ranging from 4.60-4.65 were observed, whereas the related ester *rac-19d* with a propyl spacer proved to be

less biologically active at mGAT1-mGAT3 and to have an identical activity at mGAT4. Finally, compound *rac-19f* displaying phenyl residues, a C₃-bridge ($m = 2$) and a propyl spacer ($n = 0$) had a considerably higher activity at mGAT2 and mGAT3 with pIC₅₀ values of 4.28 and 4.97, respectively, but also a lower one at mGAT4 as compared to the analogous ester *rac-19m* with a butyl spacer, who had pIC₅₀ of 4.33 at mGAT4. Unfortunately, these results did not indicate a universal trend for the inhibitory potency at mGAT1-mGAT4 when the spacer length was altered.

Further analysis of the biological activity of carboxylic acids *rac-11a-m* by comparing structures deviating only in their attached residues R¹, being either methyl or phenyl residues, showed that for most of the carboxylic acids the residue had a very small to negligible effect on the inhibitory potency at mGAT1-mGAT4 (compare *rac-11a* and *rac-11b*; *rac-11c* and *rac-11d*; *rac-11e* and *rac-11f*; *rac-11i* and *rac-11m*). Exceptions are the methyl substituted nipecotic acid derivative *rac-11g* with a butyl spacer ($n = 1$) and a methylene bridge ($m = 0$), which had an improved inhibitory potency at mGAT1 with a pIC₅₀ of 4.25 as compared to its phenyl substituted analogue *rac-11h*, and the phenyl substituted nipecotic acid derivative *rac-11k* with a butyl spacer ($n = 1$) and a C₂-bridge ($m = 1$), that had a higher biological activity at mGAT1 and mGAT2 with a pIC₅₀ of 4.40 and a remaining [³H]GABA uptake of 45%, respectively, as compared to its related methyl substituted carboxylic acid *rac-11j*.

When taking a look at the carboxylic acid esters *rac-19a-m* it became evident that almost always the phenyl substituted esters had higher inhibitory potencies at mGAT1-mGAT4 than their otherwise identical methyl substituted analogues. This observation is nicely highlighted by ester *rac-19k* with pIC₅₀ values in a range of 4.60 to 4.65 at mGAT1-mGAT4, which are in strong contrast to the biological results obtained for the related, basically inactive methyl substituted ester *rac-19j*. Obviously, the aromatic phenyl residue in the nipecotic acid ester derived GAT inhibitors seems to be necessary as structural element to achieve a reasonable activity at all GAT subtypes.

The examination of the influence of the bridge size (m) on the biological activity of the carboxylic acids *rac-11a-m* at mGAT1-mGAT4 led to contradictory results. For the methyl substituted nipecotic acid derivatives *rac-11a*, *rac-11c* and *rac-11e* with a propyl spacer ($n = 0$) no significant effect of the bridge size on the inhibitory potencies at mGAT1-mGAT4 could be observed. Also, the methyl substituted carboxylic acids *rac-11g*, *rac-11j* and *rac-11i* with a butyl spacer ($n = 1$) showed similar biological activities at mGAT2-mGAT4 despite their

varying bridge size ($m = 0-2$) and only at mGAT1 a preference for the carboxylic acid *rac-11g* with the smallest bridge size ($m = 0$), for which a pIC_{50} of 4.25 was found, could be noticed. The comparison of the phenyl substituted carboxylic acids *rac-11b*, *rac-11d* and *rac-11f* with a propyl spacer ($n = 0$) among each other indicated a preference for structures with smaller bridge sizes with regard to biological activity at mGAT1 and mGAT3 as the remaining [3H]GABA uptake declined from 82% to 52% at mGAT1 and from 90% to 67% at mGAT3 with decreasing bridge size. For these structures at mGAT4 no influence of the bridge size on the biological activity was observed and at mGAT2 only a weak preference for carboxylic acid *rac-11f* with a C_3 -bridge was recognized. The comparative analysis of the phenyl substituted carboxylic acids *rac-11h*, *rac-11k* and *rac-11m* with a butyl spacer ($n = 1$), in contrast, showed a preference for the medium sized bridge ($m = 1$) for the biological activity at mGAT1-mGAT3, as the best inhibitory potencies with a pIC_{50} value of 4.40 at mGAT1 and remaining [3H]GABA uptakes of 45%-58% at mGAT2-mGAT3 were determined for carboxylic acid *rac-11k*.

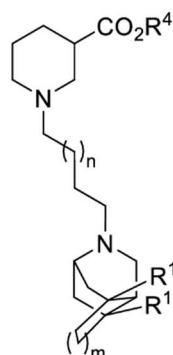
In addition, the influence of the bridge size (m) on the biological activity was studied for the carboxylic acid esters *rac-19a-m*. When the esters *rac-19a*, *rac-19c* and *rac-19e*, all equipped with methyl residues and a propyl spacer ($n = 0$), were compared among each other, only for the inhibitory potency at mGAT4 the bridge size seemed to be important to some extent. Here ester *rac-19c* with a medium sized C_2 -bridge ($m = 1$) reducing the remaining [3H]GABA uptake to 54% at a test compound concentration of 100 μM proved to be best. Also, the biological activity of the methyl substituted esters *rac-19g*, *rac-19j* and *rac-19l* with a butyl spacer ($n = 1$) at mGAT2-mGAT4 appeared to be rather unaffected by the bridge size of these compounds. Solely, according to the results of the inhibitory potencies at mGAT1, a methylene bridge ($m = 0$) mediates a slightly higher potency at this GAT subtype (see ester *rac-19g*). The comparative analysis of the test results of the phenyl substituted esters *rac-19b*, *rac-19d* and *rac-19f* with a C_3 -spacer ($n = 0$) showed, that ester *rac-19f* with the largest bridge size ($m = 2$) turned out best to address mGAT3, with a pIC_{50} value of 4.97, whereas, in order to address mGAT2, ester *rac-19b* with the smallest bridge size ($m = 0$) led to the best result (pIC_{50} of 4.53). The esters *rac-19b*, *rac-19d* with a small or medium sized bridge were equally suited to address mGAT4. As the esters *rac-19b*, *rac-19d* and *rac-19f* displayed almost equal inhibitory potencies at mGAT1, no effect of the bridge size on the biological activity at this GAT subtype could be noticed. Finally, the structurally related phenyl substituted esters *rac-19h*, *rac-19k* and *rac-19m* with a butyl spacer ($n = 1$) were compared among each other to study the influence of the bridge size on the biological activity for these compounds. Ester *rac-19k* with a medium

sized bridge ($m = 1$) demonstrated to be superior as compared to esters *rac-19h* and *rac-19m* with regard to inhibitory activities at mGAT1-mGAT3. Since at mGAT4 the inhibitory potency of esters *rac-19h*, *rac-19k* and *rac-19m* was decreasing with an increase in bridge size, the ester *rac-19h* led with a pIC_{50} value of 4.89 to the best result. However, by the above obtained results no general correlation between the biological activity at a certain GAT subtype and the bridge size (m) in the lipophilic domain of the tested carboxylic acids *rac-11a-m* or their corresponding esters *rac-19a-m* could be concluded.

Interestingly, all phenyl substituted nipecotic acid ester derivatives, i.e. *rac-19b*, *rac-19d*, *rac-19f*, *rac-19h*, *rac-19k* and *rac-19m* exhibited higher inhibitory potencies at mGAT1-mGAT4 than their corresponding carboxylic acids. For the methyl substituted nipecotic acid ester derivatives no such universal effect was observed. The former phenyl substituted nipecotic acid derivatives showed rather equal inhibitory potencies at all four GAT subtypes (Table 4, see entries for compounds *rac-19b*, *rac-19d*, *rac-19k* and *rac-19m*), but also a weak subtype selectivity for mGAT3 and for mGAT4 was achieved with ester *rac-19f* (pIC_{50} value of 4.97 at mGAT3; Table 4, entry 11) and ester *rac-19h* (pIC_{50} value of 4.89 at mGAT4; Table 4, entry 15), respectively. These esters, *rac-19f* and *rac-19h*, represent the first subtype selective GAT inhibitors carrying a cage unit in the lipophilic domain.

Still to be mentioned is the fact, that the binding affinities at mGAT1 determined in binding assays often do not correlate with the inhibitory potencies from mGAT1 uptake assays. This phenomenon, the cause of which is still to be clarified, can be seen for example in case of ester *rac-19k*. This compound, *rac-19k*, exhibits a pIC_{50} value of 4.60 at mGAT1 in the uptake assay, but a reduction of remaining NO711 marker binding in the binding assay to 84% only (at a test compound concentration of 100 μ M).

Table 4: Nipecotic acid derivatives possessing various tricyclic amines as substituents and their binding affinities and inhibitory potencies.



Entry	Compound	R ¹	m	n	R ⁴	pK _i [a]		pIC ₅₀ [a]		
						mGAT1	mGAT1	mGAT2	mGAT3	mGAT4
1	<i>rac</i> - 19a	Me	0	0	Et	95%	66%	61%	81%	69%
2	<i>rac</i> - 11a	Me	0	0	H	82%	66%	78%	73%	81%
3	<i>rac</i> - 19b	Ph	0	0	Et	4.62	4.32	4.53	4.46	4.59
4	<i>rac</i> - 11b	Ph	0	0	H	68%	52%	79%	67%	68%
5	<i>rac</i> - 19c	Me	1	0	Et	72%	86%	50%	60%	54%
6	<i>rac</i> - 11c	Me	1	0	H	76%	50%	83%	75%	77%
7	<i>rac</i> - 19d	Ph	1	0	Et	60%	4.37	58%	4.29	4.65
8	<i>rac</i> - 11d	Ph	1	0	H	104%	66%	79%	79%	69%
9	<i>rac</i> - 19e	Me	2	0	Et	89%	69%	76%	77%	89%
10	<i>rac</i> - 11e	Me	2	0	H	88%	62%	72%	74%	87%
11	<i>rac</i> - 19f	Ph	2	0	Et	78%	4.14	4.28	4.97	62%
12	<i>rac</i> - 11f	Ph	2	0	H	98%	83%	57%	90%	71%
13	<i>rac</i> - 19g	Me	0	1	Et	95%	59%	60%	77%	62%
14	<i>rac</i> - 11g	Me	0	1	H	84%	4.25	80%	61%	71%
15	<i>rac</i> - 19h	Ph	0	1	Et	81%	4.35	4.00	4.13	4.89
16	<i>rac</i> - 11h	Ph	0	1	H	82%	67%	79%	77%	80%
17	<i>rac</i> - 19j	Me	1	1	Et	106%	88%	81%	90%	86%
18	<i>rac</i> - 11j	Me	1	1	H	84%	74%	102%	71%	96%
19	<i>rac</i> - 19k	Ph	1	1	Et	84%	4.60	4.61	4.65	4.64
20	<i>rac</i> - 11k	Ph	1	1	H	71%	4.40	45%	58%	83%
21	<i>rac</i> - 19l	Me	2	1	Et	101%	83%	73%	86%	74%

22	<i>rac-11l</i>	Me	2	1	H	89%	78%	85%	79%	86%
23	<i>rac-19m</i>	Ph	2	1	Et	72%	4.18	59%	53%	4.33
24	<i>rac-11m</i>	Ph	2	1	H	104%	83%	76%	105%	76%

[a] All values were determined in one experiment performed in triplicate. The results of the MS binding assay are given as pK_i , the results of the [3H]GABA uptake assay as pIC_{50} . Percent values indicate remaining specific NO711 binding or remaining [3H]GABA uptake, respectively, in presence of 100 μM test compound.

Conclusion

Inspired by the drug Deramciclane (*rac-9*), a new class of GABA uptake inhibitors with bulky and highly rigid tricyclic subunits in the lipophilic domain delineated from the 2-azabicyclo[2.2.2]octane scaffold by the presence of an additional carbon bridge was developed. The polycyclic subunits are connected via a plain hydrocarbon spacer with the amino nitrogen of nipecotic acid or that of the corresponding ethyl ester. For the synthesis of the new compounds, nipecotic acid derivatives with an *N*-alkyl residue displaying a terminal aldehyde function, were connected with symmetric tricyclic amines by reductive amination. The tricyclic amines used were either generated in situ from tricyclic imines serving as precursors directly before the reductive amination by the same reducing agent or they were generated from the tricyclic imines in a separate reaction step. The new GAT inhibitors varied in regard to the spacer length, the size of one of the bridges of the tricyclic skeleton of the lipophilic domain and the substituents attached to the latter. Whereas the nipecotic acid derived GAT inhibitors displayed only weak inhibitory potencies and binding affinities at the four different GABA transporter subtypes, all phenyl substituted nipecotic acid ethyl ester derivatives exhibited moderate biological activity at mGAT1-mGAT4. The structure activity relationship of these GAT inhibitors demonstrated the importance of the phenyl residues and the ester function for the biological activity. Two of the phenyl substituted nipecotic acid ethyl ester derivatives, *rac-19f* and *rac-19h*, being equipped with either a propyl spacer and a C_3 -bridge (*rac-19f*) or a butyl spacer and a methylene bridge (*rac-19h*), showed even moderate subtype selectivity at mGAT3 and mGAT4 respectively. As demonstrated by the obtained results tricyclic cage structures represent promising subunits for the construction of novel GAT inhibitors.

Conflict of interest

The authors declare that they have no conflict of interest.

References

Abdel-Magid AF, Carson KG, Harris BD, Maryanoff CA, Shah RD (1996) Reductive Amination of Aldehydes and Ketones with Sodium Triacetoxyborohydride. Studies on Direct and Indirect Reductive Amination Procedures. *J Org Chem* 61: 3849-3862.

Abdel-Magid AF, Mehrman SJ (2006) A Review on the Use of Sodium Triacetoxyborohydride in the Reductive Amination of Ketones and Aldehydes. *Org Proc Res Dev* 10: 971-1031.

Andersen KE, Braestrup C, Grønwald FC, Jørgensen AS, Nielsen EB, Sonnewald U, Sørensen PO, Suzdak PD, Knutsen LJS (1993) The Synthesis of Novel GABA Uptake Inhibitors. 1. Elucidation of the Structure-Activity Studies Leading to the Choice of (*R*)-1-[4,4-Bis(3-methyl-2-thienyl)-3-butenyl]-3-piperidinecarboxylic Acid (Tiagabine) as an Anticonvulsant Drug Candidate. *J Med Chem* 36: 1716-1725.

Andersen KE, Lau J, Lundt BF, Petersen H, Huusfeldt PO, Suzdak PD, Swedberg MDB (2001) Synthesis of Novel GABA Uptake Inhibitors. Part 6: Preparation and Evaluation of *N*- Ω Asymmetrically Substituted Nipecotic Acid Derivatives. *Bioorg Med Chem* 9: 2773-2785.

Andersen, KE, Sørensen JL, Huusfeldt PO, Knutsen LJS, Lau J, Lundt BF, Petersen H, Suzdak PD, Swedberg MDB (1999) Synthesis of Novel GABA Uptake Inhibitors. 4. Bioisosteric Transformation and Successive Optimization of Known GABA Uptake Inhibitors Leading to a Series of Potent Anticonvulsant Drug Candidates. *J Med Chem* 42: 4281-4291.

Andersen, KE, Sørensen JL, Lau J, Lundt BF, Petersen H, Huusfeldt PO, Suzdak PD, Swedberg MDB (2001) Synthesis of Novel γ -Aminobutyric Acid (GABA) Uptake Inhibitors. 5. Preparation and Structure-Activity Studies of Tricyclic Analogues of Known GABA Uptake Inhibitors. *J Med Chem* 44: 2152-2163.

Błaszczak, JW (2016) Parkinson's Disease and Neurodegeneration: GABA-Collapse Hypothesis. *Front Neurosci* 10 (269).

Böck, MC, Höfner G, Wanner KT (2020) N-Substituted Nipecotic Acids as (*S*)-SNAP-5114 Analogues with Modified Lipophilic Domains. *ChemMedChem* 15: 1-17.

Borden, LA (1996) GABA TRANSPORTER HETEROGENEITY: PHARMACOLOGY AND CELLULAR LOCALIZATION. *Neurochem Int* 29: 335-356.

Brookes, KB, Hickmott PW, Jutle KK, Schreyer CA (1992) Introduction of pharmacophoric groups into polycyclic systems. Part 4. Aziridine, oxiran and tertiary β -hydroxyethylamine derivatives of adamantane. *S Afr J Chem* 45: 8-11.

Christiansen, B, Meinild AK, Jensen AA, Bräuner-Osborne H (2007) Cloning and Characterization of a Functional Human γ -Aminobutyric Acid (GABA) Transporter, Human GAT-2. *J Biol Chem* 282: 19331-19341.

Conti, F, Minelli A, Melone M (2004) GABA transporters in the mammalian cerebral cortex: localization, development and pathological implications. *Brain Res Rev* 45: 196-212.

Denmark SE, Gomez L (2003) Tandem Double Intramolecular [4+2]/[3+2] Cycloadditions of Nitroalkenes. The Fused/Bridged Mode. *J Org Chem* 68: 8015-8024.

Dhar TGM, Borden LA, Tyagarajan S, Smith KE, Branchek TA, Weinshank RL, Gluchowski C (1994) Design, Synthesis and Evaluation of Substituted Triarylnipeptotic Acid Derivatives as GABA Uptake Inhibitors: Identification of a Ligand with Moderate Affinity and Selectivity for the Cloned Human GABA Transporter GAT-3. *J Med Chem* 37: 2334-2342.

Firbank MJ, Parikh J, Murphy N, Killen A, Allan CL, Collerton D, Blamire AM, Taylor JP (2018) Reduced occipital GABA in Parkinson disease with visual hallucinations. *Neurology* 91: 675-685.

Fujioka H, Sawama Y, Murata N, Okitsu T, Kubo O, Matsuda S, Kita Y (2004) Unexpected Highly Chemoselective Deprotection of the Acetals from Aldehydes and Not Ketones: TESOTf-2,6-Lutidine Combination. *J Am Chem Soc* 126: 11800-11801.

Fulmer GR, Miller AJM, Sherden NH, Gottlieb HE, Nudelman A, Stoltz BM, Bercaw JE, Goldberg KI (2010) NMR Chemical Shifts of Trace Impurities: Common Laboratory Solvents, Organics, and Gases in Deuterated Solvents Relevant to the Organometallic Chemist. *Organometallics* 29: 2176–2179.

Gether U, Andersen PH, Larsson OM, Schousboe A (2006) Neurotransmitter transporters: molecular function of important drug targets. *Trends Pharmacol Sci* 27: 375-383.

Guzmán BCF, Vinnakota C, Govindpani K, Waldvogel HJ, Faull RLM, Kwakowsky A (2018) The GABAergic system as a therapeutic target for Alzheimer's disease. *J Neurochem* 146: 649-669.

Jin XT, Galvan A, Wichmann T, Smith Y (2011) Localization and function of GABA transporters GAT-1 and GAT-3 in the basal ganglia. *Front Syst Neurosci* 5 63.

Joubert J, Geldenhuys WJ, van der Schyf CJ, Oliver DW, Kruger HG, Govender T, Malan SF (2012) Polycyclic cage structures as lipophilic scaffolds for neuroactive drugs. *ChemMedChem* 7: 375-384.

Kalueff AV, Nutt DJ (2007) ROLE OF GABA IN ANXIETY AND DEPRESSION. *Depression and Anxiety* 24: 495-517.

Kerscher-Hack S, Renukappa-Gutke T, Höfner G, Wanner KT (2016) Synthesis and biological evaluation of a series of N-alkylated imidazole alcanoic acids as mGAT3 selective GABA uptake inhibitors. *Eur J Med Chem* 124: 852-880.

Kleppner SR, Tobin AJ (2001) GABA signalling: therapeutic targets for epilepsy, Parkinson's disease and Huntington's disease. *Expert Opin Ther Targets* 5: 219-239.

- Knutsen LJS, Andersen KE, Lau J, Lundt BF, Henry RF, Morton HE, Nærum L, Petersen H, Stephensen H, Suzdak PD, Swedberg MDB, Thomsen C, Sørensen PO (1999) Synthesis of Novel GABA Uptake Inhibitors. 3. Diaryloxime and Diarylvinyl Ether Derivatives of Nipecotnic Acid and Guvacine as Anticonvulsant Agents. *J Med Chem* 42: 3447-3462.
- Kovács I, Maksay G, Simonyi M (1989) Inhibition of high-affinity synaptosomal uptake of gamma-aminobutyric acid by a bicyclo-heptane derivative. *Arzneimittelforschung* 39: 295-297.
- Kragler A, Höfner G, Wanner KT (2008) Synthesis and biological evaluation of aminomethylphenol derivatives as inhibitors of the murine GABA transporters mGAT1-GAT4. *Eur J Med Chem* 43: 2404-2411.
- Kristensen AS, Andersen J, Jorgensen TN, Sorensen L, Eriksen J, Loland CJ, Stromgaard K, Gether U (2011) SLC6 Neurotransmitter Transporters: Structure, Function, and Regulation. *Pharmacol Rev* 63: 585-640.
- Krogsgaard-Larsen P (1988) GABA Synaptic Mechanisms: Stereochemical and Conformational Requirements. *Med Res Rev* 8: 27-56.
- Lancot KL, Herrmann N, Mazzotta P, Khan LR, Ingber N (2004) GABAergic Function in Alzheimer's Disease: Evidence for Dysfunction and Potential as a Therapeutic Target for the Treatment of Behavioural and Psychological Symptoms of Dementia. *Can J Psychiatry* 49: 439-453.
- Leppik IE, Gram L, Deaton R, Sommerville KW (1999) Safety of tiagabine: summary of 53 trials. *Epilepsy Res* 33: 235-246.
- Liu QR, López-Corcuera B, Mandiyan S, Nelson H, Nelson N (1993) Molecular Characterization of Four Pharmacologically Distinct α -Aminobutyric Acid Transporters in Mouse Brain. *J Biol Chem* 268: 2106-2112.
- Lüllmann H, Mohr K, Hein L (2010) *Pharmakologie und Toxikologie*. Georg Thieme Verlag, Stuttgart.
- Madsen KK, Clausen RP, Larsson OM, Krogsgaard-Larsen P, Schousboe A, White HS (2009) Synaptic and extrasynaptic GABA transporters as targets for anti-epileptic drugs. *J Neurochem* 109: 139-144.
- Madsen KK, White HS, Schousboe A (2010) Neuronal and non-neuronal GABA transporters as targets for antiepileptic drugs. *Pharmacol Ther* 125: 394-401.
- Minelli A, DeBiasi S, Brecha NC, Zuccarello LV, Conti F (1996) GAT-3, a High-Affinity GABA Plasma Membrane Transporter, Is Localized to Astrocytic Processes, and It Is Not Confined to the Vicinity of GABAergic Synapses in the Cerebral Cortex. *J Neurosci* 16: 6255-6264.
- Pabel J, Faust M, Prehn C, Wörlein B, Allmendinger L, Höfner G, Wanner KT (2012) Development of an (*S*)-1-{2-[Tris(4-methoxyphenyl)methoxy]ethyl}piperidine-3-carboxylic acid [(*S*)-SNAP-5114] Carba Analogue Inhibitor for Murine γ -Aminobutyric Acid Transporter Type 4. *ChemMedChem* 7: 1245-1255.

Palacín M, Estévez R, Bertran J, Zorzano A (1998) Molecular Biology of Mammalian Plasma Membrane Amino Acid Transporters. *Physiol Rev* 78: 969-1054.

Pauli GF, Chen S-N, Simmler C, Lankin DC, Gödecke T, Jaki BU, Friesen JB, McAlpine JB, Napolitano JG (2014) Importance of Purity Evaluation and the Potential of Quantitative ¹H NMR as a Purity Assay. *J Med Chem* 57: 9220-9231.

Perrin DD, Armarego WLF (1988) Purification of Laboratory Chemicals. Pergamon, New York.

Rancati F, Rizzi A, Carzaniga L, Linney I, Walden S, Knight C, Schmidt W (2016) COMPOUNDS HAVING MUSCARINIC RECEPTOR ANTAGONIST AND BETA2 ADRENERGIC RECEPTOR AGONST ACTIVITY. US Patent 2016-0235734, filed Feb 10, 2016, issued Aug 18, 2016.

Rudy HKA, Mayer P, Wanner KT (2020) Synthesis of 1,5-Ring fused Imidazoles from Cyclic Imines and TosMIC – Identification of in situ generated *N*-methyleneformamide as a Catalyst in the van Leusen Imidazole Synthesis. *Eur J Org Chem* online.

Rudy HKA, Wanner KT (2019) Accessing Tricyclic Imines Comprising a 2-Azabicyclo[2.2.2]octane Scaffold by Intramolecular Hetero-Diels–Alder Reaction of 4-Alkenyl-Substituted *N*-Silyl-1,4-dihydropyridines. *Synthesis* 51: 4296-4310.

Sałat K, Podkowa A, Kowalczyk P, Kulig K, Dziubina A, Filipek B, Librowski T (2015) Anticonvulsant active inhibitor of GABA transporter subtype 1, tiagabine, with activity in mouse models of anxiety, pain and depression. *Pharmacol Rep* 67: 465-472.

Schaarschmidt M, Höfner G, Wanner KT (2019) Synthesis and Biological Evaluation of Nipecotnic Acid and Guvacine Derived 1,3-Disubstituted Allenes as Inhibitors of Murine GABA Transporter mGAT1. *ChemMedChem* 14: 1135-1151.

Scheschonka A, Betz H, Becker CM (2007) Chemische Signalübertragung zwischen Neuronen. In: Löffler G, Petrides PE, Heinrich PC (ed) *Biochemie und Pathobiochemie*. Springer, Heidelberg, pp 1036-1045.

Schmaunz CE, Mayer P, Wanner KT (2014) Inter- and Intramolecular [4+2]-Cycloaddition Reactions with 4,4-Disubstituted *N*-Silyl-1,4-dihydropyridines as Precursors for *N*-Protonated 2-Azabutadiene Intermediates. *Synthesis* 46: 1630-1638.

Schousboe A, Madsen KK, Barker-Haliski ML, White HS (2014) The GABA Synapse as a Target for Antiepileptic Drugs: A Historical Overview Focused on GABA Transporters. *Neurochem Res* 39: 1980-1987.

Sen SE, Roach SL, Boggs JK, Ewing GJ, Magrath J (1997) Ferric Chloride Hexahydrate: A Mild Hydrolytic Agent for the Deprotection of Acetals. *J Org Chem* 62: 6684-6686.

Skovstrup S, Taboureau O, Bräuner-Osborne H, Jørgenson FS (2010) Homology Modelling of the GABA Transporter and Analysis of Tiagabine Binding. *ChemMedChem* 5: 968-1000.

Stockdale TP, Williams CM (2015) Pharmaceuticals that contain polycyclic hydrocarbon scaffolds. *Chem Soc Rev* 44: 7737-7763.

Sun J, Dong Y, Cao L, Wang X, Wang S, Hu Y (2004) Highly Efficient Chemoselective Deprotection of O,O-Acetals and O,O-Ketals Catalyzed by Molecular Iodine in Acetone. *J Org Chem* 69: 8932-8934.

Wein T, Petrera M, Allmendinger L, Höfner G, Pabel J, Wanner KT (2016) Different Binding Modes of Small and Large Binders of GAT1. *ChemMedChem* 11: 509-518.

Tóth K, Höfner G, Wanner KT (2018) Synthesis and biological evaluation of novel N-substituted nipecotic acid derivatives with a trans-alkene spacer as potent GABA uptake inhibitors. *Bioorg Med Chem* 26: 5944-5961.

Tóth K, Höfner G, Wanner KT (2018) Synthesis and biological evaluation of novel N-substituted nipecotic acid derivatives with an alkyl spacer as GABA uptake inhibitors. *Bioorg Med Chem* 26: 3668-3687.

Treimann DM (2001) GABAergic Mechanisms in Epilepsy. *Epilepsia* 42: 8-12.

van Nuland AJM, den Ouden HEM, Zach H, Dirkx MFM, van Asten JJA, Scheenen TWJ, Toni I, Cools R, Helmich RC (2020) GABAergic changes in the thalamocortical circuit in Parkinson's disease. *Hum Brain Mapp* 41: 1017-1029.

Willford SL, Anderson CM, Spencer SR, Eskandari S (2015) Evidence for a Revised Ion/Substrate Coupling Stoichiometry of GABA Transporters. *J Membrane Biol* 248: 795-810.

Wipf P, Skoda EM, Mann A (2015) *The Practice of Medicinal Chemistry*. Academic Press, London, San Diego, Waltham, Oxford.

Zafar S, Jabeen I (2018) Structure, Function, and Modulation of γ -Aminobutyric Acid Transporter 1 (GAT1) in Neurological Disorders: A Pharmacoinformatic Prospective. *Front Chem* 6(397).

Zepperitz C, Höfner G, Wanner KT (2006) MS-Binding Assays: Kinetic, Saturation, and Competitive Experiments Based on Quantitation of Bound Marker as Exemplified by the GABA Transporter mGAT1. *ChemMedChem* 1: 208-217.

Zheng Y, Tice CM, Singh SB (2014) The use of spirocyclic scaffolds in drug discovery. *Bioorg Med Chem Lett* 24: 3673-3682.

Zhou Y, Holmseth S, Guo C, Hassel B, Höfner G, Huitfeldt HS, Wanner KT, Danbolt NC (2012) Deletion of the γ -Aminobutyric Acid Transporter 2 (GAT2 and SLC6A13) Gene in Mice Leads to Changes in Liver and Brain Taurine Contents. *J Biol Chem* 287: 35733-35746.

Zhou Y, Holmseth S, Hua R, Lehre AC, Olofsson AM, Poblete-Naredo I, Kempson SA, Danbolt NC (2012) The betaine-GABA transporter (BGT1, slc6a12) is predominantly expressed in the liver and at lower levels in the kidneys and at the brain surface. *Am J Physiol Renal Physiol* 302: 316-328.

Supporting Information

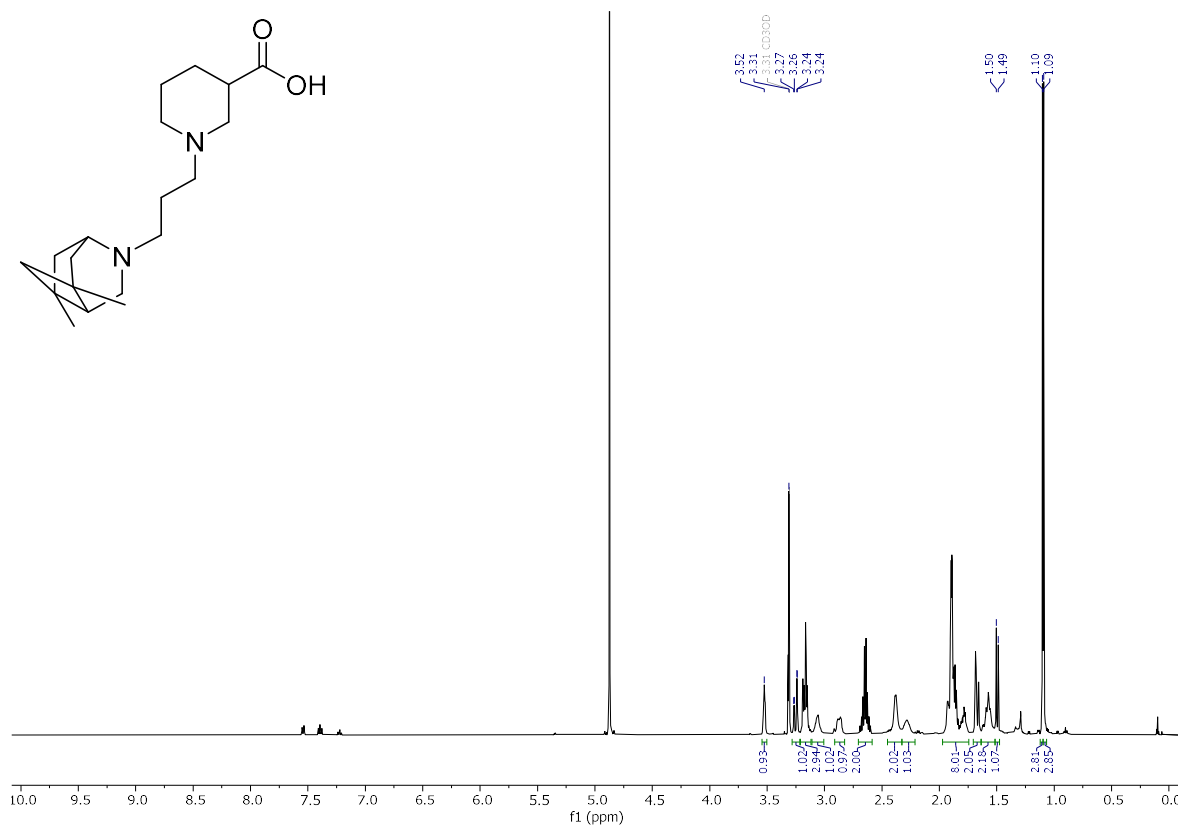
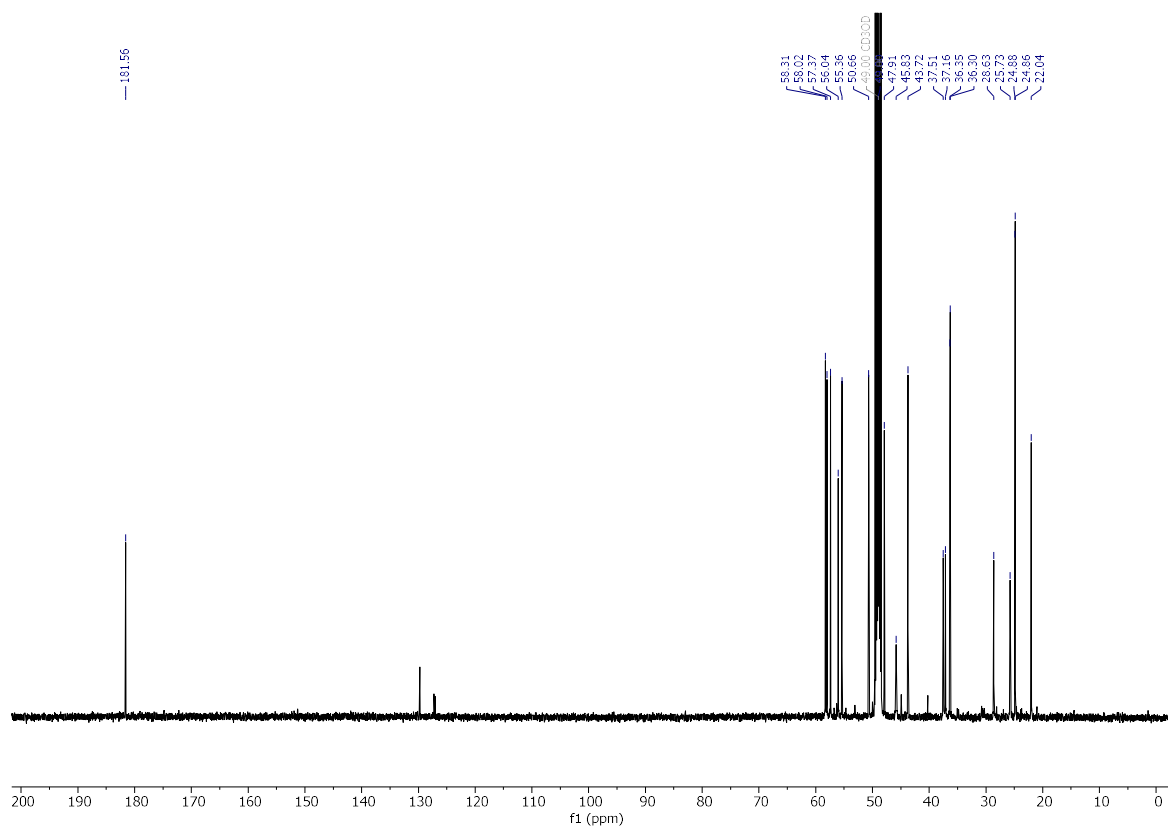
Synthesis and biological evaluation of novel *N*-substituted nipecotic acid derivatives with tricyclic cage structures in the lipophilic domain as GABA uptake inhibitors

Heinrich-Karl A. Rudy, Georg Höfner, Klaus T. Wanner

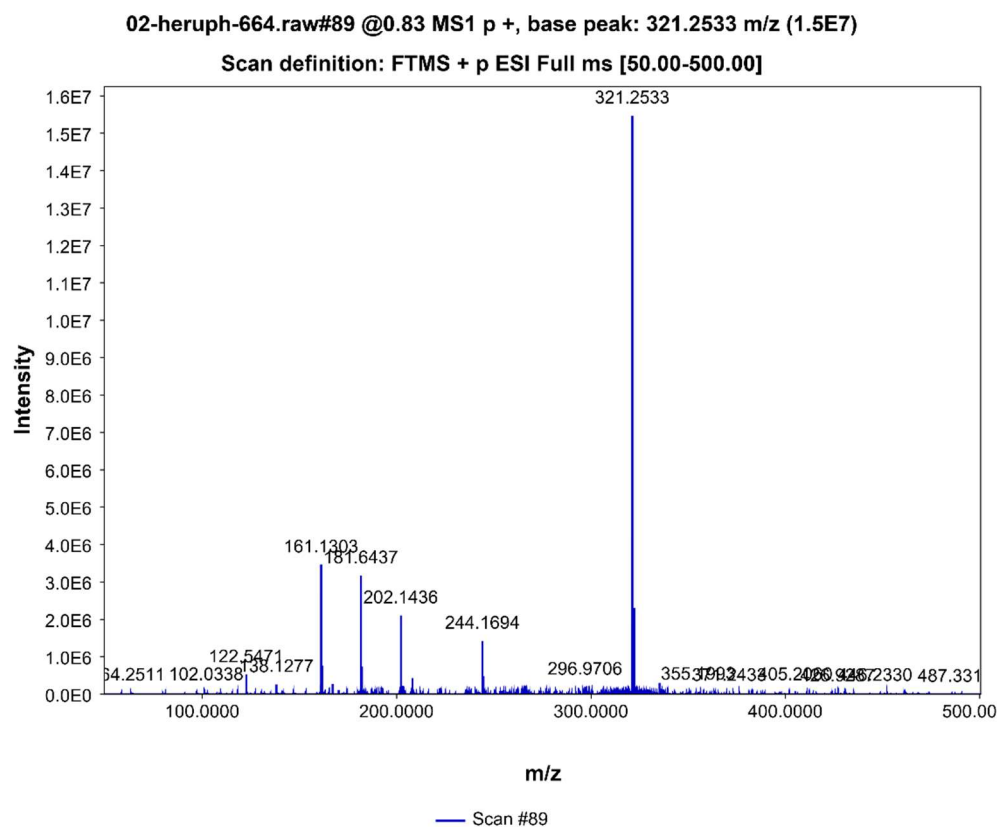
Ludwig-Maximilians-Universität München, Department of Pharmacy – Center for Drug Research, Butenandtstraße 5-13, Haus C, 81377 Munich, Germany

✉ Klaus T. Wanner

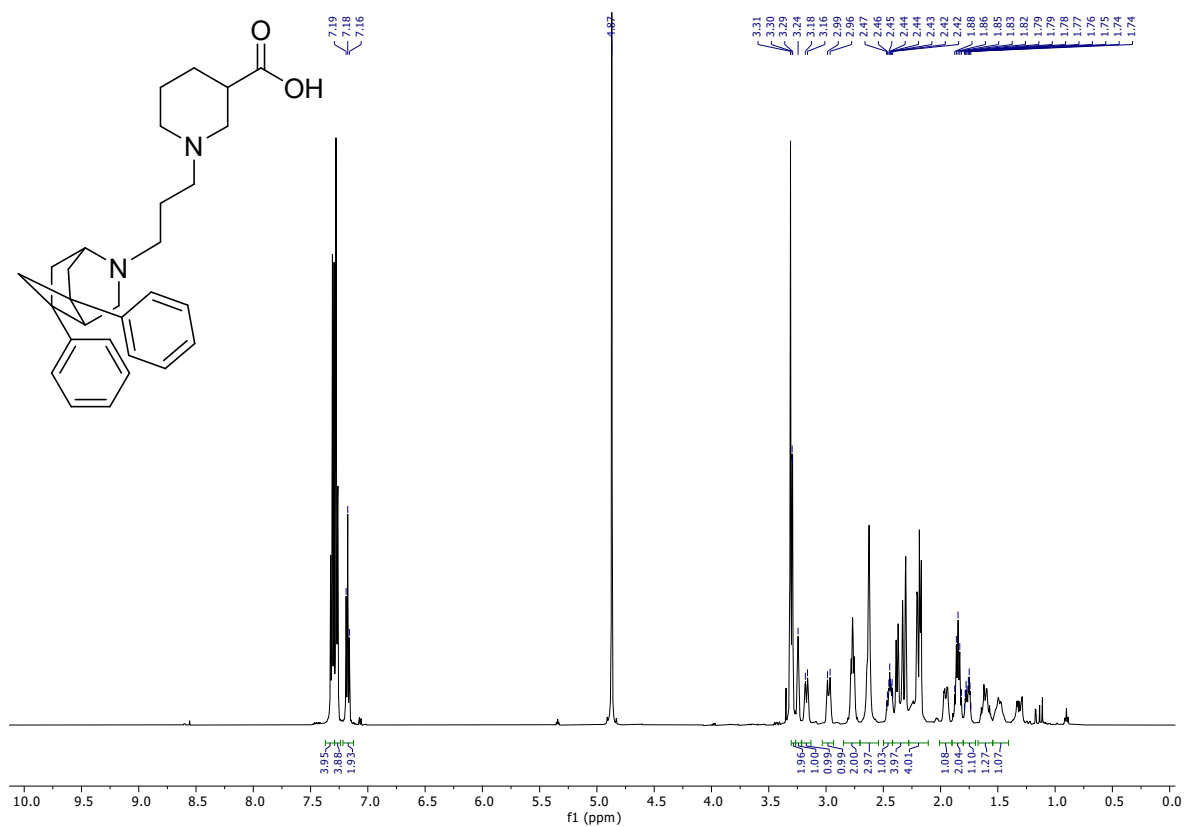
klaus.wanner@cup.uni-muenchen.de

^1H NMR, ^{13}C NMR and Mass spectra*rac*-11a (^1H):*rac*-11a (^{13}C):

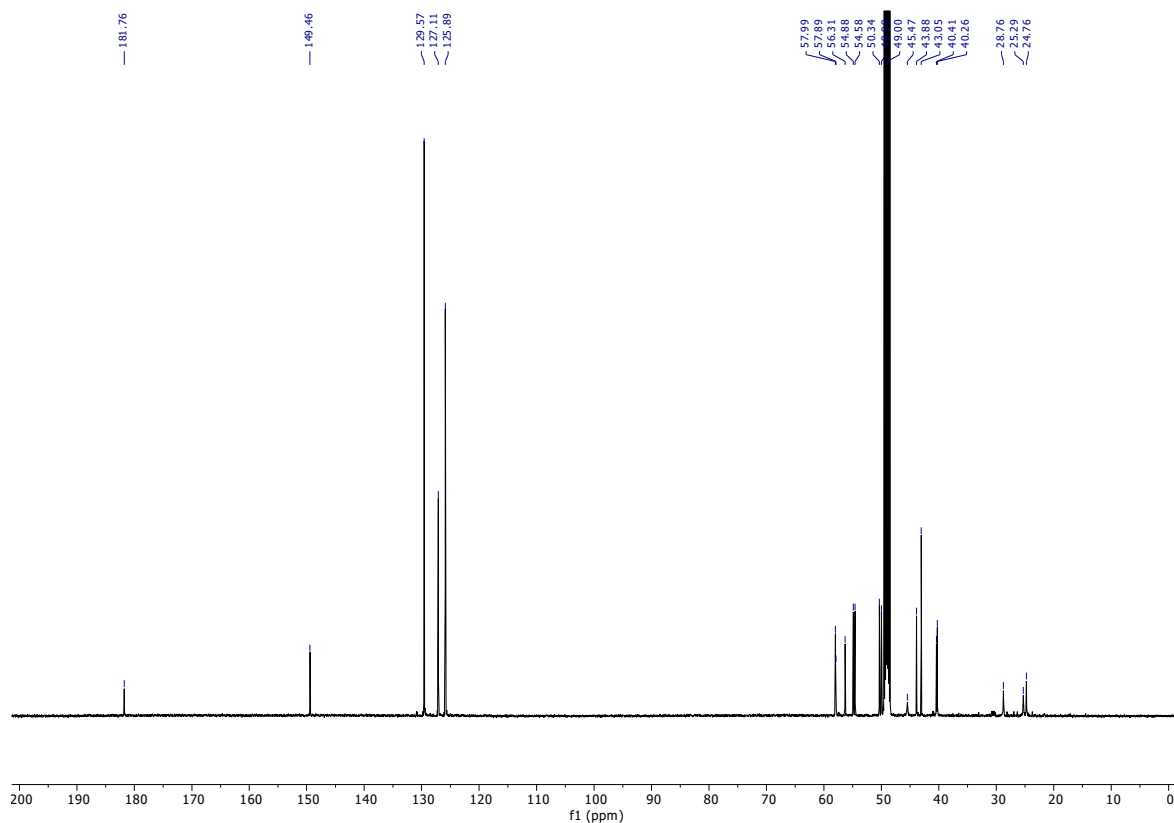
rac-11a (HRESIMS):



rac-11b (^1H):



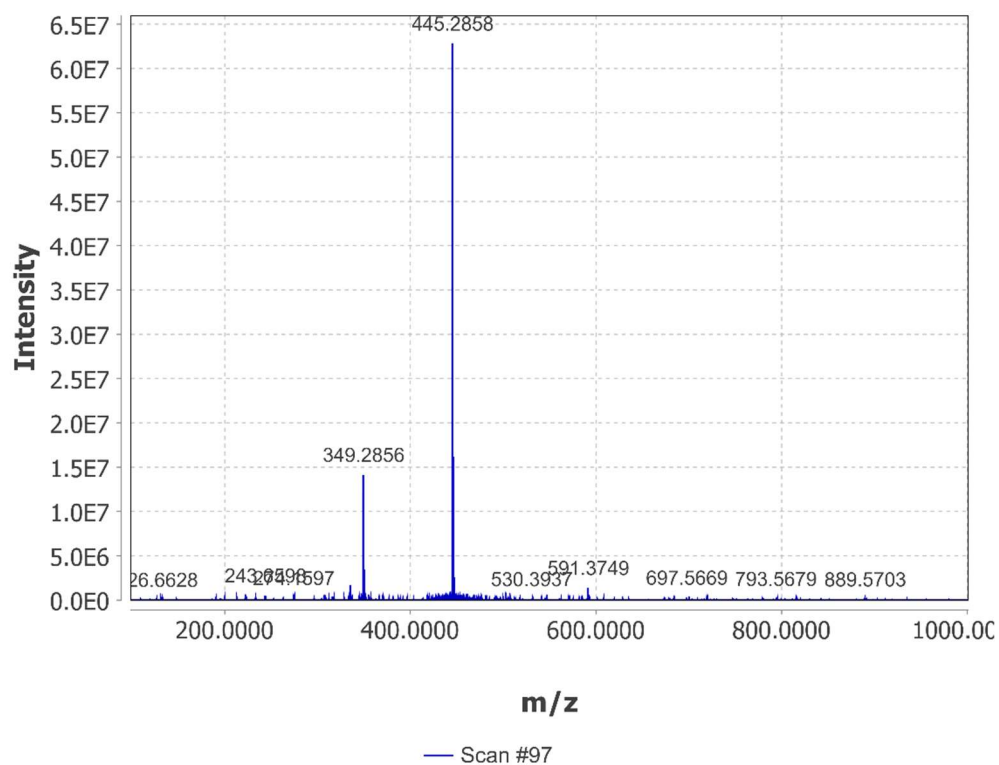
rac-11b (^{13}C):



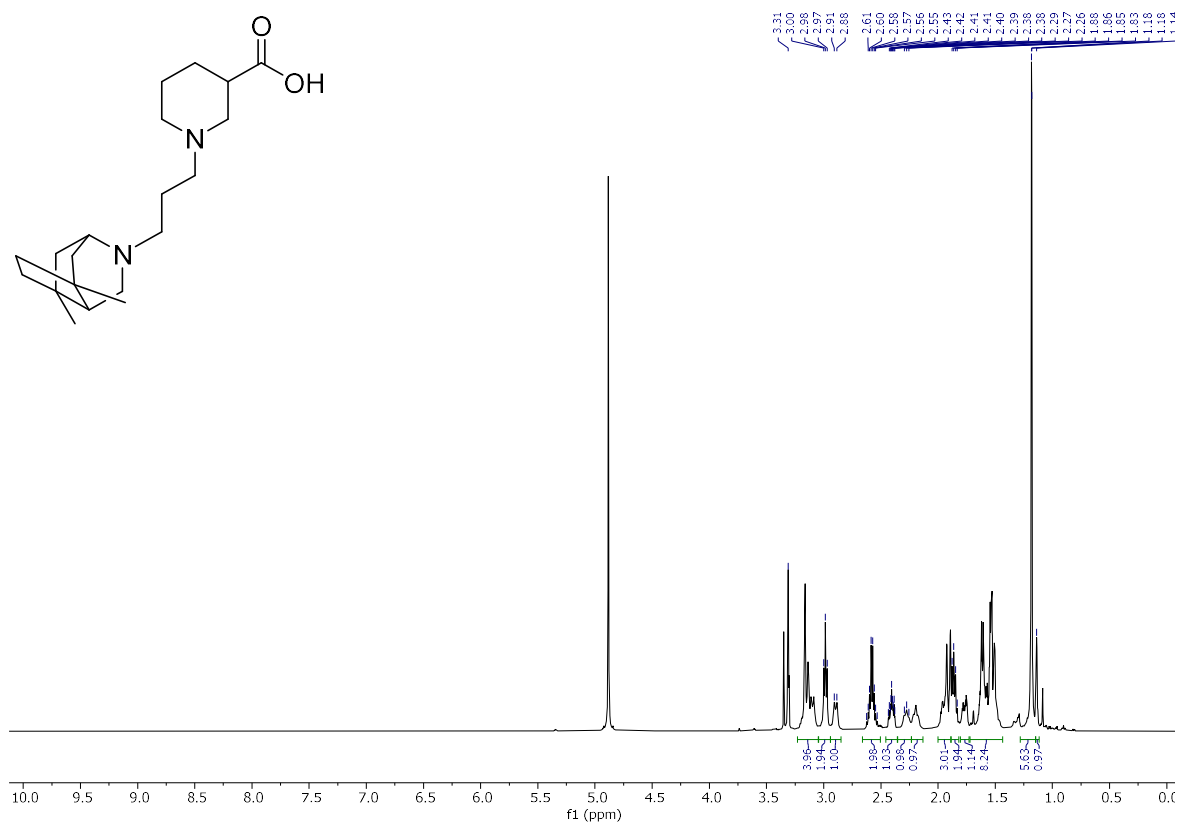
rac-11b (HRESIMS):

06-heruph-638.raw#97 @0.78 MS1 p +, base peak: 445.2858 m/z (6.3E7)

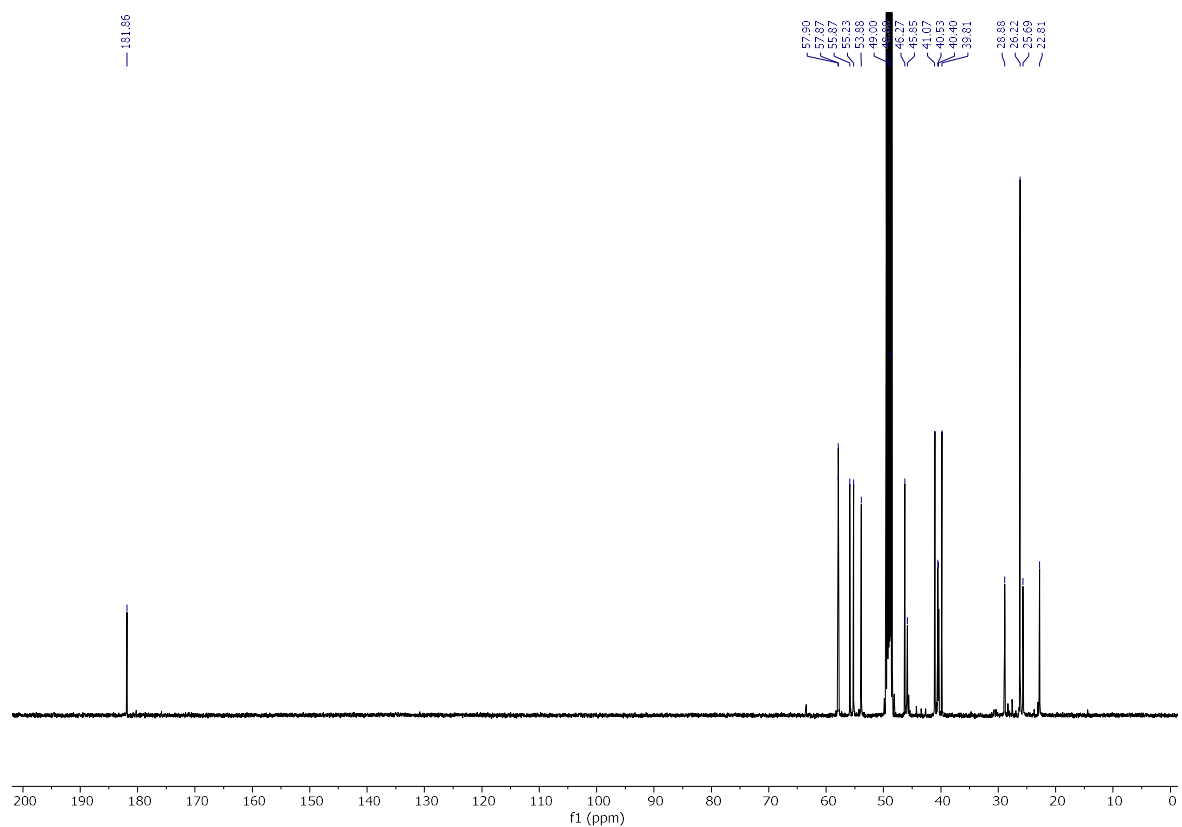
Scan definition: FTMS + p ESI Full ms [100.00-1000.00]



rac-**11c** (^1H):



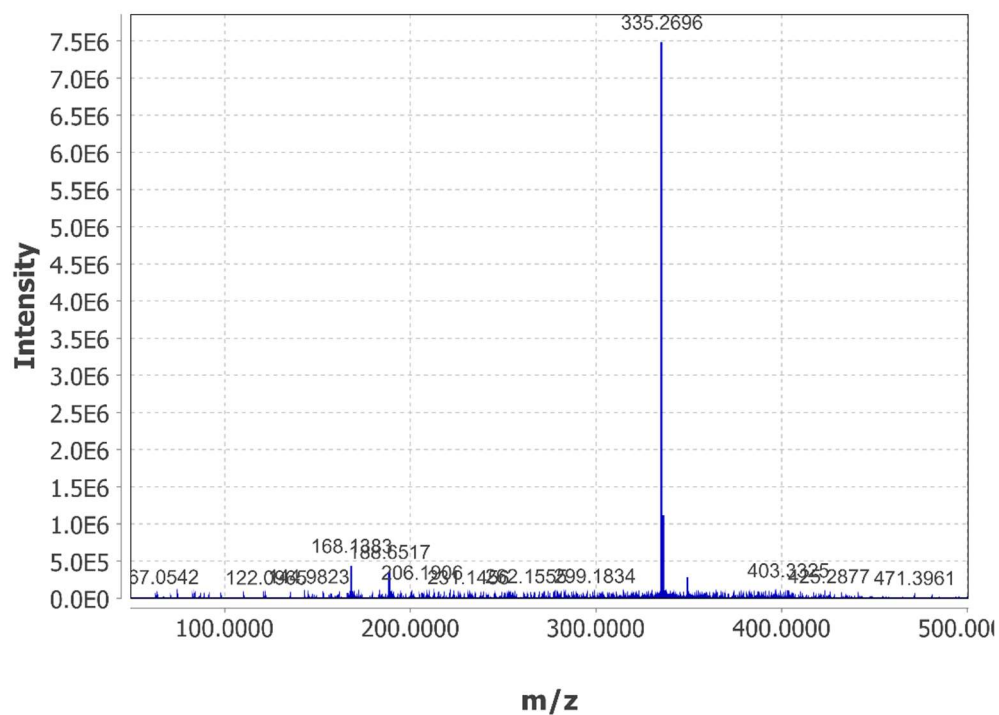
rac-**11c** (^{13}C):



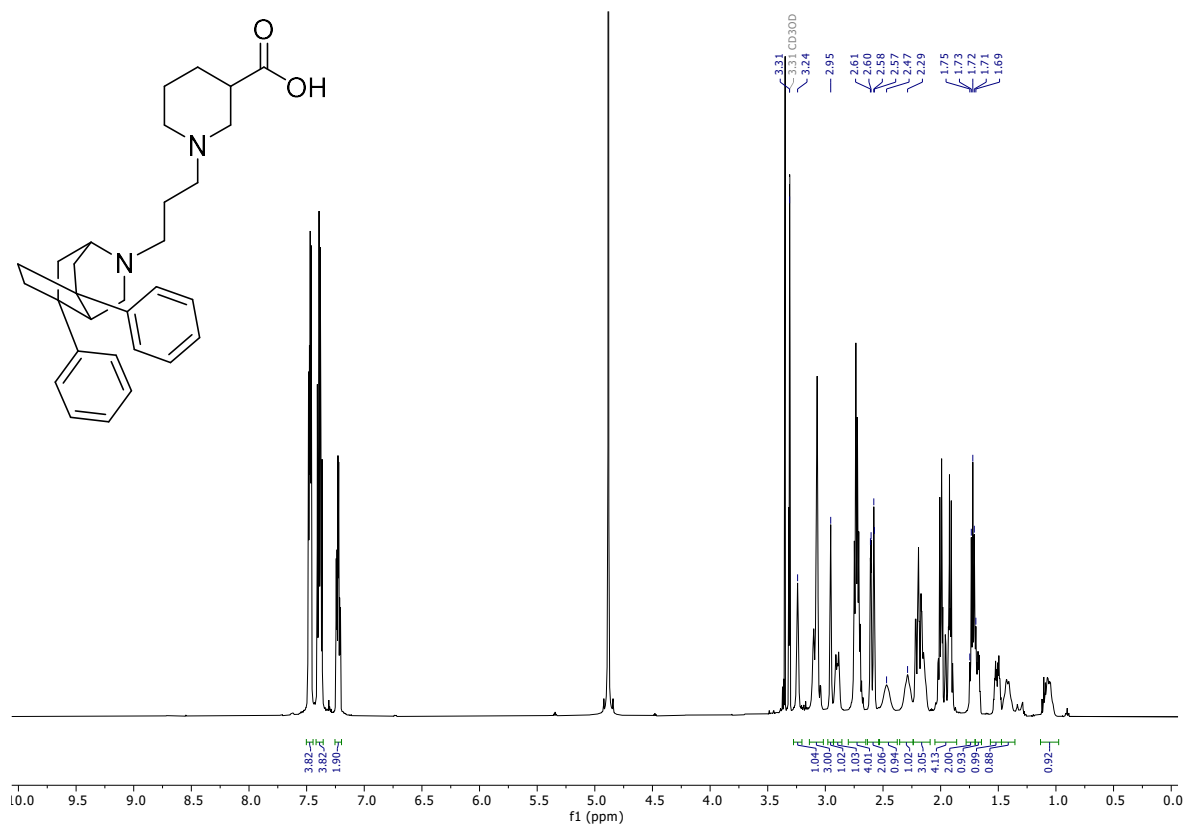
rac-11c (HRESIMS):

06-heruph-639.raw#233 @2.03 MS1 p +, base peak: 335.2696 m/z (7.5E6)

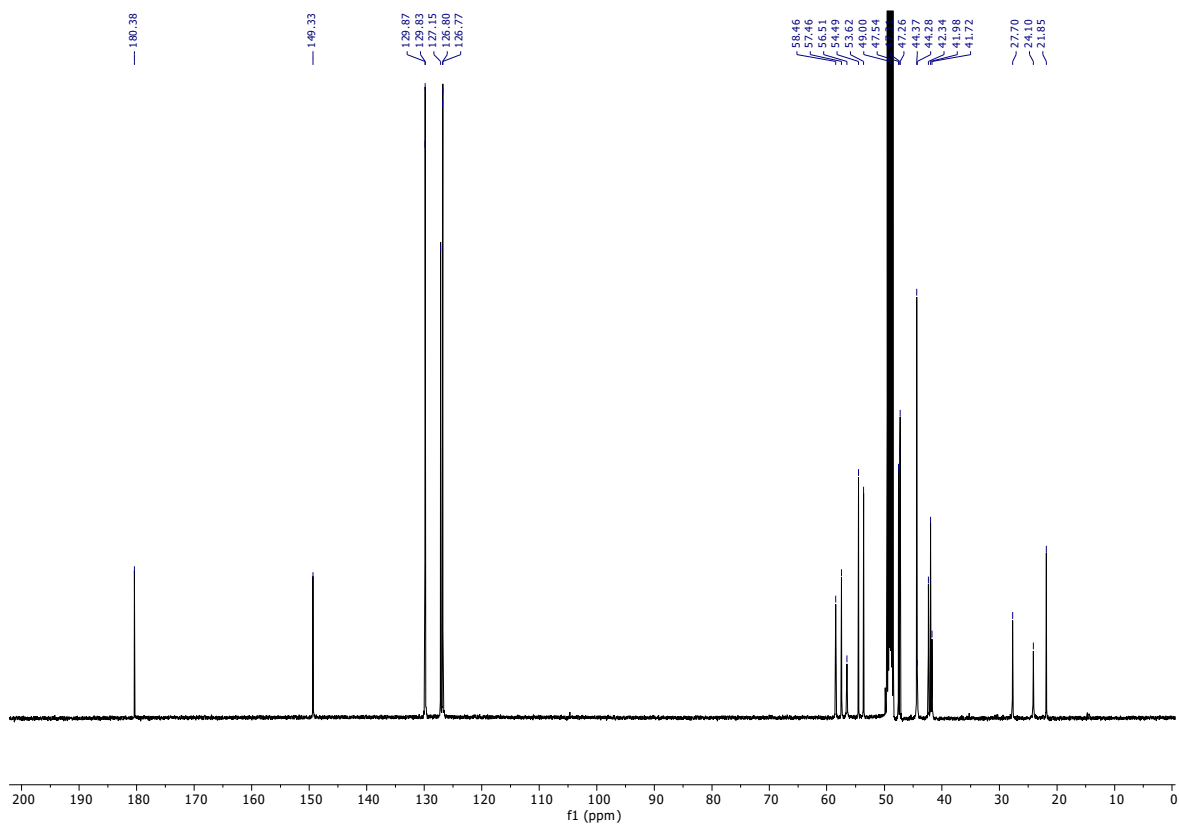
Scan definition: FTMS + p ESI Full ms [50.00-500.00]



rac-11d (^1H):



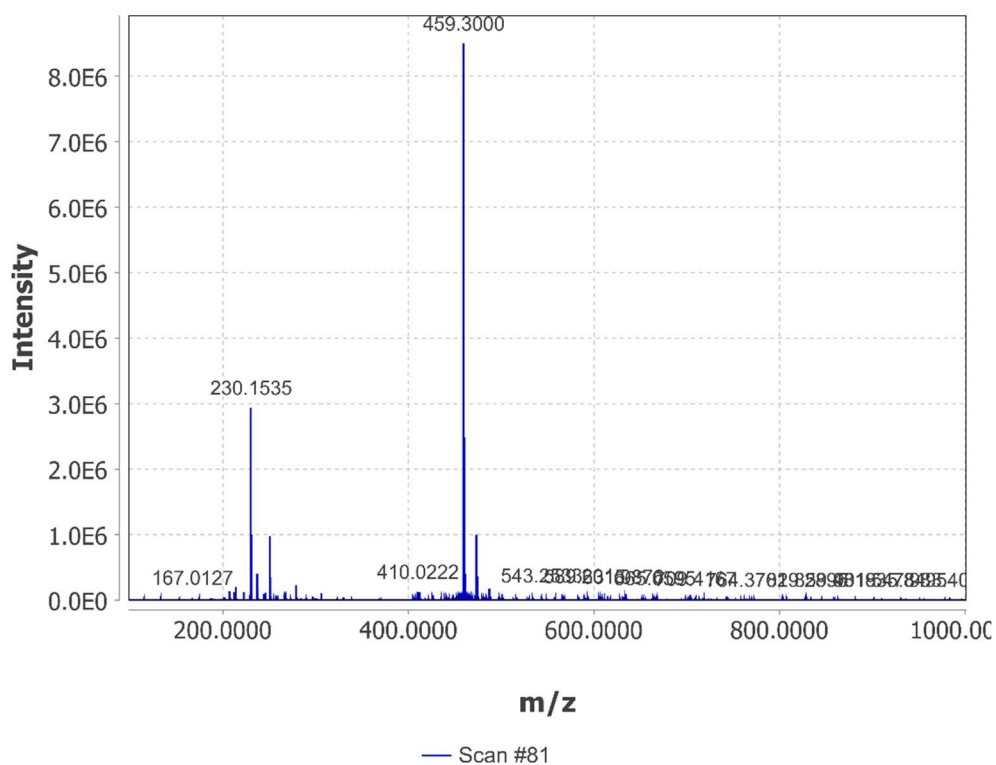
rac-11d (^{13}C):



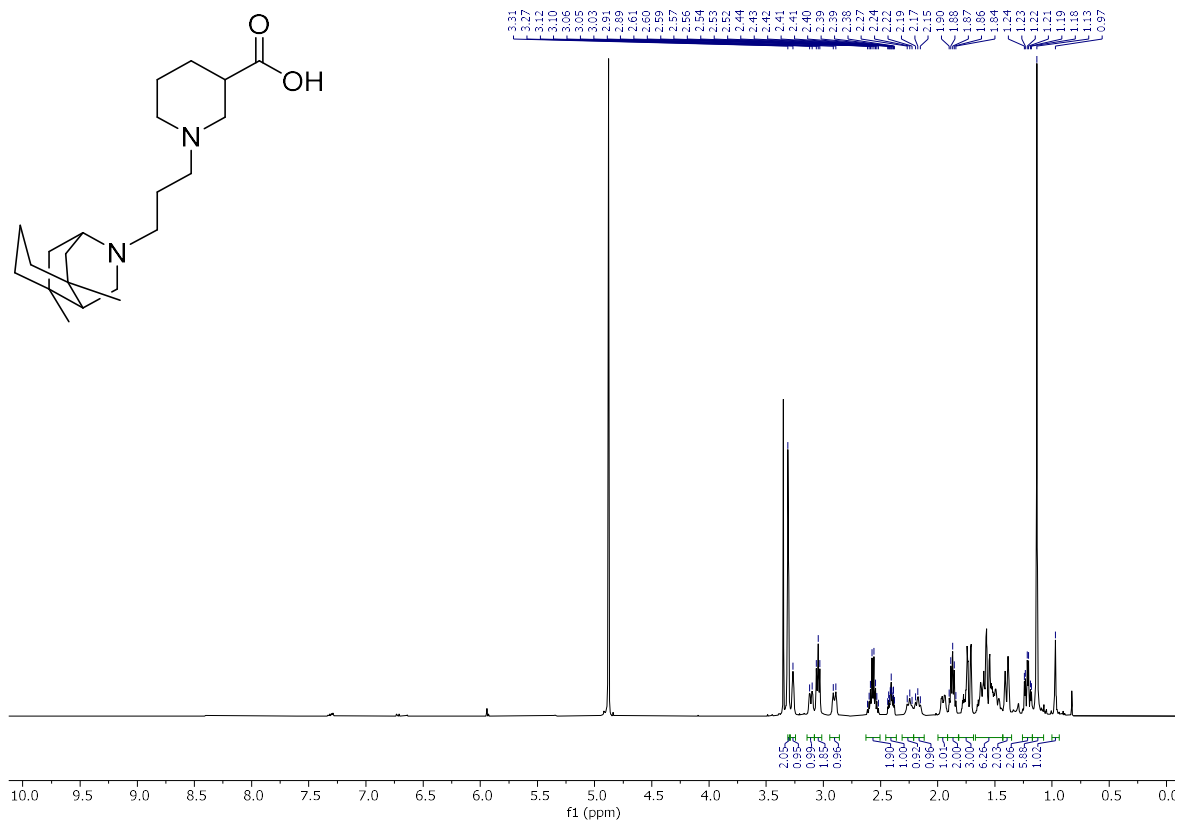
rac-11d (HRESIMS):

02-heruph-657.raw#81 @0.76 MS1 p +, base peak: 459.3000 m/z (8.5E6)

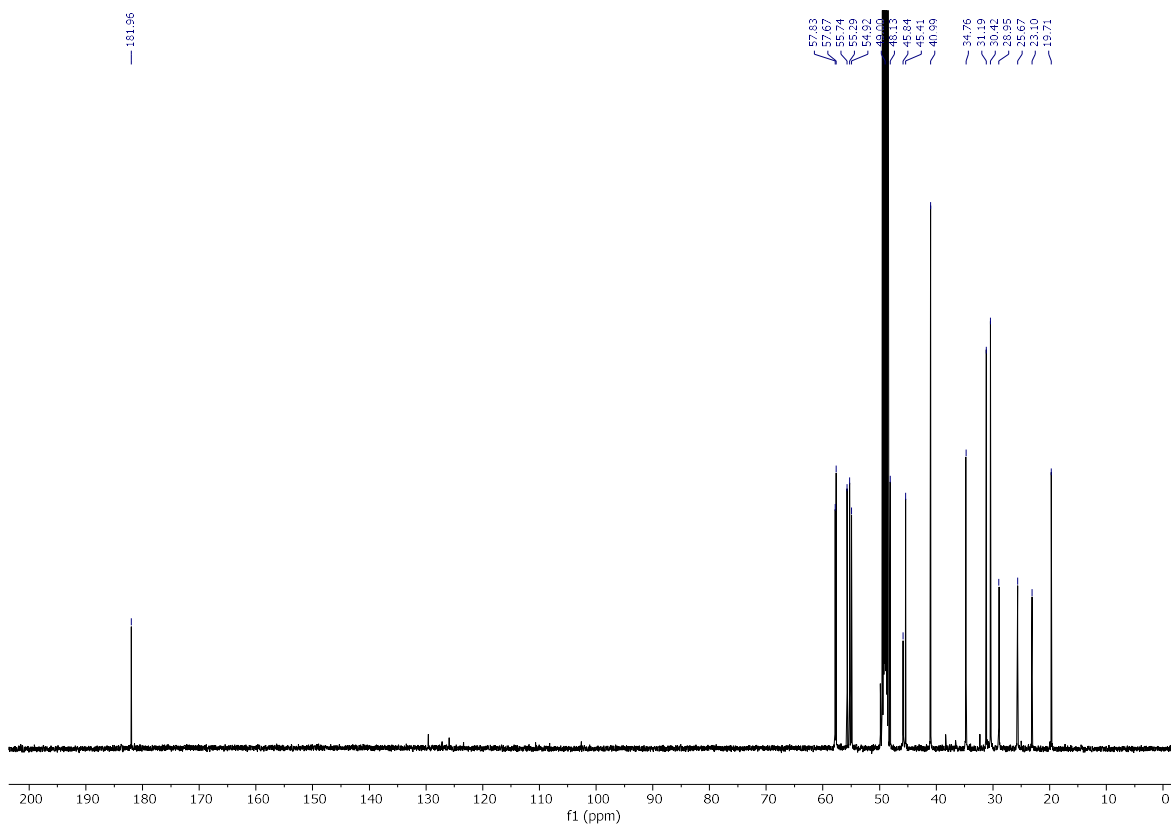
Scan definition: FTMS + p ESI Full ms [100.00-1000.00]



rac-**11e** (^1H):



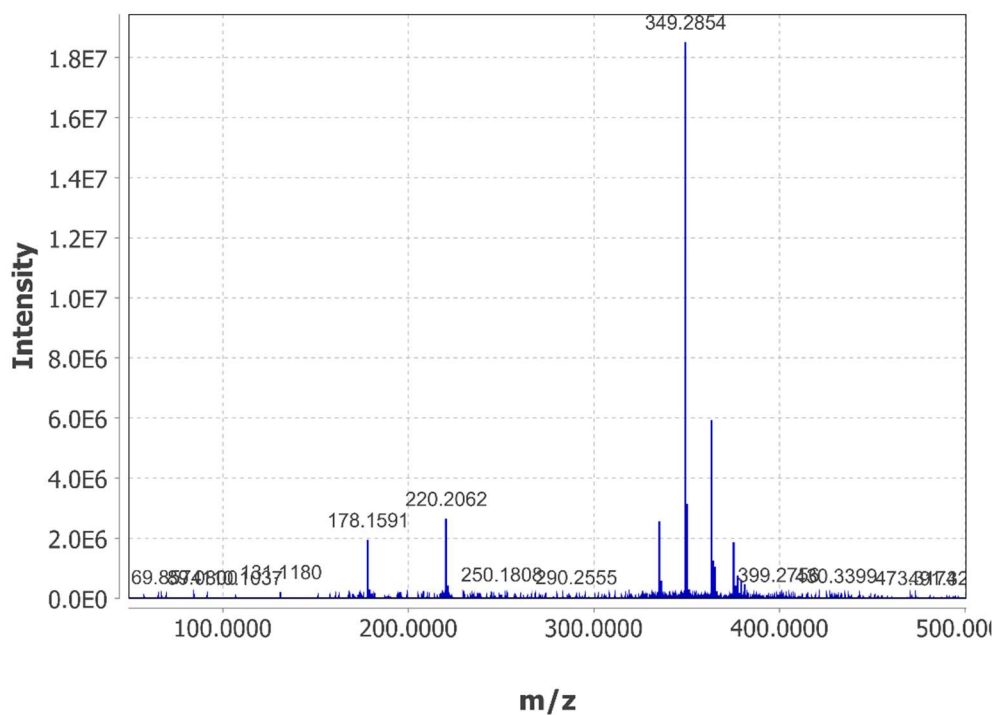
rac-**11e** (^{13}C):



rac-11e (HRESIMS):

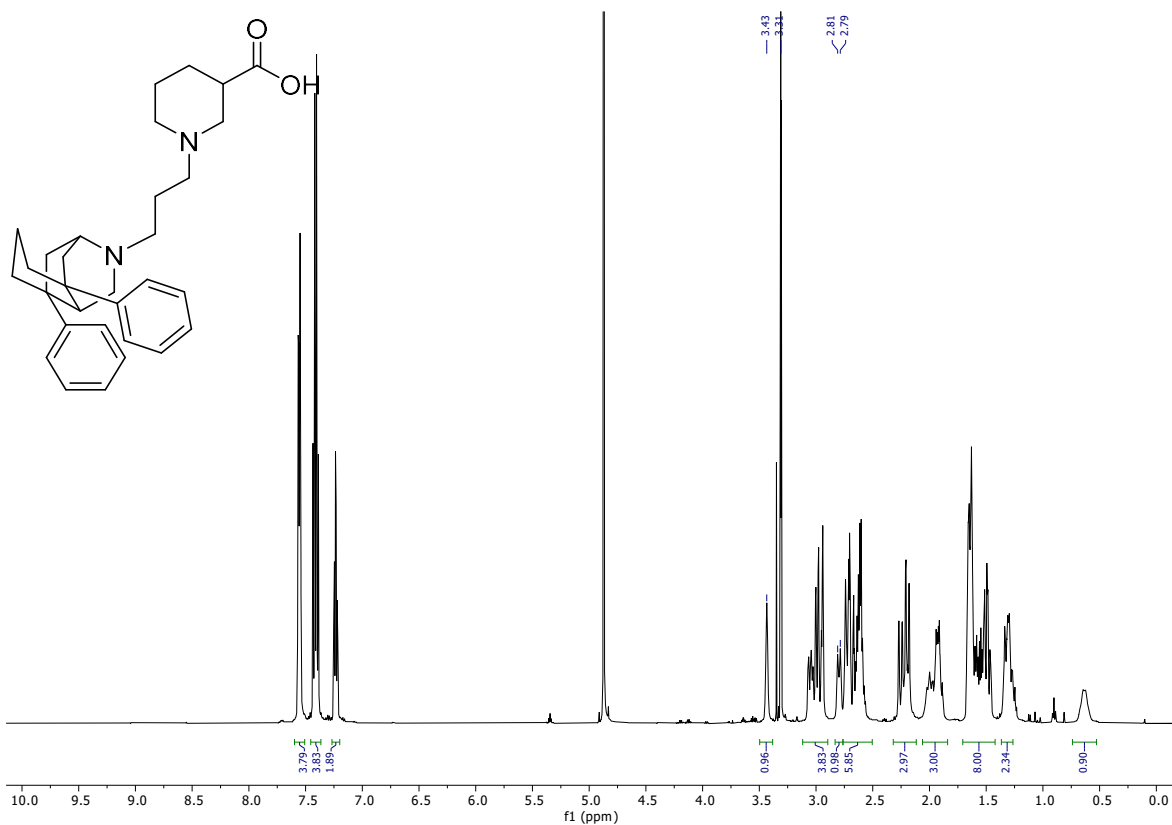
06-heruph-640_190617131704.raw#89 @0.82 MS1 p +, base peak: 349.2854 m/z (1.9E7)

Scan definition: FTMS + p ESI Full ms [50.00-500.00]

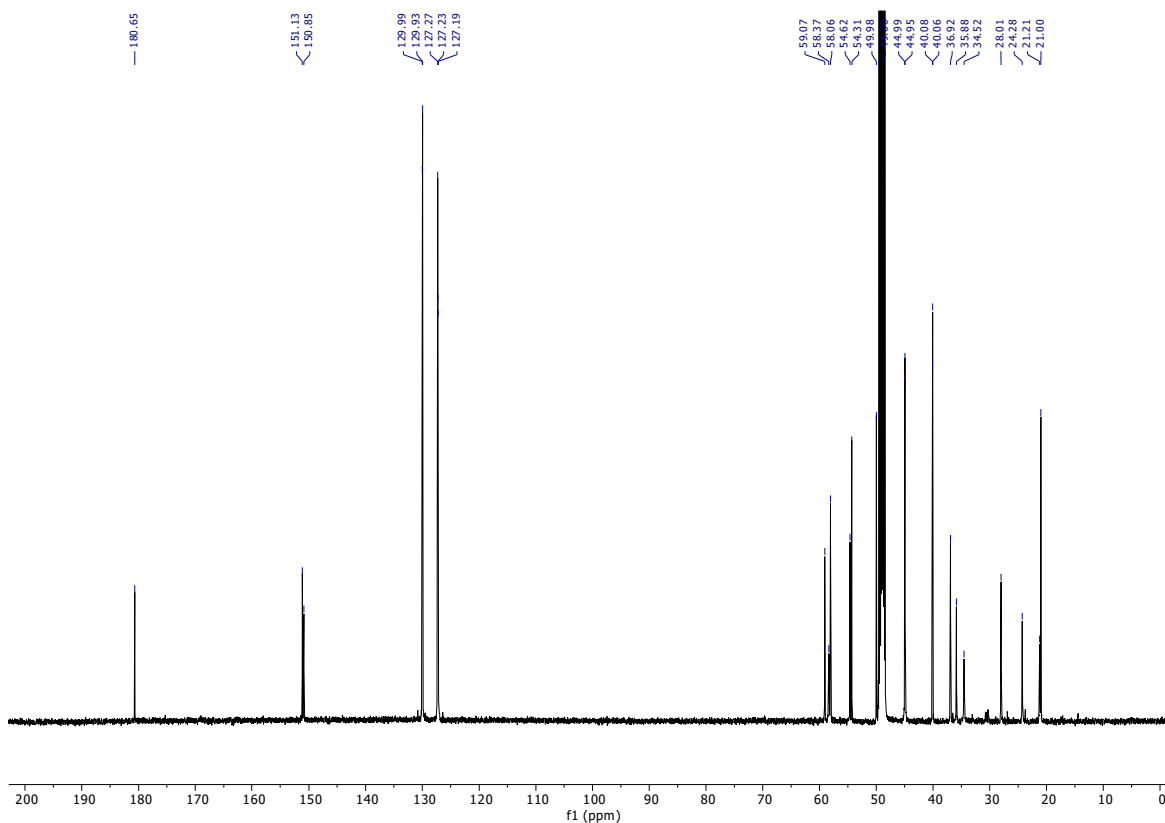


— Scan #89

rac-11f (^1H):



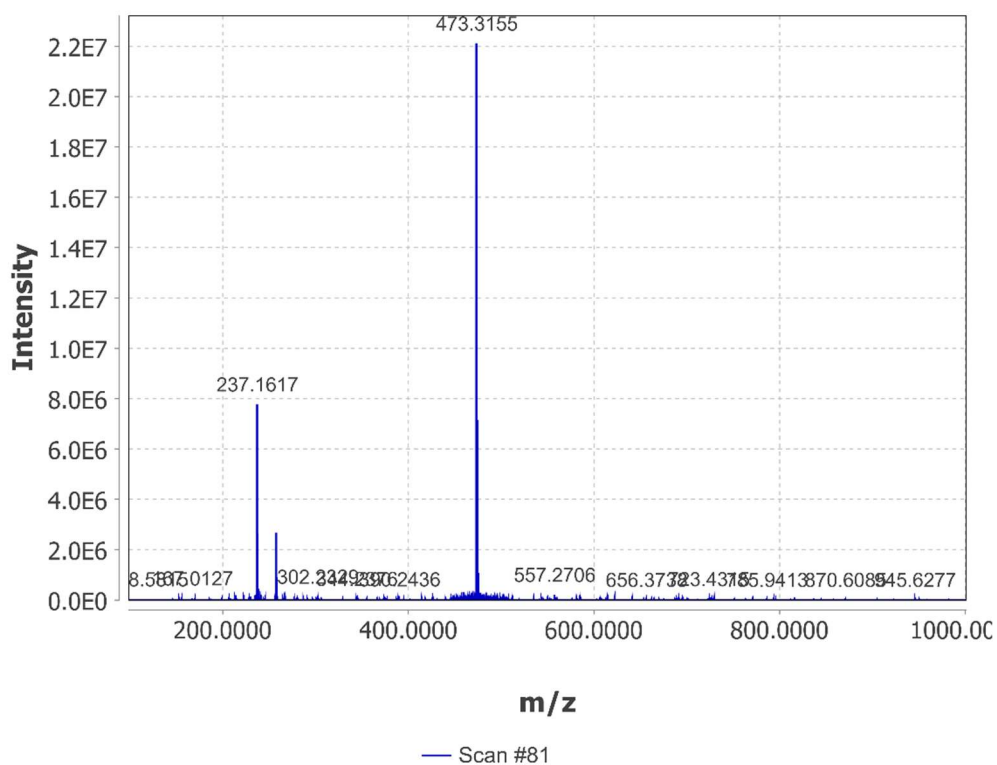
rac-11f (^{13}C):



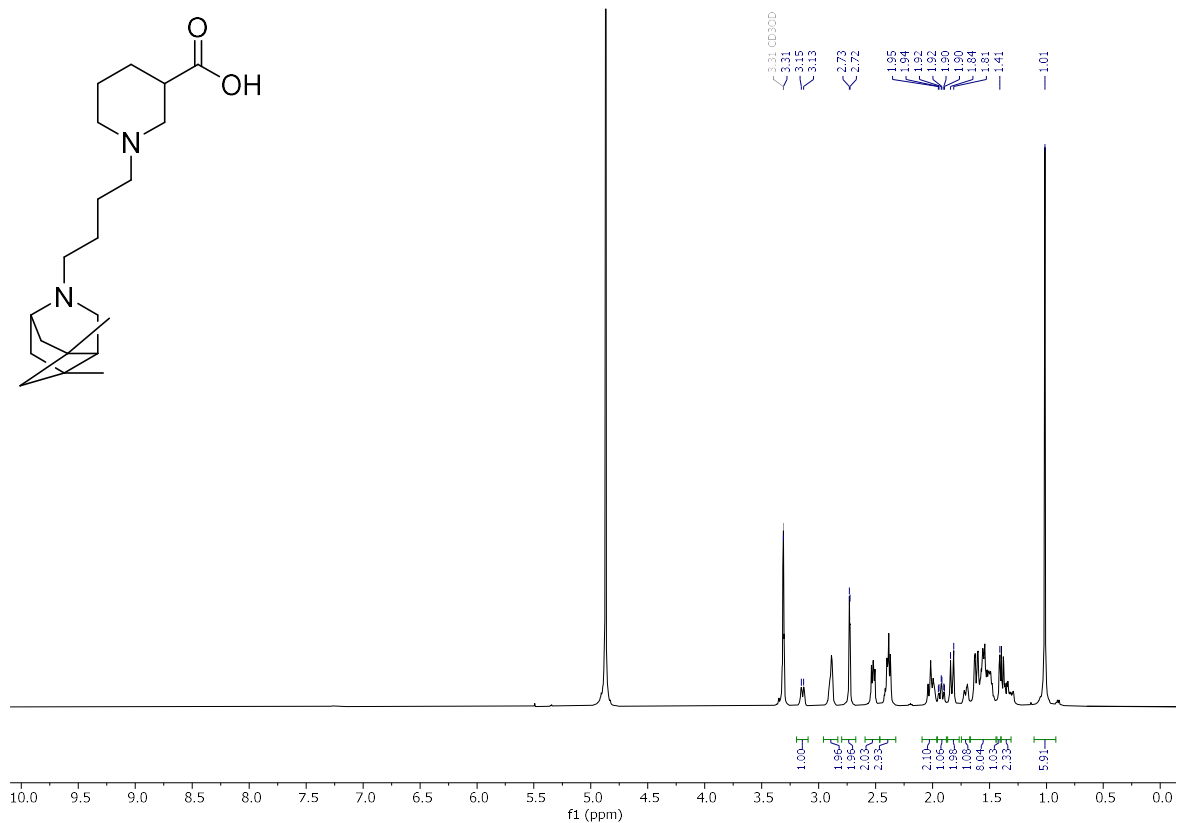
rac-11f (HRESIMS):

02-heruph-655.raw#81 @0.74 MS1 p +, base peak: 473.3155 m/z (2.2E7)

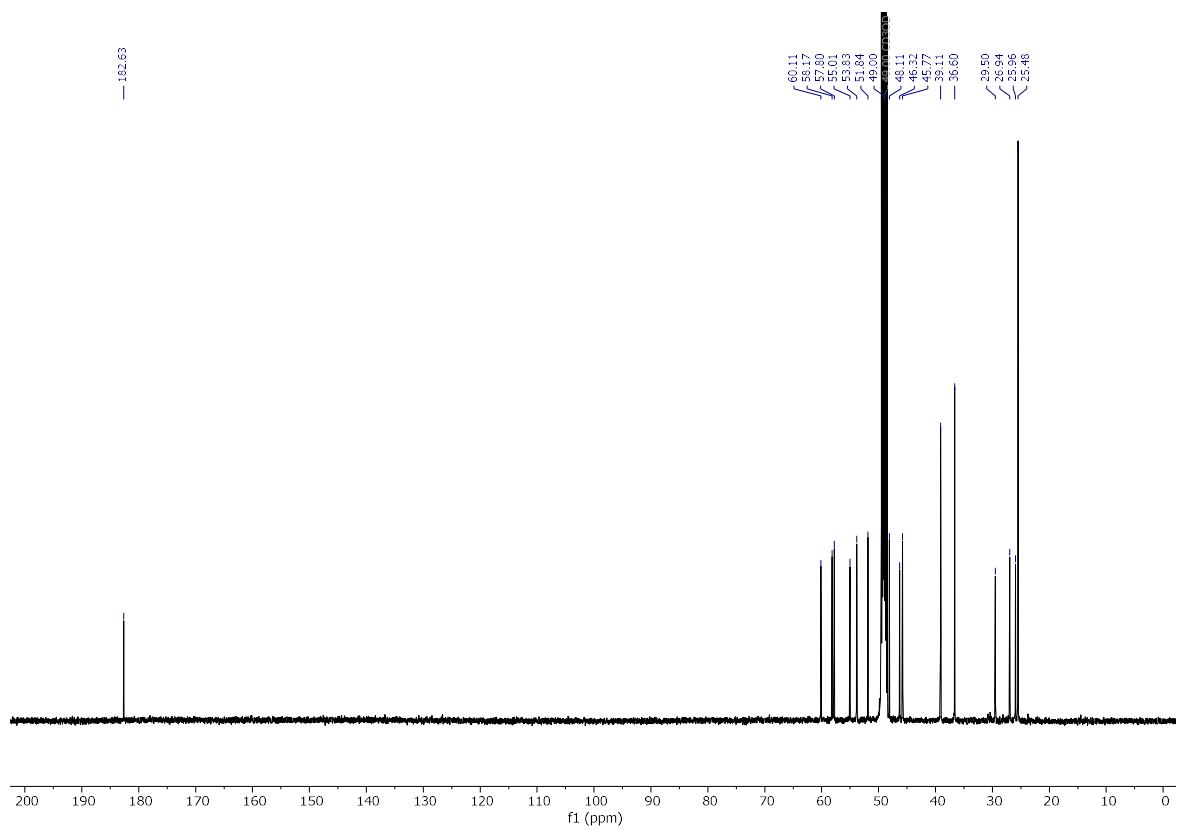
Scan definition: FTMS + p ESI Full ms [100.00-1000.00]



rac-**11g** (^1H):

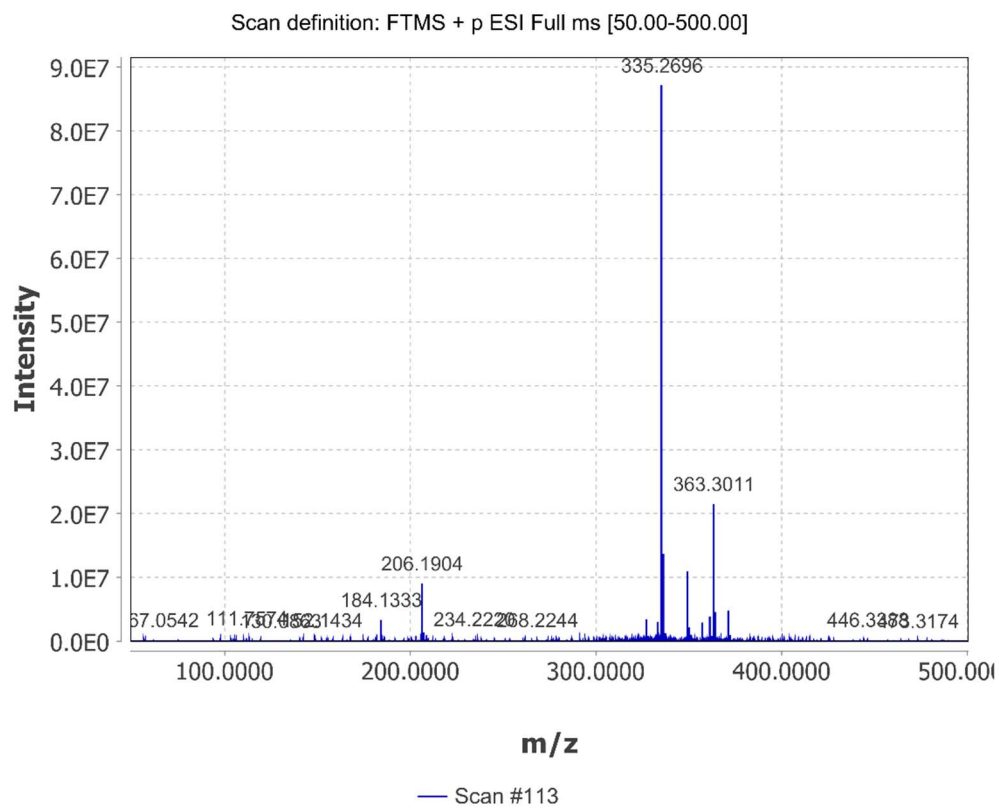


rac-**11g** (^{13}C):

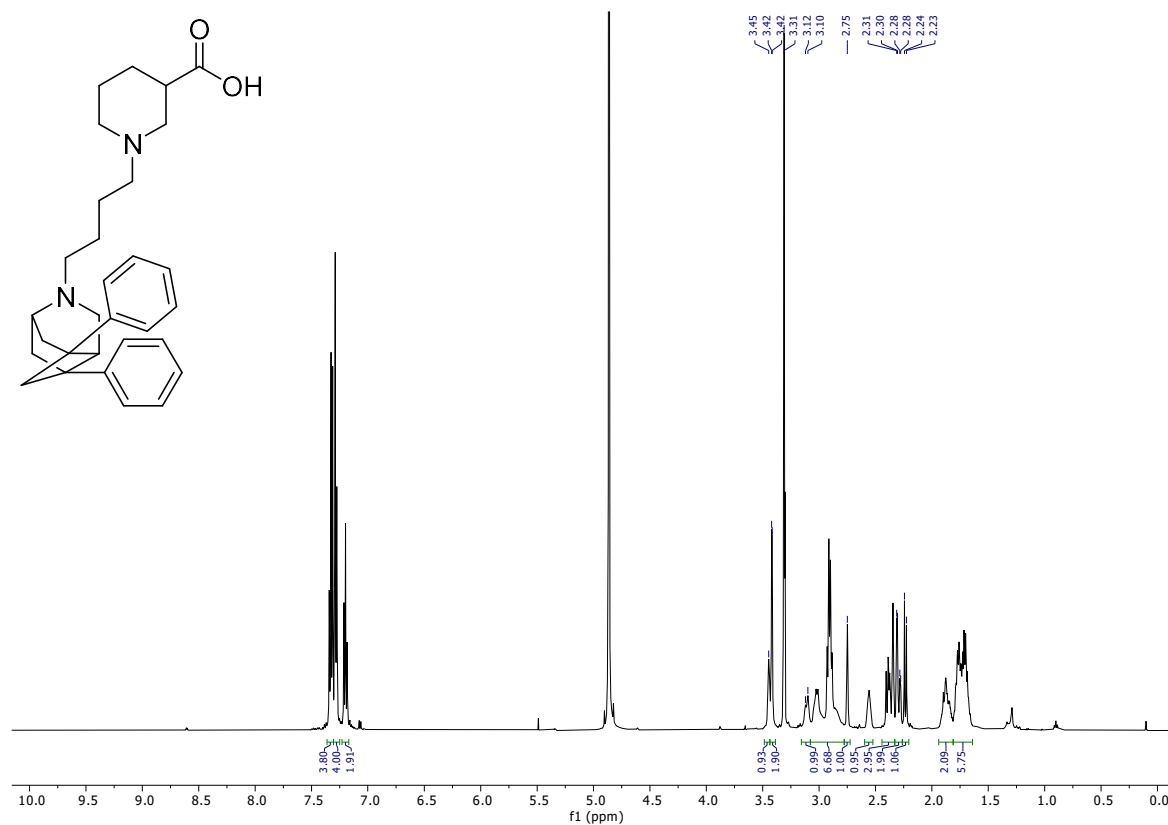


rac-11g (HRESIMS):

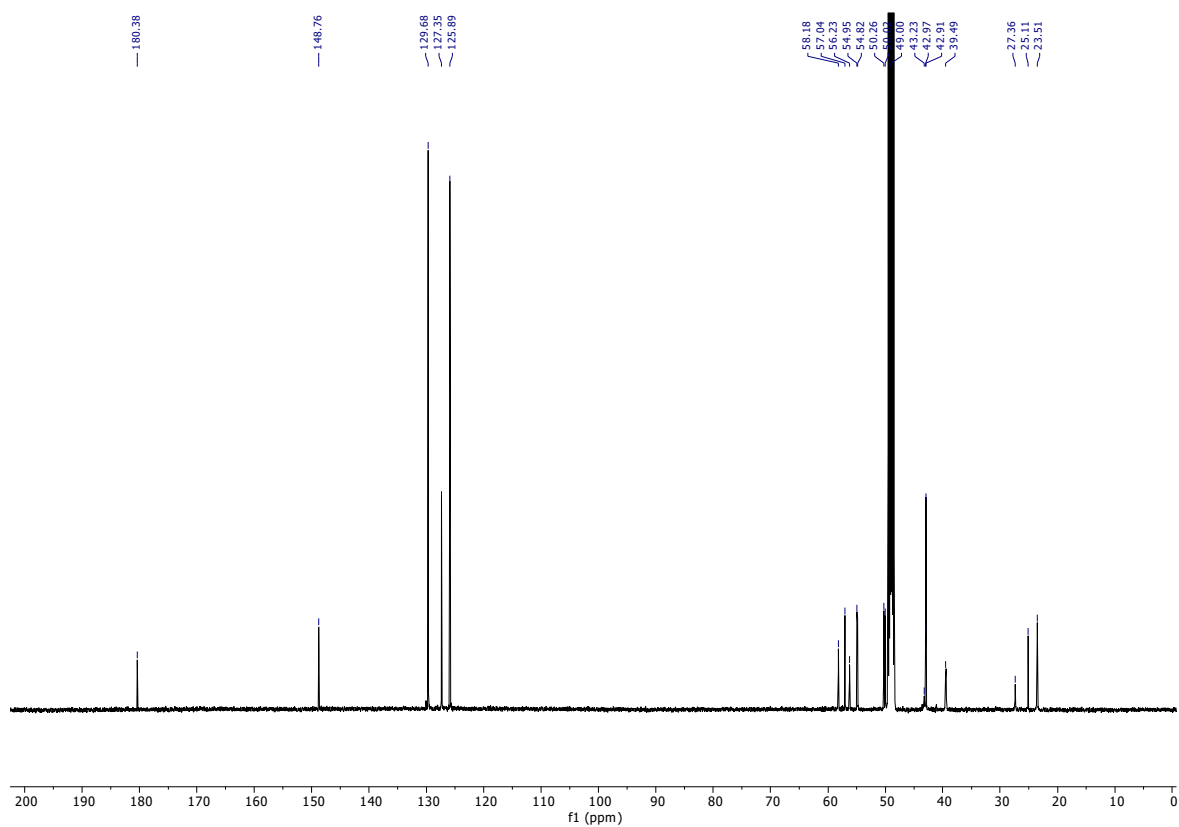
06-heruph-634_190606151534.raw#113 @0.91 MS1 p +, base peak: 335.2696 m/z (8.7E7)



rac-11h (^1H):



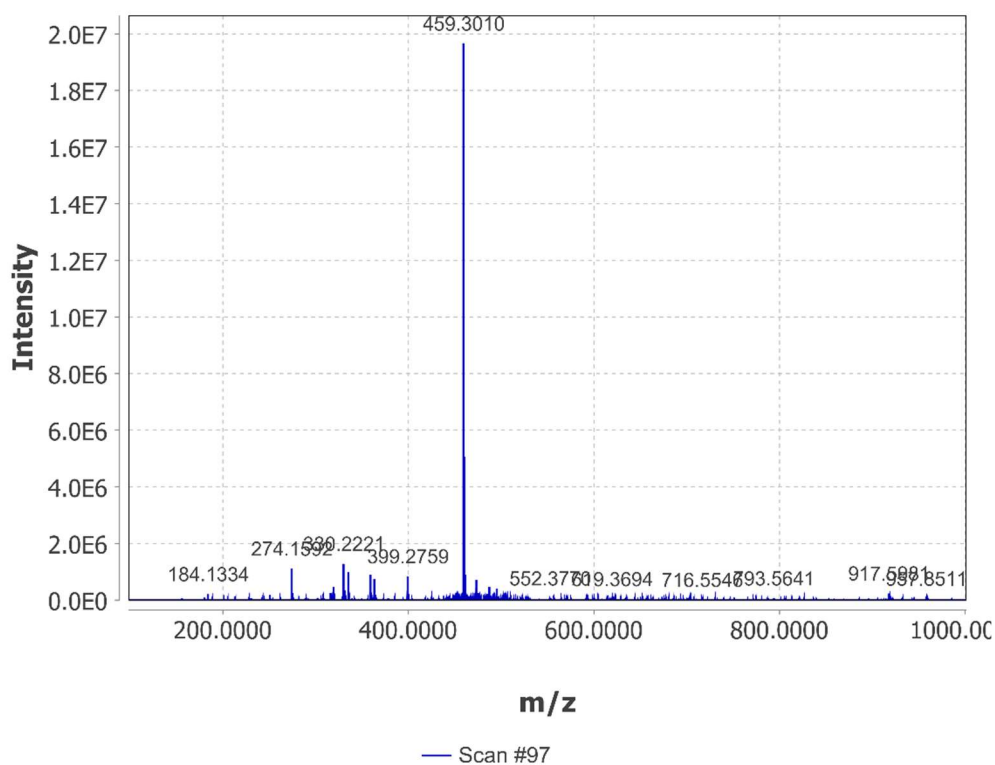
rac-11h (^{13}C):



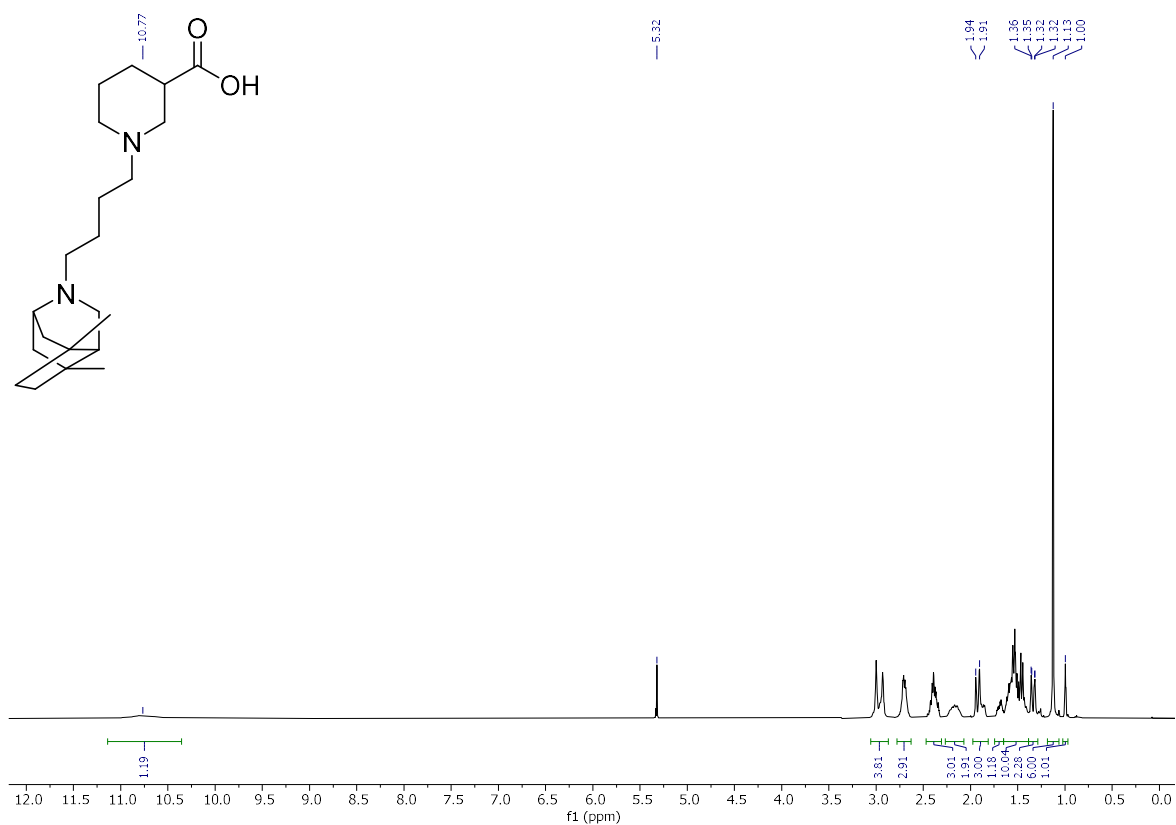
rac-11h (HRESIMS):

05-herup-635.raw#97 @0.83 MS1 p +, base peak: 459.3010 m/z (2.0E7)

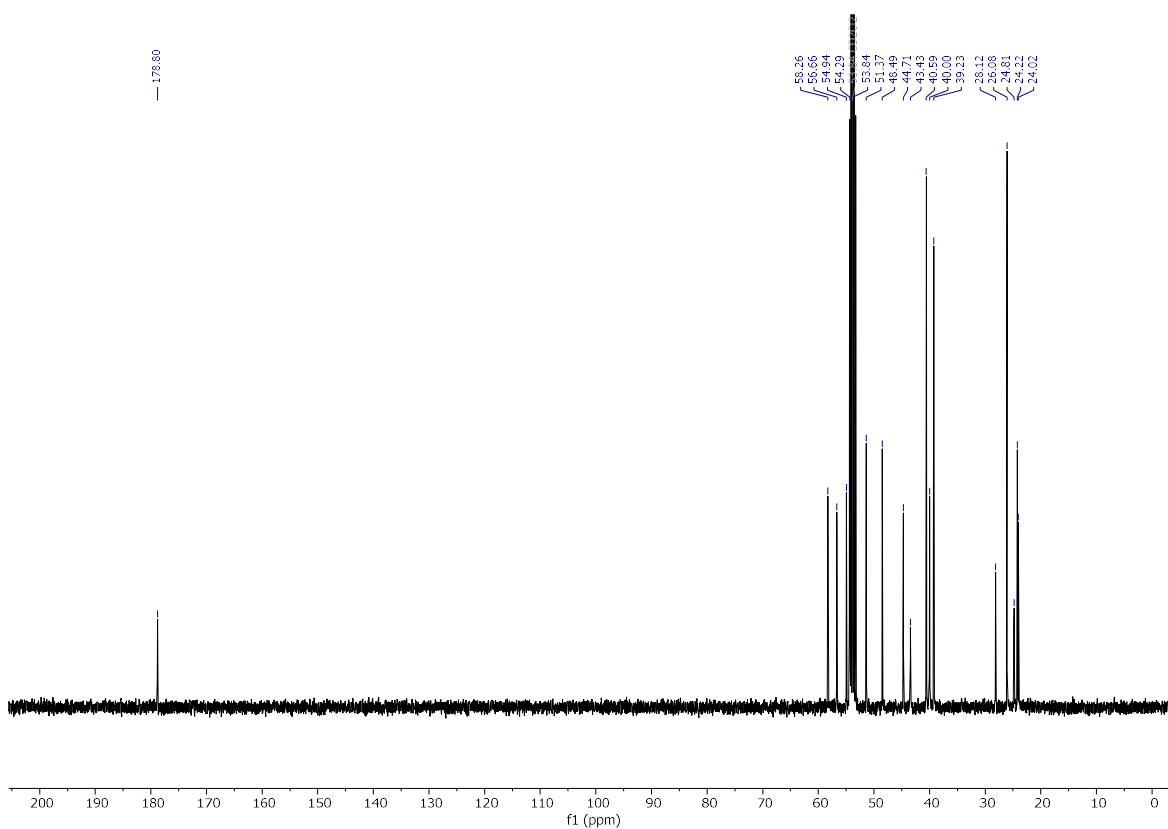
Scan definition: FTMS + p ESI Full ms [100.00-1000.00]



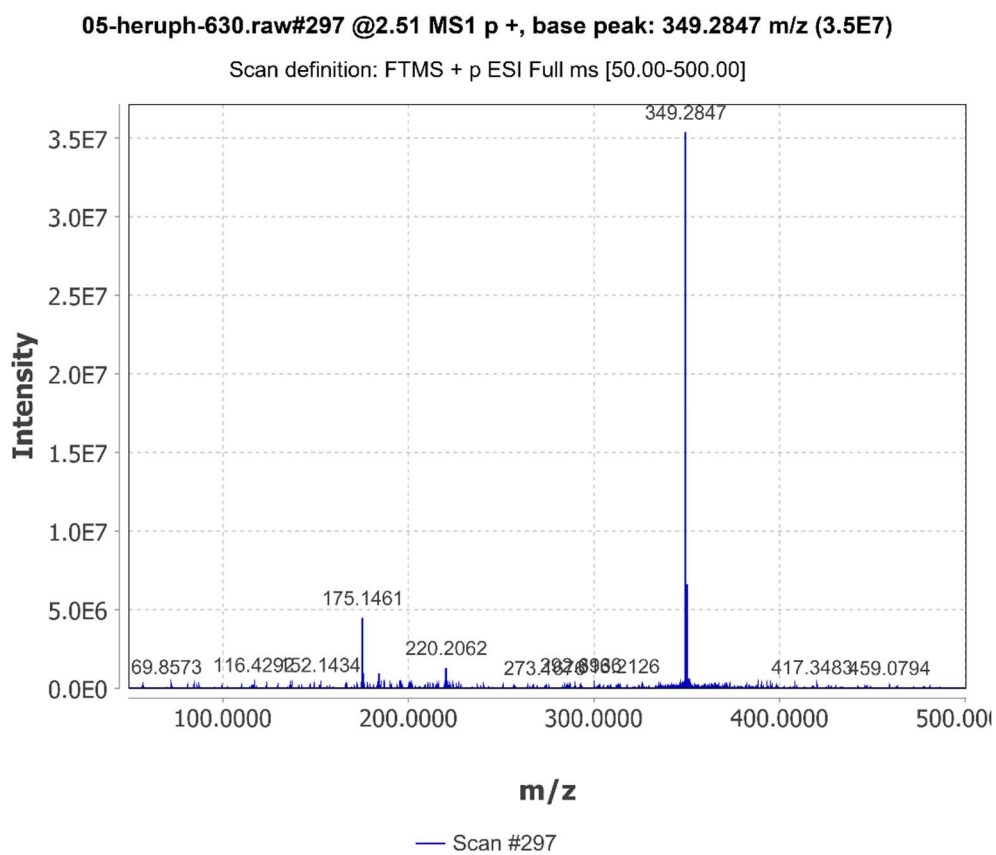
rac-11j (^1H):



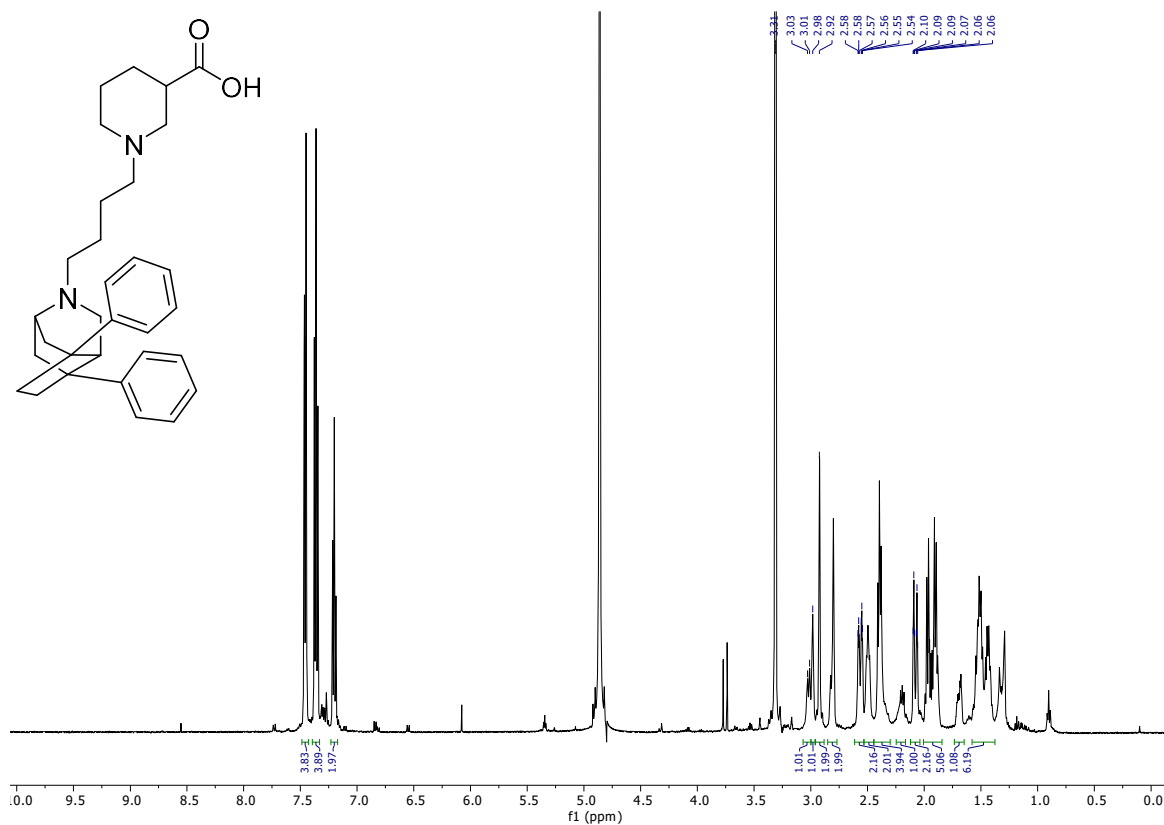
rac-11j (^{13}C):



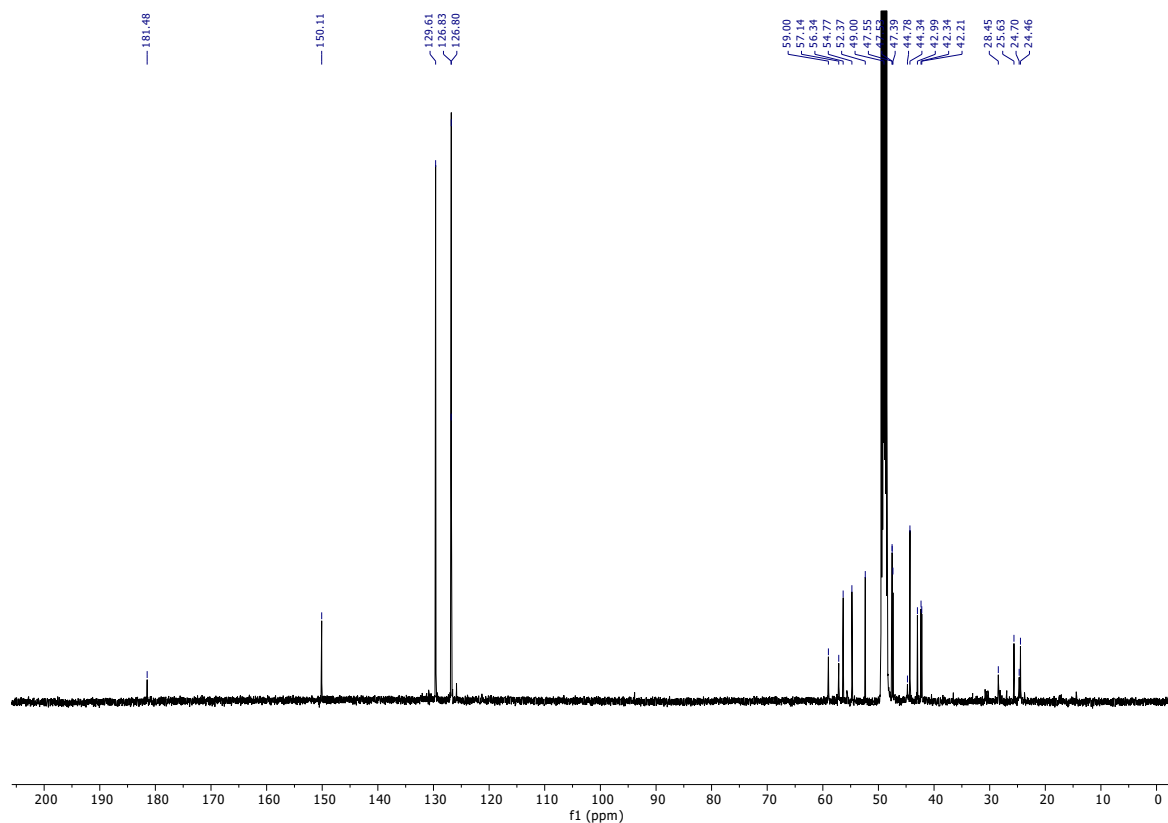
rac-11j (HRESIMS):



rac-11k (^1H):



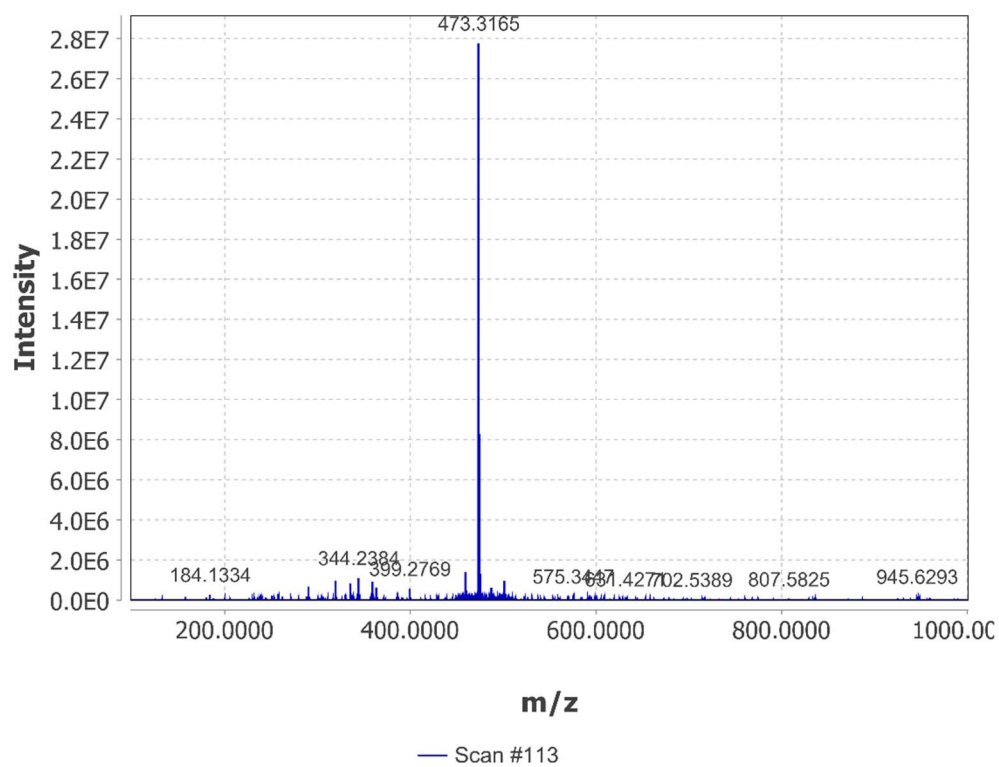
rac-11k (^{13}C):



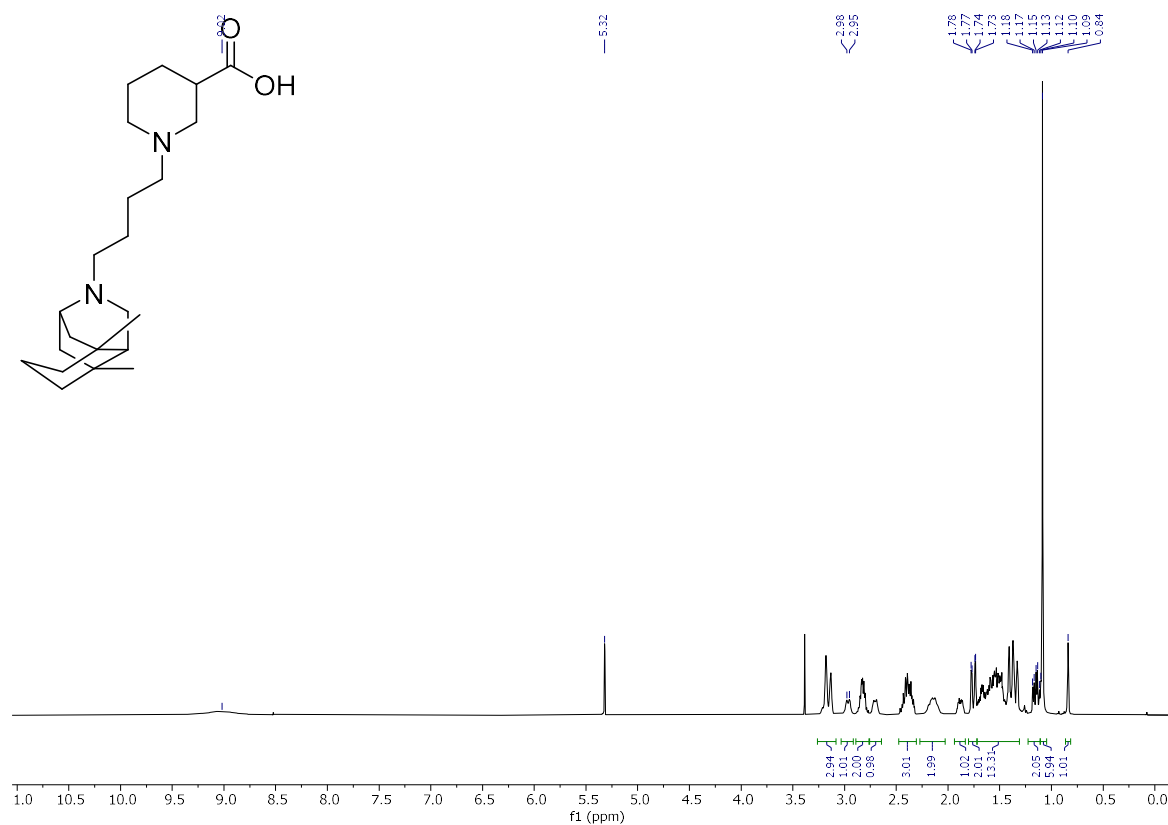
rac-11k (HRESIMS):

05-heruph-632.raw#113 @0.93 MS1 p +, base peak: 473.3165 m/z (2.8E7)

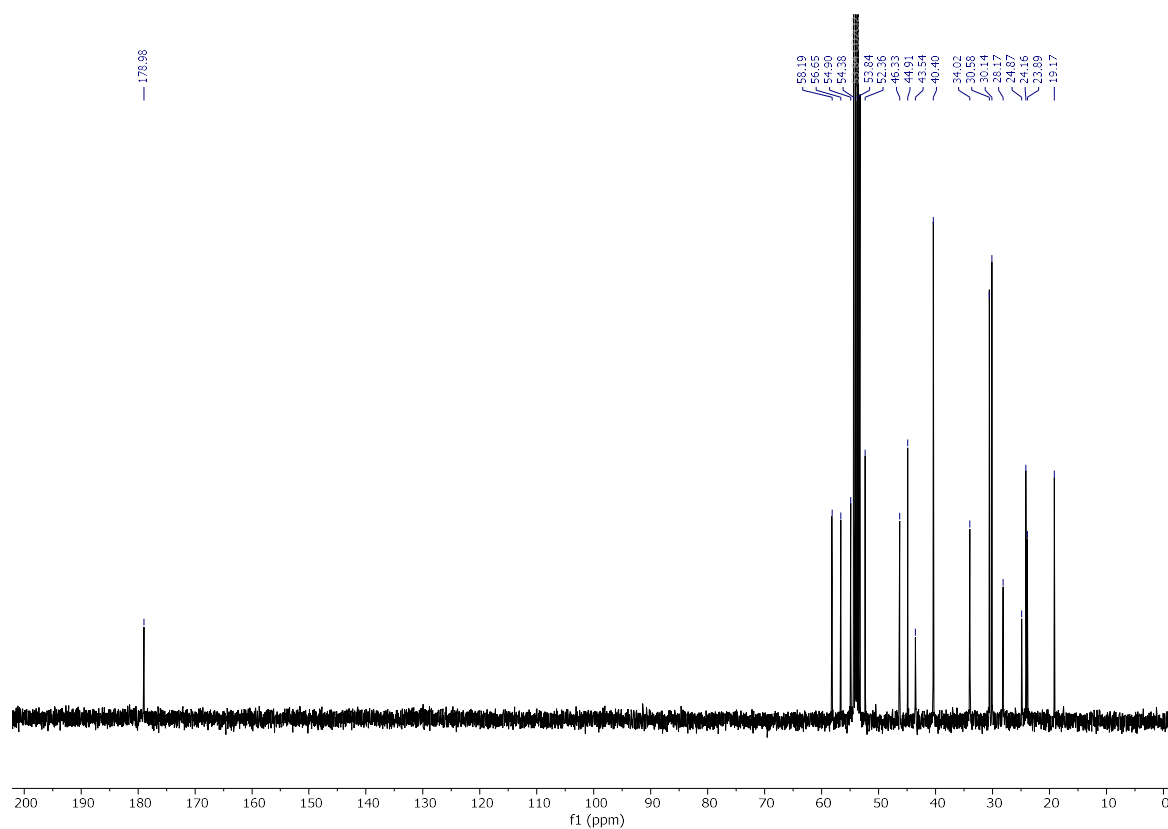
Scan definition: FTMS + p ESI Full ms [100.00-1000.00]



rac-**11l** (^1H):



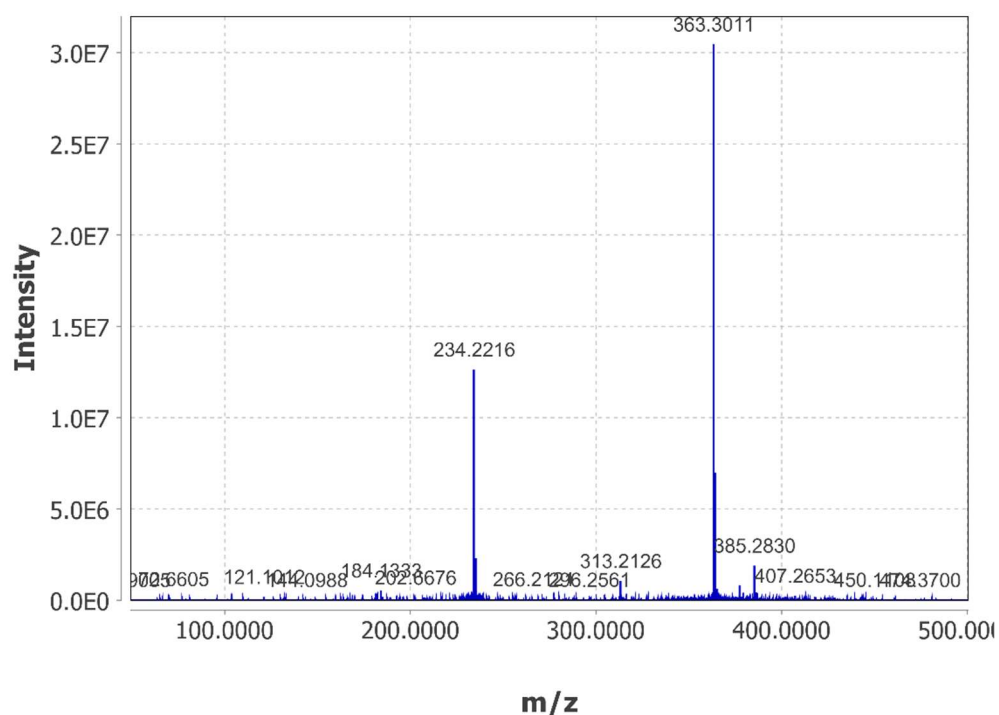
rac-**11l** (^{13}C):



rac-11l (HRESIMS):

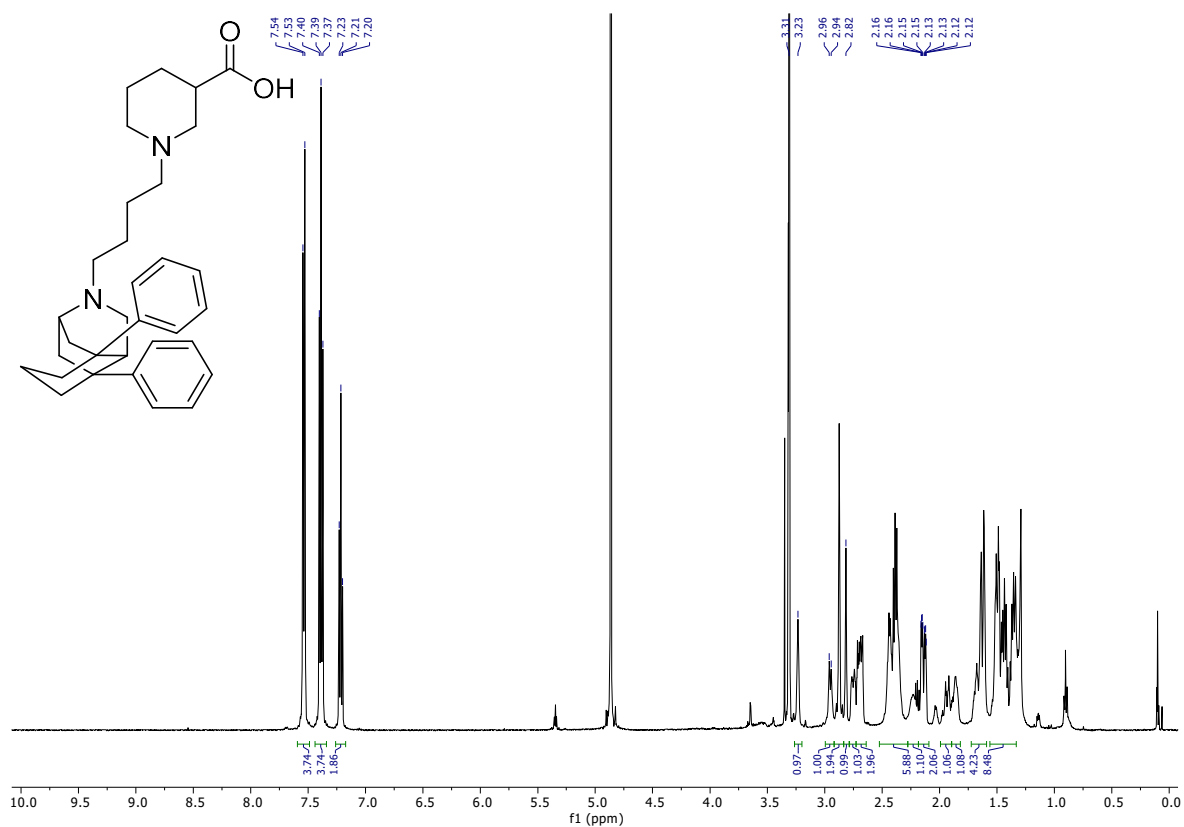
06-heruph-633_190606145418.raw#105 @0.95 MS1 p +, base peak: 363.3011 m/z (3.0E7)

Scan definition: FTMS + p ESI Full ms [50.00-500.00]

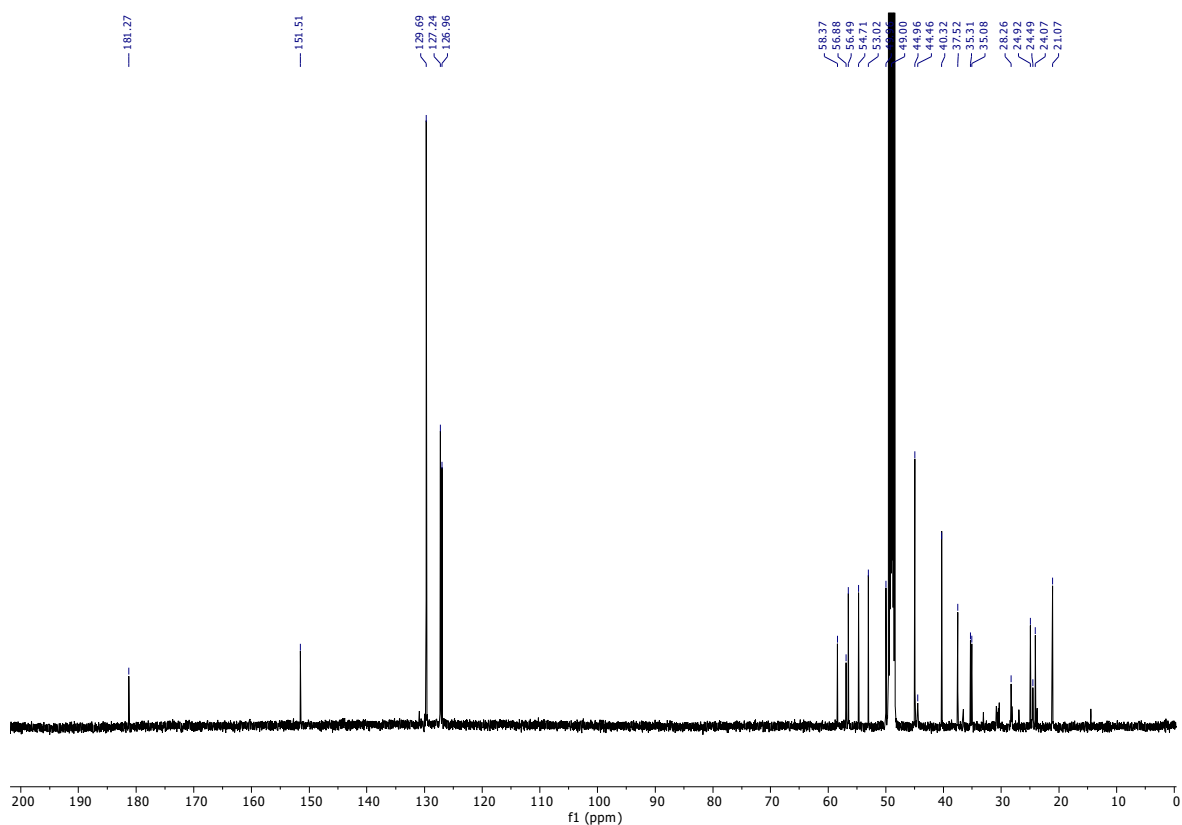


— Scan #105

rac-11m (^1H):



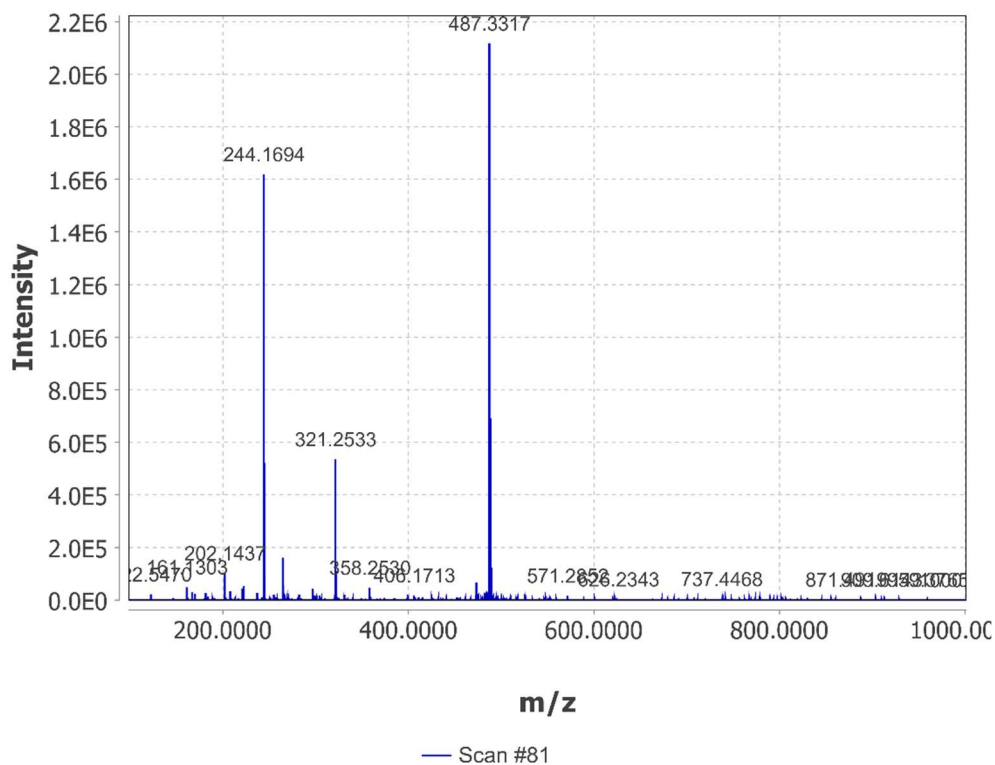
rac-11m (^{13}C):

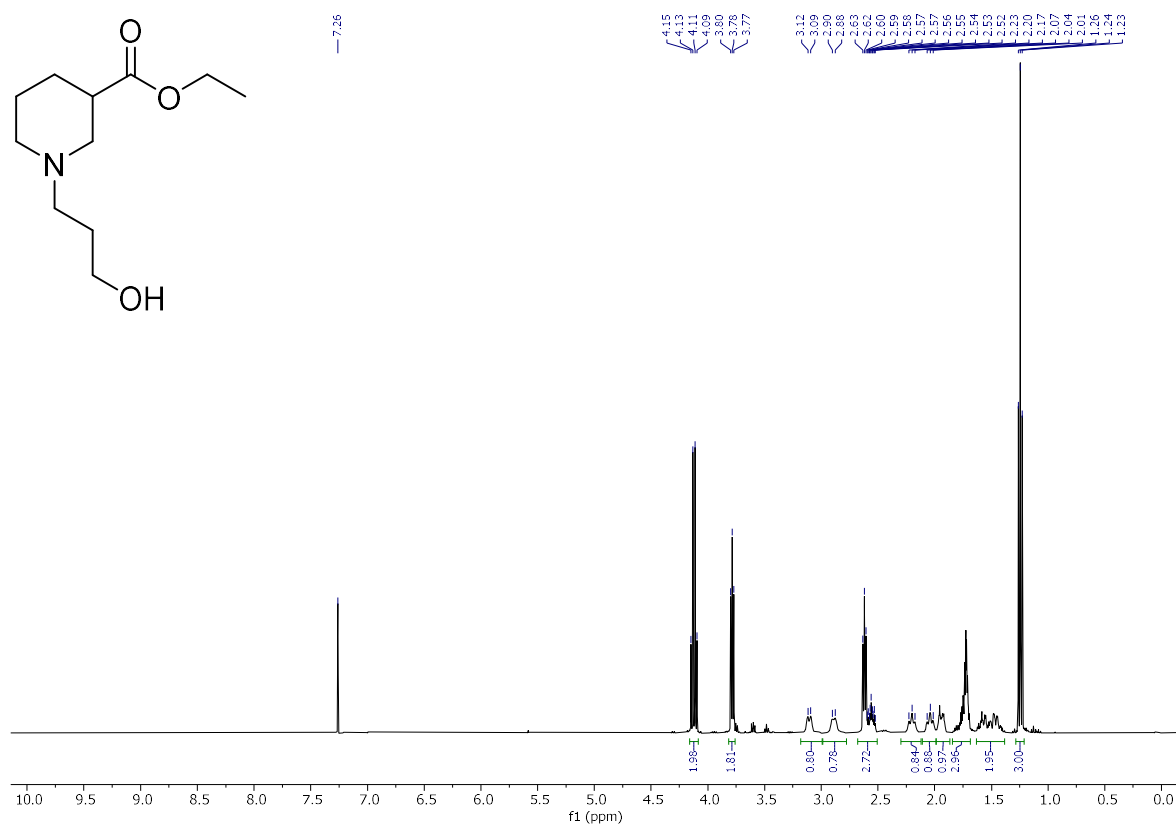
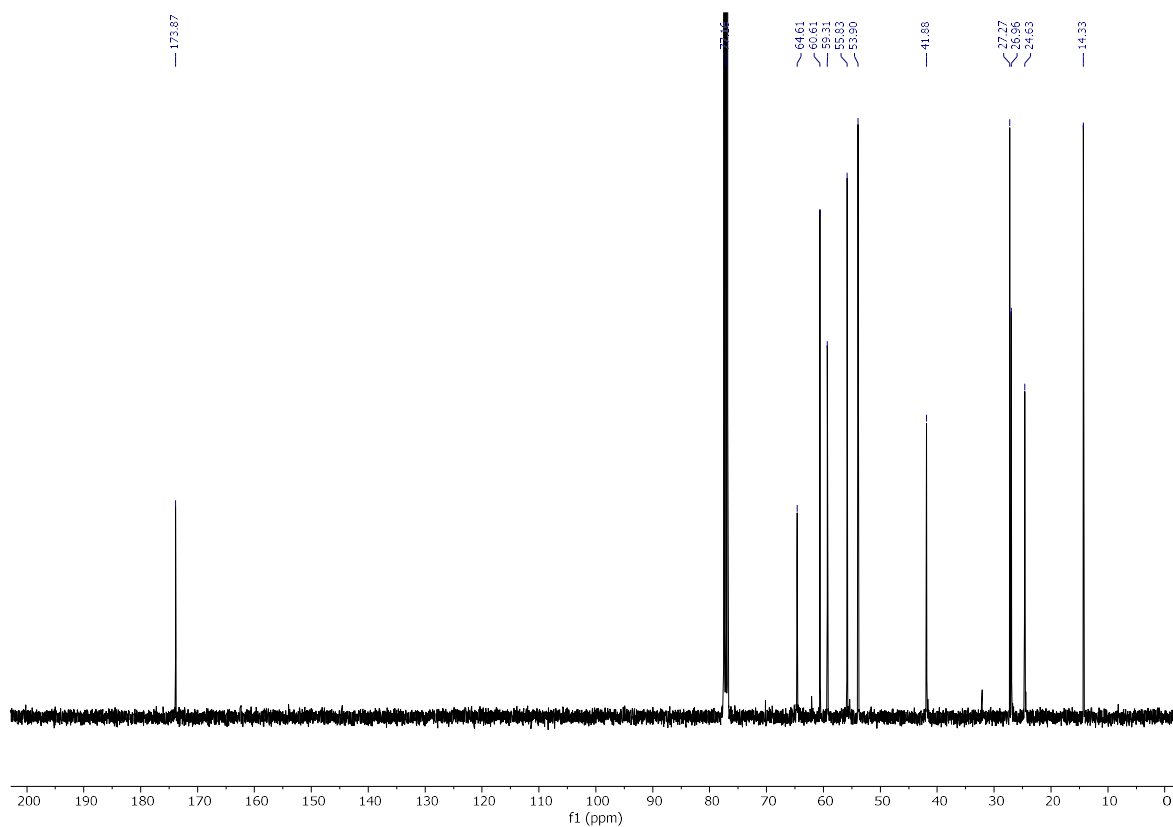


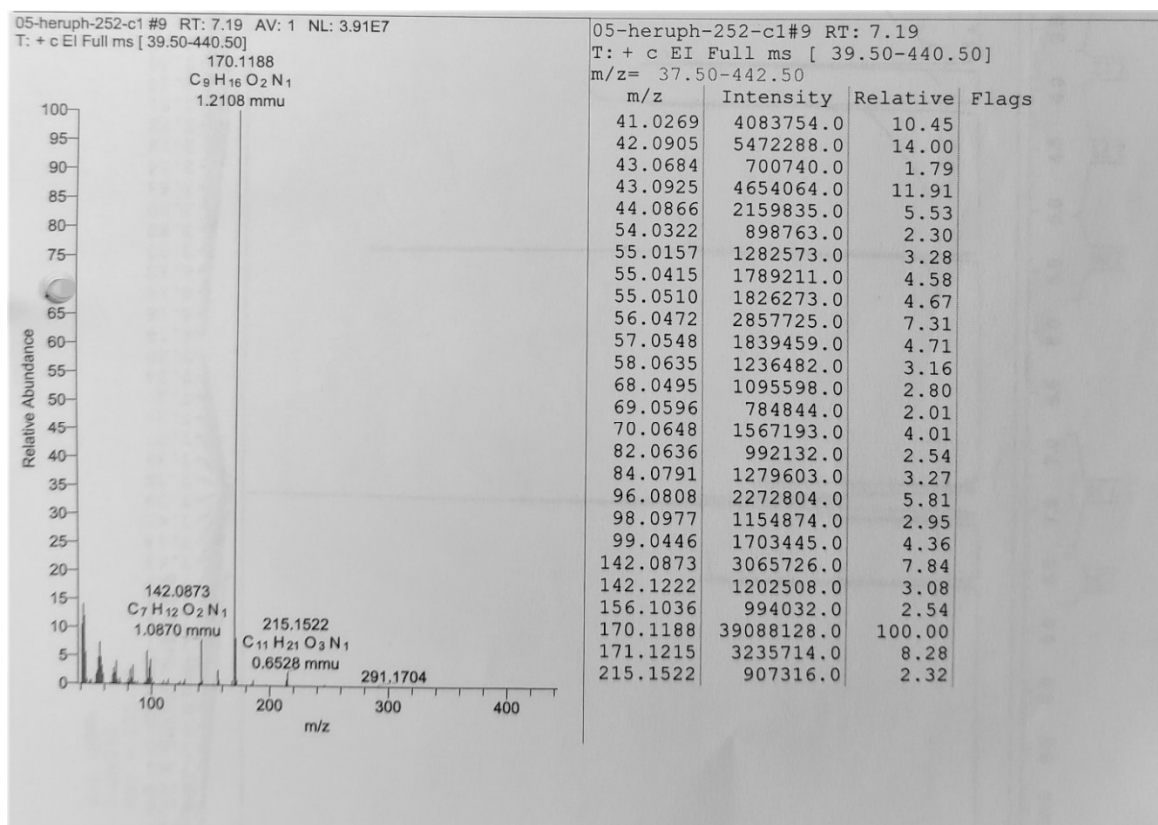
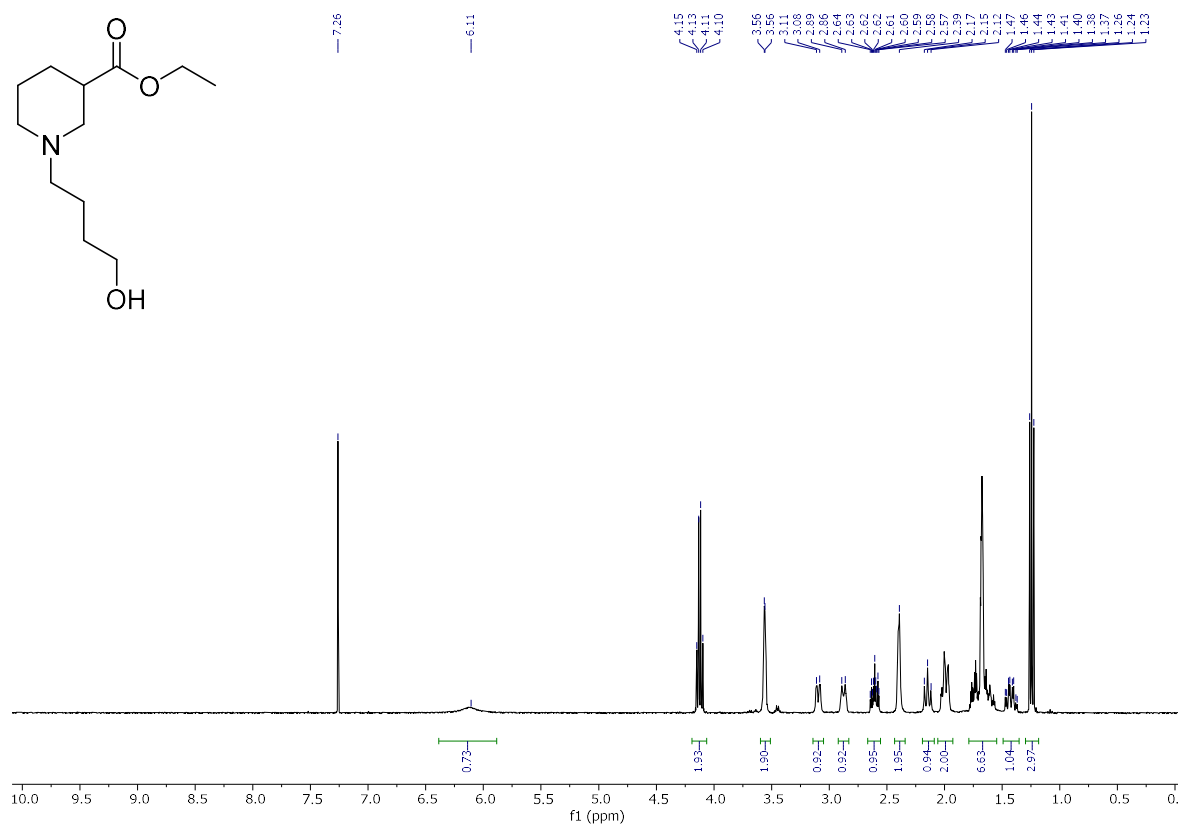
rac-11m (HRESIMS):

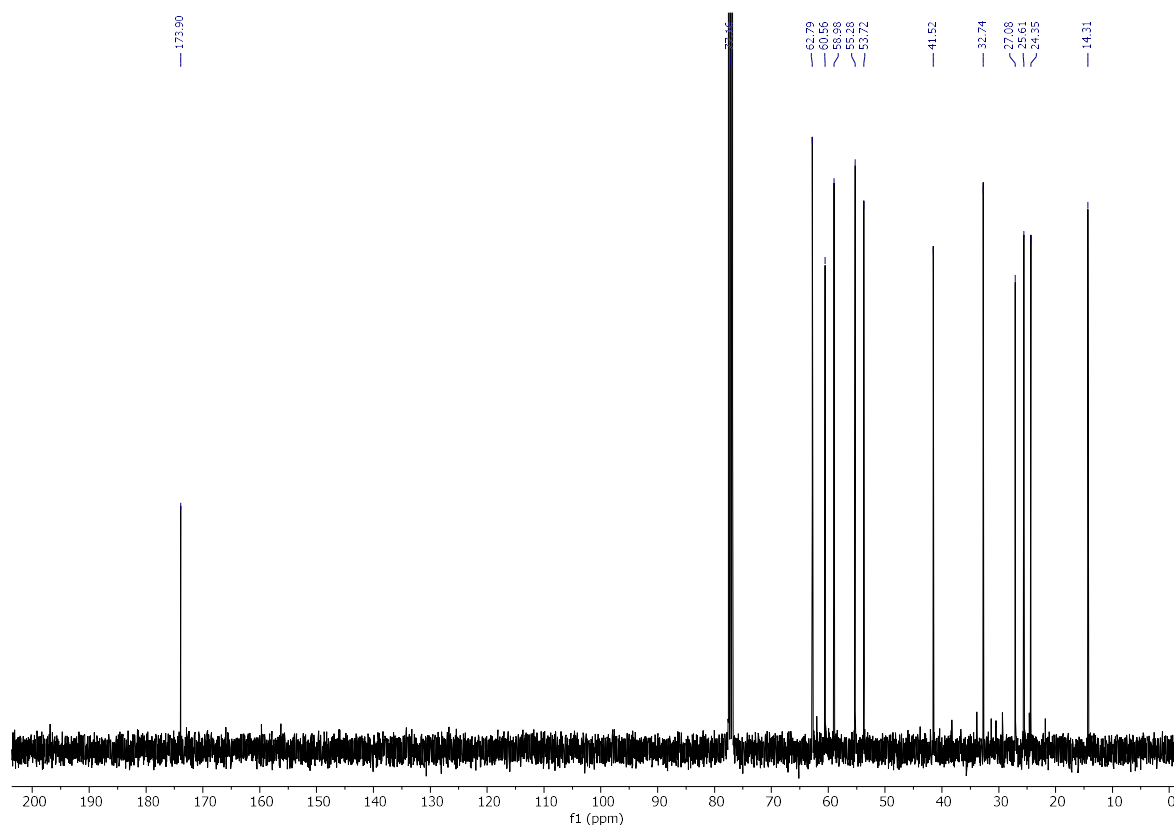
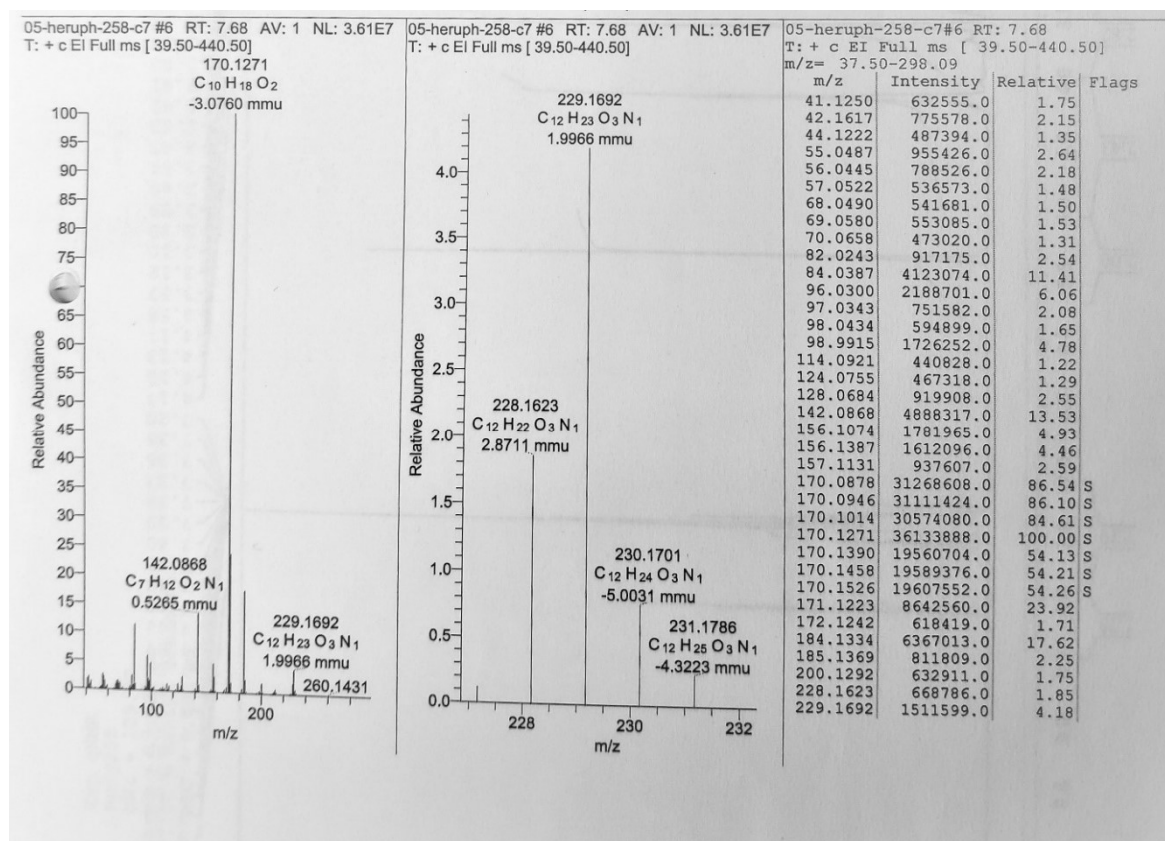
02-heruph-656.raw#81 @0.77 MS1 p +, base peak: 487.3317 m/z (2.1E6)

Scan definition: FTMS + p ESI Full ms [100.00-1000.00]

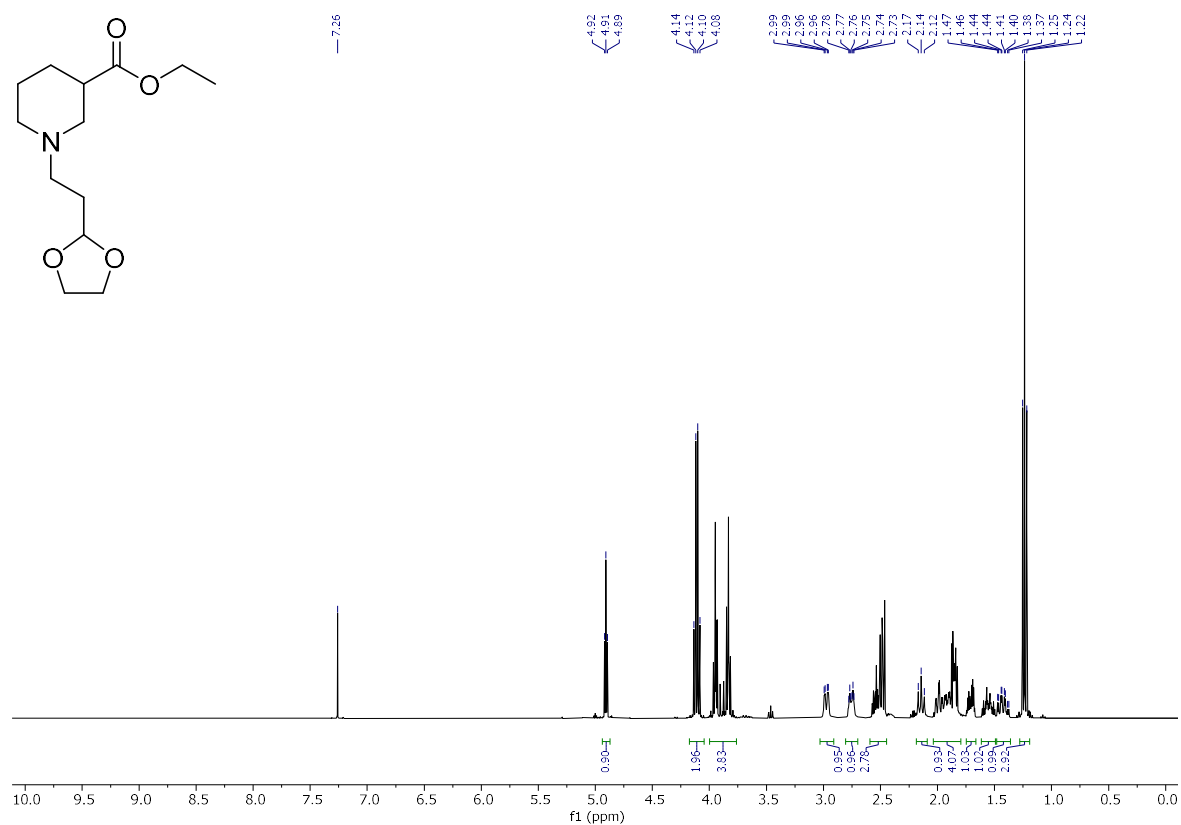


rac-15a (^1H):*rac-15a* (^{13}C):

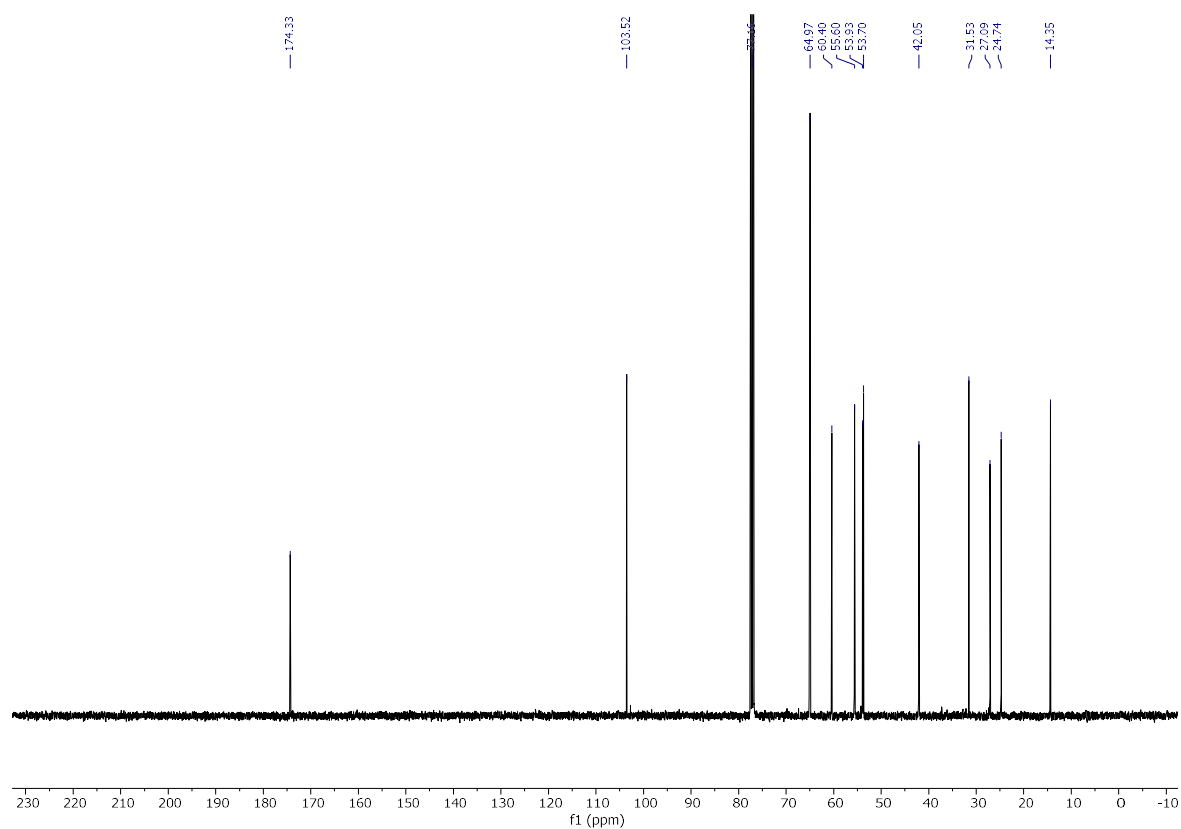
rac-15a (HREIMS):*rac-15b* (¹H):

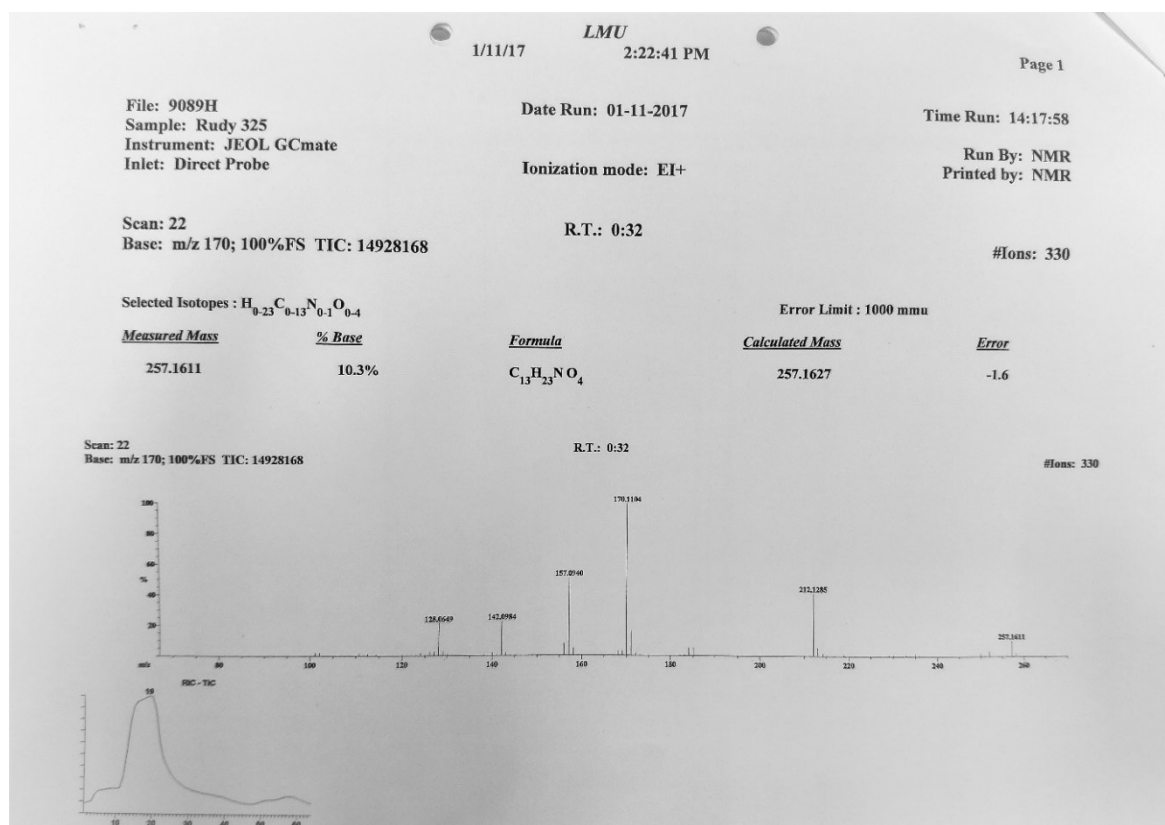
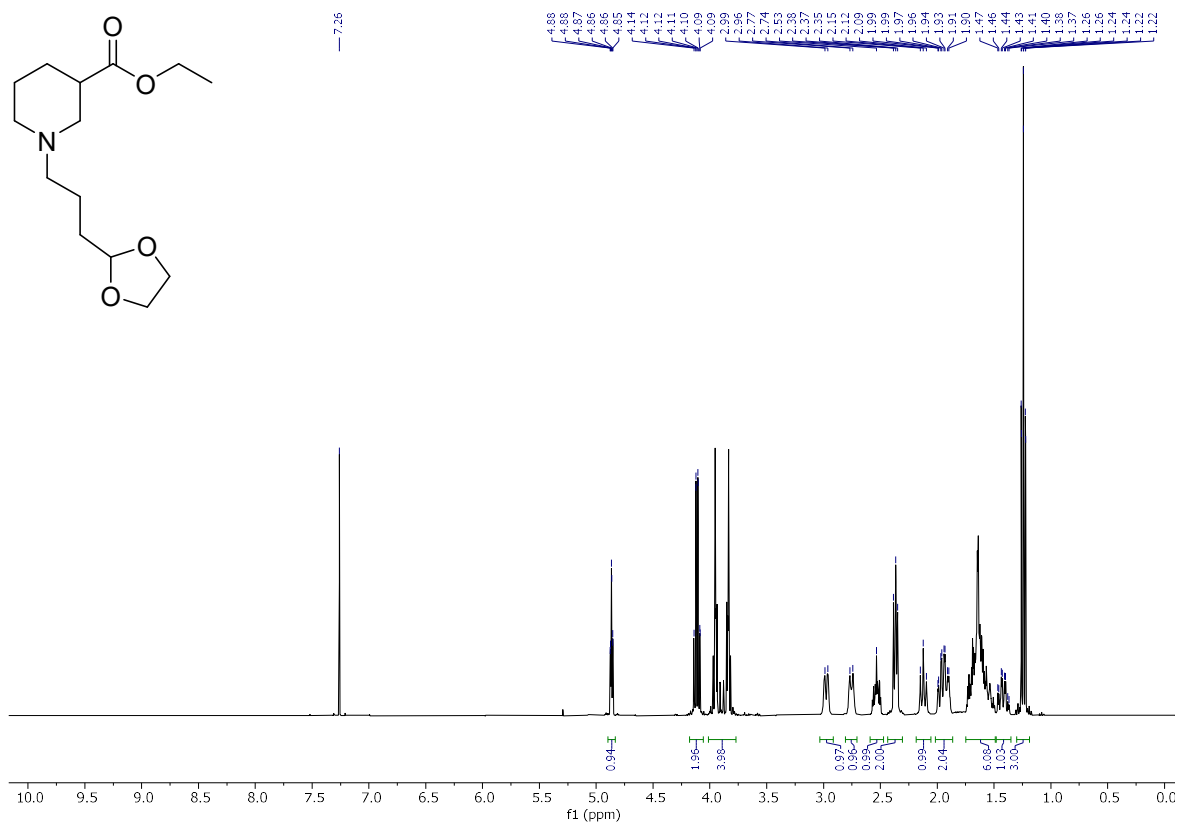
rac-15b (^{13}C):*rac*-15b (HREIMS):

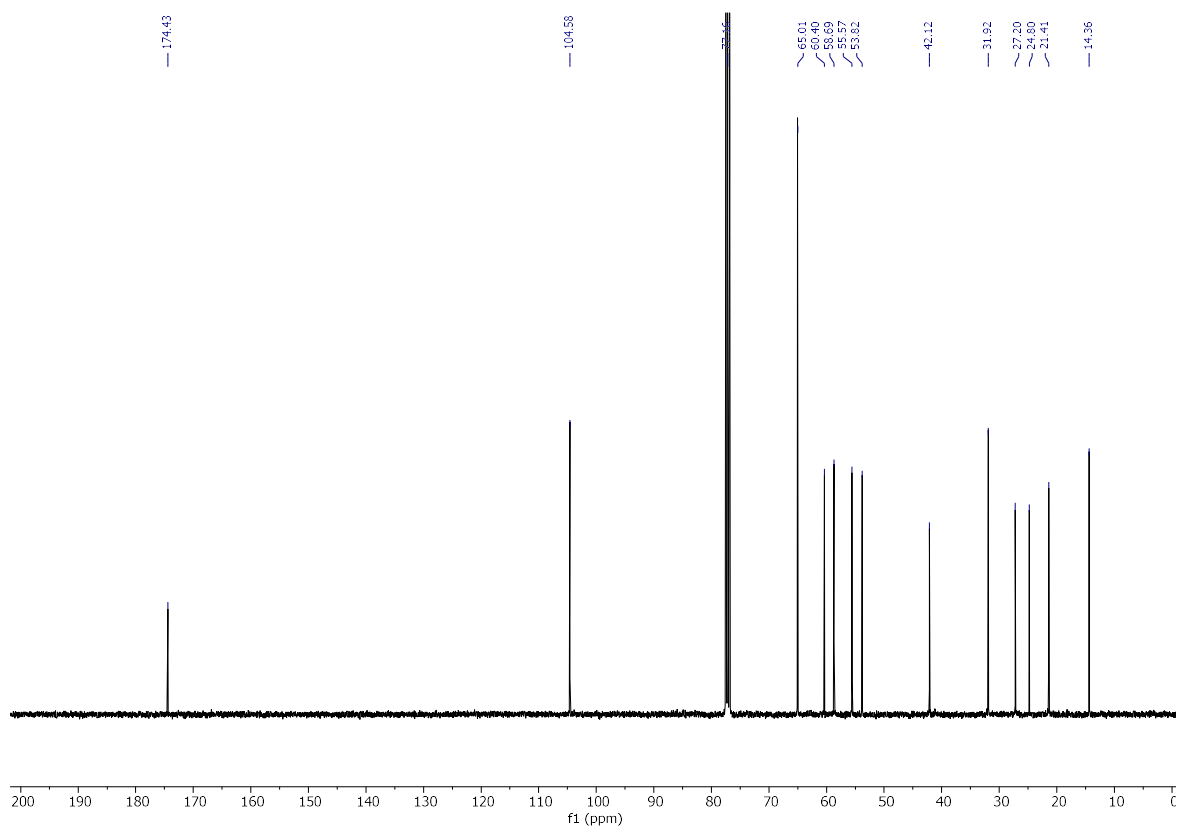
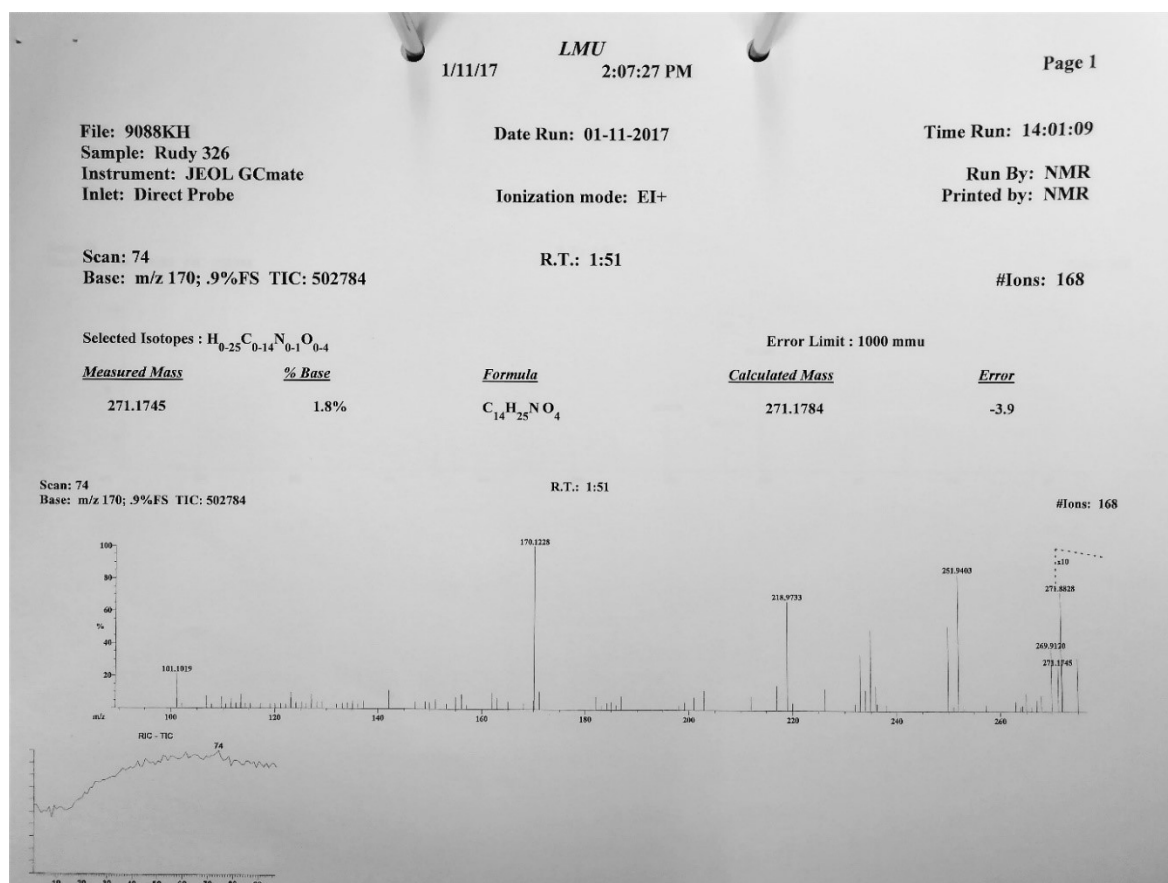
rac-**15c** (^1H):



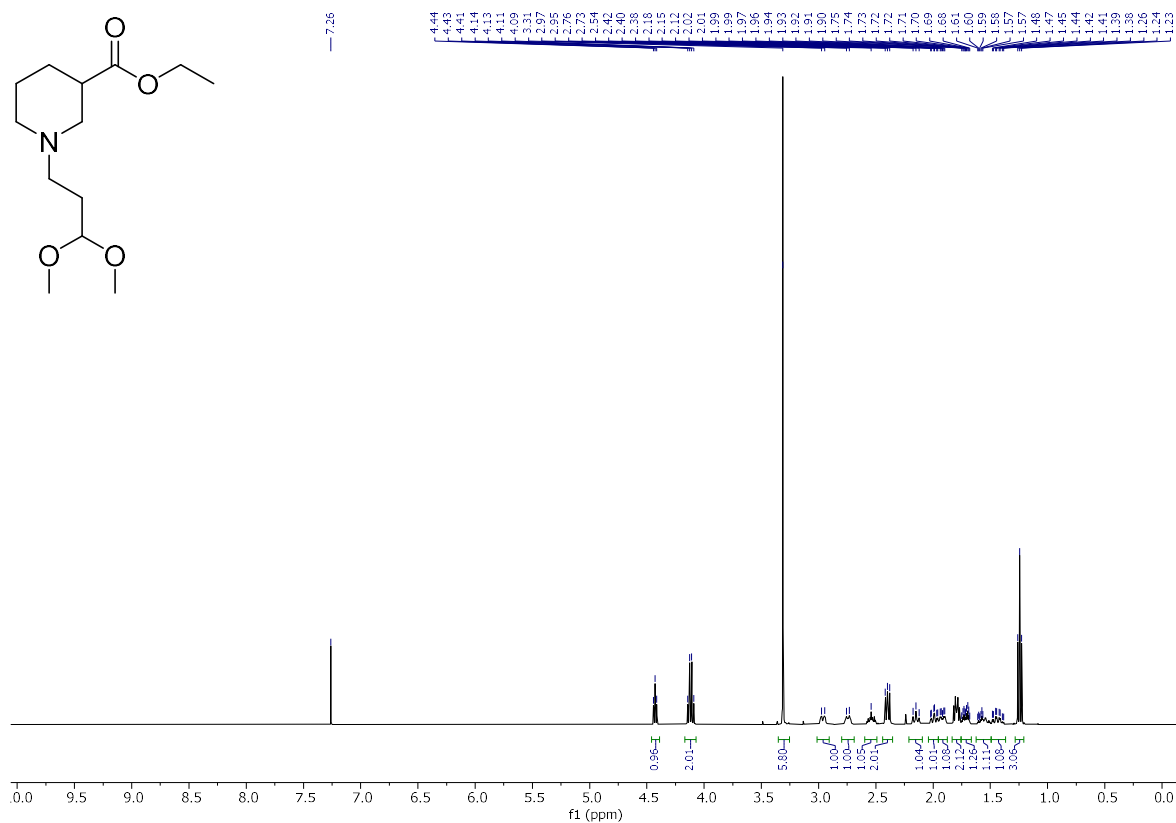
rac-**15c** (^{13}C):



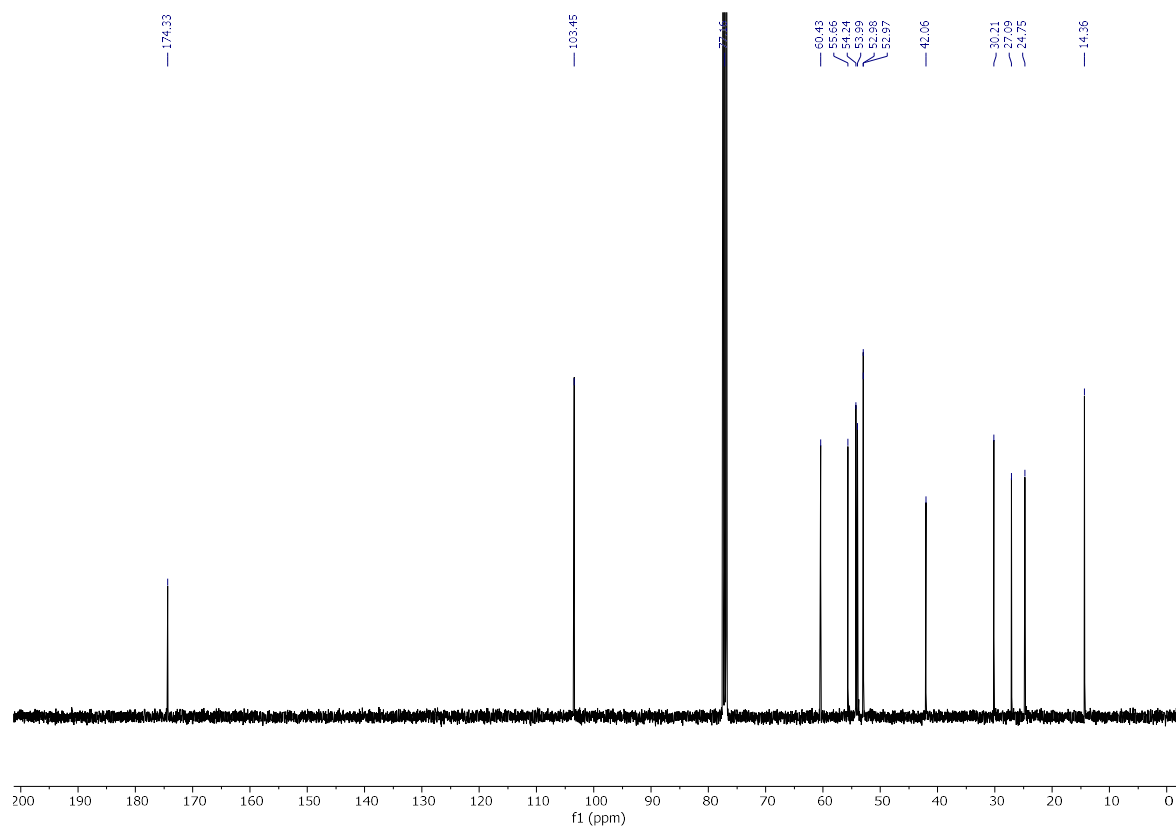
rac-15c (HREIMS):*rac-15d* (1H):

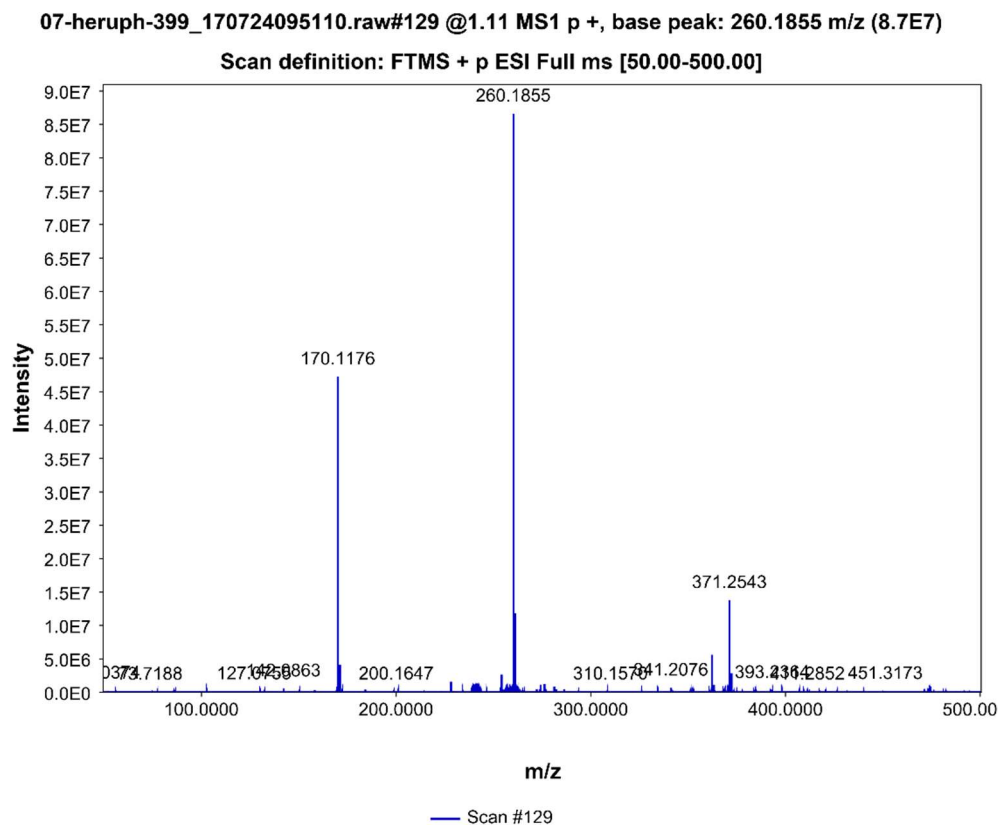
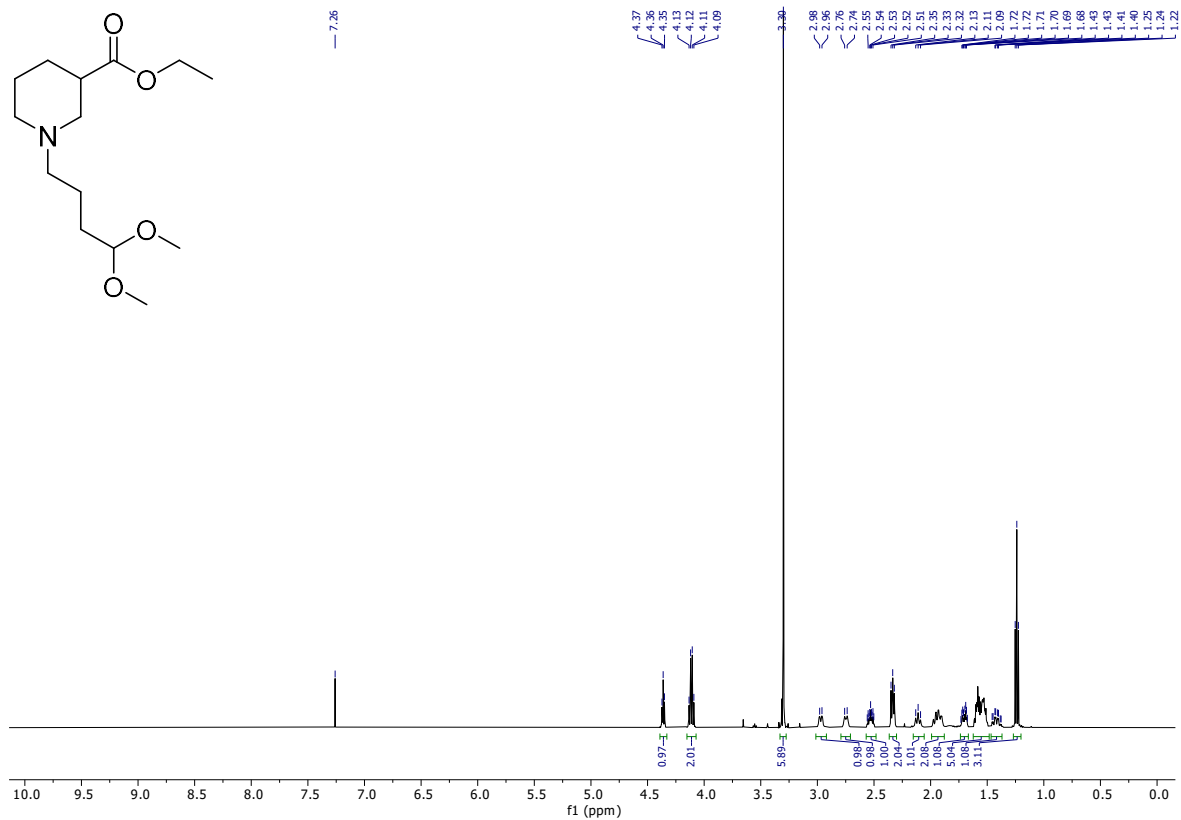
rac-15d (^{13}C):*rac*-15d (HREIMS):

rac-15e (^1H):

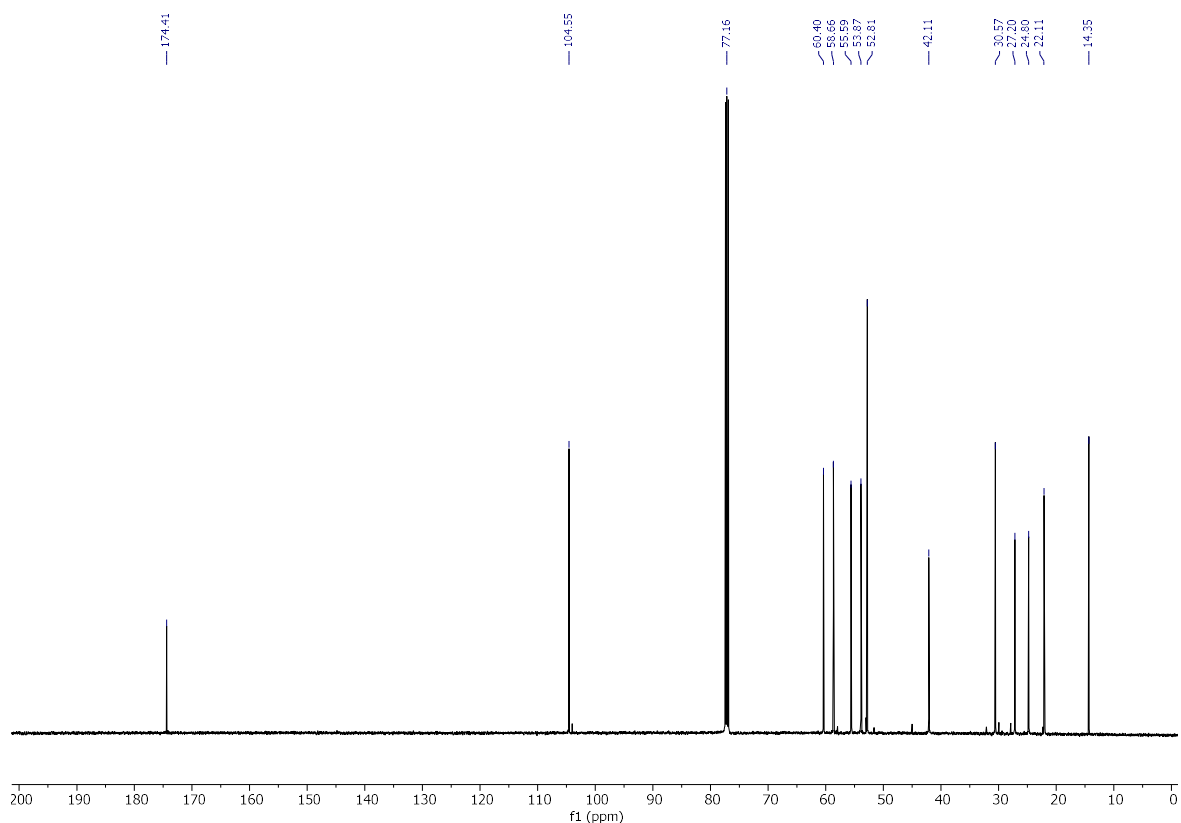


rac-15e (^{13}C):

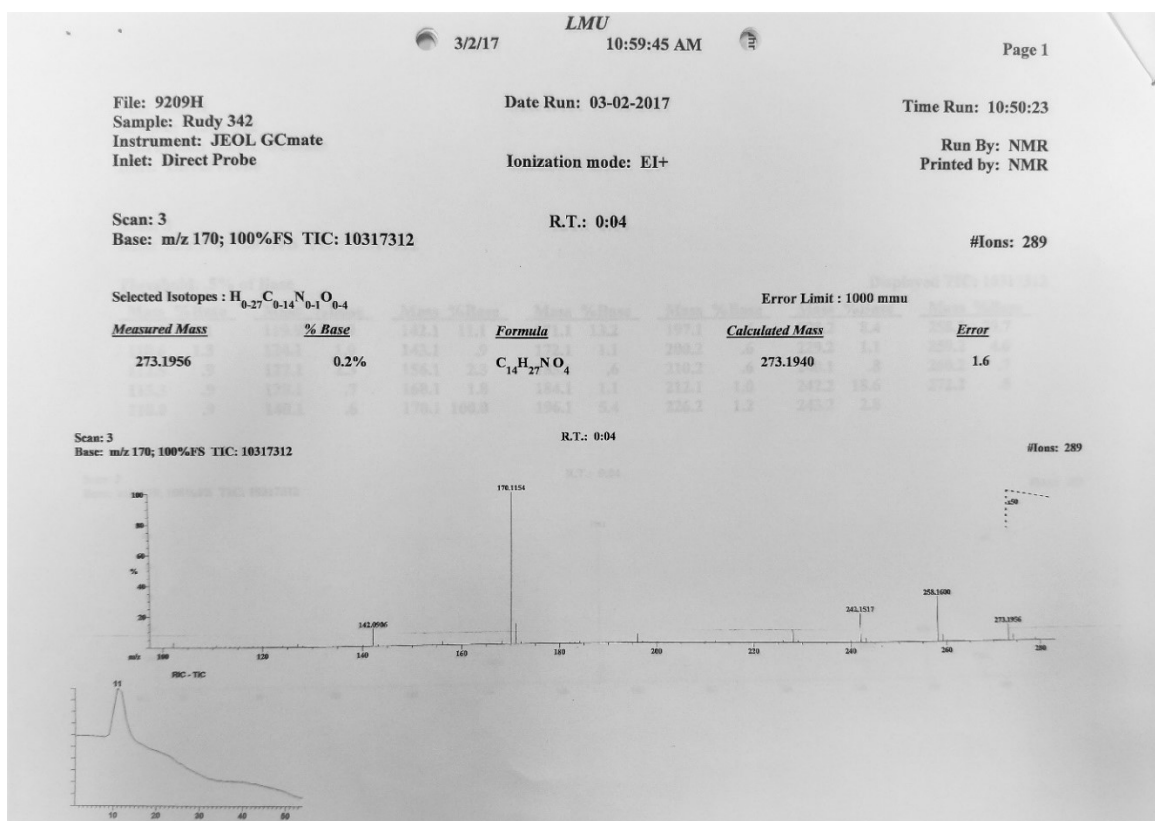


rac-15e (HRESIMS):*rac-15f* (^1H):

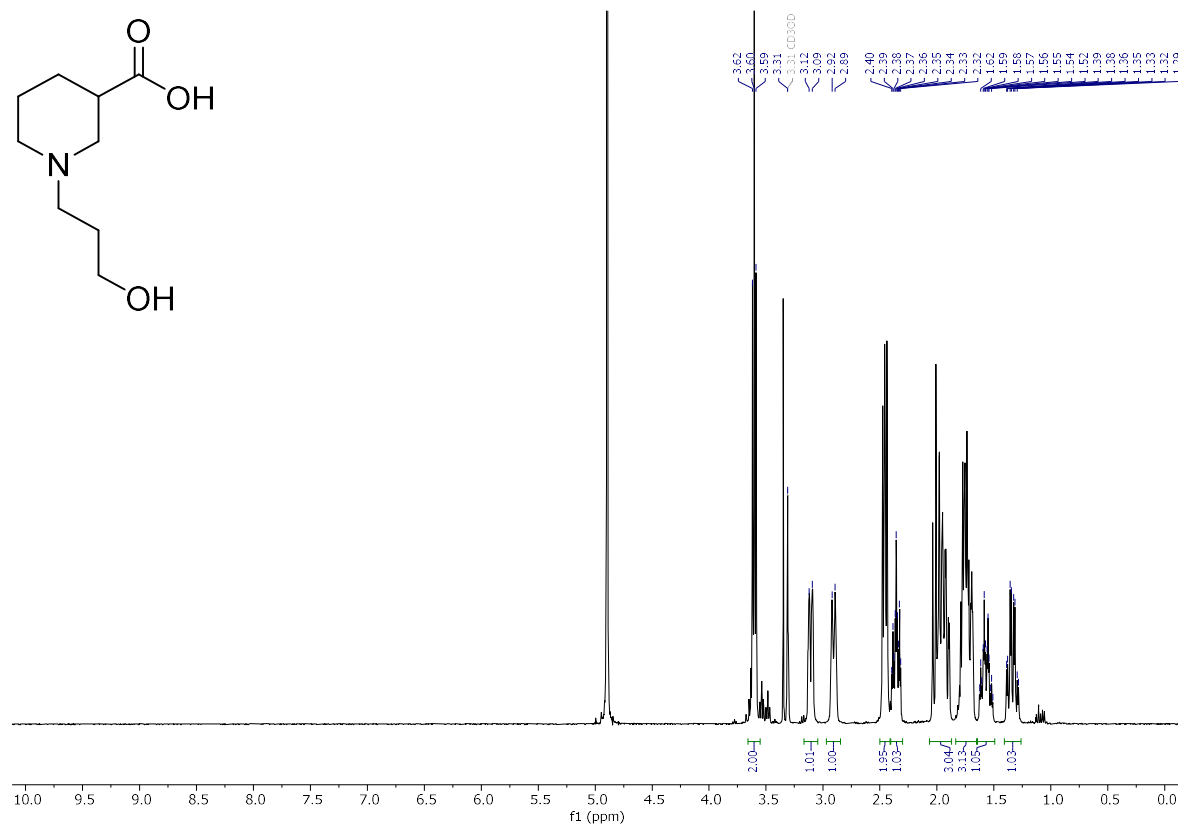
rac-15f (¹³C):



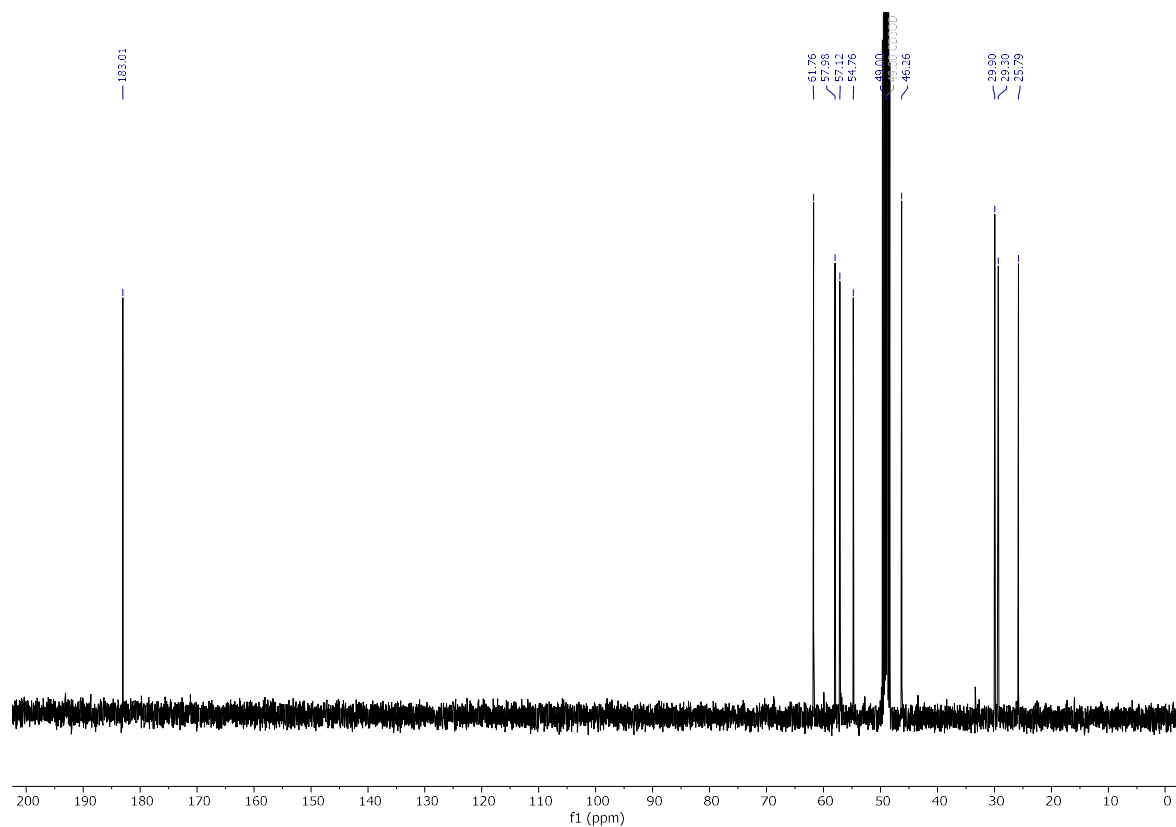
rac-15f (HREIMS):



rac-18a (^1H):



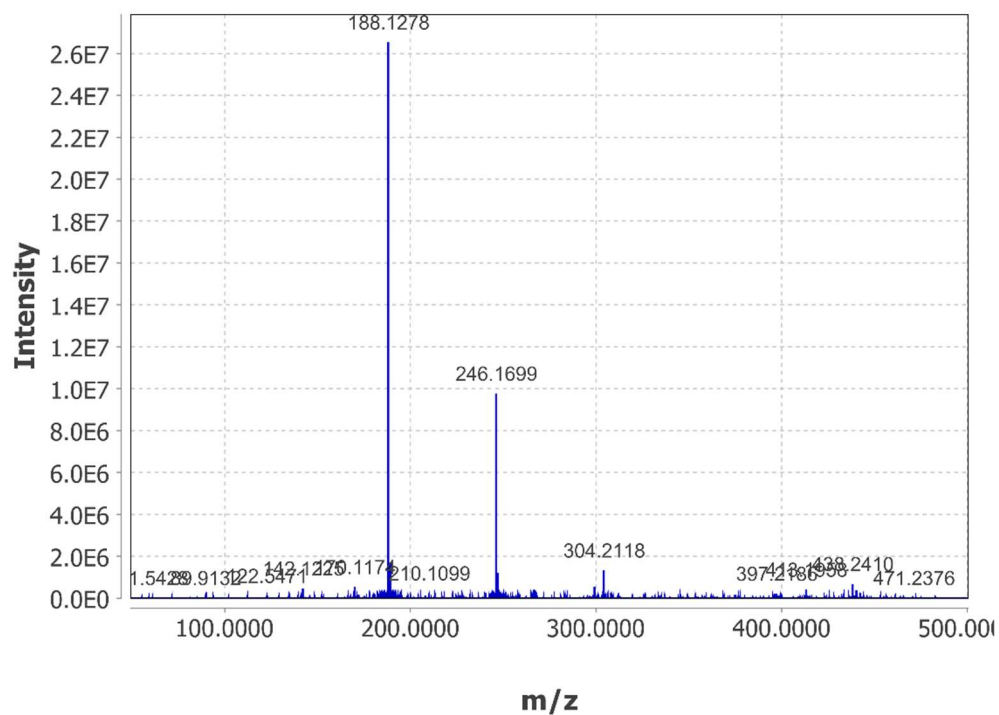
rac-18a (^{13}C):



rac-18a (HRESIMS):

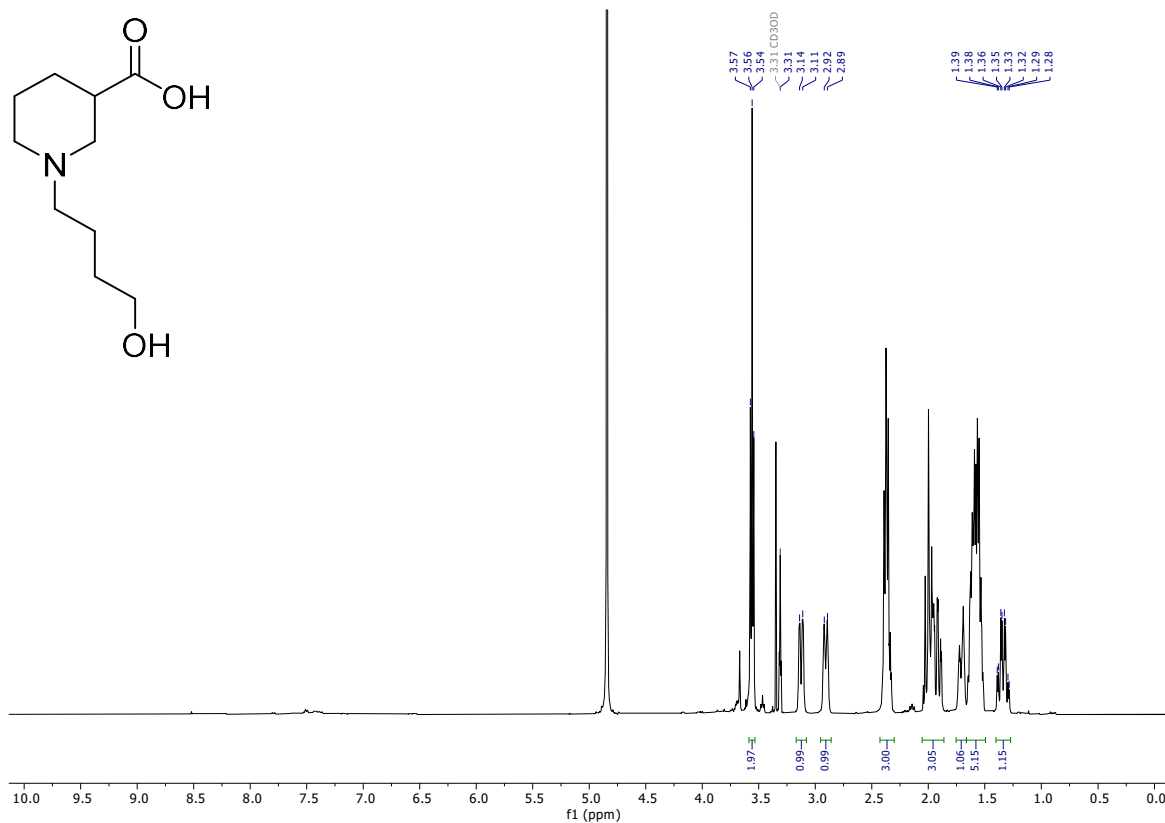
02-heruph-663.raw#89 @0.81 MS1 p +, base peak: 188.1278 m/z (2.7E7)

Scan definition: FTMS + p ESI Full ms [50.00-500.00]

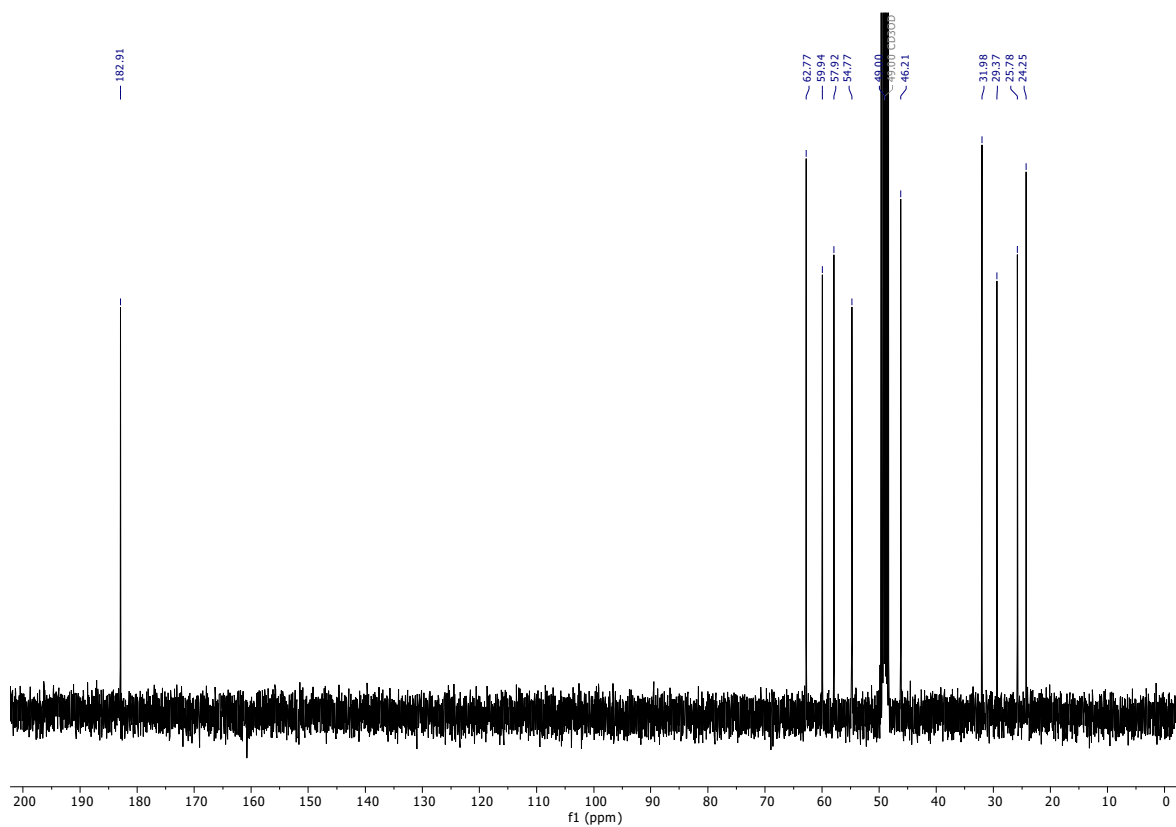


— Scan #89

rac-18b (^1H):



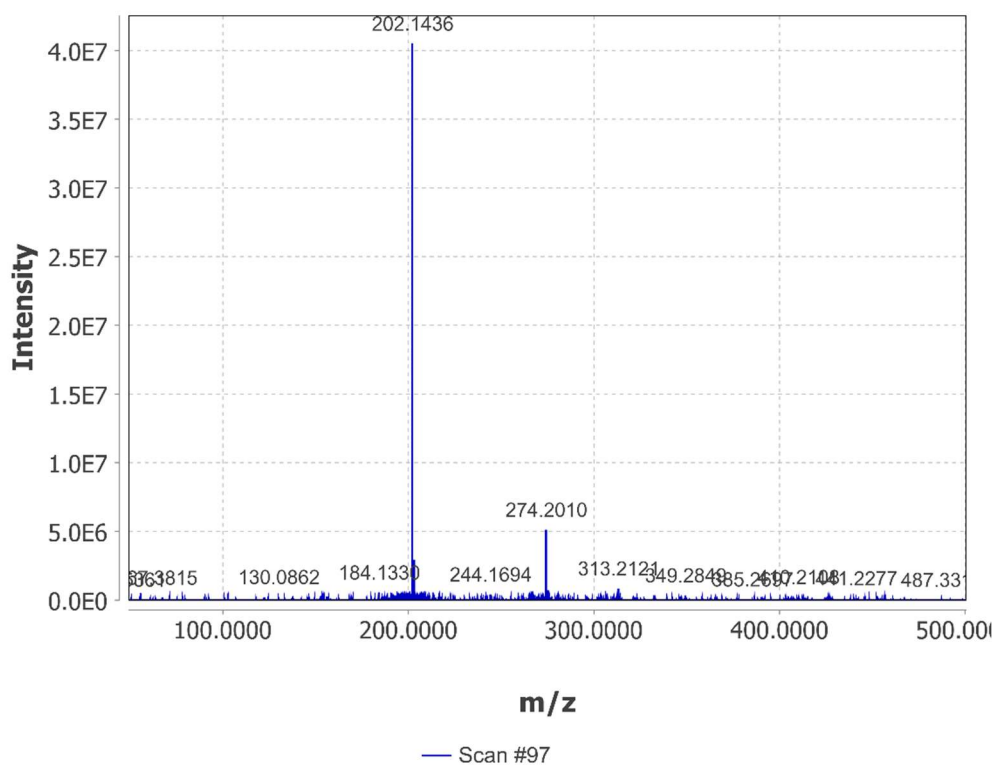
rac-**18b** (^{13}C):



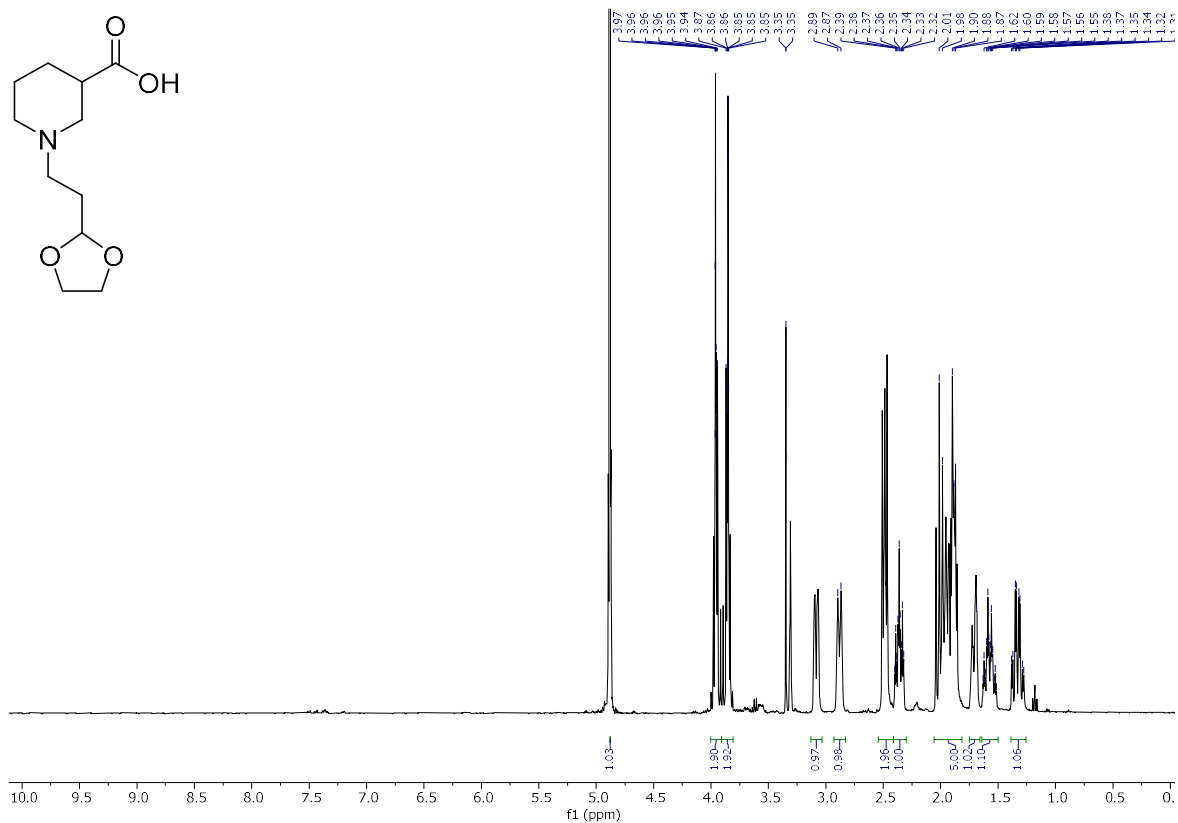
rac-**18b** (HRESIMS):

02-heruph-662.raw#97 @0.87 MS1 p +, base peak: 202.1436 m/z (4.1E7)

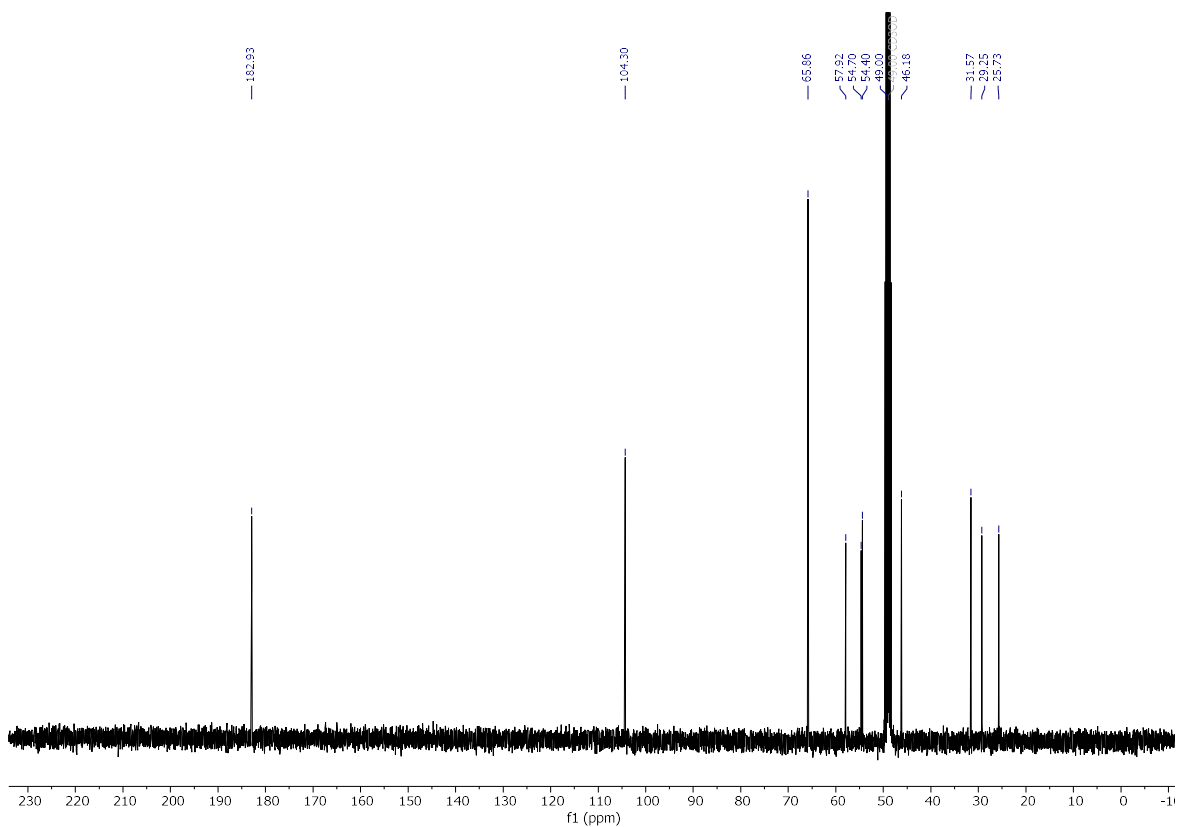
Scan definition: FTMS + p ESI Full ms [50.00-500.00]



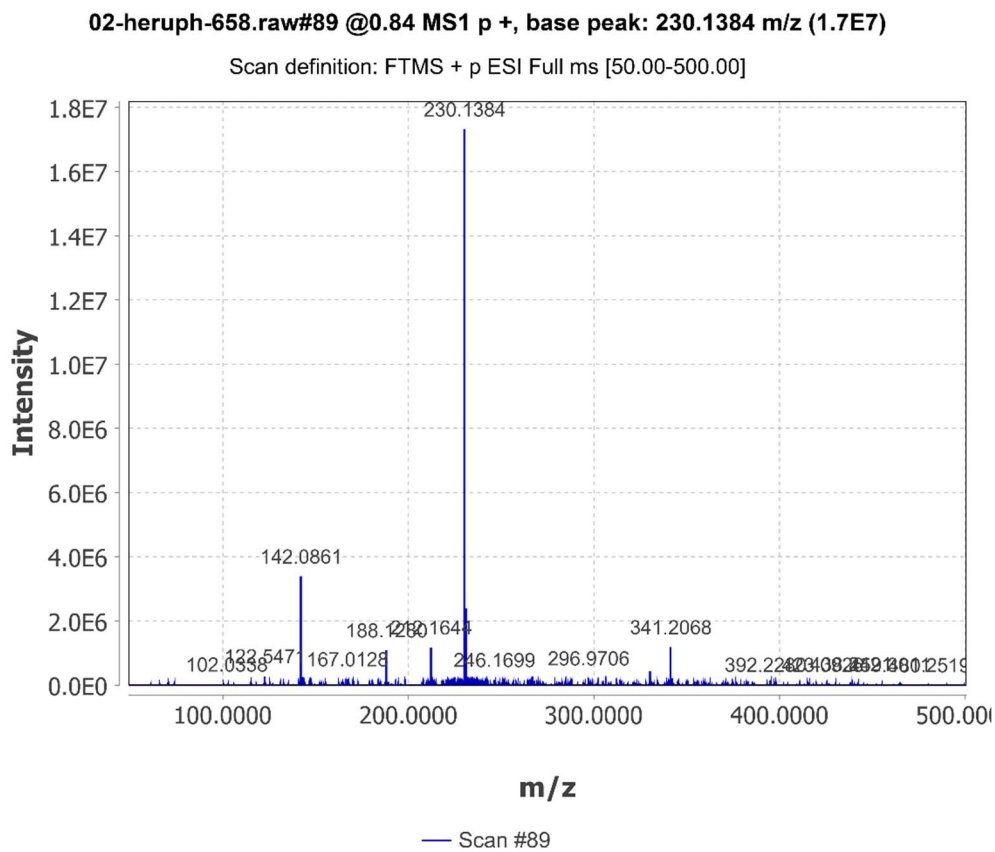
rac-18c (^1H):



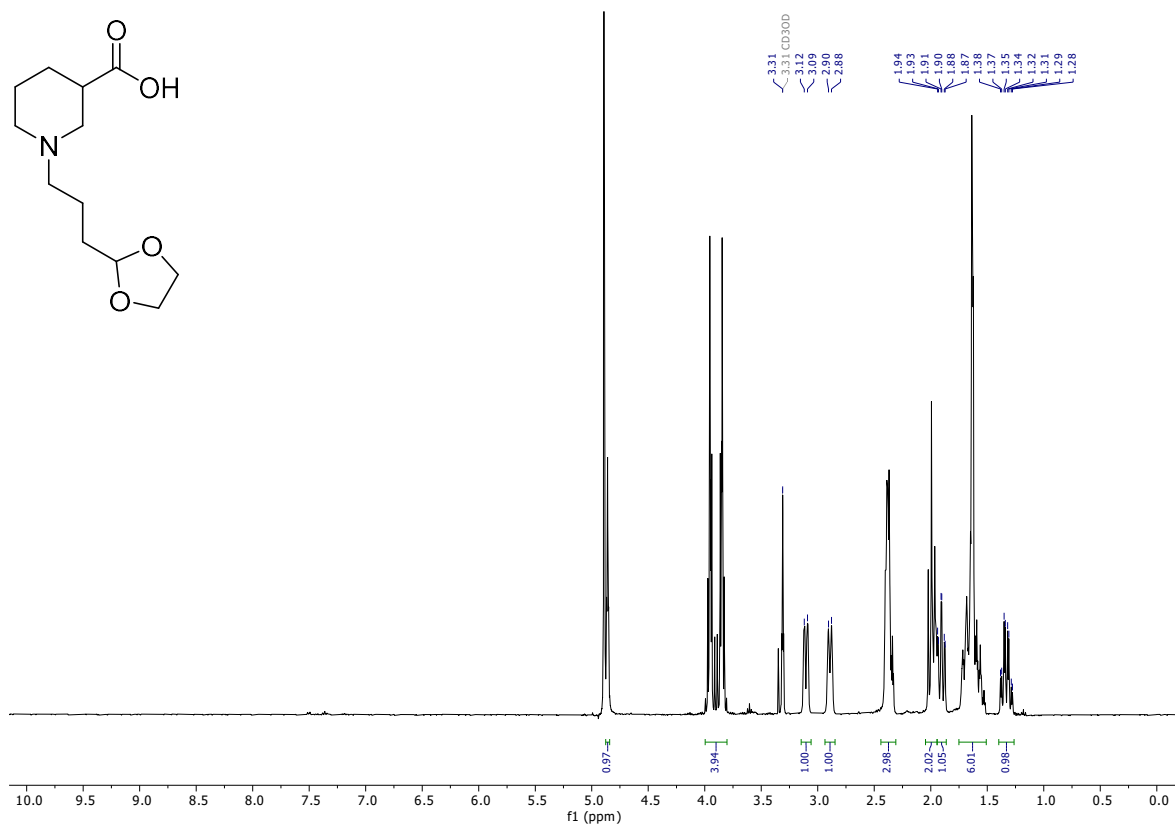
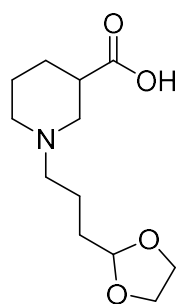
rac-18c (^{13}C):



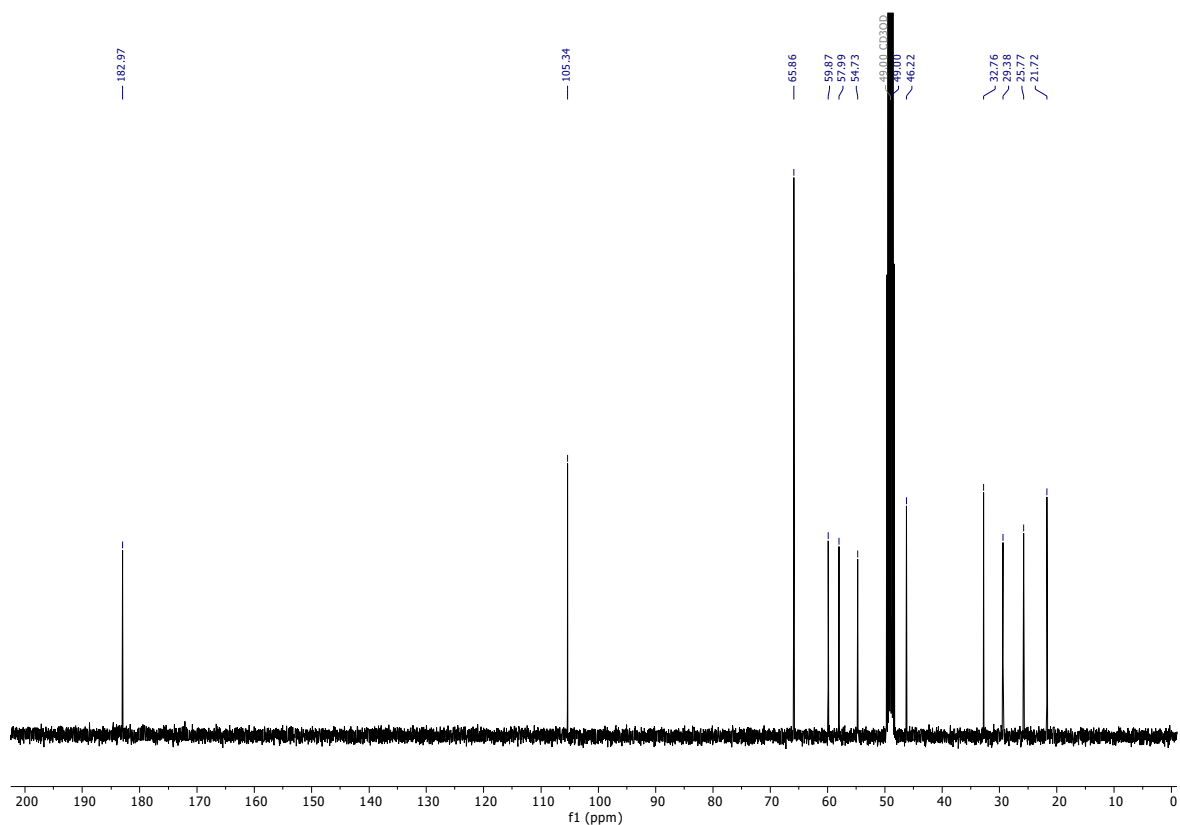
rac-18c (HRESIMS):



rac-18d (^1H):



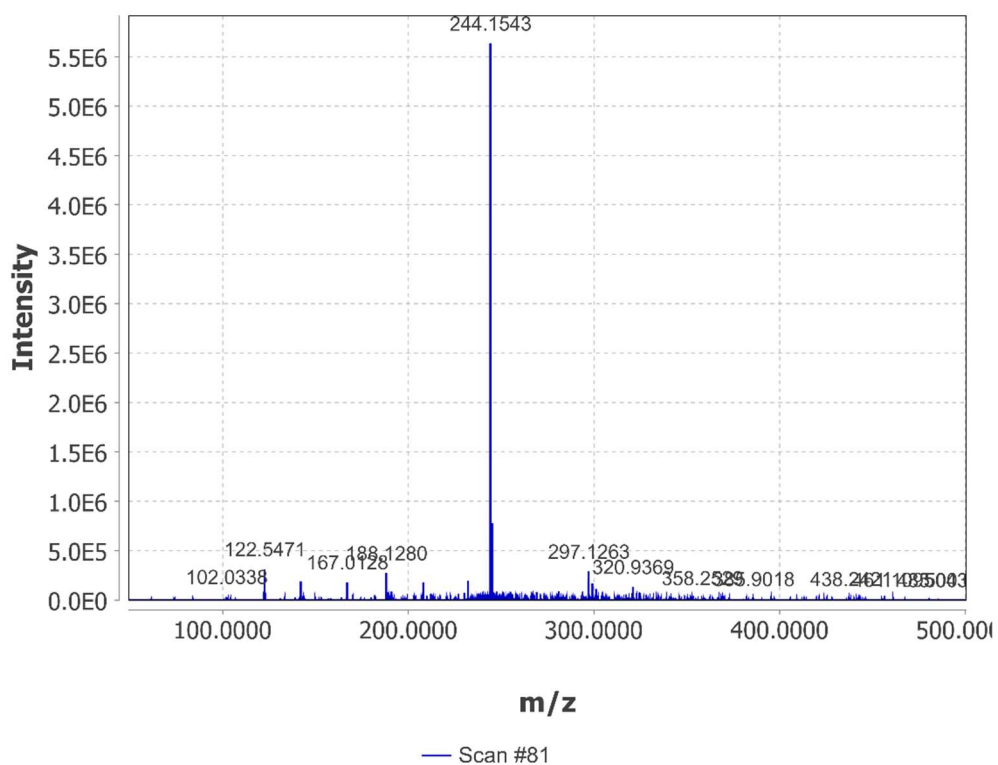
rac-18d (^{13}C):



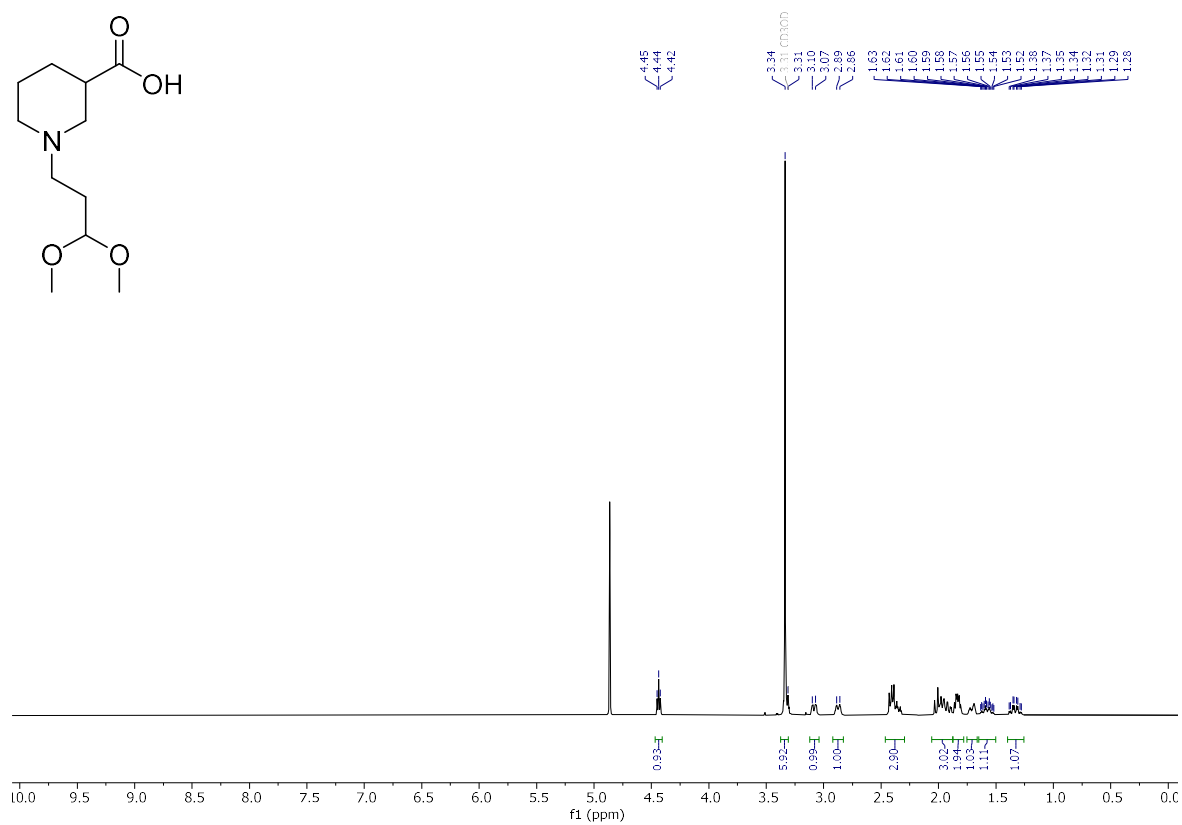
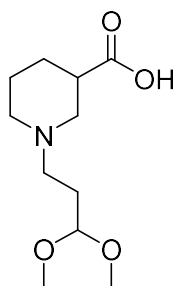
rac-18d (HRESIMS):

02-heruph-659.raw#81 @0.77 MS1 p +, base peak: 244.1543 m/z (5.6E6)

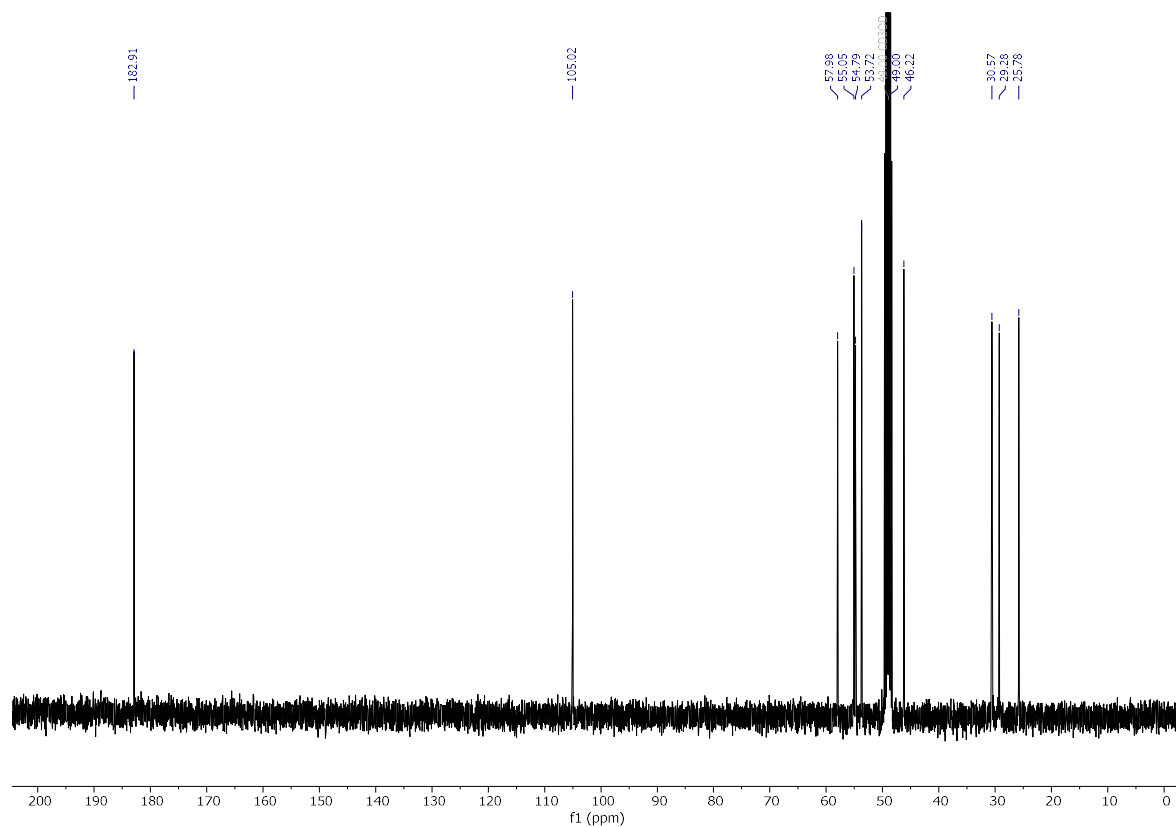
Scan definition: FTMS + p ESI Full ms [50.00-500.00]



rac-**18e** (^1H):



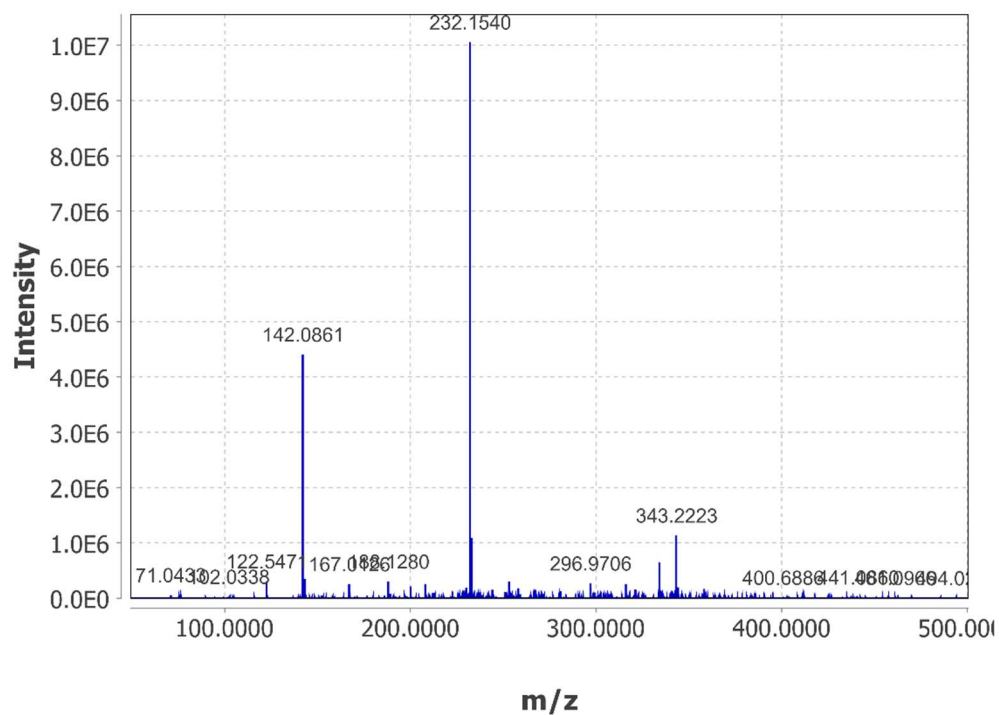
rac-**18e** (^{13}C):



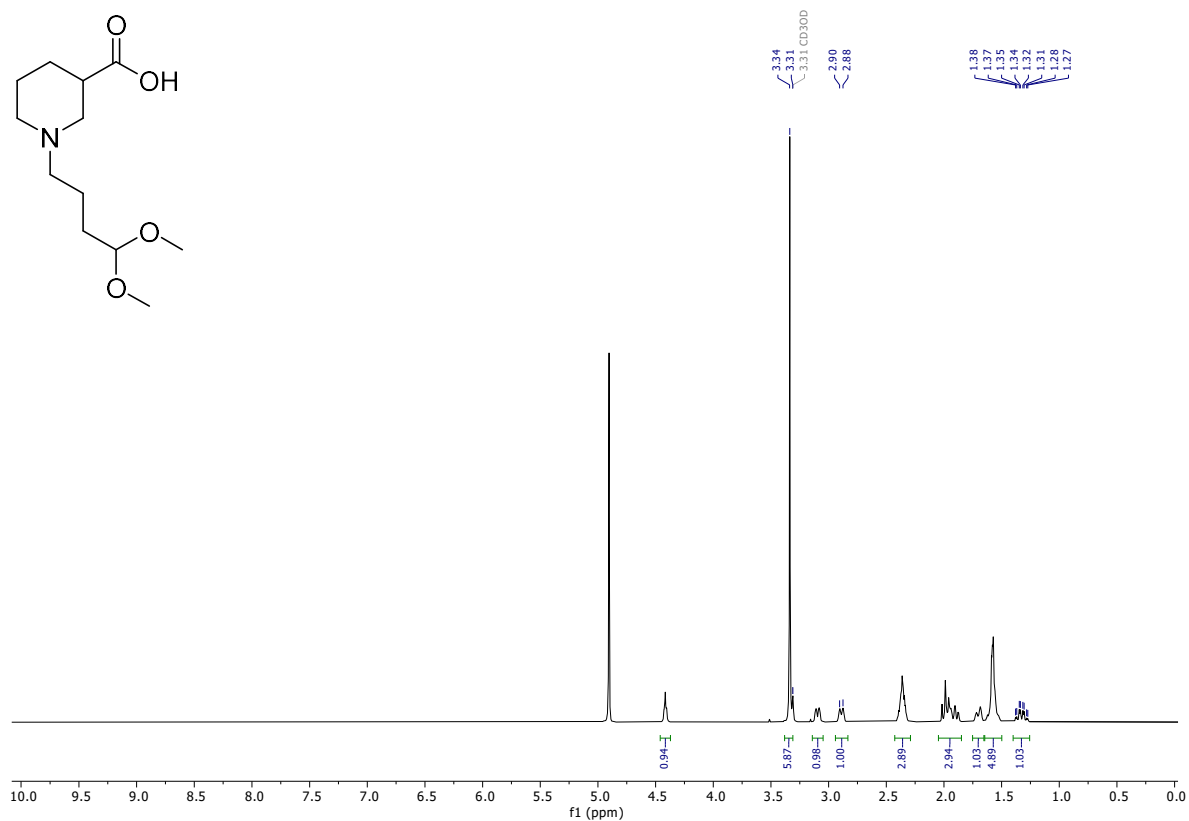
rac-18e (HRESIMS):

02-heruph-660.raw#89 @0.83 MS1 p +, base peak: 232.1540 m/z (1.0E7)

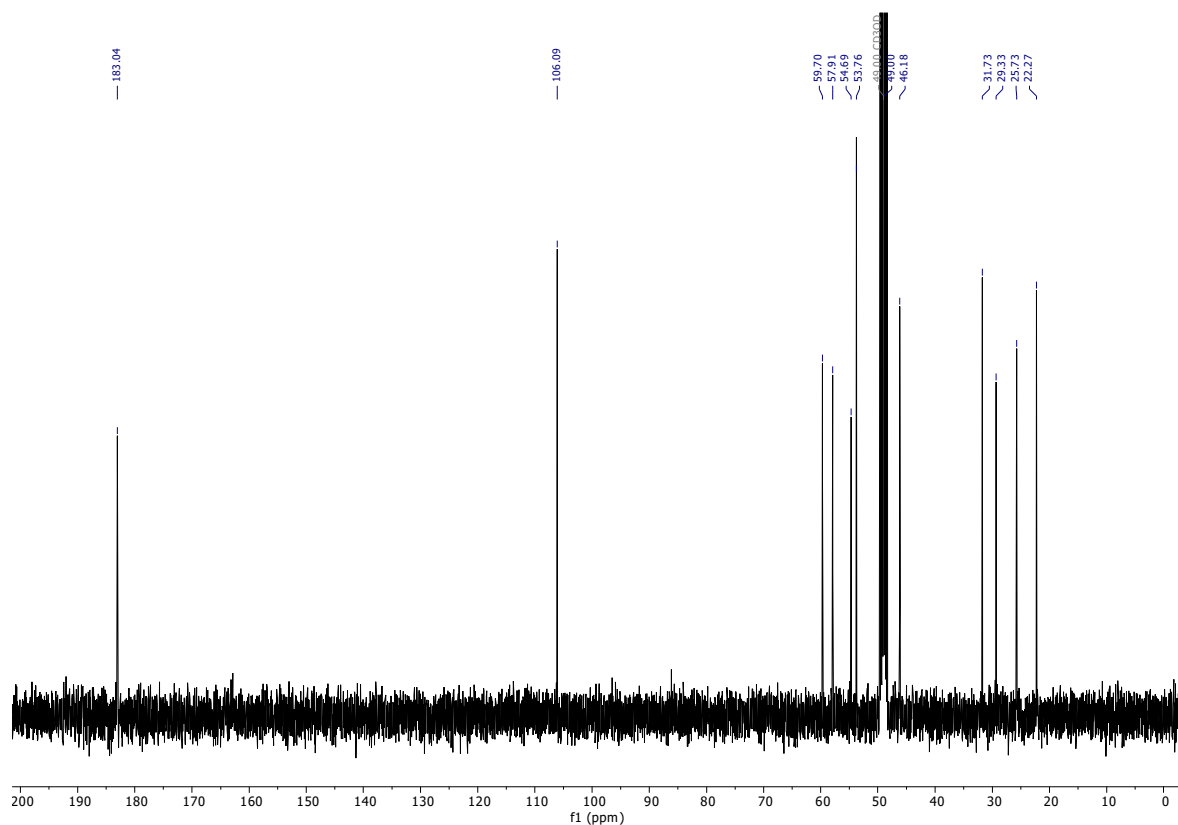
Scan definition: FTMS + p ESI Full ms [50.00-500.00]



rac-18f (^1H):



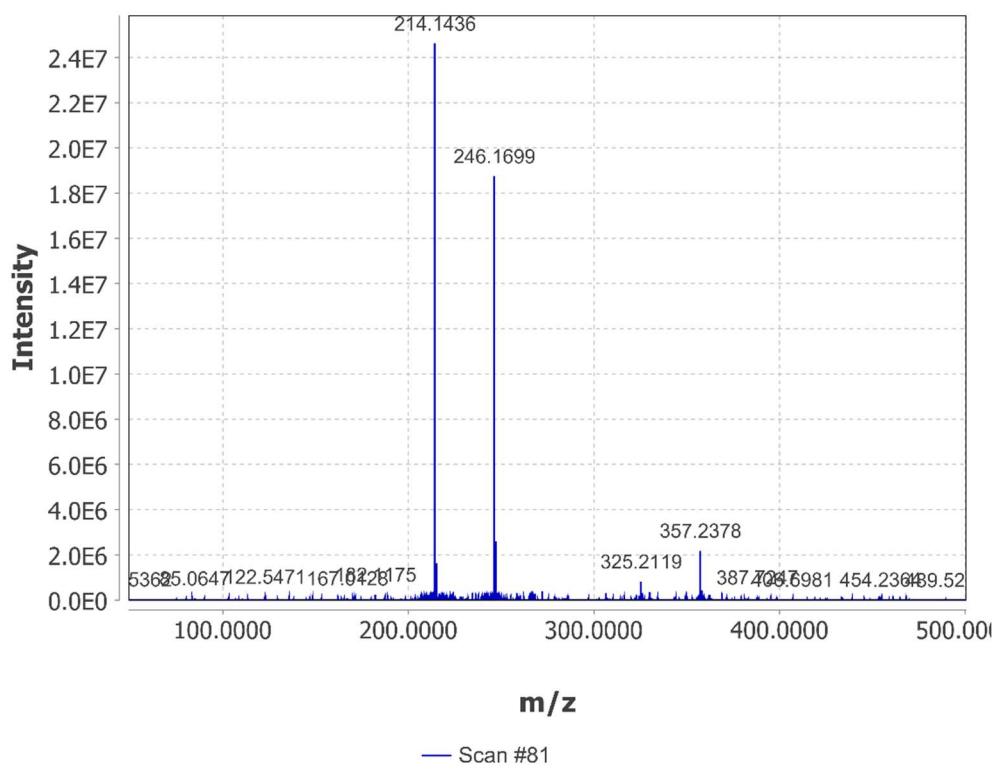
rac-**18f** (^{13}C):



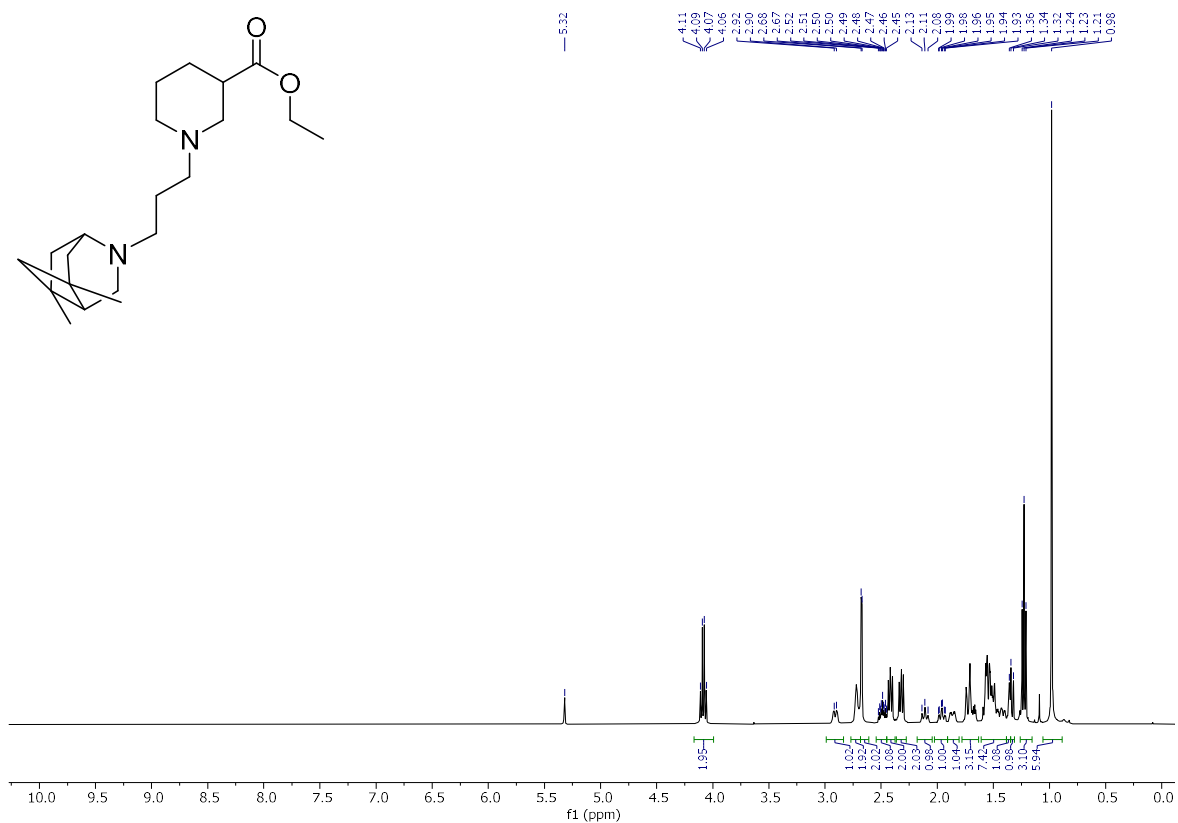
rac-**18f** (HRESIMS):

02-heruph-661.raw#81 @0.75 MS1 p +, base peak: 214.1436 m/z (2.5E7)

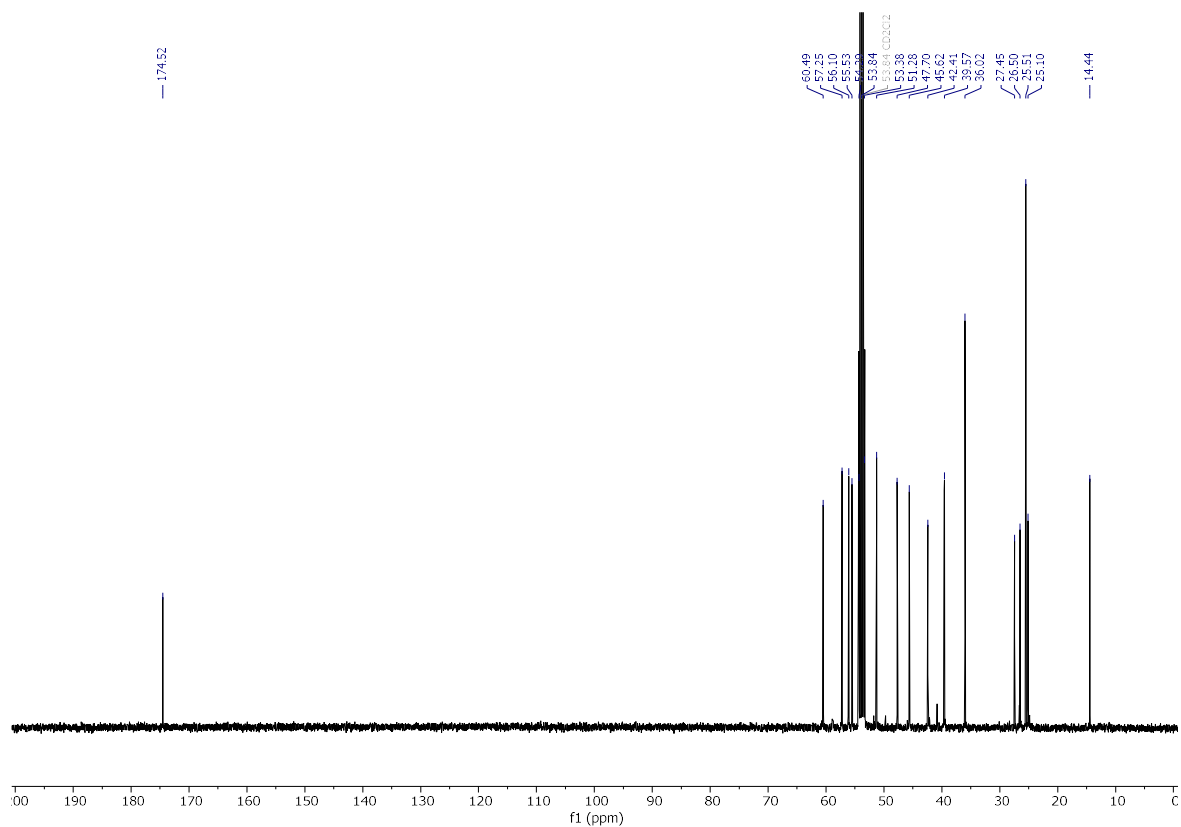
Scan definition: FTMS + p ESI Full ms [50.00-500.00]



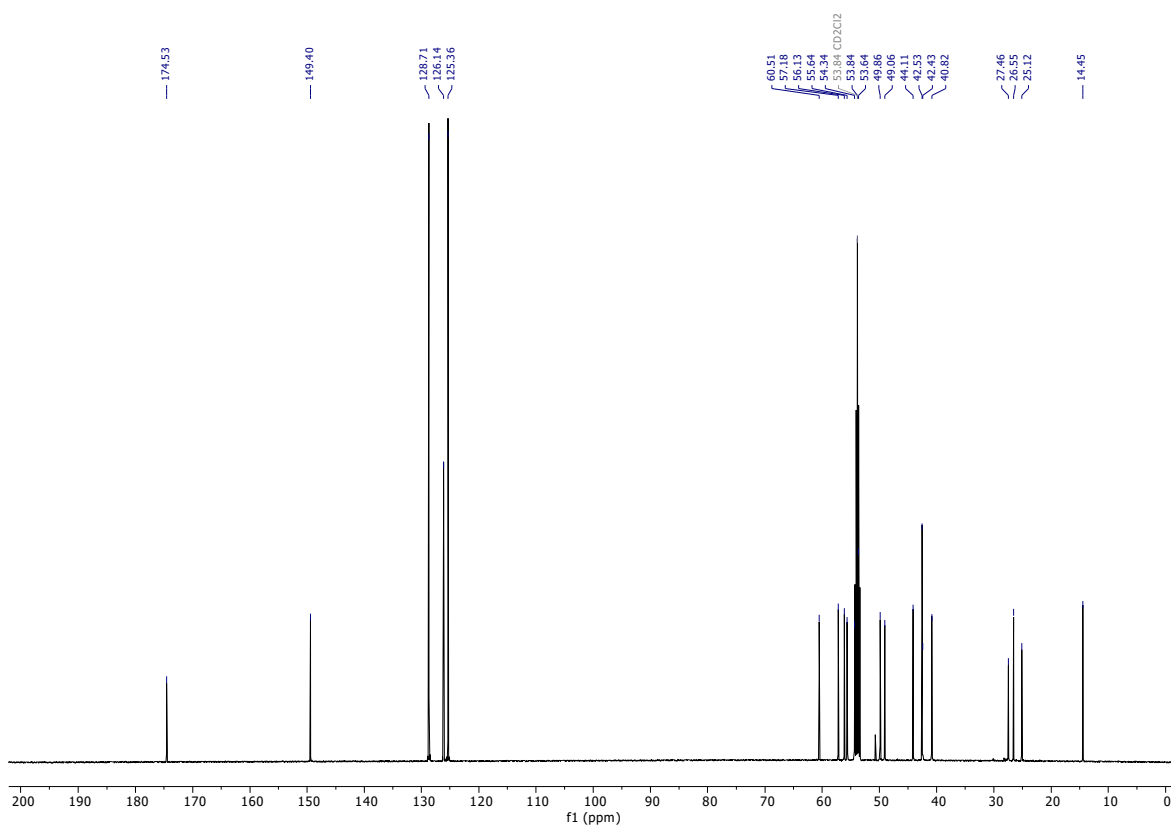
rac-**19a** (^1H):



rac-**19a** (^{13}C):



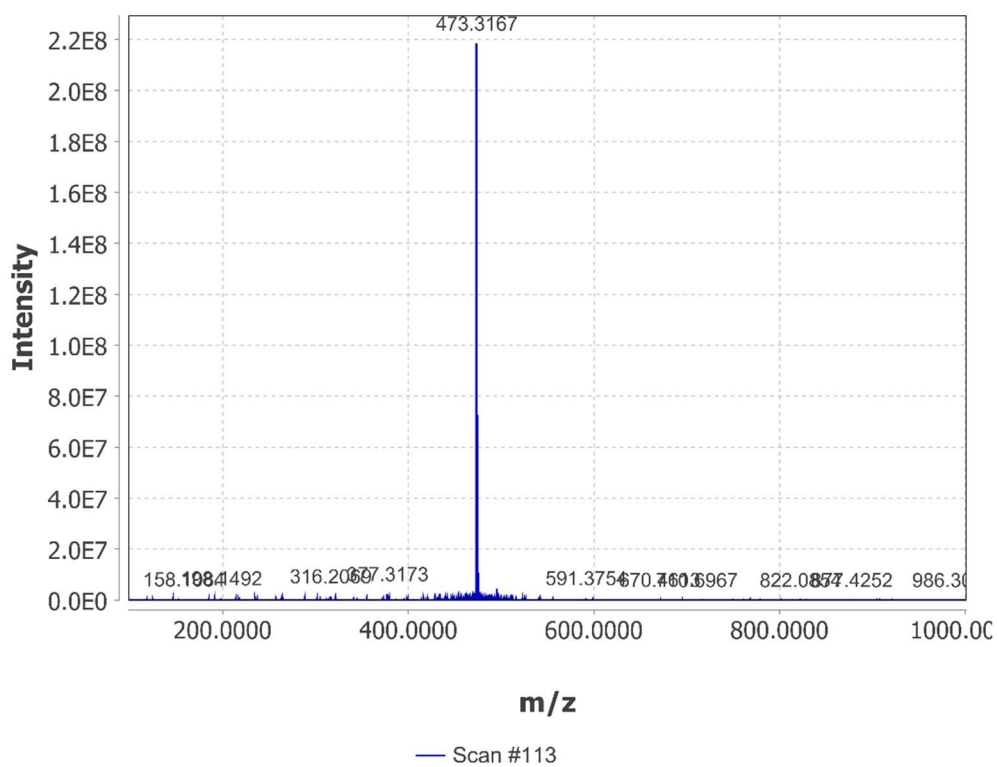
rac-19b (^{13}C):



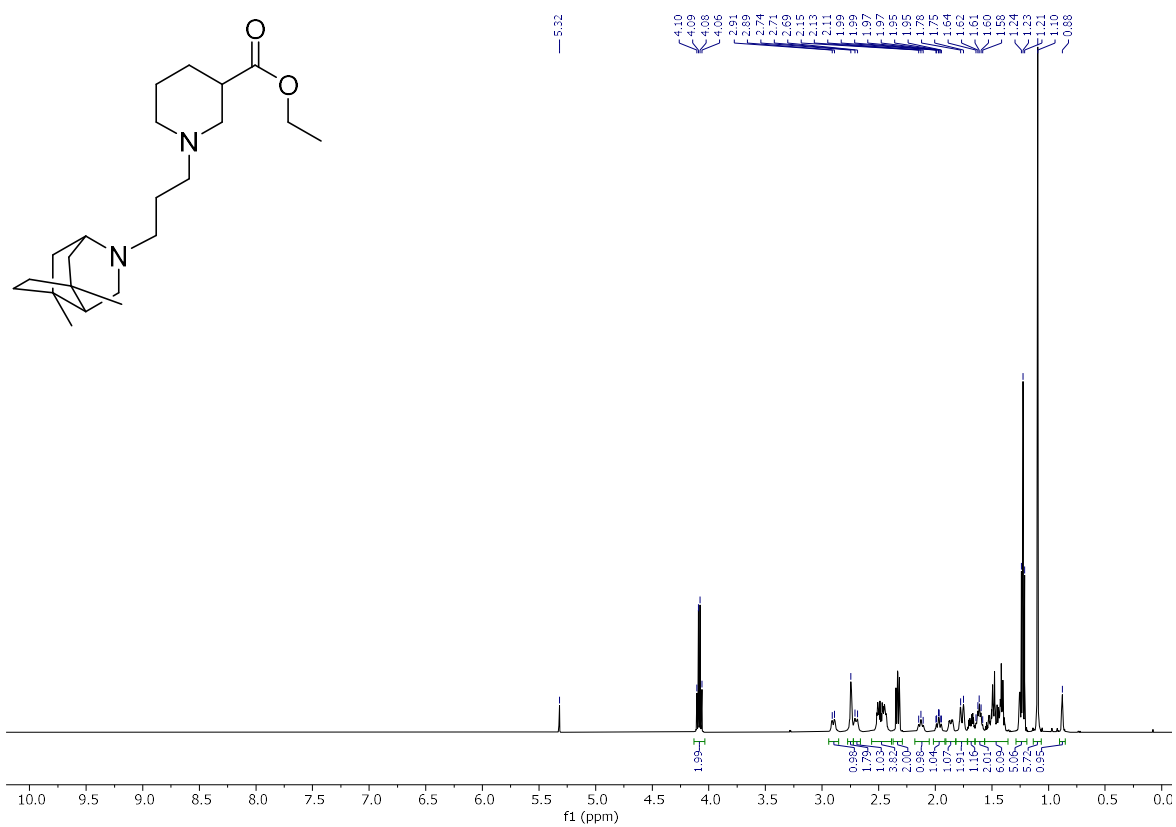
rac-19b (HRESIMS):

01-heruph-598.raw#113 @0.96 MS1 p +, base peak: 473.3167 m/z (2.2E8)

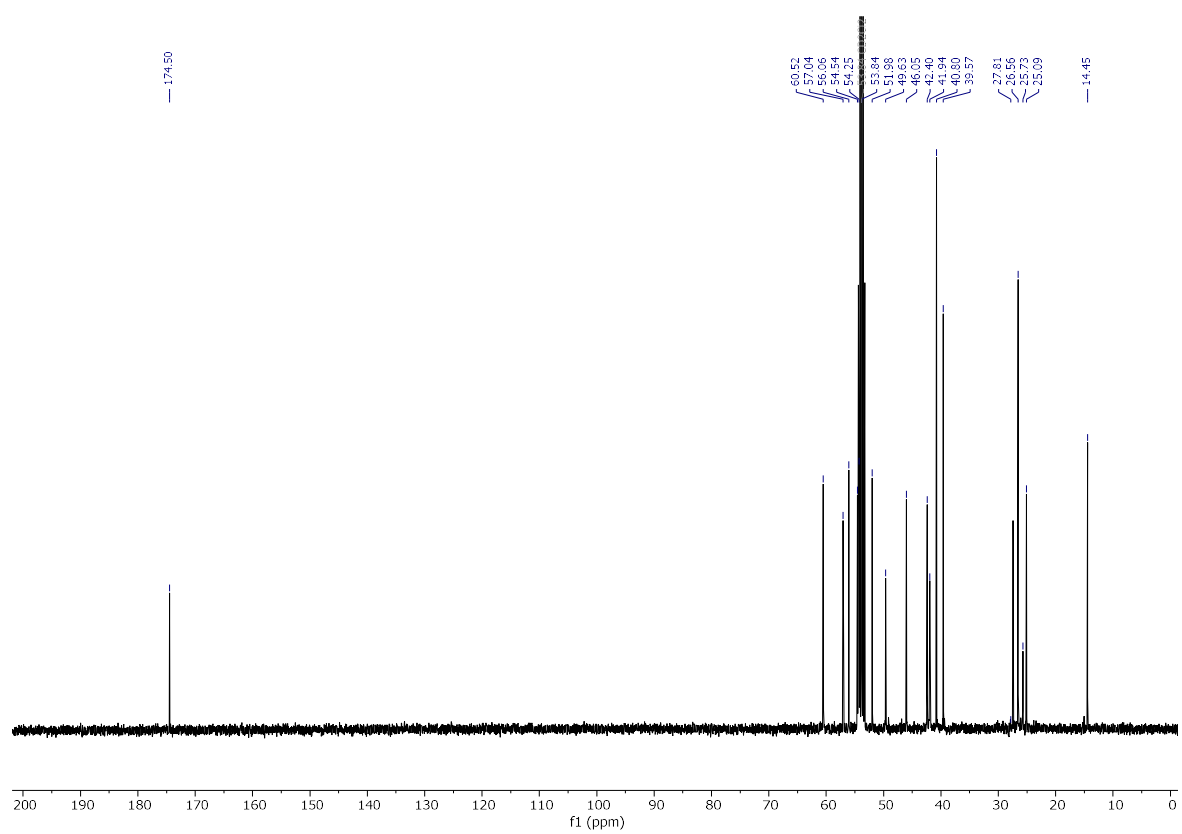
Scan definition: FTMS + p ESI Full ms [100.00-1000.00]



rac-19c (^1H):

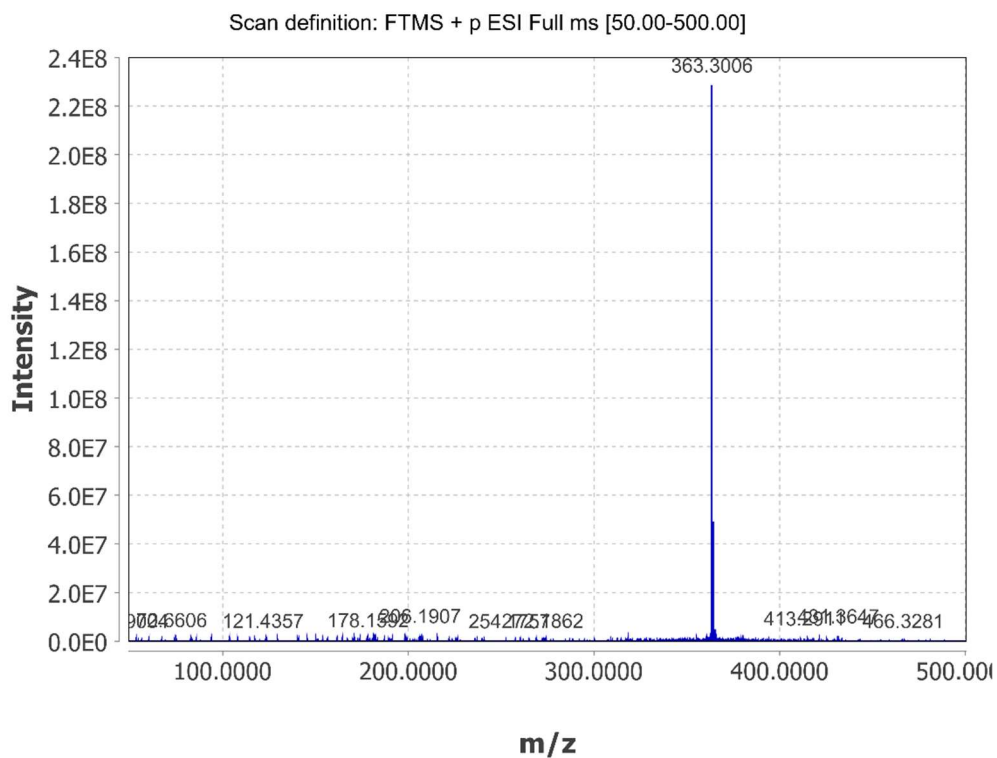


rac-19c (^{13}C):

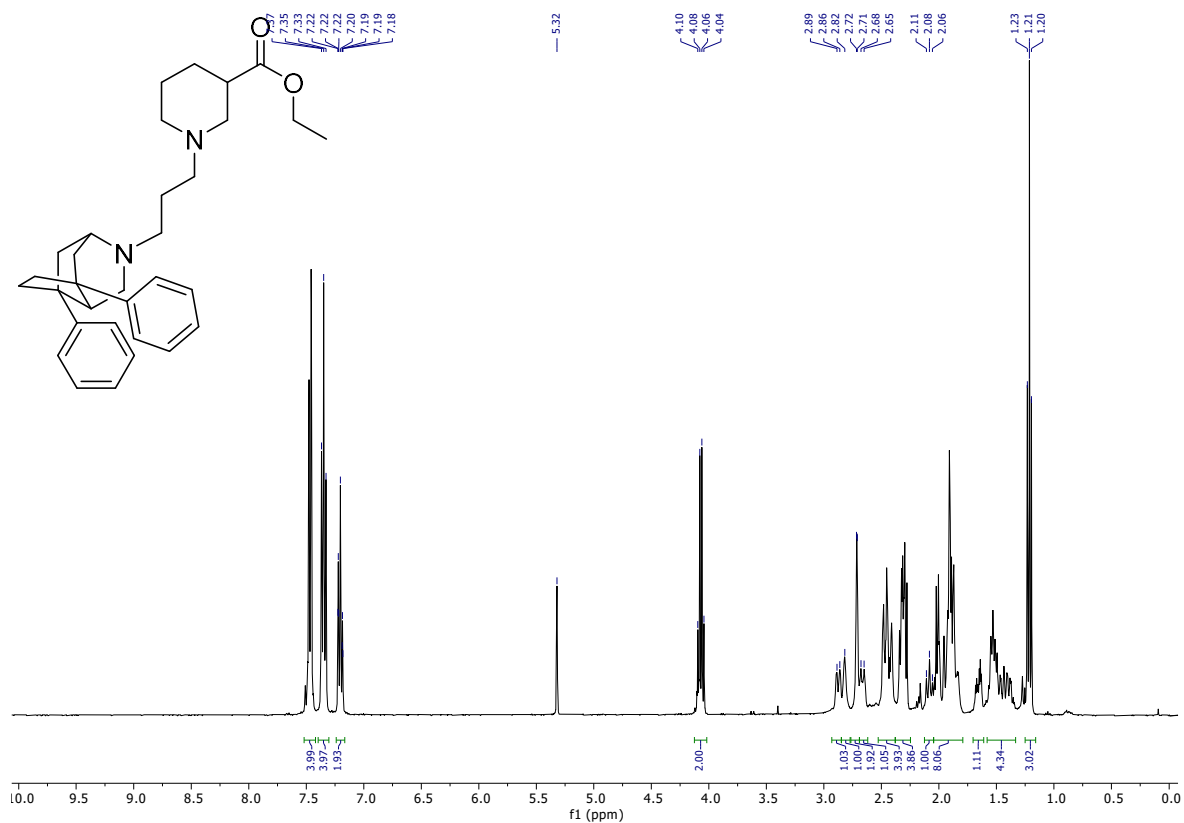


rac-19c (HRESIMS):

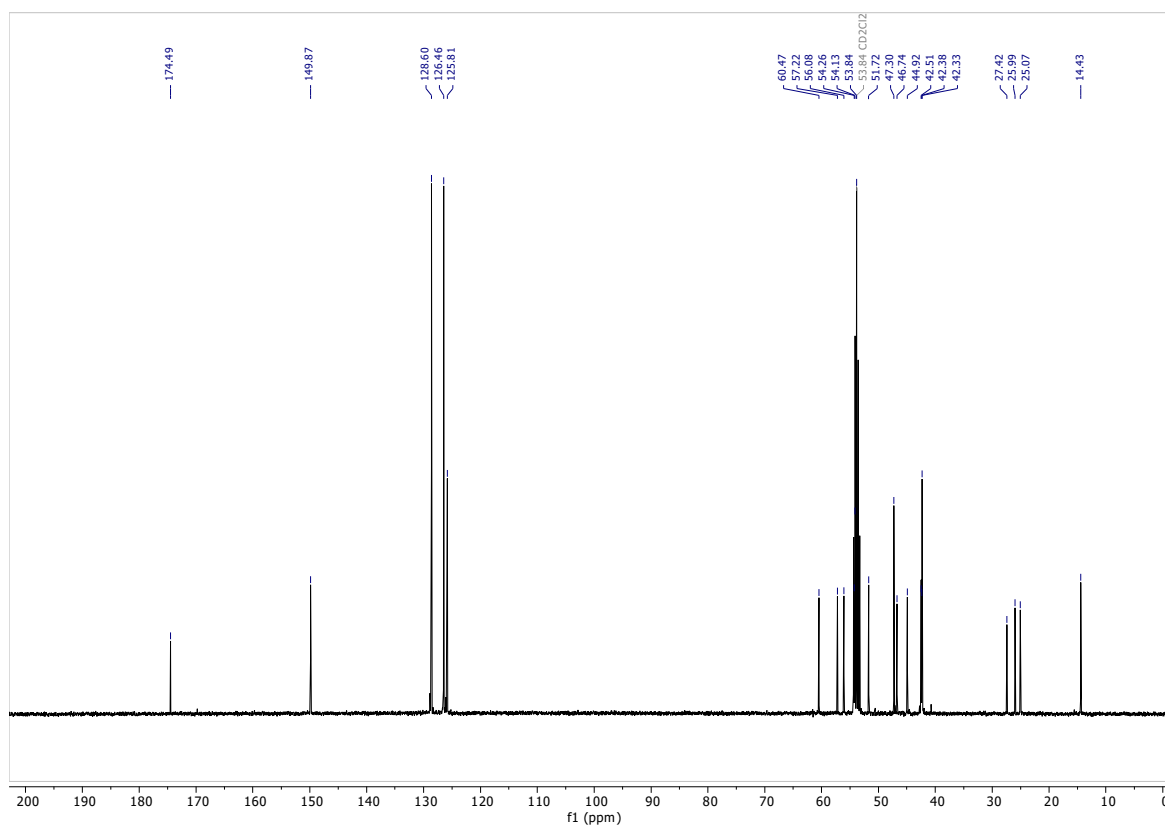
12-heruph-574.raw#97 @0.89 MS1 p +, base peak: 363.3006 m/z (2.3E8)



rac-19d (^1H):



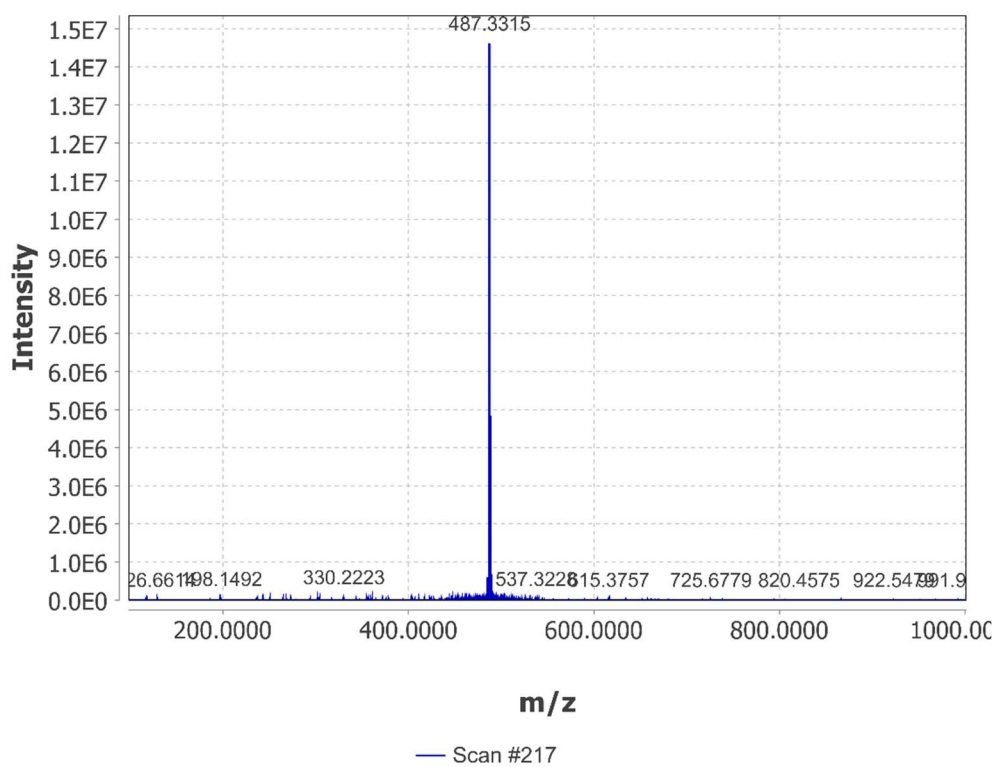
rac-19d (^{13}C):



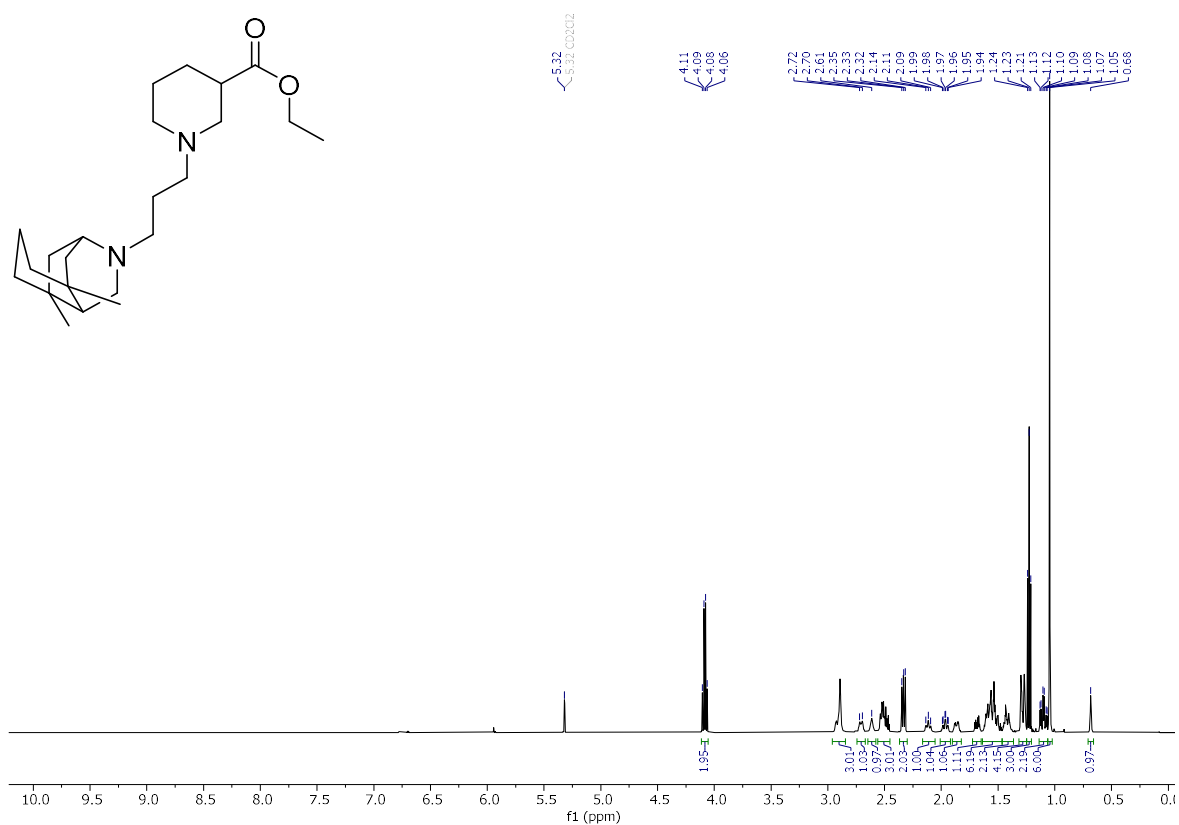
rac-19d (HRESIMS):

12-heruph-573.raw#217 @1.93 MS1 p +, base peak: 487.3315 m/z (1.5E7)

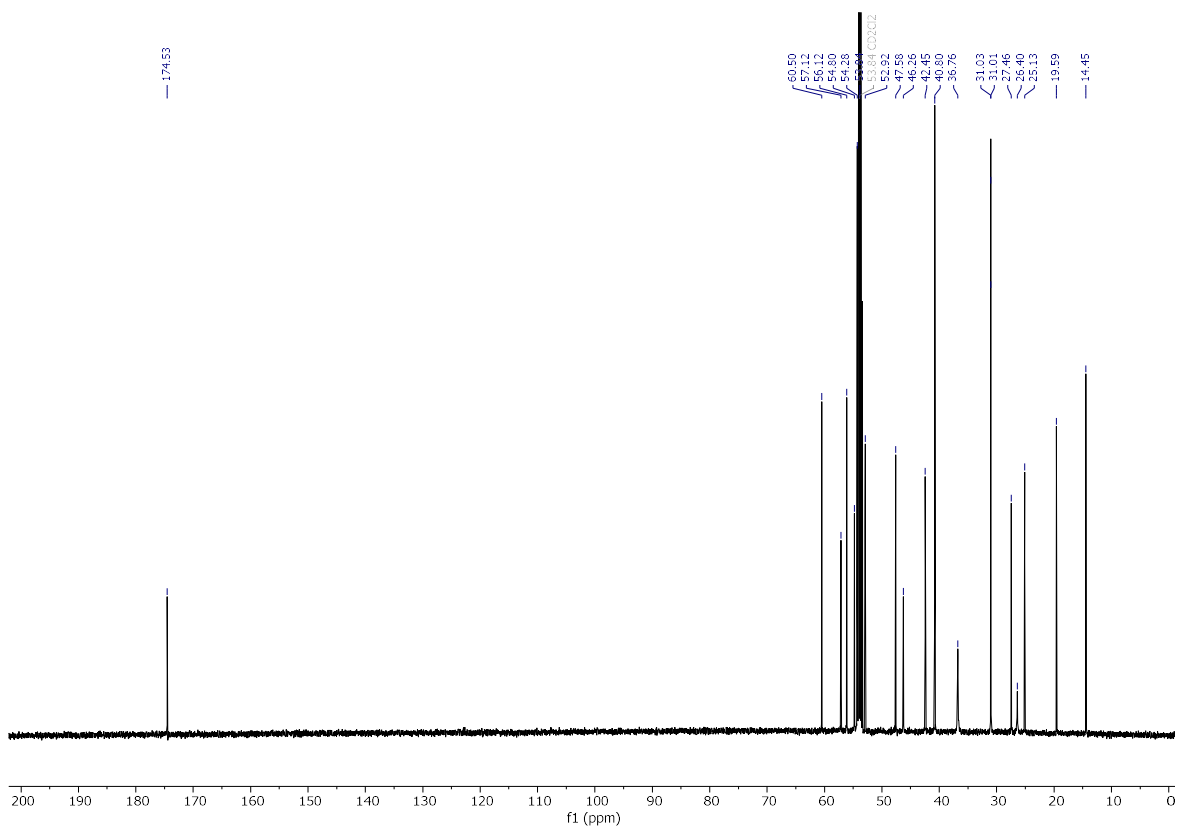
Scan definition: FTMS + p ESI Full ms [100.00-1000.00]



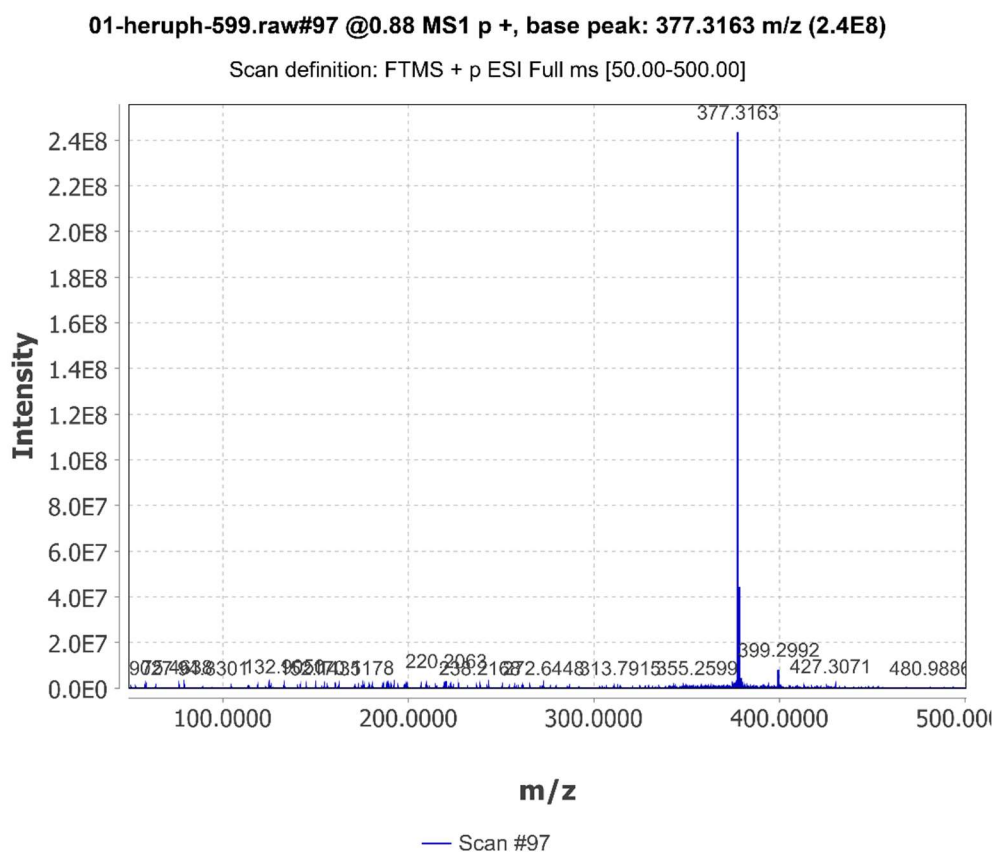
rac-19e (^1H):



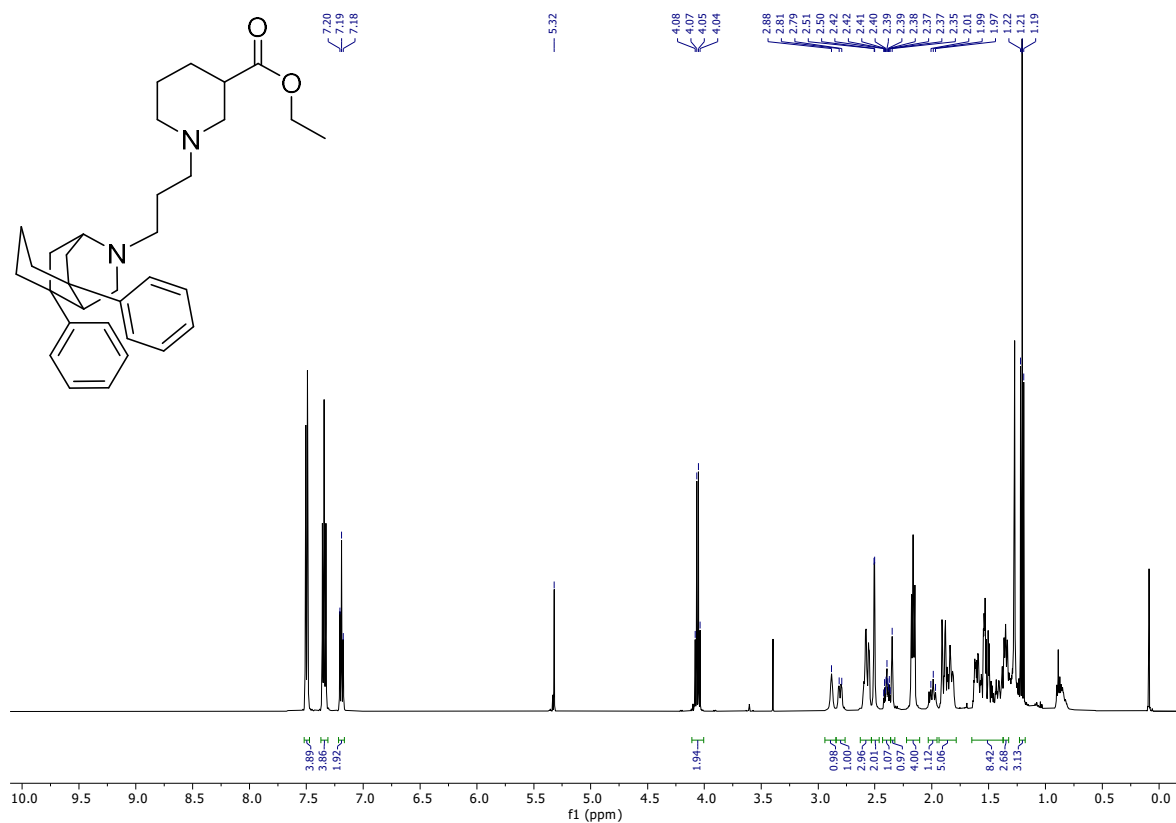
rac-19e (^{13}C):



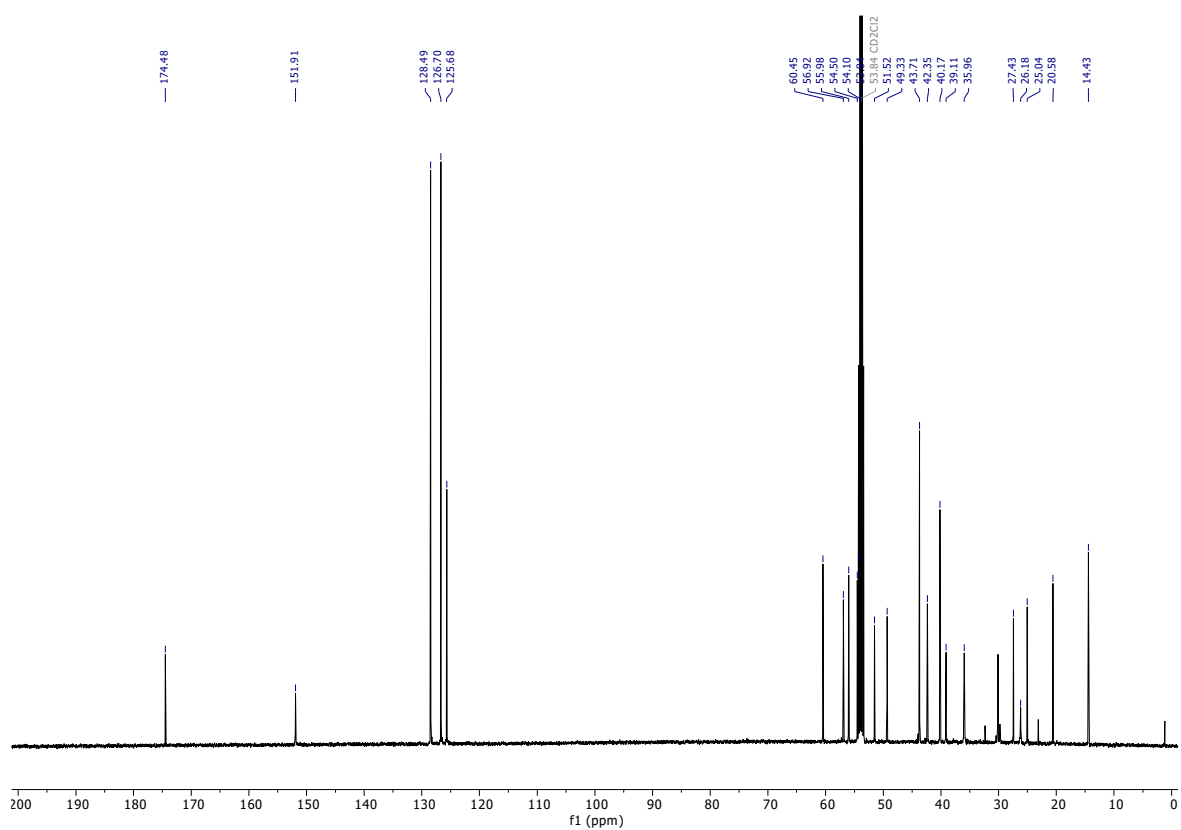
rac-19e (HRESIMS):



rac-19f (^1H):



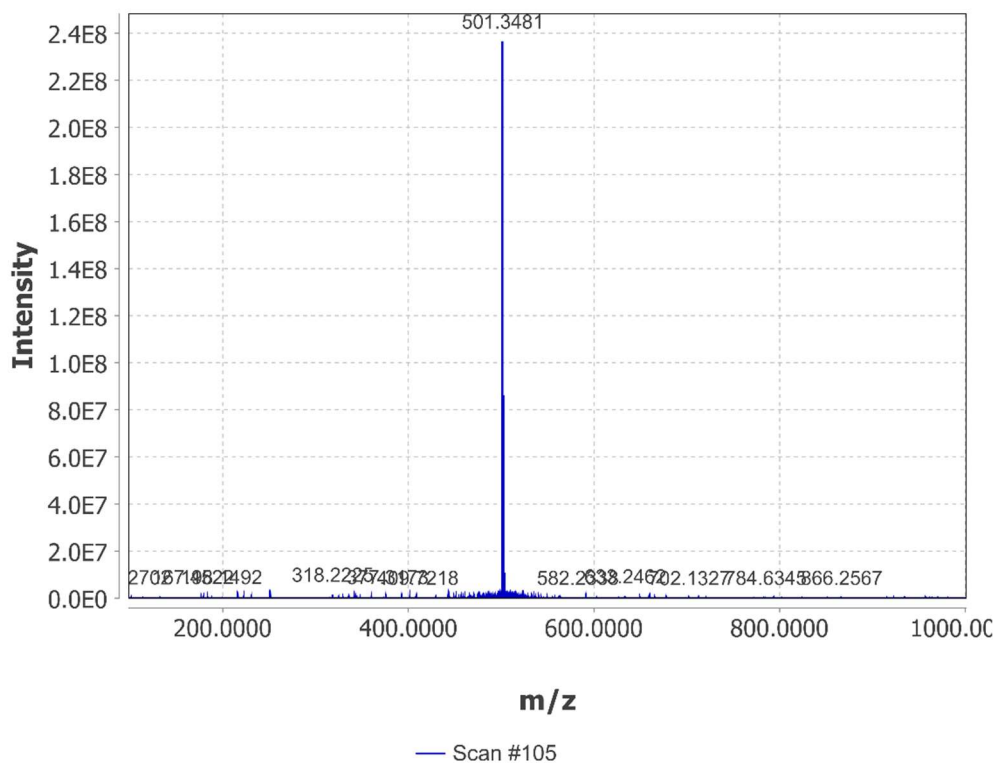
rac-**19f** (^{13}C):



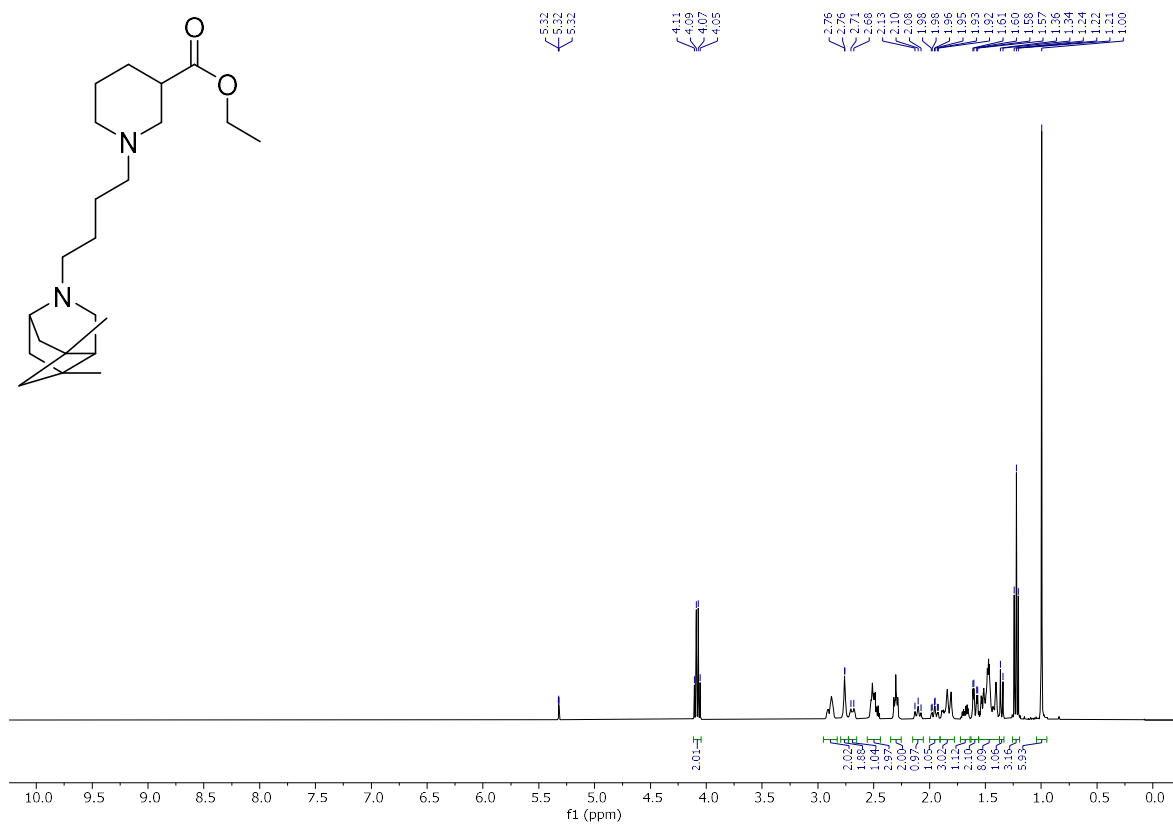
rac-**19f** (HRESIMS):

01-heruph-600.raw#105 @0.87 MS1 p +, base peak: 501.3481 m/z (2.4E8)

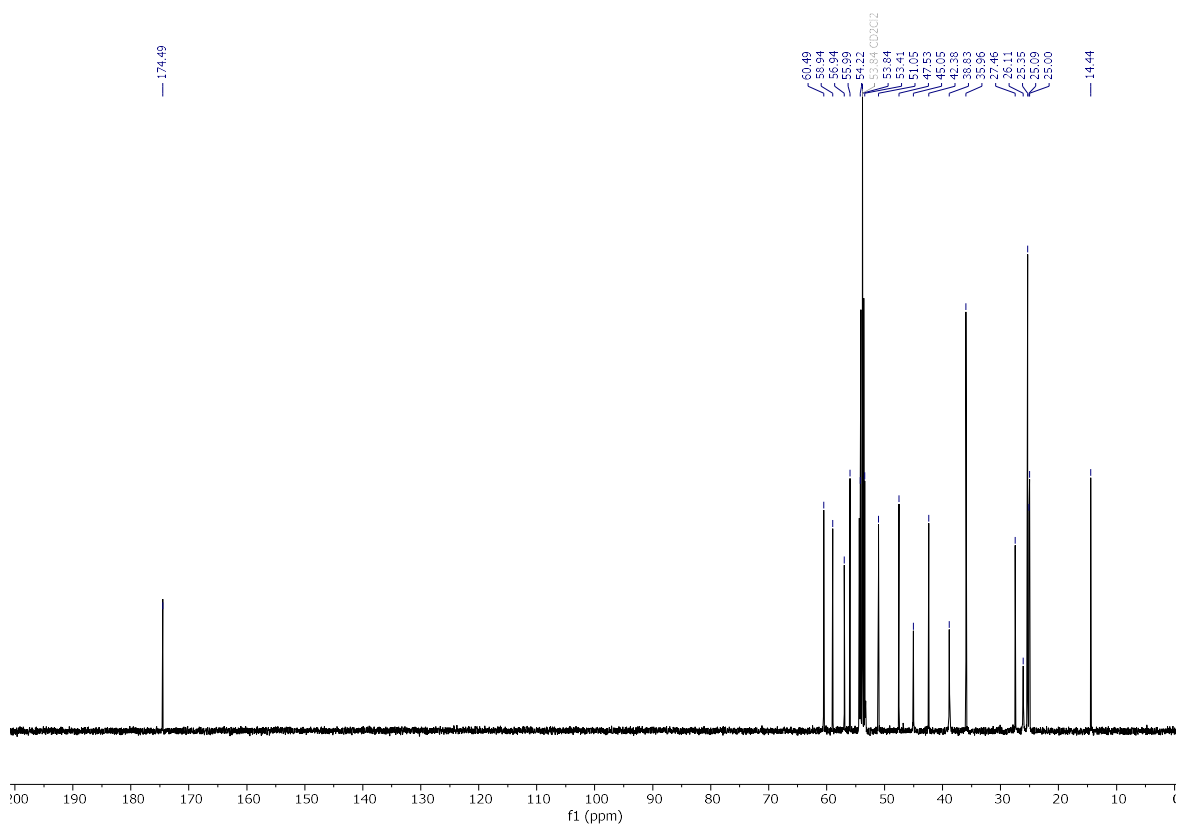
Scan definition: FTMS + p ESI Full ms [100.00-1000.00]



rac-**19g** (^1H):



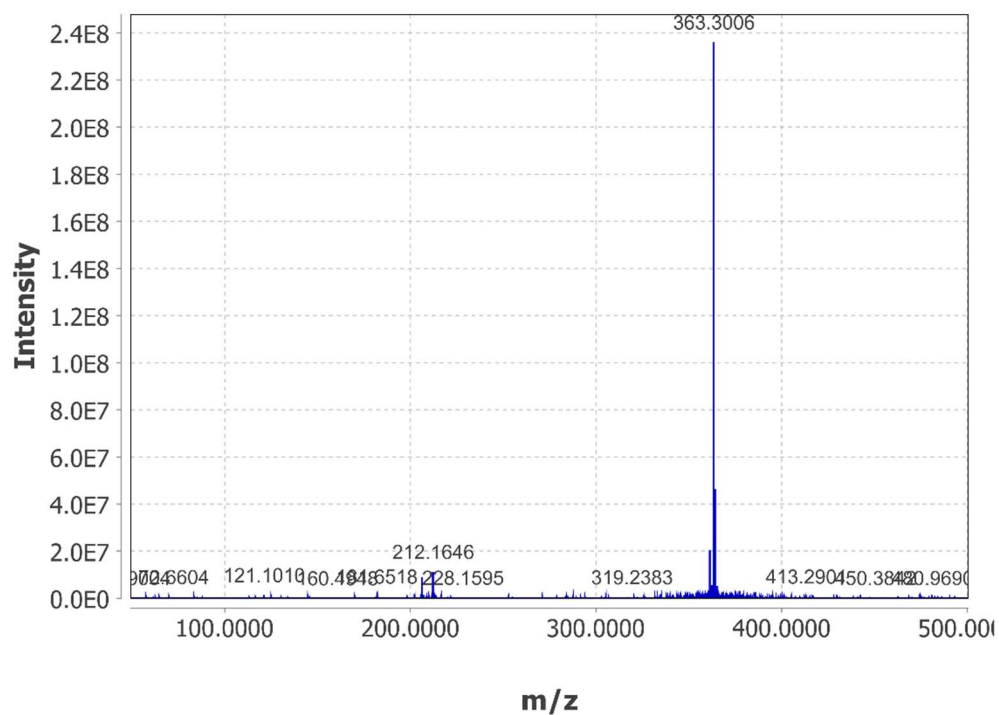
rac-**19g** (^{13}C):



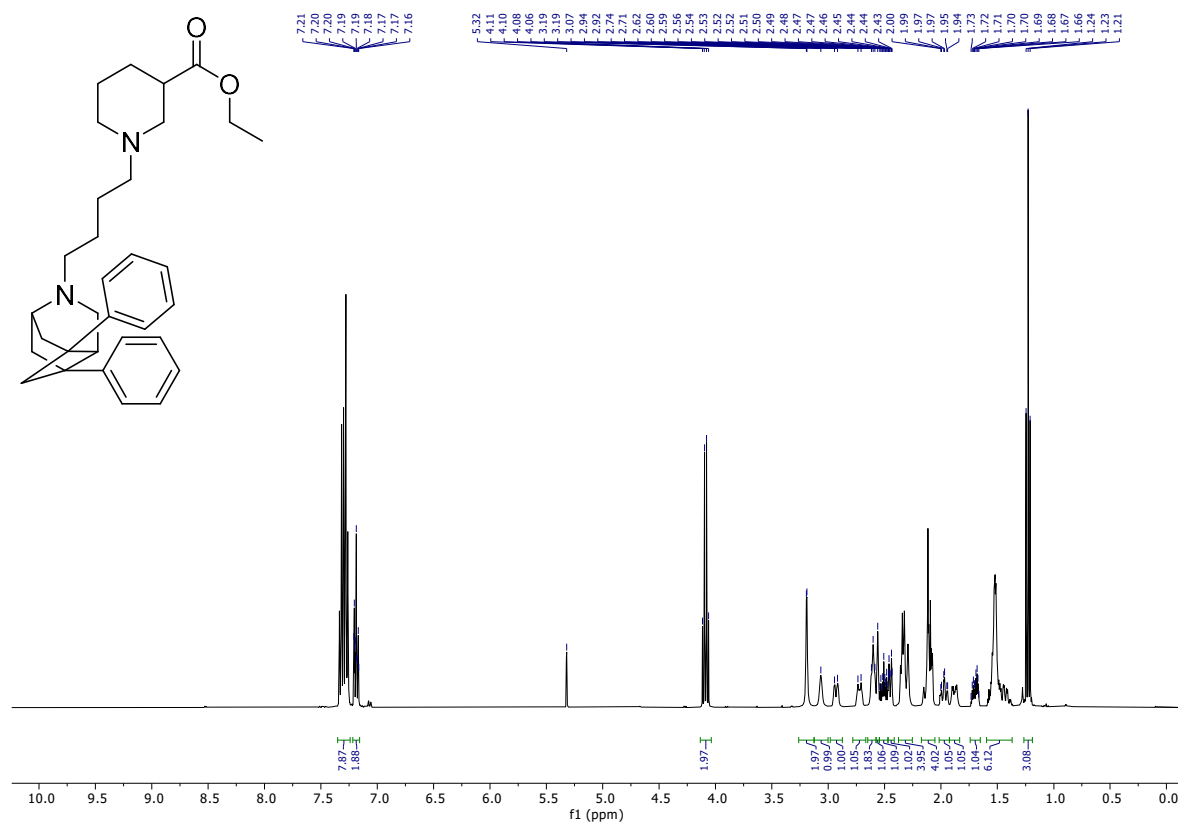
rac-19g (HRESIMS):

11-heruph-571.raw#97 @0.88 MS1 p +, base peak: 363.3006 m/z (2.4E8)

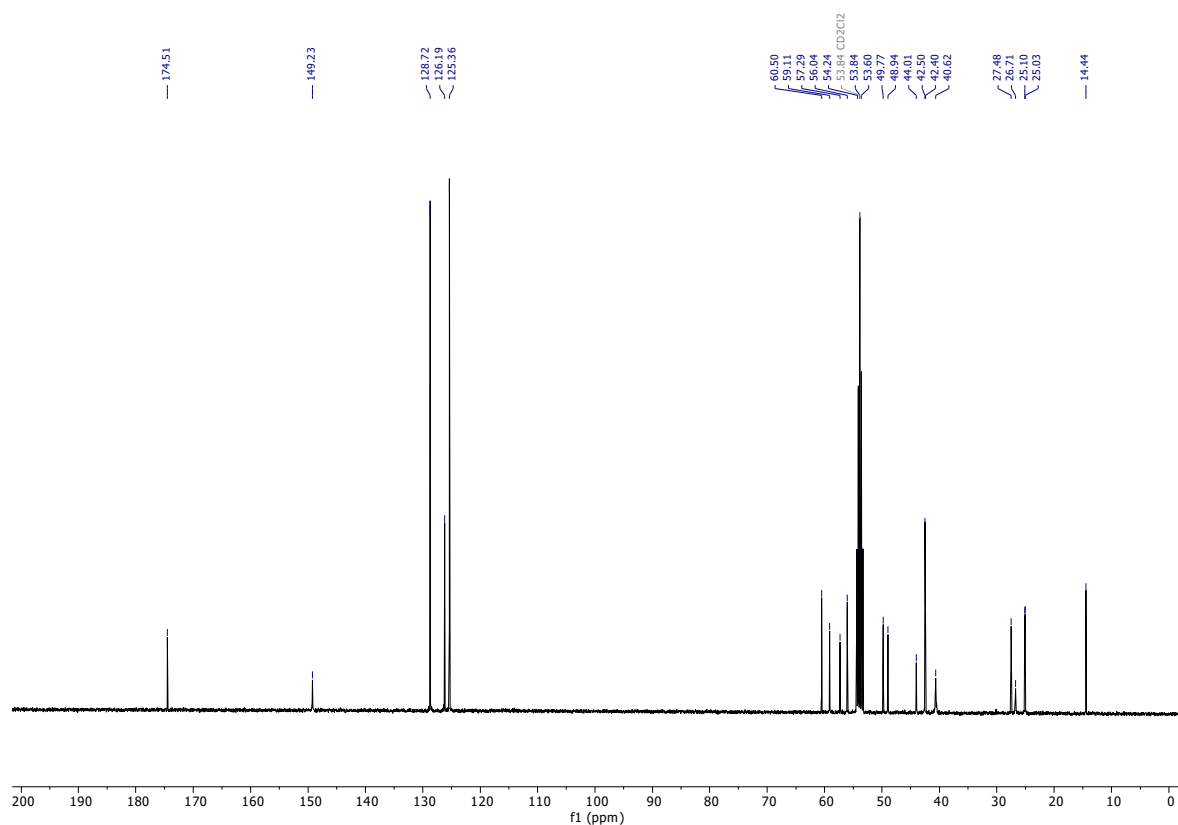
Scan definition: FTMS + p ESI Full ms [50.00-500.00]



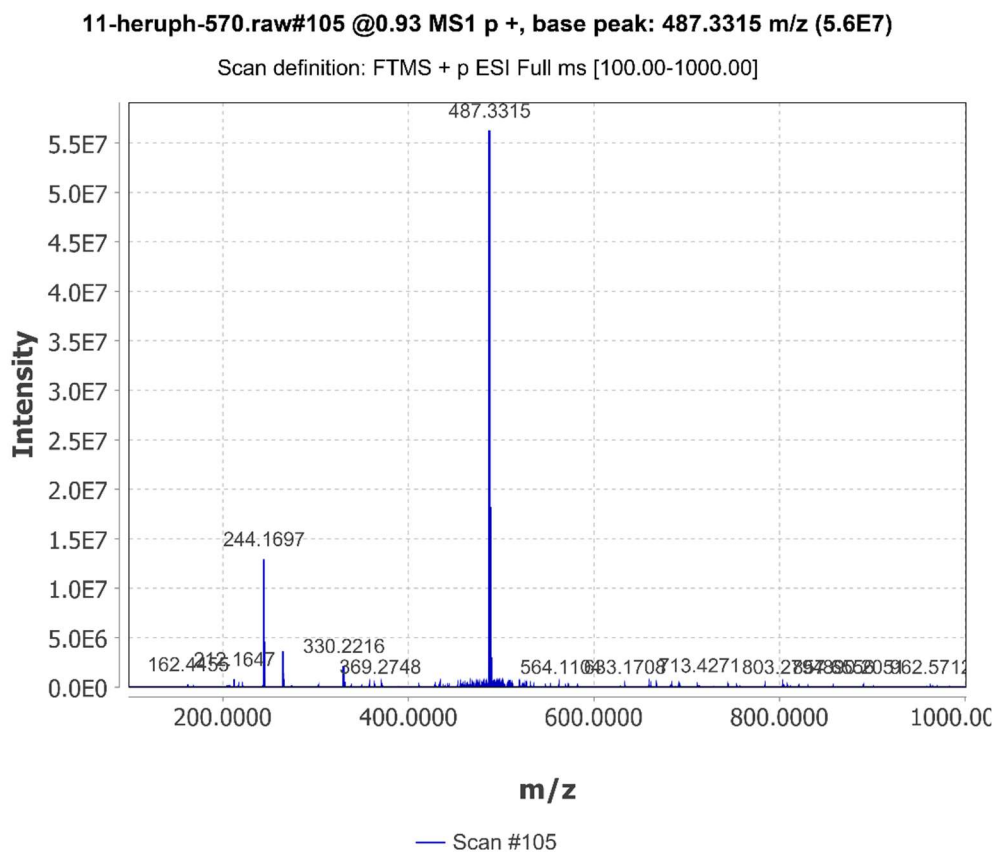
rac-19h (^1H):



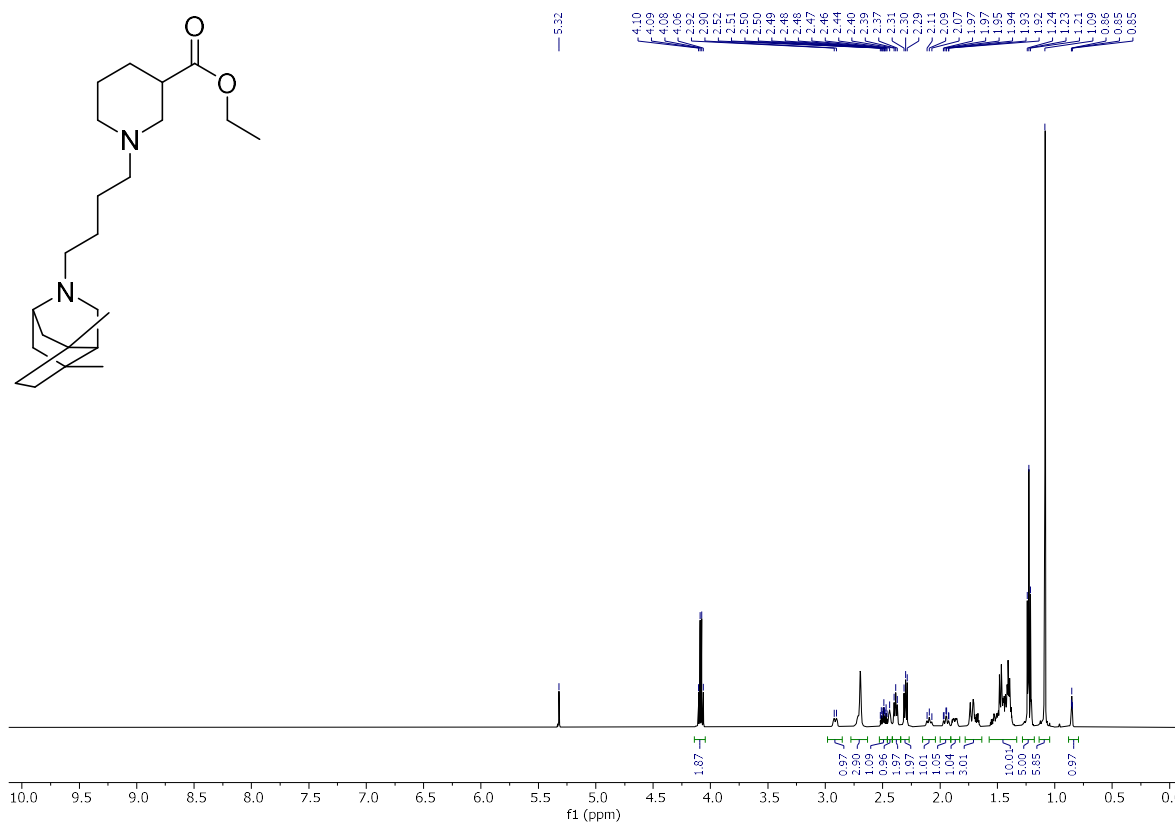
rac-**19h** (^{13}C):



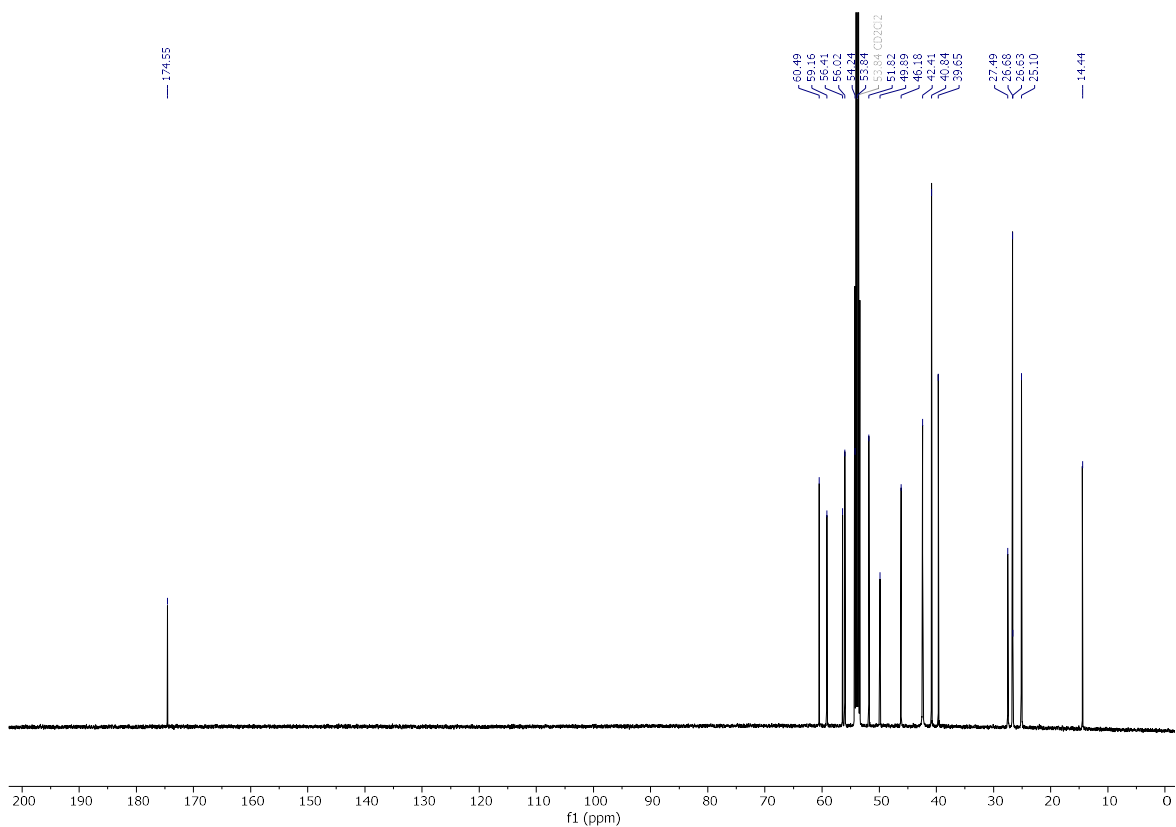
rac-**19h** (HRESIMS):



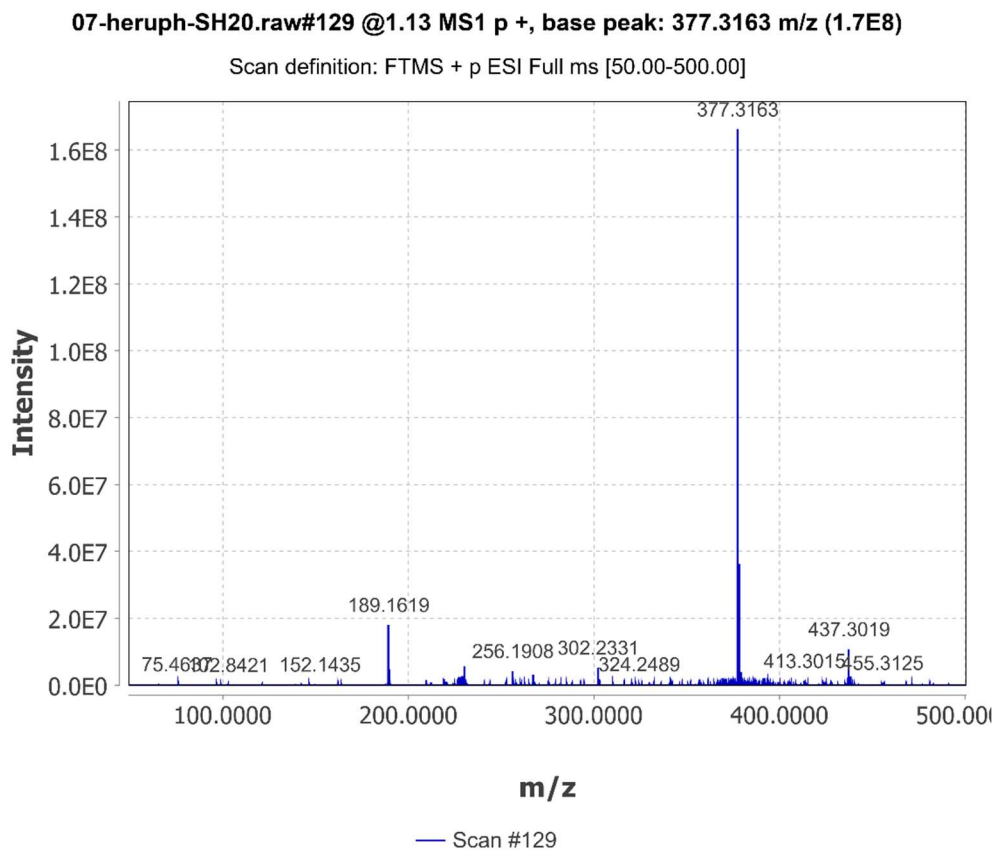
rac-**19j** (^1H):



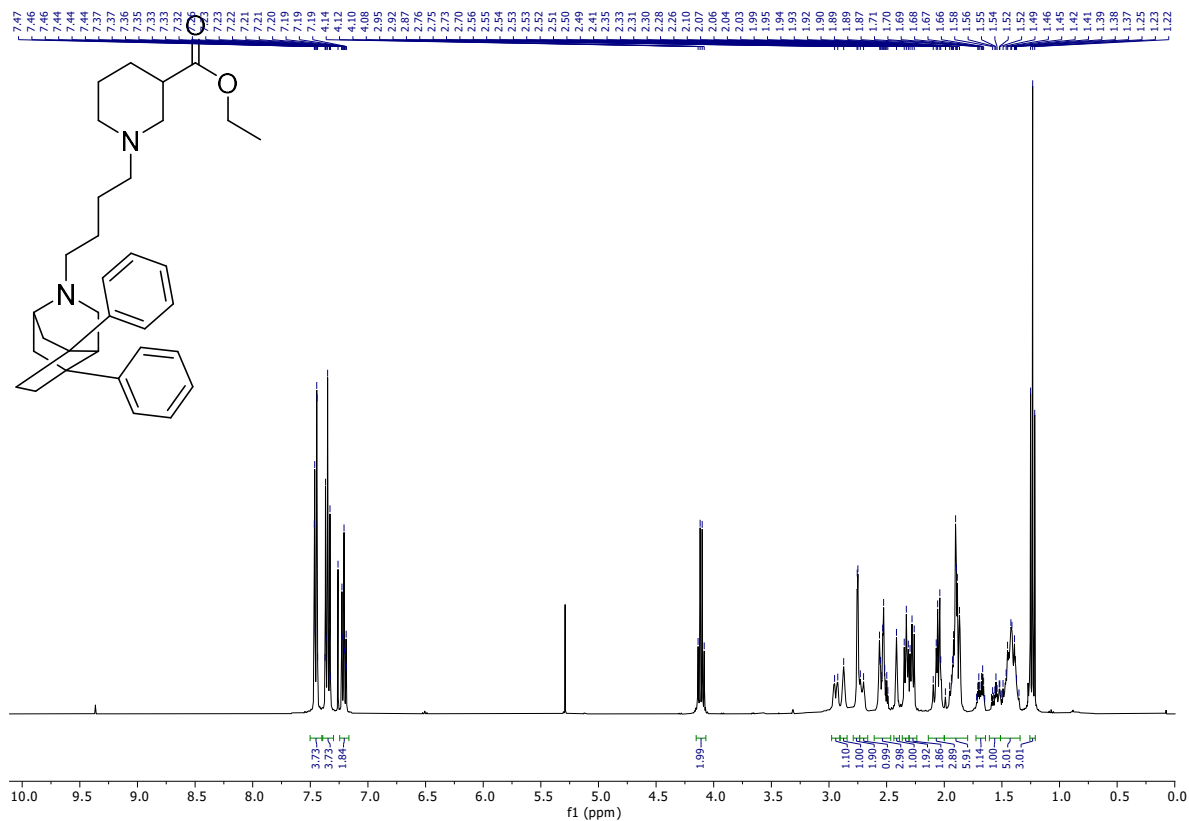
rac-**19j** (^{13}C):



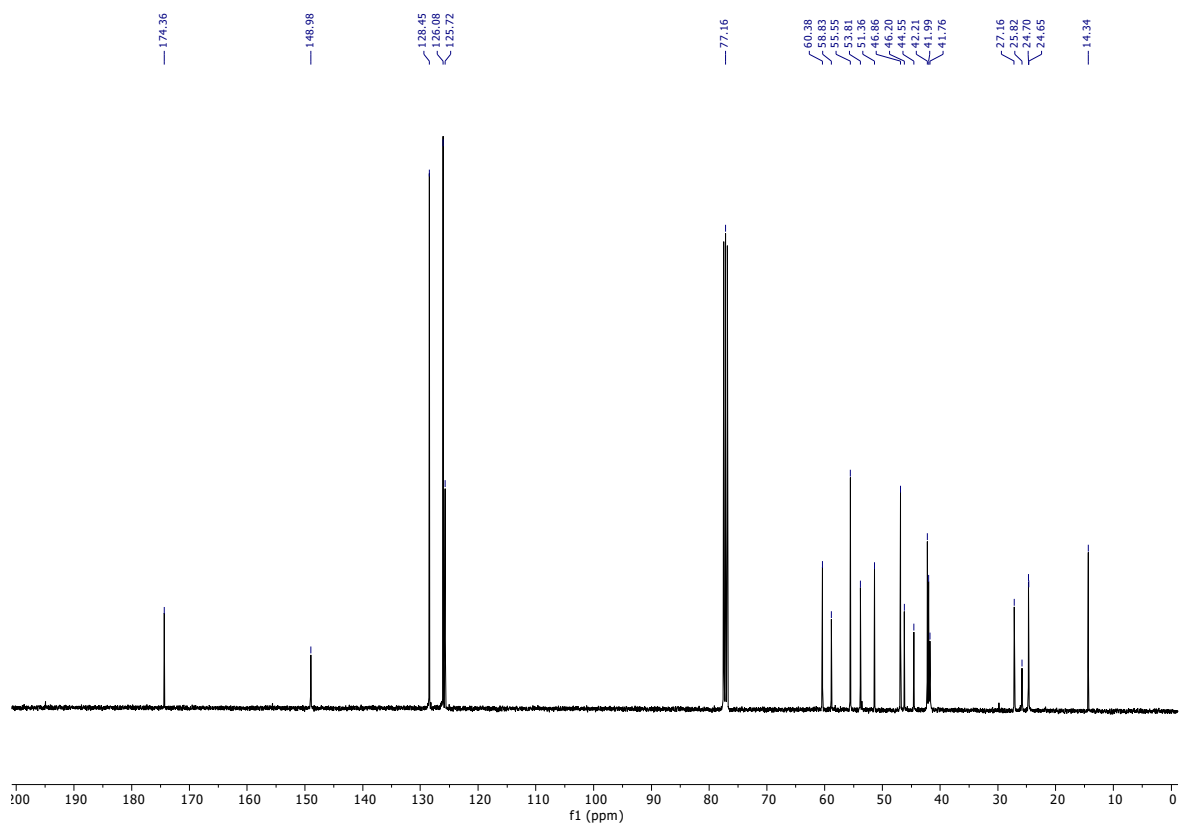
rac-19j (HRESIMS):



rac-19k (^1H):



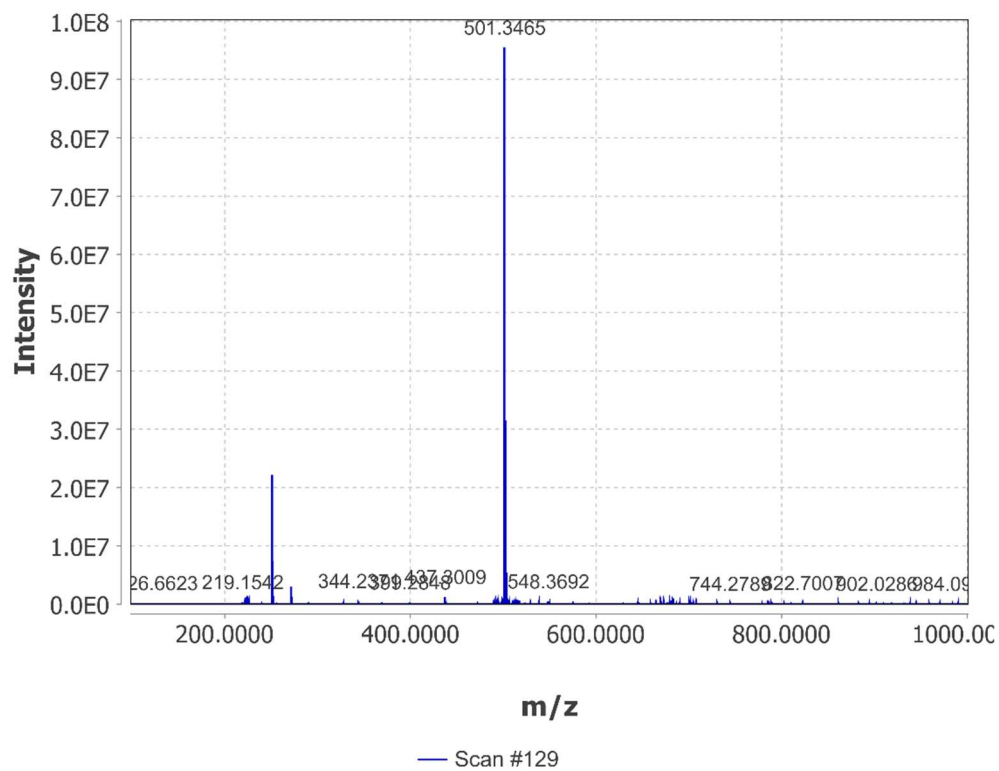
rac-19k (^{13}C):



rac-19k (HRESIMS):

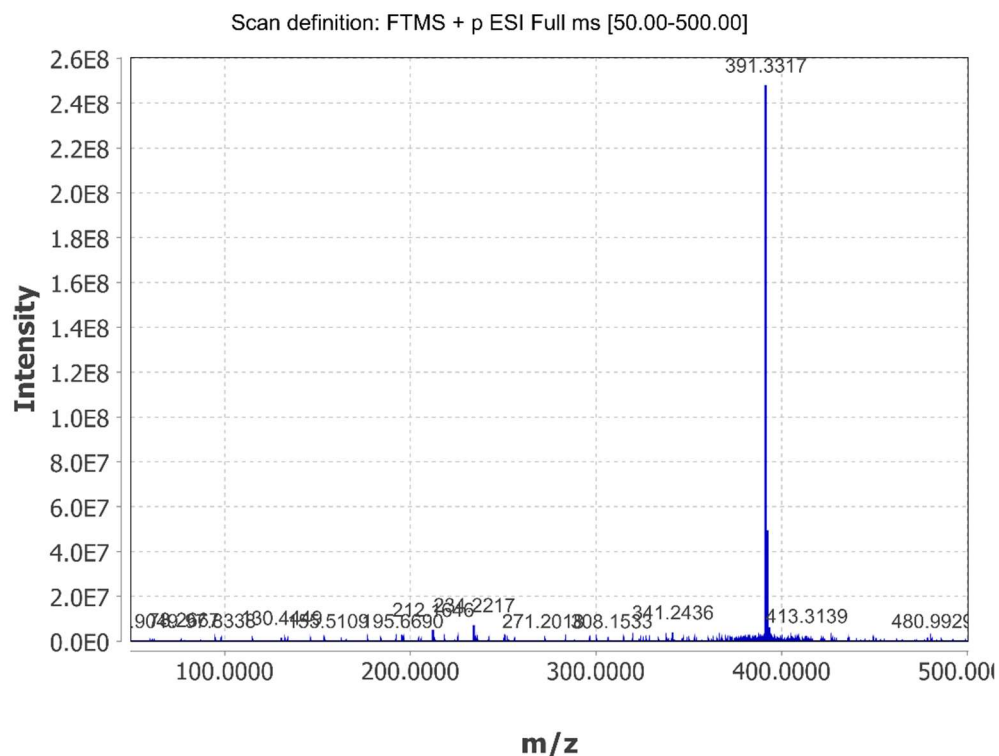
07-heruph-SH19.raw#129 @1.12 MS1 p +, base peak: 501.3465 m/z (9.6E7)

Scan definition: FTMS + p ESI Full ms [100.00-1000.00]

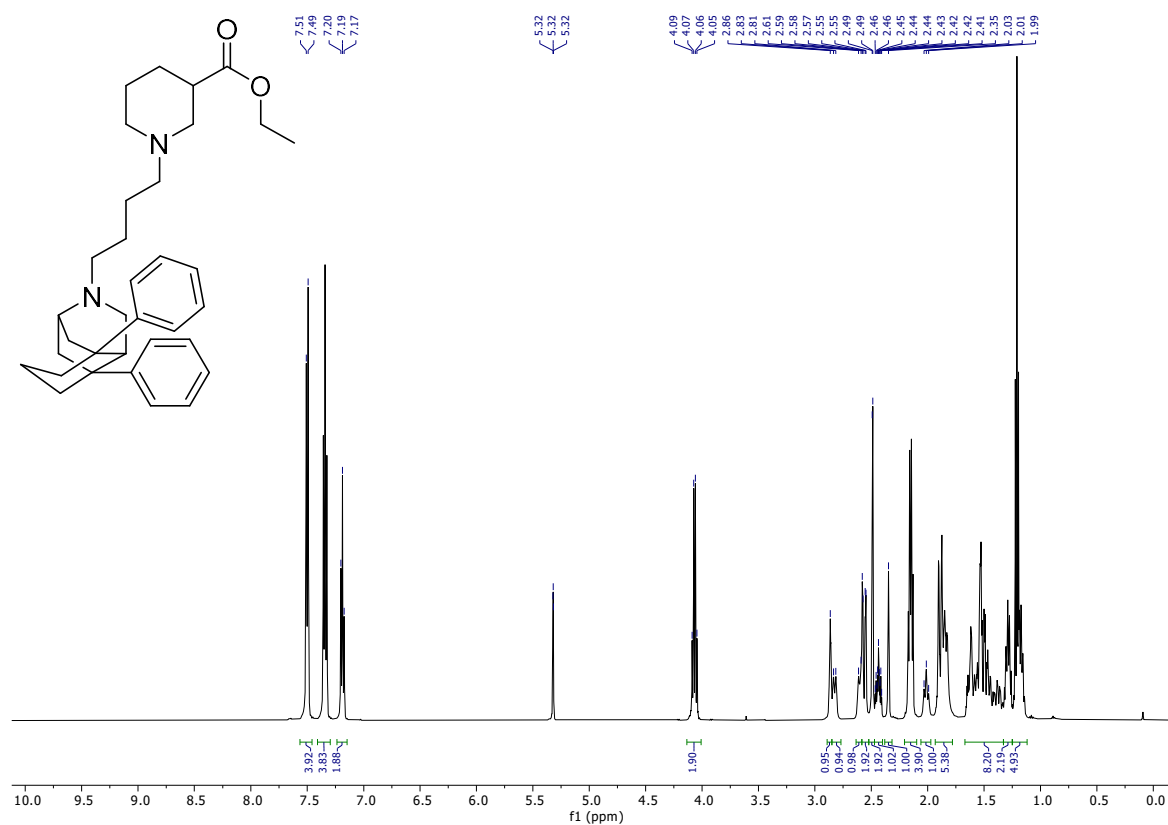


rac-19l (HRESIMS):

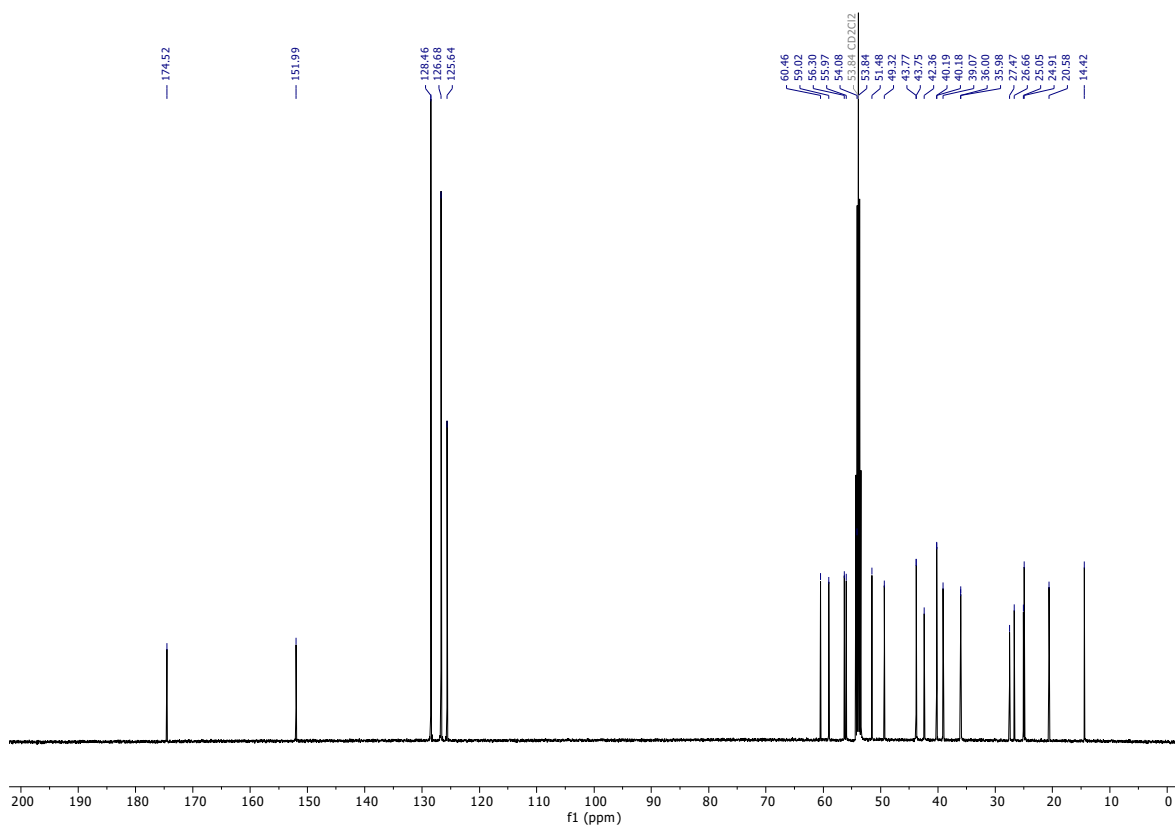
11-heruph-569_181128101823.raw#97 @0.89 MS1 p +, base peak: 391.3317 m/z (2.5E8)



rac-19m (^1H):



rac-19m (^{13}C):



rac-19m (HRESIMS):

04-heruph-613.raw#105 @0.89 MS1 p +, base peak: 515.3640 m/z (6.5E7)

Scan definition: FTMS + p ESI Full ms [100.00-1000.00]

